Edited by Nazario Martín and
Francesco Giacalone

WILEY-VCH

Fullerene Polymers

Synthesis, Properties and Applications

With a Foreword by Maurizio Prato

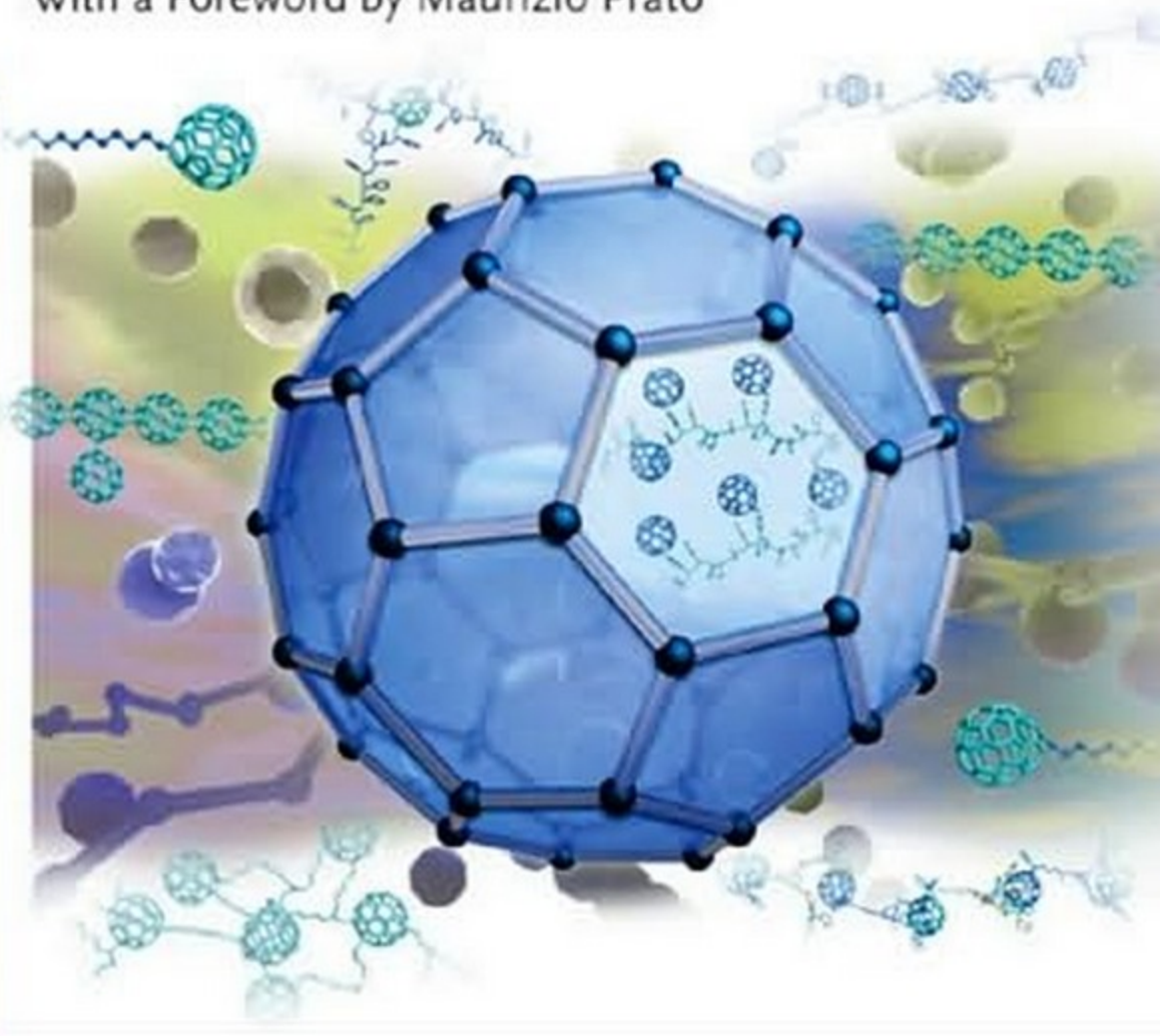

Fullerene Polymers

Edited by
Nazario Martín and
Francesco Giacalone

Further Reading

Dubois, P., Coulembier, O., Raquez, J.-M. (eds.)
Handbook of Ring-Opening Polymerization
2009
ISBN: 978-3-527-31953-4

Atwood, J. L., Steed, J. W. (eds.)
Organic Nanostructures
2008
ISBN: 978-3-527-31836-0

Barner-Kowollik, C. (ed.)
Handbook of RAFT Polymerization
2008
ISBN: 978-3-527-31924-4

Schnabel, W.
Polymers and Light
Fundamentals and Technical Applications
2007
ISBN: 978-3-527-31866-7

Müller, T. J. J., Bunz, U. H. F. (eds.)
Functional Organic Materials
Syntheses, Strategies and Applications
2007
ISBN: 978-3-527-31302-0

Hadziioannou, G., Malliaras, G. G. (eds.)
Semiconducting Polymers
Chemistry, Physics and Engineering
2007
ISBN: 978-3-527-31271-9

Fullerene Polymers

Synthesis, Properties and Applications

Edited by
Nazario Martín and Francesco Giacalone

WILEY-VCH Verlag GmbH & Co. KGaA

The Editors

Prof. Dr. Nazario Martín
Facultad de Quimica
Universidad Complutense
Ciudad Universitaria s/n
28040 Madrid
Spain

Dr. Francesco Giacalone
Univ. degli Studi di Palermo
Dept. of Organic Chemistry
Parco d'Orleans II
90128 Palermo
Italy

Library of Congress Card No.: applied for

British Library Cataloguing-in-Publication Data
A catalogue record for this book is available from the British Library.

Bibliographic information published by the Deutsche Nationalbibliothek
The Deutsche Nationalbibliothek lists this publication in the Deutsche Nationalbibliografie; detailed bibliographic data are available on the Internet at <http://dnb.d-nb.de>.

Composition SNP Best-set Typesetters Ltd., Hong Kong
Printing Betz-Druck GmbH, Darmstadt
Bookbinding Litges & Dopf GmbH, Heppenheim
Cover Design Formgeber, Eppelheim

Printed in the Federal Republic of Germany
Printed on acid-free paper

ISBN: 978-3-527-32282-4

Foreword

From a non-technical point of view, we can think of this book as a treatise on nanojewelry. What makes nanojewels so precious is the combination of two classes of unique materials, polymers and fullerenes. Put together, these building blocks can form nanobracelets or nanonecklaces, such as illustrated below, using the creativity typical of organic chemists.

In fact, this book is a pure gem. The work, realized by Nazario Martín and Francesco Giacalone, fills a gap in the scientific topic of advanced materials. The various synthetic approaches and the new properties exhibited by the fullerene-polymers are described in this beautiful monograph, which gathers together first-class contributions from authorities in the field.

All the different geometries and the related properties of the resulting materials are discussed in depth. The processability and wide applicability of polymers is enriched with the geometrical, electronic and photophysical properties of fullerenes. The result is a unique class of novel materials with huge potential in composite science and electronics.

This book is aimed at the broad community of scientists working in various fields of chemistry, physics, materials science and engineering, but is also valuable for graduate students who wish to approach this very interdisciplinary field.

Trieste, June 2009 *Maurizio Prato*

Fullerene Polymers. Synthesis, Properties and Applications. Edited by Nazario Martín and Francesco Giacalone

ISBN: 978-3-527-32282-4

Contents

Fullerene Polymers. Synthesis, Properties and Applications. Edited by Nazario Martín and Francesco Giacalone

ISBN: 978-3-527-32282-4

Preface

Polymers are everywhere! These macromolecules formed by repeating units are in the base of life as constituents of all living organisms and are widely spread in nature. On the other hand, chemists have also been able to prepare non-natural polymers to fabricate a Pleiades of new materials to create new objects and devices with unprecedented properties. Actually, polymers represent one of the most outstanding contributions of science to society, strongly influencing the development of practical technological applications.

A more recent scientific achievement occurred in 1985 when R. F. Curl, H. W. Kroto and R. E. Smalley reported the discovery of the first molecular carbon allotrope constituted by 60 carbon atoms organized in a perfect spherical cage formed by 12 pentagons and 20 hexagons with an I_h symmetry. Soon afterwards, Krästchmer and Huffman reported in 1990 the first preparation of the C_{60} molecule in multigram amounts, thus opening the avenue to the chemical modification and, therefore, to the preparation of new fullerene derivatives exhibiting properties modulated at will. The interest and expectations of these new molecules for many purposes made them the most studied chemical compounds during the last two decades. Because of this excitement, the discoverers of fullerenes were awarded the Nobel Prize in Chemistry in 1996.

The combination of the unique fullerenes with highly versatile polymer chemistry has given rise to a new interdisciplinary field. Thus, all the knowledge on the synthesis, mechanical strength, processing and ease of manipulation of natural as well as artificial macromolecules has been applied to fullerenes to achieve new fullerene-based architectures in the search for new materials exhibiting unprecedented properties.

Because of the interest of this topic, several reviews have been reported previously in the literature, most of them focusing on partial aspects or considered within a broader context of general studies on fullerenes. However, no single volume has so far been compiled on the topic of fullerene polymers chemically synthesized, authored by prominent experts in this hybrid field. Therefore, this book aims to highlight and update the most recent advances in this topic, gathering the huge amount of work reported along the years in a rational and systematic way.

Fullerene Polymers. Synthesis, Properties and Applications. Edited by Nazario Martín and Francesco Giacalone

ISBN: 978-3-527-32282-4

The book contains 12 chapters, compiling the different types of polymers bearing fullerenes, which have been organized according to the position of the fullerene units within the polymer (side-chain, main-chain, end-capped or star polymers), or, alternatively, focusing on a specific aspect where the combination of fullerenes and polymers has created a new scenario from structural (fullerene-containing helical polymers) or applied (electroactive C_{60}-polymer systems or polyfullerene-based organic solar cells) viewpoints. Furthermore, because of the tremendous advance experienced by systems in which fullerenes and polymers are brought together by means of supramolecular interactions, a chapter has been specifically dedicated to this new type of materials governed by noncovalent forces. The mosaic is completed with the presence of two chapters devoted to related chemical systems such as C_{60}-based dendrimers and liquid crystals endowed with fullerenes, as well as a final chapter in which the polymers are associated with carbon nanotubes, instead of fullerenes, as another form of carbon nanostructures.

We hope that this volume will serve not only the specialists but also as a reference work for a broad audience of non-specialists by gathering together a large part of the extensive literature related to this field.

We are grateful to all the invited contributors who readily accepted the idea of writing a chapter, convinced that each review would be a guideline to further establish this emerging field where fullerenes and polymers converge.

We express our sincere gratitude to all those scientists who have contributed their time and effort to the work cited in this book. Last, but not least, our gratitude is also extended to Wiley-VCH for their support and enthusiasm with our idea of editing this work, as well as their interest in the preparation of this book.

Nazario Martín
Francesco Giacalone

Contributors

Antonio Cravino
University of Angers
CIMA
CNRS UMR 6200
Group Linear Conjugated
Systems
2 Bd. Lavoisier
49045 Anges
France

Sheng Dai
University of Adelaide
School of Chemical Engineering
Adelaide SA 5005
Australia

Robert Deschenaux
Université de Neuchâtel
Institut de Chimie
Avenue de Bellevaux 51
2009 Neuchâtel
Switzerland

Bertrand Donnio
Institut de Physique et Chimie des
Matériaux de Strasbourg
Groupe des Matériaux Organiques
23 Rue du Loess
F-67034 Strasbourg
France

Francesco Giacalone
Università degli Studi di Palermo
Dipartimento di Chimica Organica
"E. Paternò"
Via delle Scienze
Parco d'Orleans – Padiglione 17
90100 Palermo
Italy

Suat Hong Goh
National University of Singapore
Department of Chemistry
Singapore 117543
Singapore

Daniel Guillon
Institut de Physique et Chimie des
Matériaux de Strasbourg
Groupe des Matériaux Organiques
23 Rue du Loess
F-67034 Strasbourg
France

Fullerene Polymers. Synthesis, Properties and Applications. Edited by Nazario Martín and Francesco Giacalone

ISBN: 978-3-527-32282-4

Takeharu Haino
Hiroshima University
Department of Chemistry
Graduate School of Science
1-3-1 Kagamiyama
Higashi-Hiroshima
739-8526
Japan

Mª Ángeles Herranz
Universidad Complutense de Madrid
Departamento de Química Orgánica
Facultad de Ciencias Químicas
28040 Madrid
Spain

Changshui Huang
Chinese Academy of Sciences
Institute of Chemistry
CAS Key Laboratory of Organic Solids Institute of Chemistry
Beijing 100190
China

Yuliang Li
Chinese Academy of Sciences
Institute of Chemistry
CAS Key Laboratory of Organic Solids Institute of Chemistry
Beijing 100190
China

Katsuhiro Maeda
Kanazawa University
Graduate School of Natural Science and Technology
Kakuma-machi
Kanazawa 920-1192
Japan

Nazario Martín
Universidad Complutense de Madrid
Departamento de Química Orgánica
Facultad de Ciencias Químicas
28040 Madrid
Spain

Claude Mathis
Institut Charles Sadron
CNRS – Université de Strasbourg
23 Rue du Loess
BP 84047
67034 Strasbourg Cedex 2
France

Jean-François Nierengarten
Université de Strasbourg
Ecole Européenne de Chimie Polymères et Matériaux (ECPM)
Laboratoire de Chimie des Matériaux Moléculaires
25 rue Becquerel
67087 Strasbourg Cedex 2
France

Palaniswamy Ravi
Nanyang Technological University
Singapore – MIT
School of Medical and Aerospace Engineering
50 Nanyang Avenue
Singapore 639798
Republic of Singapore

Niyazi Serdar Sariciftci
Johannes Kepler University Linz
Linz Institute for Organic Solar Cells (LIOS)
Physical Chemistry
Altenbergerstraβe 69
4040 Linz
Austria

Kam Chiu Tam
University of Waterloo
Department of Chemical Engineering
200 University Avenue West
Waterloo
Ontario
Canada N2L 3G1

Fred Wudl
University of California
Department of Chemistry and Biochemistry
Santa Barbara, CA 93106
USA

Eiji Yashima
Nagoya University
Department of Molecular Design and Engineering
Graduate School of Engineering
Chikusa-ku
Nagoya 464-8603
Japan

Weidong Zhou
Chinese Academy of Sciences
Institute of Chemistry
CAS Key Laboratory of Organic Solids
Institute of Chemistry
Beijing 100190
China

1
Fullerene-Containing Polymers: An Overview

Francesco Giacalone, Nazario Martín, and Fred Wudl

1.1
Polyfullerenes: A Brief History

Fullerenes, the new molecular allotrope of carbon, were discovered in 1985 by H. W. Kroto, R. F. Curl and R. E. Smalley [1], who were awarded the Nobel Prize in Chemistry in 1996 due to this seminal scientific finding. However, it was not until 1990 that C_{60} became available in multigram amounts with the preparation procedure of Krätschmer and Huffman [2]. Since then, "the chemistry of fullerenes" [3] has only been limited by the imagination of chemists. Thus, the development of chemical reactions able to modify the chemical structure of C_{60} led to new fullerene derivatives [4] with outstanding structural [5], magnetic [6], superconducting [7], electrochemical [8] and photophysical properties [9].

Soon after the discovery of fullerenes, the first fullerene-containing polymer was synthesized; thus a new and powerful type of material emerged that can combine the processability, ease of handling and toughness of polymers with the rather unique geometrical and electronic properties of fullerenes. To the best of our knowledge, the first reported example of a polyfullerene compound is due to G. A. Olah, who reacted a C_{60}/C_{70} mixture to react with monodispersed polystyrene using $AlCl_3$ as a catalyst in a Friedel–Crafts reaction [10].

Since then, a huge number of very different C_{60}-polymers have been prepared, and their literature has been widely reviewed [11]. Furthermore, as expected, several polymers showed outstanding properties such as optical limiting [12] or photoinduced electron transfer [13] to name just a few. Notably, however, several polyfullerenes have been employed as active materials in electroluminescent devices [14], non-volatile flash devices [15], as well as in one of the most realistic applications of fullerenes, photovoltaic solar cells [16].

In this introductory chapter we summarize the various types of polyfullerenes, resuming the main synthetic strategies employed for their preparation. Moreover, for each family, the first examples have been emphasized as well as some more recently reported remarkable examples, to give a more precise idea about where the field is moving to.

Fullerene Polymers. Synthesis, Properties and Applications. Edited by Nazario Martín and Francesco Giacalone

ISBN: 978-3-527-32282-4

1.2 Classification of Polyfullerenes

This section overviews the different types of [60]fullerene-containing polymers according to their chemical structure (Figure 1.1). Moreover, a general insight into their principal synthetic routes is shown to provide the reader with a practical summary.

As a criterion for the classification, we have ordered the many families of polyfullerenes taking into account both their increasing chemical complexity and the difficulty in synthesizing them. In this sense, all-C_{60} and organometallic polymers are presented first, followed by the random crosslinked ones, since their synthesis

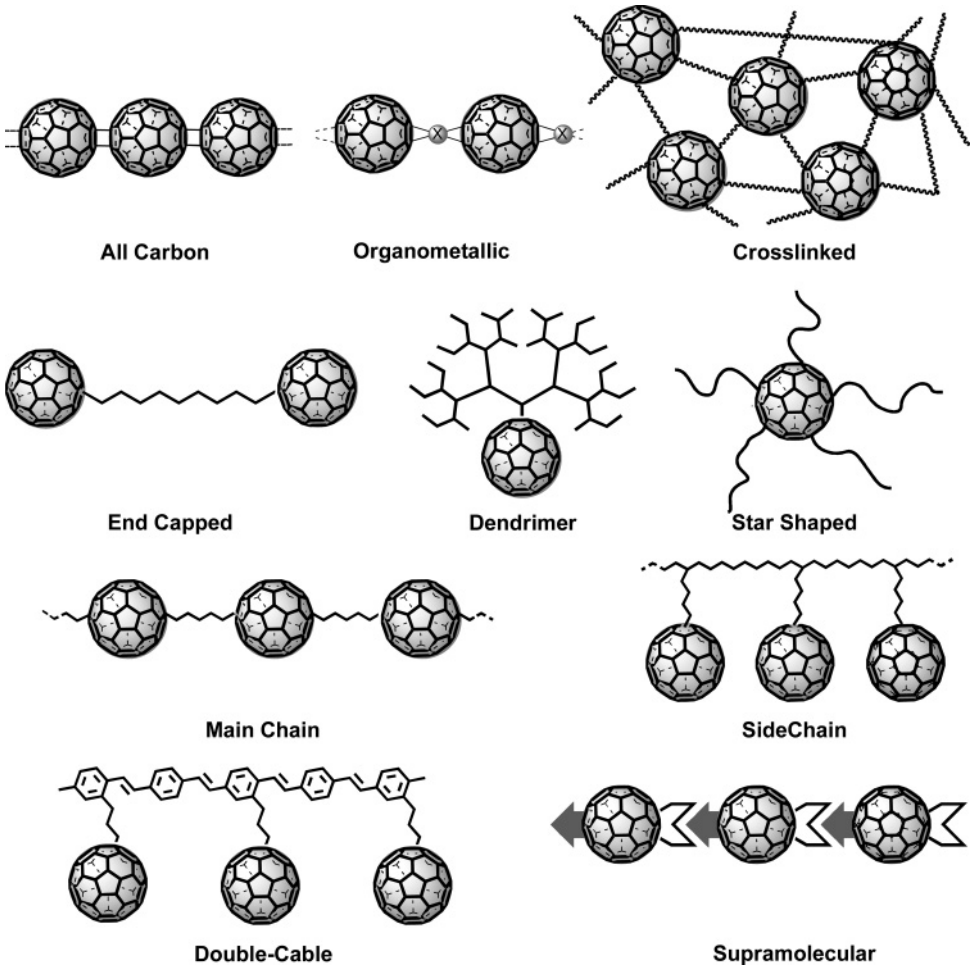

Figure 1.1 Schematic representation of the different types of C_{60}-containing polymers.

often requires lower chemical control. We then focus on those polymers in which only a few units of C_{60} are present, such as end-capped, star-polymers and the related dendrimers. Hence, the subsequent classes are those that require a higher level of synthetic control and represent the major challenge for the chemist, namely main-chain and side-chain polymers, including the so-called double-cable polymers. Finally, we show the more recent supramolecular polymers, in which aggregation and organization stems from the interaction of complementary units properly designed for self-assembly.

1.2.1
All-C_{60} Polymers

With the term all-fullerene polymers are intended specifically those materials or structures constituted exclusively by fullerene units covalently linked to each other. Some authors refer to them as "intrinsic polymers" [17].

The first example was described by Rao in 1993 who, after exposure of C_{60} to visible light, obtained an insoluble photopolymerized film [18]. Soon thereafter, the first piezopolymerized polyfullerene was also reported [19]. Beside polymerizations carried out in the presence of light or with pressure, electron beam-induced [20] and plasma-induced polymerization [21] are also known.

The mechanism of the polymerization process involves [2 + 2] cycloadditions between two 6-6 double bonds of neighboring C_{60} molecules to form cyclobutane rings connecting the two fullerene cages [22] (Figure 1.2).

More recently, a new frontier was opened up by filling single-walled carbon nanotubes with C_{60} to form the so-called "fullerene peapods" [23]. In 2003, Terrones *et al.* studied fullerene coalescence to a polyfullerene induced by electron irradiation on pristine nanotube peapods [24], paving the way to new highly conducting and semiconducting tubular structures with specific electronic characteristics (Figure 1.3).

1.2.2
Organometallic Polymers

Often, this class is considered as a subclass of all-C_{60} polymers that should be considered as heteroatom-containing polymers, since their structures contain metals or elements other than carbon. In 1994, Forró discovered that the fulleride

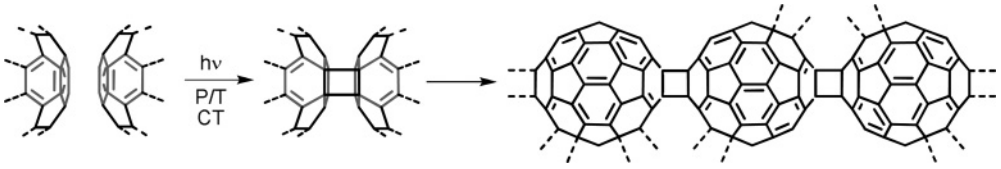

Figure 1.2 Formation of all-C_{60} polyfullerenes by [2 + 2] cycloaddition reactions.

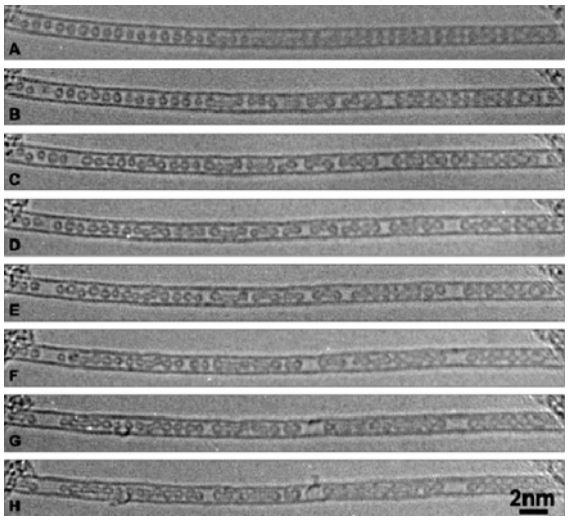

Figure 1.3 Sequence of TEM micrographs showing irradiation-induced coalescence of C_{60} within the lumen of an isolated single-walled carbon nanotube. (a) Starting configuration after a minimal electron dose; (b–h) consecutive images recorded at 60–90 s intervals. (Reprinted from Reference [24] with the permission of the American Chemical Society.)

phases AC_{60} (A = K, Rb, Rb or Cs), undergo [2 + 2] cycloadditions producing polyfullerenes with alkali metals in the crystal voids [25]. For organometallic polymers, metal doping of C_{60} affords the corresponding charge-transfer polymer [26].

To date several different metals have been copolymerized with fullerene but, among them, palladium has led to the most promising copolymers with outstanding properties. In fact, in 1992 Nagashima *et al*. reported the first examples of poly-(C_{60}:Pd) in which the change in the Pd : C_{60} ratio affects the dimensionality of the resulting polymer (from one-dimensional to three-dimensional) [27]. Furthermore, they found that the polymer $(C_{60}Pd_3)_n$ catalyzes heterogeneous hydrogenation reactions of alkenes [28].

On the other hand, much work has been devoted by Balch to the study of the electrochemical formation and properties of redox-active films formed from fullerenes, or a fullerene derivative, and selected transition-metal complexes of Pd(II), Pt(II), Rh(II) and Ir(I) [29]. These organometallic films may find potential application as charge storage materials for batteries, photovoltaic devices and electrochemical sensors.

1.2.3 Crosslinked Polymers

The synthesis of crosslinked polymers usually proceeds from random and quick reactions that take place in three dimensions with the help of the C_{60} sphere.

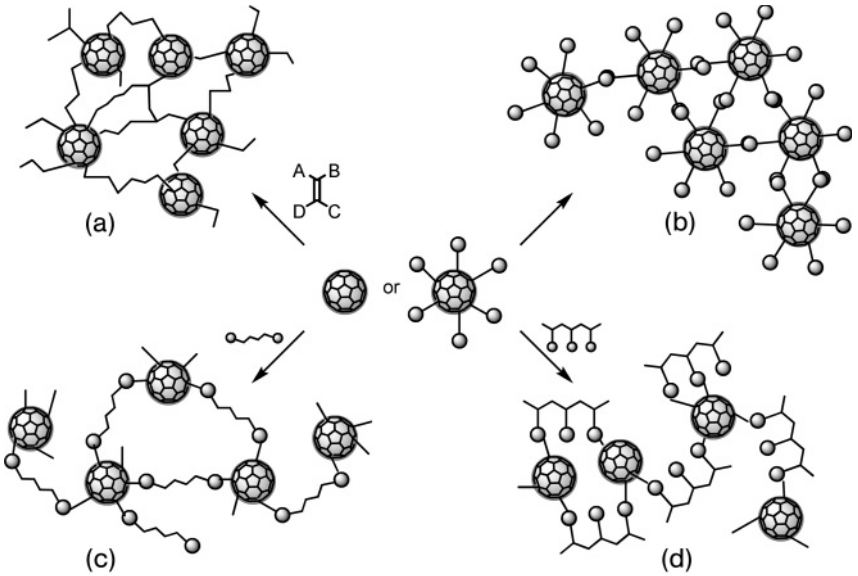

Figure 1.4 Synthetic strategies for the synthesis of C_{60}-crosslinked polymers.

However, a certain level of control of the addition reactions to the 30 fullerene double bonds is required to avoid a drastic intractability of the final products, which severely prevents characterization of the obtained material.

Crosslinked C_{60}-containing polymers can be prepared by four main pathways (Figure 1.4):

1 C_{60} or a C_{60} derivative and a monomer are mixed together and allowed to react randomly (Figure 1.4a);
2 a multisubstituted C_{60} derivative is homopolymerized in three-dimensions (Figure 1.4b);
3 a preformed polymer properly functionalized at the end termini is allowed to react with C_{60} or a multisubstituted C_{60} derivative (Figure 1.4c);
4 polymers endowed with pendant reacting moieties are allowed to react with C_{60} (Figure 1.4d).

Most of the first examples of crosslinked C_{60}-polymers have been prepared by means of free-radical and "living" anionic polymerization. In some cases, the materials thus obtained showed an increase in tensile strength and in thermal mechanical stability [30], some of them exhibiting a good nonlinear optical (NLO) response [12d–e, 31].

1.2.4
End-Capped Polymers

This interesting class of polymers, which could be considered telechelic, is one of the clear examples in which the introduction of only one or two units of C_{60} at the

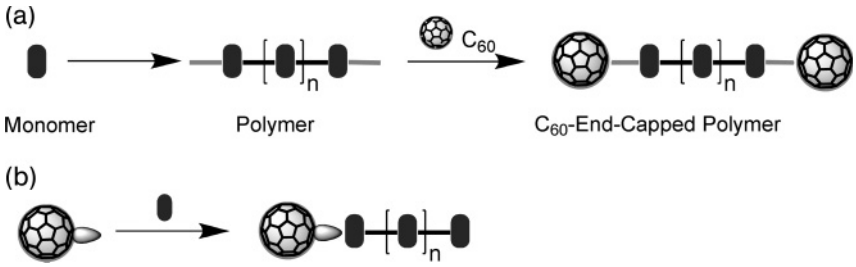

Figure 1.5 Synthetic strategies for the synthesis of C_{60}-end-capped polymers.

terminal positions of the polymeric backbone may strongly influence both molecular and bulk behavior of well-established polymers. In fact, the presence of fullerene moieties at the end of the polymeric chain can modify the hydrophobicity of the parent polymer and, subsequently, its properties.

Two synthetic strategies have been followed to prepare these polymers (Figure 1.5): (a) synthesis of the polymer first, followed by incorporation of fullerenes, by far the most widely employed, and (b) growth of the polymeric chain from a C_{60} derivative as starting material.

The first example of polystyrenes capped with a C_{60} moiety was reported in 1995 by Frey [32]. All the materials easily formed transparent and homogeneous films with increased conductivity.

Nevertheless, two groups have strongly helped the development of this class of polyfullerenes: Goh's, which has focused mainly on the mechanical behavior, miscibility properties and interpolymer complexes of C_{60}-end-capped polymers (Chapter 4) [33], and Tam's, which has emphasized the aggregation behavior and self-assembly of end-capped polymers under appropriate conditions (Chapter 3) [34].

However, other groups are still working on this topic and, recently, an interesting thermosensitive end-capped C_{60}-polymer with radical scavenging properties [35] has been reported, as well as the first example of a telechelic C_{60}-polymer prepared by "click" chemistry [36].

1.2.5
C_{60}-Dendrimers

Although dendrimers are, strictly speaking, oligomers, often, especially in their higher generation, they reach high molecular weights. Moreover, dendrimers may be considered as polymers with a polydispersity of 1.0 – suitable as model compounds for the parent polymers. In addition, fullerene appears to be a natural candidate as core for hosting several dendrons due to its spherical shape, which easily leads to globular structures.

Four types of fullerodendrimers are found in the literature (Figure 1.6):

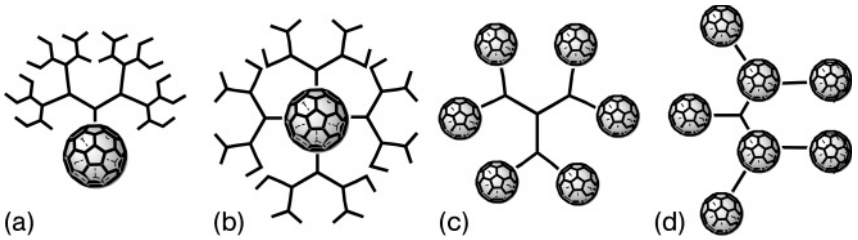

Figure 1.6 Different kinds of fullerodendrimers.

1 a dendrimer is anchored to the fullerene surface (Figure 1.6a);
2 a fullerene is employed as the core, to which several dendrons are attached, forming a globular structure (Figure 1.6b);
3 a fullerene is linked to the peripheral position of the dendrimer (Figure 1.6c);
4 a fullerene is located at the connection points (Figure 1.6d).

The first example of a fullerene covalently linked to a dendrimer was reported by Fréchet and Wudl in 1993 [37]. Since then, several studies have been carried out, mainly by the groups of Hirsch, who have focused on the synthesis and properties of water-soluble C_{60}-dendrimers and on globular dendrimers [38], Nierengarten, who have developed several synthetic routes for a number of different fullerodendrimers and their applications (Chapter 10) [39], and Deschenaux, who have studied, in detail, all aspects regarding C_{60}-dendrimers with liquid crystal properties (Chapter 11) [40].

Very recently, a highly active fullerodendrimer catalyst able to mimic the superoxide dismutase enzyme has been reported [41]. On the other hand, Martín and his research group have recently reported a new supramolecular approach to C_{60}-dendrimers, self-assembled by concave–convex interactions [42].

1.2.6 Star-Shaped Polymers

In this family of C_{60}-polymers, two to twelve long and flexible polymer chains are covalently linked to a fullerene unit with topologies similar to that of sea-stars. Such polymers have also been called "flagellenes," in the first example reported in 1992, since its shape resembles that of flagellated-unicellular protozoa [43].

To date, they have been synthesized by two pathways (Figure 1.7): (a) the "graft-in" approach, in which preformed polymers are linked to the fullerene unit, and (b) the "graft-from" approach, in which the polymeric chains grow-up from the surface of properly functionalized fullerene-derivatives. Notably, both approaches have also been employed for the covalent functionalization of single-walled carbon nanotubes (Chapter 12).

This field has been mainly explored by the group of Mathis (Chapter 5), who have developed several syntheses of a number of flagellanes and studied their chemical and physical properties [44].

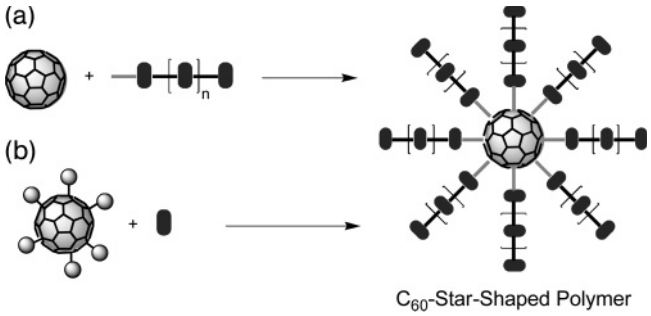

Figure 1.7 Synthetic strategies for the synthesis of C_{60}-star-shaped polymers.

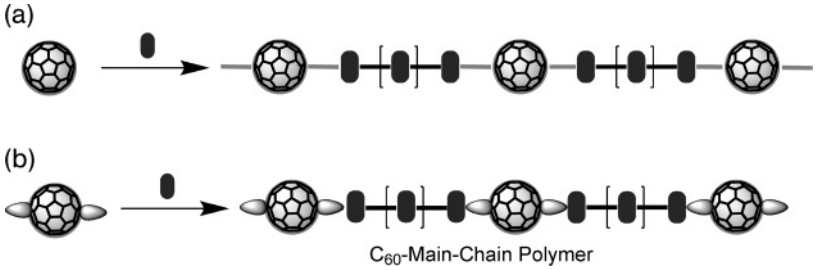

Figure 1.8 Synthetic strategies for the synthesis of C_{60}-main-chain polymers.

Recently, several groups have focused on the preparation of water-soluble C_{60}-star polymers as potential photochemotherapeutic agents for the photodynamic therapy of cancer [45].

1.2.7 Main-Chain Polymers

In this family of C_{60}-polymers, also called "in-chain" or "pearl necklace" [11b], the fullerene units are located in the polymer backbone, forming a necklace-type structure. They have been synthesized by two different strategies (Figure 1.8): (a) direct reaction between the C_{60} cage and a symmetrically difunctionalized monomer and (b) polycondensation between a fullerene bisadduct (or a mixture) and a difunctionalized monomer; the latter is by far the most employed.

Owing to the low control of the double-addition to C_{60} that leads to eight possible isomers, and the difficult preparation of pure bis-adducts, this class of compounds has been perhaps the least explored among all the polyfullerenes (Chapter 2).

Nevertheless, a series of water-soluble poly(fullerocyclodextrin)s has been prepared that shows good performances as a DNA-cleaving agent [46].

1.2.8 Side-Chain Polymers

Without doubt, this is by far the most studied family of C_{60}-polymers, also called "on-chain" or "charm-bracelet," with a wide range of potential applications (Chapter 2).

Although many examples have been reported, the synthetic strategies followed for the preparation of side-chain polymers can be summarized as two different approaches (Figure 1.9): (a) direct introduction of fullerene itself or a C_{60}-derivative into a preformed polymer and (b) synthesis of a C_{60} derivative that can be, in turn, directly homopolymerized or copolymerized together with other monomer(s).

The first example belonging to this category was reported by the group of Wudl in 1992 [47]. Among the recent literature, we emphasize the outstanding performances showed by two recent examples of side-chain C_{60}-polymer-based organic solar cells reported by Sariciftci (2.0% efficiency) [48] and Fréchet (2.8% efficiency) [49].

1.2.8.1 Double-Cable Polymers

In this subclass of side-chain polymers, the main chain always consists of a π-conjugated backbone with electron-donating characteristics, the so-called p-type cable, to which several electron-accepting fullerene cages, or an n-type cable, are covalently linked. Owing to its intrinsic electronic properties, numerous double-cable-polymers (D-C) have been employed in electro-optical devices, namely photovoltaic devices (Chapters 7 and 8) [50].

The chemical strategies followed for the synthesis of D-C-polymers are the same as those described for side-chain C_{60}-polymers. In addition, they can be prepared by electropolymerization of a suitable monomer.

The first example was reported in 1994 by Diederich, who electropolymerized a bis(1,3-dialkyne)methanofullerene to obtain conductive films [51]. Nowadays, several research groups are engaged in the synthesis and study of D-C polymers, especially in the search for more efficient organic photovoltaic solar devices [52].

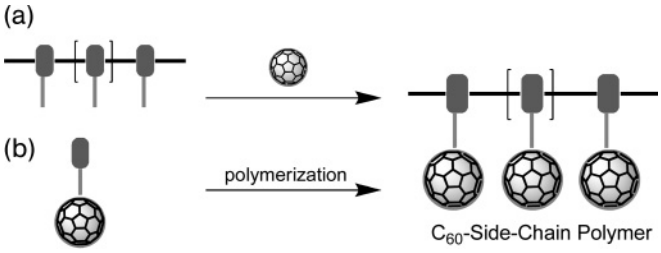

Figure 1.9 Synthetic strategies for the synthesis of side-chain C_{60}-polymers.

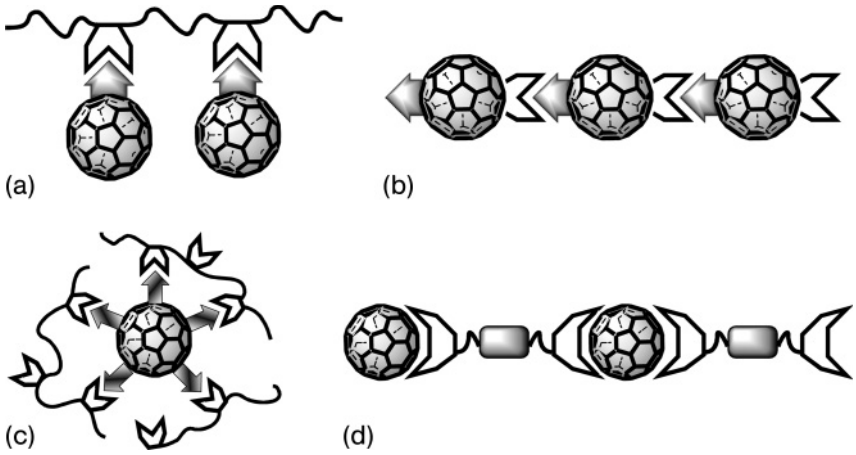

Figure 1.10 Different forms of C_{60}-supramolecular polymers.

1.2.9
Supramolecular Polymers

Although the supramolecular chemistry of fullerene derivatives is a well explored and established field [53], surprisingly, fullerene-containing supramolecular polymer systems have been scarcely studied. In fact, this family can be considered as the most recently explored among the other polyfullerenes, and it is now experiencing growing interest.

According to their syntheses, four kinds of C_{60} supramolecular polymers can be formed (Figure 1.10) (Chapter 9): (a) systems obtained by interactions between functionalized polymers and C_{60} derivatives or fullerene itself; (b) assembly of self-complementary C_{60} derivatives; (c) multisubstituted fullerene derivatives and complementary polymeric backbones; and (d) assemblies between ditopic concave guests and C_{60} by means of concave–convex complementary interactions.

As stated, this has been the last family to appear since the first example was reported in 1999 by the group of Dai, regarding the significant enhancement in the conduction experienced by polyanilines when mixed with polysulfonated fullerene [54]. Recently, other interesting examples of supramolecular helical polymers have been reported (Chapter 6) [55] as well as head-to-tail donor–acceptor supramolecular polymers based in π,π concave–convex interactions [56].

1.3
Outlook and Perspective

Implementing the chemistry of fullerenes in macromolecular chemistry has received a great deal of attention in the last decade and, as a result, new polymer materials exhibiting unusual structural, electrochemical and photophysical

properties have been obtained. The preparation of these fullerene-containing macromolecules has required much synthetic effort in which well-known synthetic protocols in modern organic synthesis have allowed the preparation of a wide variety of chemical structures, limited only by the imagination of chemists.

We are at the dawn of a new interdisciplinary field in which C_{60}-based polymers should afford unprecedented materials in which the presence of fullerenes as photo- and electroactive components of the polymer structure should give rise to new properties of interest for the development of technological applications. In fact, in some cases very promising materials have already been prepared, representing the tip of the iceberg that will become more visible during the next few years. Polymers are certainly among the most important achievements that chemistry has given to society in terms of practical applications and, surely, the presence of fullerenes will open up new avenues for remarkable materials.

The following chapters will convince the reader of the fascinating new scientific scenario exhibited by fullerene-containing polymers. For that purpose, leading scientists will provide the most recent perspective of their different fields of expertise, thus enhancing the scope of the short overview presented in this chapter.

References

1 Kroto, H.W., Heath, J.R., O'Brien, S.C., Curl, R.F. and Smalley, R.E. (1985) *Nature*, **318**, 162.

2 Kratschmer, W., Lamb, L.D., Fostiropoulos, K. and Huffman, D.R. (1990) *Nature*, **347**, 354.

3 (a) Hirsch, A. and Brettreich, M. (2006) *Fullerenes: Chemistry and Reactions*, Wiley-VCH Verlag GmbH, Weinheim, Germany.
(b) Lippard, S.J. and Berg, J.M. (1994) *Principles of Bioinorganic Chemistry*, University Science Books, USA.
(c) Guldi, D.M. and Martín, N. (eds) (2002) *Fullerenes: From Synthesis to Optoelectronic Properties*, Kluwer Academic Publishers, Dordrecht, The Netherlands.

4 Martín, N. (2006) New challenges in fullerene chemistry. *Chem. Commun.*, 2093.

5 (a) Hammond, G.S. and Kuck, V.J. (eds) (1992) *Fullerenes: Synthesis, Properties, and Chemistry of Large Carbon Clusters*, ACS Symposium Series 481, American Chemical Society, Washington, DC.
(b) Hebard, A.F. (1993) *Annu. Rev. Mater. Sci.*, **23**, 159.

6 (a) Allemand, P.M., Khemani, K.C., Koch, A., Wudl, F., Holczer, K., Donovan, S., Grüner, G. and Thompson, J.D. (1991) *Science*, **253**, 301.
(b) Lappas, A., Prassides, K., Vavekis, K., Arcon, D., Blinc, R., Cevc, P., Amato, A., Feyerherm, R., Gygax, F.N. and Schenck, A. (1995) *Science*, **267**, 1799.
(c) Narymbetov, B., Omerzu, A., Kabanov, V.V., Tokumoto, M., Kobayashi, H. and Mihailovic, D. (2000) *Nature*, **407**, 883.
(d) Makarova, T.L., Sundqvist, B., Hohne, R., Esquinazi, P., Kopelevich, Y., Scharff, P., Davydov, V.A., Kashevarova, L.S. and Rakhmanina, A.V. (2001) *Nature*, **413**, 716.

7 (a) Hebard, A.F., Rosseinsky, M.J., Haddon, R.C., Murphy, D.W., Glarum, S.H., Palstra, T.T.M., Ramirez, A.P. and Kortan, A.R. (1991) *Nature*, **350**, 600.
(b) Schon, J., Kloc, C. and Batlogg, B. (2001) *Science*, **293**, 2432.
(c) Dagotto, E. (2001) *Science*, **293**, 2410.
(d) Grant, P. (2001) *Nature*, **413**, 264.

8 (a) Xie, Q., Pérez-Cordero, E. and Echegoyen, L. (1992) *J. Am. Chem. Soc.*, **114**, 3978.
(b) Echegoyen, L. and Echegoyen, L.E. (1998) *Acc. Chem. Res.*, **31**, 593.

9 (a) Guldi, D.M. (2000) *Chem. Commun.*, 321.

(b) Guldi, D.M. and Prato, M. (2000) *Acc. Chem. Res.*, **33**, 695.

10 Olah, G.A., Bucsi, I., Lambert, C., Aniszfeld, R., Trivedi, N.J., Sensharma, D.K. and Prakash, G.K.S. (1991) *J. Am. Chem. Soc.*, **113**, 9387.

11 (a) Prato, M. (1997) *J. Mater. Chem.*, **7**, 1097.
(b) Chen, Y., Huang, Z.-E., Cai, R.-F. and Yu, B.-C. (1998) *Eur. Polym. J.*, **34**, 137.
(c) Dai, L. (1999) *J. Macromol. Sci. Rev. Macromol. Chem. Phys. C*, **39**, 273.
(d) Dai, L. (1999) *Polym. Adv. Technol.*, **10**, 357.
(e) Geckeler, K.E. and Samal, S. (1999) *Polym. Int.*, **48**, 743.
(f) Geckeler, K.E. and Samal, S. (2000) *Macromol. Sci. Rev. Macromol. Chem. Phys.*, **C40**, 193.
(g) Dai, L. and Mau, A.W.H. (2001) *Adv. Mater.*, **13**, 899.
(h) Wang, C., Guo, Z.-X., Fu, S., Wu, W. and Zhu, D. (2004) *Prog. Polym. Sci.*, **29**, 1079.
(i) Giacalone, F. and Martín, N. (2006) *Chem. Rev.*, **106**, 5136.

12 (a) Tutt, L.W. and Kost, A. (1992) *Nature*, **356**, 225.
(b) Ma, B., Riggs, J.E. and Sun, Y.-P. (1998) *J. Phys. Chem. B*, **102**, 5999.
(c) Bunker, C.E., Lawson, G.E. and Sun, Y.P. (1995) *Macromolecules*, **28**, 3744.
(d) Luang, L., Chen, Q., Sargent, E.H. and Wang, Z.Y. (2003) *J. Am. Chem. Soc.*, **125**, 13648.
(e) Chen, Q., Luang, L., Wang, Z.Y. and Sargent, E.H. (2004) *Nano Lett.*, **9**, 1673.

13 (a) Chen, Y., Huang, Z.-E. and Cai, R.-F. (1996) *J. Polym. Sci. B Polym. Phys.*, **34**, 631.
(b) Chen, Y., Huang, Z.-E., Cai, R.-F., Yu, B.-C., Ito, O., Zhang, J., Ma, W.-W., Zhong, C.-F., Zhao, L., Li, Y.-F., Zhu, L., Fujitsuka, M. and Watanabe, A. (1997) *J. Polym. Sci. B Polym. Phys.*, **35**, 1185.

14 (a) Cloutet, E., Fillaut, J.-L., Gnanou, Y. and Astruc, D. (1994) *J. Chem. Soc., Chem. Commun.*, 2433.
(b) Fedurco, M., Costa, D.A., Balch, A.L. and Fawcett, W.R. (1995) *Angew. Chem. Int. Ed. Engl.*, **34**, 194.
(c) Chen, X., Gholamkhass, B., Han, X., Vamvounis, G. and Holdcroft, S. (2007) *Macromol. Rapid Commun.*, **28**, 1792.
(d) Nanjo, M., Cyr, P.W., Liu, K., Sargent, E.H. and Manners, I. (2008) *Adv. Funct. Mater.*, **18**, 470.

15 Ling, Q.-D., Lim, S.-L., Song, Y., Zhu, C.-X., Chan, D.S.-H., Kang, E.-T. and Neoh, K.-G. (2007) *Langmuir*, **23**, 312.

16 (a) Sariciftci, N.S., Smilowitz, L., Heeger, A.J. and Wudl, F. (1992) *Science*, **258**, 1474.
(b) Yu, G., Gao, J., Hummelen, J.C., Wudl, F. and Heeger, A.J. (1995) *Science*, **270**, 1789.
(c) Gutiérrez-Nava, M., Setayesh, S., Rameau, A., Masson, P. and Nierengarten, J.-F. (2002) *New J. Chem.*, **26**, 584.
(d) Mwaura, J.K., Pinto, M.R., Witker, D., Ananthakrishnan, N., Schanze, K.S. and Reynolds, J.R. (2005) *Langmuir*, **21**, 10119.
(e) Adamopoulos, G., Heiser, T., Giovannella, U., Ould-Saad, S., van de Wetering, K.I., Brochon, C., Zorba, T., Paraskevopoulos, K.M. and Hadziioannou, G. (2006) *Thin Solid Films*, **511–12**, 371.
(f) Wang, N., Lu, F., Huang, C., Li. Y., Yuan, M., Liu, X., Liu, H., Gan, L., Jiang, L. and Zhu, D. (2006) *J. Polym. Sci. Part A Polym. Chem.*, **44**, 5863.
(g) De la Escosura, A., Martínez-Díaz, M.V., Torres, T., Grubbs, R.H., Guldi, D.M., Neugebauer, H., Winder, C., Drees, M. and Sariciftci, N.S. (2007) *Chem. Asian J.*, **1–2**, 148.

17 For detailed treatises on this topic:
(a) Special issue on polymeric fullerenes (1997) *Appl. Phys. A: Mater. Sci. Process.*, **64** (3).
(b) Sundqvist, B. (1999) *Adv. Phys.*, **48**, 1.
(c) Blank, V.D., Buga, S.G., Dubitsky, G.A., Serebryanaya, N.R., Yu Popov, M. and Sundqvist, B. (1998) *Carbon*, **36**, 319.

18 Rao, A.M., Zhou, P., Wang, K.-A., Hager, G.T., Holden, J.M., Wang, Y., Lee, W.-T., Bi, X.-X., Eklund, P.C., Cornett, D.S., Duncan, M.A. and Amster, I.J. (1993) *Science*, **259**, 955.

19 Iwasa, Y., Arima, T., Fleming, R.M., Siegrist, T., Zhou, O., Haddon, R.C., Rothberg, L.J., Lyons, K.B., Carter, H.L. Jr., Hebard, A.F., Tycko, R., Dabbagh, G., Krajewski, J.J., Thomas, G.A. and Yagi, T. (1994) *Science*, **264**, 1570.

20 Rao, A.M., Eklund, P.C., Hodeau, J.L., Marques, L. and Nuñez-Regueiro, M. (1997) *Phys. Rev. B*, **55**, 4766.

21 (a) Takahashi, N., Dock, H., Matsuzawa, N. and Ata, M. (1993) *J. Appl. Phys.*, **74**, 5790.
(b) Zou, Y.J., Zhang, X.W., Li, Y.L., Wang, B., Yan, H., Cui, J.Z., Liu, L.M. and Da, D.A. (2002) *J. Mater. Sci.*, **37**, 1043.

22 Nuñez-Regueiro, M., Marques, L., Hodeau, J.L., Béthoux, O. and Perroux, M. (1995) *Phys. Rev. Lett.*, **74**, 278.

23 (a) Smith, B.W. and Luzzi, D.E. (2000) *Chem. Phys. Lett.*, **321**, 169.
(b) Service, R.F. (2001) *Science*, **292**, 45.

24 Hernández, E., Meunier, V., Smith, B.W., Rurali, R., Terrones, H., Buongiorno Nardelli, M., Terrones, M., Luzzi, D.E. and Charlier, J.-C. (2003) *Nano Lett.*, **3**, 1037.

25 (a) Stephens, P.W., Bortel, G., Faigel, G., Tegze, M., Janossy, A., Pekker, S., Oszlányi, G. and Forró, L. (1994) *Nature*, **370**, 636.
(b) Pekker, S., Forró, L., Mihaly, L. and Janossy, A. (1994) *Solid State Commun.*, **90**, 349.

26 Rao, A.M., Eklund, P.C., Venkateswaran, U.D., Tucker, J., Duncan, M.A., Bendele, G.M., Stephens, P.W., Houdeau, J.-L., Marques, L., Nuñez-Regueiro, M., Bashkin, I.O., Ponyatovsky, E.G. and Morovsky, A.P. (1997) *Appl. Phys. A: Mater. Sci. Process.*, **64**, 231.

27 Nagashima, H., Nakaoka, A., Saito, Y., Kato, M., Kawanishi, T. and Itoh, K. (1992) *J. Chem. Soc. Chem. Commun.*, 377.

28 Nagashima, H., Nahaoka, A., Tajima, S., Saito, Y. and Itoh, K. (1992) *Chem. Lett.*, 1361.

29 (a) Winkler, K. and Balch, A.L. (2006) *C. R. Chim.*, **9**, 928.
(b) Balch, A.L., Costa, D.A. and Winkler, K. (1998) *J. Am. Chem. Soc.*, **120**, 9614.
(c) Winkler, K., de Bettencourt-Dias, A. and Balch, A.L. (2000) *Chem. Mater.*, **12**, 1386.
(d) Plonska, M.A., de Bettencourt-Dias, A., Balch, A.L. and Winkler, K. (2003) *Chem. Mater.*, **15**, 4122.

30 Chiang, L.Y., Wang, L.Y. and Kuo, C.-S. (1995) *Macromolecules*, **28**, 7574.

31 (a) Bunker, C.E., Lawson, G.E. and Sun, Y.P. (1995) *Macromolecules*, **28**, 3744.
(b) Kojima, Y., Matsuoka, T., Takahashi, H. and Karauchi, T. (1995) *Macromolecules*, **28**, 8868.
(c) Chen, Q., Luang, L., Sargent, E.H. and Wang, Z.Y. (2003) *Appl. Phys. Lett.*, **83**, 2115.

32 Weis, C., Friedrich, C., Mulhaupt, R. and Frey, H. (1995) *Macromolecules*, **28** (**8**), 403.

33 (a) Huang, X.-D., Goh, S.H. and Lee, S.Y. (2000) *Macromol. Chem. Phys.*, **201**, 2660.
(b) Huang, X.-D. and Goh, S.H. (2000) *Macromolecules*, **33**, 8894.
(c) Song, T., Goh, S.H. and Lee, S.Y. (2003) *Polymer*, **44**, 2563.

34 Ravi, P., Dai, S., Wang, C. and Tam, K.C. (2007) *J. Nanosci. Nanotechnol.*, **7**, 1176.

35 Zhou, G., Harruna, I.I., Zhou, W.L., Aicher, W.K. and Geckeler, K.E. (2007) *Chem. Eur. J.*, **13**, 569.

36 Zhang, W.-B., Tu, Y., Ranjan, R., Van Horn, R.M., Leng, S., Wang, J., Polce, M.J., Wesdemiotis, C., Quirk, R.P., Newkome, G.R. and Cheng, S.Z.D. (2008) *Macromolecules*, **41**, 515.

37 Wooley, K.L., Hawker, C.J., Fréchet, J.M.J., Wudl, F., Srdanov, G., Shi, S., Li, C. and Kao, M. (1993) *J. Am. Chem. Soc.*, **115**, 9836.

38 (a) Camps, X., Schönberger, H. and Hirsch, A. (1997) *Chem. Eur. J.*, **3**, 561.
(b) Brettreich, M. and Hirsch, A. (1999) *Tetrahedron Lett.*, **39**, 2731.
(c) Hirsch, A. and Vostrowsky, O. (2001) *Eur. J. Org. Chem.*, 829.

39 (a) Nierengarten, J.-F., Habicher, T., Kessinger, R., Cardullo, F., Diederich, F., Gramlich, V., Gisselbrecht, J.-P., Boudon, C. and Gross, M. (1997) *Helv. Chim. Acta*, **80**, 2238.
(b) Nierengarten, J.-F. (2000) *Chem. Eur. J.*, **6**, 3667.
(c) Nierengarten, J.-F., Armaroli, N., Accorsi, G., Rio, Y. and Eckert, J.-F. (2003) *Chem. Eur. J.*, **9**, 36.

40 (a) Dardel, B., Deschenaux, R., Even, M. and Serrano, E. (1999) *Macromolecules*, **32**, 5193.
(b) Dardel, B., Guillon, D., Heinrich, B. and Deschenaux, R. (2001) *J. Mater. Chem.*, **11**, 2814.

41 Liu, G.-F., Filipović, M., Ivanović-Burmazović, I., Beuerle, F., Witte, P. and Hirsch, A. (2008) *Angew. Chem. Int. Ed.*, **47**, 3991.

42 (a) Fernández, G., Pérez, E.M., Sánchez, L. and Martín, N. (2008) *J. Am. Chem. Soc.*, **130**, 2410.
(b) Fernández, G., Pérez, E.M., Sánchez, L. and Martín, N. (2008) *J. Am. Chem. Soc.*, **130**, 10674.

43 Samulski, E.T., DeSimone, J.M., Hunt, M.O., Jr., Menceloglu, Y.Z., Jarnagin, R.C., York, G.A., Labat, K.B. and Wang, H. (1992) *Chem. Mater.*, **4**, 1153.

44 (a) Mathis, C., Schmaltz, B. and Brinkmann, M. (2006) *C. R. Chim.*, **9**, 1075.
(b) Ederlé, Y. and Mathis, C. (1997) *Macromolecules*, **30**, 2546.
(c) Ederlé, Y. and Mathis, C. (1997) *Macromolecules*, **30**, 4262.
(d) Ederlé, Y. and Mathis, C. (1999) *Macromolecules*, **32**, 554.

45 (a) Stoilova, O., Jrme, C., Detrembleur, C., Mouithys-Mickalad, A., Manolova, N., Rashkov, I. and Jrme, R. (2006) *Chem. Mater.*, **18**, 4917.
(b) Jiang, G., Zheng, Q. and Yang, D. (2006) *J. Appl. Polym. Sci.*, **99**, 2874.
(c) Stoilova, O., Jerome, C., Detrembleur, C., Mouithys-Mickalad, A., Manolova, N. and Rashkov, I. (2007) *Polymer*, **48**, 1835.

46 Samal, S., Choi, B.-J. and Geckeler, K.E. (2001) *Macromol. Biosci.*, **1**, 329.

47 Shi, S., Khemani, K.C., Li, Q. and Wudl, F. (1992) *J. Am. Chem. Soc.*, **14**, 10656.

48 Drees, M., Hoppe, H., Winder, C., Neugebauer, H., Sariciftci, N.S., Schwinger, W., Schäffler, F., Topf, C., Scharber, M.C., Zhu, Z. and Gaudiana, R. (2005) *J. Mater. Chem.*, **15**, 5158.

49 Sivula, K., Ball, Z.T., Watanabe, N. and Fréchet, J.M.J. (2006) *Adv. Mater.*, **18**, 206.

50 (a) Cravino, A. and Sariciftci, N.S. (2002) *J. Mater. Chem.*, **12**, 1931.
(b) Cravino, A. and Sariciftci, N.S. (2003) *Nat. Mater.*, **2**, 360.
(c) Cravino, A. (2007) *Polym. Int.*, **56**, 943.

51 Anderson, H.L., Boudon, C., Diederich, F., Gisselbrecht, J.-P., Gross, M. and Seiler, P. (1994) *Angew. Chem. Int. Ed. Engl.*, **33**, 1628.

52 (a) Tan, Z., Hou, J., He, Y., Zhou, E., Yang, C. and Li, Y. (2007) *Macromolecules*, **40**, 1868.
(b) Ouhib, F., Khoukh, A., Ledeuil, J.-B., Martinez, H., Desbrières, J. and Dagron-Lartigau, C. (2008) *Macromolecules*, **41**, 9736.

53 (a) Martín, N. and Guldi, D.M. (2002) *J. Mater. Chem.*, **12**, 1978.
(b) Sánchez, L., Martín, N. and Guldi, D.M. (2005) *Angew. Chem. Int. Ed.*, **44**, 5374.
(c) Martín, N., Solladié, N. and Nierengarten, J.-F. (2006) *Electrochem. Soc. Interface*, **15**, 29.
(d) Diederich, F. and Gómez-López, M. (1999) *Chem. Soc. Rev.*, **28**, 263.

54 (a) Dai, L., Lu, J., Matthews, B. and Mau, A.W.H. (1998) *J. Phys. Chem. B*, **102**, 4049.
(b) Lu, J., Dai, L. and Mau, A.W.H. (1998) *Acta Polym.*, **49**, 371.

55 (a) Yashima, E. and Maeda, K. (2008) *Macromolecules*, **41**, 3.
(b) Kawauchi, T., Kumaki, J., Kitaura, A., Okoshi, K., Kusanagi, H., Kobayashi, K., Sugai, T., Shinohara, H. and Yashima, E. (2008) *Angew. Chem. Int. Ed.*, **47**, 515.
(c) Nishimura, T., Tsuchiya, K., Ohsawa, S., Maeda, K., Yashima, E., Nakamura, Y. and Nishimura, J. (2004) *J. Am. Chem. Soc.*, **126**, 11711.

56 (a) Fernández, G., Pérez, E.M., Sánchez, L. and Martín, N. (2008) *Angew. Chem. Int. Ed.*, **47**, 1094.
(b) Pérez, E.M. and Martín, N. (2008) *Chem. Soc. Rev.*, **37**, 1512.

2
Main-Chain and Side-Chain C_{60}-Polymers

Francesco Giacalone and Nazario Martín

2.1
Introduction

Soon after the production of fullerenes in multigram amounts by Krätschmer and Huffman in 1990 [1], the first polymers endowed with the new spherical molecule were reported [2]. Among these first examples, polymers bearing the fullerene unit forming part of the polymer chain (main-chain polymers), or as a pendant unit from the main polymer chain (side-chain polymers), were readily synthesized.

Since then, a wide variety of these two types of fullerene polymers have been prepared, involving most of the well-known basic polymers (polystyrenes, polyethers, polyacrylates, etc.). The expected properties for the new materials stem from the outstanding photo- [3], electro-chemical [4] and photophysical [5] properties of fullerenes with the ease of processability as well as the good thermal and chemical stability of the polymers. As a result, great excitement has always been present in the search for practical applications in various different fields, ranging from materials science [6] to biomedical purposes [7].

To rationalize the number of polymers prepared so far, we have gathered the lesser number of main-chain polymers in the next section, followed by the larger class of side-chain polymers, which are ordered according to their nature. In both cases, the synthetic challenges as well as their potential applications are discussed when available in the literature.

2.2
Main-Chain Polymers

This type of polymer is characterized by the presence of the fullerene spheres in the polymer backbone forming a necklace-type structure. However, the double addition on the C_{60} cage yields complex regioisomeric mixtures (up to eight isomers), and the formation of crosslinking products by multiple additions is also possible. Main-chain polymers are prepared by following two different synthetic

Fullerene Polymers. Synthesis, Properties and Applications. Edited by Nazario Martín and Francesco Giacalone

ISBN: 978-3-527-32282-4

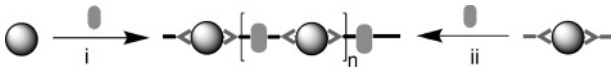

Figure 2.1 Synthetic strategies followed for the synthesis of C_{60}-main-chain polymers.

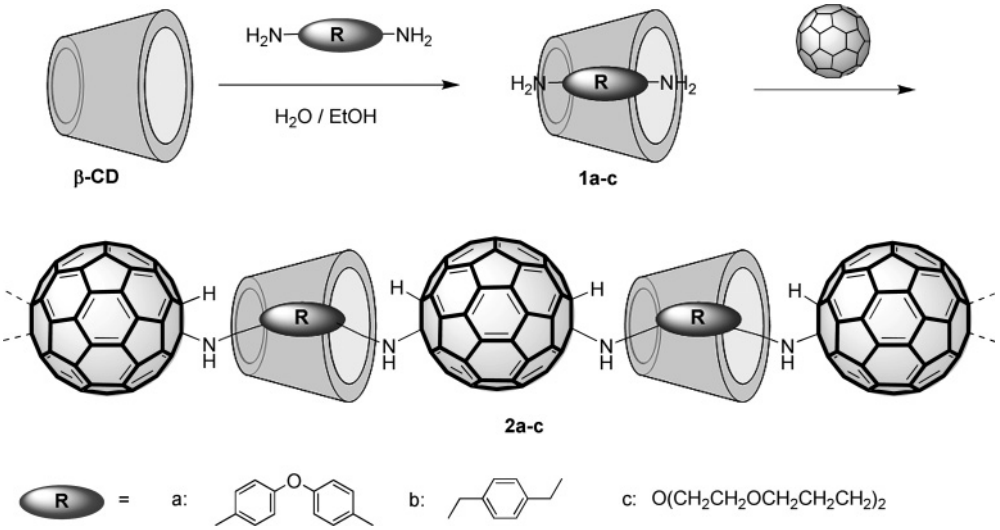

Scheme 2.1 Synthesis of main-chain polymers **2a–c**.

strategies: (i) direct reaction between the C_{60} cage and a suitable symmetrically difunctionalized monomer and (ii) polycondensation between a fullerene bisadduct (or a mixture) and a difunctionalized monomer (Figure 2.1); the latter is the most widely employed.

With the first strategy a series of water-soluble poly(fullerocyclodextrin)s (**2a–c**) have been prepared by Geckeler and coworkers by reacting the β-cyclodextrin-bisamino complexes **1a–c** directly with C_{60} via nucleophilic polyaddition reactions (Scheme 2.1) [8].

These polyrotaxanes showed a good solubility in water (>10 mg mL^{-1}) as well as an excellent DNA-cleaving activity [9]. In fact, small amounts of these polymers can cleave DNA in the presence of visible light with quantitative yields. Therefore, these smart polymers are potential candidates for practical applications in photodynamic cancer therapy [10].

In 1997, Rotello and Nie prepared a thermoreversible main-chain C_{60}-polymer, introducing a poly-Diels–Alder cycloaddition strategy [11a]. They reacted [60]fullerene with bis-anthracene derivative **3** in a 1 : 1 molar ratio at room temperature, obtaining polymer **4** in moderate yield (Scheme 2.2).

This new material showed thermoreversible properties since, after heating at 60–75 °C, it readily cycloreverts into the starting reagents. Interestingly, this process can be repeated several times and no decomposition was observed. This

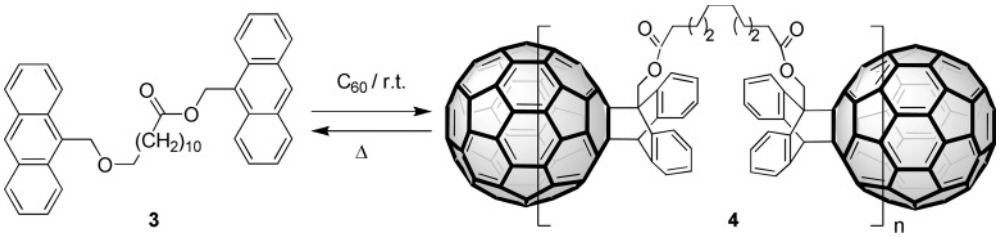

Scheme 2.2 Synthesis of thermoreversible polymer **4**.

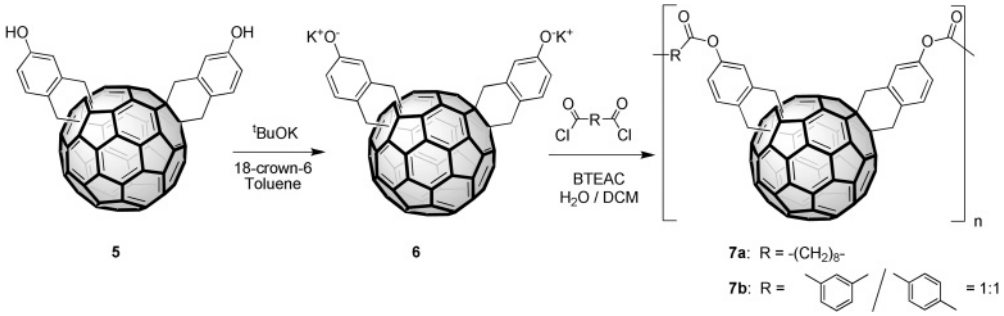

Scheme 2.3 Synthesis of main-chain polymers **7a, b**.

approach has led to the new idea of recyclable and thermally processable C_{60}-based materials, although the low range of temperatures between polymerization and depolymerization is the major problem with these polymers.

As stated, several examples have been reported for the second synthetic strategy in which a fullerene-bisadduct reacts as AA monomer together with a suitably functionalized BB monomer. This reaction can be carried out by employing either a mixture of bisadducts or chromatographically separated isomerically pure bisadducts.

In 1997, Taki *et al*. prepared two in-chain polymers by reacting a mixture of C_{60} bisphenol (**5**) with an equimolar amount of dibasic acid dichloride (sebacoyl dichloride or a 1 : 1 mixture of isophthaloyl chloride/terephthaloyl chloride) at room temperature to afford linear main chain-polyesters **7a, b**, which are soluble in DMF (Scheme 2.3) [12].

Following a similar strategy, two new examples of fullerene-main-chain polymers were later reported (Scheme 2.4) [13].

Polymers **11** and **12** were synthesized by a condensation reaction between an isomeric mixture of 61,61′-bis(*p*-hydroxyphenylmethano)[60]fullerene (**8**) and bisphenol A (**9**) or 1,20-bis(bisphenoxy-A)-eicosane (**10**) in the presence of NaOH. These macromolecules were soluble in organic solvents, with good thermal stability and presented a relatively high M_w (**11**: 151 200; **12**: 18 170).

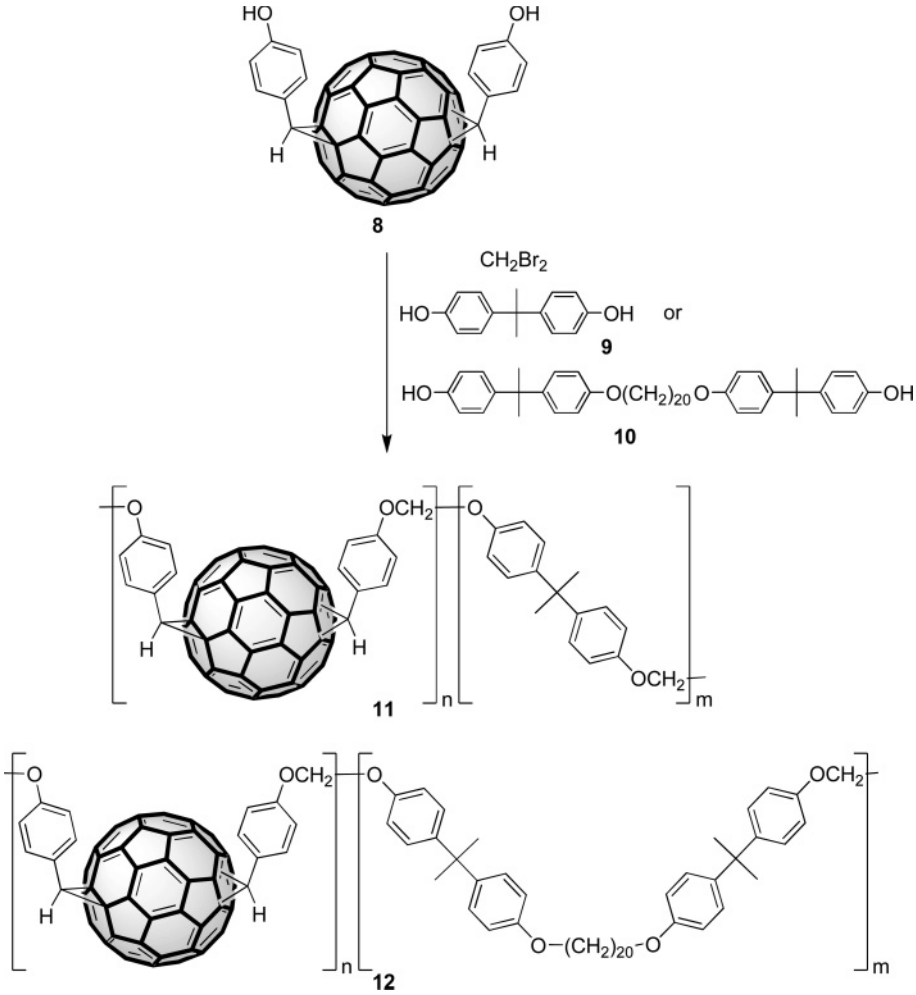

Scheme 2.4 Synthesis of main-chain polymers **11** and **12**.

In the same year, Müllen and coworkers incorporated C_{60} into a poly(dimethylsiloxane) (PDMS) to prepare an extremely soluble in-chain fullerene polymer with a high thermal stability (Scheme 2.5) [14].

Polymer **16** was synthesized through a poly-S_{NA} reaction between the commercially available aminopropyl-end-capped-PDMS **15** (M_w 35 000) and a mixture of C_{60}-bis adducts **14**, which was in turn prepared by the *o*-xylylene method [15]. After SEC purification, the resulting material presented a high average molecular weight (>50 000) and a M_w of 150 000.

In contrast, Saigo has focused on the synthesis of main-chain polymers starting from pure fullerene regioisomers. A new class of C_{60}-based-polyamides has been

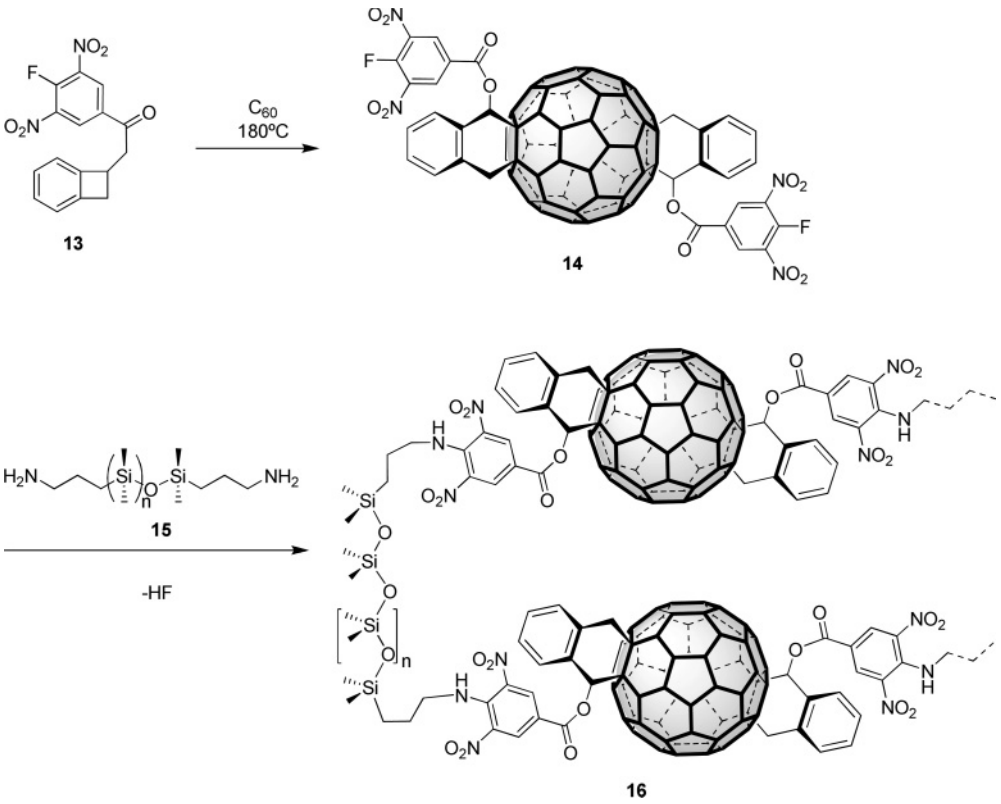

Scheme 2.5 Synthesis of polysiloxane **16**.

prepared by using a direct polycondensation method in the presence of triphenylphosphite and pyridine (Scheme 2.6).

First, the trans-2 isomer **17a** was reacted together with 4,4′-diaminobenzophenone to afford polymer **18** [16, 17], with a M_w of 53 000. The use of LiCl avoids the exclusive formation of oligomers, cleaving the inter- and intramolecular hydrogen bonds, and thus improving polymer solubility.

When the equatorial isomer **17b** and isophthalic acid (molar ratio 1 : 50; 1 : 5; 1 : 1; 1 : 0) were reacted with an equimolar amount of di(4-aminophenyl) ether, polymers **19a–d** were obtained in shapes that ranged from fibers to powder [18]. The M_w decreases linearly with **17b** content ($3 \times 10^5 - 3 \times 10^3$), as well as the thermal stability, as observed by TGA and DSC analyses.

Finally, pearl-necklace polyiminofullerenes have been prepared, starting from enantiopure equatorial bis(formylmethano)[60]fullerenes (e-**22**) or from the corresponding cis-3 isomer (cis-3-**23**) and the aromatic diamine 4,4″-diamino-2′,5′-bis(dodecyloxy)-*p*-terphenyl (**21**) (Scheme 2.7) [19]. The macromolecular products obtained showed excellent processability.

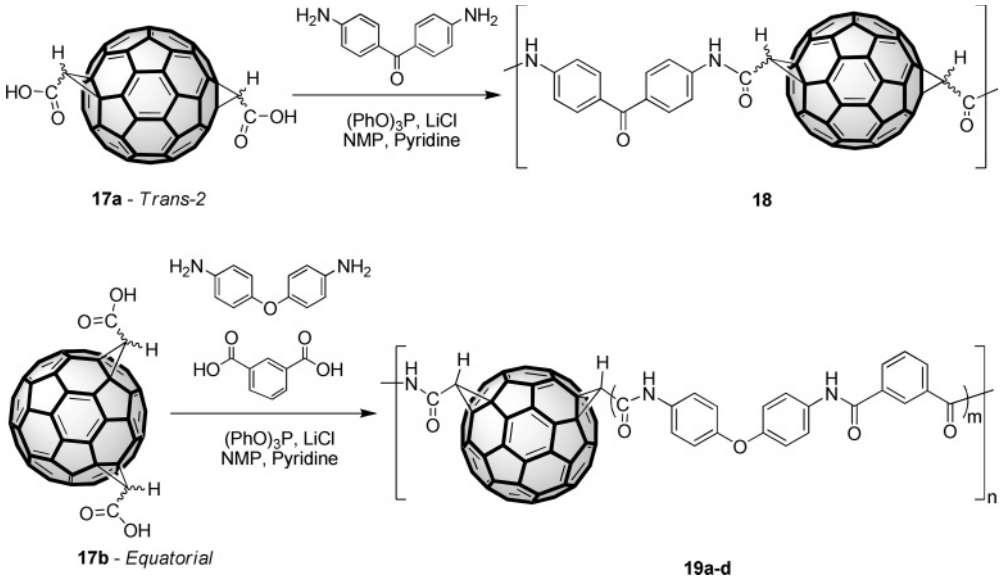

Scheme 2.6 Synthesis of polymers **18** and **19a–d**.

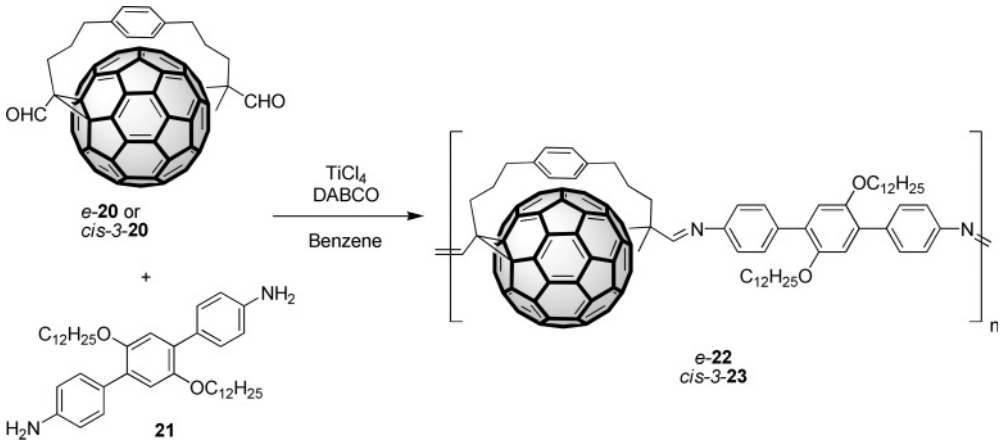

Scheme 2.7 Synthesis of polyiminofullerenes e-**22** and cis-3-**23**.

2.3
Side-Chain Polymers

2.3.1
Polystyrene-C_{60} Polymers

The ready access to polystyrene (PS) copolymer derivatives made this class of macromolecules a good candidate for side functionalization with C_{60}. Several

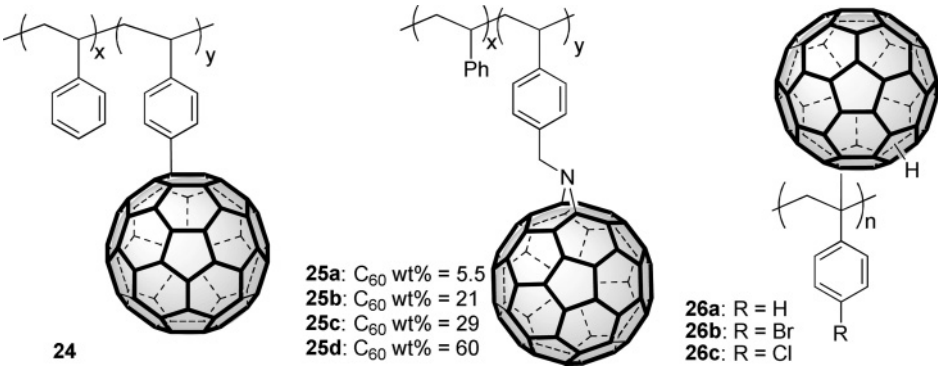

Figure 2.2 Chemical structures for polystyrenes **24–26**.

approaches have been explored to incorporate fullerene moieties both in the aliphatic backbone and in the lateral phenyl groups (Figure 2.2).

One approach involves the grafting of C_{60} via Friedel–Crafts reaction, leading to high weight polymers that, in some cases, could be due to crosslinking (**24**) [20].

On the other hand, Hawker and Hadziioannou independently modulated the C_{60} content in the final polymer by simply modifying the styrene/*p*-azidomethylstyrene ratio in the precursor copolymer feed [21]. Thus, polymers **25a–d** with a fullerene content between 5.5 and 60 wt% have been synthesized; they show very good solubility properties.

Reaction between fullerene and carbanion intermediates of PS [22], poly(bromostyrene) [23] or poly(vinylbenzyl chloride) [24] has afforded the corresponding polymers fullerenated directly on the main chain (**26a–c**). In these cases, polymer stereo-electronic effects as well as the steric hindrance of C_{60} units greatly influence the structure and physical properties of the polymers.

In contrast, Cao and coworkers have reported self-assembled ultrathin films using a C_{60}-tricarboxylic acid (**27**) together with a diazonium resin (**28**) via electrostatic interaction in aqueous solution (Scheme 2.8) [25]. Subsequently, by irradiating with UV light, the bonds between the layers changed from ionic to covalent (**29**). The film so formed was very stable towards polar solvents and, in addition, investigation of the microtribological properties revealed that C_{60} in the film affords load-bearing capacity. Furthermore, the authors incorporated poly(acrylic acid) with the aim of forming a ternary composite film with enhanced lubricative properties. Such ternary polymer-bound C_{60} films displayed very load-bearing as well as low friction properties.

An elegant approach for the synthesis of an electroactive block copolymer has been proposed by Hadziioannou and coworkers (Scheme 2.9) [26, 27]. They first prepared the PPV-based block (**31**) via a Siegrist polycondensation [28]. By this method, oligo-PPVs (oPPVs) of narrow molecular weight range with only one formyl group per molecule are obtained (up to ten repeating units). The covalent linkage of the ATRA (atom transfer radical addition) initiator to the oPPV

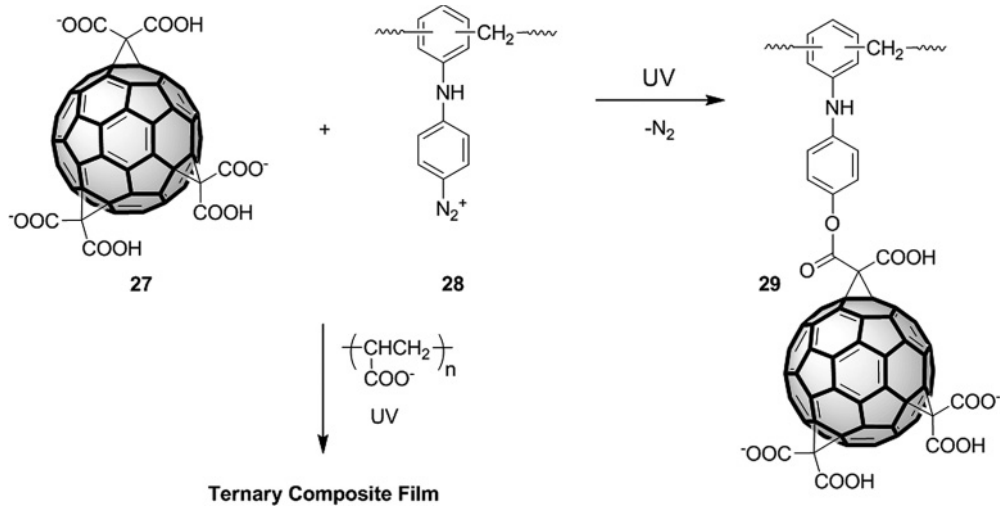

Scheme 2.8 Synthesis of polymer **29**.

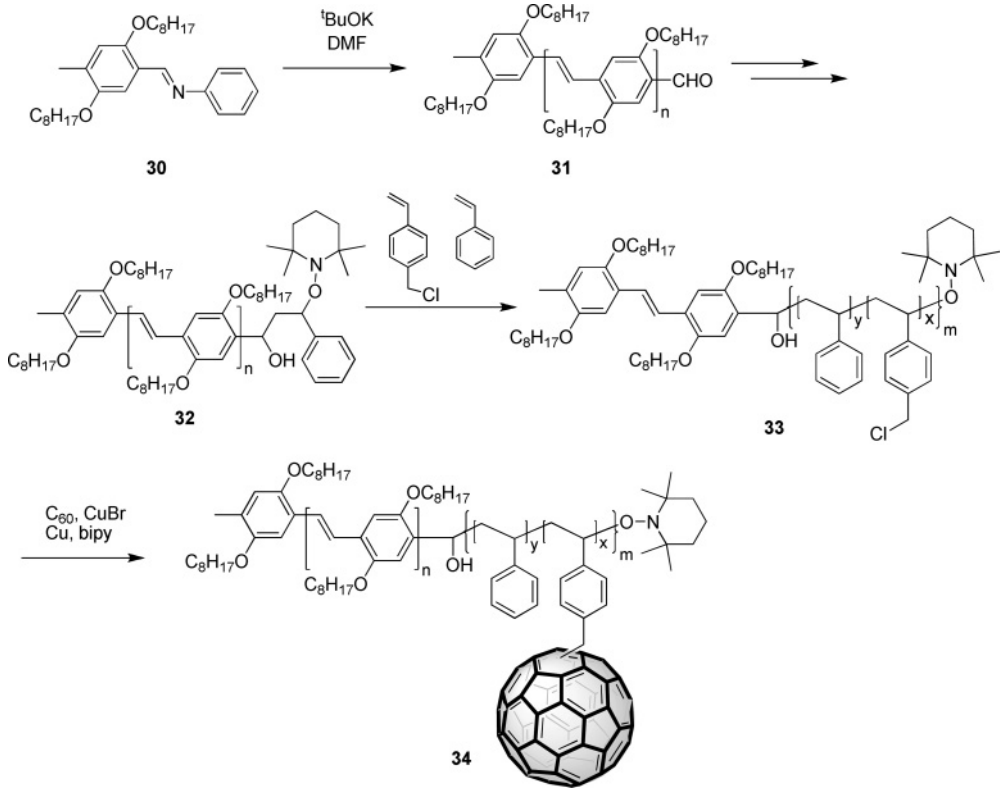

Scheme 2.9

(poly(*p*-phenyle vinylene)) moiety allows the subsequent controlled "living" radical polymerization in the presence of styrene and chloromethylstyrene to form **33**. Finally, the acceptor C_{60} is incorporated through a new atom transfer radical addition to the 4-chloromethylstyrene units to afford the rod-coil polymer **34**.

TGA analysis revealed a 46 wt% content of fullerene in the final product, indicating an average of 15 C_{60} molecules per chain, revealing also that one of every two chloromethyl moieties reacted with the acceptor. Interestingly, upon casting films of **34** from CS_2 solutions, the formation of honeycomb patterns on a micrometer scale was observed.

The suitability of the type of such block-copolymer for application in photovoltaic devices relies, among other aspects, on the abilities of the respective blocks to function as electron donor and acceptor, as well as a good charge transport media. When C_{60} is incorporated in the final polymer, the photoluminescence intensity in the film is reduced by three orders of magnitude, this being evidence for an efficient and very rapid electron transfer from the donor block (PPV) to the acceptor (PS-C_{60}). Photovoltaic cells have been fabricated using **34** or a blend of PPV homopolymer **31** and a statistical copolymer of styrene incorporating C_{60} for comparative purposes but, unfortunately, low efficiencies were achieved. Recently, an analogue series of block-copolymer, incorporating this time C_{60} through azido groups, has been prepared [29]. The authors observed that the addition of fullerene strongly affects the polymer self-assembly due to the growth of C_{60} nanocrystals. The latter hinder the formation of the lamellar phase by pinning the coils. Despite the presence of a large donor–acceptor interface, as evidenced by strong photoluminescence quenching, the resulting thin film nanostructure remains inappropriate for the target bulk heterojunction photovoltaic device.

In 2007, Holdcroft and coworkers presented polythiophene-based main-chain polymers bearing polystyrene-side chains in which fullerene moieties were grafted (Scheme 2.10) [30].

The brominated regioregular P3HT **35** was reacted with the boronic ester of TEMPO (**36**). The macroinitiator **37** was then used for the polymerization of styrene and chloromethylstyrene by nitroxide-mediated living polymerization to afford the comb-like polymer **38**. Finally, C_{60} was grafted via ATRA reaction to yield polymer **39** with a fullerene content of 47 wt%.

2.3.2
Polyacrylate- and Methacrylate-C_{60} Polymers and Copolymers

Figure 2.3 summarizes the structures for "classical" polymers carrying C_{60} as side substituent such as polymethacrylates (**40a, b**) [31], derivatized poly(alkyl methacrylate)s **41a, b** [32, 33] and **42a, b** [34] or poly(hydroxyethyl methacrylate) (PHEMA) **43a–f** [35].

Interestingly, for all polymers depicted in Figure 2.3 the fullerene units have been grafted via the "azido" route [36] as a viable manner to join C_{60} and to limit bis- and tris-addition and avoid subsequent crosslinking. In this way, C_{60}-containing poly(alkyl methacrylate)s presented a very narrow polydispersity,

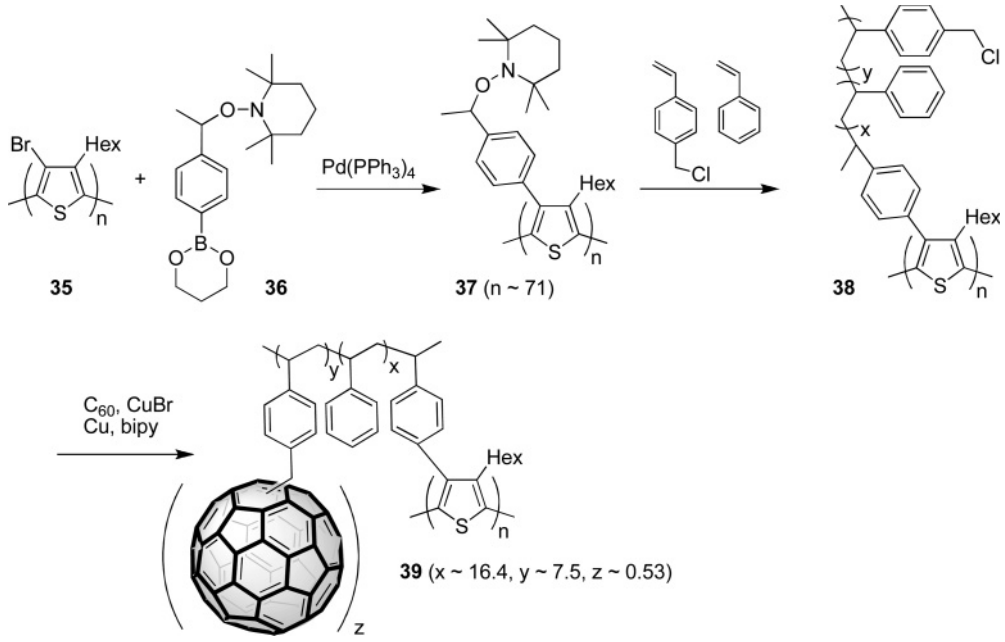

Scheme 2.10

whereas C_{60}-PHEMA (**43a–f**) showed a stronger influence of solubility with C_{60} content. Thus, polymers carrying more than 3.2 wt% of C_{60} have a limited solubility. Samples of **43a–f** formed successfully interpolymer complexes when mixed together with poly(4-vinylpyridine) (P4VPy) and poly(1-vinylimidazole) (PVI) as proton-acceptor polymer [35, 37]. Interpolymer complexes have also been formed between poly(vinylidene fluoride) (PVDF) and samples of C_{60}-containing poly(ethyl methacrylate), poly(methyl acrylate), poly(ethyl acrylate) [38] and poly(methyl methacrylate) [39]. In contrast, when C_{60} is incorporated into poly(ethyl methacrylate), the surface behavior of the polymer suffers a dramatic effect since it becomes more hydrophobic when the C_{60} content increases, as shown by an increase in the water contact angles [34].

Another effective manner to graft C_{60} to a polymeric backbone is represented by [4 + 2] cycloaddition reaction between fullerene and side-chain reactive dienes. This strategy has been employed by Wang and coworkers, who prepared several vinyl polymers with different contents of benzocyclobutenone-containing (BCBO) monomer **44** (Scheme 2.11) [40]. Such moieties, upon thermal activation in *o*DCB, generate a reactive diene, which subsequently undergoes a [4 + 2] cycloaddition with C_{60}, leading to soluble macromolecules (**46a–c**) with a 22.5–44 wt% content in fullerene.

Finally, good photoconductivities have been measured for styrene/acrylamide copolymers carrying C_{60} units directly linked to the hanging amido-groups; the photoconductivity could be enhanced by increasing the fullerene content [41].

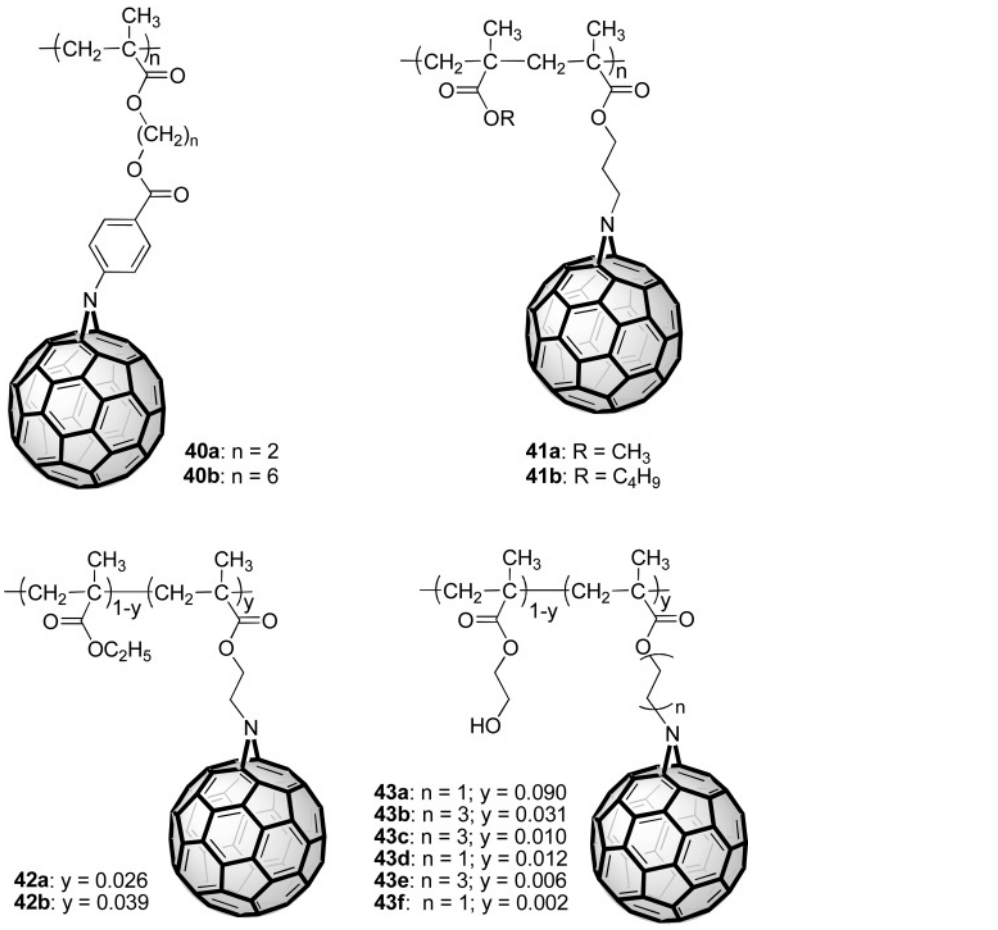

Figure 2.3 Chemical structures for polymers **40–43**.

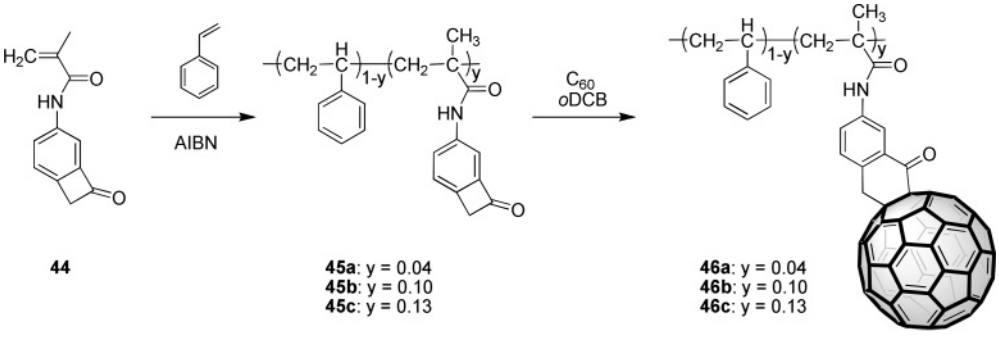

Scheme 2.11 Synthesis of copolymers **46a–c**.

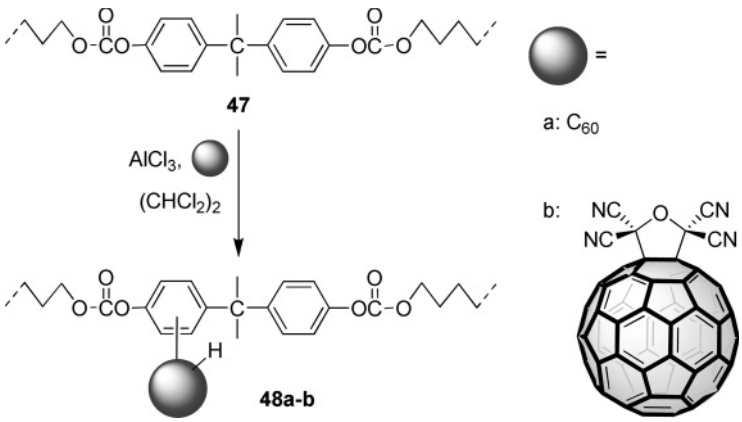

Scheme 2.12 Synthesis of C_{60}-containing polycarbonates **48a, b**.

2.3.3
Polycarbonate-C_{60} Polymers

An interesting class of C_{60}-side-chain polymers includes fullerenated polycarbonates (PCs). Despite previous attempts to incorporate C_{60} into PCs by simple irradiation [42], or the more recent direct grafting under microwave irradiation in the presence of AIBN [43], better results have been obtained by using a one-pot straightforward Friedel–Crafts experimental procedures (Scheme 2.12) [44, 45].

These parallel studies, in which C_{60} or TCNEO-C_{60} were incorporated into PC, reported very similar results, showing outstanding optical limiting properties and, at the same time, improved the C_{60} processability of such materials. In both cases, the calculated M_w were lower than that of the starting PC, indicating that some chain cleavage is involved in the fullerenation reaction. Comparing these two polymers, the optical limiting properties of TCNEO-C_{60}-PC **48b** show a remarkable improvement, suggesting that an increase in the electron-accepting ability of the C_{60} derivative leads to stronger intermolecular interaction between the C_{60} derivative and the PC. Fullerene has also been incorporated on PC chains as its derivative 61-(*p*-hydroxyphenyl)methano-1,2-[60]fullerene [46].

2.3.4
Aminofishing Side-Chain Polymers

One of the first classes of side-chain polymers studied includes the amino- or imino-functionalized polymers, due to the well-known reaction of amine addition to fullerene double bonds [47, 48]. Figure 2.4 summarizes the different chemical structures for C_{60}-side-chain polymers derived from the corresponding amino-polymers.

The first examples were reported in 1993 by Geckeler and Hirsch, who synthesized **49** and **50** by titration of C_{60} with poly(ethylene imine) and poly{4-[(2-

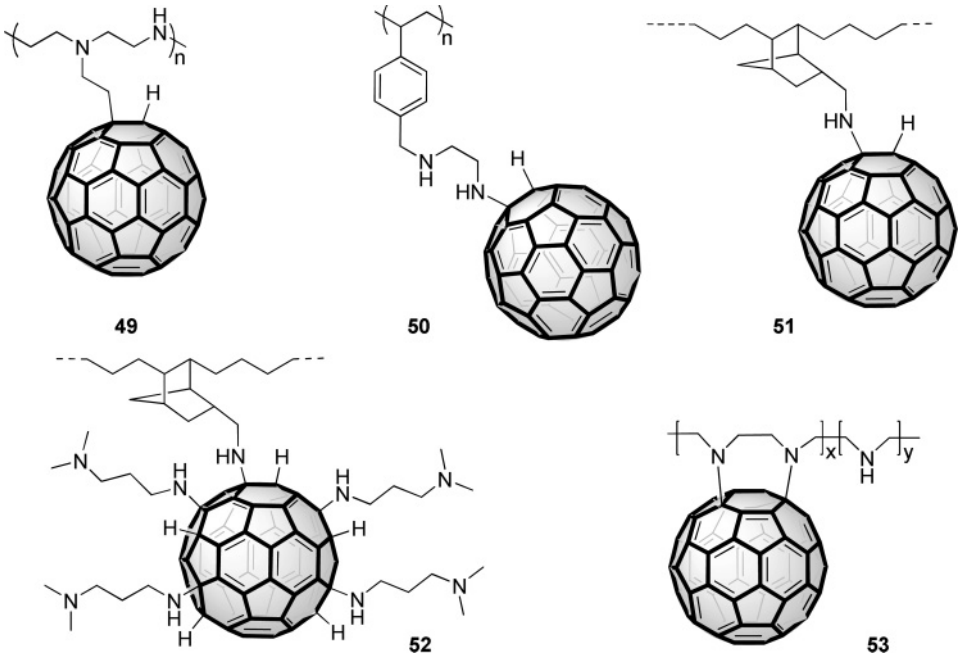

Figure 2.4 Examples of aminofishing C_{60}-polymers.

aminoethyl)imino]methyl}styrene, respectively [49]. Polymer **50** was soluble in CS_2 and toluene, representing the first example of a soluble C_{60}-containing polymer.

Other remarkable examples of C_{60} functionalized amino-polymers are **51** [50], **52** [51] and **53** [52, 53]. The latter was obtained by photochemical reaction between C_{60} and the secondary amine of poly(ethylene imine), following a photo-induced electron transfer–proton transfer mechanism. In this way, the authors prepared water-soluble materials with a C_{60} content of up to 37 wt%, which showed fluorescence quenching via intrapolymer electron transfer.

Water-soluble pendant C_{60} polymers have also been prepared by following a different approach. Sun and coworkers employed the secondary amino-groups of the linear (propionyl-ethylene-imine-*co*-ethylene-imine) (PPEI-EI) as attachment sites for different fullerene pendant groups (Scheme 2.13) [54, 55].

After partial hydrolysis under acidic conditions of the poly(propionyl-ethylene imine) (PPEI), condensation with C_{60} derivatives **55a–c**, using 1-ethyl-3-(dimethylaminopropyl)carbodiimide (EDAC) as coupling agent, led to the fullerene-containing polymers **56a–c**. Such polymers displayed a M_w of ~49 000 with a C_{60} content of ~11%. GPC (gel-permeation chromatography) analysis of **56b** did not show significant crosslinking despite possessing two different carboxylic groups. In addition, such materials presented impressive water solubility, >90 mg mL^{-1}, representing an effective way to afford water-soluble compounds for biological studies.

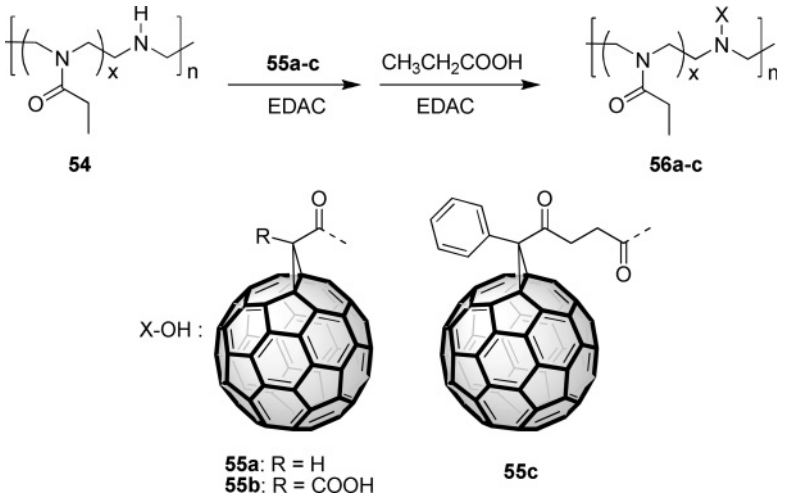

Scheme 2.13 Synthesis of polymers **56a–c**.

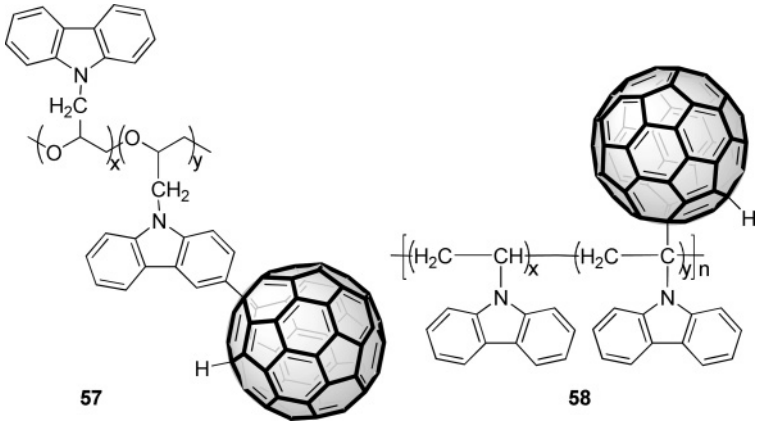

Figure 2.5 Polyvinylcarbazoles **57** and **58**.

2.3.5
Polyvinylcarbazoles

The side fullerenation of poly(epoxypropylcarbazole) (PEPC) **57** has been achieved by grafting C_{60} via a Friedel–Crafts reaction (Figure 2.5) [56]. Analogously, the same synthetic strategy applied to polyvinylcarbazole (PVK) led to C_{60} chemically modified PVK copolymer, in which, after laser flash photolysis, photoinduced electron transfer between C_{60} and inter- and intrachain carbazole units takes place (polymer **58** – Figure 2.5) [57]. Kang and coworkers have exploited this behavior

to fabricate a nonvolatile flash device [58]. In fact, the device with architecture ITO/PVK-C_{60}/Al behaved as a rewritable memory with accessible electronic states that could be written, read and erased, working for more than 100 million read cycles.

2.3.6 Polyphosphazenes and Polysiloxanes

Up to now we have exclusively shown organic C_{60}-based polymers, but a few examples of C_{60}-based inorganic polymers are also known, which are of great interest. In past decades polymers with inorganic backbones aroused curiosity and interest because of their special properties and due to some advantages they present over some carbon-chain polymers [59]. Among them, polyphosphazenes and polysiloxanes are particularly noticeable [60]. The former have been used not only as flame-retarding materials [61] but also as liquid crystals [62], photoconductors [63] and nonlinear optical materials [64], whereas the latter show an exceptional chain mobility that affords good solubility [65].

Qin and coworkers have described the synthesis and characterization of four different C_{60}-containing polyphosphazenes (Scheme 2.14) [66, 67].

From Scheme 2.14, it can be seen that the syntheses of polymers **61a, b**, **63** and **66** is straightforward, involving ordinary solvents and reagents. Initially, poly(dichlorophosphazene) is prepared by ring-opening polymerization of phosphonitrile chloride trimer, providing a material with double sites for further functionalization. In this way, two subsequent reactions allow us to introduce solubilizing chains and reactive sites that, in turn, react with C_{60} to give polymers **61a, b**, **63** and **66**. In all cases, good M_w and narrow polydispersity indexes have been calculated, and C_{60}-contents of ~2 and ~7% have been calculated for **61b** and **66**, respectively.

In contrast, attempts to graft C_{60} onto a siloxane copolymer using (divinyltetramethyldisiloxane)platinum(0) failed, affording a fullerene cage surrounded by two siloxane chains multiply attached [68]. Better results have been obtained by Kraus and Müllen, who first reported side-chain polysiloxanes with pendant C_{60} units (Scheme 2.15) [14].

Polymer **69** was prepared by following two different routes: in the first, C_{60} was incorporated directly to a suitably functionalized polymer (**68**) by the *o*-quinodimethane method [15]. The second strategy deals with the incorporation of a C_{60}-derivative (**70**) directly into an amino-functionalized polysiloxane (**67**). In both cases, the polymers show identical M_w values and a remarkable content in [60]fullerene as high as 30 wt%. This new material displayed a M_w analogue to those of **69** (~35 000) as well as a high thermal stability of up to 435 °C.

In 2003, two new examples of polysiloxanes side-functionalized with fullerene units were described (Scheme 2.16) [69].

Again, C_{60} was loaded into the polymer by means of pendant aminofishing groups, giving rise to low weight macromolecules with moderate C_{60}-contents

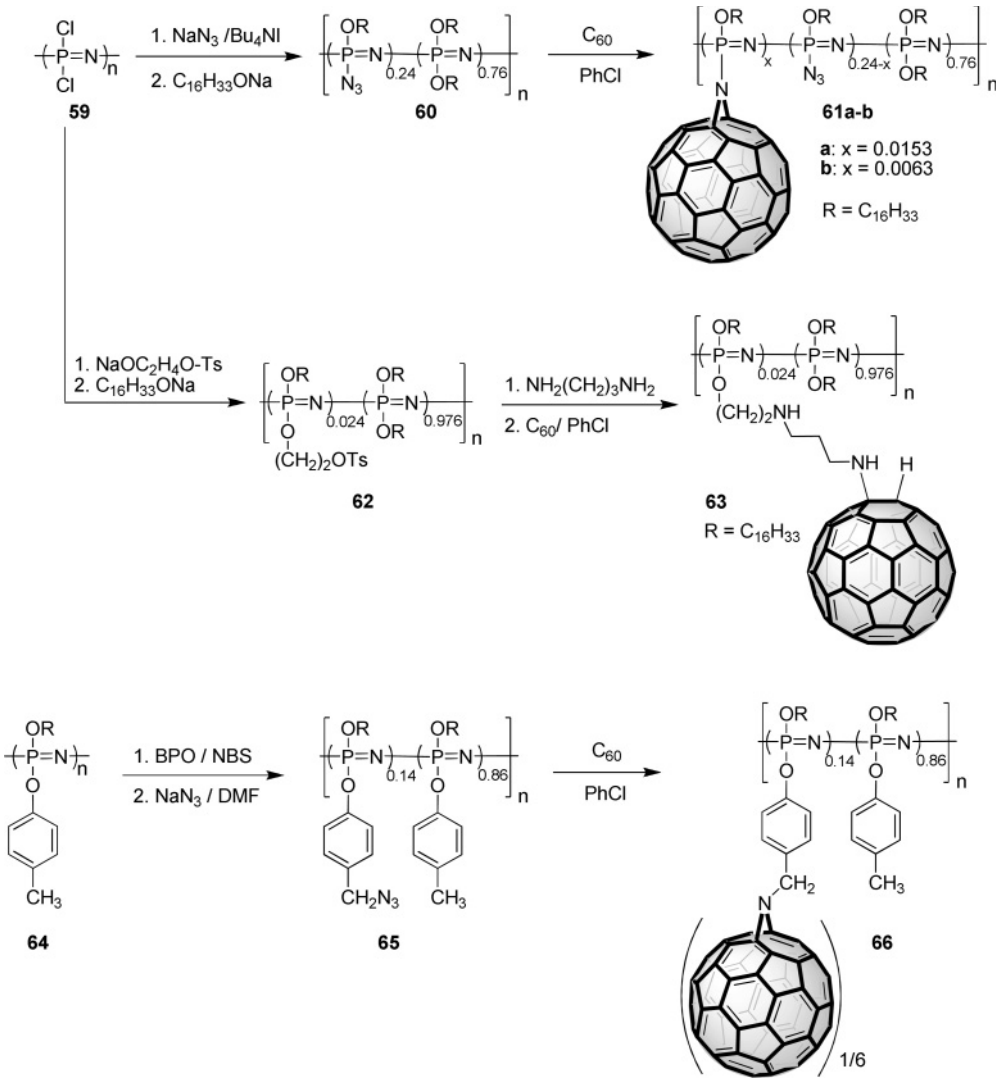

Scheme 2.14 Synthesis of polyphosphazenes **61a, b, 63** and **66**.

(**73a**: 2.5%; **73b**: 3.9%). However, more recently, the first example in which a C_{60}-containing siloxane monomer (**75**) is polymerized to give the corresponding homopolymer (**76**) has been reported (Scheme 2.17) [70] The polymerization was carried out using triflic acid as initiator and GPC revealed a high M_n (95 000).

Recently, Manners, Sargent *et al.* have reported the synthesis of a series of polyferrocenylsilane random copolymers containing covalently bound pendant [60]fullerene cages [71].

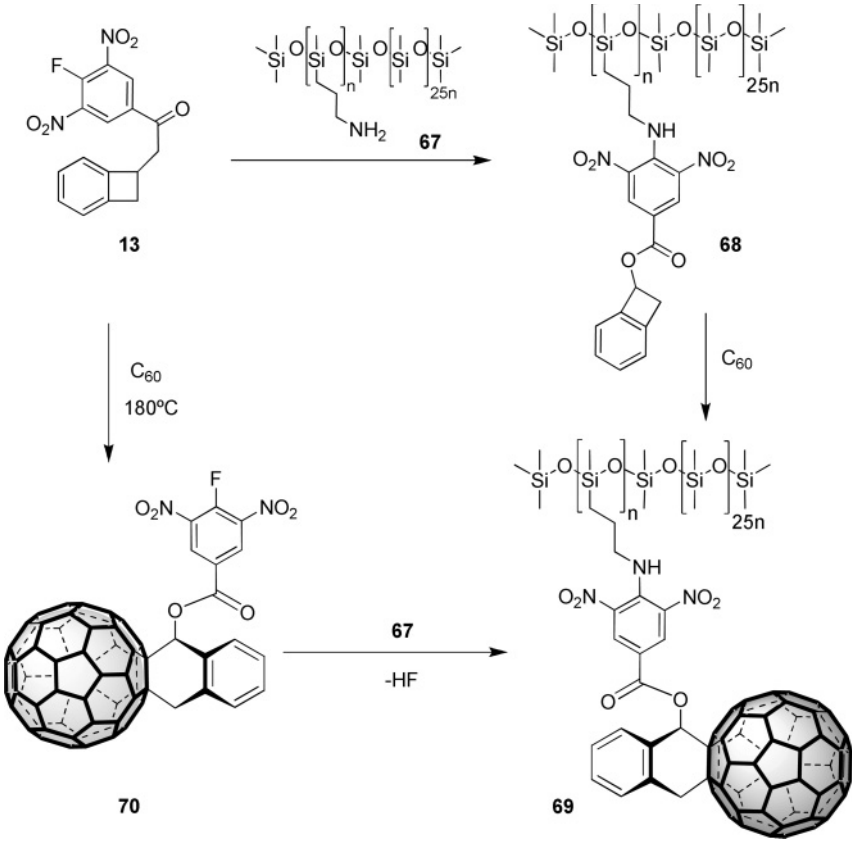

Scheme 2.15 Synthesis of polysiloxane **69**.

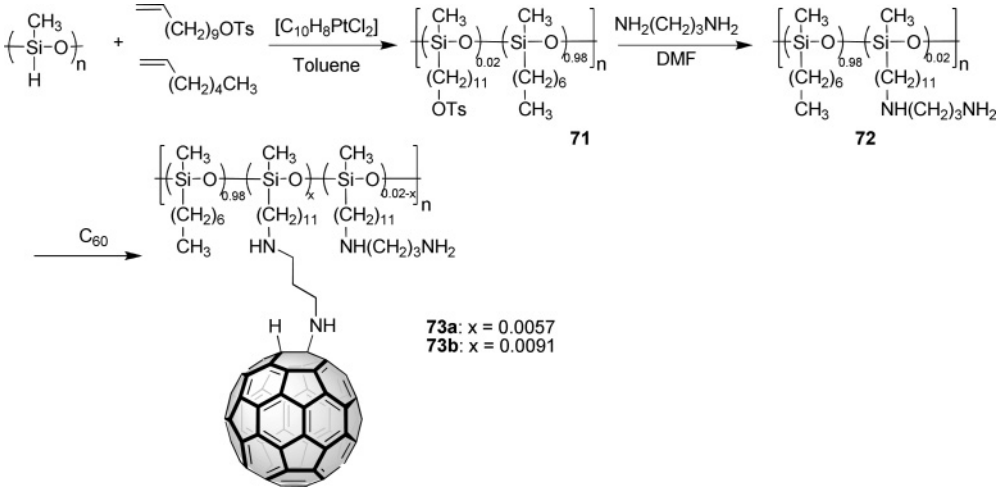

Scheme 2.16 Synthesis of aminofishing polysiloxanes **73a, b**.

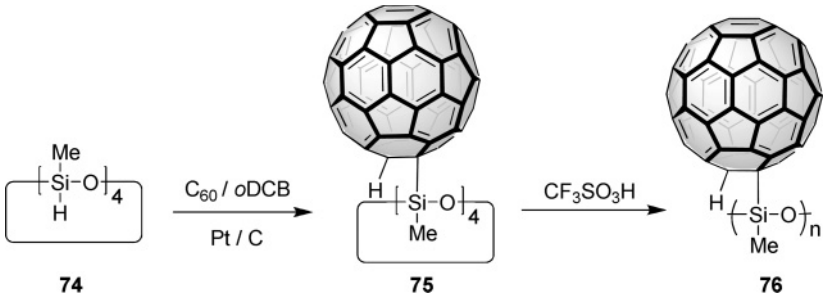

74 75 76

Scheme 2.17 Synthesis of polymer **76**.

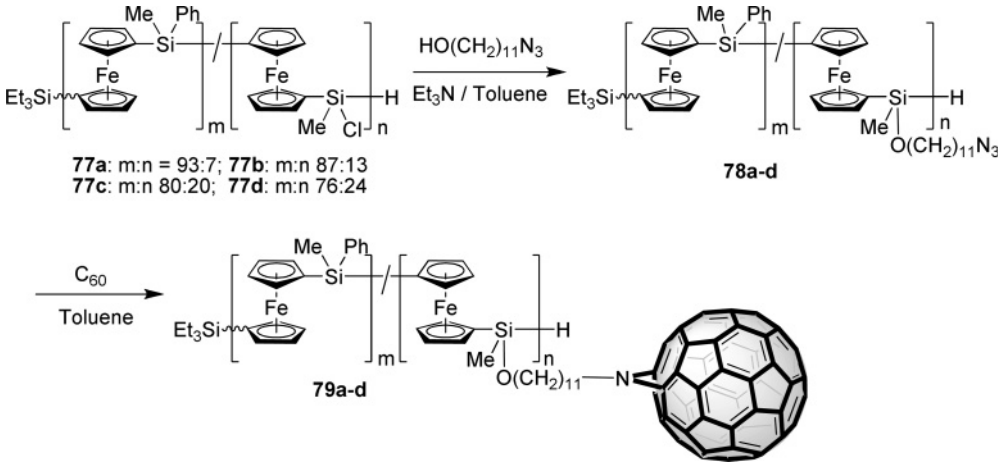

Scheme 2.18 Synthesis of polyferrocenylsilanes **79a–d**.

Scheme 2.18 depicts the syntheses performed. After preparing polymers **77a–d** by Pt-catalyzed ring-opening polymerization, the resulting copolymers were functionalized with 11-azido-1-undecanol in the presence of triethylamine and, finally, reacted with C_{60}. The so-obtained polymers **79a–d** were air-stable and soluble in several solvents. Hence, the C_{60}-containing polyferrocenylsilanes were explored as the active layer in an all-solid-state photodiode. The device showed photoconductive and photovoltaic responses under white light illumination.

2.3.7
Side-Chain C_{60}-Polysaccarides

The first example reported in the literature deals with the synthesis of water-soluble pullulans (a non-ionic water-soluble polymer constituted by α-1,6-linked maltotriose units) bearing pendant fullerene moieties. C_{60} was incorporated into the pullulan as depicted in Scheme 2.19 and involves two different degrees of chlorination to obtain polymers with different C_{60} contents [72].

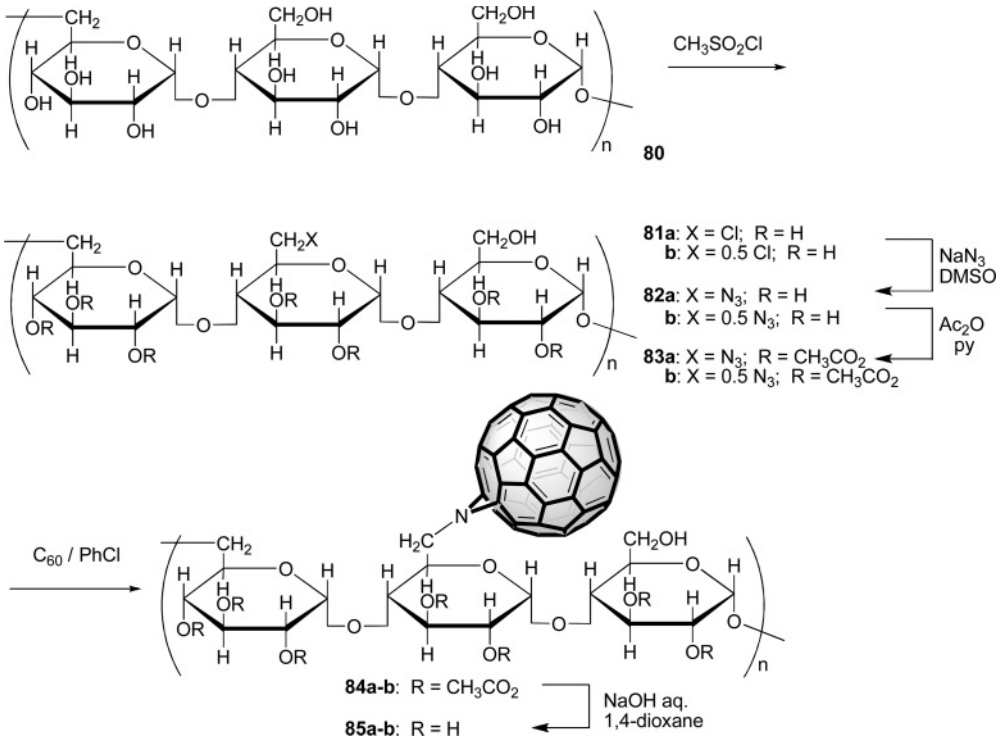

Scheme 2.19 Synthesis of pullulans-C_{60} conjugates **85a, b**.

A new polysaccaride–C_{60} system was reported in 2007. This time curdlan sulfates was the saccharide of choice because of its high solubility in water and its strong anti-HIV activity (Figure 2.6) [73].

2.3.8
Polyether-C_{60} Polymers

Side-chain polymers containing C_{60}, as seen above, have been employed as donor–acceptor materials for potential use in photovoltaic devices. In this regard, Nierengarten *et al.* have prepared three different polyesters, **88** and **89a** and **b**, starting from the same C_{60}-containing diacyl chloride (Figure 2.7) [74]. In the case of the oligo-PPV-containing polymer **88**, the material preserved the optical and electrochemical properties of both electroactive units. A M_w of 63 000 g mol^{-1} ($M_w/M_n = 1.1$) was calculated by analytical SEC (size-exclusion chromatography) coupled with a light-scattering detector for this polymer.

On the other hand, polymers **89a** and **b** were obtained in high yields and high M_w (66 000 and 70 000, respectively) [75]. Polymer **89a** was blended together with MDMO-PPV and spin-coated to prepare organic solar cells. However,

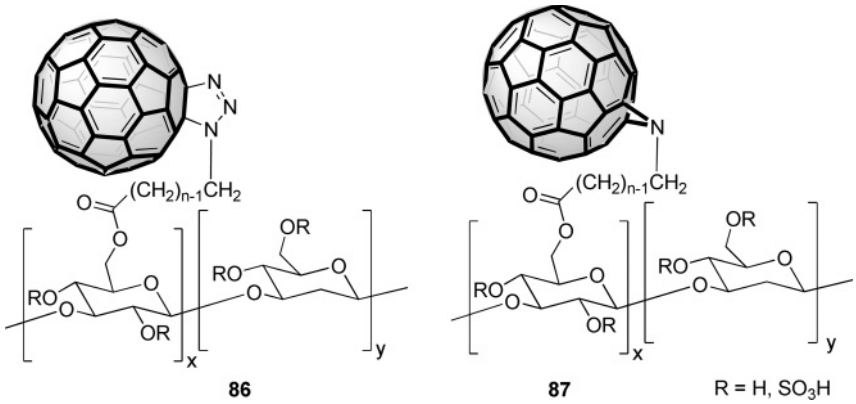

Figure 2.6 New polysaccaride-C_{60} curdlan sulfates **86** and **87**.

although some photovoltaic activity has been found, the overall performance was very low.

Improved performances of polyfullerene-containing organic solar cells have been reported by Drees, Sariciftci and coworkers [76]. They successfully tried a new approach in which first the glycidol ester of [6,6]-phenyl C_{61}-butyric acid (PCBG – **90**) was prepolymerized in the presence of the Lewis acid tris(pentafluorophenyl)borane as the initiator (Scheme 2.20). After spin-coating the prepolymer in blend with poly(3-hexylthiophene) (P3HT), the ring-opening polymerization was completed by heating the photovoltaic device. In this way, a very promising 2% conversion energy efficiency value was obtained, probably due to the morphological stabilization of the bulk heterojunction, which prevents its long-term high temperature instability.

Another interesting example of a C_{60}-containing polyether involves the synthesis of poly(2,6-dimethyl-1,4-phenylene oxide) (PPO) endowed with fullerene moieties for use in the fabrication of membranes for gas separation [77] and for blending and miscibility studies with styrenic polymers [78]. The synthesis took place by partial bromination of the methyl groups which, in turn, were substituted for azido-groups (Scheme 2.21). In this way, by controlling the initial bromine content, it was possible to prepare a series of C_{60}-containing PPO. Experiments of gas permeability carried out on pure PPO sample, a blend of PPO and C_{60} and C_{60} linked to PPO (**95**) showed that the latter exhibited a significantly higher permeability, which in some cases reaches 80% without compromising the selectivity.

2.3.9
Side-Chain Polymers Prepared by Organometallic Catalysis

Given the presence in the literature of several heterogeneous examples of side-chain C_{60}-containing polymers, it is often hard to classify them in a rational way. Nevertheless, after a detailed examination of the syntheses of such polymers, a

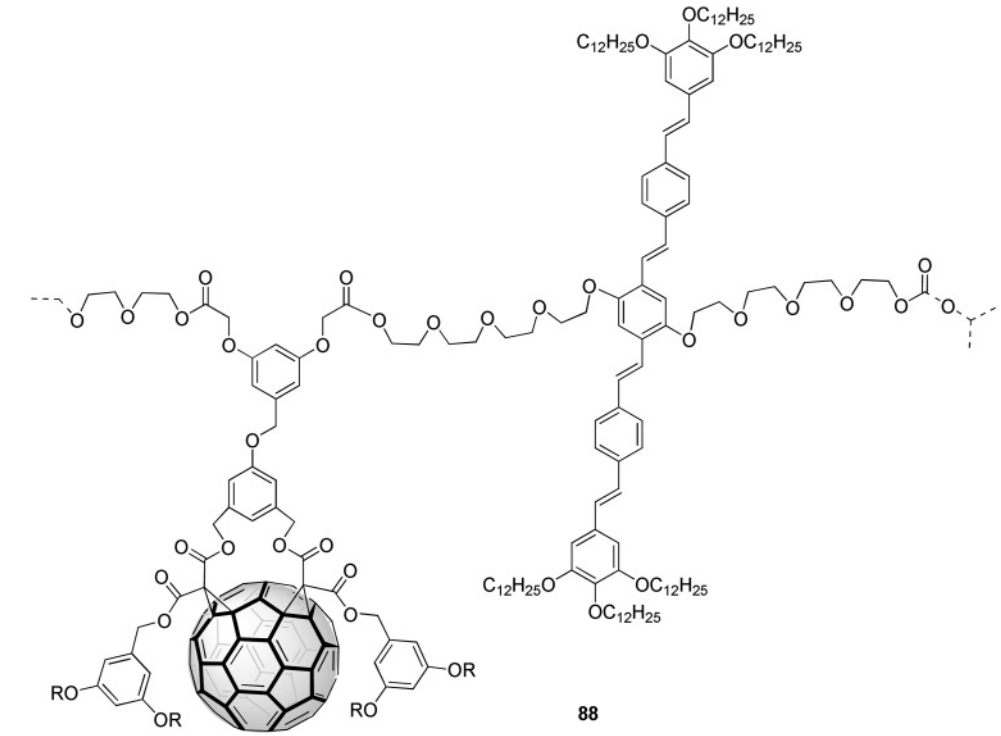

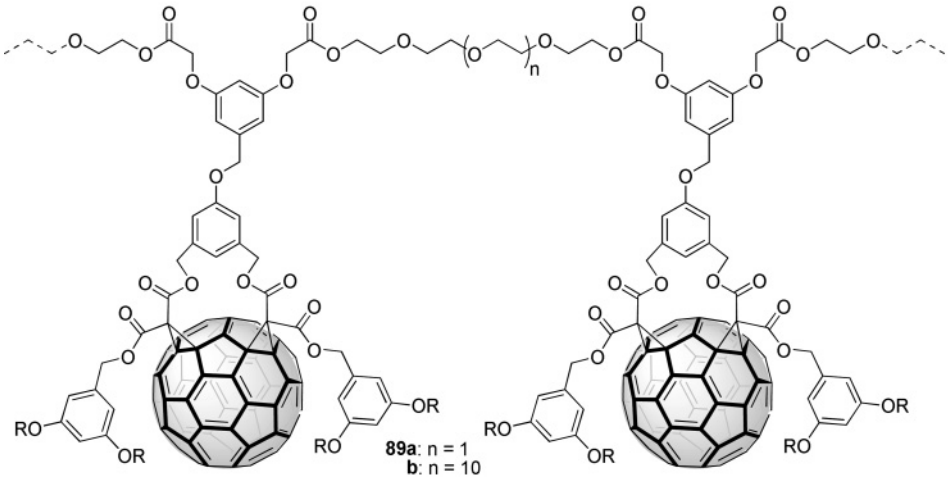

Figure 2.7 Chemical structures for polymers **88** and **89a, b**.

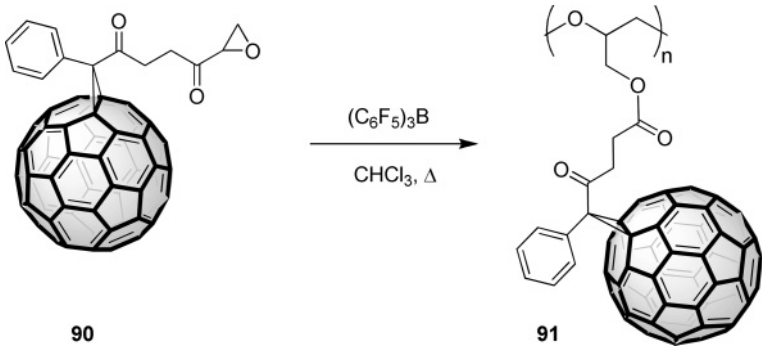

Scheme 2.20 Synthesis of polyether **91**.

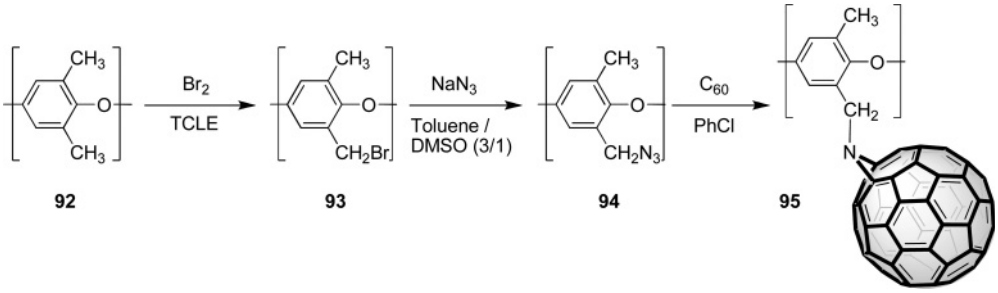

Scheme 2.21 Synthesis of PPO-C_{60} polymer **95**.

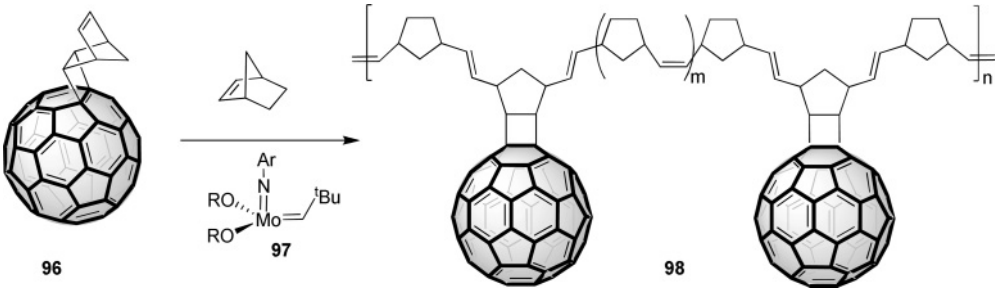

Scheme 2.22 Synthesis of polymer **98**.

kind of leitmotiv emerges when one considers the catalysts employed in the polymerization: the presence of an organometallic catalyst. The use of such compounds in the preparation of C_{60}-polymers first appeared in work by Wudl, Prato, Maggini and coworkers in 1995 [79]. They employed Mo(CH-Bu^t)(NAr)[OCMe$(CF_3)_2]_2$ as catalyst for a ring-opening metathesis copolymerization (ROMP) between the norbornene modified C_{60} **96** and an excess of norbornene (1 mol% of **96**) (Scheme 2.22).

The material so-obtained (**98**) showed a cis/trans isomer ratio of 6 : 2 with a remarkable M_w, as high as ~103 000, and presented crosslinking processes when heated at 70 °C in the solid state.

Recently, Fréchet *et al.* have described other examples of ruthenium-catalyzed ROMP [80]. They used this strategy to synthesize a polymer containing 50 wt% of C_{60} (**101**) as well as the diblock copolymers **103a** and **b** and **105** by using the sterically demanding monomer **102** (Scheme 2.23). In the former case, fullerene is incorporated at every repeat of monomer, leading to short inter-fullerene distances in a soluble polymer. In contrast, the copolymer **103a** exhibited micellar aggregation in solution but phase separation with interpenetrating C_{60}-domains in the solid state. The new amphiphilic diblock copolymer **105** was designed to control the blend morphology of the active layer of an organic solar cell (Scheme 2.23) [81].

The incorporation in the polymer backbone of fragments of P3HT, which act as compatibilizer between PCBM and P3HT, reduces the interfacial energy between the immiscible components in the solid state. In this way, once added to a blend of PCBM:P3HT at 17 wt%, polymer **105** leads to photovoltaic devices with comparable performances in terms of efficiency (~2.8%) but with enhanced stability against destructive thermal phase segregation, hence improving the disposal longevity.

An elegant approach to incorporate fullerenes into a saturated alkylic polymer has been reported recently by Hessen *et al.* [82]. They prepared a polyethene endowed with fullerene moieties pendant on short-chain branches by catalytic polymerization of ethene and a C_{60}-containing vinylic monomer (**106**), employing $(C_5Me_4SiMe_2NBu^t)TiCl_2$ (**107**)/methylalumoxane (MAO) as catalytic system (Scheme 2.24).

2.4 Conclusions and Further Perspectives

In summary, we have reviewed the main synthetic efforts carried out to introduce the fullerene sphere into a polymer chain, either into the main chain or as pendant units. Comparatively, fewer main-chain polymers have been reported in the literature, probably due to the greater synthetic difficulties as well as to the mixture of regioisomers resulting from the reaction and, often, the formation of crosslinking products.

Despite these drawbacks, highly soluble and thermally stable main-chain polymers have been prepared and, in a few cases, polymers endowed with pure fullerene regioisomers have been produced that show excellent processability.

In contrast to main-chain polymers, wide synthetic effort has been applied to the preparation of fullerene polymers in which the C_{60} moiety is pendant from the main polymer chain (side-chain polymer). With the aim of ordering the wide variety of these fullerene-containing polymers, we have classified them according to the nature of the polymer. Thus, polymers such as polystyrenes, polyacrylates

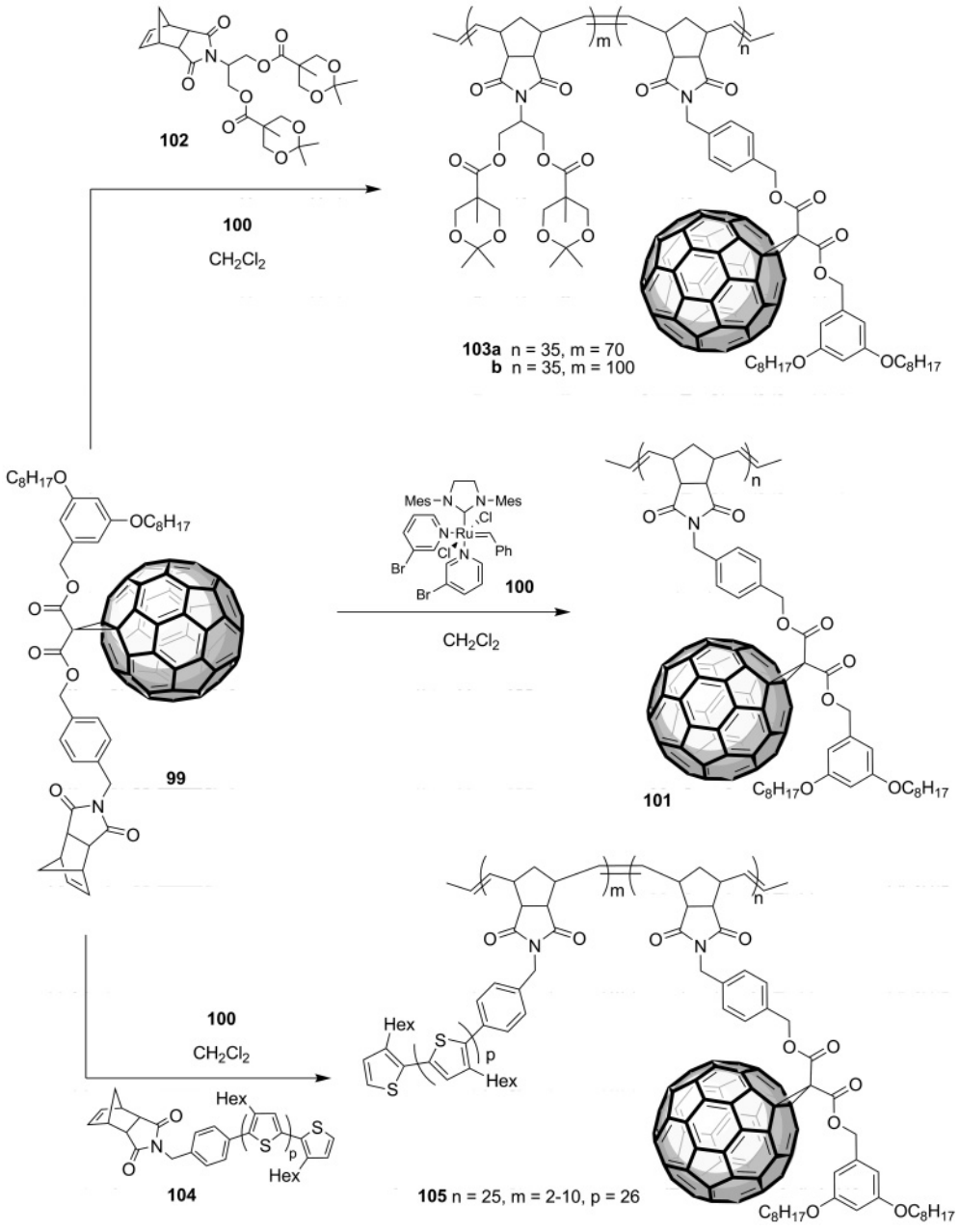

Scheme 2.23 Synthesis of polymers **101, 103a, b** and **105**.

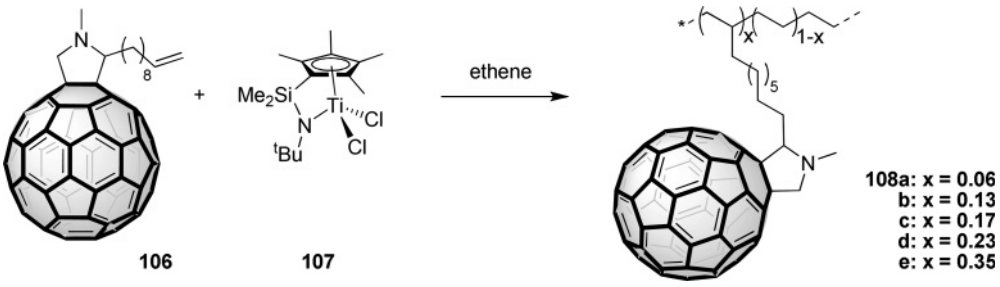

Scheme 2.24 Synthesis of polymers **108a–e**.

and polymethacrylates, polycarbonates, polyalkylamines, polyvinylcarbazoles, polyphosphazenes, polysiloxanes, polysaccharides and polyethers have been extensively studied during the last 15 years, which has allowed the preparation of a huge number of polymers endowed with fullerenes – where the imagination of the chemist is the only limit.

Some of the above polymers have been studied for several applications (low friction, water solubility, photoconductivity, all-solid-state photodiodes, photovoltaics, biological properties, gas permeability), which has led to very appealing materials by combining the outstanding properties of fullerenes with those of polymers. In particular, the processability of the fullerene-containing polymers renders them compounds of choice for the development of new materials for the preparation of unprecedented optoelectronic devices.

References

1 Krätschmer, W., Lamb, L.D., Fostiropoulos, K. and Huffman, D.R. (1990) *Nature*, **347**, 354.

2 (a) Shi, S., Khemani, K.C., Li, Q. and Wudl, F. (1992) *J. Am. Chem. Soc.*, **114**, 10656.
(b) Nagashima, H., Nakaoka, A., Saito, Y., Kato, M., Kawanishi, T. and Itoh, K. (1992) *J. Chem. Soc., Chem. Commun.*, 377.
(c) Loy, D.A. and Assink, R.A. (1992) *J. Am. Chem. Soc.*, **11**, 3977.
(d) Giacalone, F. and Martín, N. (2006) *Chem. Rev.*, **106**, 5136.

3 (a) Foote, C.S. (1994) *Top. Curr. Chem.*, **169**, 347.
(b) Sun, Y.-P. (1997) *Molecular and Supramolecular Photochemistry*, vol. **1** (eds V. Ramamurthy and K.S. Schanze), Marcel Dekker, New York, pp. 325.

4 Echegoyen, L. and Echegoyen, L.E. (1998) *Acc. Chem. Res.*, **31**, 593.

5 (a) Guldi, D.M. (2000) *Chem. Commun.*, 321.
(b) Guldi, D.M. and Prato, M. (2000) *Acc. Chem. Res.*, **33**, 695.

6 (a) Prato, M. (1997) *J. Mater. Chem.*, **7**, 1097.
(b) Guldi, D.M. and Martín, N. (2002) *Fullerenes: From Synthesis to Optoelectronic Properties*, Kluwer Academic, Dordrecht.
(c) Special issue on "functionalised fullerene materials" Prato, M. and Martín, N. (eds) (2002) *J. Mater. Chem.*, **12**, 1931.
(d) Martín, N. (2006) *Chem. Commun.*, 2093.

7 (a) Jensen, A.W., Wilson, S.R. and Schuster, D.I. (1996) *Bioorg. Med. Chem.*, **4**, 767.
(b) Da Ros, T. and Prato, M. (1999) *Chem. Commun.*, 663.

8 Samal, S., Choi, B.-J. and Geckeler, K.E. (2000) *Chem. Commun.*, 1373.

9 Samal, S., Choi, B.-J. and Geckeler, K.E. (2001) *Macromol. Biosci.*, **1**, 329.

10 (a) Pass, H.I. (1993) *J. Natl. Cancer Inst.*, **85**, 443.
(b) Dougherty, T.J., Gomer, C.J., Henderson, B.W., Jori, G., Kessel, D., Korbelik, M., Moan, J. and Peng, Q. (1998) *J. Natl. Cancer Inst.*, **90**, 889.
(c) Dolmans, D.E., Fukumura, D. and Jain, R.K. (2003) *Nat. Rev. Cancer*, **3**, 380.

11 (a) Nie, B. and Rotello, V.M. (1997) *Macromolecules*, **30**, 3949.
(b) Ilhan, F. and Rotello, V.M. (1999) *J. Org. Chem.*, **64**, 1455.

12 Taki, M., Takigami, S., Watanabe, Y., Nakamura, Y. and Nishimura, J. (1997) *Polym. J.*, **29**, 1020.

13 Scamporrino, E., Vitalini, D. and Mineo, P. (1999) *Macromolecules*, **32**, 4247.

14 Kraus, A. and Müllen, K. (1999) *Macromolecules*, **32**, 4214.

15 (a) Belik, P., Gügel, A., Spickermann, J. and Müllen, K. (1993) *Angew. Chem. Int. Ed. Engl.*, **32**, 95.

(b) Gügel, A., Kraus, A., Spickcrmann, J., Belik, P. and Müllen, K. (1994) *Angew. Chem. Int. Ed. Engl.*, **33**, 559.
(c) Anderson, L.J., An, Y.-Z., Rubin, Y. and Foote, C.S. (1994) *J. Am. Chem. Soc.*, **116**, 9763.
(d) Fernández-Paniagua, U.M., Illescas, B., Martín, N., Seoane, C., de la Cruz, P., de la Hoz, A. and Langa, F. (1997) *J. Org. Chem.*, **62**, 3705.
(e) Martín, N., Pérez, I., Sánchez, L. and Seoane, C. (1997) *J. Org. Chem.*, **62**, 5690.
(f) Segura, J.L. and Martín, N. (1999) *Chem. Rev.*, **99**, 3199.

16 Li, J., Yoshizawa, T., Ikuta, M., Ozawa, M., Nakahara, K., Hasegawa, T., Kitazawa, K., Hayashi, M., Kinbara, K., Nohara, M. and Saigo, K. (1997) *Chem. Lett.*, 1037.

17 Xiao, L., Shimotani, H., Ozawa, M., Li, J., Dragoe, N., Saigo, K. and Kitazawa, K. (1999) *J. Polym. Sci. Part A Polym. Chem.*, **37**, 3632.

18 Ozawa, M., Li, J., Ankara, K., Xiao, L., Sugawara, H., Kitazawa, K., Kinbara, K. and Saigo, K. (1998) *J. Polym. Sci. Part A Polym. Chem.*, **36**, 3139.

19 Ito, H., Ishida, Y. and Saigo, K. (2006) *Tetrahedron Lett.*, **47**, 3095.

20 Liu, B., Bunker, C.E. and Sun, T.-P. (1996) *Chem. Commun.*, 1241.

21 (a) Hawker, C.J. (1994) *Macromolecules*, **27**, 4836.
(b) Adamopoulos, G., Heiser, T., Giovanella, U., Ould-Saad, S., van de Wetering, K.I., Brochon, C., Zorba, T., Paraskevopoulos, K.M. and Hadziioannou, G. (2006) *Thin Solid Films*, **511–512**, 371.

22 Chen, Y., Cai, R.-F., Huang, Z.-E. and Kong, S.-Q. (1995) *Polym. Bull.*, **35**, 705.

23 Chen, Y., Huang, Z.-E., Cai, R.-F., Kong, S.-Q., Chen, S., Shao, Q., Yan, X., Zhao, F. and Fu, D. (1996) *J. Polym. Sci. Part A Polym. Chem.*, **34**, 3297.

24 Chen, Y., Huang, Z.-E., Cai, R.-F., Yu, B.-C., Ma, W., Chen, S., Shao, Q., Yan, X. and Huang, Y. (1997) *Eur. Polym. J.*, **33**, 291.

25 Cao, T., Wei, F., Yang, Y., Huang, L., Zhao, X. and Cao, W. (2002) *Langmuir*, **18**, 5186.

26 Stalmach, U., de Boer, B., Videlot, C., van Hutten, P.F. and Hadziioannou, G. (2000) *J. Am. Chem. Soc.*, **122**, 5464.

27 de Boer, B., Stalmach, U., van Hutten, P.F., Melzer, C., Krasnikov, V.V. and Hadziioannou, G. (2001) *Polymer*, **72**, 9097.

28 (a) Siegrist, A.E., Liechti, P., Meyer, H.R. and Weber, K. (1969) *Helv. Chim. Acta*, **52**, 2521.
(b) Siegrist, A.E. (1981) *Helv. Chem. Acta*, **64**, 662.
(c) Kretzschmann, H. and Meier, H. (1991) *Tetrahedron Lett.*, **32**, 5059.
(d) Meier, H., Stalmach, U. and Kolshorn, H. (1997) *Acta Polym.*, **48**, 379.

29 Barrau, S., Heiser, T., Richard, F., Brochon, C., Ngov, C., van de Wetering, K., Hadziioannou, G., Anokhin, D.V. and Ivanov, D.A. (2008) *Macromolecules*, **41**, 2701.

30 Chen, X., Gholamkhass, B., Han, X., Vamvounis, G. and Holdcroft, S. (2007) *Macromol. Rapid Commun.*, **28**, 1792.

31 Sato, H., Matsuda, D. and Ogino, K. (1998) *Polym. J.*, **30**, 904.

32 Zheng, J., Goh, S.H. and Lee, S.Y. (1997) *Polym. Bull.*, **39**, 79.

33 Lu, Z.H., Goh, S.H. and Lee, S.Y. (1997) *Polym. Bull.*, **39**, 661.

34 Huang, H.L., Goh, S.H., Zheng, J.W., Lai, D.M.Y. and Huan, C.H.A. (2003) *Langmuir*, **19**, 5332.

35 Goh, H.W., Goh, S.H. and Xu, G.Q. (2002) *J. Polym. Sci. Part A Polym. Chem.*, **40**, 1157.

36 Prato, M., Li, Q.C., Wudl, F. and Lucchini, V. (1993) *J. Am. Chem. Soc.*, **115**, 1148.

37 Goh, H.W., Goh, S.H. and Xu, G.Q. (2002) *J. Polym. Sci. Part A Polym. Chem.*, **40**, 4316.

38 Zheng, J.W., Goh, S.H. and Lee, S.Y. (2000) *J. Appl. Polym. Sci.*, **75**, 1393.

39 Zheng, J.W., Goh, S.H. and Lee, S.Y. (2001) *Fullerene Sci. Technol.*, **9**, 487.

40 Wang, Z.Y., Kuang, L., Meng, X.S. and Gao, J.P. (1998) *Macromolecules*, **31**, 5556.

41 Wang, C., Tao, Z., Yang, W. and Fu, S. (2001) *Macromol. Rapid Commun.*, **22**, 98.

42 Tang, B.Z., Leung, S.M., Peng, H. and Yu, N.-T. (1997) *Macromolecules*, **30**, 2848.

43 (a) Tong, R., Wu, H., Li, B., Zhu, R., You, G., Qian, S., Lin, Y. and Cai, R.-F. (2005) *Physica B*, **366**, 192.

(b) Wu, H., Li, F., Lin, Y., Cai, R.-F., Wu, H., Tong, R. and Qian, S. (2006) *Polym. Eng. Sci.*, **46**, 399.
44 Tang, B.Z., Peng, H., Leung, S.M., Au, C.F., Poon, W.H., Chen, H., Wu, X., Fok, M.W., Yu, N.-T., Hiraoka, H., Song, C., Fu, J., Ge, W., Wong, G.K.L., Monde, T., Nemoto, F. and Su, K.C. (1998) *Macromolecules*, **31**, 103.
45 Li, F., Li, Y., Ge, Z., Zhu, D., Song, Y. and Fang, G. (2000) *J. Phys. Chem. Solids*, **61**, 1101.
46 Vitalini, D., Mineo, P., Iudicelli, V., Scamporrino, E. and Troina, G. (2000) *Macromolecules*, **33**, 7300.
47 Wudl, F. (1992) *Acc. Chem. Res.*, **25**, 157.
48 Wudl, F., Hirsch, A., Khemani, K.C., Suzuki, T., Allemand, P.-M., Koch, A., Eckert, H., Srdanov, G. and Webb, H.M. (1992) *Fullerenes: Synthesis. Properties and Chemistry of Large Carbon Clusters* (eds G.S. Hammond and V.J. Kuck), American Chemical Society, Washington, DC, p. 161.
49 Geckeler, K.E. and Hirsch, A. (1993) *J. Am. Chem. Soc.*, **115**, 3850.
50 Patil, A.O., Schriver, G.W., Carstensen, B. and Lundberg, R.D. (1993) *Polym. Bull.*, **30**, 187.
51 Patil, A.O. and Schriver, G.W. (1995) *Macromol. Symp.*, **91**, 73.
52 Sun, Y.-P., Bunker, C.E. and Liu, B. (1997) *Chem. Phys. Lett.*, **272**, 25.
53 Sun, Y.-P., Liu, B. and Lawson, G.E. (1997) *Photochem. Photobiol.*, **66**, 301.
54 Sun, Y.-P., Liu, B. and Moton, D.K. (1996) *Chem. Commun.*, 2669.
55 Sun, Y.-P., Lawson, G.E., Huang, W., Wright, A.D. and Moton, D.K. (1999) *Macromolecules*, **32**, 8747.
56 Gu, T., Chen, W.-X. and Xu, Z.-D. (1999) *Polym. Bull.*, **42**, 191.
57 (a) Chen, Y., Huang, Z.-E. and Cai, R.-F. (1996) *J. Polym. Sci. B Polym. Phys.*, **34**, 631.
(b) Chen, Y., Huang, Z.-E., Cai, R.-F., Yu, B.-C., Ito, O., Zhang, J., Ma, W.-W., Zhong, C.-F., Zhao, L., Li, Y.-F., Zhu, L., Fujitsuka, M. and Watanabe, A. (1997) *J. Polym. Sci. B Polym. Phys.*, **35**, 1185.
58 Ling, Q.-D., Lim, S.-L., Song, Y., Zhu, C.-X., Chan, D.S.-H., Kang, E.-T. and Neoh, K.-G. (2007) *Langmuir*, **23**, 312.
59 Manners, I. (1996) *Angew. Chem. Int. Ed. Engl.*, **35**, 1602.
60 (a) Allcock, H.R. (1976) *Science*, **193**, 1214.
(b) Neilson, R.H. and Neilson, P.W. (1988) *Chem. Rev.*, **88**, 541.
61 Kumar, D., Gupta, A.D. and Khullar, M. (1993) *J. Polym. Sci. Part A Polym. Chem.*, **31**, 707.
62 Allcock, H.R. and Kim, C. (1990) *Macromolecules*, **23**, 3881.
63 Marco, P.D., Giro, G., Lora, S. and Gleria, M. (1985) *Mol. Cryst. Liq. Cryst.*, **118**, 439.
64 Allcock, H.R., Ravikiran, R. and Olshavsky, M.A. (1998) *Macromolecules*, **31**, 5206.
65 Rotello, V.M., Howard, J.B., Yadav, T., Conn, M.M., Viani, E., Giovane, L.M. and Lafleur, A.L. (1993) *Tetrahedron Lett.*, **34**, 1561.
66 Li, Z. and Qin, J. (2004) *J. Polym. Sci. Part A Polym. Chem.*, **42**, 194.
67 Li, Z., Qin, J. and Xu, X. (2004) *J. Polym. Sci. Part A Polym. Chem.*, **42**, 2877.
68 Miller, M.L. and West, R. (1999) *Chem. Commun.*, 1797.
69 Li, Z. and Qin, J. (2003) *J. Appl. Polym. Sci.*, **89**, 2068.
70 Ungurenasu, C. and Pinteala, M. (2005) *Macromol. Rapid Commun.*, **26**, 707.
71 Nanjo, M., Cyr, P.W., Liu, K., Sargent, E.H. and Manners, I. (2008) *Adv. Funct. Mater.*, **18**, 470.
72 Okamura, H., Miyazono, K., Minoda, M. and Miyamoto, T. (1999) *Macromol. Rapid Commun.*, **20**, 41.
73 Ungurenasu, C. and Pienteala, M. (2007) *J. Polym. Sci. Part A Polym. Chem.*, **45**, 3124.
74 Gutiérrez-Nava, M., Masson, P. and Nierengarten, J.-F. (2003) *Tetrahedron Lett.*, **44**, 4487.
75 Gutiérrez-Nava, M., Setayesh, S., Rameau, A., Masson, P. and Nierengarten, J.-F. (2002) *New J. Chem.*, **26**, 584.
76 Drees, M., Hoppe, H., Winder, C., Neugebauer, H., Sariciftci, N.S., Schwinger, W., Schäffler, F., Topf, C., Scharber, M.C., Zhu, Z. and Gaudiana, R. (2005) *J. Mater. Chem.*, **15**, 5158.
77 (a) Sterescu, D.M., Bolhuis-Versteeg, L., van der Vegt, N.F.A., Stamatialis, D.F. and Wessling, M. (2004) *Macromol. Rapid Commun.*, **25**, 1674.
(b) Sterescu, D.M., Stamatialis, D.F., Mendes, E., Wibbenhorst, M. and

Wessling, M. (2006) *Macromolecules*, **39**, 9234.
78 Goh, S.H., Zheng, J.W. and Lee, S.Y. (2000) *Polymer*, **41**, 8721.
79 Zhang, N., Schricker, S.R., Wudl, F., Prato, M., Maggini, M. and Scorrano, G. (1995) *Chem. Mater.*, **7**, 441.
80 Ball, Z.T., Sivula, K. and Fréchet, J.M.J. (2006) *Macromolecules*, **39**, 70.
81 Sivula, K., Ball, Z.T., Watanabe, N. and Fréchet, J.M.J. (2006) *Adv. Mater.*, **18**, 206.
82 Zhang, X., Sieval, A.B., Hummelen, J.C. and Hessen, B. (2005) *Chem. Commun.*, 1616.

3
Acrylate and Methacrylate C_{60}-End-Capped Polymers

Palaniswamy Ravi, Sheng Dai, and Kam Chiu Tam

3.1
Introduction

Since the discovery of buckminsterfullerene (C_{60}) in 1985 by Kroto, Curl and Smalley [1], the scientific and industrial communities have devoted significant effort to exploit and use fullerenes for the synthesis of various types of functional nanostructured materials. Among various forms of fullerene molecules, [60]fullerene (C_{60}) and its derivatives possess a diverse range of attractive properties, such as electronic, conducting and magnetic properties due to its unusual symmetry and electron conjugate characteristic [2–4]. As a result, the number of studies in this field has grown steadily; especially, the applications of C_{60} in biological [5] and materials chemistry [6] have received increasing attention recently. However, most potential large scale applications are hampered by the strong cohesive nature and poor solubility in common organic solvents. Therefore, numerous strategies have been explored to enhance its solubility so as to broaden and expand its end-use applications [7]; for example, (i) conjugating C_{60} with functional groups such as carboxylic acids [8], amines [9] or alcohols [10]; (ii) solubilizing or encapsulating via the formation of complexes with surfactants, cyclodextrins, calixarenes, phospholipids and liposomes [11–16]; (iii) producing charge-transfer (CT) complexes with organic compounds bearing electron-donating groups through electron donor and acceptor interaction [17]. Among these, water-soluble fullerene systems are undoubtedly of great interest, particularly for biomedical applications [18–21]. In general, water-compatible C_{60} derivatives could be obtained by modifying C_{60} with polar functional groups, such as carboxyl, hydroxyl [22, 23] or amino groups [24], and by interaction with hydrophilic polymers [25]. Geckeler *et al.* have synthesized water-soluble and biocompatible fullerenes by nucleophilic addition of cyclodextrin-iminoalkyl and iminoaryl monoamines to C_{60}, where their potential interaction with DNA has been elucidated [12]. A star-like water-soluble fullerene derivative, hexa(sulfonbutyl)fullerene ($C_{60}[(CH_2)_4SO_3^-]_6$), with six negatively charged sulfonate arms has been synthesized and used to selectively precipitate positively charged surfactants, amino acids, peptides and proteins [26].

Fullerene Polymers. Synthesis, Properties and Applications. Edited by Nazario Martín and Francesco Giacalone

ISBN: 978-3-527-32282-4

In addition, many water-soluble fullerene polymeric composites have been developed by exploiting the donor–acceptor properties of nitrogen-containing polymers and C_{60} [27]. C_{60} can also be solubilized by encapsulating it in block copolymer micelles [28]. For example, Jenekhe and Chen have investigated the solubilization of C_{60} by encapsulating it inside spherical aggregates consisting of the rod-coil amphiphilic block copolymer poly(phenylquinoline)-*block*-polystyrene [29]. These types of functionalization of C_{60} have yielded potentially new materials with appealing and technologically promising characteristics. However, derivatizing C_{60} with multiple functional groups unavoidably damages the π–π conjugation, which partially disrupts the physical properties of C_{60}. To retain the unique properties of C_{60}, the functionalization of C_{60} with a lower degree of substitution (DS) is desirable. The promising strategy to enhance its solubility with a lower DS is to graft long polymer chains onto the surface of C_{60} [30].

C_{60}-containing polymeric systems show solvent-selective character in solution and form different nanoscale aggregates with interesting morphologies [31]. Synthesizing novel nanoscopic materials by combining the unique properties of C_{60} with specific properties of polymers extends their desired end-use applications [32]. In the past several years, the development of nanostructured materials based on well-defined C_{60}-containing polymers has been reported. For example, a novel salt-derivatized C_{60} pyrrolidine nitroxide has been synthesized, and it readily self-assembled into 80–130 nm ball-like nanoparticles in 10 : 1 chlorobenzene/methanol [33]. Nanospheres and nanorods composed of C_{60}-containing polymers have also been prepared, using cationic amphiphiles, for biomedical applications [34]. The chemical modifications and applications of C_{60} derivatives are described in other chapters of this book and in some early reviews [35]. In this chapter, we emphasize current developments in the synthesis and physicochemical properties of acrylate and methacrylate C_{60}-end-capped polymers in aqueous solution or selective solvents.

3.2 Synthesis of C_{60}-End-Capped Polymers

3.2.1 General Synthetic Approaches for C_{60}-Containing Polymers

In general, C_{60}-containing polymers can be prepared using different synthetic approaches, including copolymerization of polymerizable monomers with C_{60}, *in situ* polymerization of monomers initiated from C_{60} functionalized initiators, and substitution or end-capping of C_{60} with end-functionalized precursor polymers. Depending on the synthetic methodologies used, these synthetic approaches could produce different structures, such as C_{60} on the main polymeric chain, C_{60} on the side chain of the polymers, hyperbranched C_{60}-containing polymers, star-like polymers, mono-end-capped polymers, telechelic polymers, dendrimers and so on. A more detailed description of the preparation of C_{60}-containing polymers and

their physicochemical properties in solution is given in reviews by Geckler *et al.* [36], Wang *et al.* [37], Ravi *et al.* [38] and Giacalone and Martin [39].

Using the multiple reactive double bonds, C_{60} can be employed as a co-monomer in an *in situ* polymerization process with various vinyl based monomers through addition polymerization. For example, Mourey *et al.* have used radical chain polymerization with AIBN as initiator in 1,2-dichlorobenzene to produce branched structures of C_{60} and both PMMA [poly(methyl methacrylate)] and PS (polystyrene) [40]. Details of the structure and radical mechanism for the formation of copolymers of C_{60} with styrene or methyl methacrylate have been proposed by Ford and coworkers [41]. The free radical copolymerization of C_{60} with various monomers, such as methyl methacrylate, vinyl acetate and *N*-vinylcarbazole has been investigated by Wang [42]. However, it is impossible to obtain well-defined C_{60}-containing polymers using such techniques. Consequently, various methodologies have been developed for grafting C_{60} to the preformed polymers because C_{60} is prone to react with nucleophiles. Chen *et al.* have proposed a nucleophilic addition reaction to synthesize fullerenated polymers [43–45]. In this technique, the living polymeric active carbanion intermediates generated by conventional anionic polymerization react with C_{60} to form C_{60} end-capped polymers [46–48]. The anionic mechanism allows the production of a well-defined polymer grafted C_{60} [49]. Chen *et al.* have prepared highly soluble star-shaped C_{60}-*p*-methylstyrene copolymers with different amounts of C_{60} by the addition of active poly(*p*-methylstyrene) carbanion to C_{60} [50]. A polymeric photoconductor composed of C_{60}-poly(*N*-vinylcarbazole) can be synthesized using anionic polymerization by introducing C_{60} to the active carbanion moiety [51, 52]; the resulting C_{60} derivative exhibited a remarkable photoconducting properties. Yashima *et al.* have synthesized highly isotactic PMMA-C_{60} (*mm* ~ 98%) with a narrow molecular weight distribution by the stereospecific anionic living polymerization of a methacrylate followed by end-capping with C_{60}. The C_{60} end-capped PMMA was successfully isolated through self-assembly in a polar solvent and by size exclusion chromatography (SEC) (Scheme 3.1) [53]. A water-soluble C_{60}-containing polyphosphazene has been synthesized by Li and Qin using cycloaddition reaction of azide-terminated polyphosphazenes intermediate with C_{60} [54].

The most facile and widely used technique to derivatize C_{60} with well-defined polymer is azido coupling with C_{60}. The stoichiometry of C_{60} and azide-terminated polymers determine the degree of polymer substitution on the C_{60}. Azido coupling with excess C_{60} results in mono-substitution of the polymer with C_{60}. The reaction of azido-substituted polymers with C_{60} produces water-soluble C_{60} with a well-controlled macromolecular architecture. A well-defined, water-soluble, fullerene end-capped poly(ethylene oxide) (PEO) can be synthesized by azido coupling of azide-terminated PEO with C_{60} [55, 56]. The reaction of polymers containing amine groups with C_{60} has also attracted significant attention, due to the mild reaction conditions, which permit the preparation of well-defined, water-soluble mono-substituted polymeric C_{60} derivatives [57–59]. Water-soluble poly(azomethine) has been end-capped with C_{60} by reacting amine-terminated poly(azomethine) with C_{60} in a DMF/toluene solvent mixture [60], where the C_{60} was used as end-capping

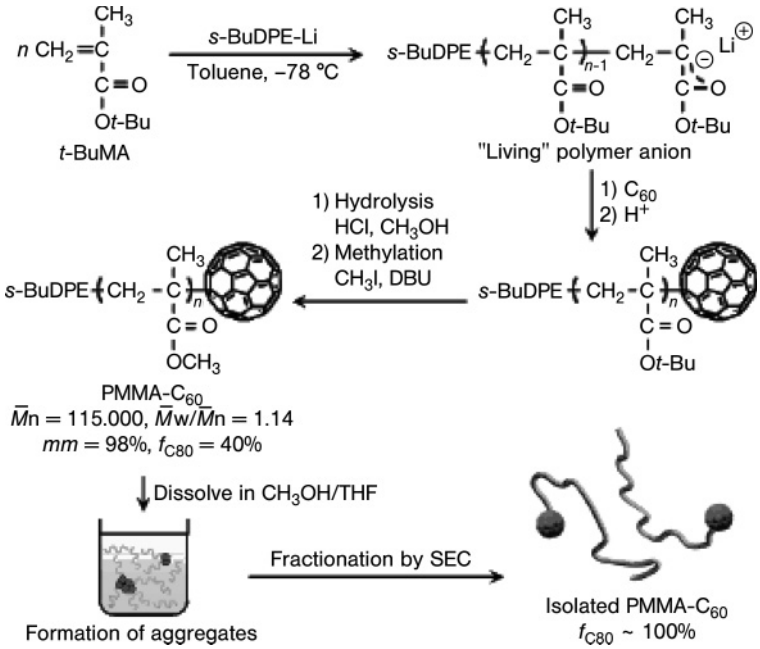

Scheme 3.1 Synthesis route for the preparation of well-defined isotactic PMMA end-capped C_{60}. (Reprinted with permission from Reference [53]. Copyright © American Chemical Society.)

agent with self-dopant for polyrotaxane. The "living" active ends of well-defined polymers prepared either by anionic or controlled radical polymerization can be used to end-cap C_{60} to yield C_{60} with a controlled polymeric architecture, such as C_{60}-polybutadiene and C_{60}-poly(butadiene-*co*-styrene). These polymers have been synthesized through anionic polymerization of butadiene and styrene in hexane, where the living ends were capped with C_{60} via epoxybutane bridging [61]. Stereospecific anionic polymerization has been applied to synthesize isotactic- and syndiotactic-PMMA-C_{60} polymers by living polymerization of MMA followed by end-capping with C_{60} [62]. A poly(3-hexylthiophene), bearing a nitroxide moiety on each thienyl unit, has been synthesized and used as the macro-initiator to initiate the nitroxide-mediated radical polymerization (NMP) of styrene and chloromethylstyrene (CMS) from the polythienyl. Finally, C_{60} has been attached to the CMS component by ATRP (atom transfer radical polymerization) in the presence of CuBr/bipy to form polythiophene-*graft*-(styrene-*g*-C_{60}) copolymers [63].

3.2.2
Well-Defined C_{60} End-Capped Polymers by Controlled Radical Polymerization

To synthesize C_{60}-containing polymers with narrow molar mass distribution, the preformed polymer that is conjugated to C_{60} must be prepared by living polymerization. However, there have been few reports on the synthesis of well-defined C_{60}-containing polymers using living polymerization because of the strin-

gent reaction conditions. The number of polymeric chains attached to C_{60} depends on the amount of reactants, counterions and solvent [64]. Controlled/"living" radical polymerization offers an attractive route to synthesize polymers with predictable molecular weights and low polydispersity. The living end-groups can be further initiated to form macro-radicals, and such macro-radicals can be used to produce well-defined block copolymers or to perform radical addition reaction of the initiated polymeric radical to vinyl groups (living radical addition). The living radical addition process can be used as an attractive pathway to produce well-controlled polymeric architecture end-capped with C_{60}. Fukuda *et al*. have proposed the synthesis of well-defined, di-substituted polymer derivatives of C_{60} by a radical addition mechanism [65]. Later, narrow polydispersed polystyryl adducts with TEMPO (2,2,6,6-tetramethylpiperidinyl-1-oxy) were heated with excess C_{60} to yield a well-controlled 1,4-dipolystyryldihydro-C_{60}. In addition, they also synthesized well-defined, C_{60}-containing two-arm poly(vinylphenol) [$(PVP)_2$-C_{60}] and a diblock copolymer of (PS-*b*-PVP)$_2$-C_{60} using TEMPO-mediated polymerization [66]. Ford *et al*. have succeeded in producing well-defined mono- and di-substituted polystyrene with C_{60} using the TEMPO-mediated polymerization technique [67]. Hadziioannou *et al*. have demonstrated the successful synthesis of well-defined rod-coil block copolymers containing a poly(*p*-phenylenevinylene) (PPV) block as the rigid part and PS as a flexible coil obtained by means of nitroxide-mediated "living" radical polymerization [68]. Further, the block copolymer was functionalized with C_{60}, using an atom transfer radical addition (ATRA) reaction to obtain a well-controlled (PPV-*b*-PS)-C_{60}.

The development of a novel and innovative ATRP technique by Matyjaszewski and coworkers offers polymer chemists an attractive and efficient method for preparing well-defined polymers [69, 70]. Developments in ATRP have provided flexible synthetic routes to aid macromolecular design and engineering of well-defined C_{60}-polymer derivatives. Zhou *et al*. have used the ATRP technique to synthesize well-defined PS and PMMA end-capped with C_{60} (Scheme 3.2) [71]. First, well-defined, monodispersed Br-terminated PS and PMMA macro-initiators were synthesized by ATRP of styrene and MMA using 1-phenylethyl bromide and

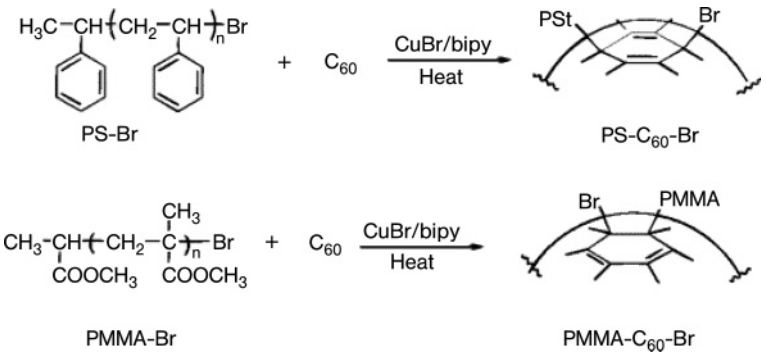

Scheme 3.2 Synthesis scheme of C_{60} end-bonded, well-defined PS and PMMA by ATRP (Reprinted with permission from Reference [71]. Copyright © American Chemical Society.)

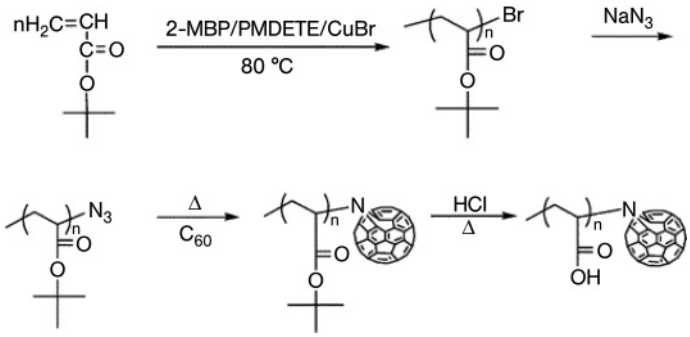

Scheme 3.3 Synthesis scheme of well-defined PAA-*b*-C_{60} (Reprinted with permission from Reference [74]. Copyright © American Chemical Society.)

methyl 2-bromopropionate as initiators, respectively, and CuBr/bipyridine (CuBr/bipy) as the catalyst system. Subsequently, ATRA of PS and PMMA macro-radicals to C_{60} was performed in the presence of an excess of C_{60} using a CuBr/bipy catalyst system in 1,2-dichlorobenzene at 90 and 110 °C, respectively, for MAA and styrene to produce well-defined mono end-capped PMMA-*b*-C_{60} and PS-*b*-C_{60} with narrow polydispersity. Mathis *et al*. have demonstrated the synthesis of well-controlled, even-numbered PS chains (di and tetra adduct) attached to C_{60} by direct addition of PS macro-radicals prepared by the ATRP onto C_{60} in the presence of CuBr/bipy at 100 °C [72].

ATRP has also been used to synthesize mono end-caped C_{60} with rod-coil block copolymers of terfluorene-*b*-PS segments in the presence of CuBr/bipy catalyst system in *o*-dichlorobenzene at 110 °C [73]. The resulting C_{60} end-capped polymer exhibited a stable emission of blue light. Wang *et al*. have used ATRP combined with azido coupling to synthesize water-soluble poly(acrylic acid)-*b*-C_{60} (PAA-*b*-C_{60}) polymer with narrow polydispersity [74]. Well-defined poly(*tert*-butyl acrylate) (P*t*BA) with narrow polydispersity was first synthesized by ATRP followed by azide substitution of the Br end groups to yield P*t*BA-N_3. Fullerenation of P*t*BA-N_3 in the presence of C_{60} using azido coupling, followed by hydrolysis, produced a well-defined PAA-*b*-C_{60} polymer (Scheme 3.3). Chu *et al*. have synthesized a novel water-soluble C_{60} anchored with a two-arm PAA polymer using a ATRP technique based on the Bingel reaction [75]. A multi-step synthetic strategy was adopted in which a dibromo-functionalized initiator bearing a malonate ester core was synthesized and used for the polymerization of *t*BA. Finally, C_{60} was functionalized with the polymer via a Bingel cyclopropanation on the C_{60} to produce C_{60} containing two arm P*t*BA. A well-defined amphiphilic block copolymer of PAA-*b*-PS-*b*-C_{60} could be prepared using ATRP followed by the azido coupling reaction [76]. First, C_{60} end-capped P*t*BA-*b*-PS copolymer was synthesized by reacting C_{60} with azide-functionalized copolymer that was prepared by ATRP. Hydrolysis of the resulting P*t*BA-*b*-PS-C_{60} copolymer produced a well-defined water-soluble amphiphilic block copolymer that exhibited good photoconducting properties. ATRP also provides flexibility in tailor-

ing multiple block copolymers of a desirable macromolecular architecture. Well-defined telechelic C_{60}-containing polymers can be produced by ATRP. For the synthesis of a well-defined polymer with dual end-capped C_{60}, two-arm well-defined polymers can be prepared starting from the dual initiator system. Subsequently, azido coupling can be performed, followed by heating with an excess of C_{60} to obtain a dual C_{60} end-capped, well-defined polymer. Recently, Tam and coworkers have synthesized well-defined pH-responsive mono- (PAA-*b*-C_{60}) and di-substituted C_{60} (C_{60}-*b*-PAA-*b*-C_{60}) end-capped polyelectrolytes with identical molecular weights using a combination of ATRP and cycloazido addition reaction [77]. For the synthesis of di-substituted C_{60} with PAA, well-defined Br-P*t*BA-Br was first synthesized using a bifunctional initiator of diethyl *meso*-2,5-dibromoadipate (DEDBA) in anisole at 60 °C. The bromine end-groups were converted into the corresponding azide-terminated P*t*BA and, subsequently, P*t*BA end-capped with C_{60} was obtained by refluxing the azide-terminated N_3-P*t*BA-N_3 with excess C_{60} in 1,2-dichlorobenzene for 24 h. The di-substituted C_{60}-*b*-P*t*BA-*b*-C_{60} was soluble in most organic solvents. Finally, the *tert*-butyl protecting groups were removed by hydrolysis in the presence of trifluoroacetic acid in dichloromethane at room temperature to yield a well-defined C_{60}-*b*-PAA-*b*-C_{60}. Goh *et al.* have synthesized the dual Br-terminated poly(*n*-butyl methacrylate) (PBMA) using dibromo-*p*-xylene as an initiator and CuBr/bipy catalyst followed by reaction with trimethylsilyl amide to obtain dual Br-PBMA-Br. Finally, C_{60}-PBMA-C_{60} was obtained by heating the Br-PBMA-Br with excess C_{60} [78]. The same technique has been used to synthesize dual end-capped C_{60}-PDMAEMA-C_{60}, starting from the PEO-based dual initiator [79]. A triblock copolymer of dual C_{60} end-capped ABA type can also prepared in a similar manner. The synthesis of an amphiphilic ABA type double hydrophilic triblock copolymer of poly[2-(dimethylamino)ethyl methacrylate]-*block*-poly(ethylene oxide)-*block*-poly[2-(dimethylamino)ethyl methacrylate] (PDMAEMA-*b*-PEO-*b*-PDMAEMA) with C_{60} (C_{60}-$PDMAEMA_{60}$-*b*-PEO_{105}-*b*-$PDMAEMA_{60}$-C_{60}) using the combination of ATRP followed by azido coupling has also been reported [80]. To synthesize this polymer, a Br-PEO-Br macro-initiator was synthesized and used for the polymerization of DMAEMA in aqueous medium in the presence of CuCl/HMTETA (1,1,4,7,10,10-hexamethyltriethylenetetramine) catalyst. Subsequently, azide substitution of the triblock copolymer followed by the azido coupling addition with C_{60} afforded the well-defined polymer end-capped with C_{60}. Four-arm, well-defined, star-like polymers with C_{60} end-capped PS and PMMA polymers were sought by Cai *et al.* by synthesizing the respective Br-terminated four-arm polymers, using 1,2,4,5-tetrakis(bromomethyl)benzene as an initiator, by ATRP [81]. The synthesized C_{60} end-capped PS and PMMA showed optical limiting response.

Recently, we have synthesized a series of well-defined stimuli responsive, water-soluble, fullerene-containing polymers using ATRP. A well-defined alkali-soluble C_{60} end-capped poly(methacrylic acid) was synthesized by ATRP using group protecting chemistry [82]. A well-defined, stable Cl-terminated poly(*tert*-butyl methacrylate) (P*t*BMA) was synthesized using *p*-toluenesulfonic acid (*p*-TSA) as an initiator in the presence of CuCl/HMTETA catalyst complex at 90 °C. The Cl-terminated P*t*BMA was further used to perform in the presence of excess of C_{60}

to produce a well-defined P*t*BMA-*b*-C_{60}. Subsequently, the alkali-soluble C_{60}-containing polyelectrolyte (PMAA-*b*-C_{60}) was obtained by deprotecting the *tert*-butyl groups by hydrolysis in the presence of concentrated HCl in 1,4-dioxane at 80 °C. The well-defined C_{60} coupled to poly[2-(dimethylamino)ethyl methacrylate] (PDMAEMA) polymer, which exhibits temperature-responsive behavior, has been synthesized using ATRA by reacting PDMAEMA radical, initiated by a CuCl/HMTETA catalyst complex system, with C_{60} in 1,2-dichlorobenzene [83]. The room temperature ATRP of DMAEMA was performed using *p*-TSA initiator in the presence of CuCl/HMTETA in an aqueous methanol (1 : 4 water/methanol) system to obtain monodispersed PDMAEMA-Cl macroinitiator [84]. The temperature- and salt-responsive C_{60}-containing poly-zwitterionic polymers were further synthesized by the betainization of PDMAEMA-*b*-C_{60} [85]. The tertiary amine residues on the PDMAEMA can be betainized quantitatively using 1,3-sulfobetaine in THF under mild reaction condition (room temperature) (Scheme 3.4). ^{1}H NMR studies indicated that quantitative betainization (>95%) of the PDMAEMA-*b*-C_{60} was achieved. The poly-zwitterionic betainized-PDMAEMA-*b*-C_{60} (*Bet*-PDMAEMA-*b*-C_{60}) polymer showed responsiveness to both temperature [upper critical solution temperature (UCST)] and electrolyte (salt).

Ampholytic block copolymer contains both positive and negative charges on different segments of the diblock copolymer. Stimuli responsive, water-soluble polyampholyte-C_{60} polymer has also been synthesized by ATRP [86]. First, a well-defined, stable Cl-terminated P(*t*BMA_{102}-*b*-$DMAEMA_{67}$)-Cl block copolymer was prepared by ATRP in the presence of the CuCl/HMTETA catalyst system [87]. ATRA of P(*t*BMA-*b*-DMAEMA)-Cl macro-initiator to excess C_{60} using the same catalyst system at 90 °C offered a well-defined block copolymer-C_{60} (Scheme 3.5). Subsequently, the specific hydrolysis of P(*t*BMA-*b*-DMAEMA)-*b*-C_{60} to remove the tert-butyl group in the presence of concentrated HCl in 1,4-dioxane offered well-defined polyampholyte P(MAA-*b*-DMAEMA)-*b*-C_{60} polymer, which is responsive to both pH and temperature.

In addition, Cai *et al*. have proposed a reverse atom transfer radical polymerization (RATRP) approach to prepare end-functionalized PMMA with C_{60} and C_{70} [88]. The Cl-terminated PMMA-Cl as reaction precursor was synthesized through RATRP in the presence of an AIBN/$FeCl_3$/PPh_3 initiating system in solution and in bulk, respectively. The polymer was then functionalized with C_{60} or C_{70} by ATRA using Cu/CuBr/bipy or $FeCl_2$/bipy as catalyst to form well-defined PMMA-C_{60}.

3.3 Aggregation of C_{60}-End-Capped Polymers in Solution

3.3.1 Self-Assembly of C_{60}-End-Capped Polymers in Organic Solvents

C_{60}-containing polymers are attractive systems with self-assembly properties that are of particular interests in academic and industrial laboratories. Various

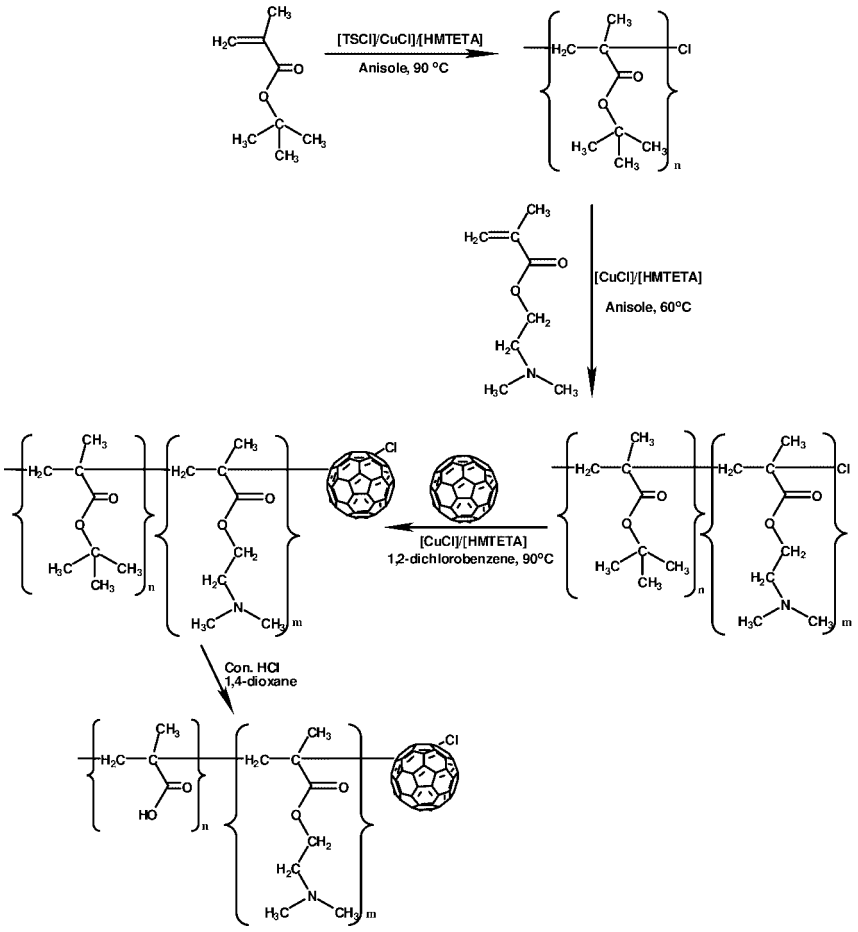

Scheme 3.4 Synthesis scheme of well-defined *Bet*-PDMAEMA-*b*-C_{60}. (Reprinted with permission from Reference [85]. Copyright © American Chemical Society.)

strategies can be adopted to control the formation of different types of aggregate in solution [89]. The development of these aggregates is a physical process controlled by both kinetics and thermodynamics of self-aggregation phenomenon. Owing to the special chemical and physical properties of C_{60} [90], the chemical structure, molecular weight, concentration and solvent character play critical roles in controlling the morphology of C_{60}-containing polymeric aggregates in solution [91]. Sunamoto *et al.* have produced fairly stable monodispersed nanoparticles via the self-assembly of a C_{60}/hydrophobized polysaccharide (CHP) complex in PBS to study the effect of C_{60} in a biological environment [92]. Sol–gel polycondensation of tetraethoxysilane in the presence of C_{60}/poly(*N*-vinylpyrrolidone) (PVP) complex yielded novel silica particles that contained of C_{60} with a particle diameter of 50–150 nm [93]. Core–shell micelles possessing different aggregation

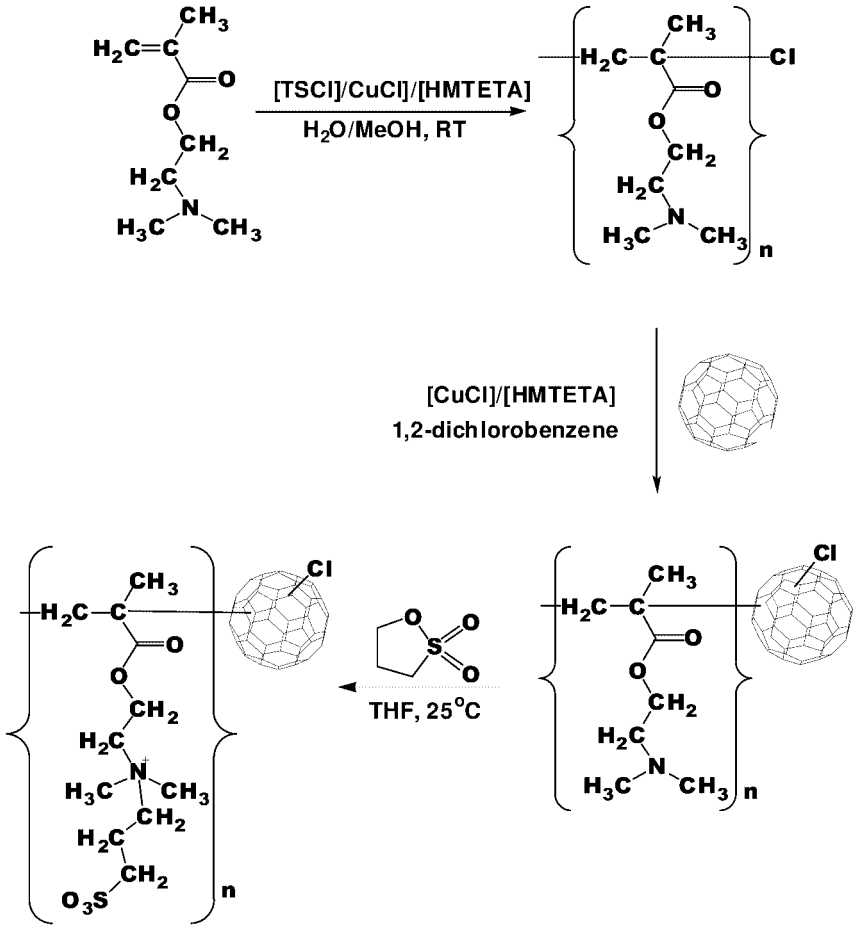

Scheme 3.5 Synthesis scheme of well-defined P(MAA-*b*-DMAEMA)-*b*-C_{60}. (Reprinted with permission from Reference [86]. Copyright © American Chemical Society.)

numbers with a hydrodynamic radius (R_h) of 70 nm and a radius of gyration (R_g) of 50 nm, and R_g/R_h of 0.7, have been reported for well-defined C_{60}-PMMA and C_{60}-P*n*BMA in THF solution [94]. The chemical structure and composition of the polymers along with their solubility controls the micellization behaviors of C_{60}-containing poly(alkyl methacrylate) based polymers in THF. There is an equilibrium between individual polymer chains and micelles for C_{60}-containing poly(alkyl methacrylate)s in THF (Figure 3.1). C_{60} grafted with two well-defined $(PVP)_2$-C_{60} [poly(*p*-vinylphenol)$_2$-C_{60}] and $(PS\text{-}b\text{-}PVP)_2$-$C_{60}$ arms with identical molecular weight have been synthesized and the micellization behavior in THF examined [66]. A laser light scattering study indicated that both $(PVP)_2$-C_{60} and $(PS\text{-}PVP)_2$-C_{60} formed stable micelles in dilute solution ($10^{-3} < c < 10^{-2}$ g mL^{-1}) with apparent aggregation numbers of about 20 and 6, respectively. However, $(PS)_2$-C_{60} showed

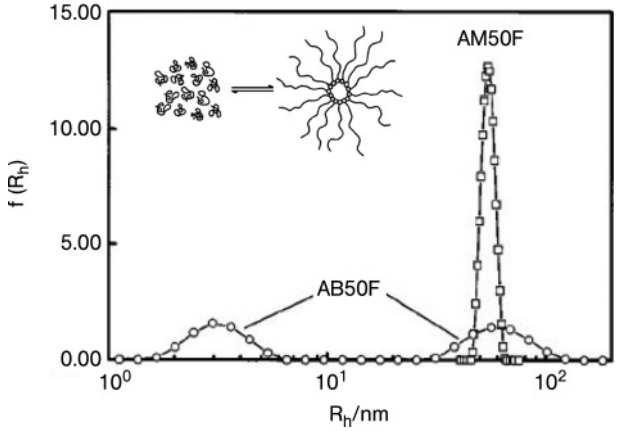

Figure 3.1 Typical normalized R_h distributions of C_{60}-containing poly(methyl methacrylate) (□) and poly(*n*-butyl methacrylate) (○) in THF; the polymer concentrations are 4.25×10^{-3} and 4.04×10^{-3} g mL^{-1}, respectively. (Reprinted with permission from Reference [94], copyright © American Chemical Society.)

no indication of association in THF, at least in dilute solution. The difference in the micellization behaviors was attributed to the solubilities of the individual polymers.

Our group has studied the self-assembly behavior of well-defined mono end-capped C_{60}-containing polymers in mixed selective solvents. For example, a well-defined C_{60} end-capped with P*t*BMA-*b*-C_{60} of number-averaged molecular weight (M_n) of 14 000 Da was synthesized using ATRP and the self-assembly behavior examined in chlorobenzene/ethyl acetate (CB/EA) solvent mixtures [31]. Chlorobenzene (CB) is a good solvent for both P*t*BMA and C_{60} and ethyl acetate (EA) is a selective solvent for only P*t*BMA [95]. In CB/EA solvent mixtures of various CB/EA compositions, P*t*BMA-*b*-C_{60} chains self-assemble to produce interesting morphologies. Both dynamic (DLS) and static (SLS) light scattering studies revealed conformational changes at different molar ratios of CB : EA. For example, the R_h of the aggregates decreased from ~110 to ~80 nm when the EA molar composition (X_{EA}) was increased from 0.7 to 0.84 and then increased sharply to ~120 nm at X_{EA} = 0.88 and to ~130 nm at X_{EA} = 0.95. However, R_g decreased from ~90 to ~70 nm as X_{EA} increased from 0.7 to 0.84 and then increased sharply to ~170 nm at X_{EA} = 0.88 and gradually to ~200 nm at X_{EA} = 0.95. The value of R_g/R_h, remained essentially constant at ~0.8 for X_{EA} in the range 0.7–0.84 and increased sharply to ~1.5 for X_{EA} between 0.84 and 0.88; thereafter R_g/R_h remained constant (Figure 3.2). Such a transition signifies a step change in the conformation and compactness of P*t*BMA-*b*-C_{60} aggregates. These aggregates were attributed to the formation of large compound vesicles (LCVs) in CB/EA solvent mixtures, which was confirmed by transmission electron microscopy (TEM).

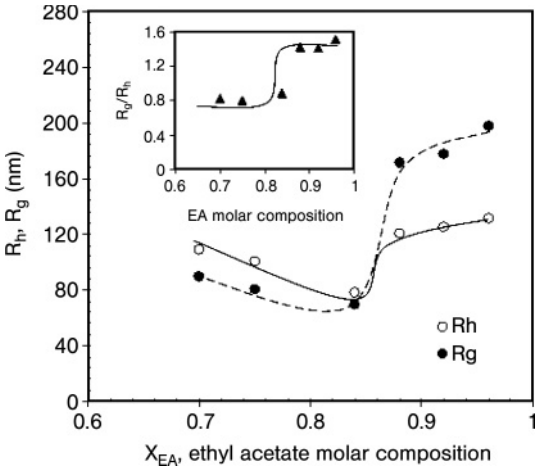

Figure 3.2 Hydrodynamic radius $<R_h>$ (○) and radius of gyration $<R_g>$ (●) of 0.7 wt% P*t*BMA-*b*-C_{60} aggregates in different solvent mixtures of ethyl acetate and chlorobenzene. Inset: R_g/R_h (▲) in different solvent mixtures. (Reprinted with permission from Reference [31], copyright © American Chemical Society.)

"Dimple-like" and "fractured" large compound vesicles were observed from the TEM micrographs (Figure 3.3); the dimple-like structures were mainly attributed to the drying of solvent during the sample preparation for TEM analyses. When the LCV started to dry, the chlorobenzene molecules diffuse to the interface of the P(*t*BMA) film and penetrate the dried P(*t*BMA) film, thereby producing the "dimple-like structure." The size of the "dimples" decreased significantly as the ethyl acetate molar composition increased from 0.84 to 0.88, where the R_g/R_h increased from 0.8 to 1.5.

Similarly, well-defined mono end-capped C_{60}-containing PMMA has been synthesized and the self-assembly behavior in various molar ratios of ethyl acetate/decalin (EA/DC) mixture has also been studied [96]. In 100% EA, PMMA-*b*-C_{60} existed as uniform aggregates. However, in solvent mixtures, the large aggregates coexisted in dynamic equilibrium with core–shell micelles and unimers. For each solvent mixture, the sizes of the aggregates were independent of concentration, indicating that self-assembly occurs via the closed association mechanism. The molecular weights of the aggregates range from 6.67×10^6 to 9.46×10^7 g mol^{-1} for the various solvent mixtures (Figure 3.4). The R_h of the particles varied from 90 to 111 nm, while R_g changed from 244 to 264 nm. The R_g/R_h value for each solvent mixture is about 2.3. The results indicate the formation of polydispersed large compound micelles (LCMs), which is independent of decalin content in the mixed solvents, but the aggregation number of the LCM increased with increasing decalin composition.

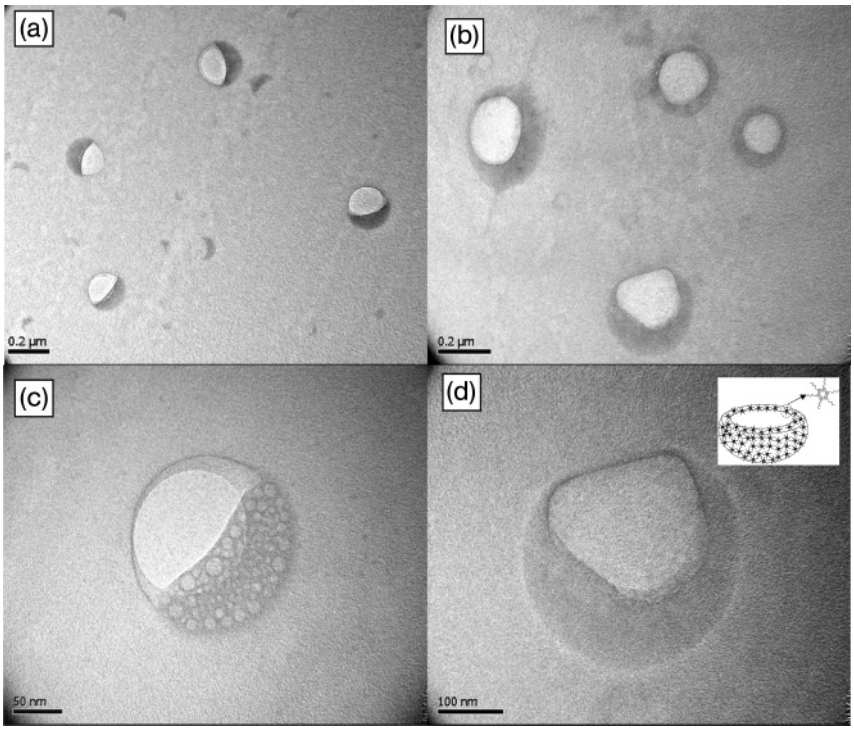

Figure 3.3 Typical transmission electron microscopy micrographs: (a) 0.5 wt% P*t*BMA-*b*-C_{60} in 0.75 ethyl acetate molar composition; (b) 1.0 wt% P*t*BMA-*b*-C_{60} in 0.92 ethyl acetate molar composition; (c) close up view of a single aggregate of 0.5 wt% P*t*BMA-*b*-C_{60} in 0.75 ethyl acetate molar composition; (d) close up view of a single aggregate of 1.0 wt% P*t*BMA-*b*-C_{60} in 0.92 ethyl acetate molar composition. Inset of (d): pictorial representation of a large compound vesicle. (Reprinted with permission from Reference [31], copyright © American Chemical Society.)

3.3.2 Aggregation of C_{60}-End-Capped Polymers in Aqueous Solution

3.3.2.1 pH-Responsive C_{60}-Containing Polymers

C_{60} attached to a water-soluble polymeric system behaves like an amphiphilic polymer consisting of hydrophobic C_{60} and a hydrophilic water-soluble polymer. In aqueous solution, these C_{60}-containing polymers may form core–shell micelles that consist of a C_{60} core and a hydrophilic polyelectrolyte shell or aggregates of other shapes. Depending on the polyelectrolyte chain length and C_{60} content, various morphologies can be attained. The self-assembly behavior of many well-defined polyelectrolyte-containing block copolymers has been elucidated [76, 97]; however, there are few published reports on the self-assembly behavior of mono-substituted water-soluble C_{60}-containing polyelectrolyte systems. In aqueous solution, PAA-*b*-C_{60} produced core–shell micelles, ~191 nm in diameter with a

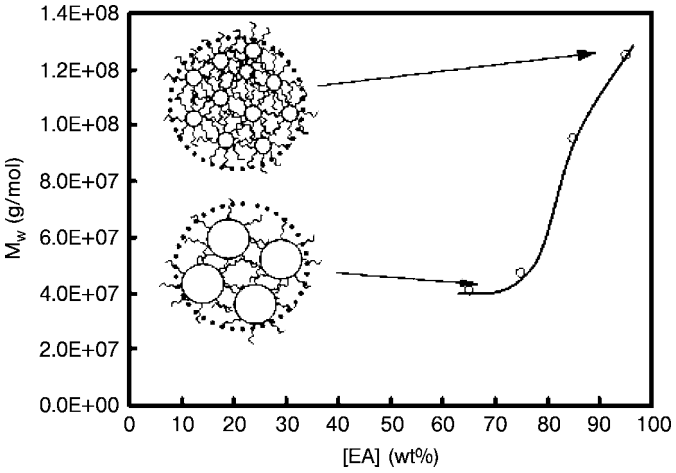

Figure 3.4 Possible aggregation mechanisms for the formation of PMMA-*b*-C_{60} LCM in different solvent mixtures of ethyl acetate and decalin (from Reference [96], copyright © 2005 Elsevier Ltd.).

polydispersity of 0.42, consisting of a C_{60} moiety forming the compact core and ionized PAA forming the shell at high pH (Figure 3.5) [74]. The polymeric film formed from PAA-*b*-C_{60} was found to enhance the photoconductivity of the film.

Recently, Tam and coworkers synthesized a series of mono- and di-substituted C_{60}-PAA systems with identical molecular weights and demonstrated the formation of different types of morphology in aqueous solution [77]. Both PAA_{83}-*b*-C_{60} and C_{60}-*b*-PAA_{85}-*b*-C_{60} showed pH-responsive properties and were water-soluble at high pH. At complete neutralized conditions, a core–shell micellar structure was obtained for PAA-*b*-C_{60}, with a R_h of 102 nm, that consists of a hydrophobic C_{60} core and ionized PAA shell. However, C_{60}-*b*-PAA-*b*-C_{60} self-assembled to form LCM under complete neutralization conditions, with a R_h of ~128 nm (Figure 3.6). The formation of LCM was further confirmed by TEM. The M_w of the LCM and core–shell micelle determined from a Berry plot was $\sim 3.50 \times 10^7$ and 3.42×10^6, respectively. The aggregation number (N_{agg}) for C_{60}-*b*-PAA-*b*-C_{60} was much higher (~4670) than that for PAA-*b*-C_{60} (~456) to form LCM and core–shell micelle. The hydrophilic–lipophilic balance (HLB) for both mono- and di-substituted C_{60} end-capped PAA system dictates the types of morphologies produced.

Well-defined mono end-capped C_{60}-containing alkali-soluble PMAA (PMAA-*b*-C_{60}) polymer also self-assembled into nanoscale aggregates in aqueous solution [82]. PMAA-*b*-C_{60} was soluble at high pH and showed pH-responsive properties. In dilute solution, the micelles coexisted with large secondary aggregates. These secondary aggregates consist of individual micelles that possess a microstructure similar to LCMs. Both the micelles and LCMs were formed via the closed association mechanism. The R_h of the micelles increased from 6 to 10 nm with increasing

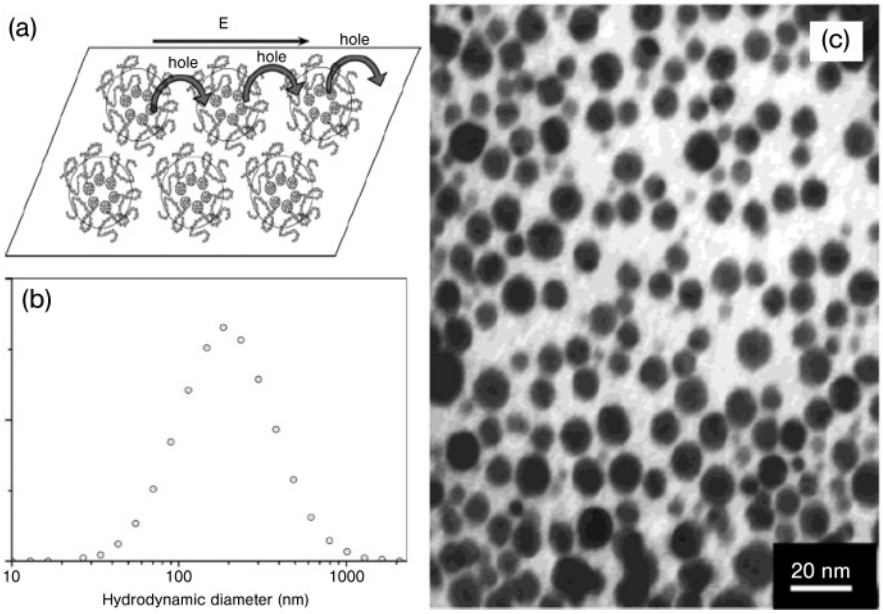

Figure 3.5 (a) Schematic represent of the aggregates of PAA-C_{60} in aqueous solution; (b) hydrodynamic diameter curve of the PAA-C_{60} in water; (c) TEM images of PAA-C_{60} film cast from water solution. (Reprinted with permission from Reference [74], copyright © American Chemical Society.)

degree of neutralization (α) and remained constant at 10 nm in the presence of salt. Addition of NaCl shields the electrostatic interaction between charged polyelectrolyte segments, enhancing the chain flexibility of PMAA segments and at the same time increases solvent polarity. The increase in aggregation number and the reduction in hydrodynamic size of fully neutralized PMAA segments maintained a small micellar size with increasing NaCl concentration.

R_h and R_g of the LCM increased from 91 to 153 nm and 210 to 335 nm, respectively, with increasing α while M_w of the LCM (~4.0×10^7 g mol^{-1}) and R_g/R_h values (~2.30) remained unchanged. However, R_h and R_g of the LCM decreased from 153 to 105 nm and 335 to 168 nm, respectively, with increasing NaCl concentration (Figure 3.7). The LCMs were stabilized by electrostatic interactions from charged polyelectrolyte backbones and counterions. At high salt concentrations, the carboxylate groups are shielded by oppositely charged counterions, and the PMAA chains shrink, causing a reduction in particle size of the LCM. TEM studies revealed the formation of a LCM microstructure that consists of individual micelles.

3.3.2.2 Temperature-Responsive C_{60}-Containing Polymers

Poly(dimethylaminoethyl methacrylate) (PDMAEMA) exhibits both pH and thermo-responsive properties. At low pH the protonated PDMAEMA chains yields

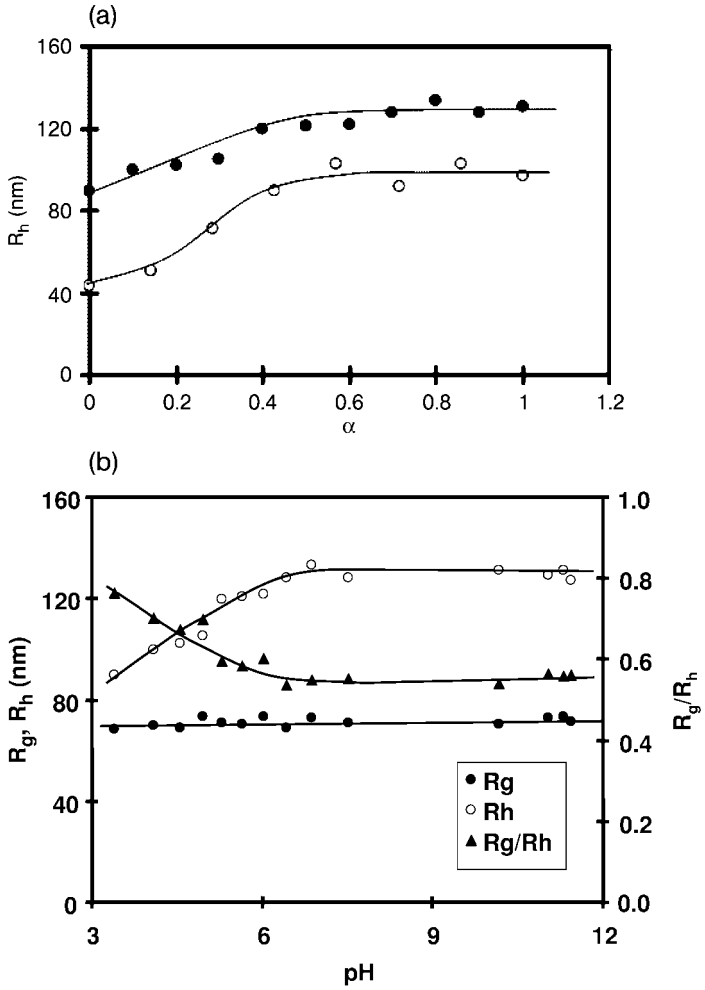

Figure 3.6 (a) Dependence of R_h on α (the degree of neutralization) for 0.1 wt% PAA-C_{60} (●) and C_{60}-PAA-C_{60} (●) in 0.1 M NaCl solution; (b) dependence of R_h (○), R_g (●) and R_g/R_h (▲) on pH for 0.1 wt% C_{60}-PAA-C_{60} in 0.1 M NaCl solution. (Reprinted with permission from Reference [77], copyright © American Chemical Society.)

a water-soluble polyelectrolyte, while at high pH the PDMAEMA chains are deprotonated and become water-insoluble when the temperature exceeds the lower critical solution temperature (LCST) [98]. PDMAEMA exhibits a LCST at around 45°C, and this temperature depends on the chain length and solution concentration [99]. The exploitation of PDMAEMA as biomaterials and polymeric electrolytes has been investigated extensively. Examination of the self-assembly behavior of well-defined C_{60} end-capped PDMAEMA is very important since both materials are biocompatible and the aqueous solution behavior of well-defined

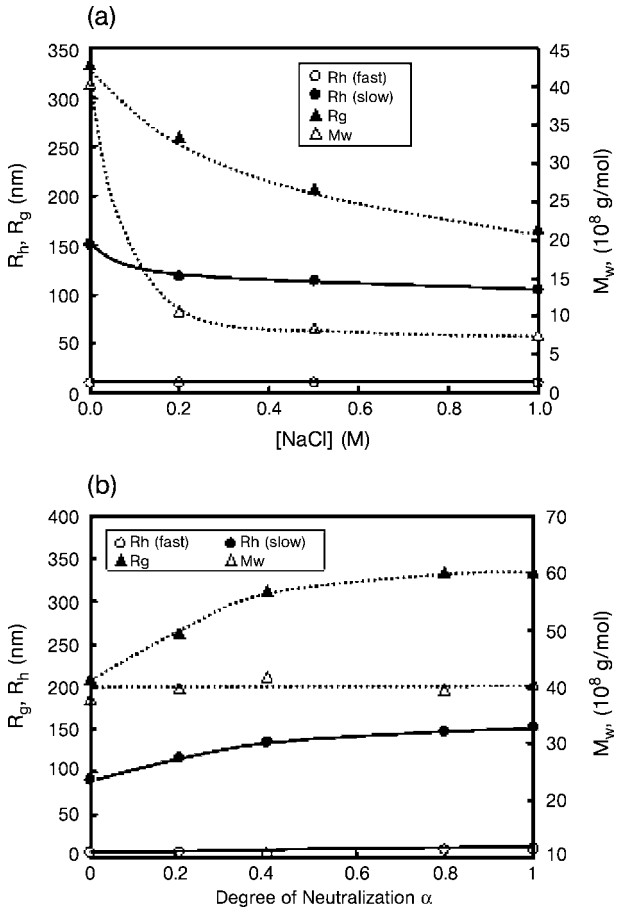

Figure 3.7 (a) Effect of salt concentration on R_h and R_g for 0.2 wt% PMAA-*b*-C_{60} at $\alpha = 1$; (b) dependence of R_h and R_g on degree of neutralization α for 0.2 wt% PMAA-*b*-C_{60} in aqueous solution. (Reprinted with permission from Reference [82], copyright © American Chemical Society.)

C_{60} end-capped PDMAEMA has been studied extensively. Tam and coworkers have reported the synthesis and physical properties of well-defined mono end-capped C_{60}-containing PDMAEMA in aqueous solution.

The PDMAEMA-*b*-C_{60} with a M_n of 18 000 Da also exhibited both pH- and temperature-responsive properties [83]. The LCST of PDMAEMA-*b*-C_{60} determined from light transmittance (UV/vis) was ~45 °C. However, the light transmittance of PDMAEMA-*b*-C_{60} was independent of pH at low temperatures but dependent on pH at high temperatures. At 55 °C, the PDMAEMA-*b*-C_{60} became water-insoluble at pH >7.8. Laser-light scattering studies of PDMAEMA-*b*-C_{60} in aqueous solutions at different temperatures and pH indicated that the

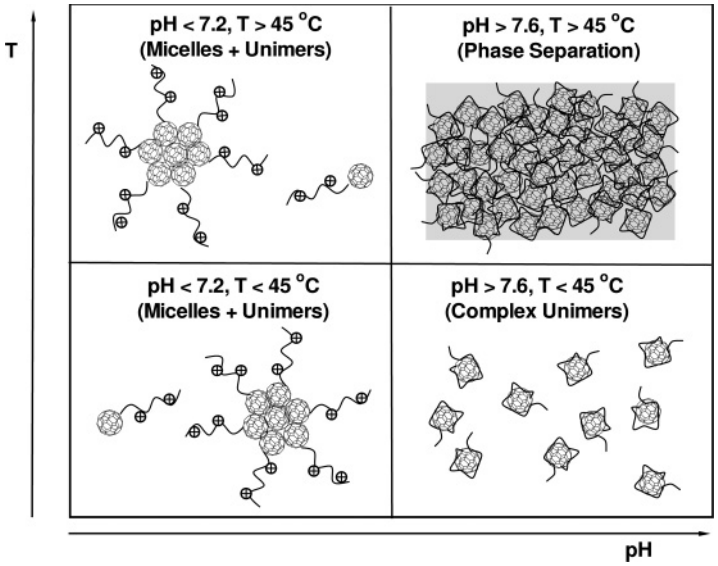

Figure 3.8 Phase diagram of PDMAEMA-*b*-C_{60} in aqueous solutions at different temperatures and pH values. (Reprinted with permission from Reference [83], copyright © American Chemical Society.)

hydrodynamic radius (R_h) did not change with temperature, but decreased with pH. At low pH, protonated PDMAEMA chains behave as a positively charged polyelectrolyte, resulting in an apparent increase in R_h. At pH 3 core–shell micelles with R_h ~55 nm coexisted with a substantial proportion of unimers (R_h = 5.5 nm) at 25 and 55 °C; the micellar formation was driven by the amphiphilic properties of PDMAEMA-*b*-C_{60}. Interestingly, only unimers with a R_h of ~4 nm were present at pH of 10 and 25 °C in aqueous solution. At high pH (>9) and low temperature, the deprotonated PDMAEMA chains (electron donor) formed a charge-transfer (CT) complex with the C_{60} (electron acceptor) [100]; formation of the CT complex of C_{60} with PDMAEMA was confirmed by UV/vis measurements. Such interaction precluded the formation of a micellar aggregate as the PDMAEMA/C_{60} charge-transfer complex, resulting in the formation of isolated stable fullerene particles. Based on the results obtained by LLS, potentiometric and conductometric titrations and UV/vis, the aggregation behavior and microstructure of PDMAEMA-*b*-C_{60} in aqueous solution at various pH and temperatures were elucidated and are summarized in the phase diagram shown in Figure 3.8.

3.3.2.3 C_{60}-Containing Polyampholytes

Polyampholytic block copolymers possess block rather than statistical architectures, consisting of different ionizable segments having different pK_a on the

respective blocks, which tend to precipitate around the isoelectric point (IEP). The difference between the pK_a of two blocks is the reason for their interesting self-assembly behavior that results in the formation of complex microstructure, depending on the block copolymer composition, molecular weight and types of monomer [101]. Synthetic polyampholytes have many potential applications, especially in the purification/complexation of different proteins as, described by Patrickios *et al*. [102, 103], for example, PMAA-*b*-PMMA-*b*-PDMAEMA. Both PMAA and PDMAEMA are biocompatible and possess stimuli-responsive properties [104, 105]. Attachment of C_{60} to well-defined polyampholyte makes the system P(MAA-*b*-DMAEMA)-*b*-C_{60} be more attractive as a drug delivery vehicle and the self-assembly of this system has not been exploited. Tam and coworkers conducted a systematic study on the self-assembly behavior of a well-defined P(MAA-*b*-DMAEMA)-*b*-C_{60} polyampholyte as functions of pH and concentration [86]. In aqueous solution, different electronic environments around the C_{60} were present at pH 3 and 11, as evidenced from the variation in UV/vis absorption spectra that show a disparity in the aggregation phenomena. At high pH, the formation of DMAEMA/C_{60} CT complex perturbed the localization of conjugated bonds, which resulted in the continuous absorption from 200 to 400 nm. The electronic environments around C_{60} were not altered by temperature, as evidenced from the absorption spectra measured at 55 °C, at pH of 3 and 11, which were similar to the corresponding spectra at 25 °C. The copolymer became insoluble in the pH range 5.4–8.8 due the overall charge neutralization near its IEP [97, 106] and the water-soluble P(MAA-*b*-DMAEMA)-*b*-C_{60} retained the polyampholyte behavior of P(MAA-*b*-DMAEMA).

At both high and low pH at 25 °C, the unimers were in dynamic equilibrium with large aggregates of R_h ~120 nm and the size of the aggregate was largely unaffected by variations in pH due to the difference in pK_a of MAA (~4.7–5.5) and PDMAEMA (~7.5–8.5) monomers. Thus, the copolymer aggregation microstructure was, to a large degree, stable below and above the insoluble pH range, and charge neutralization effects become significant only when the solution pH is close to the phase separation regime. The average size of the unimers in the copolymer solution remained constant at ~5 nm, which was independent of the pH. Figure 3.9 illustrates the temperature and pH dependence of P(MAA-*b*-DMAEMA)-*b*-C_{60}.

At pH 3, 25 °C, the balance of hydrophobic attraction and electrostatic repulsion arising from $-NH^+(CH_3)_2$ accounts for the association of P(MAA-*b*-DMAEMA)-*b*-C_{60}, giving rise to the formation of aggregates. Instead of forming simple core–shell micelles, the aggregates possessed a microgel-like structure with two hydrophobic domains composed of C_{60} and PMAA segments interconnected by charged hydrophilic PDMAEMA segments. At 55 °C, the R_h distribution was nearly identical to the one produced at 25 °C, with R_h of ~120 nm (large aggregates) and ~5 nm (unimers) coexisting in solution.

At pH 11, 25 °C, both unimers and aggregates are in equilibrium, with R_h of ~5 and ~120 nm, respectively. Both the ionized COO^- and deprotonated PDMAEMA segments are hydrophilic at this temperature, while the C_{60} is hydrophobic. Some

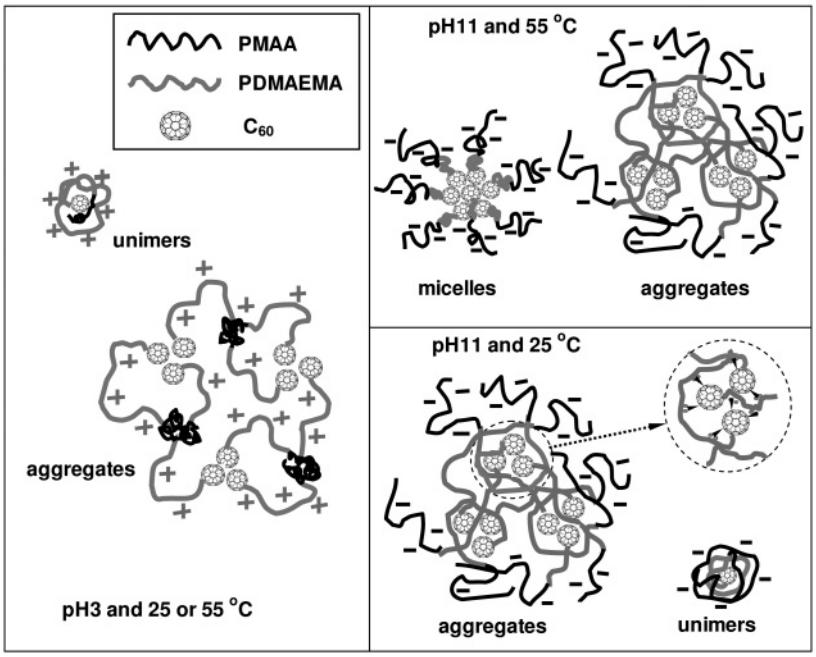

Figure 3.9 Schematic representation of the possible microstructures of P(MAA_{102}-*b*-$DMAEMA_{67}$)-*b*-C_{60} in aqueous solutions at different pH and temperatures. Inset: enlargement of the charge-transfer complex section. (Reprinted with permission from Reference [86], copyright © American Chemical Society.)

of the C_{60} molecules self-aggregated through hydrophobic interaction, while the others formed CT complex with PDMAEMA segments, and they acted as physical crosslinkers. At pH of 11, between 25 and 45 °C, unimers and aggregates coexist without changes in their sizes. Above 50 °C, R_h corresponding to small particle disappeared and an intermediate particle size with R_h of ~13 nm appeared, while the size of large aggregates decreased to about 90 nm. The appearance of the intermediate particle size, disappearance of unimers, and decrease in aggregate R_h occurred between 45 and 50 °C. As the temperature increased, C_{60} and PDMAEMA (LCST ~45 °C) form a continuous hydrophobic domain at higher temperatures with ionized PMAA as the hydrophilic shell. The intermediate size resulted in the tendency for micelle formation (R_h ~13 nm), with C_{60} and PDMAEMA comprising the hydrophobic core and ionized PMAA the hydrophilic shell. The formation of different microstructures both at low and high pH was further confirmed by TEM.

Poly-zwitterions differ from polyampholytes in that both the cationic and anionic species are on the same monomer residue, consisting of a quaternary ammonium, which is a cationic moiety, and sulfonate (sulfobetaines), carboxylate (carbo- or

carboxybetaines), phosphate/phosphonate/phosphinate (phosphobetaines), and so on as the anionic group [107]. The most interesting property of poly-zwitterionic polymers is that they can be used to mimic naturally occurring ampholytic polymers, such as protein near the IEP or DNA at low pH [108] and their characteristics can respond to external stimuli such as temperature or ionic strength of the solution[109]. Another interesting characteristic of these polymers is their lack of solubility in water at low temperature due to the formation of strong intra- or intermolecular electrostatic attraction, resulting in an ionically crosslinked network structure. Addition of small electrolytes (e.g., NaCl) not only destroys the electrostatic interaction, which enhances solubility, but induces an "anti-polyelectrolyte effect" that results in chain expansion [110]. Though the aqueous solution properties of different polybetaines have been made, few studies have reported on DMAEMA based block copolymeric polybetaines [111, 112].

For C_{60}-containing poly-zwitterionic polymer, the chemical structure, molecular weight, polymer concentration, ionic strength and temperature play important roles in controlling the self-assembly behavior of the system. At room temperature, *Bet*-PDMAEMA-*b*-C_{60} was water-insoluble due to a strong electrostatic attractive force from oppositely charged ion pairs along the polymer chains. When the temperature was increased to a critical value where the thermal energy exceeds the electrostatic attractive force, *Bet*-PDMAEMA-*b*-C_{60} becomes water-soluble at a temperature denoted as the upper critical solution temperature (UCST) [113]. *Bet*-PDMAEMA-*b*-C_{60} exhibits a UCST of ~32 °C, which is much higher than for *Bet*-PDMAEMA (<20 °C) [113]. Attachment of C_{60} hydrophobic moieties to the polymer alters the phase behavior of *Bet*-PDMAEMA to yield a higher UCST. The temperature-dependent solubility (UCST) of the *Bet*-PDMAEMA-*b*-C_{60} was further confirmed by ^{1}H NMR spectroscopy, where the chemical shift peaks corresponding to *Bet*-PDMAEMA segments became less pronounced at low temperature and the peaks shifted to lower fields, with more pronounced peaks at temperatures greater than the UCST.

An interesting behavior corresponding to the "polyelectrolyte effect" and "anti-polyelectrolyte effect" has been observed for the first time for *Bet*-PDMAEMA-*b*-C_{60} as a function of NaCl concentrations. Addition of small amounts of salt led to an initial increase in the UCST of *Bet*-PDMAEMA-*b*-C_{60} in the low salt concentration regime; after attaining a maximum of 49 °C at 0.35 wt% (NaCl), the UCST then decreased at higher salt regime, which was also supported by both viscometric and light transmittance studies (Figure 3.10). Below the UCST, the strong inherent energy due to intermolecular electrostatic attraction produced a compact chain conformation, which causes the polymer to phase separate. However, there are small amounts of ion pairs that are exposed in bulk water due to its zwitterionic property. At low salt concentration, the small electrolyte ions bind to these exposed ion pairs, resulting the shrinkage of the polymeric chains. Such behavior is similar to the addition of salt to the polyelectrolyte solution, which not only enhances the intermolecular electrostatic interaction but also decreases the solubility of zwitterionic polymers in water. When the salt concentration was saturated with the exposed ions, a maximum UCST was observed. A further increase in salt

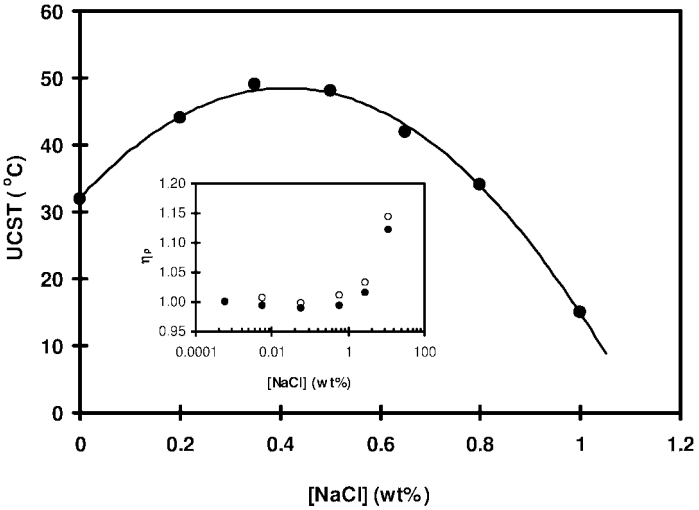

Figure 3.10 Effect of salt on the UCST of *Bet*-PDMAEMA-*b*-C_{60}. Insert: NaCl concentration dependence of the relative viscosity of 0.3 wt% *Bet*-PDMAEMA-*b*-C_{60} (●) and *Bet*-PDMAEMA (○), respectively. (Reprinted with permission from Reference [85], copyright © American Chemical Society.)

concentration (>0.35 wt% NaCl) resulted in the shielding of intermolecular electrostatic attraction, which facilitates the dissolution of polymer chains ("anti-polyelectrolyte"). *Bet*-PDMAEMA-*b*-C_{60} also tends to form micelles in 0.5 M NaCl aqueous solution at room temperature. These micelles, with a R_h of ~47 nm, are in dynamic equilibrium with unimers having a R_h of ~5 nm. However, *Bet*-PDMAEMA existed as unimers with a R_h of ~5 nm. The hydrophobic C_{60} induces the formation of uniform micelles with a more compact structure. The averaged apparent M_w calculated from a Berry plot was ~1.60×10^5 g mol^{-1}, with a *z*-averaged radius of gyration (R_g) of ~42 nm and an apparent aggregation number of ~25. Figure 3.11 illustrates the mechanism describing the salt dependence of *Bet*-PDMAEMA-*b*-C_{60} and the "anti-polyelectrolyte" effect.

3.3.2.4 Supramolecular Fractal Patterning

Micro- to macroscopic branched fractal structures constitute many spontaneous pattern formations in nature [114]. The fractal morphology observed from the growth of clusters and aggregates is usually a consequence of a non-equilibrium process. Unique "seahorse" fractal patterns were first prepared by employing an ionized cluster-beam deposition method, using C_{60} tetracyanoquinodimethane (C_{60}-TCNQ) multilayered thin films [115]. The growth of the fractal patterns was compared to the cluster-diffusion-limited-aggregation (CDLA) model. The formation mechanism of the fractals was discussed and proposed. Negatively charged fullerene-grafted polymeric systems can serve as excellent nano-templates for the

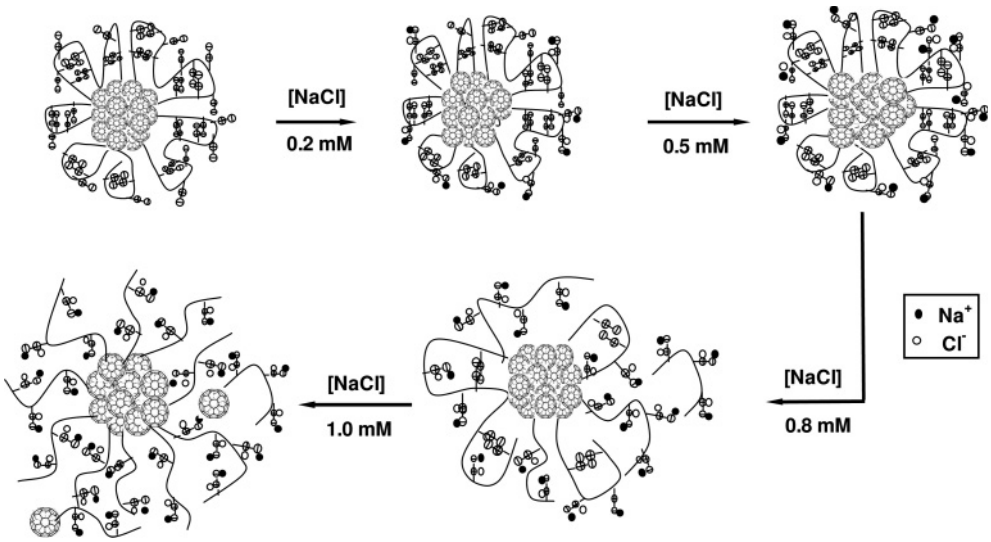

Figure 3.11 Schematic representation of *Bet*-PDMAEMA-*b*-C_{60} in the presence of different concentrations of NaCl. (Reprinted with permission from Reference [85], copyright © American Chemical Society.)

controlled growth of inorganic crystals at the nano- to micrometer length scale. The formation of fractal patterns at the nano- to microscopic dimension induced by PMAA-*b*-C_{60} has been reported by Tam and coworkers [116]. PMAA-*b*-C_{60} self-assembles to form the LCM in aqueous solution, consisting of smaller individual core–shell micellar aggregates. The radii of LCMs in the $\alpha = 1$ condition vary from 125 to 165 nm, which are in good agreement with dynamic light scattering (DLS) measurements.

PMAA-*b*-C_{60} in the presence of NaCl at $\alpha = 1$ forms interesting morphologies. Fractal patterns were observed when the sample was dried at room temperature on a copper grid. Under isothermal conditions, crystallization of NaCl is controlled by the concentration of diffusing ionic species. The development of such fractal morphology is governed by a competition between reaction or diffusion limited transport processes and interfacial phenomenon radiating from the heterogeneous nucleation site [117]. In the present system, the LCMs act as nucleation sites, resulting in the controlled growth of nano-structured, morphology such as the diverse fractal patterns observed (Figure 3.12). In the presence of larger amounts of NaCl, the growth of fractal pattern becomes denser and more closely packed. Interestingly, such fractal pattern could not be observed for the unneutralized PMAA-*b*-C_{60} system ($\alpha = 0$). The LCMs serve as nucleating sites for the crystallization of NaCl, and the growth of NaCl crystals becomes denser with increasing NaCl. Since no fractal pattern was observed for the unneutralized PMAA-*b*-C_{60} system, it was deduced that the negative charges on the surface of LCMs are critical

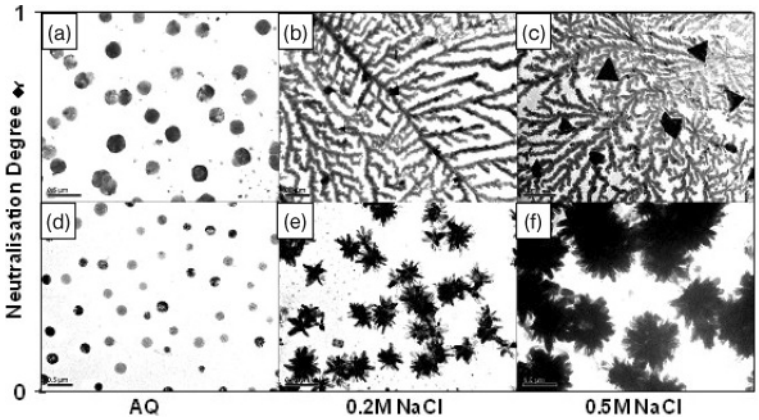

Figure 3.12 Phase diagram of PMAA-*b*-C_{60}. (a) Aggregates exist as charged LCM at $\alpha = 1$; (b) fractal pattern formed with the addition of NaCl; (c) fractal pattern becomes denser with the addition of more NaCl; (d) aggregates exist as uncharged LCM at $\alpha = 0$; (e) salt crystallizes on the LCM; (f) crystallization of the salt becomes denser. (Reprinted with permission from Reference [116], copyright © American Chemical Society.)

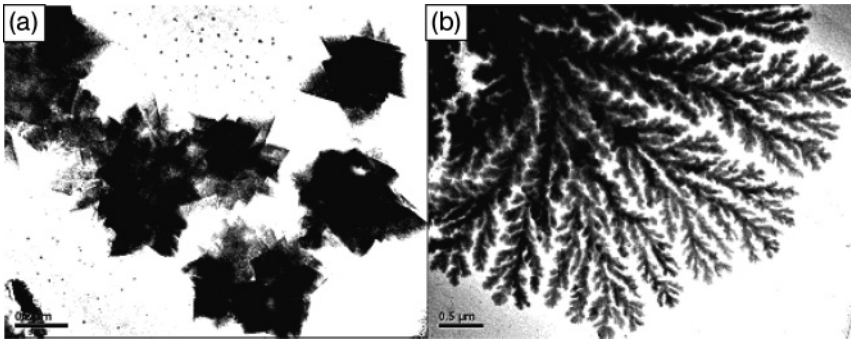

Figure 3.13 Formation of fractal patterns from (a) C_{60}-containing polycations and (b) C_{60}-containing polyanions. (Reprinted with permission from Reference [116], copyright © American Chemical Society.)

for the fractal growth process. For the fully neutralized PMAA-*b*-C_{60} system ($\alpha = 1$), carboxylate groups are ionized, producing negative charges on the surface of LCMs. When NaCl is introduced, sodium ions are attracted and condensed on the external surface of LCMs together with chloride ions, driven by electrostatic forces. Each LCM becomes a nucleating site that controls the crystallization of sodium chloride. The progressive diffusion control growth of sodium chloride crystals during the drying process produces the nanoscale fractal patterns observed in Figure 3.12. However, the fractal pattern was not observed for the fully protonated PDMAEMA-*b*-C_{60} in the presence of salt. Figure 3.13 compares the formation of

the fractal pattern. At the same time, *Bet*-PDMAEMA-*b*-C_{60} could also produce the fractal pattern when the TEM samples were prepared in presence of 0.5 M NaCl [85]. In this case the $-SO_3^-Na^+$ induces the formation of a controlled fractal pattern in aqueous salt solution when it is dried. From the results, it seems that the negative charges on the polymer control the formation of a fractal pattern. The utility of such templating and patterning methodology will be further extended to other salt systems and this can potentially be exploited for various applications.

3.3.2.5 Surfactant Induced Nano-Structures

Surfactant micelles, such as TX100, can successfully disperse fullerene molecules in aqueous medium [118, 119]. Intrigued by the strong affinity between tert-octylphenyl deca-ethylene glycol ester (TX100) and fullerenes and motivated by the potential applications of nanomaterials in drug delivery and microbiological devices, studies on the interaction of PAA-*b*-C_{60} and C_{60}-PAA-*b*-C_{60} with aromatic non-ionic surfactant TX100 at different degrees of neutralization have been carried out ($\alpha = 0$ corresponds to the unneutralized state of PAA, and $\alpha = 1$ represents the fully neutralized state of PAA) [120, 121]. To understand the detailed mechanism of the interactions, mono- and di-end-capped telechelic PAA with identical molecular weight were synthesized through ATRP and group protection chemistry (PAA_{85}-*b*-C_{60} and C_{60}-PAA_{83}-*b*-C_{60}). Strong binding of TX100 to PAA_{85}-*b*-C_{60} and C_{60}-PAA_{83}-*b*-C_{60} and unusual morphological transformations of the polymer in the course of binding were observed. These polymers were soluble in basic aqueous solution. The enthalpy profiles and particle sizes obtained from isothermal titration calorimetric (ITC) and DLS, respectively, showed that strong binding interaction and binding-induced complexation are only observed when the surfactant contains an aromatic ring (e.g., TX100) and the polymer contains fullerene (PAA_{85}-*b*-C_{60} and C_{60}-PAA_{83}-*b*-C_{60}). However, DLS studies confirmed that PAA_{85}-*b*-C_{60} did not produce a structural reorganization or conformational change with the addition of the aliphatic non-ionic surfactant of polyoxyethylene lauryl ether ($C_{12}E_9$). It was noticed that the aromatic character of the hydrophobic moiety of TX100 and fullerene grafted on PAA enhanced the binding interaction, allowing the micelles of TX100 to partition to the fullerene domains of aggregates of C_{60} end-capped PAA polymers rather than binding unselectively to hydrophobic segments of the polymer aggregates. The results from both ITC and UV/vis studies confirmed that the interaction between TX100 and fullerene-end-capped PAA was initiated by hydrophobic forces. The excellent compatibility and π–π conjugation between the phenyl group of the surfactant and fullerene moieties that localized TX100 molecules near the fullerene domains will trigger the specific binding and induce the observed structural reorganization.

DLS studies also confirmed the unique specific binding of TX100 to fullerene domains within the LCM of PAA_{85}-*b*-C_{60} and C_{60}-*b*-PAA_{83}-*b*-C_{60}, which induced a structural transformation of polymeric micelles. These types of interactions open the possibility of tuning the morphology and solubility of C_{60}-containing polymers using an aromatic non-ionic surfactant. Both polymers existed as LCM (in the absence of TX100) and formed polymer/surfactant complex (PSC) precipitates in the presence of TX100; the precipitates were re-solubilized by a wetting layer of

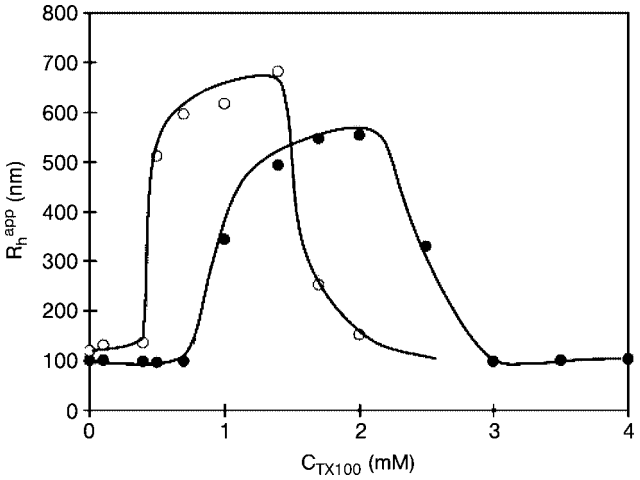

Figure 3.14 Dependencies of R_h^{app} on the TX100 concentration for 5 mM PAA_{85}-*b*-C_{60} (○) and C_{60}-*b*-PAA_{83}-*b*-C_{60} (●) at $\alpha = 0$ (Reprinted with permission from Reference [120], copyright © American Chemical Society.)

bound TX100 molecules. However, the morphology of the polymer surfactant complex (PSC) was different, depending on the polymer architecture (Figures 3.14–3.16). For PAA_{85}-*b*-C_{60}, $R_{h\text{-}app}$ increased sharply from ~134 to ~510 nm at C_{TX100} ~0.4 mM, whereas the $R_{h\text{-}app}$ of C_{60}-*b*-PAA_{83}-*b*-C_{60} increased from ~98 to ~344 nm at C_{TX100} ~1 mM (Figure 3.14). Complexation of C_{60}-*b*-PAA_{83}-*b*-C_{60} occurred at higher TX100 concentrations, and the PSC was smaller than that of PAA_{85}-*b*-C_{60}. This is caused by a higher proportion of fullerene, which resulted in a stronger hydrophobic association of fullerene moieties, requiring more surfactant molecules to induce the structural transformation of the polymeric micelles. With further addition of TX100, $R_{h\text{-}app}$ decreased rapidly from ~680 to ~250 nm at C_{TX100} ~1.6 mM and from ~608 to ~96 nm at C_{TX100} ~3 mM for PAA_{85}-*b*-C_{60} and C_{60}-*b*-PAA_{83}-*b*-C_{60}, respectively. Apparently, the binding-induced complexation of di-end-capped C_{60}-*b*-PAA_{83}-*b*-C_{60} took place over a broader range of TX100 concentration. In excess amounts of surfactant, the complexes for both polymers were dissociated by polymer-bound TX100 micelles, with their hydrophilic head groups extending outward, resulting in re-solubilization.

Figures 3.15 and 3.16 show a series of TEM images describing the morphology changes of 5 mM un-ionized PAA_{85}-*b*-C_{60} and C_{60}-*b*-PAA_{83}-*b*-C_{60}, respectively, in different amounts of TX100. Correspondingly, Figure 3.17 shows a schematic describing the mechanism for the binding and morphological evolution of the complex with PAA_{85}-*b*-C_{60}. (It should be stressed that the schematics shown in Figure 3.17 are meant to illustrate the possible aggregation phenomenon; quantitative assessment of these structures will require SAXS or SANS studies.) Figures 3.15a and 3.17a show the LCMs of un-ionized PAA_{85}-*b*-C_{60} with a radius of 100 nm, which is consistent with the particle size obtained from light scattering measure-

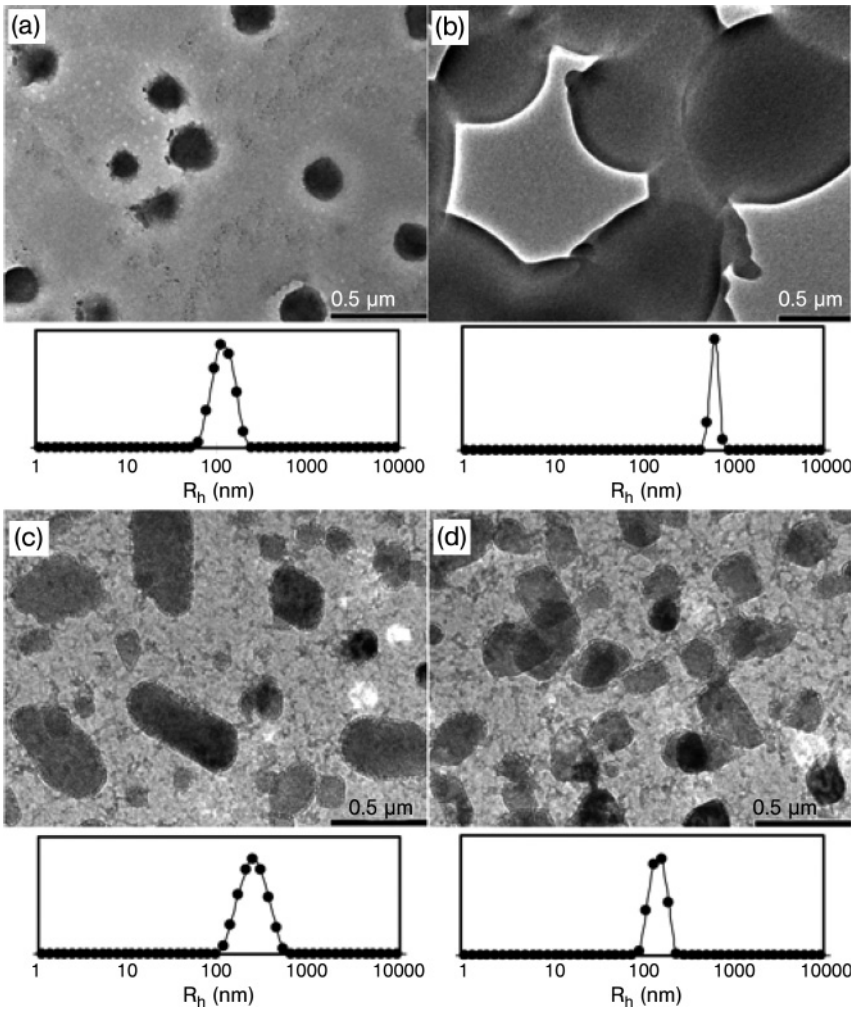

Figure 3.15 Particle size distributions and micrographs demonstrating the morphology change of un-ionized PAA_{85}-*b*-C_{60} induced by the binding of TX100. C_{TX100} = (a) 0; (b) 1; (c) 1.7; (d) 2 mM. (Reprinted with permission from Reference [121], copyright © American Chemical Society.)

ments. When the TX100 concentration was increased to 1.0 mM, spherical, dense particles with a smooth surface and much larger size were observed, characterizing the formation of a precipitated PSC induced by surfactant binding. The hydrophobic binding is strengthened by the good compatibility between the hydrophobic segment of TX100 and fullerene; thus, the surfactant micelles can encapsulate the fullerene clusters within the LCMs. The selective binding may expand the fullerene clusters and release some fullerene moieties. The "free" polymer chains

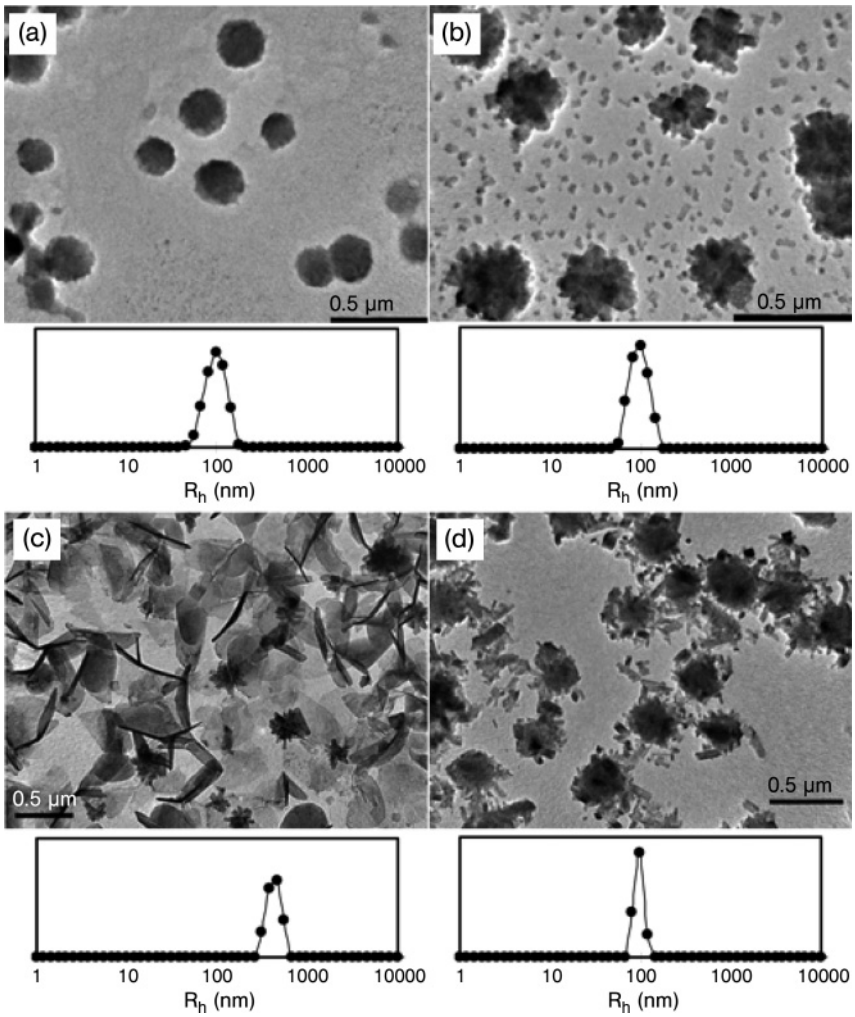

Figure 3.16 Particle size distributions and micrographs demonstrating the morphology change of un-ionized di-end-capped C_{60}-*b*-PAA_{83}-*b*-C_{60} induced by the binding of TX100. C_{TX100} = (a) 0; (b) 0.7; (c) 1.7; (d) 3.5 mM. (Reprinted with permission from Reference [121], copyright © American Chemical Society.)

together with bound TX100 molecules may associate and act as physical cross-linkers that enhance interparticle association between the polymeric micelles, resulting in the formation of a flocculated PSC as shown in Figures 3.15b and 3.17b. The radii of the PSCs vary from 450 to 600 nm, which is in good agreement with the size determined from DLS. With further addition of TX100 to 1.7 mM, more surfactant micelles are bound on the fullerene clusters within the LCMs with

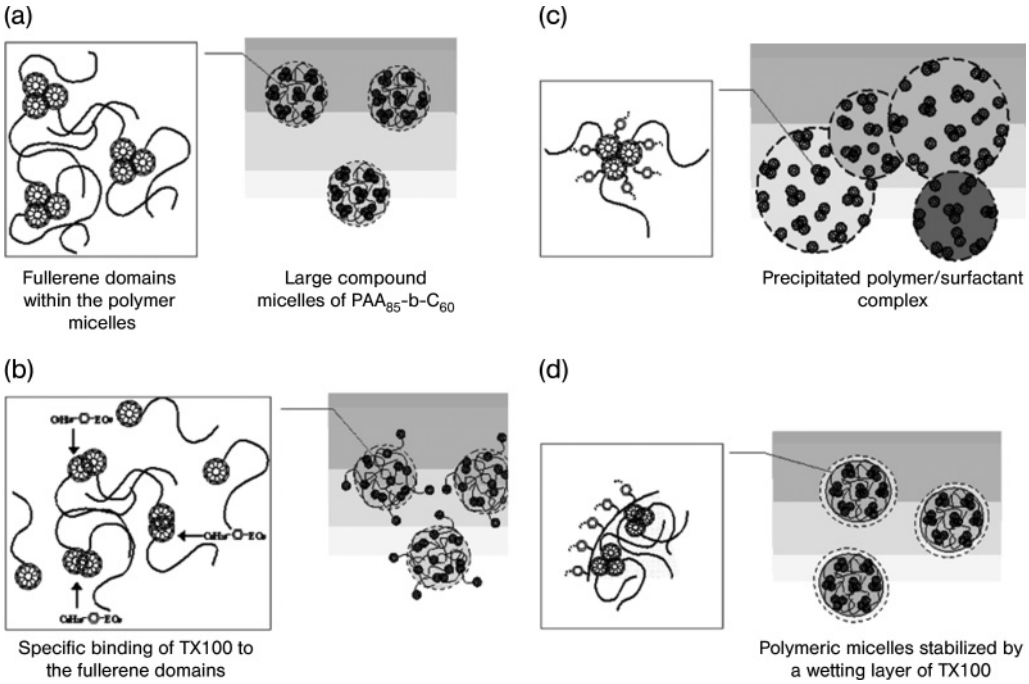

Figure 3.17 Mechanism of the binding and induced morphological change of the PAA_{85}-*b*-C_{60}/TX100 system at $\alpha = 0$ in an aqueous medium: (a) $C_{TX100} = 0$ mM, large compound micelle of PAA_{85}-*b*-C_{60}; (b) $C_{TX100} = 0.5$ mM, selective binding of TX100 to fullerene domains, which releases polymer chains; (c) 0.5 mM < C_{TX100} < 1.7 mM, precipitated polymer/surfactant complex; (d) $C_{TX100} > 1.7$ mM, LCMs stabilized by a wetting layer of TX100 in an excess amount of surfactant. (Reprinted with permission from Reference [121], copyright © American Chemical Society.)

their hydrophilic head groups extending outward to enhance the overall hydrophilicity of the particles. Thus, the dense precipitates of the PSC disintegrated into smaller aggregates with a broad size distribution and irregular shapes (Figures 3.15c and 3.17c). When the concentration of TX100 exceeded 1.7 mM, the complex dissociated completely into smaller particles with radii in the range 60–100 nm. The polymeric micelles were coated and stabilized by a wetting layer of bound TX100 as shown in the micrograph (Figures 3.15d and 3.17d). These results demonstrated that the addition of TX100 significantly influenced the self-assembly of fullerene-containing polymers and is an effective way of tuning the size, shape and solubility of the polymeric micelles.

Figure 3.16 shows a series of micrographs, together with particle size distributions, depicting the morphology change of 5 mM di-end-capped C_{60}-*b*-PAA_{83}-*b*-C_{60} induced by the binding of TX100. Correspondingly, a schematic depicting the probable aggregation behavior is shown in Figure 3.18. The polymer formed LCMs in the absence of TX100 (Figures 3.16a and 3.18a), where an abundance of

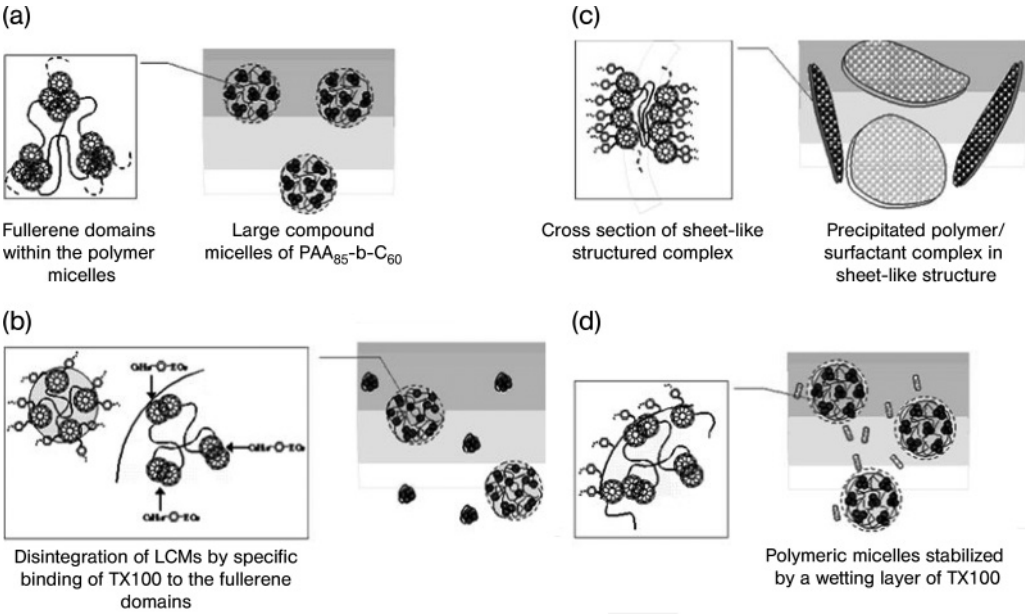

Figure 3.18 Mechanism of the binding and induced morphological change of the C_{60}-*b*-PAA_{83}-*b*-C_{60}/TX100 system at $\alpha = 0$ in aqueous medium: (a) $C_{TX100} = 0$ mM, large compound micelle of PAA_{85}-*b*-C_{60}; (b) $C_{TX100} = 0.7$ mM, selective binding of TX100 to fullerene domains, which releases polymer chains; (c) 0.7 mM < C_{TX100} < 2.5 mM, precipitated polymer/surfactant complex; (d) $C_{TX100} > 2.5$ mM, LCMs stabilized by a wetting layer of TX100 in an excess amount of surfactant. (Reprinted with permission from Reference [121], copyright © American Chemical Society.)

spherical particles with smooth surface and uniform size was observed. The micellar radius ranges from ~90 to 100 nm, which is consistent with the size determined from DLS. With the addition of 0.7 mM TX100 to the polymer solution, small polymer clusters with a diameter of ~10 nm were released from the LCMs, caused by the specific binding of TX100 to the fullerene domains within the polymeric micelles, which disrupted the compound micelles and slightly reduced their size to ~90 nm (Figures 3.16b and 3.18b). With a further increase in TX100 concentration to 1.7 mM, the C_{60}-*b*-PAA_{83}-*b*-C_{60}/TX100 mixture formed a precipitated complex (Figures 3.16c and 3.18c). The continuous partitioning of TX100 into the fullerene domains released additional smaller polymeric clusters from the compound micelles. The "free" fullerene moieties with bound TX100 together with the un-ionized PAA blocks tend to associate with each other, driven by hydrophobic interaction, which induced the formation of a flocculated PSC. However, the morphology of the PSC was completely different from that of the mono end-capped PAA_{85}-*b*-C_{60}/TX100 system; the PSC was arranged into a lamellar structure with a dimension of ~500 nm and a thickness of ~10 nm (Figures 3.16c and 3.18c). Aggregation of fullerene pendants at both sides of the PAA blocks was stabilized

and solubilized by TX100 molecules; this expanded the PAA segments and promoted the formation of sheet-like structures, which are similar to the lamellar stack structure observed in amphiphilic block copolymers and complexes between oligomeric amphiphiles and polymers [122–124]. When the concentration of TX100 reached 3.5 mM, the precipitated PSCs were resolubilized as more TX100 molecules were bound to the polymer with their hydrophiles pointing outward, and the PSC dissociated and the structure rearranged into a spherical structure that possessed lower interfacial energy and was more stable in an aqueous medium (as shown in Figures 3.16d and 3.18d). The radii of the spherical particles varied from ~90 to 120 nm.

This finding provides a new and simple approach to directly control the assembly of fullerene-containing polymers using aromatic surfactants, which may find important applications in drug delivery, nanoscale patterning, miniaturized biological devices and many others.

3.4 Summary

C_{60} and its derivatives continue to attract the attention of researchers due to their special physicochemical properties and potential applications in various fields. Fullerene-containing polymers are one of the most attractive fullerene derivatives recently introduced because they not only make C_{60} soluble in aqueous or common organic solvents but also retain its conjugating properties. C_{60}-containing polymers can be produced through direct copolymerization in the presence of C_{60} using the conventional radical polymerization technique, *in situ* polymerization of monomers initiated from C_{60}-based initiators using the conventional or "living" polymerization technique, and substitution or end-capping of C_{60} with end-functionalized precursor polymer. Depending on the synthetic methodologies used, all these approaches could produce C_{60} on the main polymer chain, C_{60} on the side chain of the polymers, hyper-branched C_{60}-containing polymers, star-like polymers, mono end-capped polymers, telechelic polymers and dendrimers. C_{60}-containing polymers to become soluble in solution. However, due to the high hydrophobicity and large bulk volume of C_{60}, large aggregates are present in both aqueous and organic solutions. Blocking functional polymers onto C_{60} retains the physicochemical properties of both functional polymers and C_{60}. For C_{60}-containing, water-soluble polymers, altering the solution conditions, such as pH, temperature, salt and co-solvents, results in a change of the morphologies of aggregates. Anionic C_{60}-containing polymers could induce the formation of a nano- to microscale fractal pattern in solution, while a cationic polymer could not. The development in the synthesis of novel C_{60}-containing polymers and the understanding of the solution properties of C_{60}-containing polymers could provide the basis for fullerene materials.

Research on water-soluble, fullerene-containing polymers has received increasing attention in the last 10 years. As a result of the development of controlled radical polymerization, particularly ATRP and RAFT, it is now possible to tailor

the development of well-defined polymeric grafted C_{60} with different polymer composition and architecture. Interesting C_{60}-containing self-assembled macromolecular systems are emerging using controlled radical polymerization techniques. Although the self-assembled behavior of C_{60} with different types of polymeric architectures has been studied, the biological activity of these systems has not been investigated in detail. Preliminary biological investigations of various types of fullerene derivatives have been carried out that have produced encouraging results [5]. A well-defined, stimuli responsive, fullerene-containing polymeric system is an important class of polymers that has potential biomedical applications. Studies on the biological activity of fullerene grafted with stimuli responsive polymers could provide detailed information for the future development of fullerene-grafted polymeric materials for biomedical applications. Systematic studies on the cytotoxicity of stimuli-responsive fullerene polymeric self-assembled nanoparticles are also important for their use in drug delivery systems. The binding of doxorubincin with well-defined C_{60}-containing PAA systems and the release kinetics are under investigation. The science of targeted drug delivery systems using ligand attached C_{60}-containing stimuli-responsive polymers is another important field of research. Polymer chemists need to seriously consider the design, synthesis and biological studies on the targeted drug delivery systems of well-defined stimuli-responsive C_{60}-containing polymers. The research in this field is new and is expected to undergo an important break-through in the near future.

References

1 Kroto, H.W., Heath, J.R., O'Brien, S.C., Curl, R.F. and Smalley, R.F. (1985) *Nature*, **318**, 6042.

2 Rosseinsky, M.J. (1995) *J. Mater. Chem.*, **5**, 1489.

3 Stephens, P.W., Cox, D., Lauher, J.W., Mihaly, L., Wiley, J.B., Allemande, P.M., Hirsh, A., Holczer, K., Li, Q., Thompson, J.D. and Wudl, F. (1992) *Nature*, **331**, 355.

4 Konarev, D.V. and Lyubovskaya, R.N. (1999) *Russ. Chem. Rev.*, **68**, 19.

5 Bosi, S., Ros, T.D., Spalluto, G. and Prato, M. (2003) *Eur. J. Med. Chem.*, **38**, 913.

6 (a) Dardel, B., Guillon, D., Heinrich, B. and Deschenaux, R. (2001) *J. Mater. Chem.*, **11**, 2814.
(b) Koppe, M., Scharber, M., Brabec, C., Duffy, W., Heeney, M. and Mcculloch, I. (2007) *Adv. Funct. Mater.*, **17**, 1371.

7 Karaulova, E.N. and Bagrii, E.I. (1999) *Russ. Chem. Rev.*, **68**, 889.

8 Cerar, J. and Skerjanc, J. (2003) *J. Phys. Chem. B*, **10**, 8255.

9 Richardson, C.F., Schuster, D.I. and Wilson, S.R. (2000) *Org. Lett.*, **2**, 1011.

10 Chiang, L.Y., Bhonsle, J.B., Wang, L., Shu, S.F., Chang, T.M. and Hwu, J.R. (1996) *Tetrahedron*, **52**, 4963.

11 Filippone, S., Heimann, F. and Rassat, A. (2002) *Chem. Commun.*, 1508.

12 Samal, S. and Geckeler, K.E. (2000) *Chem. Commun.*, 1101.

13 Atwood, J.L., Koutsantonis, G.A. and Raston, C.L. (1994) *Nature*, **368**, 229.

14 Moussa, F., Trivin, F., Ceolin, R., Hadchuouel, M., Siaret, P.Y., Greugny, V., Fabre, C., Rassat, A. and Szwarc, H. (1996) *Fullerene Sci. Technol.*, **4**, 21.

15 Hwang, K.C. and Mauzerall, D. (1992) *J. Am. Chem. Soc.*, **114**, 9705.

16 Bensasson, R.V., Bienvenue, F., Dellinger, S., Leach, S. and Seta, P. (1994) *J. Phys. Chem.*, **98**, 3492.

17 Konarev, D.V. and Lyubovskaya, R.N. (1999) *Russ. Chem. Rev.*, **68**, 19.
18 Kasermann, F. and Kempf, C. (1997) *Antiviral. Res.*, **34**, 65.
19 Ueng, T.H., Kang, J.J., Wang, H.W., Cheng, Y.W. and Chiang, L.Y. (1997) *Toxicol. Lett.*, **93**, 29.
20 Da Ros, T. and Prato, M. (1999) *Chem. Commun.*, 663.
21 Friedman, S.H., De Camp, D.L., Sijbesma, R.P., Srdanov, G., Wudl, F. and Kenyon, G.I. (1993) *J. Am. Chem. Soc.*, **115**, 6506.
22 Wang, L.Y., Wu, J.S., Tseng, S.M., Kuo, C.S., Sich, K.H., Liau, W.B. and Chiang, L.Y. (1996) *Polym. Res.*, **3**, 1.
23 Meier, M.S. and Kiegiel, J. (2001) *Org. Lett.*, **3**, 1717.
24 Vaknin, D. (1996) *Physica B*, **221**, 152.
25 Taton, D., Angot, S., Gnanou, Y., Wolert, E., Setz, S. and Duran, R. (1998) *Macromolecules*, **31**, 6030.
26 Shiea, J., Huang, J.P., Teng, C.F., Jeng, J., Wang, L.Y. and Chiang, L.Y. (2003) *Anal. Chem.*, **75**, 3587.
27 Tarassova, E., Aseyev, V., Tenhu, H. and Klenin, S. (2003) *Polymer*, **44**, 4823.
28 Chen, X.L. and Jenekhe, S.A. (1999) *Langmuir*, **15**, 8007.
29 Jenekhe, S.A. and Chen, X.L. (2001) *Science*, **279**, 1903.
30 Yang, D., Li, L. and Wang, C. (2004) *Mater. Chem. Phys.*, **87**, 114.
31 Tan, C.H., Ravi, P., Dai, S., Tam, K.C. and Gan, L.H. (2004) *Langmuir*, **20**, 9882.
32 Goswami, T.H., Singh, R., Alam, S. and Mathur, G.N. (2004) *Chem. Mater.*, **16**, 2442.
33 Shi, Z., Jin, J., Li, Y., Guo, Z., Wang, S., Jiang, L. and Zhu, D. (2001) *New J. Chem.*, **25**, 670.
34 Georgakilas, V., Pellarini, F., Prato, M., Guldi, D.M., Franco, M. and Zerbetto, F. (2002) *Proc. Natl. Acad. Sci. U.S.A.*, **99**, 5075.
35 Prato, M. and Maggini, M. (1998) *Acc. Chem. Res.*, **31**, 519.
36 Geckler, K.E. and Samal, S. (1999) *Polym. Int.*, **48**, 743.
37 Wang, C., Guo, Z.X., Fu, S., Wu, W. and Zhu, D. (2004) *Prog. Polym. Sci.*, **29**, 1079.
38 Ravi, P., Dai, S., Wang, C. and Tam, K.C. (2007) *Journal of Nanoscience and Nanotechnology*, **17**, 5988.
39 Giacalone, F. and Martín, N. (2006) *Chem. Rev.*, **106**, 5136.
40 Ford, W.T., Graham, T.D. and Mourey, H.T. (1997) *Macromolecules*, **30**, 6422.
41 Ford, W.T., Nishioka, T., McCleskey, S.C., Mourey, T.H. and Kahol, P. (2000) *Macromolecules*, **33**, 2413.
42 Wang, C.C. (1996) *Synthesis, characterization and photoconductivity of C_{60}-containing polymer materials*. Ph.D thesis, Fudan University, China.
43 Chen, Y., Huang, Z.E., Cai, R.F., Yu, B.C., Ma, W.W., Chen, S.M., Shao, Q.F., Yan, X.M. and Huang, Y.F. (1997) *Eur. Polym. J.*, **33**, 291.
44 Chen, Y., Huang, Z.E. and Cai, R.F. (1996) *J. Polym. Sci. Pol. Phys.*, **34**, 631.
45 Chen, Y., Huang, Z.E., Cai, R.F., Kong, S.Q., Chen, S., Shao, Q., Yan, X., Zhao, F. and Fu, D. (1996) *J. Polym. Sci. Pol. Chem.*, **34**, 3297.
46 Wignall, G.D., Affholter, K.A., Bunick, G.J., Hunt, M.O., Menceloglu, Y.Z., Jaarnagin, J.M. Jr., Desimone, J.M. and Samulski, E.T. (1995) *Macromolecules*, **28**, 6000.
47 Chen, Y., Huang, W.S., Huang, Z.E., Cai, R.F., Yu, H.K., Chen, S.M. and Yan, X.M. (1997) *Eur. Polym. J.*, **33**, 823.
48 Samulski, E.T., Desimone, J.M., Hunt, M.O. Jr., Menceloglu, Y.Z., Jarnagin, R.C., York, G.A., Labat, K.B. and Wang, H. (1992) *Chem. Mater.*, **4**, 1153.
49 Ederlé, Y. and Mathis, C. (1997) *Macromolecules*, **30**, 2546.
50 Chen, Y., Wang, J.X., Yu, B.C., Cai, R.F., Huang, Z.E. and Zhang, J.M. (1999) *J. Phys. Chem. Solids*, **60**, 949.
51 Chen, Y., Huang, Z.E., Cai, R.F., Fan, D., Hou, X., Yan, X., Chen, S., Jin, W., Pan, D. and Wang, S. (1996) *J. Appl. Polym. Sci.*, **61**, 2185.
52 Huang, Z.E., Chen, H., Cai, R.F., Rui, C.G. and Zhang, F.P. (1996) *J. Appl. Polym. Sci.*, **60**, 573.
53 Kawauchi, T., Kumaki, J. and Yashima, E. (2005) *J. Am. Chem. Soc.*, **127**, 9950.
54 Li, Z. and Qin, J.G. (2004) *J. Polym. Sci. Pol. Chem.*, **42**, 194.

55 (a) Song, T., Dai, S., Tam, K.C., Lee, S.Y. and Goh, S.H. (2003) *Langmuir*, **19**, 4798. (b) Song, T., Dai, S., Tam, K.C., Lee, S.Y. and Goh, S.H. (2003) *Polymer*, **44**, 2529.

56 (a) Huang, X.D., Goh, S.H. and Lee, S.Y. (2000) *Maromol. Chem. Phys.*, **201**, 2660. (b) Song, T., Goh, S.H. and Lee, S.Y. (2002) *Macromolecules*, **35**, 4133.

57 Geckeler, K.E. and Hirsch, A. (1993) *J. Am. Chem. Soc.*, **115**, 3850.

58 Manolova, N., Rashkov, I., Damme, V.V. and Begum, F. (1994) *Polym. Bull.*, **33**, 175.

59 Weis, C., Friedrich, C., Muthaupt, R. and Frey, H. (1995) *Macromolecules*, **28**, 403.

60 Nepal, D., Samal, S., and Geckeler, K.E. (2003) *Macromolecules*, **36**, 3800.

61 Wang, X. and Yan, Y.Y. (2006) *Polymer*, **47**, 6267.

62 Kawauchi, T., Kumaki, J. and Yashima, E. (2006) *J. Am. Chem. Soc.*, **128**, 10560.

63 Chen, X., Gholamkhass, B., Han, X., Vamvounis, G. and Holdcroft, S. (2007) *Macromol. Rapid Commun.*, **28**, 1792.

64 Ederlé, Y. and Mathis, C. (1997) *Macromolecules*, **30**, 4262.

65 Okamura, H., Terauchi, T., Minoda, M., Fukuda, T. and Komatsu, K. (1997) *Macromolecules*, **30**, 5279.

66 Okamura, H., Ide, N., Minoda, M., Komatsu, K. and Fukuda, T. (1998) *Macromolecules*, **31**, 1859.

67 Ford, W.T., Lary, A.L. and Mourey, T.H. (2001) *Macromolecules*, **34**, 5819.

68 Stalmach, U., de Boer, B., Videlot, C., van Hutten, P.F. and Hadziioannou, G. (2000) *J. Am. Chem. Soc.*, **122**, 5464.

69 Wang, J.S. and Matyjaszewski, K. (1995) *J. Am. Chem. Soc.*, **117**, 5614.

70 Matyjaszewski, K. and Xia, J.H. (2001) *Chem. Rev.*, **101**, 2921.

71 Zhou, P., Chen, G., Hong, H., Du, F., Li, Z. and Li, F. (2000) *Macromolecules*, **33**, 1948.

72 Audouin, F., Nuffer, R. and Mathis, C. (2004) *J. Polym. Sci. Pol. Chem.*, **42**, 3456.

73 Chochos, C.L., Kallitsis, J.K. and Gregoriou, V. (2005) *J. Phys. Chem. B*, **109**, 8755.

74 Yang, J., Li, L. and Wang, C. (2003) *Macromolecules*, **36**, 6060.

75 Chu, C.C., Wang, L. and Ho, T.I. (2005) *Macromol. Rapid Commun.*, **26**, 1179.

76 Yang, D., Li, L. and Wang, C. (2004) *Mater. Chem. Phys.*, **87**, 114.

77 Ravi, P., Wang, C., Dai, S. and Tam, K.C. (2006) *Langmuir*, **22**, 7167.

78 Wang, M., Pramoda, K.P. and Goh, S.H. (2006) *Macromolecules*, **39**, 4932.

79 Yu, H., Gan, L.H., Hu, X. and Gan, Y.Y. (2007) *Polymer*, **42**, 2312.

80 Yu, H., Gan, L.H., Hu, X., Venkatraman, S.S., Tam, K.C. and Gan, Y.Y. (2005) *Macromolecules*, **38**, 9889.

81 Wu, H.X., Cao, W.M., Cai, R.F., Song, Y.L. and Zhao, L. (2007) *J. Mater. Sci.*, **42**, 6515.

82 Ravi, P., Dai, S., Tan, C.H. and Tam, K.C. (2005) *Macromolecules*, **38**, 933.

83 Dai, S., Ravi, P., Tan, C.H. and Tam, K.C. (2004) *Langmuir*, **20**, 8569.

84 Mao, B.W., Gan, L.H., Gan, Y.Y., Lee, X.S., Ravi, P. and Tam, K.C. (2004) *J. Polym. Sci. Pol. Chem.*, **42**, 5161.

85 Ravi, P., Dai, S. and Tam, K.C. (2005) *J. Phys. Chem. B*, **109**, 22791.

86 Teoh, S.K., Ravi, P., Dai, S. and Tam, K.C. (2005) *J. Phys. Chem. B*, **109**, 4431.

87 Dai, S., Ravi, P., Tam, K.C., Mao, B.W. and Gan, L.H. (2003) *Langmuir*, **19**, 5175.

88 Guo, C.D., Teng, W.R., Wu, H.X., Shen, J.Z., Deng, X.M. and Cai, R.F. (2005) *Chin. J. Chem.*, **23**, 1113.

89 Ding, J. and Liu, G. (1997) *Macromolecules*, **30**, 655.

90 Diederich, F. and Thilgen, C. (1996) *Science*, **271**, 317.

91 Riegel, I.C. and Eisenberg, A. (2002) *Langmuir*, **18**, 3358.

92 Lai, D.T., Neumann, M.A., Matsumoto, M. and Sunamoto, J. (2000) *Chem. Lett.*, 64.

93 Shinkai, S., Asai, M. and Futija, N. (2003) *Chem. Lett.*, 186.

94 Wang, X., Goh, S.H., Lu, Z.H., Lee, S.Y. and Wu, C. (1999) *Macromolecules*, **32**, 2786.

95 Bezmel'nitsyn, V.N., Eletskii, A.V. and Okun, M.V. (1998) *Physics-Uspekhi*, **41**, 1091.

96 Ravi, P., Dai, S., Hong, K.M., Tam, K.C. and Gan, L.H. (2005) *Polymer*, **46**, 4714.

97 Lowe, A.B., Billingham, N.C. and Armes, S.P. (1998) *Macromolecules*, **31**, 5991.

98 Lowe, A.B., Billingham, N.C. and Armes, S.P. (1997) *Chem. Commun.*, 1035.

99 Lee, S.B., Russell, A.J. and Matyjaszewski, K. (2003) *Biomacromolecules*, **4**, 1386.
100 Wang, Y. (1992) *J. Phys. Chem.*, **96**, 764.
101 Gohy, J.F., Antoun, S. and Jérôme, R. (2001) *Macromolecules*, **34**, 7435.
102 Patrickios, C.S., Gadam, S.D., Cramer, S.M., Hertler, W.R. and Hatton, T.A. (1995) *Biotechnol. Prog.*, **11**, 33.
103 Patrickios, C.S., Sharma, L.R., Armes, S.P. and Billingham, N.C. (1999) *Langmuir*, **15**, 1613.
104 Wetering, P.V.D., Cherng, J.-Y., Talsma, H. and Hennink, W.E. (1997) *J. Controlled Release*, **49**, 59.
105 Torres-Lugo, M., Garcý, M.A., Record, R. and Peppas, N.A. (2002) *J. Controlled Release*, **80**, 197.
106 Gohy, J.F., Creutz, S., Garcia, M., Mahltig, B., Stamm, M. and Jérôme, R. (2000) *Macromolecules*, **33**, 6378.
107 Lowe, A.B. and McCormick, C.L. (2002) *Chem. Rev.*, **102**, 4177.
108 Favresse, P. and Laschewsky, A. (2001) *Polymer*, **42**, 2755.
109 Kudaibergenov, S.E. (1999) *Adv. Polym. Sci.*, **144**, 115.
110 Lowe, A.B. and McCormick, C.L. (2001) *Stimuli-Responsive Water-Soluble and Amphiphelic Copolymers*. In *Advances in Chemistry Series*, No. 780 (ed. C.L. Mccormick), American Chemical Society, Washington, D.C., p. 1.
111 Tuzar, Z., Pospisil, H., Plestil, J., Lowe, A.B., Baines, F.L., Billingham, N.C. and Armes, S.P. (1997) *Macromolecules*, **30**, 2509.
112 Lowe, A.B., Billingham, N.C. and Armes, S.P. (1999) *Macromolecules*, **32**, 2141.
113 Weaver, J.V.M., Armes, S.P. and Butun, V. (2002) *Chem. Commun.*, 2122.
114 Ball, P. (1999) *The Self-Made Tapestry*, Oxford University Press Inc., New York.
115 Gao, H.J., Xue, Z.Q., Wu, Q.D. and Pang, S.J. (1996) *Solid State Commun.*, **97**, 579.
116 Tan, C.H., Ravi, P., Dai, S. and Tam, K.C. (2004) *Langmuir*, **20**, 9901.
117 Vicsek, T. (1992) *Fractal Growth Phenomenon*, 2nd edn, World Scientific, Singapore.
118 Bensasson, R.V., Blenvenue, E., Dellinger, M., Leach, S. and Patrick, S. (1994) *J. Phys. Chem.*, **98**, 3492.
119 Guldi, D.M. (1997) *J. Phys. Chem. A*, **101**, 3895.
120 Wang, C., Ravi, P. and Tam, K.C. (2006) *Langmuir*, **22**, 2927.
121 Wang, C., Ravi, P. and Tam, K.C. (2007) *Langmuir*, **27**, 8798.
122 Ikkala, O. and Brinke, G. (2002) *Science*, **295**, 29.
123 Wei, Z., Laitinen, T., Smarsly, B., Ikkala, O. and Faul, C.F.J. (2005) *Angew. Chem. Int. Ed.*, **44**, 751.
124 Ikkala, O. and Brinke, G. (2004) *Chem. Commun.*, 2131.

4
Semi-Interpenetrating Polymer Networks Involving C_{60}-Polymers

Suat Hong Goh

4.1
Introduction

A semi-interpenetrating polymer network (SIPN) is a combination of a network polymer and a linear polymer. A SIPN is usually prepared by the polymerization of a multifunctional monomer in the presence of a linear polymer [1]. C_{60} derivatives and C_{60}-containing polymers form aggregates in solution and in the solid state [2–18]. For double-C_{60}-end-capped polymers in which both ends of each polymer chain are capped with C_{60}, the aggregation of C_{60} leads to a network-like material. Therefore, a combination of a double-C_{60}-end-capped polymer and a linear polymer produces a material resembling a SIPN and is termed a pseudo-SIPN. This chapter discusses the mechanical and optical properties of some pseudo-SIPNs involving double-C_{60}-end-capped polymers.

4.2
Synthesis and Properties of Double-C_{60}-End-Capped Polymers

A polymer chain can be end-capped with C_{60} by several methods. The reaction between a polymeric living carbanion and C_{60} enables the attachment of C_{60} at the polymer chain end [19–22]. End-capping is also achieved through reaction between amine-terminated polymer and C_{60} [23, 24]. However, the most widely used method makes use of the reaction between an azide group and C_{60}. Organic azides can serve as 1,3-dipoles and undergo [3+2]cycloadditions to C_{60}, leading to aza-bridged fullerenes. The addition reaction proceeds primarily through mono-addition, with little or no higher addition products being observed [25–27]. As a result, double-C_{60}-end-capped polymers can be prepared by reactions between C_{60} and double-azido-terminated polymers. For example, the terminal hydroxyl groups of poly(ethylene oxide) (PEO) have been converted into chlorine groups through reaction with thionyl chloride. The double-chloro-terminated PEO was then reacted with sodium azide to form double-azido-terminated PEO, which subsequently

Fullerene Polymers. Synthesis, Properties and Applications. Edited by Nazario Martín and Francesco Giacalone

ISBN: 978-3-527-32282-4

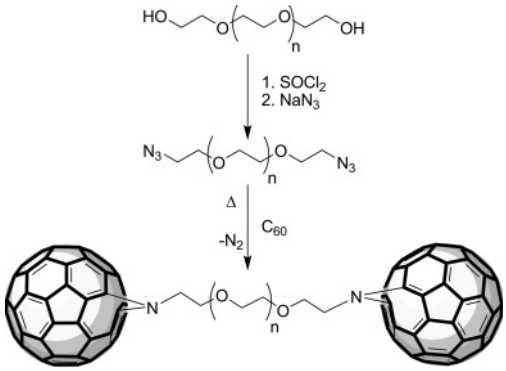

Scheme 4.1 Synthetic route to double-C_{60}-end-capped poly(ethylene oxide).

underwent cycloaddition with C_{60} to afford double-C_{60}-end-capped PEO (Scheme 4.1) [28]. In general, the precursor polymers were first prepared by atom transfer radical polymerization (ATRP). Depending on the choice of initiators, one or both ends of a polymer chain were terminated with bromine or chlorine groups. The terminal chlorine or bromine groups were then converted into azido groups, followed by cycloaddition with C_{60} [9–18, 29–31]. Recently, Zhang *et al.* have reported the synthesis of C_{60}-end-capped polystyrene (PS) using a "click chemistry" approach [32]. C_{60} was functionalized to possess a terminal alkyne group. Bromine-terminated PS prepared by ATRP was converted into azido-terminated PS. The "click" reaction between alkyne and azido groups led to the attachment of C_{60} to the PS chain end. The "click" reaction is mild and high yielding, producing single-C_{60}-end-capped PS with narrow polydispersity (~1.01) and free of multiadducts.

The use of C_{60} and its derivatives as reinforcing materials has been explored. Ma *et al.* have studied the mechanical properties of blends of a Novolac-type phenolic resin with fullerenol polyurethane or linear polyurethane [33]. Fullerenol polyurethane offers a better improvement in terms of the impact strength of phenolic resin (54.3%) than linear polyurethane (27.4%). The storage modulus of a blend of poly(styrene-*co*-4-vinylpyridine) and poly(styrene-*co*-butadiene) at room temperature increases by about 20% upon the addition of 10 wt% of a C_{60} derivative [34]. Another study found that the storage modulus of low-density polyethylene at room temperature increased by about 40% upon the addition of 5 wt% multifunctional benzylaminofullerene [35]. It is envisaged that the mechanical properties of a polymer are likely to change upon end-capping with C_{60}.

The tensile properties of double-C_{60}-end-capped PEO (FPEOF) have been studied by Song *et al.* [36]. The parent PEO10 and PEO20 (the number after PEO denotes the molecular weight of PEO in $kg\,mol^{-1}$) are wax-like materials, but the two FPEOF samples possess very good tensile properties (Table 4.1). For comparison the tensile properties of PEO300 reported by Tsou *et al.* [37] are included in Table 4.1. While PEO300 breaks at about 1.5% strain before yielding, the two FPEOF samples do not break even at 640% strain, the limit of the testing instrument.

Table 4.1 Tensile properties of double-C_{60}-end-capped PEOs (FPEOFs).

Polymer	Tensile strength (MPa)	Tensile modulus (MPa)	Yield strength (MPa)	Toughness ($MJ\,m^{-3}$)
FPEO10F	24.1	283	15.9	119
FPEO20F	20.1	258	16.0	110
PEO300	5.5	650	[a]	0.04

a Fracture occurred at about 1.5% strain before yielding. (Reprinted with permission from Reference [36]. Copyright 2003 Elsevier Science Ltd.)

Apart from the tensile modulus, the two FPEOF samples are superior to PEO300, especially the toughness as measured by the total area under the stress–strain curve. Interestingly, THF-cast films of FPEOF can not dissolve in water even though PEO is water soluble [36]. The films become fully swollen in water in about 1 min, and take up water amounting to 7–9 times their initial weight. The films show shape recovery ability. The swollen films recover completely their original shapes and sizes without loss in mechanical performance after drying at 55 °C for 1 h. Irregularly drawn FPEOF films also fully recover their original shapes and sizes after being heated at 55 °C for just ~10 min. The results suggest that FPEOF possess a network-like structure that can be disrupted and reformed. Although the THF-cast FPEOF films can not be dissolved in water, they are soluble in hot chlorobenzene. Water is a poor solvent for C_{60} so that it can not disrupt the C_{60} aggregates. In contrast, chlorobenzene is a good solvent for both C_{60} and PEO, and the aggregation of C_{60} can be disrupted by chlorobenzene. Single-C_{60}-end-capped PEO (FPEO) is a wax-like material, just like its parent polymer poly(ethylene oxide) monomethyl ether. Although FPEO also undergoes aggregation in water and THF, the C_{60} aggregates are not interconnected to form a network-like structure.

The tensile properties of double-C_{60}-end-capped poly(*n*-butyl methacrylate) (FPBMAF) have been studied by Wang *et al.* [38]. As shown by the stress–strain curves in Figure 4.1, the tensile strength of FPBMAF is 240% higher than that of the parent poly(*n*-butyl methacrylate) (PBMA). The toughness of PBMA is increased by 190% upon end-capping with C_{60}. Wang *et al.* also found that the storage modulus of FPBMAF at 20 °C is more than double that of PBMA (Figure 4.2). However, the end-capping with C_{60} of other poly(alkyl methacrylate)s such as poly(methyl methacrylate) (PMMA), poly(ethyl methacrylate) (PEMA) and poly(*n*-propyl methacrylate) (PPMA) does not produce significant improvements in the mechanical properties. The glass transition temperatures (T_gs) of PMMA (105 °C), PEMA (60 °C) and PPMA (45 °C) are higher than the room temperature (30 °C) at which tensile measurements were made. In contrast, the T_gs of PBMA and PEO are 20 °C and −75 °C, respectively, which are lower than room temperature. The results appear to suggest that end-capping with C_{60} is beneficial to polymers with low T_gs. However, poly(*n*-butyl acrylate) (PBA, T_g = −50 °C) remains weak after

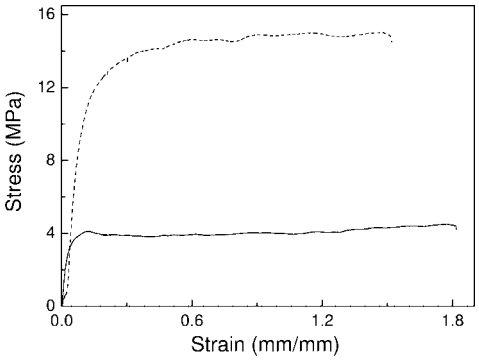

Figure 4.1 Stress–strain curves of PBMA (lower curve) and FPBMAF (upper curve). (Reprinted with permission from Reference [38]. Copyright 2006 American Chemical Society.)

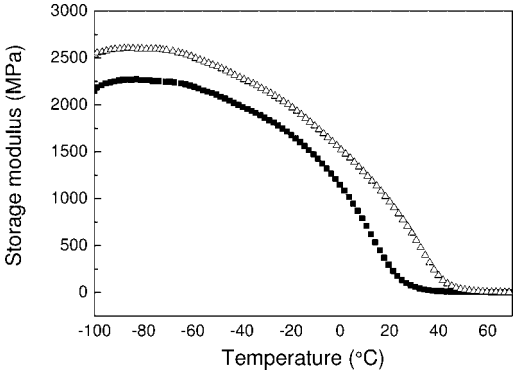

Figure 4.2 Storage moduli of PBMA (■) and FPBMAF (△). (Reprinted with permission from Reference [38]. Copyright 2006 American Chemical Society.)

end-capping with C_{60}. The differences between the effects of end-capping with C_{60} for PEO and PBA may be attributed to the semi-crystalline nature of PEO. Although the T_g of PEO is even lower than that of PBA, PEO is semi-crystalline with a melting temperature of 55 °C.

However, a recent study by Inoue and coworkers has shown that end-capping of semi-crystalline poly(ε-caprolactone) (PCL, $T_g = -51$ °C and $T_m = 30$ °C) with C_{60} produces a detrimental effect on the mechanical properties [39]. The storage modulus of PCL is higher than those of single- and double-C_{60}-end-capped PCL at a temperature below T_g. At a temperature higher than the T_g, the storage modulus of C_{60}-end-capped PCL is higher than that of PCL. The mechanical properties of PCL are significantly reduced when both chain ends are capped with C_{60}. The

Young's modulus and the ultimate strain of PCL change from 240 MPa and 620% to 170 MPa and 70%, respectively, upon end-capping with C_{60}.

From the results discussed so far, it appears that the end-capping of a polymer with C_{60} does not necessarily bring about improvements in mechanical properties. For PEO, the benefits of end-capping with C_{60} are tremendous, whereas for PCL the mechanical properties deteriorate. At this stage, it is not clear what types of polymers would definitely benefit from end-capping with C_{60}.

4.3 Mechanical Properties of Pseudo-SIPNs

4.3.1 FPEOF/PMMA Pseudo-SIPNs

The mechanical properties of FPEOF/PMMA pseudo-SIPNs have been reported by Wang *et al.* [40]. Two series of pseudo-SIPNs were prepared, one based on FPEO5F (samples A, B and C) and the other based on FPEO12F (samples D, E and F). The FPEOF contents are 9.1, 14.9, 25.0, 8.7, 11.9 and 35.9 wt% for samples A–F, respectively; the corresponding C_{60} contents are 1.6, 2.7, 4.5, 1.1, 1.5 and 4.6 wt%, respectively.

Figure 4.3 shows the storage moduli of PMMA and three PMMA/PEO5 blends. The storage modulus of PMMA decreases progressively upon the addition of PEO5. Since PEO has a low T_g of –75 °C and is miscible with PMMA, PEO serves as a plasticizer and softens the PMMA matrix, leading to a lower storage modulus. For the FPEO5F/PMMA pseudo-SIPNs as shown in Figure 4.3, samples A and B possess slightly higher storage moduli than PMMA. However, sample C, which has the highest FPEO5F content, has a storage modulus lower than that of PMMA. Apparently, at a higher FPEO5F content, the reinforcing effect of C_{60} has been offset by the plasticizing effect of PEO chains. On the other hand, the storage

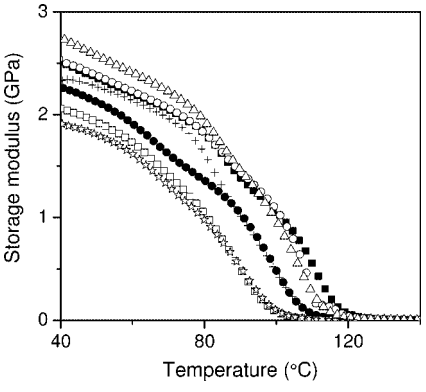

Figure 4.3 Storage moduli of PMMA, PEO5/PMMA blends and FPEO5F/PMMA pseudo-SIPNs. (○) A; (△) B; (+) C; (■) PMMA; (●) PEO5/PMMA (5:95); (□) PEO5/PMMA (10:90); (☆) PEO5/PMMA (20:80); see text for composition of samples A–C. (Reprinted with permission from Reference [40]. Copyright 2004 American Chemical Society.)

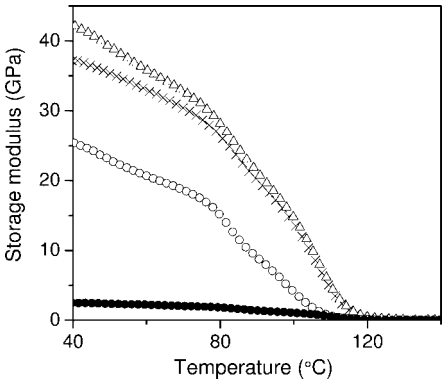

Figure 4.4 Storage moduli of PMMA and FPEO12F/PMMA pseudo-SIPNs. (×) D; (△)E; (○) F; (●) PMMA; see text for composition of samples D–F. (Reprinted with permission from Reference [40]. Copyright 2004 American Chemical Society.)

moduli of the three FPEO12F/PMMA pseudo-SIPNs are substantially larger than that of PMMA (Figure 4.4). The storage modulus of sample E is 42 GPa at 40 °C, representing an astonishing 16-fold increase over PMMA. Such a remarkable enhancement of the storage modulus of a polymer by an additive is uncommon. Hwang *et al.* have reported that the storage modulus of PMMA at 20 °C was improved by 12 times upon the addition of 20 wt% of PMMA-grafted multiwalled carbon nanotubes [41]. The storage modulus of a thermoplastic polymer such as PMMA decreases rapidly when it is heated through the glass transition temperature, as shown in Figure 4.3. The storage moduli of pseudo-SIPNs also begin to decrease rapidly at 80 °C. However, even at 100 °C, the storage moduli of samples D and E are still 10 times larger than that of PMMA. As shown in Figures 4.3 and 4.4, the storage modulus of pseudo-SIPN is affected by the chain length of the parent PEO. The aggregation of FPEOF is affected by the polarity of solvent and the PEO chain length. The size of C_{60} aggregates in sample B ranges from 200 to 800 nm, whereas that of sample D is in the range 50–150 nm [40]. Smaller filler particles generally have a better strengthening effect on polymer than bigger particles [42]. Therefore, the better performance of pseudo-SIPNs based on FPEO12F is partly due to the smaller size of the C_{60} aggregates.

Table 4.2 summarizes the tensile properties of PMMA and the six pseudo-SIPNs. The Young's modulus of PMMA is increased by 50–100% upon the incorporation of FPEOF, whereas the tensile strength, ultimate strain and toughness are decreased slightly. There also appears to be an optimum FPEOF content in the pseudo-SIPN, above which the tensile properties start to decrease.

4.3.2
FPEOF/Poly(L-Lactic Acid) Pseudo-SIPNs

Poly(L-lactic acid) (PLLA) is a biodegradable polymer that is widely used in biomedical applications. However, the low ultimate strain of 3% makes PLLA very brittle and difficult to process. PEO has been added to PLLA to improve its process-

Table 4.2 Strain–stress properties of PMMA and pseudo-SIPNs (A–F).

Sample code	Tensile strength (MPa)	Ultimate strain (mm mm^{-1})	Young's modulus (MPa)	Toughness (MJ m^{-3})
PMMA	51.3	0.0627	1180	1.96
A	41.2	0.0279	1980	0.77
B	28.6	0.0216	1680	0.34
C	28.0	0.0250	1580	0.44
D	31.4	0.0220	2020	0.43
E	43.3	0.0250	2430	0.61
F	34.2	0.0238	1940	0.46

ability [43–45]. Although the ultimate strain of PLLA is increased significantly by the addition of PEO, its Young's modulus and yield stress are substantially reduced [44, 45]. The PEO/PLLA blends become more rigid (with increasing modulus and reduced ductility) upon standing at room temperature due to the crystallization of PEO.

The effects of aging on the dynamic and tensile properties of FPEOF/PLLA pseudo-SIPNs have been studied by Inoue and coworkers [46, 47]. The dynamic behavior of FPEOF/PLLA pseudo-SIPNs differs from that of FPEOF/PMMA pseudo-SIPNs. For FPEOF/PLLA pseudo-SIPNs, the storage modulus of PLLA decreases upon the addition of FPEOF. In contrast, the storage modulus of PMMA increases upon the addition of FPEOF, as mentioned earlier.

Similarly, the effects of FPEOF on the tensile properties of PLLA are also different from that on PMMA. Tables 4.3 and 4.4 show the tensile properties of FPEOF/PLLA pseudo-SIPNs aged at room temperature and at 90 °C, respectively [46, 47]. The Young's modulus and yield stress of various pseudo-SIPNs are lower than those of PLLA. However, the ultimate strains of the pseudo-SIPNs are remarkably higher than that of PLLA. For PLLA/FPEO20F6 (FPEO20F content of 6 wt%), the ultimate strain of the pseudo-SIPN aged at room temperature is 340%, which is 85 times larger than that of PLLA. Similar to what was observed by Wang *et al.* [40], the chain length of PEO in FPEOF has some effects on the tensile property of the pseudo-SIPNs. The tensile properties of pseudo-SIPNs based on FPEO20F are marginally better than those based on FPEO4F.

There is an optimum amount of FPEOF to achieve maximum ductility [46, 47]. At a low FPEOF content, the number of C_{60} aggregates is too low to support the whole PLLA matrix, and hence the ultimate strain is increased slightly. An increased amount of FPEOF results in the formation of a loose PEO network that can sustain a higher strain. However, at an even higher FPEOF content, the density of C_{60} aggregates is too high, which results in the brittleness of the network.

Table 4.3 Tensile properties of PLLA and PLLA/FPEOF pseudo-SIPNs aged at room temperature.

Sample[a]	Young's modulus (MPa)	Yield stress (MPa)	Ultimate strain (%)
PLLA	1600 ± 30	52 ± 2	4 ± 1
PLLA/FPEO4F2.5	1300 ± 40	20 ± 2	15 ± 3
PLLA/FPEO4F6	1250 ± 30	36 ± 2	100 ± 10
PLLA/FPEO4F12	1200 ± 10	34 ± 1	45 ± 5
PLLA/FPEO4F17	1100 ± 20	30 ± 1	20 ± 5
PLLA/FPEO20F3	1450 ± 30	47 ± 2	20 ± 3
PLLA/FPEO20F6	1400 ± 30	37 ± 1	340 ± 30
PLLA/FPEO20F10	1300 ± 20	35 ± 1	200 ± 20
PLLA/PEO4-6	1350 ± 30	43 ± 2	4 ± 1
PLLA/PEO20-6	1450 ± 30	45 ± 2	4 ± 1

a The number x in FPEOxF denotes the molecular weight in kg mol^{-1} of parent PEO; the number after FPEOxF denotes the weight percentage of FPEOxF in pseudo-SIPN. (From Reference [47].)

Table 4.4 Tensile properties of PLLA/FPEOF pseudo-SIPNs aged at 90 °C.

Sample	Young's modulus (MPa)	Yield stress (MPa)	Ultimate strain (%)
PLLA	1600 ± 40	60 ± 2	4 ± 1
PLLA/FPEO4F2.5	1400 ± 30	46 ± 3	10 ± 2
PLLA/FPEO4F6	1300 ± 30	40 ± 1	22 ± 3
PLLA/FPEO4F12	1100 ± 10	33 ± 2	34 ± 5
PLLA/FPEO4F17	900 ± 20	26 ± 1	16 ± 4
PLLA/FPEO20F3	1500 ± 20	49 ± 1	8 ± 2
PLLA/FPEO20F6	1450 ± 30	45 ± 1	18 ± 5
PLLA/FPEO20F10	1400 ± 20	39 ± 1	25 ± 3

The number x in FPEOxF denotes the molecular weight in kg mol^{-1} of parent PEO; the number after FPEOxF denotes the weight percentage of FPEOxF in pseudo-SIPN.
(From Reference [47].)

As shown in Tables 4.3 and 4.4, aging at 90 °C produces no significant effects on Young's modulus and yield stress. However, the ultimate strain is greatly reduced. Nevertheless, the ultimate strains of pseudo-SIPNs are still significantly larger that that of PLLA. For samples aged at room temperature, PLLA is amorphous. Since PLLA is miscible with PEO, the pseudo-SIPNs are homogeneous. The introduction of a network into PLLA enables a quick transfer of force exerted on the sample to the whole sample through the network to avoid stress concentration. Moreover, the network formed in PLLA can render large deformation, arising from the excellent deformation ability of the network. As a result, the pseudo-

SIPNs possess excellent ductility. In contrast, PLLA in the pseudo-SIPNs crystallizes upon aging at 90 °C. The network formed is confined by crystalline PLLA, resulting in a significant reduction in ductility.

4.3.3 FPBMAF/PVC Pseudo-SIPNs

Wang *et al*. have studied the mechanical properties of FPBMAF/poly(vinyl chloride) (PVC) pseudo-SIPNs [38]. The molecular weight of PBMA in FPBMAF is 60 kg mol^{-1}. Two pseudo-SIPNs were prepared by solution casting from THF, and the effective C_{60} contents of the samples were 0.06 and 0.10 wt%. As shown in Figure 4.5, the storage moduli of the pseudo-SIPNs are significantly larger than that of PVC. At 60 °C, the storage modulus of the pseudo-SIPN with an effective C_{60} content of 0.10 wt% is about twice as that of PVC.

Figure 4.6 shows the stress–strain curves of PVC and the two pseudo-SIPNs; Table 4.5 summarizes the tensile properties. For the pseudo-SIPN with an effective content of 0.1 wt%, the Young's modulus, yield stress, tensile strength, ultimate strain and toughness are better than those of PVC. FPBMAF is more effective than carbon black and nano-$CaCO_3$ in enhancing the mechanical properties of PVC. The yield stress, tensile strength and Young's modulus of PVC are improved marginally from 39, 39 and 952 MPa, respectively, to 40, 40 and 1010 MPa, respectively, upon the addition of 3 wt% of carbon black [48]. For PVC/nano-$CaCO_3$ nanocomposites, the ultimate strain and tensile strength decrease with increasing filler content, although the notched Izod impact strength increases

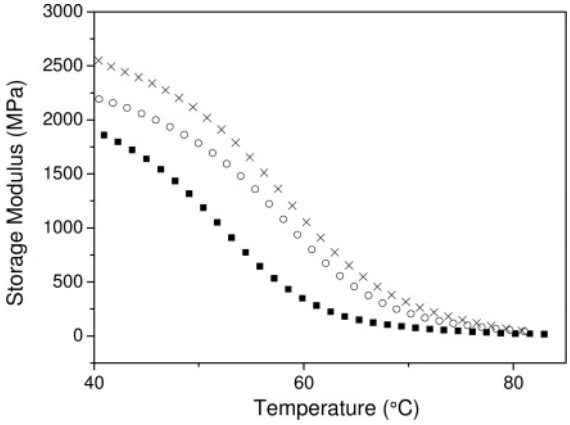

Figure 4.5 Storage moduli of PVC (■) and PVC/FPBMAF pseudo-SIPNs: sample A with C_{60} content of 0.06 wt% (○); sample B with C_{60} content of 0.10 wt% (×). (Reprinted with permission from Reference [38]. Copyright 2006 American Chemical Society.)

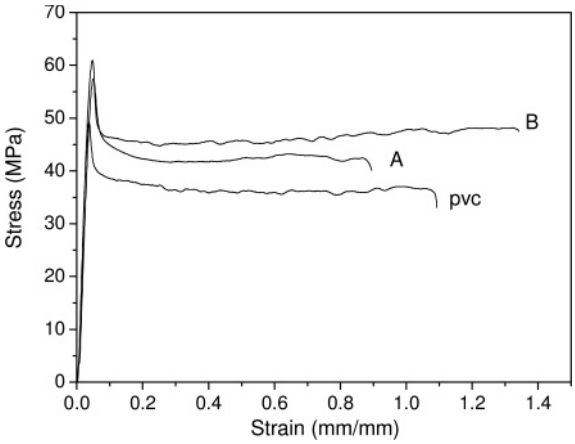

Figure 4.6 Stress–strain curves of PVC and PVC/FPBMAF pseudo-SIPN sample A with a C_{60} content of 0.06 wt% and sample B with a C_{60} content of 0.10 wt%. (Reprinted with permission from Reference [38]. Copyright 2006 American Chemical Society.)

Table 4.5 Mechanical properties of PVC and PVC/FPBMAF pseudo-SIPNs.

Sample	Effective C_{60} content (wt%)	Tensile strength (MPa)	Yield stress (MPa)	Ultimate strain (mm mm^{-1})	Young's modulus (MPa)	Toughness ($MJ\,m^{-3}$)
PVC	0	36.3	49.2	1.08	1470	39.7
A	0.06%	42.4	57.5	0.903	1570	38.1
B	0.1%	47.9	61.0	1.34	1680	61.8

(Reprinted with permission from Reference [38]. Copyright 2006 American Chemical Society.)

[49, 50]. Therefore the strengthening and toughening effects of FPBMAF on PVC are noteworthy.

4.4 Optical Transmission Characteristics of Pseudo-SIPNs

The optical limiting properties of C_{60} and its derivatives have attracted much attention in view of their potential uses in optoelectronics [51–55]. Tang and coworkers have studied the optical transmission characteristics of several C_{60}-containing polymers [56, 57]. The materials show light transmission spectra resembling those of cutoff filters, and the cutoff wavelength (λ_c, defined as the wavelength at which the transmittance falls to 0.1%) varies with C_{60} concentration in a semi-logarithmic

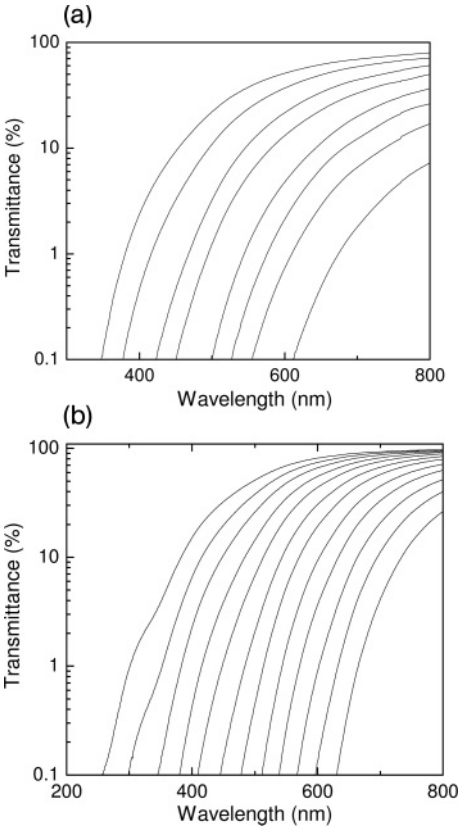

Figure 4.7 (a) Light transmission spectra of FPEO2 (C_{60} content: 24 wt%) in water; polymer concentration (mg mL^{-1}) – from right to left: 5, 3.33, 2.5, 1.67, 1.25, 0.83, 0.625 and 0.417; (b) light transmission spectra FPEO2F (C_{60} content: 40 wt%) in water; polymer concentration (mg mL^{-1}) – from right to left: 4.5, 3, 2.25, 1.5, 1.12, 0.75, 0.562, 0.375, 0.281, 0.187, 0.140 and 0.094.

manner. Therefore, the materials are potentially excellent optical filters that can be used to cut off light over a very wide spectral region.

Figure 4.7 shows the optical transmission characteristics of aqueous solutions of single- and double-C_{60}-end-capped PEO (FPEO2 and FPEO2F, respectively; the molecular weight of PEO is 2 kg mol^{-1}[11]). The spectrum shifts continuously to a longer wavelength over a wavelength range of 250–650 nm with increasing polymer concentration. In other words, λ_c increases with increasing FPEO2/FPEO2F concentration of the solution. Since the sizes of C_{60} aggregates of FPEO2 and FPEO2F in water increase with increasing polymer concentration [5], λ_c appears to be related to the size of aggregates. Figure 4.7 also shows that, at the same effective C_{60} content of 1.2 mg mL^{-1}, FPEO2 (polymer concentration of 5 mg mL^{-1}) cuts off light at a longer wavelength of 613 nm as compared to 597 nm by FPEO2F (polymer concentration of 3 mg mL^{-1}). The TEM micrographs (Figure 4.8) show that the sizes of C_{60} aggregates of FPEO2 in water are in the range 400–500 nm, whereas those of FPEO2F are in the range 150–300 nm. FPEO2 is more mobile than FPEO2F, whose mobility is restricted by two bulky C_{60} at both

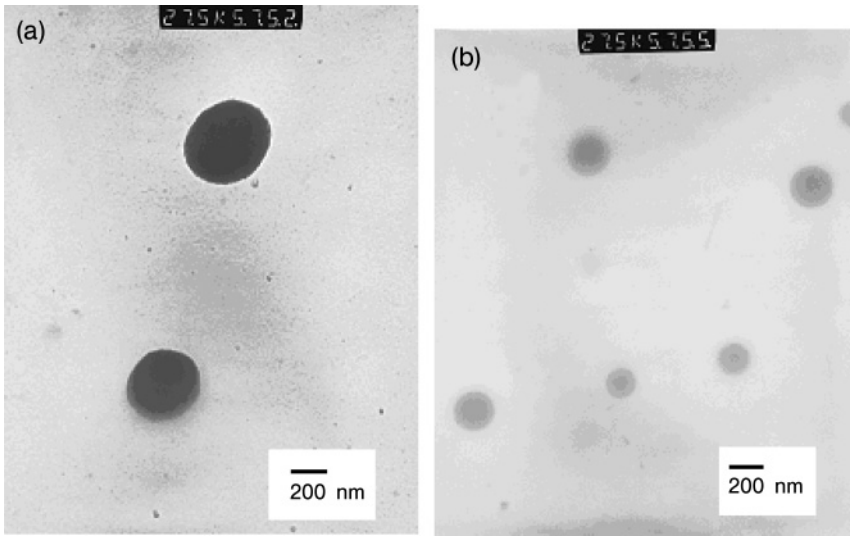

Figure 4.8 TEM micrographs: (a) FPEO2 in water ×27 500; (b) FPEO2F in water ×27 500.

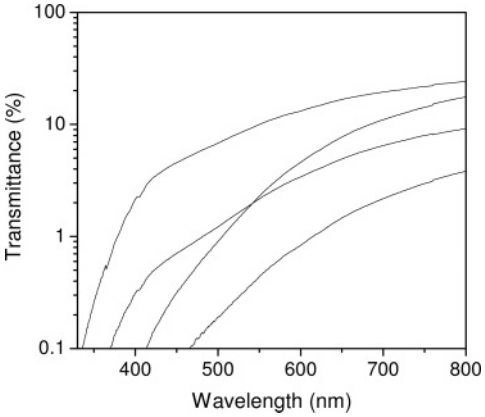

Figure 4.9 Light transmission spectra of PMMA/FPEOF pseudo-SIPN films (see text for details). Path length: 0.2 mm. C_{60} concentration (wt%) – from right to left: 1.1, 1.5, 2.7 and 4.5.

ends, and hence FPEO2 forms larger aggregates. The results show that λ_c is closely related to the size of C_{60} aggregates in solution.

The optical transmission characteristics of the following four FPEOF/PMMA pseudo-SIPNs have also been studied: FPEO12F/PMMA (C_{60} content = 1.1%), FPEO12F/PMMA (C_{60} content = 1.5%), FPEO20F/PMMA (C_{60} content = 2.7%) and FPEO5F/PMMA (C_{60} content = 4.5%). Figure 4.9 shows the transmission spectra of solid films of the four pseudo-SIPNs. Similarly, the spectrum also red-

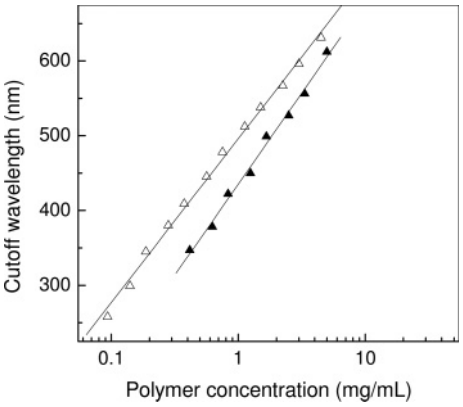

Figure 4.10 Cutoff wavelength as a function of polymer concentration of aqueous solutions of FPEO2 (▲) and FPEO2F (△).

Table 4.6 Values of *a* and *k* for various C_{60}-containing polymers.

Polymer	Solvent or polymer	*a*	*k*
FPEO2	H_2O	243	435 (600)[a]
FPEO2F	H_2O	219	496 (582)[a]
FPBMAF	THF	211	277 (546)[a]
C_{60}-PMMA	THF	168[b]	174[b] (514)[a]
C_{60}-PC	THF	158[b]	200[b] (486)[a]
FPEOF	PMMA	207	1095
C_{60}-CR39	—	48[b]	632[b]

a Value in parentheses shows *k* value based on actual C_{60} content.
b Value calculated from Reference [57].

shifts with increasing C_{60} content in the pseudo-SIPN. The size of C_{60} aggregates in the pseudo-SIPN as measured by TEM also increases with increasing C_{60} content. Once again, the cutoff wavelength increases with increasing size of C_{60} aggregates.

As shown in Figure 4.10, the cutoff wavelengths of C_{60}-end-capped polymer solutions are concentration dependent, obeying the semi-logarithmic relationship previously reported by Tang and coworkers [57]:

$$\lambda_c = a\log(bc) + k$$

The use of 1-cm quartz cells means that the path length of light (*b*) is 1 cm, and the equation is simplified to $\lambda_c = a\log(c) + k$, where *c* denotes the concentration of C_{60}-end-capped polymer. Table 4.6 lists the values of *a* and *k* obtained from the gradient and intercept of the straight line, respectively. From Figure 4.10, it is

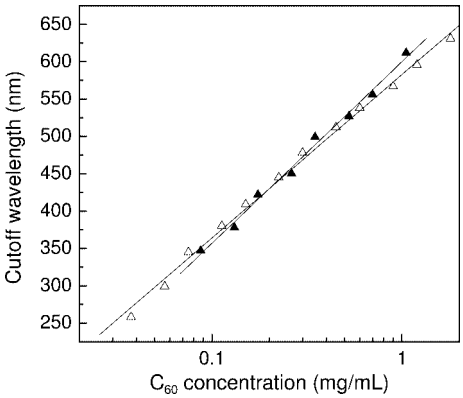

Figure 4.11 Cutoff wavelength as a function of C_{60} concentration of aqueous solutions of FPEO2 (▲) and FPEO2F (△).

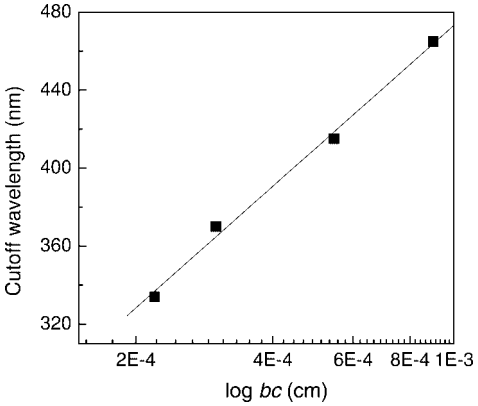

Figure 4.12 Cutoff wavelength of PMMA/FPEOF pseudo-SIPN films; b = 0.020 cm and c (weight fraction of C_{60} in sample) = 0.011, 0.015, 0.027 or 0.045.

noted that, to cut off a certain wavelength, a more concentrated solution is needed for polymer with a lower C_{60} content. However, when the cutoff wavelength is plotted against the actual C_{60} content of the solution, the two lines nearly superimpose (Figure 4.11). In other words, the a and k values of the two polymers are about the same. Similarly, a linear relationship between λ_c and log(bc) is also observed for solid FPEOF/PMMA pseudo-SIPNs, where b is the thickness of the film (Figure 4.12).

Table 4.6 summarizes the a and k values of various C_{60}-containing polymeric materials. The a values of THF solutions of C_{60}-containing PMMA (C_{60}-PMMA) and C_{60}-containing polycarbonate (C_{60}-PC), where C_{60} are randomly attached on the polymer chains, reported by Peng *et al.* [57], are included for comparison. Also

included is the *a* value of a solid sample of fullerenated CR-39 resin (polymer of diethylene glycol diallyl carbonate). A larger *a* value means that λ_c increases more rapidly with increasing concentration of C_{60} or C_{60}-containing polymer. The *a* value of the aqueous solutions of FPEO2 and FPEO2F, and the FPEOF/PMMA pseudo-SIPNs are around 220, which are larger than those of 168 and 158 for C_{60}-PMMA and C_{60}-PC, respectively. The *a* value of 48 for CR-39 resin is even smaller. The *a* values appear to reflect the ease of aggregation of C_{60} moieties. For C_{60}-end-capped polymers, C_{60} aggregates easily, as in the case of conventional surfactants. In comparison, the aggregation of C_{60} in C_{60}-PMMA and C_{60}-PC is more difficult as C_{60} is linked to the polymer main chains. The crosslinked nature of CR-39 is likely to make it even more difficult for the C_{60} moieties to aggregate.

The *k* value is the cutoff wavelength when the concentration is 1 mg C_{60}-polymer mL^{-1} or 1 mg C_{60} mL^{-1}. The *k* values of FPEO2 and FPEO2F are larger than those of C_{60}-PMMA and C_{60}-PC. The *k* values indicate that at a C_{60} concentration of 1 mg mL^{-1}, C_{60}-end-capped polymers cut off light of longer wavelength than polymer with C_{60} attached to the main polymer chains. The *k* value of pseudo-SIPN is twice that of the FPEO2 and FPEO2F solutions. However, the comparison is inappropriate as the path lengths of the samples are different from those of the solution samples. Nevertheless, the *k* value of the pseudo-SIPN is nearly twice of that of solid C_{60}-CR-39 resin. Thus, the *k* value may similarly reflect the ease of aggregation of C_{60} moieties. It is then suggested that, because of the ease of aggregation, the *a* and *k* values of C_{60}-end-capped polymers and their pseudo-SIPNs are larger than those of polymer with C_{60} attached to the main polymer chains. Since PMMA is used as lenses and for optical applications, FPEOF/PMMA pseudo-SIPNs may have potential applications as excellent optical filters.

4.5 Conclusions

The aggregation of C_{60} moieties in a double-C_{60}-end-capped polymer affords a network-like material that possesses interesting mechanical and optical properties. A combination of a double-C_{60}-end-capped polymer and a linear polymer gives rise to a pseudo-SIPN. Pseudo-SIPNs based on FPEOF/PMMA, FPEOF/PLLA and FPBMAF/PVC possess outstanding mechanical properties. FPEOF/PMMA pseudo-SIPNs are potentially useful optical filters as they are able to cut off light. The cutoff wavelength can be adjusted by changing the C_{60} content of the material.

References

1 Sperling, L.H. (2002) Interpenetrating polymer networks, in *Polymer Blends Handbook*, Chapter 6 (ed. L.A. Utracki), Kluwer Academic Publishers, Dordrecht.

2 Zhou, S.Q., Buger, C., Chu, B., Sawamura, M., Nagahama, N., Toganoh, M., Hackler, U.E., Isobe, H. and Nakamura, E. (2001) *Science*, **291**, 1944.

3 Okamura, H., Ide, N., Minoda, M., Komatsu, K. and Fududa, T. (1998) *Macromolecules*, **31**, 1859.
4 Wang, X.H., Goh, S.H., Lu, Z.H., Lee, S.Y. and Wu, C. (1999) *Macromolecules*, **32**, 2786.
5 Song, T., Dai, S., Tam, K.C., Lee, S.Y. and Goh, S.H. (2003) *Langmuir*, **19**, 4789.
6 Song, T., Dai, S., Tam, K.C., Lee, S.Y. and Goh, S.H. (2003) *Polymer*, **44**, 2529.
7 Hou, H., Goh, S.H. and Ngai, T. (2007) *Langmuir*, **23**, 12067.
8 Ravi, P., Dai, S., Wang, C. and Tam, K.C. (2007) *J. Nanosci. Nanotechnol.*, **7**, 1176.
9 Ravi, P., Dai, S., Tan, C.H. and Tam, K.C. (2005) *Macromolecules*, **38**, 933.
10 Yu, H., Gan, L.H., Hu, X., Venkatraman, S.S. and Tam, K.C. (2005) *Macromolecules*, **38**, 9889.
11 Ravi, P., Dai, S., Hong, K.M., Tam, K.C. and Gan, L.H. (2005) *Polymer*, **46**, 4714.
12 Ravi, P., Wang, C., Dai, S. and Tam, K.C. (2006) *Langmuir*, **22**, 7167.
13 Tan, C.H., Ravi, P., Dai, S., Tam, K.C. and Gan, L.H. (2004) *Langmuir*, **20**, 9882.
14 Dai, S., Ravi, P., Tan, C.H. and Tam, K.C. (2004) *Langmuir*, **20**, 8569.
15 Ravi, P., Dai, S. and Tam, K.C. (2005) *J. Phys. Chem. B*, **109**, 22791.
16 Teoh, S.K., Ravi, P., Dai, S. and Tam, K.C. (2005) *J. Phys. Chem. B*, **109**, 4431.
17 Yu, H., Gan, L.H., Hu, X. and Gan, Y.Y. (2007) *Polymer*, **48**, 2312.
18 Yang, J., Li, L. and Wang, C. (2003) *Macromolecules*, **36**, 6060.
19 Samulski, E.T., DeSimone, J.M., Hunt, M.O. Jr., Menceloglu, Y.Z., Jarnagin, R.C., York, G.A., Labat, K.B. and Wang, H. (1992) *Chem. Mater.*, **4**, 1153.
20 Wignall, G.D., Affholter, K.A., Bunick, G.J., Hunt, M.O. Jr., Menceloglu, Y.Z., DeSimone, J.M. and Samulski, E.T. (1995) *Macromolecules*, **28**, 6000.
21 Kawauchi, T., Kumaki, J. and Yashima, E. (2005) *J. Am. Chem. Soc.*, **127**, 9550.
22 Kawauchi, T., Kumaki, J. and Yashima, E. (2006) *J. Am. Chem. Soc.*, **128**, 10560.
23 Weis, C., Friedrich, C., Mulhaupt, R. and Frey, H. (1995) *Macromolecules*, **28**, 403.
24 Nepal, D., Samal, S. and Geckeler, K.E. (2003) *Macromolecules*, **36**, 3800.
25 Prato, M., Li, Q.C., Wudl, F. and Lucchini, V. (1993) *J. Am. Chem. Soc.*, **115**, 1148.
26 Hawker, C.J., Wooley, K.L. and Frechet, J.M.J. (1994) *Chem. Commun.*, 925.
27 Hawker, C.J. (1994) *Macromolecules*, **27**, 4836.
28 Huang, X.D. and Goh, S.H. (2000) *Macromolecules*, **33**, 8894.
29 Li, L., Wang, C., Long, Z. and Fu, S. (2000) *J. Polym. Sci. Part A: Polym. Chem.*, **38**, 4519.
30 Zhou, P., Chen, G.Q., Hong, H., Du, F.S., Li, Z.C. and Li, F.M. (2000) *Macromolecules*, **33**, 1948.
31 Wu, H., Li, F., Lin, Y., Yang, M., Chen, W. and Cai, R. (2006) *J. Appl. Polym. Sci.*, **99**, 828.
32 Zhang, W.B., Tu, Y., Ranjan, R., van Horn, R.M., Leng, S., Wang, J., Polce, M.J., Wesdemiotis, C., Quirk, R.P., Newkome, G.R. and Cheng, S.Z.D. (2008) *Macromolecules*, **41**, 515.
33 Ma, C.C.M., Sung, S.C., Wang, F.Y., Chiang, L.Y., Wang, L.Y. and Chiang, C.L. (2001) *J. Polym. Sci. Part B: Polym. Phys.*, **39**, 2436.
34 Ouyang, J.Y., Goh, S.H. and Li, Y. (2001) *Chem. Phys. Lett.*, **347**, 344.
35 Lu, Z., He, C. and Chung, T.S. (2001) *Polymer*, **42**, 5233.
36 Song, T., Goh, S.H. and Lee, S.Y. (2003) *Polymer*, **44**, 2563.
37 Tsou, L., Sauer, J.A. and Hara, M. (2000) *J. Polym. Sci. Part B: Polym. Phys.*, **38**, 1377.
38 Wang, M., Pramoda, K.P. and Goh, S.H. (2006) *Macromolecules*, **39**, 4932.
39 Kai, W., Hua, L., Dong, T., Pan, P., Zhu, B. and Inoue, Y. (2008) *Macromol. Chem. Phys.*, **209**, 104.
40 Wang, M., Pramoda, K.P. and Goh, S.H. (2004) *Chem. Mater.*, **16**, 3452.
41 Hwang, G.L., Shieh, Y.T. and Hwang, K.C. (2004) *Adv. Funct. Mater.*, **14**, 487.
42 Nelson, L.E. and Landel, R.F. (1994) *Mechanical Properties of Polymers and Composites*, Chapter 7, Marcel-Dekker, New York.
43 Nijenhuis, A., Colstee, E., Grijpma, D.W. and Pennings, A.J. (1996) *Polymer*, **37**, 5849.
44 Hu, Y., Rogunova, M., Topolkaraev, V., Hiltner, A. and Baer, E. (2003) *Polymer*, **44**, 5701.
45 Hu, Y., Hu, Y.S., Topolkaraev, V., Hiltner, A. and Baer, B. (2003) *Polymer*, **44**, 5711.

46 Kai, W., Zhao, L., Zhu, B. and Inoue, Y. (2006) *Macromol. Rapid Commun.*, **27**, 109.
47 Kai, W., Zhao, L., Zhu, B. and Inoue, Y. (2006) *Macromol. Chem. Phys.*, **207**, 746.
48 Chen, C.H., Li, H.C., Teng, C.C. and Yang, C.H. (2006) *J. Appl. Polym. Sci.*, **99**, 2167.
49 Tian, M., Chen, G. and Guo, S. (2005) *Macromol. Mater. Eng.*, **290**, 927.
50 Sun, S., Li, C., Zhang, L., Du, H.L. and Burnell-Gray, J.S. (2006) *Polym. Int.*, **55**, 158.
51 Sun, Y.P. and Riggs, J.E. (1997) *J. Chem. Soc., Faraday Trans.*, **93**, 1965.
52 Sun, Y.P., Riggs, J.E. and Liu, B. (1997) *Chem. Mater.*, **9**, 1268.
53 Sun, Y.P. and Riggs, J.E. (1999) *Int. Rev. Phys. Chem.*, **18**, 43.
54 Ouyang, J.Y., Goh, S.H., Elim, H.I., Meng, G.C. and Ji, W. (2002) *Chem. Phys. Lett.*, **366**, 224.
55 Elim, H.I., Ouyang, J.Y., He, J., Goh, S.H., Tang, S.H. and Ji, W. (2003) *Chem. Phys. Lett.*, **369**, 281.
56 Tang, B.Z., Peng, H., Leung, S.M., Au, C.F., Poon, W.H., Chen, H., Wu, X., Fok, M.W., Yu, N.T., Hiraoka, H., Song, C., Fu, J., Ge, W., Wong, G.L., Monde, T., Nemoto, F. and Su, K.C. (1998) *Macromolecules*, **31**, 103.
57 Peng, H., Leung, F.S.M., Wu, A.X., Dong, Y., Dong, Y., Yu, N.T., Feng, X. and Tang, B.Z. (2004) *Chem. Mater.*, **16**, 4790.

5
Star-Shaped Polymers with a Fullerene Core

Claude Mathis

5.1
Introduction

Among the great diversity of fullerene-based macromolecular architectures [1] polymer-stars with a fullerene as the central core have been particularly well studied. Interest in them stems first from the potentialities of these new materials to combine the electronic properties of C_{60} with the well-known advantages of polymers but also from the opportunities offered by the specific chemical reactivity of this fullerene to build new "model" star-shaped architectures.

These multi-adducts can be prepared by three main synthetic strategies: (i) direct addition onto C_{60} of preformed linear polymer chains bearing on one end a chemical function able to react with one of the 6-6 bonds of the fullerene, (ii) polymerization of a monomer using charged or functionalized fullerenes as initiators and (iii) addition of linear end-functionalized polymer chains to multi-substituted fullerenes. This wide range of synthetic methods has been used extensively to prepare $(polymer)_xC_{60}$ stars with various numbers of arms (2 to about 10) of different chemical nature. In this chapter, the di-adducts will be considered as stars with the lowest number of arms; even so, they are actually linear macromolecules.

The fact that these multi-adducts may be obtained as mixtures of stereoisomers is not a drawback in material chemistry. Nevertheless, it has to be stressed that any addition imposes the opening of one of the thirty 6-6 bonds on the fullerene, which consequently induces a change in its electronic properties. To produce materials where the properties of the incorporated C_{60} are well defined, it is essential that the number of grafted chains (i.e., the number of opened double bonds) is perfectly controlled and is identical for all the fullerenes. Furthermore, as, for a given functionality x of the $(polymer)_xC_{60}$ stars, the load of C_{60} and the inter-fullerene distances will directly depend on the length of the grafted chains, it is also essential to be able to control the molar mass of the polymer and keep its polydispersity as low as possible.

Fullerene Polymers. Synthesis, Properties and Applications. Edited by Nazario Martín and Francesco Giacalone

ISBN: 978-3-527-32282-4

Of all the polymerization methods, the anionic [2] and "controlled" radical polymerizations [3] give the best control over the chain length and produce polymers with the lowest polydispersities. In addition, polymers prepared through these routes bear a terminal function that can add to one of the "double" bonds (6-6 bonds) of C_{60}: respectively, a carbanion, a stabilized radical or a bond that can be converted into a radical. Furthermore, it is possible to take advantage of the specific shape and chemical reactivity of C_{60} to perfectly control the number of polymer chains grafted onto the fullerene using these two types of addition. This is why the mechanism of these two addition reactions will be discussed in more detail.

In this chapter we review the various synthetic routes toward polymer stars with a fullerene core. We also illustrate by a few examples how it is possible to take advantage of the presence of polymer or block copolymer chains grafted on the C_{60} core to obtain a special organization of this fullerene in a polymer matrix. Finally, we address the thermal stability of these materials as this consideration is of prime importance for any application.

5.2 Grafting of Linear Polymer Chains onto C_{60}

The direct addition of an end-functionalized linear polymer chain onto a 6-6 bond on C_{60} is the most commonly employed method to synthesize star-shaped polymers with a fullerene core. This grafting can occur via radicals, nucleophilic addition or insertion.

5.2.1 Grafting via Radicals

5.2.1.1 Radical Copolymerization of Fullerenes with Vinyl Monomers

The grafting of radicals to form multi-adducts R_nC_{60} (n = 1 to at least 15) [4] was one of the first addition reactions described in the literature. On the other hand, radical polymerization using 2,2′-azobis(isobutyronitrile) (AIBN), benzoyl peroxide and so on as initiators is one of the easiest and most commonly used methods to prepare polymer chains. Therefore, it was a logical step to try to incorporate C_{60} into a polymer by running such a radical polymerization in the presence of this strong radical acceptor. This "free radical copolymerization" of C_{60} has been studied by several groups and for various vinyl monomers (xylylene [5], styrene [6–13], methyl methacrylate [14, 15], 4-vinylbenzoic acid [16], maleic anhydride [17], etc.) and leads to branched star-like structures [6]. This very simple way to incorporate fullerenes in a polymer applies for many monomers; however, its mechanism is very complicated as many simultaneous reactions may take place (Scheme 5.1). The C_{60} acts first as an inhibitor for the radical polymerization of the vinyl monomer by scavenging the primary radicals (Scheme 5.1c) arising from cleavage of the initiator (Scheme 5.1a). Only after enough primary radicals have

Initiation

$$I \rightarrow 2R^{\bullet} \quad \text{(a)}$$

$$R^{\bullet} + M \rightarrow RM^{\bullet} \quad \text{(b)}$$

$$nR^{\bullet} + C_{60} \rightarrow (R)_nC_{60}^{\bullet} \quad \text{(c)}$$

Propagation

$$RM^{\bullet} + (x\text{-}1)M \rightarrow RM_x^{\bullet} \quad \text{(d)}$$

$$RM^{\bullet} + C_{60} \rightarrow RMC_{60}^{\bullet} \quad \text{(e)}$$

$$(R)_nC_{60}^{\bullet} + yM \rightarrow (R)_nC_{60}M_y^{\bullet} \quad \text{(f)}$$

Termination

$$(R)_nC_{60}^{\bullet} \xrightarrow[+\,mR^{\bullet}]{+\,zRM_x^{\bullet}} (R)_{n+m}C_{60}(RM_x)_z \quad \text{(g)}$$

Scheme 5.1 Simplified reaction scheme for the radical copolymerization of C_{60} with a vinyl monomer (M) [11]. I = initiator, $R^{\bullet}$ = primary radical, $RM_x^{\bullet}$ = growing polymer chains. For a complete reaction scheme see Reference [15].

been added to the fullerenes to adequately decrease their radical-affinity can the initiation (Scheme 5.1b) and the polymerization of the monomer proceed (Scheme 5.1d). At this point, competition between the addition of primary and propagating radicals takes place (Scheme 5.1c and 5.1e). Therefore, the polymers obtained are rather ill-defined as they consist of mixtures of stars with undefined numbers of arms of various lengths (from the primary small radical to the whole range of molar masses of the growing polymer chains). Polymerization through initiation by radicals located on the fullerenes (Scheme 5.1f) is not very likely as these radicals are probably too delocalized on the C_{60} [18] to be able to open the double bond of a monomer. Such a reaction would lead to coupling between stars and finally to reticulation.

To prepare star-shaped macromolecules with a well-defined number of arms of about the same length it is necessary to separate the polymerization step from the addition onto the fullerene. This can be done using "controlled" radical polymerization or macro-initiators.

5.2.1.2 Addition of Macro-radicals Obtained by "Controlled" Radical Polymerization

This type of chemistry towards well-defined star-shaped $(polymer)_xC_{60}$ is closely linked to progress made during this last decade in radical polymerization [3]. Indeed, the various "controlled radical polymerizations" such as nitroxide-mediated polymerization (NMP) or atom transfer radical polymerization (ATRP) allow us to produce polymer chains with tailored chain length and low polydispersities. Furthermore, the "as-prepared" chains bear at their end a function (stable radical or C—halogen bond) that can be converted under the right conditions into a macro-radical. If this latter is produced in the presence of C_{60}, several chains should add to the fullerene.

The first results reported in the literature concerned the addition onto C_{60} of polymer chains produced through NMP. A mono-adduct was obtained by reacting

C_{60} with a 4-hydroxy-2,2,6,6-tetramethylpiperidine-*N*-oxyl (TEMPOL) terminated polystyrene (PS) (M_n = 12 000 g mol^{-1}, M_w/M_n = 1.16) at 95 °C in toluene [19]. In a similar reaction, but with 2,2,6,6-tetramethylpiperidine-*N*-oxyl (TEMPO) as the stable counter radical, a di-adduct was formed in high yield even when a four-fold excess of C_{60} per PS-TEMPO was used [20]. The two chains are attached in the 1,4 positions on the same six-membered ring, only one double bond is opened and no TEMPO is present on the fullerene (Scheme 5.2).

The predominant formation of the di-adduct was confirmed by another group [21]. Scheme 5.3 shows the proposed addition mechanism.

The macro-radical PS$^\bullet$ produced upon heating (Scheme 5.3a) adds to the fullerene (Scheme 5.3b) and a PS-C_{60}-TEMPO is formed (Scheme 5.3c). However, it is very likely that the interaction between the stable radical TEMPO and the radical on the fullerene (Scheme 5.3c) is weaker than with the less delocalized PS radical (Scheme 5.3a). Therefore, at the temperature used, enough PS-$C_{60}^\bullet$ radicals will always be present when a PS$^\bullet$ radical is formed so that their recombination is highly favored (Scheme 5.3d), leading preferentially to the di-adduct. This peculiar behavior is a direct consequence of the spherical shape and conjugated nature of the fullerene molecule. At the working temperature PSC_{60}-C_{60}PS is not likely to be formed as the C_{60}—C_{60} bond should be very unstable (Scheme 5.3e). Control experiments without fullerene have shown that the recombination of PS$^\bullet$ radicals to form di-adduct with no incorporated C_{60} is a minor side product (Scheme 5.3f).

This synthetic route has been extended to the production of other well-defined di-adducts: [poly(*p*-vinylphenol)]$_2C_{60}$ and [(poly(*p*-vinylphenol)-*b*-polystyrene]$_2C_{60}$ [22, 23]. The solubility and micellization behavior of these two-arm stars in THF,

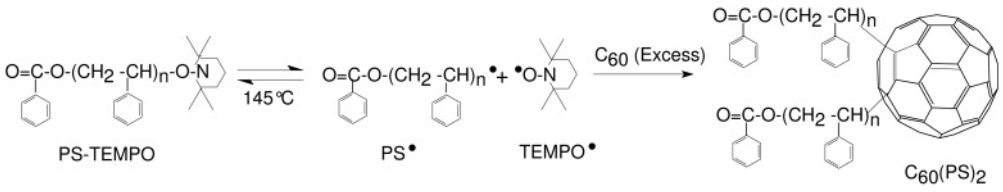

Scheme 5.2 Synthesis of di-adduct $(PS)_2C_{60}$ using a nitroxide-mediated (TEMPO) radical addition.

$$\text{PS-TEMPO} \leftrightarrows \text{PS}^\bullet + \text{TEMPO}^\bullet \quad \text{(a)}$$
$$\text{PS}^\bullet + C_{60} \rightarrow \text{PS-}C_{60}^\bullet \quad \text{(b)}$$
$$\text{PS-}C_{60}^\bullet + \text{TEMPO}^\bullet \leftrightarrows \text{PS-}C_{60}\text{-TEMPO} \quad \text{(c)}$$
$$\text{PS-}C_{60}^\bullet + \text{PS}^\bullet \rightarrow (\text{PS})_2\text{-}C_{60}^\bullet \quad \text{(d)}$$
$$\text{PS-}C_{60}^\bullet + \text{PS-}C_{60}^\bullet \leftrightarrows \text{PS-}C_{60}\text{-}C_{60}\text{PS} \quad \text{(e)}$$
$$\text{PS}^\bullet + \text{PS}^\bullet \rightarrow (\text{PS})_2 \quad \text{(f)}$$

Scheme 5.3 Proposed mechanism for the formation of a bis-adduct upon reacting PS-TEMPO with an excess of C_{60}.

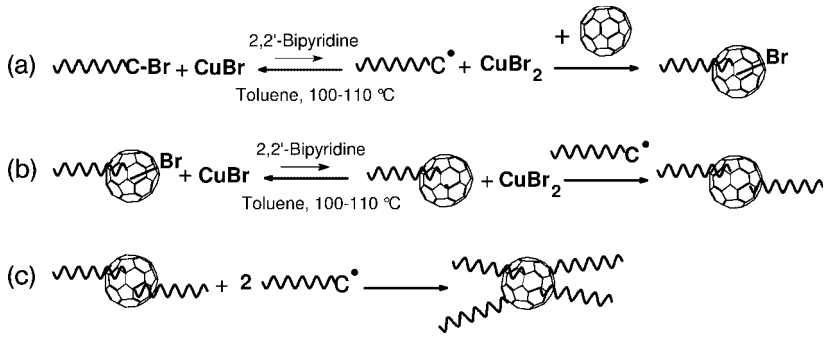

Scheme 5.4 Addition mechanism of PSBr onto C_{60} through atom transfer radical addition.

where C_{60} is insoluble, have been studied [22]. The di-adducts aggregate even in dilute solution to form stable micelles containing 6 to 20 molecules. Their solubility in a polystyrene matrix has also been examined [24].

Atom transfer radical addition (ATRA) is an alternative route to graft macro-radicals onto C_{60}. In the first reported work [25], Br-terminated polystyrenes and poly(methyl methacrylate)s (PMMAs) of low molar masses prepared by ATRP were reacted with C_{60} in chlorobenzene at around 100 °C using CuBr/2,2′-bipyridine as the catalytic system.

Under such conditions, the covalent C—Br bond is in equilibrium with the free radical form (Scheme 5.4a). The generated macro-radical adds to the fullerene (Scheme 5.4a) and a Br is located on the C_{60}. In all cases, an increase of the molar mass of the PS-C_{60}-Br or the PMMA-C_{60}-Br, determined by size exclusion chromatography (SEC) using a polystyrene calibration, was observed. The authors attributed this mass increase, of about 1000 g mol^{-1}, to the attached fullerene and concluded that mono-adducts were formed. However, the apparent molar mass of C_{60} measured by SEC (using toluene as the eluent) is considerably lower than its actual mass, much lower even than that of a styrene monomer [20, 26]. Therefore, this interpretation can be questioned and the experimental data point rather to the formation of di-adducts. The preferential formation of di-adducts using ATRA was demonstrated a year later [27] with PS-Br of larger molar masses and low polydispersities. Indeed, only two-arm stars and no detectable mono-adducts were obtained even when the C_{60} was in a ten-fold excess over PS-Br (Figure 5.1a).

The fact that no mono-adduct is observed under conditions where this product should be the only one formed points to a peculiar addition mechanism in which the addition of a second chain is highly favored once a first one is grafted. In addition, no Br could be found in the addition products, even when using very short PS chains [26]. This is reminiscent of the results reported for nitroxide-mediated addition (Scheme 5.3) [20, 21]. Such behavior is further confirmed by the observation that only tetra-adducts are formed if a ratio PS-Br/C_{60} equal to or larger then 4 is used (Figure 5.1b). In fact, whatever the stoichiometry of PSBr/C_{60} is, only

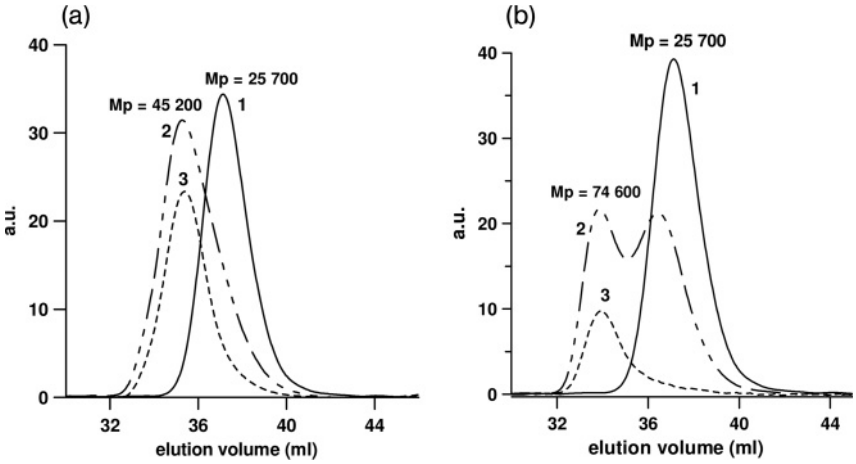

Figure 5.1 (a) SEC analysis of the addition product formed upon reacting 1 PSBr with 10 C_{60} in toluene at 100 °C for 53 h in the presence of CuBr/bipyridine: 1 – RI trace of the pristine PSBr (M_n = 19 600), 2 – RI trace of product, 3 – UV trace at 320 nm (where only fullerene-containing molecules are detected) of product [26]; (b) SEC analysis of the products formed upon reacting 8 PSBr with 1 C_{60} in toluene at 100 °C for 135.5 h in the presence of CuBr/bipyridine: 1 – RI trace of the pristine PSBr (M_{wLS} = 25 200), 2 – RI trace of products, 3 – UV trace at 320 nm of products (M_{wLS} = 87 000) (M_{wLS} mass determined by light scattering) [26].

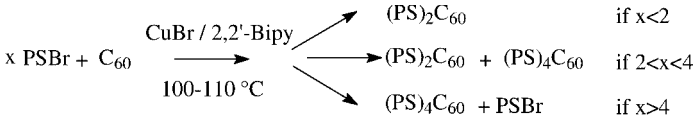

Scheme 5.5 Influence on the ratio PS-Br/C_{60} on the production of di- and tetra-adducts.

even numbers of PS chains are grafted to the fullerene using ATRA (Scheme 5.5) and, for each pair, the chains are attached at 1,4 positions on the same hexagon [26]. At this point it is important to stress that only one double bond is opened on the C_{60} core of a di-adduct $(PS)_2C_{60}$ and only two in tetra-adducts $(PS)_4C_{60}$, thereby keeping the perturbation of the electronic properties of the fullerene to a minimum.

The addition of an even number of arms is easily explained if one takes into account that a direct bond to C_{60} is generally less stable than the corresponding "normal" bond. In other words, the fullerene—Br bond formed after addition of the first macro-radical (Scheme 5.4a) is more easily converted into the radical form (Scheme 5.4b) than PS-Br. Therefore, the relative concentration of PS-$C_{60}^{\bullet}$ radicals is always much higher than the concentration of PS$^{\bullet}$, leading to a highly preferential recombination of PS$^{\bullet}$ with PS-$C_{60}^{\bullet}$ to produce the di-adduct (Scheme 5.4b). The formation of the tetra-adduct follows the same pathway once all the fullerenes are converted into $(PS)_2C_{60}$ (Scheme 5.4c).

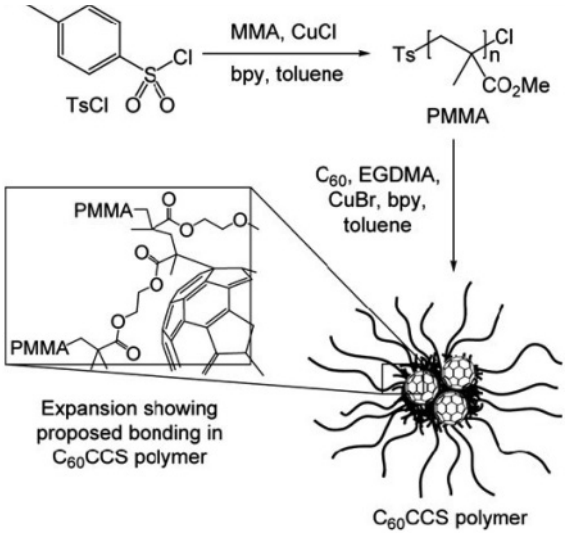

Scheme 5.6 Synthesis of C_{60} functionalized CCS polymer, including expansion, showing the proposed bonding of C_{60} to the crosslinked core [29].

The mechanism becomes more complicated in halogenated solvents. For example, a non-negligible amount of mono-adducts were observed in chlorobenzene [27], indicating their participation the ATRA reaction. The grafting of poly(methyl methacrylate) or poly(methacrylic acid) also shows some deviation from the above mechanism as the mono-adducts are favored [28]. That may be a consequence of the reactivity of the radicals stemming from these polymers.

C_{60}-functionalized core crosslinked polymer stars have been obtained via an arms-first approach. This preparation involves first the synthesis of poly(methyl methacrylate)-Cl by ATRP followed by crosslinking with a di-functional monomer (ethylene glycol dimethacrylate – EGDMA) in the presence of C_{60} under ATRA conditions (Scheme 5.6). The PMMA$^{\bullet}$ radicals react with the crosslinker via ATRP and then add to C_{60}. From the increase in molar mass determined by light scattering (LS) it was concluded that the resulting product is a star with a mean number of grafted arms around 30 and multiple molecules of C_{60} incorporated in its poly(EGDMA) core [29]. However, the actual number of arms, the size of the EGDMA micro-gel core and the number and electronic state (depending on the number of opened double bonds, i.e., grafts) of the incorporated C_{60} in each star is ill-defined.

Four-arm stars [poly(vinyl acetate)]$_4C_{60}$ have been prepared by cobalt-mediated radical polymerization of vinyl acetate (VAc) followed by addition of the PVAc-Co(acetylacetonate)$_2$ chains to the fullerene [30]. The photoactive water-soluble [poly(vinyl alcohol)]$_4C_{60}$ was then obtained by hydrolysis of the PVAc arms. Because

of their photoactivity and very low cytotoxicity, this type of water-soluble nanohybrid may be very promising for photodynamic cancer therapy.

5.2.1.3 Addition of Macro-radicals Obtained by Cleavage of Macro-initiators

Another way to separate the polymerization step from the addition onto the fullerene has been described in a recent paper [31]. First a macroazo initiator, PEO-R-N=N-R-PEO [with M_n of poly(ethylene oxide) being 550 or 2000 g mol^{-1}], was prepared by reacting 4,4′-azobis(4-cyanopentanoyl chloride) with PEO-Me. The macro-initiator was then cleaved at 70 °C in *o*-dichlorobenzene in the presence of C_{60} and the PEO$^{\bullet}$ macro-radicals added to the fullerene. Both a di-adduct $(PEO_{550})_2C_{60}$ and a tetra-adduct $(PEO_{550})_4C_{60}$ were obtained when the molar mass of the PEO was low but only a di-adduct $(PEO_{2000})_2C_{60}$ was formed for the longer polymer. Interestingly, in this case also only even numbers of chains are attached.

Therefore, it appears that the grafting of chains by pairs is a general rule for the addition of macro-radicals onto C_{60}.

5.2.2 Grafting via Nucleophilic Addition

5.2.2.1 Grafting of Neutral Nucleophiles

Amines can add to C_{60}. An early paper showed that up to 15 amine molecules may be added to the fullerene, but the hexa-adduct with the chains attached to the central double bond of the six pyracyclene unit constituting the C_{60} seems favored [32]. This addition has been used to graft C_{60} on poly(ethylene imine) and poly(4-{[(2-aminoethyl)imino]methyl}styrene) [33] or amine functionalized ethylene propylene terpolymer [34] to obtain side-chain fullerene polymers. Amino-terminated polystyrene with very narrow molar mass distributions, synthesized using anionic polymerization followed by end functionalization, can add to C_{60} to form multi-arm stars (Scheme 5.7). Even, if a ratio C_{60}/PS-NH_2 of 2 : 1 is used in order to favor the mono-adduct, about 20% of di-adducts as well as small amounts of higher adducts are obtained [35].

Fullerene core star-like polymers, with an average number of arms ranging from 2 to 6, have also been prepared through addition of monoaminopolyethers [36].

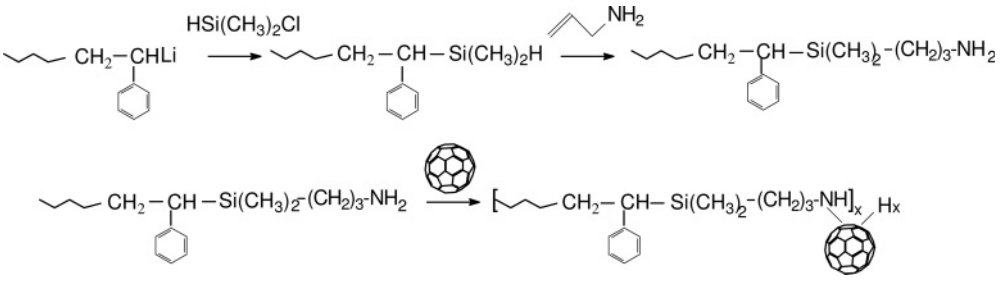

Scheme 5.7 Amine functionalization of a PSLi and grafting onto C_{60}.

Poly(vinylpyrrolidone)$_x$C$_{60}$ with $x \leq 10$ were obtained through grafting of poly(vinylpyrrolidone) chains bearing a terminal amino group [37, 38]. More recently, commercially available *o*-(2-aminoethyl)-*o*′-(2-hydroxyethyl)poly(ethylene glycol) (H_2NPEG) as well as specifically synthesized amino-poly(caprolactone) (H_2NPCL) were grafted onto C_{60}. H_xC_{60}(NPEG)$_x$ and H_xC_{60}(NPCL)$_x$ stars with an average of six grafted chains were obtained. These compounds can generate singlet oxygen upon photoactivation, making them promising materials for photodynamic therapy of tumors and treatment of multi-drug resistant pathogens [39]. When the poly(oxyethylene) or poly(oxypropylene) bear a NH_2 group at both ends the chain can add to two different fullerenes. As each C_{60} can react with several amine-terminated chains, the use of such α,ω-functional polymers leads to mixtures of architectures, where several fullerenes are linked together by chains, and ultimately to the formation of insoluble networks [40].

5.2.2.2 Grafting of Charged Nucleophiles

The tendency for carbanions to add onto 6-6 bonds was first demonstrated by reacting *tert*-butyllithium with C_{60} in a non-polar organic solvent [41, 42]. If the organolithium is used in excess, a mixture of adducts of various functionalities is obtained but no adduct higher than the hexa-adduct was observed. Considering these results, it was logical to try to graft "living" polystyrene-Li (PSLi) prepared through anionic polymerization initiated by *sec*-BuLi in a non-polar solvent. Indeed, not only the PSLi has a final carbanion that should be able to add to C_{60} but the molar mass of the polymer chain can be varied within a large range (from 100 up to $>10^6\,g\,mol^{-1}$) while keeping the polydispersity at a very low value [2]. Of all the polymerization methods, anionic polymerization allows us to get the closest possible to the ideal situation where all the chains have the same length. Therefore, the functionality of the star can be accurately determined by comparing its molar mass to that of the arm, providing that the mass of the star is determined by an absolute method such as light scattering (LS). Indeed, as a branched architecture is more compact in solution than a linear chain of same molar mass, the apparent molar mass of a star, determined by SEC using a linear PS calibration, is underestimated. In addition, this deviation varies with the number of arms [43].

The first (PS)$_x$C$_{60}$ stars, called flagellene, were prepared by reacting polystyryllithium with C_{60} in toluene following the synthetic route shown in Scheme 5.8 [44]. Mixtures of multi-adducts were obtained and analyzed by SEC. Using a UV/Vis detector set at a wavelength where only the fullerene-containing molecules are detected, it could be shown that the number of arms increases with the ratio PSLi/C_{60}. The maximum number of PS chains grafted onto the C_{60} was estimated to be in the range 4–10 and the amount of mono-adducts remained very low even if the fullerene was used in excess. This addition reaction of PSLi onto C_{60} in toluene has also been studied by other groups, who concluded that the product obtained was a mixture of tetra-, hexa- and octa-adducts [45] or even that the grafting is limited to two chains due to steric hindrance [46].

In an attempt to favor the mono-adduct, a polar solvent (THF) was added to the reaction media [47]. The aim was to break up the aggregates (PSLi)$_x$ that exist in

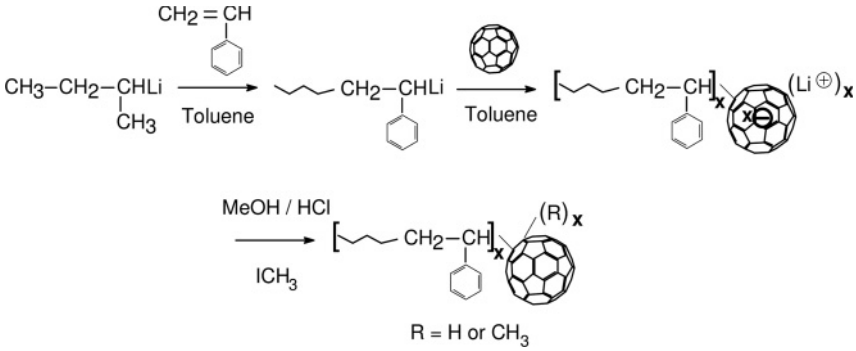

Scheme 5.8 Anionic polymerization of PSLi and addition onto C_{60} in a non-polar solvent.

non-polar solvents [48] and were supposed to be responsible for multiple additions. In fact, it is known that in non-polar solvents the aggregates $(PSLi)_x$ are in equilibrium with isolated PSLi and that only these latter can add to a double bond [2, 48]. Therefore, it could be anticipated that the dissociation of the aggregates by THF would not favor much the formation of mono-adducts, as confirmed by the experimental data [47]. However, the presence of a polar solvent has a much more disturbing effect: it favors electron transfer. As fullerenes are strong electron-acceptors, electron transfer from a carbanion to C_{60} can be expected in a polar solvent, leading to complex reactions.

The actual grafting mechanisms of anionic polymers onto C_{60} in polar and non-polar solvents have been established using high purity conditions: all experiments were performed in glass apparatus sealed under high vacuum, using the break-seal technique [2] and the C_{60} used was carefully purified [49–51].

5.2.2.2.1 **Grafting Mechanism in Polar Solvents** As mentioned above, with C_{60} being one of the best electron acceptors, the mechanism of the reaction between this fullerene and a "living" anionic polymer becomes complicated in a polar solvent like THF where both electron transfer and addition can occur. In THF, polystyrylpotassium (PS^-K^+), prepared through initiation by potassium 1-phenylethylide, has been reacted with C_{60} rather than PS^-Li^+ because of its better stability in polar solvents. By adding increasing amounts of PS^-K^+ to C_{60} it has been shown, using UV/Vis/NIR spectroscopy, that the fullerene is converted quantitatively first into the mono-anion $C_{60}^{\bullet-}K^+$ (Scheme 5.9a) and then to the dianion $C_{60}^{2-}(K^+)_2$ (Scheme 5.9b) through electron transfer from the carbanion. The $PS^\bullet$ radicals formed upon this electron transfer recombine and a polymer PS-PS with twice the molar mass of the arm but with no incorporated C_{60} is produced (Scheme 5.9a). When the ratio PS^-Li^+/C_{60} became higher than 2, no $C_{60}^{x-}(K^+)_x$ with $x > 2$ could be detected, but adducts with up to four chains were formed. Therefore, it appears that once all the fullerenes are converted into dianions their electron affinity is reduced enough to allow the addition reaction of the polystyryl carbanion onto a double bond of the fullerene to become predominant over electron transfer [51]

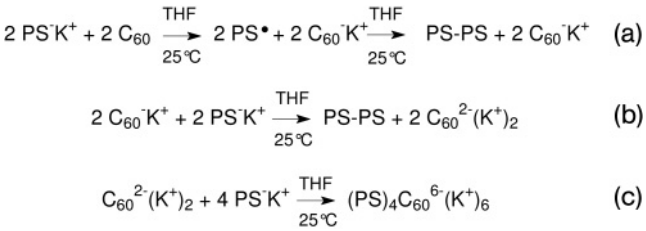

Scheme 5.9 Addition mechanism in THF: pure electron transfer from PS^-K^+ to C_{60} up to a total conversion into dianions $C_{60}^{2-}(K^+)_2$ followed by addition of four PS chains to this latter.

(Scheme 5.9c). The stars obtained under such condition are a mixture of $(PS)_xC_{60}^{(x+2)-}$ (with $x \leq 4$, depending on the ratio PSK/C_{60}) and PS-PS. After deactivation with MeOH or HCl, and separation of the PS-PS chains by polymer fractionation, $(PS)_xC_{60}(H)_{x+2}$ stars are obtained. Of course, if the "living" polymer and the fullerene are mixed at once the products are even less defined as electron transfer and addition interfere.

The electron transfer step can be completely separated from the addition step by reacting PS^-K^+ directly with $C_{60}^{2-}(K^+)_2$ prepared separately by electron transfer from potassium naphthalenide. This allows the preparation of pure tetra-adducts where the C_{60} core bears six negative charges [51], leading, after deactivation of the carbanions, to well-defined $(PS)_4C_{60}(H)_6$.

Through initiation by electron transfer from potassium naphthalenide to styrene in THF, α,ω-dicarbanionic "living" polystyrenes K^{+-}PS-PS$^-K^+$ can be prepared. By reacting these dicarbanionic chains with the plurifunctional C_{60} ($f > 3$) a network with fullerenes as the reticulation points is expected. Nevertheless, such a network is not obtained if K^{+-}PS-PS$^-K^+$ is mixed with C_{60}. In fact, to get a gel at least three chains need to be attached to each fullerene and the polymer chains have to remain perfectly dicarbanionic during all the addition reaction. This is not the case if electron transfer from a terminal carbanion to the fullerene occurs as it affords monocarbanionic chains and it is well known that addition of such chains to the reticulation points reduces drastically the mechanical strength of the network or even prevents its formation. Therefore, complete separation of electron transfer and addition is also necessary to produce networks through this route. Good quality polystyrene networks where each fullerene knot was linked to four PS chains have been prepared by reacting a dicarbanionic K^{+-}PS-PS$^-K^+$ with the dianion $C_{60}^{2-}(K^+)_2$ according to Scheme 5.10 [52].

This apparently complicated route toward networks is a consequence of the difficulty of preparing dicarbanionic chains in non-polar solvents due to the lack of well-defined difunctional initiators soluble in such solvents.

Electron transfer from carbanions to the fullerene occurs already when only a few percent of polar solvents are added to a non-polar one [51]. This limits the possibility of preparing well-defined star architectures through addition of "living"

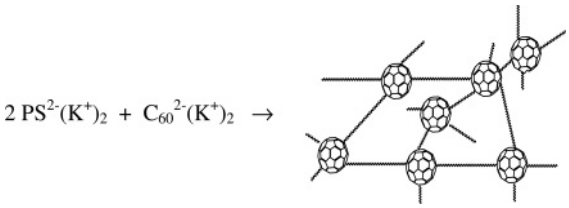

Scheme 5.10 Synthesis of networks with C_{60} knots through addition of dicarbanionic "living" polystyrene chains onto $C_{60}^{2-}(K^+)_2$ dianions in THF.

carbanionic polymer chains onto C_{60} or C_{70} [53] in the presence of polar solvents. Several "living" polymers, such as polyacrylonitrile [54], poly(vinylcarbazole) [55, 56], poly(*p*-methylstyrene) [57] and poly(*α*-methylstyrene) [58], have been reacted with C_{60} in pure non-polar solvents or mixtures containing polar solvents. Therefore, "star-happed" products were obtained but with no accurate determination of the actual number of arms or opened double bonds. Nevertheless, the poly(vinylcarbazole)$_x$C$_{60}$ stars (*x* estimated to about 3) have been used as the hole-transporting layer in an electroluminescent ITO/(PVK)3C60/CPDHFPV/liF/Al device (CPDHFPV = poly(9,9′-dihexylfluorene-2,7-divinylene-*m*-phenylenevinylene-*stat*-*p*-phenylenevinylene), resulting in quenching of the electroluminescence [56]. Conversely, when a new PVK layer was added the new device showed a three-fold improvement in the emitted light power.

The grafting of water-soluble chains like poly(ethylene oxide) (PEO) onto C_{60} by reacting this fullerene with a "living" PEO^-K^+ was also attempted in pure THF [59] or in mixed solvents [60]. Higher adducts were formed, but it was difficult to ascertain the actual functionality of the $(PEO)_xC_{60}$ stars. This determination is complicated by the tendency of fullerene functionalized PEO to aggregate. In fact, the grafting mechanism in THF is much more complicated as electron transfer from the oxanions of PEO^-K^+ to C_{60}, producing mono- and di-anions, has been demonstrated [59]. During this electron transfer, $PEO^•$ radicals are formed that can also add to C_{60} or its anions. In addition, ungrafted PEO chains could not be avoided and these are very difficult to remove. Therefore, no well-defined $(PEO)_xC_{60}$ stars could be produced.

Grafting conjugated polymers onto C_{60} is also an interesting issue as it should allow the association within a single molecule of an electron donor and an electron acceptor. Therefore, poly(phenyl vinyl sulfoxide)$^-K^+$ (PPVS – a precursor polymer for polyacetylene) and the block copolymer polystyrene-*b*-poly(phenyl vinyl sulfoxide)$^-K^+$ (PS-*b*-PPVS), prepared through anionic polymerization in THF, were reacted with C_{60}. Up to three PS-*b*-PPVS chains could be grafted to the fullerene and the PPVS converted into polyacetylene, producing a star shaped (PS-*b*-PA)$_3$C$_{60}$ [61]. The use of a polar solvent limits the control over the architecture of these stars. No charge transfer between the fullerene and the polyacetylene could be detected in these materials.

5.2.2.2.2 **Grafting Mechanism in Non-polar Solvents** In a non-polar solvent, where no electron transfer can take place, the reaction between PS^-Li^+ and C_{60} is a pure addition reaction of the terminal carbanion to one of the 30 double bonds of the fullerene (Scheme 5.8). It could be demonstrated that a maximum of six PSLi add to the C_{60} (Figure 5.2) as the molar mass of the adduct stays unchanged if the ratio PSLi/C_{60} is varied from 6.5 to 8; only the amount of ungrafted PSLi increases in the proportions expected from the stoichiometry assuming the formation of a pure hexa-adduct. In addition, the polydispersity of the stars ($M_w/M_n \leq 1.1$) is as low as or even lower than that of the starting PS, indicating that there is no mixture of functionality.

The formation of pure hexa-adducts when PSLi/C_{60} is higher than 6 was further confirmed by the fact that their molar masses (determined by LS) are six times that of the arms [49, 51, 62]. Six-arm stars with a C_{60} core and very high molar masses (over 2 million) could be obtained, thus excluding any steric limitation on the functionality [62].

The upper limit of six grafted chains when C_{60} is reacted with a "living" PSLi is a direct consequence of the specific shape of the C_{60} molecule and the fact that each addition introduces on the fullerene core a negative charge that delocalizes on the conjugated cage [49]. As illustrated in Scheme 5.11a, the carbanion on the fullerene is delocalized over the pyracyclene unit including in its center the double

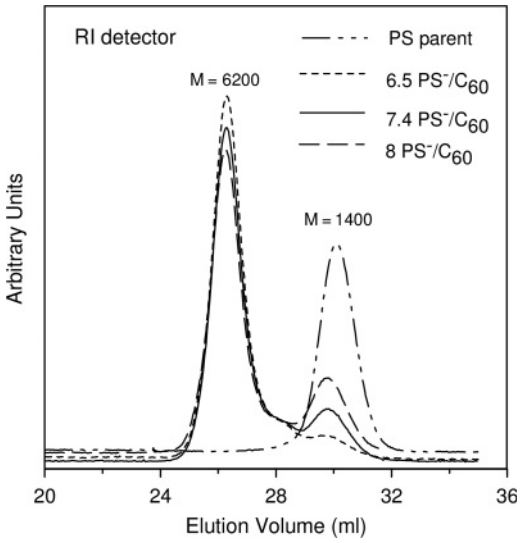

Figure 5.2 SEC characterization of the addition products obtained by reacting 6.5, 7.4 and 8 PSLi per C_{60}. The experimental amounts of ungrafted chains, deduced from the deconvolution of the RI traces of, respectively, 10, 17 and 22% compare well with the values expected from the stoichiometry, 7.7, 19 and 25% [51].

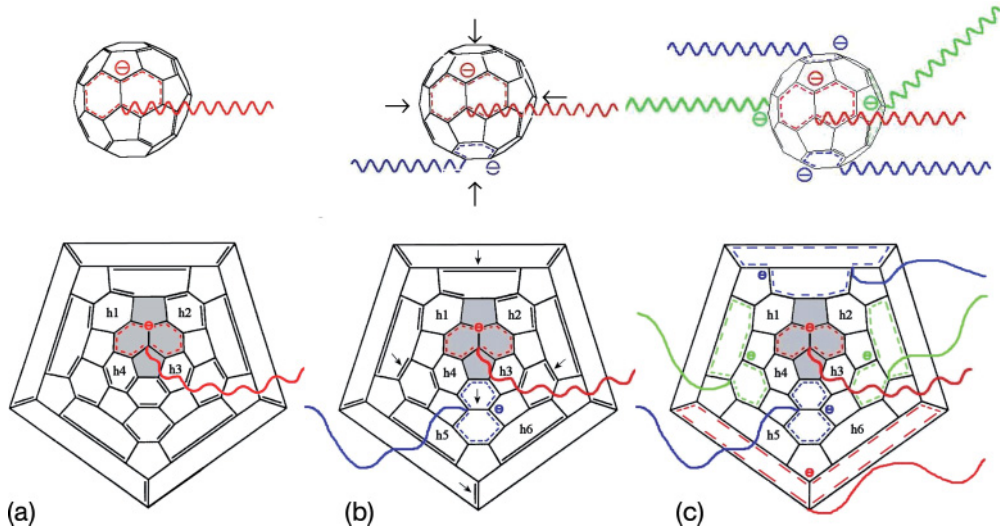

Scheme 5.11 Delocalization of the carbanions introduced on C_{60} upon addition of PSLi. Explanation of the upper limit of six grafted chains (see text).

bond to which the first PSLi adds, so that no further addition can take place on this part of the C_{60} molecule. Even the addition of a second "living" chain to one of the double bonds of the four adjacent hexagons h1, h2, h3, and h4 surrounding the pyracyclene unit is not likely as it would lead to strong interaction of the two negative charges. Considering the geometry of the C_{60}, the most favorable place for the second addition would be on the central double bond of one of the adjacent pyracyclenes (arrows in Scheme 5.11b).

Indeed, this allows the two carbanions introduced on the C_{60} to delocalize without direct interference (Scheme 5.11b). Once, a PSLi chain has attached to the central bond of the six pyracyclene units constituting the C_{60}, the whole conjugated fullerene molecule is covered by the six delocalized carbanions (Scheme 5.11c) and no further addition can take place. A theoretical approach for this grafting mechanism onto C_{60} has been proposed using a so-called "umbrella effect" that protects the double bonds surrounding the grafting point from further addition and taking into account the architecture of the fullerene. The calculations and computer simulations showed that conditions can be found where the hexa-adducts are highly favored [63].

Pure tri-, tetra-, penta- and hexa-adducts can be prepared simply by controlling the stoichiometry PSLi/C_{60} [50, 51]. Pure mono- or di-adducts could not be obtained through this route as the decrease of reactivity of C_{60} after the first and the second addition is not pronounced enough.

This specific addition mechanism allows us to prepare PS stars with exactly six arms and a C_{60} core just by using an excess of PSLi over the fullerene higher than

six. After quenching of the carbanions on the fullerene core by protonation, the ungrafted chains can be easily removed by classical polymer fractionation. The six-arm stars with a fullerene core obtained through this route are among the best-defined polymer star architectures reported. The dimensions of these hexa-adducts in solution are in good agreement with those expected for stars with six arms and, upon decreasing the molar mass of the arm, an evolution from a random coil type behavior towards that of a dense sphere can be observed [62]. Furthermore, it is possible to vary the molar mass of these stars over about three orders of magnitudes without changing their functionality. This enabled a detailed study of their conformation in dilute solution and the structural behavior in semi-dilute solution by small-angle neutron scattering, adding new knowledge in the field of physical chemistry of polymer stars [64]. The influence of the molar mass on the formation of membranes with a honeycomb pore organization upon evaporation of carbon disulfide solutions of $(PS)_6C_{60}$ in a humid atmosphere could also be demonstrated [65]. The photophysical [66], optical limiting and nonlinear optical properties [67, 68] of these stars have also been studied in solution and in the solid state as a function of molar mass and number of arms. The PS grafts prevent intermolecular interactions between the fullerene cores, leading to enhanced third-order NLO properties and an ultrafast NLO response [67]. However, PS is not the best matrix as the damage threshold is rapidly reached [68].

The grafting of PSLi in non-polar solvents has been extended to higher fullerenes like C_{70}, C_{84} and C_{96}. Despite a decrease in reactivity with size, star-shaped polymers were always obtained and in all cases the maximum number of grafts attached to the fullerene was found to be six [69]. This upper limit may be a consequence of the fact that the number of pentagons stays constant.

Grafting of other "living" anionic polymers has also been reported and it was found that the maximum number of grafted chains depends on the nucleophilicity of the terminal carbanion [51]. This behavior is not unexpected as the reactivity of the fullerene decreases with each addition. For example, for the carbanions isoprenyl and 1,3-cyclohexadienyl, which have about the same reactivity as the carbanion styryl, a maximum of six polyisoprene (PI) or poly(1,3-cyclohexadiene) chains are attached to the C_{60} upon reaction with, respectively, polyisoprenyllithium (PILi) [51, 70] and poly 1,3-cyclohexadienyllithium [71] in a non-polar solvent. Some other factors like steric effects or stability of the carbanion may interfere in this latter case, and a recent publication concluded that only four arms are attached, based on a ratio $M_{star}/M_{arm} = 4.37$ [72]. However, these molar masses were determined by SEC using linear PS standards and such a ratio is very close to what is expected for a six-arm star [43]. If the terminal carbanion is the more delocalized 1,1-diphenylethylyl, only three chains are grafted [51].

As mentioned above, stoichiometric control allows the preparation of tri-, tetra- and penta-adducts. With the upper limit of the number of grafts being six, it becomes possible to add, respectively, three, two or one additional PS or PI arms. This has been used to prepare asymmetric stars $(PS_a)_{6-n}C_{60}(PS_b)_n$ or mikto-arm stars $(PS)_{6-n}C_{60}(PI)_n$ by reacting such adducts of lower functionality with an excess of PSLi that has a different molar mass or with polyisoprenyllithium (Scheme 5.12) [73].

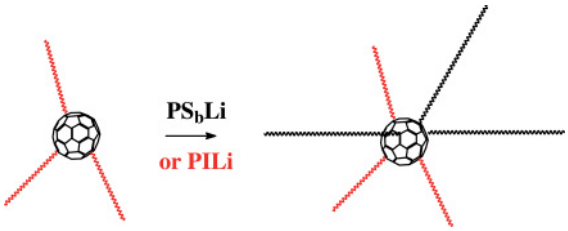

Scheme 5.12 A six-arm asymmetric star $(PS_a)_xC_{60}(PS_b)_{6-x}$ or mikto-arm star $(PS_a)_xC_{60}(PI)_{6-x}$ obtained by "saturation" of a polystyrene star $(PS_a)_xC_{60}$ with an excess of PS_bLi or PILi. The number of arms of the non-saturated star ($x < 6$) is controlled by adjusting the stoichiometry PS_a/C_{60}.

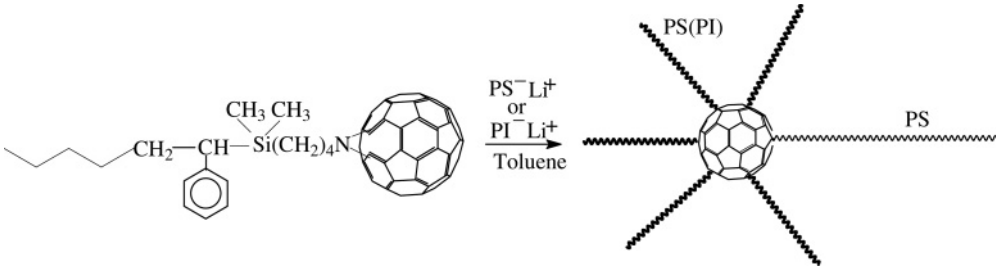

Scheme 5.13 A six-arm asymmetric star $(PS_a)C_{60}(PS_b)_5$ or mikto-arm star $(PS_a)C_{60}(PI)_5$ obtained by "saturation" of a mono-adduct PS-C_{60} with an excess of PS_bLi or PILi.

The same approach was used to add five additional PS or PI chains on a mono-adduct PS-C_{60} prepared by reacting the fullerene with an azide-terminated polystyrene (Scheme 5.13) [74].

This "saturation" of the C_{60} already attached to one or x chains ($x < 6$) by a "living" anionic polymer can be used in many cases. For example, respectively, five, four and two additional PS chains have been grafted on poly(methyl methacrylate)C_{60}, $(PS)_2C_{60}$ and $(PS)_4C_{60}$ prepared by atom transfer radical addition.

Another interesting possibility offered by the anionic polymerization is the synthesis of "living" block-copolymers that can be further attached to the fullerene. Six-arm star copolymers (PS-*b*-PI)$_6C_{60}$ or (PI-*b*-PS)$_6C_{60}$ [49, 66] as well as (PS_H-*b*-PS_D)$_6C_{60}$ [64] have been prepared and characterized. However, as the C_{60}-isoprene bond is rather unstable as compared to C_{60}-styrene [70], it is more appropriate to graft the copolymer chains by their PSLi end. A very interesting synthetic strategy has been used for the synthesis of star block copolymers [poly(1,4-phenylene)-*b*-PS]$_6C_{60}$ and (PS-*b*-PPP-styrene)$_6C_{60}$, incorporating in the same molecule conjugated poly(1,4-phenylene) (PPP) blocks and fullerenes [71]. "Living" block copolymers poly(1,3-cyclohexadiene)-*b*-PSLi (PCHD-*b*-PSLi) and PS-*b*-PCHD-

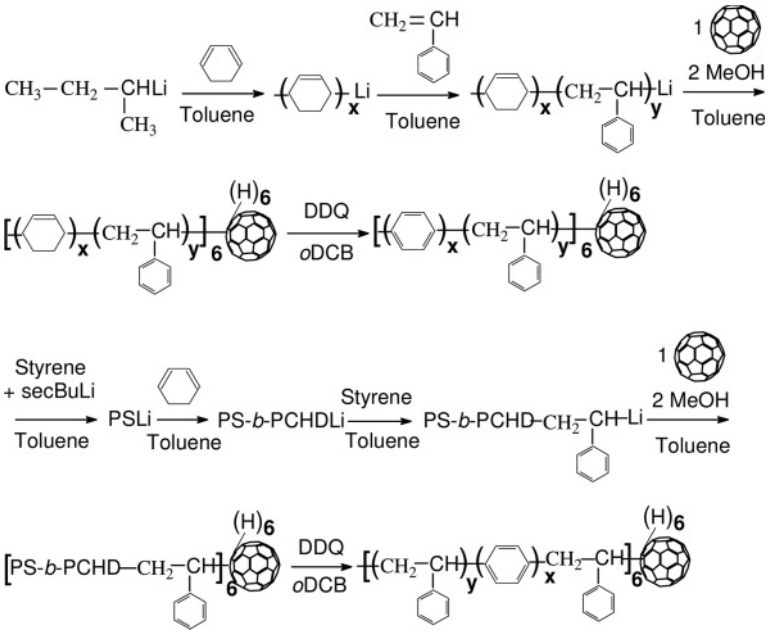

Scheme 5.14 Synthesis of $(PPP\text{-}b\text{-}PS)_6C_{60}$ and $(PS\text{-}b\text{-}PPP\text{-}styrene)_6C_{60}$.

styryllithium were first prepared through anionic copolymerization and then reacted in excess with C_{60} (Scheme 5.14). The stars were further oxidized with DDQ to afford $(PPP\text{-}b\text{-}PS)_6C_{60}$ and $(PS\text{-}b\text{-}PPP\text{-styrene})_6C_{60}$. These compounds showed an effective quenching of PPP fluorescence that was considered indicative for a charge transfer from the donor fragment PPP to the acceptor C_{60} despite the fact that six double bonds have been opened on the latter.

The most interesting aspect of block-copolymers made of two incompatible blocks is their self-organization in the solid state in order to minimize the interface between the incompatible domains. Depending on the respective molar masses of the blocks, various morphologies (spheres, hexagonal array of cylinders, gyroïd, lamellae) are formed [75]. The possibility of synthesizing well-defined homopolystyrene stars $C_{60}(PS)_f$ ($f = 2$, 4 and 6) as well as block-copolymer stars $C_{60}(PS\text{-b-PI})_6$ opens up new and interesting possibilities for the nanoscale organization of C_{60} in a polymer matrix.

The addition of homopolystyrene (hPS) to a diblock copolymer PS-b-PI can result in the selective solubilization of the hPS into the PS domains of the microphase separated structure of the diblock copolymer [76]. Following the same approach, homopolystyrene stars $C_{60}(PS)_x$ ($x = 2$, 4 and 6) have been selectively incorporated in the PS lamellae of a symmetric PS-b-PI copolymer, creating a periodic nanoscale organization of C_{60} in a copolymer matrix (schematized in Figure 5.3) with a typical lamellar periodicity D in the range 20–100 nm [77]. As

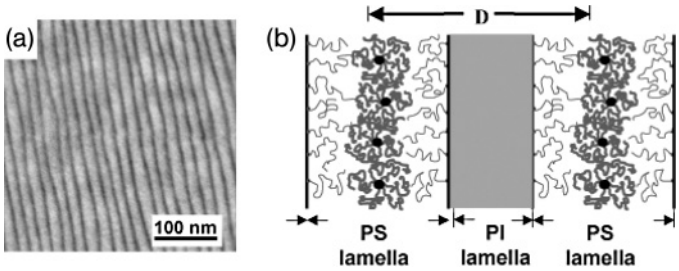

Figure 5.3 (a) TEM micrograph showing the swollen lamellar morphology of a PS_{30000}-b-PI_{30000} copolymer blended with 40 wt% of a $C_{60}(PS)_6$ star with $M_w = 18000\,g\,mol^{-1}$; (b) schematic view of the localized solubilization of the $C_{60}(PS)_6$ stars in the PS lamellae of the symmetric block copolymer. Note that the PI lamella appear dark (OsO_4 staining).

an example, the swollen lamellar morphology observed by transmission electron microscopy (TEM) for blends of a PS_{30000}-b-PI_{30000} copolymer with 40% wt of a $C_{60}(PS)_6$ star with $M_w = 18000\,g\,mol^{-1}$ is given in Figure 5.3.

This first approach involves blends of a structurating copolymer matrix and $C_{60}(PS)_x$ stars. However, no blending is necessary if a well-controlled number of PI-*b*-PS chains with low polydispersities are grafted through the PS sequence (for better stability) onto the C_{60} core like in (PI-*b*-PS)$_6C_{60}$ (Figure 5.4a). Indeed, these copolymer stars themselves self-assemble in bulk to form the various morphologies mentioned above, depending on the respective length of the two blocks. Furthermore, due to the symmetry of the (PI-*b*-PS)$_6C_{60}$ stars, the fullerene cores localize themselves towards the middle of the PS lamellae or cylinders. Figure 5.4 illustrates a lamellar structure (b), a hexagonal array of PS cylinders in a PI matrix (c) and a gyroïd structure with PS as the minor phase forming the two interpenetrating networks (d). In these organized polymer matrixes the fullerene cores of the stars are localized in the central plains of the PS lamellae, the central "threads" of the PS cylinders or of the two interpenetrated 3D PS channels [78]. The major benefit of this organization is the reduced inter-fullerene distances, despite the very low load of C_{60}.

5.2.3 Other Grafting Reactions

It has been reported that the reaction of azides with C_{60} proceeds primarily through mono-addition; this has been widely used to attach fullerenes onto the side chains of polymers or copolymers [79–81]. Star-shaped macromolecules were obtained when PS chains prepared by atom transfer radical polymerization were converted into PS-N_3 before reaction with C_{60}. Even so, the mono-adducts were predominant,

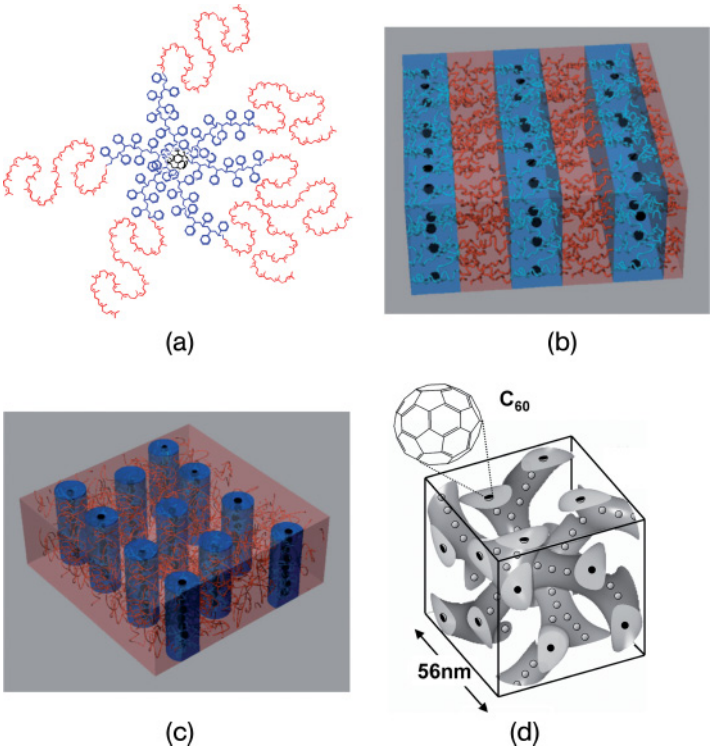

Figure 5.4 Schematic illustration of the organization and the location of the fullerene core for block copolymer stars $(PI\text{-}b\text{-}PS)_6C_{60}$ (a) as a function of the length of the two blocks; (b) lamellar morphology formed by $(PI_{25\,000}\text{-}b\text{-}PS_{25\,000})C_{60}$ – the fullerenes are located in the central plain of the PS lamellae; (c) hexagonal packing of PS cylinders in a PI matrix obtained with $(PI_{34\,000}\text{-}b\text{-}PS_{11\,000})C_{60}$ – the fullerenes are located in the central "threads" of the PS cylinders; (d) gyroïd structure showing the two interpenetrated PS networks in a PI matrix obtained with $(PI_{21\,000}\text{-}b\text{-}PS_{12\,000})C_{60}$ – the fullerenes are located in the central "threads" of the two interpenetrated PS channels.

although di-adducts were also formed [82]. The addition of monoazidopolyethers of various lengths onto C_{60} produced $(CH_3OPOE)_xC_{60}$ stars with up to seven arms. These compounds form stable emulsions of the water-in-oil type in a water/toluene system and show herbicidal activity [83]. By optimizing the experimental conditions and the stoichiometry, six poly(ε-caprolactone) (PCL) chains could be grafted onto C_{60}. These $(PCL)_6C_{60}$ generate singlet oxygen upon irradiation and could be encapsulated within the core of micelles formed by biocompatible block copolymers in water. Micro/nanosized polymer fibers could also be prepared with these biodegradable materials by electrospinning [84].

A well-defined C_{60}-anchored two-arm poly(*t*-butyl acrylate) has been synthesized by a Bingel cyclopropanation between a two-arm poly(*t*-butyl acrylate) with a

malonate ester core prepared via ATRP and C_{60} [85]. Even if this compound has two acrylate arms, it is actually a mono-adduct.

5.3 Polymerization of a Monomer Using Charged or Functionalized Fullerenes as Initiators

In the first reported polymerization by charged fullerenes, butadiene was initiated using C_{60}^{2+} and C_{70}^{2+} cations produced by electron bombardment of C_{60} and C_{70} vapor [86]. Mono- and di-adducts were formed by addition of up to five butadienes per positive charge. This work was further extended to the trications and, despite the complexity of the mechanisms involved, multiple additions of other monomers such as allene and propyne were observed [87].

5.3.1 Controlled Radical Polymerization Using a $C_{60}(X)_n$ as Initiator

Using $C_{60}(Cl)_n$ (n = 16 to 20) [88] as a multifunctional initiator under ATRP conditions (CuCl/2,2′-bipyridine, toluene, 130 °C), styrene [89] and *N*-vinylcarbazole [90] could be polymerized (Scheme 5.15). There is experimental evidence that the resulting compounds are star shaped, but the number and length of the arms or the number of residual Cl on the fullerene could not be determined. A thermal polymerization, producing a non-negligible amount of polymer containing no fullerene, is always observed. Nevertheless, the optical-limiting behavior of $(PVK)_yC_{60}(Cl)_{x-y}$ approached that of pristine C_{60} [90]. This work was further extended to a Ni-based ATRP catalyst system and it was estimated that about two PS arms were attached to $C_{60}(Cl)_n$ [91].

Star-like polystyrene, poly(methyl methacrylate) and their copolymers with maleic anhydride with a C_{60} core have been prepared using the "iniferter" controlled radical polymerization. The plurifunctional photoiniferter $C_{60}(SR)_x$ (SR = *N*,*N*-diethyldithiocarbamate groups) was prepared starting from a polyfunctional halogenated fullerene $C_{60}(X)_x$. Upon irradiation, the polymerization proceeds by a controlled radical mechanism [92]. However, the actual functionality of the photoiniferter, the number of RS groups participating in the polymerization as well as the number and length of the arms are not known.

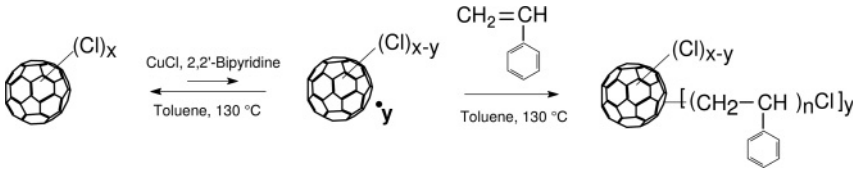

Scheme 5.15 ATRP of a monomer using $C_{60}(Cl)_n$ as a multi-functional initiator.

5.3.2
Anionic Polymerization Initiated by Fullerides $C_{60}^{x-}(M^+)_x$ or "Living" Polymer Stars with a Fullerene Core $(Polymer)_xC_{60}^{x-}(M^+)_x$ ($x \leq 6$; M = Li, Na, K)

Like radical polymerization in the presence of C_{60} (Scheme 5.1), anionic copolymerization of C_{60} with styrene or C_{70} with *p*-methylstyrene has been reported [93, 94]. In both cases, sodium naphthalenide in THF was used as the initiator. Fullerene-styrene copolymers were obtained, but their architectures are undefined, all that is known is that they are neither linear nor star like. In fact, the reaction is even more complex than in the case of radical initiation as, in addition to all the possible reactions, electron transfer from the naphthalene radical-anion to the fullerene also takes place, generating $C_{60}^{x-}(Na^+)_x$. Furthermore, because the PS chains generated by electron transfer from the naphthalene radical-anion are dicarbanionc, $Na^+{}^-PS^-Na^+$, the formation of highly branched structures or even micro-gels is favored.

Alkali metal salts of fullerenes $C_{60}^{x-}(M^+)_x$ were also tested as initiators for polymerization in polar solvents. Only the hexa-anion was able to initiate reactive monomers like methyl methacrylate, but not non-polar monomers like styrene. In all cases, the initiation proceeds through electron transfer to the monomer so that no fullerene is incorporated [95]. The reduced fullerenes initiate polymerization like classical radical anions or dianions of aromatic or conjugated molecules and therefore this synthetic route is of limited interest.

The carbanions present at the fullerene core of "living" $(PS)_xC_{60}^{x-}(Li^+)_x$ ($x \leq 6$) obtained through grafting of PSLi in non-polar solvents (I, 2, b2) offer much greater possibilities. If six carbanions are located on the fullerene core their delocalization is restricted and the negative charges become reactive enough to open the double bond of a vinyl monomer such as styrene, butadiene or isoprene [95]. But, as can be seen in Scheme 5.16, if one of the six carbanions adds to a monomer the negative charge leaves the fullerene, and the remaining charges become more delocalized [49]. In addition, it is well known that the reactivity of a carbanion

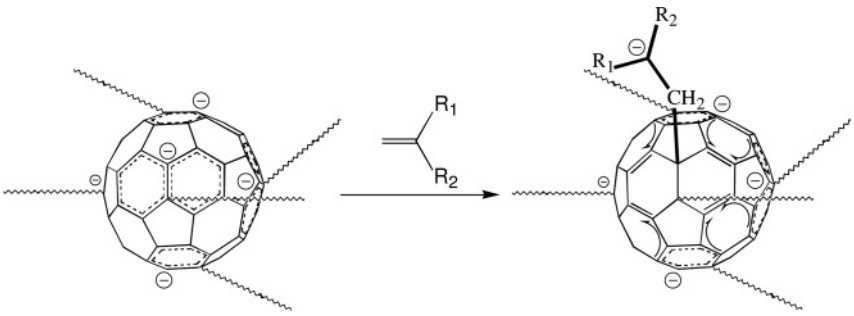

Scheme 5.16 Addition of a vinyl monomer onto one of the six carbanions on the C_{60} core of a "living" hexa-adduct and its consequences on the delocalization of the negative charges.

decreases if the delocalization of the charge increases. It was demonstrated that the reactivity of the five remaining carbanions is decreased enough so that they are no longer able to open the double bond of non-polar monomers like styrene, butadiene or isoprene [95]. Therefore, if one of these three monomers is added to a "living" hexa-adduct, only one chain grows out from the fullerene core [95, 96]. When a more reactive monomer like methyl methacrylate is used, two chains of PMMA grow out. Therefore, two carbanions have to leave the fullerene core before the four remaining become unable to open the double bond of this polar monomer [95]. As these additional chains are produced by anionic polymerization their polydispersity remains low and their molar mass can be controlled.

This very specific initiation mechanism, resulting from the fact that the six carbanions are located on the same conjugated molecule, is unique and was never encountered before in the in-out synthesis of stars by anionic polymerization. Indeed, in all other cases, the carbanions on the star core are separated by several single bonds so that they all have the same reactivity.

It therefore becomes possible to take advantage of this peculiar mechanism to prepare "palm-tree" like architectures where the C_{60} core bears six PS chains of the same length and an additional seventh chain of a different length or/and a different chemical nature (e.g., polyisoprene). Furthermore, as the out-growing chain bears a terminal carbanion more reactive than the five remaining on the core, it becomes possible to specifically couple two "palm-trees" with, for example, dibromo-*p*-xylene to form "dumbbell" type architectures where two six-arm PS stars with a fullerene core are linked together by a PS or a polyisoprene chain [97, 98]. Scheme 5.17 gives a schematic representation of these "palm-tree" and "dumbbell" architectures.

Hetero-stars $(PS)_6C_{60}(PMMA)_2$ could also be prepared [95]. A similar route has been used to produce $(PS)_xC_{60}(PMMA)_y$ but in the presence of THF. As electron transfer cannot be avoided in this polar solvent, the mechanism is more complicated and the formation of hetero-stars under such conditions may even be questioned. Nevertheless, these compounds have been used as a hole-injection layer in an electroluminescent device [99].

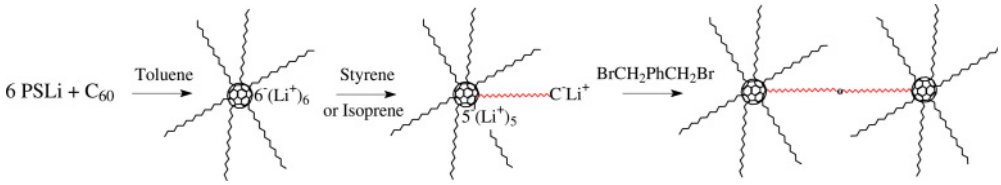

Scheme 5.17 Synthesis of a "palm tree" $(PS_a)_6C_{60}PS_b$ or $(PS_a)_6C_{60}PI$ by initiation of the anionic polymerization of styrene or isoprene with a "living" six-arm star $(PS_a)_6C_{60}^{6-}(Li^+)_6$ and of a "dumbbell" $(PS_a)_6C_{60}(PS_b)_2C_{60}(PS_a)_6$ or $(PS_a)_6C_{60}(PI)_2C_{60}(PS_a)_6$ upon coupling.

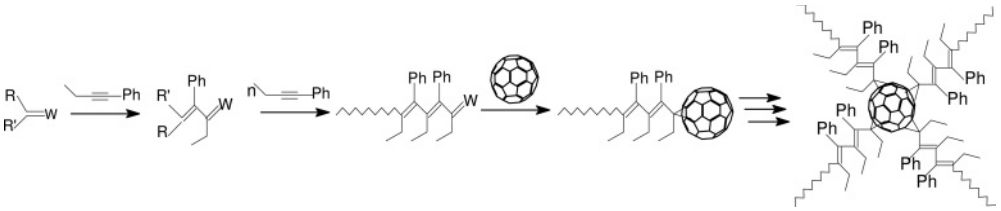

Scheme 5.18 Synthesis of star-shaped macromolecules by polymerization of 1-phenyl-1-butyne using WCl_6-Ph_4Sn as catalyst in the presence of C_{60}.

The influence of a polar solvent on the initiation mechanism has also been examined. If styrene is reacted with a "living" $(PS)_6C_{60}^{6-}(Li^+)_6$ in THF, no PS chain grows from the fullerene core. Nevertheless, PS with no incorporated C_{60} is produced [96, 100]. This points to an electron transfer from the carbanions located on the fullerene core to the monomer, followed by the classical dimerization of the so-formed ion-radicals to produce a growing di-anionic PS chain. More puzzling is the hypothesis put forward by these authors to explain some of their observations, that two arms may be released from the core of these "living" stars upon addition of THF [100].

5.3.3
C_{60} as Co-catalyst for Polymerization

C_{60} can act like a co-catalyst in the polymerization of disubstituted acetylenes using W-based catalysts. For example, only a 0.5% yield for the polymerization of 1-phenyl-1-propyne is obtained using WCl_6-Ph_4Sn while, in the presence of even small amounts of C_{60}, the yield was increased to 77%. The polydispersity of the polymer is also reduced drastically and the molar masses were increased. Scheme 5.18 shows the reaction sequence that produces a star-shaped polymer. Polymerization propagates via a tungstacarbene-mediated metathesis mechanism, and the polymeric chains are finally linked to C_{60} via a carbene addition to a double bond, producing a new cyclopropane ring. Notably, the polymer emits a strong blue light upon excitation – higher than that of pure polymer without fullerene [101, 102].

5.4
Addition of Linear Polymer Chains on Plurifunctional Fullerene Derivatives

Several parameters have to be taken into account for the preparation of well-defined stars by reacting suitably end-functionalized polymer chains with plurifunctional fullerene derivatives. The number of functional groups on these latter has to be precisely known and be the same on all the fullerene molecules, as the

actual number of opened double bonds determine their electronic properties. The molar mass of the chains should also be controlled and their polydispersity be low. In addition, the reactivity of all the functional groups on the fullerene should be, and remain, the same and their reaction with the end function of the chains should be complete. All these requirements are difficult to fulfill, setting a limit to the control of the stars prepared by this route.

Fullerenols containing multiple hydroxy groups $C_{60}(OH)_x$ (mean value of x is 10–18) are the most used multisubstituted fullerenes for the preparation of polymer stars. Commercial cycloaliphatic epoxy resins containing both epoxy and carbonyl functional groups in their structure have been reacted with $C_{60}(OH)_x$ (x = 15 − 18) in heterogeneous medium under alkaline conditions with tetrabutylammonium hydroxide (TBAH) as phase transfer catalyst (Scheme 5.19). Fullerene core ether connected epoxy star-like polymers with a mean number of around 8–10 grafts were obtained as insoluble, red-brown solid powders in high yield [103]. The number of grafted epoxy units as well as the residual unreacted OH functions on the fullerene core were estimated using thermal analysis [104].

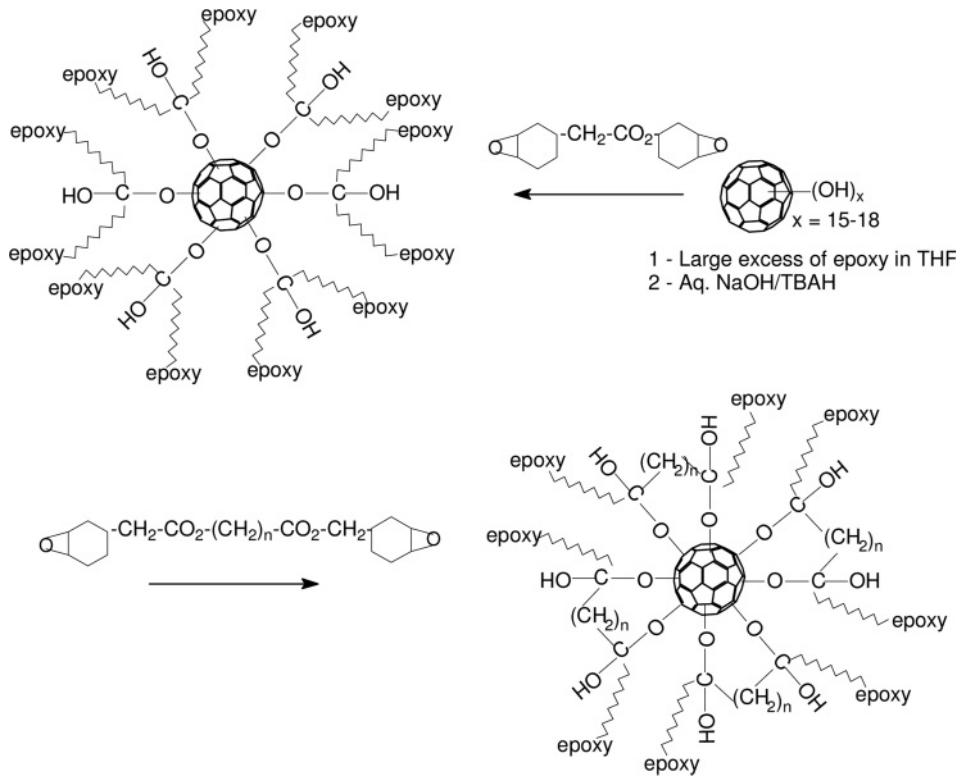

Scheme 5.19 Fullerene core ether connected epoxy star-like polymers obtained by reacting commercial cycloaliphatic epoxy resins with fullerenols.

Fullerenols with about 12 OH groups were also reacted with a diisocyanated polyether prepolymer ($M_n = 2000\,g\,mol^{-1}$, polydispersity 2.25). If the stoichiometry was adjusted to one equivalent of NCO per OH on the fullerenol, a hyper-crosslinked poly(urethane-ether) was obtained, as expected for a reaction between a difunctional polymer and a plurifunctional molecule. To limit the crosslinking and obtain soluble star-like products, an excess of the diisocyanated polyether was also used. The number of chains connected to the fullerene was estimated roughly to be six, based on the molar mass of the "star" [105, 106]. However, because the chains bear two NCO groups, coupling between two fullerenols can not be completely neglected so that the products are probably not just stars with a single C_{60} molecule.

A two-arm fullerene-containing poly(ethylene oxide) has been prepared by reacting fullerenols $C_{60}(OH)_{10-12}$ with a poly(ethylene oxide)-monoisocyanate in a 1:2 stoichiometry. The amphiphilic two-arm stars aggregate in polar solvents to form large spherical micelles containing an average of 540–1020 single polymer chains [107].

Fullerene-derived star-burst conjugated polymers have been prepared by nucleophilic substitution of the tertiary NO_2 groups (used as good leaving groups) of the hexanitrofullerene $C_{60}(NO_2)_6$ with aniline, oligoaniline, and polyaniline [108, 109].

Photo-excitation of the hexa(oligoanilino)[60]fullerene leucoemeraldines induced intramolecular electron-transfer from benzenoid moieties of oligoaniline arms to the C_{60} cage, which regenerated the emeraldine structure in oligoaniline arms. This substantiated the capability of the fullerene cage to accept multiple electrons during the irradiation process [110]. However, this conclusion is a little surprising considering the number of opened double bonds on the fullerene and the resulting decrease in its electron affinity.

A dumbbell like architecture where two C_{60}s, each bearing five hexadecaanilines, are connected by a poly(dimethylsiloxane) chain could be obtained using the same chemistry (Scheme 5.20) [110, 111]. To try to avoid addition of more than one NH_2 to the plurifunctional $C_{60}(NO_2)_6$, and so the formation of crosslinked

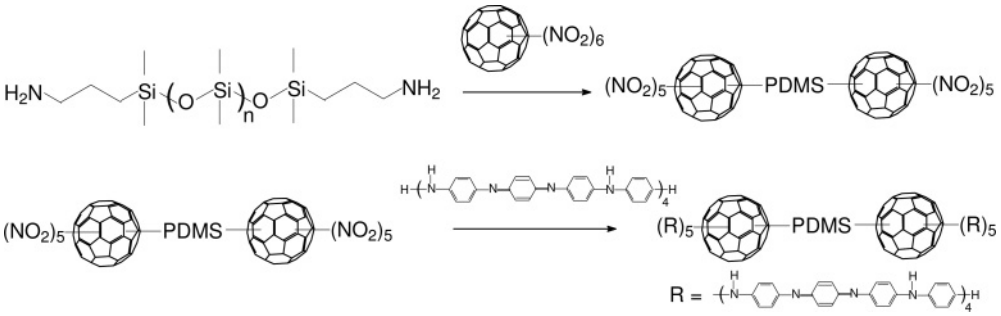

Scheme 5.20 Synthesis of a dumbbell type polymer by reacting $C_{60}(NO_2)_6$ successively with bis(3-aminopropyl)-poly(dimethylsiloxane) and with hexadecaaniline.

products where more than two fullerenes are connected through the difunctional bis(3-aminopropyl) poly(dimethylsiloxane) chains, dilute reaction conditions were used. The five remaining NO_2 on each terminal fullerene on the dumbbell were further used to graft five hexadecaanilines [112].

5.5 Stability of the C_{60}–Polymer Link

Owing to the presence of a C_{60} core, the stars described in this chapter may be of interest in many fields (optical limiting, NLO, photovoltaics, plastic electronics, cancer therapy, etc.) as already pointed out in the text above. However, for applications in most of these fields the thermal stability of these materials is a crucial issue. For this reason the thermal stability of both mixtures of various polymers with pristine C_{60}, and polymers where the chains are chemically grafted onto the fullerene, has been studied.

Several reports indicate that the introduction of pristine C_{60} in polymers increases their thermal stability [111] and has a retarding effect on their thermo-oxidative degradation [112–114]. As these degradation reactions follow radical mechanisms, unsurprisingly the presence of a very good radical acceptor like C_{60} has a beneficial effect.

The situation becomes very different if the fullerene is covalently bonded to a polymer chain. Indeed, a decreased thermal stability of polystyrene (PS) containing covalently attached fullerenes has been reported and attributed to a preferential breaking of the chain—C_{60} bond [115, 116]. Thermogravimetric analysis (TGA) has shown that the thermal decomposition of a PS star with a C_{60} core starts at about 100 °C before that of linear PS and that the thermal decomposition occurs in two steps. In addition, analysis of the volatile products by mass spectroscopy proves that styrene is produced in the low (around 350 °C) and in the high (around 500 °C) temperature domains whereas all the C_{60} is released during the low temperature step (Figure 5.5) [116–118].

That implies that all the PS—C_{60} bonds are broken in the low temperature step, confirming that they are less stable than the C—C bonds in the polystyrene chain. Therefore, the decomposition mechanism can be rationalized by taking into account the well-known thermal decomposition of PS through a radical initiated depolymerization (Scheme 5.21).

Well-defined six-arm polystyrene stars $(PS)_6C_{60}$ prepared through grafting of "living" PSLi, having very narrow polydispersities, offer a unique opportunity to study in more detail the thermal stability of the polymer–C_{60} link. Indeed, heating a toluene solution of $(PS)_6C_{60}$ at around 100 °C for several days leads to a progressive decrease of the molar mass of the star along with a quantitative release of the PS arms and no changes in the molar mass of these latter. This confirms that the polymer–C_{60} link is the weakest bond in the star and proves that the degradation reaction follows a stepwise "breaking" mechanism in which the six-arm star is first converted into a five-arm star and so on, down to C_{60} (Scheme 5.22). The

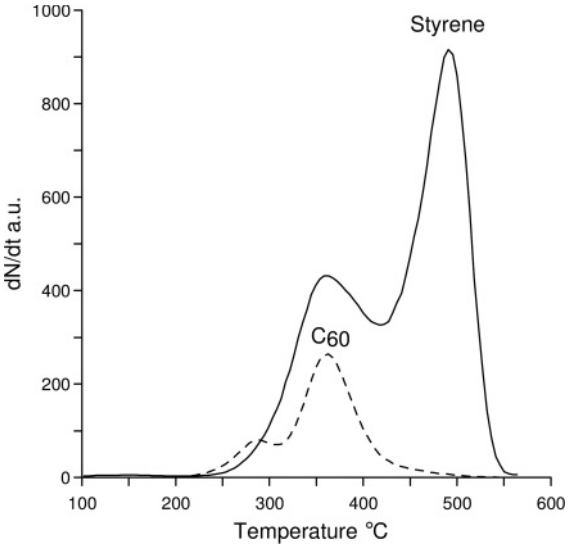

Figure 5.5 Release of styrene and C_{60} upon heating a $(PS_{3400})_6C_{60}$ film at 10 K s^{-1} (products analyzed by mass spectroscopy) [117].

Low temperature step :

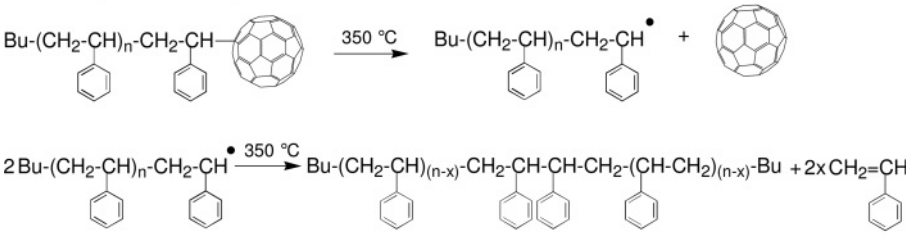

High temperature step :

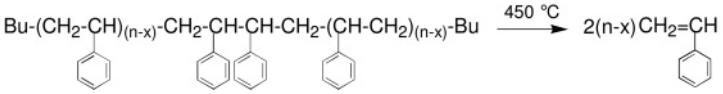

Scheme 5.21 Thermal degradation mechanism for $(PS)_6C_{60}$.

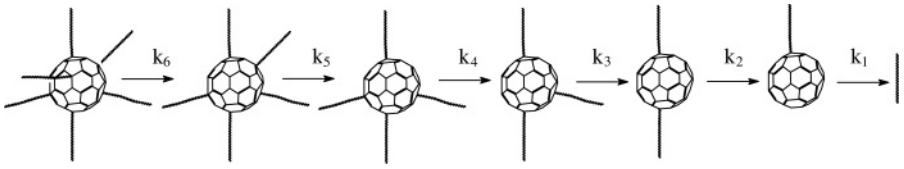

Scheme 5.22 Step wise thermal degradation mechanism of $(PS)_6C_{60}$ stars.

kinetics of the various steps in the cleavage of the polymer–C_{60} links could even be determined [119, 120].

The stability of the polymer–C_{60} link depends also on the chemical nature of the attached polymer. For example, the release of arms from copolymer stars (PS-*b*-PI)$_6C_{60}$, in which a polyisoprene chain is directly attached to the fullerene, has been observed upon storing at room temperature [70]. Furthermore, the relative weakness of the C—C_{60} bonds has been observed when stars with a fullerene core were subject to chemical reactions. For example, a poly(1,3-cyclohexadiene) can be converted into poly(*p*-phenylene) using 2,3-dichloro-5,6-dicyano-1,4-benzoquinone (DDQ) (Scheme 5.14). However, if the poly(1,3-cyclohexadiene) chains are attached directly to the fullerene, as in [poly(1,3-cyclohexadiene)]$_xC_{60}$, this reaction leads to the release of all the arms from the fullerene core [72].

Therefore, it may be wise to check the stability of fullerene-polymer adducts before considering these materials for applications where thermal stability is important.

5.6 Conclusions

Star-shaped macromolecules with a fullerene core combine in a single macromolecule the specific properties of fullerenes with the well known advantages of polymers. Therefore, these materials may find applications in many fields (optical limiting, NLO, photovoltaics, plastic electronics, cancer therapy, etc.). In addition, they can be prepared through a large variety of chemical routes. However, only a few allow for the preparation of pure adducts where a precise number of chains of a predetermined length and low polydispersity are grafted onto C_{60}. Such a control is necessary to obtain well-defined materials in which all the fullerene cores are in the same electronic state (i.e., the same number of opened double bonds) and the inter-fullerene distances are adjustable.

References

1 Giacalone, F. and Martin, N. (2006) *Chem. Rev.*, **106**, 5136–90.
2 Szwarc, M. (1968) *Carbanions, Living Polymers and Electron Transfer Processes*, John Wiley & Sons, Inc., New York.
3 Braunecker, W.A. and Matyjaszewski, K. (2007) *Prog. Polym. Sci.*, **32**, 93–146.
4 Krusic, P.J., Wasserman, E., Keizer, P.N., Morton, J.R. and Preston, K.F. (1991) *Science*, **254**, 1183–5.
5 Loy, D.A. and Assink, R.A. (1992) *J. Am. Chem. Soc.*, **114**, 3977–8.
6 Bunker, C.E., Lawson, G.E. and Sun, Y.P. (1995) *Macromolecules*, **28**, 3744–6.
7 Cao, T. and Webber, S.E. (1995) *Macromolecules*, **28**, 3741–3.
8 Camp, A.G., Lary, A. and Ford, W.T. (1995) *Macromolecules*, **28**, 7959–61.
9 Sun, Y.P., Lawson, G.E., Bunker, C.E., Johnson, R.A., Ma, B., Farmer, C., Riggs, J.E. and Kitaygorodskiy, A. (1996) *Macromolecules*, **29**, 8441–8.
10 Cao, T. and Webber, S.E. (1996) *Macromolecules*, **29**, 3826–30.

11 Arsalani, N. and Geckeler, K.E. (1996) *Fullerene Sci. Technol.*, **4**, 897–910.
12 Stewart, D. and Imrie, C.T. (1996) *Chem. Commun.*, 1383–4.
13 Chen, Y. and Lin, K.C. (1999) *J. Polym. Sci. A, Polym. Chem.*, **37**, 2969–75.
14 Ford, W.T., Graham, T.D. and Mourey, T.H. (1997) *Macromolecules*, **30**, 6422–9.
15 Ford, W.T., Nishioka, T., McCleskey, S.C., Mourey, T.H. and Kahol, P. (2000) *Macromolecules*, **33**, 2413–23.
16 Nayak, P.L., Yang, K., Dhal, P.K., Alva, S., Kumar, J. and Tripathy, S.K. (1998) *Chem. Mater.*, **10**, 2058–2066.
17 Jiang, G. and Zheng, Q. (2005) *J. Appl. Polym. Sci.*, **97**, 2182–5.
18 Morton, J.R., Preston, K.F., Krusic, P.J., Hill, S.A. and Wasserman, E. (1992) *J. Phys. Chem.*, **96**, 3576–8.
19 Wang, C.C., He, J.P., Fu, S.K., Jiang, K.J., Cheng, H.Z. and Wang, M. (1996) *Polym. Bull.*, **37**, 305.
20 Okamura, H., Terauchi, T., Minoda, M., Fukuda, T. and Komatsu, K. (1997) *Macromolecules*, **30**, 5279–84.
21 Ford, W.T. and Lary, A. (2001) *Macromolecules*, **34**, 5819–26.
22 Okamura, H., Ide, N., Minoda, M., Komatsu, K. and Fukada, T. (1998) *Macromolecules*, **31**, 1859–65.
23 Okamura, H., Takemura, T., Tsunooka, M. and Shirai, M. (2004) *Polym. Bull.*, **52**, 381–91.
24 Okamura, H., Minoda, M., Fukada, T., Miyamoto, T. and Komatsu, K. (1999) *Macromol. Rapid Commun.*, **20**, 37–40.
25 Zhou, P., Chen, G.Q., Hong, H., Du, F.S., Li, Z.C. and Li, F.M. (2000) *Macromolecules*, **33**, 1948–54.
26 Audouin, F., Nuffer, R. and Mathis, C. (2004) *J. Polym. Sci. A: Polym. Chem.*, **42**, 3456–63.
27 Audouin, F., Nunige, S., Nuffer, R. and Mathis, C. (2001) *Synth. Met.*, **121**, 1149–50.
28 Ravi, P., Dai, S., Tan, C.H. and Tam, K.C. (2005) *Macromolecules*, **38**, 933–9.
29 Blencowe, A., Kit, G.T., Best, S.P. and Qiao, G.G. (2008) *Polymer*, **49**, 825–30.
30 Detrembleur, C., Stoilova, O., Bryaskova, R., Debuigne, A., Mouithys-Mickalad, A. and Jérôme, R. (2006) *Macromol. Rapid. Commun.*, **27**, 498–504.
31 Wakai, H., Shinno, T., Yamauchi, T. and Tsubokawa, N. (2007) *Polymer*, **47**, 1972–80.
32 Hirsh, A., Li, Q. and Wudl, F. (1992) *Angew. Chem. Int. Ed. Engl.*, **30**, 1309–10.
33 Geckeler, K.E. and Hirsch, A. (1993) *J. Am. Chem. Soc.*, **115**, 3850–1.
34 Patil, O., Schriver, G.W., Carstensen, B. and Lundberg, R.D. (1993) *Polym. Bull.*, **30**, 187–90.
35 Weis, C., Friedrich, C., Mülhaupt, R. and Frey, H. (1995) *Macromolecules*, **28**, 403–5.
36 Delpeux, S., Beguin, F., Manolova, N. and Rashkov, I. (1999) *Eur. Polym. J.*, **35**, 1619–28.
37 Ryumtsev, E.I., Evlamieva, N.P., Nazarava, O.V., Bokov, S.N. and Panarin, E.F. (2003) *Dokl. Phys. Chem. (Engl. Transl.)*, **392**, 231–4.
38 Pavlov, G.M., Nazarava, O.V., Ebel, C., Mikhailova, N.A., Zaitseva, I.I., Bokov, S.N., Litvinova, L.S., Afanas'eva, E.V., Korneeva, E.V. and Panarin, E.F. (2005) *Russ. J. Appl. Chem.*, **78**, 130–6.
39 Stoilova, O., Jérôme, C., Detrembleur, C., Mouithys-Mickalad, A., Manolova, N., Rashkov, I. and Jérôme, R. (2007) *Polymer*, **48**, 1835–43.
40 Manolova, N., Rashkov, I., Van Damme, H. and Beguin, F. (1994) *Polym. Bull.*, **33**, 175–82.
41 Hirsh, A., Soi, A. and Karfunkel, H.R. (1992) *Angew. Chem. Int. Ed. Engl.*, **31**, 766–8.
42 Fagan, P.J., Krusic, P.J., Evans, D.H., Lerke, S.A. and Johnston, E.J. (1992) *J. Am. Chem. Soc.*, **114**, 9697–9.
43 Tsitsilianis, C. and Ktoridis, A. (1994) *Macromol. Rapid Commun.*, **15**, 845–50.
44 Samulski, E.T., DeSimone, J.M., Hunt, M.O., Menceloglu, Y. Jr., Jarnagin, C., York, G.A., Labat, K.B. and Wang, H. (1992) *Chem. Mater.*, **4**, 1153–7.
45 Zgonnik, V.N., Melenevskaya, E.Y., Litvinova, L.S., Kever, E.E., Vinogradova, L.V. and Terent'eva, I.V. (1996) *Polym. Sci. Ser. A*, **38**, 203–9.
46 Wang, C., Pan, B., Fu, S., Jiang, K., Chen, H. and Wang, M. (1996) *Macromol. Chem. Phys.*, **197**, 3783–90.
47 Wignall, G.D., Affholter, K.A., Bunick, G.J., Hunt, M.O., Menceloglu, Y.Z.,

DeSimone, J.M. and Samulski, E.T. (1995) *Macromolecules*, **28**, 6000–6.
48 Hsieh, H.L. and Quirk, R.P. (1996) *Anionic Polymerization: Principles and Practical Applications*, Marcel Dekker, Inc, New York.
49 Mathis, C., Schmaltz, B. and Brinkmann, M. (2006) *C. R. Chim.*, **9**, 1075–84.
50 Ederlé, Y. and Mathis, C. (1996) *Fullerene Sci. Technol.*, **4**, 1177–93.
51 Ederlé, Y. and Mathis, C. (1997) *Macromolecules*, **30**, 2546–55.
52 Nuffer, R., Ederlé, Y. and Mathis, C. (1999) *Synth. Met.*, **103**, 2376–7.
53 Chen, Y., Wang, J., Lin, Y., Cai, R. and Huang, Z. (2000) *Polymer*, **41**, 1233–6.
54 Chen, Y., Huang, W.S., Huang, Z., Cai, R., Yu, H., Chen, S. and Yan, X.M. (1997) *Eur. Polym. J.*, **33**, 823–8.
55 Chen, Y., Yang, D., Yan, X., Huang, Z., Cai, R., Zhao, Y. and Chen, S. (1998) *Eur. Polym. J.*, **34**, 1755–62.
56 Park, J.H., Park, O.O., Kim, J., Yu, J.-W., Kim, J.K. and Kim, Y.C. (2004) *Curr. Appl. Phys.*, **4**, 659–62.
57 Chen, Y., Wang, J.-X., Yu, B.-C., Cai, R.-F., Huang, Z.-E. and Zhang, J.-M. (1999) *J. Phys. Chem. Solids*, **60**, 949–56.
58 Yu, B.-C., Chen, Y., Cai, R.-F., Huang, Z.-E. and Xiao, Y.-W. (1997) *Eur. Polym. J.*, **33**, 1049–56.
59 Ederlé, Y., Mathis, C. and Nuffer, R. (1997) *Synth. Met.*, **86**, 2287–8.
60 Vinogradova, L.V., Melenevskaya, E.Y., Kever, E.E., Shibaev, L.A., Antonova, T.A. and Zgonnik, V.N. (1997) *Polym. Sci. Ser. A*, **39**, 1149–54.
61 Reibel, D. and Mathis, C. (1995) *Synth. Met.*, **70**, 1449–50.
62 Webber, V., Duval, M., Ederlé, Y. and Mathis, C. (1997) *Carbon*, **36**, 839–42.
63 Kuchanov, S., Pizik, I. and Ivanov, V. (2004) *Macromol. Theory Simul.*, **13**, 230–40.
64 Picot, C., Audouin, F. and Mathis, C. (2007) *Macromolecules*, **40**, 1643–56.
65 François, B., Ederlé, Y. and Mathis, C. (1999) *Synth. Met.*, **103**, 2362–3.
66 Janot, J.M., Eddaoudi, H., Seta, P., Ederlé, Y. and Mathis, C. (1999) *Chem. Phys. Lett.*, **302**, 103–7.
67 Koudoumas, E., Konstantaki, M., Mavromanolakis, A., Couris, S., Ederlé, Y., Mathis, C., Seta, P. and Leach, S. (2001) *Chem. Phys. Lett.*, **335**, 533–8.
68 Venturini, J., Koudoumas, E., Couris, S., Janot, J.M., Seta, P., Mathis, C. and Leach, S. (2002) *J. Mater. Chem.*, **12**, 2071–6.
69 Nuffer, R., Bartl, A., Dunsch, L. and Mathis, C. (2001) *Synth. Met.*, **121**, 1151–2.
70 Pantazis, D., Pispas, S. and Hadjichristidis, N. (2001) *J. Polym. Sci. A: Polym. Chem.*, **39**, 2494–507.
71 Mignard, E., Hiorns, R.C. and Francois, B. (2002) *Macromolecules*, **35**, 6132–41.
72 Natori, I. and Natori, S. (2008) *J. Polym. Sci. A: Polym. Chem.*, **46**, 3282–93.
73 Audouin, F., Renouard, T., Schmaltz, B., Nuffer, R. and Mathis, C. (2005) *Polymer*, **46**, 8519–27.
74 Ederlé, Y. and Mathis, C. (1998) *Macromol. Rapid Commun.*, **19**, 543–7.
75 Khandpur, A.K., Förster, S., Bates, F.S., Hamley, I.W., Ryan, A.J., Bras, W., Almdal, K. and Mortensen, K. (1995) *Macromolecules*, **28**, 8796–806.
76 Winey, J.I., Thomas, E.L. and Fetters, L.J. (1991) *Macromolecules*, **24**, 6182–8.
77 Schmaltz, B., Brinkmann, M. and Mathis, C. (2004) *Macromolecules*, **37**, 9056–63.
78 Schmaltz, B., Mathis, C. and Brinkmann, M. (2009) *Polymer*, **50**, 966–72.
79 Hawker, C.J. (1994) *Macromolecules*, **27**, 4836–7.
80 Richard, F., Brochon, C., Ngov, C., van de Wetering, K., Hadziioannou, G., Anokhin, D.V. and Ivanov, D.I.A. (2008) *Macromolecules*, **41**, 2701–10.
81 Lu, Z.H., Goh, S.H. and Lee, S.Y. (1997) *Polym. Bull.*, **39**, 661–7.
82 Li, L., Wang, C., Long, Z. and Fu, S. (2000) *J. Polym. Sci. A: Polym. Chem.*, **38**, 24519–23.
83 Delpeux, S., Beguin, F., Benoit, R., Erre, R., Manolova, N. and Rashkov, I. (1998) *Eur. Polym. J.*, **34**, 905–15.
84 Stoilova, O., Jérôme, C., Detrembleur, C., Mouithys-Mickalad, A., Manolova, N., Rashkov, I. and Jérôme, R. (2006) *Chem. Mater.*, **18**, 4917–23.
85 Chu, C.-C., Wang, L. and Ho, T.-I. (2005) *Macromol. Rapid Commun.*, **26**, 1179–84.

86 Wang, J., Javahery, G., Petrie, S. and Bohme, D.K. (1992) *J. Am. Chem. Soc.*, **114**, 9665–6.

87 Baranov, V., Wang, J., Javahery, G., Petrie, S., Hopkinson, A.C. and Bohme, D.K. (1997) *J. Am. Chem. Soc.*, **119**, 2040–6.

88 Olah, G.A., Bucsi, I., Lambert, C., Aniszfeld, R., Trivedi, N.J., Sensharma, D.K. and Surya Prakash, G.K. (1991) *J. Am. Chem. Soc.*, **113**, 9385–7.

89 Hua, J., Chen, D., Xu, L., Liu, Q., Jing, X. and Zhang, Y. (2002) *J. Appl. Polym. Sci.*, **86**, 3001–4.

90 Hua, J., Yang, W., Zhu, Y., Guo, Z., Yang, H., Xu, L. and Chen, D.-B. (2005) *Mater. Lett.*, **59**, 644–7.

91 Hua, J., Yang, H., Guo, Z., Xu, L. and Chen, D. (2005) *J Appl. Polym. Sci.*, **98**, 1215–18.

92 He, J.-D., Wang, J., Li, S.-D. and Cheung, M.-K. (2001) *J Appl. Polym. Sci.*, **81**, 1286–90.

93 Chen, Y., Zhao, Y., Cai, R., Huang, Z.-E. and Xiao, L. (1998) *J. Polym. Sci. B: Polym. Phys.*, **36**, 2653–63.

94 Shen, J., Chen, Y., Cai, R. and Huang, Z.-E. (2000) *Polymer*, **41**, 9291–8.

95 Ederlé, Y. and Mathis, C. (1997) *Macromolecules*, **30**, 4262–7.

96 Vinogradova, L.V., Amsharov, K.Y., Kever, E.E. and Zgonnik, V.N. (2003) *Polym. Sci. Ser. A*, **45**, 759–64.

97 Ederlé, Y. and Mathis, C. (1999) *Macromolecules*, **32**, 554–8.

98 Mathis, C., Ederlé, Y. and Nuffer, R. (1999) *Synth. Met.*, **103**, 2370–1.

99 Lee, T.-W., Park, O.O., Kim, J. and Kim, Y.C. (2002) *Chem. Mater.*, **14**, 4281–5.

100 Vinogradova, L.V., Ratnikova, O.V., Butorina, E.A., Kukling, D. and Adler, H.-J.P. (2006) *Russ. J. Appl. Chem.*, **79**, 647–53.

101 Tang, B.Z., Xu, H., Lam, J.W.Y., Lee, P.P.S., Xu, K., Sun, Q. and Cheuk, K.K.L. (2000) *Chem. Mater.*, **12**, 1446–55.

102 Xu, H., Sun, Q., Lee, P.P.S., Kwok, H.S. and Tang, B.Z. (2000) *Thin Solid Films*, **363**, 143–5.

103 Goswami, T.H., Nandan, B., Alam, S. and Mathur, G.N. (2003) *Polymer*, **44**, 3209–14.

104 Goswami, T.H., Singh, R., Alam, S. and Mathur, G.N. (2004) *Thermochim. Acta*, **419**, 97–104.

105 Chiang, L.Y., Wang, F.-Y. and Kuo, C.-S. (1995) *Macromolecules*, **28**, 7574–6.

106 Ma, C.-C.M., Sung, S.-C., Wang, F.-Y., Chiang, L.Y., Wanng, L.Y. and Chiang, C.-L. (2001) *J. Polym. Sci., Part B: Polym. Phys.*, **39**, 2436–43.

107 Song, T., Dai, S., Tam, K.C., Lee, S.Y. and Goh, S.H. (2003) *Polymer*, **44**, 2529–36.

108 Anantharaj, V., Wang, L.Y., Cateenwala, L. and Chiang, L.Y. (1999) *J. Chem. Soc., Perkin Trans. 1*, 3357–66.

109 Wang, L.Y., Anantharaj, V., Ashok, K. and Chiang, L.Y. (1999) *Synth. Met.*, **103**, 2350–3.

110 Canteenwala, L., Anantharaj, V., Patil, S.V., Haldar, M. and Chiang, L.Y. (2002) *J. Macromol. Sci.-Pure Appl. Chem.*, **A39**, 1069–83.

111 Troitskii, B.B., Troitskaya, L.S., Yakhnov, A.S., Lopatin, M.A. and Novikova, M.A. (1997) *Eur. Polym. J.*, **33**, 1587–90.

112 Troitskii, B.B., Troitskaya, L.S., Dmitriev, A.A. and Yakhnov, A.S. (2000) *Eur. Polym. J.*, **36**, 1073–84.

113 Zeilanov, E.B. and Kossmehl, G. (2001) *Polym. Degrad. Stabil.*, **71**, 197–202.

114 Shibaev, L.A., Ginzburg, B.M., Antanova, T.A., Ugolkov, V.L., Melenevskaya, E.Y., Vinogradova, L.V., Novoselova, A.V. and Zgonnik, V.N. (2002) *Polym. Sci. Ser. A*, **44**, 502–9.

115 Ginzburg, B.M., Pozdnyakov, A.O., Zgonnik, V.N., Pozdnyakov, O.F., Redkov, B.P., Melenevskaya, E.Y. and Vinogradova, L.V. (1996) *Tech. Phys. Lett.*, **22**, 166–7.

116 Ginzburg, B.M., Pozdnyakov, A.O., Pozdnyakov, O.F. and Redkov, B.P. (1999) *Tech. Phys. Lett.*, **25**, 812–14.

117 Pozdnyakov, O.F., Pozdnyakov, A.O., Schmaltz, B. and Mathis, C. (2006) *Polymer*, **47**, 1028–35.

118 Pozdnyakov, O.F., Redkov, B.P. and Pozdnyakov, A.O. (2002) *Tech. Phys. Lett.*, **28**, 1046–8.

119 Mathis, C., Nunige, S., Audouin, F. and Nuffer, R. (2001) *Synth. Met.*, **121**, 1153–4.

120 Audouin, F., Nuffer, R. and Mathis, C. (2004) *J. Polym. Sci., Part A: Polym. Chem.*, **42**, 4820–9.

6
Fullerene-Containing Helical Polymers

Eiji Yashima and Katsuhiro Maeda

6.1
Introduction

Fullerene-containing synthetic polymers and supramolecular polymers have been developed extensively over recent decades [1–9]. This is because the incorporation of fullerene moieties into polymer backbones or pendants through covalent or noncovalent bonding are versatile methods to produce practically useful fullerene-based materials with excellent mechanical strength and processability while maintaining the unique physical and chemical features of the fullerene molecules. Such fullerene-based polymers and supramolecules with well-defined structures may have potential applications in the wide fields of material and biological sciences [10–13]. To date, numerous fullerene-containing polymers have been synthesized by incorporating fullerene molecules into the polymers as chemically attached segments in the polymer backbone, grafting components on the pendants, a starburst polymer molecular core, and a dendritic polymer or crosslinkers in the polymer network, which have been reviewed and are described in detail elsewhere in this book. Among them, optically active fullerene-containing helical polymers are particularly intriguing and potent because, in these polymers, the fullerene units are expected to be specifically arranged in a helical array with a controlled helix-sense along the polymer backbones and, therefore, they will provide potentially useful chiral materials. Although such examples of fullerene-containing helical polymers remain rare, some of them exhibit an unambiguous induced circular dichroism (ICD) in the achiral fullerene chromophore regions, probably due to the predominantly single-handed helical array of the fullerene moieties [10, 14–18].

This chapter deals mainly with recent advances in the synthesis and structures of fullerene-containing helical polymers, in which the fullerene units are arranged in a helical array with a controlled helix-sense through covalent or noncovalent bonding along the polymer backbones (Figure 6.1a and b) or are encapsulated in a helical cavity composed of helical polymers (Figure 6.1c). Noncovalent supramolecular helical assemblies of small chiral molecules bearing fullerene moieties, an

Fullerene Polymers. Synthesis, Properties and Applications. Edited by Nazario Martín and Francesco Giacalone

ISBN: 978-3-527-32282-4

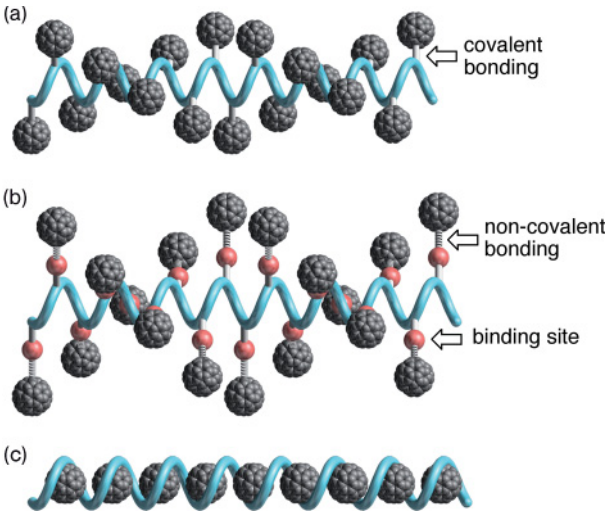

Figure 6.1 Schematic illustration of fullerene-containing helical polymers, (a) and (b), and fullerene-encapsulated helical polymers (c).

important area of emerging supramolecular chemistry, are beyond the scope of this chapter, but are described in Chapter 9.

6.2
Helical Polymers with Pendant Fullerenes via Covalent Bonds

Stereoregular (cis-transoidal) poly(phenylacetylene)s bearing an optically active substituent are known to fold into a helical conformation with an excess of one-handedness in solution, showing a characteristic induced circular dichroism (ICD) in the π–π* electronic transition regions of the conjugated polymer backbone [19–30]. In addition, copolymerization of achiral phenylacetylenes with a small amount of optically active phenylacetylenes can produce preferred-handed helical copolymers, thus showing a similar ICD in the polymer backbone regions [19, 21, 29, 30]. The ICD intensities of the copolymers increase with increasing bulkiness of the substituents attached to the phenyl groups of the achiral co-monomers. This phenomenon is a typical example of chiral amplification in a polymer and originates from the unique feature of the dynamic macromolecular helicity of poly(phenylacetylene)s like the polyisocyanates and polysilanes [27, 29, 31–34]. These dynamic helical polymers consist of an equal mixture of right- and left-handed helical segments separated by helical reversals that readily move along the polymer backbones. Therefore, a small chiral bias in the pendant chiral units covalently bonded to the main-chain is significantly amplified to induce the same helix in the major achiral monomer units, resulting in a single-handed helical

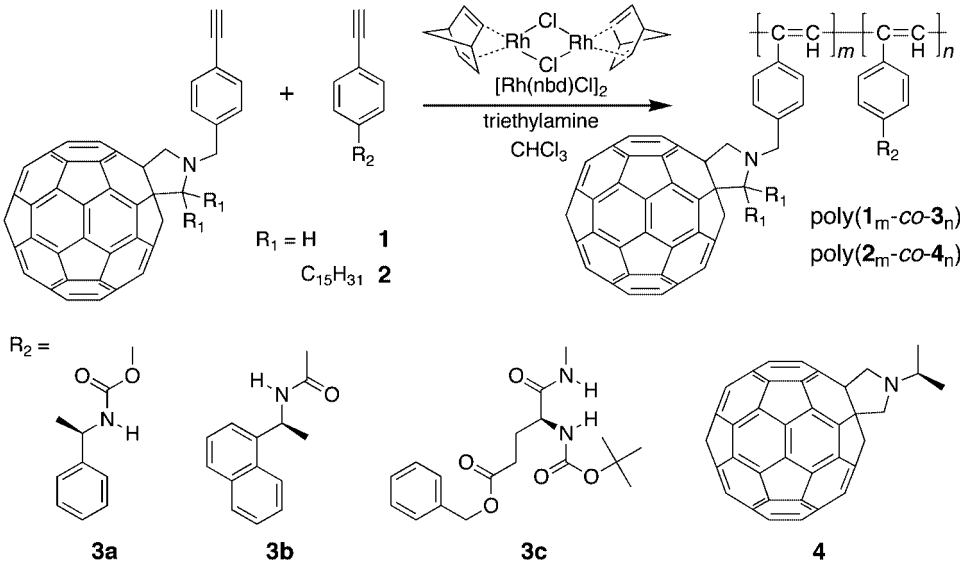

Scheme 6.1 Synthesis of fullerene-containing helical poly(phenylacetylene) derivatives.

polymer. Taking advantage of this chiral amplification property of the dynamic helical poly(phenylacetylene)s, optically active, *cis-transoidal* poly(phenylacetylene) s with C_{60} pendants have been prepared by the copolymerization of an achiral C_{60}-bound phenylacetylene (**1**) with optically active phenylacetylenes (**3a**–**3c**) using a rhodium catalyst $[Rh(nbd)Cl]_2$ (nbd = norbornadiene) (Scheme 6.1) [14, 17].

Poly($\mathbf{1}_{0.1}$-*co*-$\mathbf{3a}_{0.9}$) exhibited intense, split-type ICDs in the π-conjugated main-chain regions (280–500 nm). The magnitude of the ICDs (main-chain region) of poly($\mathbf{1}_{0.1}$-*co*-$\mathbf{3a}_{0.9}$) monotonically increased with the decreasing temperature (Figure 6.2a), indicating a preferred-handed helical conformation of the copolymer induced by cooperative interactions among the chiral and achiral pendant groups. The helical sense (right- or left-handed helix) is controlled by the pendant chirality and the excess one helical sense increased with a decrease in temperature. Interestingly, apparent and remarkable CDs were observed above 600 nm at temperatures lower than −40 °C, which are characteristic of the fullerene chromophore for the copolymer (inset in Figure 6.2a). The ICD intensities further increased at lower temperatures. Such a dramatic increase in the optical activity of the achiral C_{60} cores in the copolymer suggests a helical array of the C_{60} pendants with a one-handed screw-sense along the polymer backbone, because the C_{60} units themselves are achiral (Figure 6.2b). This is the first chirality induction in achiral fullerenes, originating from their helical arrangement in polymers.

The other copolymers [poly($\mathbf{1}_{0.1}$-*co*-$\mathbf{3b}_{0.9}$) and poly($\mathbf{1}_{0.1}$-*co*-$\mathbf{3c}_{0.9}$)] also exhibited similar ICDs in the same wavelength region (600–800 nm) as well as in the main-chain region. The observed CD magnitudes in the fullerene chromophore regions of the copolymers were calculated based on the C_{60} contents incorporated into the

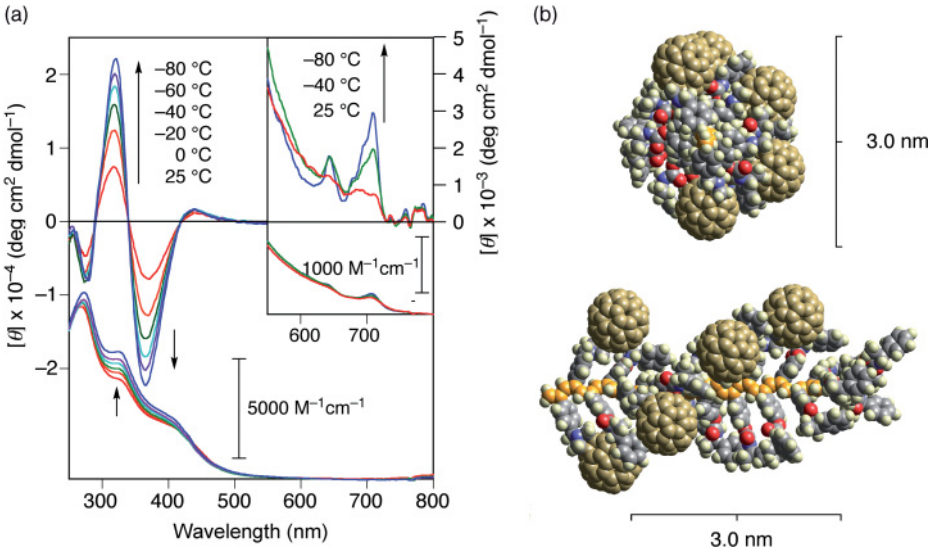

Figure 6.2 (a) CD and absorption spectra of the fullerene-containing helical poly(phenylacetylene) [poly(**1**$_{0.1}$-*co*-**3a**$_{0.9}$)] in dichloromethane (0.1 mg mL^{-1}). Insets: corresponding CD and absorption spectra in the fullerene region at a higher concentration (4.3 mg mL^{-1}); (b) possible helical structure of poly(**1**$_{0.1}$-*co*-**3a**$_{0.9}$) (20-mer); shown are space-filling models of the top (top) and side view (bottom). (Reproduced with permission from Reference [17]. Copyright 2005 Wiley-VCH Verlag GmbH & Co. KGaA.)

copolymer chains, and were as high as those for the chiral monosubstituted fullerenes [35–37] and C_1-symmetric chiral bis-substituted fullerenes [38], but were lower by one or two orders of magnitude than their C_2-symmetric counterparts [39, 40]. Especially, poly(**1**$_{0.1}$-*co*-**3c**$_{0.9}$) exhibited a rather intense ICD in the fullerene region even at 25 °C and the ICD intensity hardly changed at lower temperatures. The ICD pattern of poly(**1**$_{0.1}$-*co*-**3c**$_{0.9}$) in the fullerene region was similar to those of poly(**1**$_{0.1}$-*co*-**3a**$_{0.9}$) and poly(**1**$_{0.1}$-*co*-**3b**$_{0.9}$), indicating that the pendant fullerenes also arrange in a helical array along the helical poly(**1**$_{0.1}$-*co*-**3c**$_{0.9}$) main-chain. Probably, the bulky chiral pendant groups of **3c** may efficiently contribute to the helical arrangement of the C_{60} molecules, which are stable at 25 °C.

The structure and morphology of the helically arranged C_{60}-based copolymers have been visualized directly by atomic force microscopy (AFM) on highly oriented pyrolytic graphite (HOPG) as substrates. Figure 6.3 shows typical AFM images of poly(**1**$_{0.1}$-*co*-**3a**$_{0.9}$) cast from a dilute solution in THF on HOPG. The individual copolymer chains of poly(**1**$_{0.1}$-*co*-**3a**$_{0.9}$) (average height: 2.1 ± 0.8 nm) together with isolated particles can be seen on the HOPG (Figure 6.3a). The height profile along the copolymer chain (Figure 6.3c) is likely uneven, that is, lower (0.72 ± 0.10 nm) and higher (1.48 ± 0.21 nm) values for the poly(**1**$_{0.1}$-*co*-**3a**$_{0.9}$) segments were observed in the copolymer. Because the average height of the homopolymer of poly-**3a** was 0.71 ± 0.15 on mica, the segments with the higher height

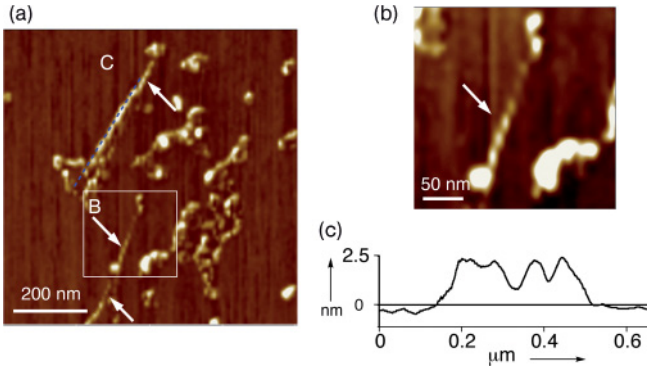

Figure 6.3 (a, b) AFM images of poly($\mathbf{1}_{0.1}$-*co*-$\mathbf{3a}_{0.9}$) cast from dilute solution of THF on HOPG – the arrows indicate the typically observed left-handed helices; (c) height profile measured along the black dashed line in the image A. (Reproduced with permission from Reference [17] Copyright 2005 Wiley-VCH Verlag GmbH & Co. KGaA.)

values appear to involve the C_{60} pendants. This means that the position of the C_{60} pendants in the copolymer chains can be predicted by AFM. The images of the copolymer poly($\mathbf{1}_{0.1}$-*co*-$\mathbf{3a}_{0.9}$) on HOPG show a particularly interesting left-handed helical shape, as marked by the arrows in Figure 6.3a. Although we could not distinguish the C_{60} and chiral pendant groups of the copolymer using AFM, these helical-shaped images seem to be related to the helical conformation of the poly(phenylacetylene), which is rather difficult to investigate using common spectroscopic methods.

The copolymerization approaches described above are certainly useful for producing optically active C_{60}-based helical polymers with the pendant C_{60} molecules in a one-handed helical array. However, the incorporation of more than 30 mol% of the C_{60} units of **1** into the copolymers produced copolymers insoluble in common organic solvents because of the low solubility of fullerene [14, 17]. To overcome this solubility problem and to produce soluble helical copolymers composed of fullerene moieties on each repeating monomer unit, we prepared an achiral C_{60}-bound phenylacetylene (**2**) by introducing two long pentadecyl chains on the pyrrolidine ring of the 3,4-fulleropyrrolidine residue, and this was copolymerized with the optically active C_{60}-bound phenylacetylene using a rhodium catalyst. The obtained stereoregular, helical copolymer [poly($\mathbf{2}_{0.9}$-*co*-$\mathbf{4}_{0.1}$)], bearing fullerene moieties on each repeating monomer unit, was totally soluble in chloroform and exhibited the characteristic ICD in the fullerene chromophore region above 600 nm as well as in the π-conjugated main-chain region (250–500 nm), and the ICD intensity hardly changed at the lower temperatures [18], whereas the optically active monomer **4** showed a very weak ICD in the same fullerene chromophore region. These results support the helical arrangement of the pendant fullerenes along the preferred-handed helical poly($\mathbf{2}_{0.9}$-*co*-$\mathbf{4}_{0.1}$) backbone. The bulky

fullerene pendants efficiently assist the helical array of the C_{60} molecules, which are stable at 25 °C. This is the first example of a totally soluble helical poly(phenylacetylene) having fullerenes as pendants on each monomer unit.

Fullerene derivatives often self-assemble to form spherical particles through the π–π* stacking interaction of the carbon cage [13, 41–45]. We anticipated that the homopolymers of **1** and **4**, poly-**1** and poly-**4**, respectively, which were insoluble in common organic solvents, might self-assemble to form aggregates with unique structures and morphologies. Figure 6.4a and c show typical scanning electron microscopy (SEM) images of the optically inactive poly-**1** and optically active poly-**4**, respectively [18]. Particles with an average diameter of about 100–200 nm were observed for poly-**1** (Figure 6.4a) and poly-**4** (Figure 6.4c) by SEM without sputter-coating with Au, suggesting that these polymers have an apparent conductivity. More detailed structure and morphology analyses of the polymers were performed by transmission electron microscopy (TEM). Smaller particles with an average diameter of about 15 and 30 nm for poly-**1** (Figure 6.4b) and poly-**4** (Figure 6.4d), respectively, can be directly visualized by the TEM [18]. Therefore, the large particles observed by SEM likely consist of smaller particles. It is presumed that poly-**1** and poly-**4** form nanometer-scale small particles, which further hierarchically aggregate to form larger particles during the polymerization (Figure 6.4e). The difference in particle sizes between these aggregates on a nanometer-scale may be connected with the difference in optical activity. Poly-**1** composed of the achiral monomer **1** may possess a dynamically racemic helical conformation (an equal mixture of right- and left-handed helices), while poly-**4** might have a preferred-handed helical conformation induced by the chiral pendant units (Figure 6.4f) as observed for other poly(phenylacetylene)s bearing the optically active pendants [19–30]. Such a one-handed helix formation in poly-**4** seems to contribute to the effective packing of the helical polymer chains with the same handedness during the aggregation process, which may result in the formation of larger particles than those of poly-**1**.

The macromolecular helicity induction in the copolymer backbones with the pendant helical array of the fullerenes, showing an optical activity in the achiral fullerenes, is generated by the optically active co-monomer introduced in the main-chain through covalent bonding during the copolymerization. An alternative way to induce macromolecular helicity in totally optically inactive poly(phenylacetylene)s is through noncovalent bonding interactions when the polymers possess functional pendant groups, such as carboxy, amino, boronate and phosphonate groups or macrocyclic host residues such as a bulky 18-crown-6 ether [20, 27, 29, 30, 34, 46–53]. Upon complexation with optically active compounds capable of interacting with the functional groups or the crown ether, the complexes exhibit a characteristic ICD in the polymer backbone regions due to a preferred-handed helical conformation induced in the polymers. In particular, the crown ether-bound poly(phenylacetylene) is highly sensitive to the amino acid chirality and forms a one-handed helix with nonracemic amino acids through a significant amplification of the chirality [51].

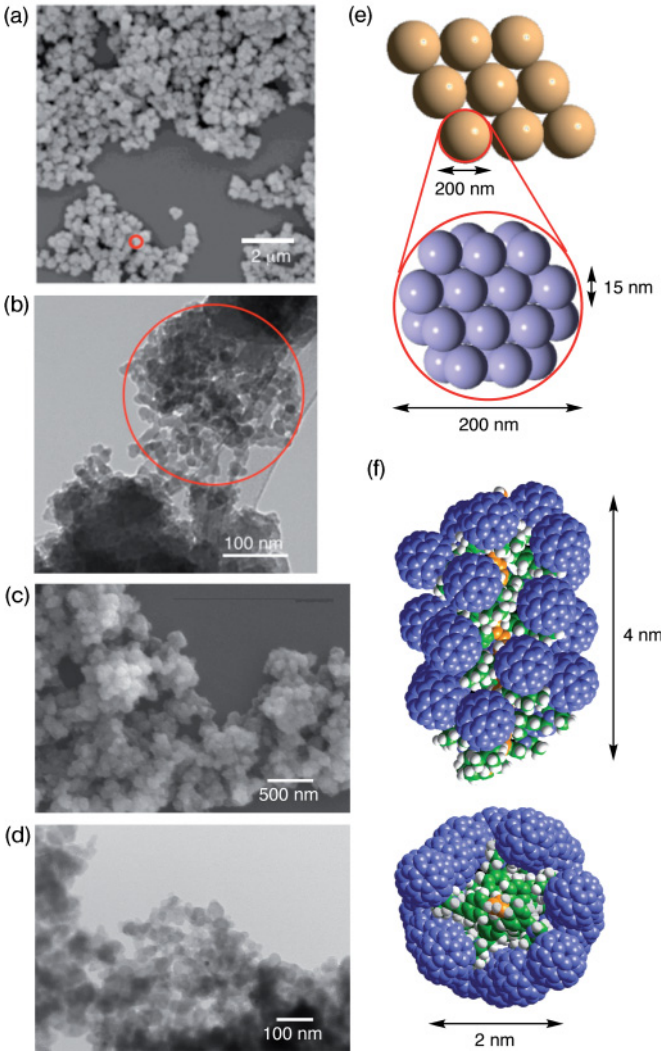

Figure 6.4 SEM, (a) and (c), and TEM images, (b) and (d), of poly-**1,** (a) and (b), and poly-**4,** (c) and (d), on HOPG; (e) schematic representation of the particles observed for poly-**1** formed by hierarchical aggregation; (f) possible helical structure of poly-**4** (20-mer) – shown are space-filling models in side (top) and top view (bottom). (Reproduced with permission from Reference [18] Copyright 2007 American Chemical Society.)

Using this helicity induction concept via noncovalent bonding interactions, we have designed and synthesized an optically inactive, cis-transoidal C_{60}-bound poly(phenylacetylene) copolymer [poly(**1**$_{0.1}$-*co*-**5**$_{0.9}$)] bearing the crown ether pendants as the amino acid binding site. Upon complexation with nonracemic amino acids, the chiral information derived from the amino acid is transmitted to the polymer backbone through a noncovalent bonding interaction with the pendant crown ethers, leading to an excess of the one-handed helical sense in the polymer backbone, which further results in a helical array of the C_{60} pendants with a preferred-handed screw-sense (Figure 6.5a) [15].

The copolymer exhibited mirror images of the split-type intense ICDs in the π-conjugated main-chain region (300–500 nm) in the presence of 2 equiv. of L- and D-alanine perchlorate (L- and D-Ala·$HClO_4$) in dichloromethane–acetonitrile (8/2, v/v), and the ICD intensities increased with the decreasing temperature (Figure 6.5b), indicating that the copolymer formed a preferred-handed helical

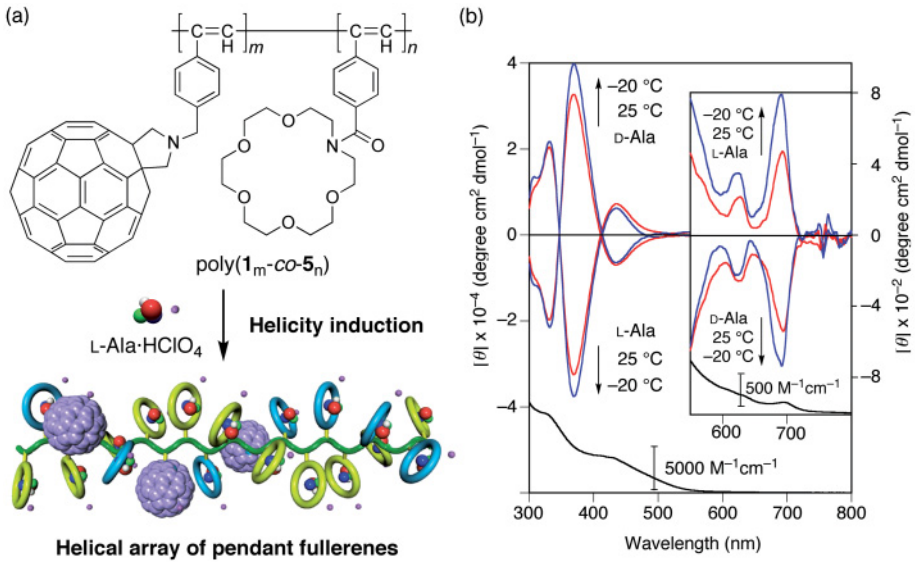

Figure 6.5 (a) Schematic representation of the macromolecular helicity induction on poly(**1** $_m$-*co*-**5** $_n$) upon complexation with L-alanine. The achiral fullerene and crown ether pendants represented by yellow and blue rings for clarity arrange in a helical array along the one-handed helical polymer backbone induced by noncovalent chiral interactions with L-alanine. (b) CD spectra of poly(**1**$_{0.1}$-*co*-**5**$_{0.9}$) with L- and D-Ala·$HClO_4$ ([Ala·$HClO_4$]/[poly(**1**$_{0.1}$-*co*-**5**$_{0.9}$)] = 2) in dichloromethane–acetonitrile (8/2, v/v) at 25 and –20 °C at a dilute concentration ([poly(**1**$_{0.1}$-*co*-**5**$_{0.9}$)] = 0.1 mg mL^{-1}). The absorption spectrum of poly(**1**$_{0.1}$-*co*-**5**$_{0.9}$) with L-Ala·$HClO_4$ at 25 °C is also shown. Inset: corresponding CD and absorption spectra in the fullerene region at a higher concentration (2.9 mg mL^{-1}). The molar concentrations were calculated based on the monomer units and fullerene units (inset). (Reproduced with permission from Reference [15]. Copyright 2004 Royal Society of Chemistry.)

conformation assisted by noncovalent complexation with the optically active Ala·$HClO_4$. In addition, the apparent CDs were also induced in the achiral fullerene chromophore regions over 600 nm, even at 25 °C, and the ICD intensity further increased with a decrease in temperature, in which the ICD patterns were similar to those of the optically active, C_{60}-containing poly(phenylacetylene)s (Figure 6.2a). These results clearly demonstrate that the achiral C_{60} pendants of the copolymer arrange in a helical array with a predominant screw-sense along the polymer backbone.

6.3
Helical Array of Fullerenes along Helical Polymer Backbone via Noncovalent Bonds

Optically active fullerenes can be used as a helicity inducer to produce a predominantly one-handed helical conformation in dynamically racemic helical poly(phenylacetylene)s when the chiral fullerenes can efficiently interact with the polymers through noncovalent bonding interactions, which may simultaneously result in a helical array of the fullerenes with an excess of the screw-sense along the polymer backbone. To this end, optically active, cationic quaternary ammonium ions of C_{60}-bisadducts, the *trans*-3, *trans*-2, and *cis*-3 regioisomers (**6**) (Figure 6.6), have been prepared and we investigated if the optically active cationic C_{60}-bisadducts could induce a macromolecular helicity on an optically inactive poly(phenylacetylene) bearing an opposite, anionic monoethyl phosphonate residue (poly-**7**) [53–55] through electrostatic interactions in aqueous solution (Figure 6.7a) [16]. Poly-**7** is highly sensitive to a chiral environment, and a small chiral bias, such as the addition of a small amount of chiral molecules that can interact with the polymer's side groups, significantly enhances the macromolecular helicity with a large amplification [53–55].

In the presence of each enantiomer of *trans*-3-**6**, ^{f,s}*A*- and ^{f,s}*C*-*trans*-3-**6** ([*trans*-3-**6**]/[poly-**7**] = 0.1), poly-**7** exhibited intense and characteristic ICDs in the π-conjugated polymer backbone region (300–500 nm) in a DMSO–water mixture (1/1, v/v) even at 25 °C, and the ICDs were mirror images of each other (Figure

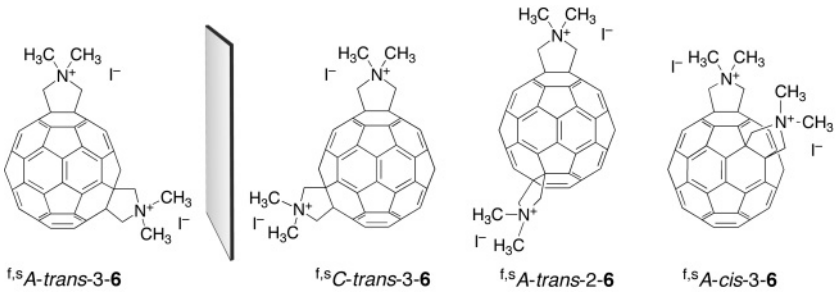

Figure 6.6 Structures of the three optically active regioisomers of C_{60}-bisadducts **6**.

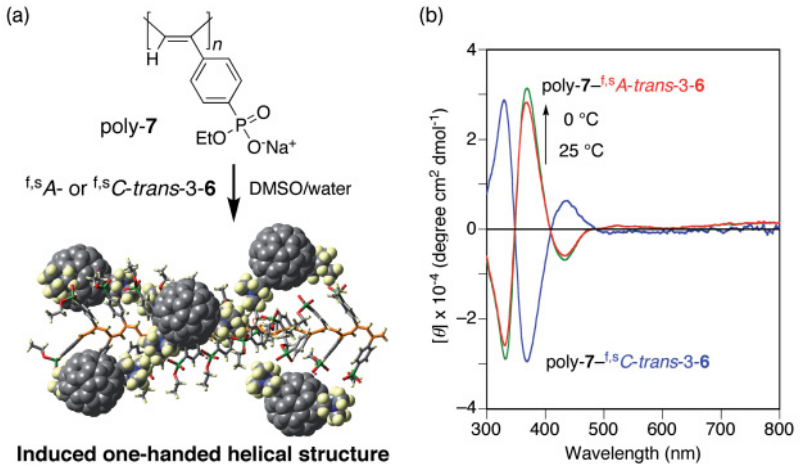

Figure 6.7 (a) Schematic representation of the macromolecular helicity induction on poly-**7** with an optically active C_{60}-bisadduct (^{f,s}*A*-*trans*-3-**6**); (b) CD spectra of poly-**7** in the presence of ^{f,s}*C*-*trans*-3-**6** at 25 °C (blue line) and ^{f,s}*A*-*trans*-3-**6** at 25 (red line) and 0 °C (green line) ([**6**]/[poly-**7**] = 0.1, [poly-**7**] = 0.5 mg mL^{-1}) in DMSO–water (1 : 1, v/v) (pH 9.5). Contributions arising from the CD absorption due to the optically active *trans*-3-**6**s themselves are subtracted from the observed CD spectra of the poly-**7**–**6** complexes. (Reproduced with permission from Reference [16]. Copyright 2004 American Chemical Society.)

6.7b). The CD spectral patterns are in fair agreement with those of the helical poly-**7** induced by optically active amines and amino acids in DMSO and water, respectively. These results indicate that a preferred-handed helical conformation was induced in poly-**7** through a noncovalent bonding interaction with the chiral C_{60}-bisadducts. The ICD intensity in the poly-**7** main-chain region decreased in the presence of increasing amounts of NaCl and was significantly influenced by the solution pH, indicating that the nature of the interaction between the poly-**7** and *trans*-3-**6** may be mainly ionic rather than hydrophobic in an aqueous solution. A possible model for the induced helical structure of poly-**7** complexed with ^{f,s}*A*-*trans*-3-**6** (Figure 6.7a) indicates that the fullerenes arrange in a helical array along the polymer backbone, and the two quaternary ammonium ion residues on the C_{60} surface can efficiently bind to the oppositely charged phosphonate pendant group of poly-**7** in a chelation-type binding manner through electrostatic interactions (Figure 6.8a).

The other chiral C_{60}-bisadducts (*trans*-2 and *cis*-3) were also used as a helix inducer for poly-**7**. However, in the presence of the optically active *cis*-3-**6** or *trans*-2-**6**, poly-**7** did not show any CD in the polymer backbone regions in a DMSO–water mixture (1/1, v/v). Molecular modeling studies suggest that the chirally arranged, two ammonium groups of *cis*-3-**6** may not be favorably located to form a complex with poly-**7** in such a way that both ammonium groups form simultaneous ionic bonding to the neighboring two phosphonate groups of

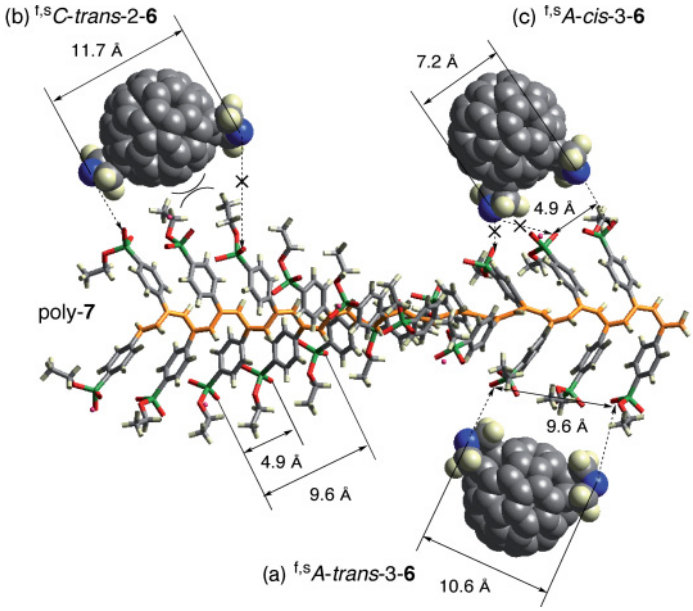

Figure 6.8 Possible interaction models of poly-**7** with optically active C_{60}-bisadduct ^{f,s}*A-trans*-3-**6** (a), ^{f,s}*C-trans*-2-**6** (b), and ^{f,s}*A-cis*-3-**6** (c). Methyl groups on the nitrogens are omitted for clarity (Reproduced with permission from Reference [16]. Copyright 2004 American Chemical Society.)

poly-**7** as in the poly-**7**–*trans*-3-**6** complexation (Figure 6.8a). In contrast, only one ammonium group of *cis*-3-**6** may participate in the ionic complexation with one phosphonate group in poly-**7** (Figure 6.8c), because the distance between the two ammonium groups in *cis*-3-**6** is longer than that between the nearest adjacent two phosphonate groups within a poly-**7** chains and shorter than that between the other two phosphonate groups within a poly-**7** chain (Figure 6.8). Similarly, for *trans*-2-**6** the two ammonium groups are too far apart to form a geometrically fitted, chelation-type complexation with the two phosphonate groups in poly-**7** (Figure 6.8b). These fullerene bisadducts are quite rigid and have no flexibility, and therefore, a structural specificity or geometric fitness is required for the C_{60}-bisadducts to form a complex with poly-**7**, leading to a preferred-handed helicity induction accompanied by a one-handed helical array of the bisadducts (Figure 6.7).

DNA is an optically active helical polyelectrolyte with negative charges. This characteristic feature may be suitable as a unique scaffold for constructing helical arrays of positively charged fullerene molecules. Tour and coworkers have reported an elegant method to construct a helical array of a water-soluble, cationic C_{60}-monoadduct (**8**) through electrostatic interactions with the phosphate groups along the DNA backbone acting as a template (Figure 6.9) [10]. The **8**–DNA complex was prepared by mixing DNA with a solution of **8**. The hybrid nano-

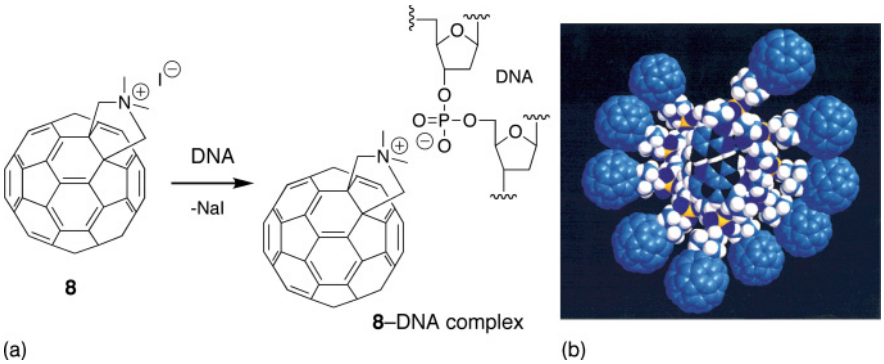

Figure 6.9 (a) Complexation of **8** with DNA by cation exchange; (b) end-on view of the space-filling model of the CG duplex hexamer of DNA complexed with **8**. (Reprinted with permission from Reference [10]. Copyright 1998 Wiley-VCH Verlag GmbH & Co. KGaA.)

architectures were visualized by TEM without heavy metals. Molecular modeling suggests a possible helical array of the fullerene molecules with a one-handed screw-sense along the DNA backbone. However, the chiroptical property of the complex has not yet been reported.

6.4 Inclusion of Fullerenes in a Helical Cavity

Syndiotactic poly(methyl methacrylate) (st-PMMA) has been reported to form a thermoreversible physical gel in aromatic solvents, such as toluene, in which the st-PMMA chains possesses a helix of 74 units per four turns (74/4 helix) with a large cavity (ca. 1 nm), in which the solvent molecules are encapsulated [56]. Recently, we found that fullerenes, such as C_{60}, were encapsulated within this helical cavity to form robust, processable peapod-like 1D regulated fullerene arrays (Figure 6.10a) [57]. The maximum C_{60} content encapsulated in the st-PMMA helical cavity was 23.5 wt% in toluene, which means that about 86% of the st-PMMA helical hollow spaces was filled with C_{60} molecules based on a possible helical structure of st-PMMA filling with C_{60} in a 1D close packing manner (Figure 6.10b). The st-PMMA/C_{60} film containing 23.5 wt% C_{60} maintained the crystal structure with a melting point over 210 °C after evaporating the solvents and showed a birefringence by polarizing optical microscopy, whereas the st-PMMA film was amorphous and showed no birefringence. In the same manner, the st-PMMA can trap C_{70} and C_{84} molecules in the hollow spaces to form crystalline films. Interestingly, the *d*-spacing value observed by X-ray diffraction (XRD) increased with increasing size of the encapsulated fullerenes, from 1.67 (C_{60}) to

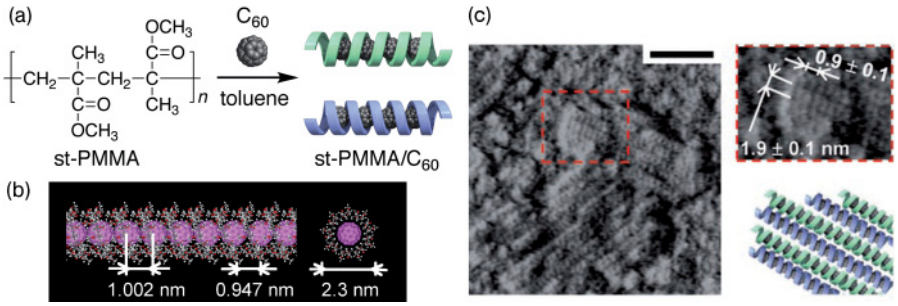

Figure 6.10 (a) Schematic illustration of the encapsulation of C_{60} in the st-PMMA helical cavity; (b) energy-minimized structure of the st-PMMA/C_{60} complex: side view (left) and top view (right); (c) left-hand side: tapping-mode AFM phase image of an LB film of the st-PMMA/C_{60} complex deposited on mica; scale bar: 10 nm; right-hand side: magnified image of the area indicated by the dotted square (top) and schematic representation of a possible bundle structure of the helical st-PMMA/C_{60} complex (bottom). (Reproduced with permission from Reference [57]. Copyright 2008 Wiley-VCH Verlag GmbH & Co. KGaA.)

1.92 (C_{70}) and 2.04 nm (C_{84}), indicating that the st-PMMA helical cavity expands upon encapsulation of the larger fullerenes [57].

The AFM image of an st-PMMA/C_{60} Langmuir–Blodgett (LB) film deposited on mica revealed helix-bundle structures, which are further resolved into individual stripe-like chains with a chain–chain lateral spacing of 1.9 ± 0.1 nm and a helical pitch of 0.9 ± 0.1 nm (Figure 6.10c). These structural features are in good agreement with those of the proposed model calculated on the basis of the reported helical structure of st-PMMA (Figure 6.10b) [56, 58] in which the C_{60} molecules are encapsulated to form a regular 1D array with an intermolecular distance of 1.0 nm.

In addition, a preferred-handed helical st-PMMA can be induced by an optically active aromatic alcohol, *(R)*- or *(S)*-1-phenylethanol (**9**), when used during the st-PMMA/C_{60} gel formation. Interestingly, the induced helical structure was retained ("memorized") after the optically active **9** was completely removed (Scheme 6.2), thus showing a vibrational CD (VCD) and ICD in the PMMA IR regions and in the encapsulated C_{60} chromophore regions, respectively, although C_{60} itself is achiral. The calculated IR and VCD spectra for the right- and left-handed helical 18/1 st-PMMAs at the B3LYP/6-31G(d) level revealed the observed spectra, suggesting that the st-PMMA helix induced by *(R)*-**9** may have a right-handed helix.

Sanders and coworkers have recently found supramolecular helical arrays of C_{60} molecules in the tubular cavity of helical organic nanotubes composed of α-amino acid functionalized naphthalenediimides (**10**), which self-assembled to form hydrogen-bonded helical nanotubes in a nonpolar solution and in the solid state (Figure 6.11) [59]. The CD spectrum of the L-**10**-C_{60} complex exhibited weak but apparent Cotton effects at 595 and 663 nm due to electronic transitions of C_{60} as

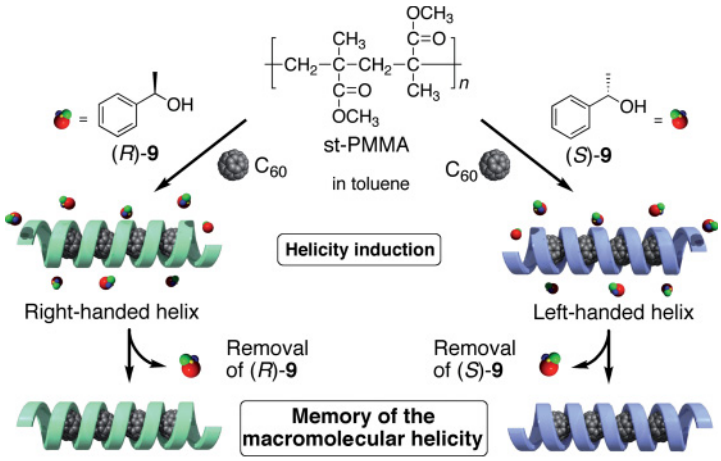

Scheme 6.2 Helicity induction in st-PMMA in the presence of C_{60} with *(S)*- or *(R)*-**9** and memory of the induced helicity after removal of **9**. (Reproduced with permission from Reference [57]. Copyright 2008 Wiley-VCH Verlag GmbH & Co. KGaA.)

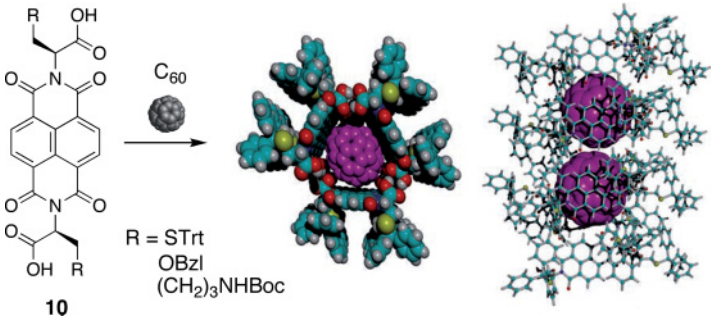

Figure 6.11 Side and top view of a possible structure of the **10**-C_{60} inclusion complex. (Reproduced with permission from Reference [59]. Copyright 2007 Wiley-VCH Verlag GmbH & Co. KGaA.)

well as at 452 nm due to chiral exciton coupling between the adjacent C_{60} molecules. These results imply a preferred-handed helical array of C_{60} molecules trapped in the tubular helical cavity.

Carbon nanotubes (CNTs) can encapsulate small and large molecules, including fullerenes [60]. Theoretical calculations by Hodak and Girifalco [61] predicted that C_{60} molecules in CNTs with a wide range of diameters can form various packing arrangements strictly defined by the size of the nanotube cavity, so that each packing arrangement can exist only in nanotubes within a certain narrow range of diameters, resembling the packing of hard macroscopic spheres inside

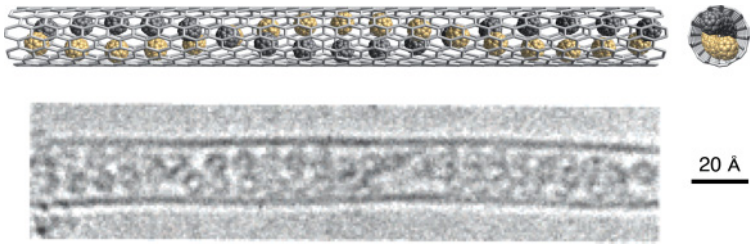

Figure 6.12 High-resolution TEM micrograph and schematic representation of the C_{60}@single-walled CNT peapod with a double helical arrangement of C_{60} molecules. (Reproduced with permission from Reference [63]. Copyright 2004 American Physical Society.)

hard cylinders [62]. According to their theoretical calculations, there is a chance for C_{60} molecules to arrange in a chiral double helical array inside the CNTs, although such a double helical packing arrangement appears to be less prominent than the zigzag one. The zigzag arrangement formed in CNTs with an internal diameter of 1.45–2.16 nm can be easily imaged by high-resolution TEM, but a more complex double helix seems to be more difficult to visualize. This is because the helical array of C_{60} molecules inside the CNTs causes a complex overlap of projections of the fullerene cages in the high-resolution TEM, which makes the micrographs difficult to interpret, especially for the double-walled CNTs in which the chiral arrays of fullerenes are surrounded by two layers of graphene. However, Khlobystov *et al*. have succeeded in observing directly the double helical array of C_{60} molecules inside a single-walled CNT by high-resolution TEM (Figure 6.12) [63, 64]. Although the helical arrays should be racemic (both right- and left-handed helices), this discovery has a great advantage for constructing a preferred-handed double helical array of C_{60} molecules since optically active CNTs with a controlled helical chirality are now available by optical resolution [65].

6.5 Conclusion

In this chapter we have mainly described the strategy and representative examples for designing and synthesizing fullerene-containing helical polymers, in which the fullerene units are arranged in a helical array with a controlled helix-sense, although such examples are still limited. The fullerene-containing helical polymers and supramolecules described in this chapter may have unique and intriguing properties that originate from their helical arrays of fullerene units and will provide potentially useful nanomaterials. Therefore, further applications of these unique fullerene-containing helical polymeric materials to organic nanodevices and optoelectronic materials will be the subject of a forthcoming investigation.

References

1 Prato, M. (1997) *J. Mater. Chem.*, **7**, 1097–109.
2 Tsukruk, V.V. (1997) *Prog. Polym. Sci.*, **22**, 247–311.
3 Chen, Y., Huang, Z.E., Cai, R.F. and Yu, B.C. (1998) *Eur. Polym. J.*, **34**, 137–52.
4 Chiang, L.Y. and Wang, L.Y. (2000) Chapter 7, in *Fullerenes: Chemistry, Physics, and Technology* (eds K.M. Kadish and R.R. Ruoff), John Wiley & Sons, Inc., New York.
5 Dai, L. and Mau, A.W.H. (2001) *Adv. Mater.*, **13**, 899–913.
6 Cravino, A. and Sariciftci, N.S. (2002) *J. Mater. Chem.*, **12**, 1931–43.
7 Wang, C., Guo, Z.-X., Fu, S., Wu, W. and Zhu, D. (2004) *Prog. Polym. Sci.*, **29**, 1079–141.
8 Giacalone, F. and Martin, N. (2006) *Chem. Rev.*, **106**, 5136–90.
9 Tashiro, K. and Aida, T. (2007) *Chem. Soc. Rev.*, **36**, 189–97.
10 Cassell, A.M., Scrivens, W.A. and Tour, J.M. (1998) *Angew. Chem. Int. Ed.*, **37**, 1528–31.
11 Wilson, S.R. (2000) Chapter 10, in *Fullerenes: Chemistry, Physics, and Technology* (eds K.M. Kadish and R.R. Ruoff), John Wiley & Sons, Inc., New York.
12 Da Ros, T., Bergamin, M., Vazquez, E., Spalluto, G., Baiti, B., Moro, S., Boutorine, A. and Prato, M. (2002) *Eur. J. Org. Chem.*, 405–13.
13 Nakamura, E. and Isobe, H. (2003) *Acc. Chem. Res.*, **36**, 807–15.
14 Nishimura, T., Takatani, K., Sakurai, S., Maeda, K. and Yashima, E. (2002) *Angew. Chem. Int. Ed.*, **41**, 3602–4.
15 Nishimura, T., Ohsawa, S., Maeda, K. and Yashima, E. (2004) *Chem. Commun.*, 646–7.
16 Nishimura, T., Tsuchiya, K., Ohsawa, S., Maeda, K., Yashima, E., Nakamura, Y. and Nishimura, J. (2004) *J. Am. Chem. Soc.*, **126**, 11711–17.
17 Nishimura, T., Maeda, K., Ohsawa, S. and Yashima, E. (2005) *Chem. Eur. J.*, **11**, 1181–90.
18 Ohsawa, S., Maeda, K. and Yashima, E. (2007) *Macromolecules*, **40**, 9244–51.
19 Yashima, E., Huang, S.L., Matsushima, T. and Okamoto, Y. (1995) *Macromolecules*, **28**, 4184–93.
20 Yashima, E. and Okamoto, Y. (2000) in *Circular Dichroism: Principles and Applications*, 2nd edn (eds K. Nakanishi, N. Berova and R.W. Woody), John Wiley & Sons, Inc., New York, Chapter 18.
21 Morino, K., Maeda, K., Okamoto, Y., Yashima, E. and Sato, T. (2002) *Chem. Eur. J.*, **8**, 5112–20.
22 Schenning, A.P.H.J., Fransen, M. and Meijer, E.W. (2002) *Macromol. Rapid Commun.*, **23**, 266–70.
23 Lam, J.W.Y. and Tang, B.Z. (2005) *Acc. Chem. Res.*, **38**, 745–54.
24 Okoshi, K., Sakajiri, K., Kumaki, J. and Yashima, E. (2005) *Macromolecules*, **38**, 4061–4.
25 Aoki, T., Kaneko, T. and Teraguchi, M. (2006) *Polymer*, **47**, 4867–92.
26 Maeda, K., Mochizuki, H., Watanabe, M. and Yashima, E. (2006) *J. Am. Chem. Soc.*, **128**, 7639–50.
27 Maeda, K. and Yashima, E. (2006) *Top. Curr. Chem.*, **265**, 47–88.
28 Rudick, J.G. and Percec, V. (2007) *New J. Chem.*, **31**, 1083–96.
29 Yashima, E. and Maeda, K. (2007) in *Foldamers: Structure, Properties, and Applications* (eds S. Hecht and I. Huc), Wiley-VCH Verlag GmbH, Weinheim, Chapter 11.
30 Yashima, E. and Maeda, K. (2008) *Macromolecules*, **41**, 3–12.
31 Green, M.M., Peterson, N.C., Sato, T., Teramoto, A., Cook, R. and Lifson, S. (1995) *Science*, **268**, 1860–6.
32 Nakano, T. and Okamoto, Y. (2001) *Chem. Rev.*, **101**, 4013–38.
33 Fujiki, M., Koe, J.R., Terao, K., Sato, T., Teramoto, A. and Watanabe, J. (2003) *Polym. J.*, **35**, 297–344.
34 Yashima, E., Maeda, K. and Nishimura, T. (2004) *Chem. Eur. J.*, **10**, 43–51.
35 Bianco, A., Maggini, M., Scorrano, G., Toniolo, C., Marconi, G., Villani, C. and Prato, M. (1996) *J. Am. Chem. Soc.*, **118**, 4072–80.
36 Schuster, D.I., Cao, J., Kaprinidis, N., Wu, Y., Jensen, A.W., Lu, Q., Wang, H. and

Wilson, S.R. (1996) *J. Am. Chem. Soc.*, **118**, 5639–47.
37 Shen, C.K.F., Chien, K.M., Juo, C.G., Her, G.R. and Luh, T.Y. (1996) *J. Org. Chem.*, **61**, 9242–4.
38 Ishi-i, T., Nakashima, K., Shinkai, S. and Ikeda, A. (1999) *J. Org. Chem.*, **64**, 984–90.
39 Nakamura, Y., O-kawa, K., Nishimura, T., Yashima, E. and Nishimura, J. (2003) *J. Org. Chem.*, **68**, 3251–7.
40 Sergeyev, S. and Diederich, F. (2004) *Angew. Chem. Int. Ed.*, **43**, 1738–40.
41 Charvet, R., Jiang, D.-L. and Aida, T. (2004) *Chem. Commun.*, 2664–5.
42 Guldi, D.M., Zerbetto, F., Georgakilas, V. and Prato, M. (2005) *Acc. Chem. Res.*, **38**, 38–43.
43 Liu, Y., Wang, N., Li, Y.J., Liu, H.B., Li, Y.L., Xiao, J.H., Xu, X.H., Huang, C.S., Cui, S. and Zhu, D.B. (2005) *Macromolecules*, **38**, 4880–7.
44 Nakanishi, T., Schmitt, W., Michinobu, T., Kurth, D.G. and Ariga, K. (2005) *Chem. Commun.*, 5982–4.
45 Murakami, H., Nakanishi, T., Morita, M., Taniguchi, N. and Nakashima, N. (2006) *Chem. Asian J.*, **1**, 860–7.
46 Yashima, E., Matsushima, T. and Okamoto, Y. (1995) *J. Am. Chem. Soc.*, **117**, 11596–7.
47 Yashima, E., Nimura, T., Matsushima, T. and Okamoto, Y. (1996) *J. Am. Chem. Soc.*, **118**, 9800–1.
48 Yashima, E., Maeda, Y., Matsushima, T. and Okamato, Y. (1997) *Chirality*, **9**, 593–600.
49 Yashima, E., Matsushima, T. and Okamoto, Y. (1997) *J. Am. Chem. Soc.*, **119**, 6345–59.
50 Yashima, E., Maeda, K. and Okamoto, Y. (1999) *Nature*, **399**, 449–51.
51 Nonokawa, R. and Yashima, E. (2003) *J. Am. Chem. Soc.*, **125**, 1278–83.
52 Maeda, K., Morino, K., Okamoto, Y., Sato, T. and Yashima, E. (2004) *J. Am. Chem. Soc.*, **126**, 4329–42.
53 Onouchi, H., Kashiwagi, D., Hayashi, K., Maeda, K. and Yashima, E. (2004) *Macromolecules*, **37**, 5495–503.
54 Onouchi, H., Hasegawa, T., Kashiwagi, D., Ishiguro, H., Maeda, K. and Yashima, E. (2005) *Macromolecules*, **38**, 8625–33.
55 Onouchi, H., Hasegawa, T., Kashiwagi, D., Ishiguro, H., Maeda, K. and Yashima, E. (2006) *J. Polym. Sci., Part A: Polym. Chem.*, **44**, 5039–48.
56 Kusuyama, H., Takase, M., Higashihata, Y., Tseng, H.-T., Chatani, Y. and Tadokoro, H. (1982) *Polymer*, **23**, 1256–8.
57 Kawauchi, T., Kumaki, J., Kitaura, A., Okoshi, K., Kusanagi, H., Kobayashi, K., Sugai, T., Shinohara, H. and Yashima, E. (2008) *Angew. Chem. Int. Ed.*, **47**, 515–19.
58 Kumaki, J., Kawauchi, T., Okoshi, K., Kusanagi, H. and Yashima, E. (2007) *Angew. Chem. Int. Ed.*, **46**, 5348–51.
59 Panto, G.D., Wietor, J.-L. and Sanders, J.K.M. (2007) *Angew. Chem. Int. Ed.*, **46**, 2238–40.
60 Kitaura, R. and Shinohara, H. (2006) *Chem. Asian J.*, **1**, 646–55.
61 Hodak, M. and Girifalco, L.A. (2003) *Phys. Rev. B.*, **67**, 075419.
62 Pickett, G.T., Gross, M. and Okuyama, H. (2000) *Phys. Rev. Lett.*, **85**, 3652–5.
63 Khlobystov, A.N., Britz, D.A., Ardavan, A. and Briggs, G.A.D. (2004) *Phys. Rev. Lett.*, **92**, 245507.
64 Khlobystov, A.N., Britz, D.A. and Briggs, G.A.D. (2005) *Acc. Chem. Res.*, **38**, 901–9.
65 Peng, X., Komatsu, N., Bhattacharya, S., Shimawaki, T., Aonuma, S., Kimura, T. and Osuka, A. (2007) *Nat. Nanotechnol.*, **2**, 361–5.

7
Electroactive C_{60}-Polymer Systems

Yuliang Li, Weidong Zhou, and Changshui Huang

7.1
Introduction

Fullerenes, first reported by Curl, Kroto and Smalley over 20 years ago [1], are highly symmetric cage-shaped molecules that consist only of carbon atoms. They have been thoroughly studied during the last two decades. Since the preparation of fullerene C_{60} in multigram amounts in 1990 [2], a wide variety of chemically modified fullerenes have been synthesized and outstanding structural [3], magnetic [4], superconducting [5], electrochemical [6] and photophysical [7] properties reported [8]. Many polymer scientists shifted their attention to this field. They tried to use this molecule as a building block to construct novel materials with unusual properties. The combination of fullerenes and polymer chemistry is a new interdisciplinary field in which all knowledge on the synthesis and study of natural as well as artificial macromolecules can be applied to fullerenes to achieve novel fullerene-based architectures with unprecedented properties and realistic applications. Because of their original structure, three-dimensional fullerenes as well as polymers are intrinsically useful scaffolds for the construction of high molecular weight structures. As we shall see later, the unique molecular structures of C_{60} can not only provide each of the carbon entities with special physicochemical properties but they also allow controlled structural modifications, leading to the formation of various advanced composite materials with appropriate polymers for many potential applications. Therefore, a combination of both systems has led to a wide variety of new materials that show appealing features based on the possibility of tuning their properties by modifying the chemical nature of the components or the chemical linkage between them. The present chapter summarizes some of the important issues on the preparation of advanced composite materials based on polymers containing fullerene C_{60}.

During the rapid development of fullerene chemistry, many types of polymeric derivatives have been prepared. Numerous chapters and reviews have been published on fullerenes [9]: some focus on their physical properties, others on their synthesis. Our aim here to give a detailed account of progress, especially recent

Fullerene Polymers. Synthesis, Properties and Applications. Edited by Nazario Martín and Francesco Giacalone

ISBN: 978-3-527-32282-4

progress, on the synthesis and properties of electroactive fullerene-containing polymers: photoinduced electron transfer, organic solar cells, potential C_{60}-polymers for photodynamic cancer therapy and so on.

7.2 Photoinduced Electron Transfer

Since the discovery of an efficient photoinduced electron transfer (PET) process from nondegenerate ground-state semiconducting π-conjugated polymers to fullerene C_{60} these materials have received a great deal of attention for various applications.

The very first example of a C_{60} moiety covalently linked to an electroactive conjugated polymer was described in 1994 by Diederich, Gross and Seiler [10]. They reported a bis(trimethylsilyl)methanofullerene (**1**) which undergoes reductive electrochemical polymerization to give the corresponding polydiacetylene **2** (Scheme 7.1). The homogeneous film so-formed deposits on the platinum cathode surface and continues to build-up during the electropolymerization of **1**, even after it has covered the electrode, implying its electrical conductance. Further proof of the conductivity of polymer **2** is given by the fact that film-covered electrodes generate an essentially normal electrochemical response with known redox systems if employed as a modified electrode.

Figure 7.1 shows three monomers suitable for electropolymerization. The choice of bithiophene as electropolymerizable unit for **3** [11, 12] and **4** [13–15] lies in the lower oxidation potential values that they present as compared to thiophene-based systems, leading to an easier and superior degree of polymerization. Notably, for poly-**4** and poly-**5** the polythiophene backbone and fullerene preserve their own electrochemical behavior, and no interactions between the electron-donor polymer and acceptor fullerene have been observed in the ground state. Photoinduced absorption (PIA) and light-induced electron spin resonance (LESR) experiments carried out on poly-**5** revealed that photoinduced electron transfer from the conjugated polymer to the pendant C_{60} occurs (Figure 7.2), thus making this material appealing for photovoltaic applications.

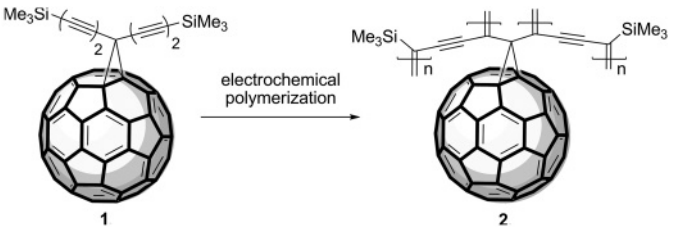

Scheme 7.1

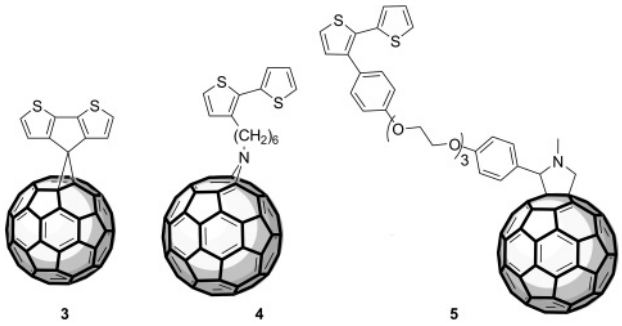

Figure 7.1 Monomers suitable for electropolymerization.

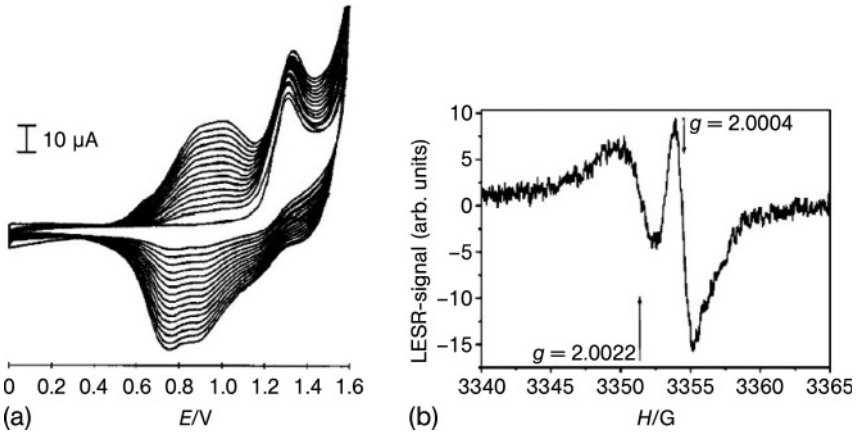

Figure 7.2 (a) Anodic cyclic voltammogram of **5** (0.1 M Bu_4NPF_6 in CH_2Cl_2); working electrode: Pt foil, quasi-reference electrode: Ag/AgCl wire (–0.44 V vs ferrocene), scan rate: 100 mV s^{-1}; (b) integrated LESR (light-on minus light-off) spectrum of poly-**5** on ITO-coated plastic foils; excitation at 488 nm (20 mW cm^{-2}), $T \approx 77$ K. The higher g factor ($g = 2.0022$) is due to the presence of positive polarons on the polythiophene backbone, while the signal at $g = 2.0004$ is typical of $C_{60}^{\bullet-}$ (Reproduced by permission of the American Chemical Society).

An original way to avoid the high C_{60}-content polymers from becoming insoluble or not processable has been suggested by Li *et al.*, who first used the supramolecular assemblies approach to obtain heterojunction materials [16, 17], and synthesized a poly-*p*-phenylenevinylenecarbazole endowed with a uracil moiety (**8**) able to link a complementary 2,6-diacylaminopyridine-C_{60} derivative (**9**) through threefold hydrogen bonding (Scheme 7.2).

Fluorescence quenching experiments mixing **8** and **9** were carried out (Figure 7.3a). For comparison, the authors also performed quenching experiments using *N*-methylfulleropyrrolidine (Fp), which does not form H bonds (Figure 7.3b). The results indicated that the fluorescence of polymer **8** was deactivated by both **9** and

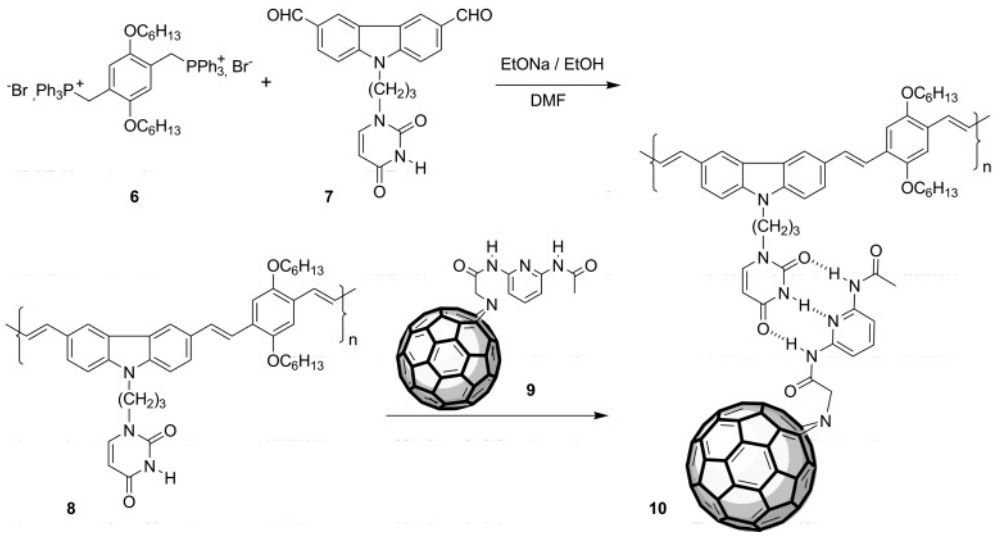

Scheme 7.2

Fp, but in the former case the Stern–Volmer constant K_{SV} was almost five-fold larger than that between **9** and Fp (5.8×10^4 vs 1.2×10^4 mol L^{-1}), suggesting that the binding force through the hydrogen links was stronger.

A hexaarm hexaazidopolystyrene star polymer has been heated with a twofold excess of C_{60} to give the hexafullerene star polymer **11** (Figure 7.4) [18]. Derivatization of the six branch termini into as many C_{60} was not hindered by steric constraints because the PS arms were large enough to avoid mutual interferences. Moreover, the cyclic voltammogram of **11** showed three reversible waves at $E = -1.00$, -1.40 and -1.90 V vs ferrocene-ferrocinium, corresponding to the three first reduction processes of fullerene-derived compounds [19], thus constituting a huge polyelectronic reservoir system.

In 2005, Gregoriou and coworkers synthesized a soluble end-capped C_{60} polymer incorporating terfluorene blocks, using the ATRP (atom transfer radical polymerization) technique (Scheme 7.3) [20]. This rod-coil polymer was prepared from the properly functionalized terfluorene oligomer **12** followed by incorporation of the polystyrene part by ATRP polymerization in two different degrees of chain extension. Subsequently, reaction of **13a** ($M_n = 9950$) and **13b** ($M_n = 18\,000$) with C_{60} in the presence of CuBr and bipyridine afforded the corresponding end-capped polymers **14a**,**b**, which exhibited excellent solubility in organic solvents and were stable materials for polymeric light-emitting diodes (PLEDs).

Using conducting polymer to prepare mono-C_{60}-end-capped polymer is also very interesting. Gu *et al.* have prepared mono-C_{60}-end-capped oligophenylenevinylene (OPE) [21]. Scheme 7.4 depicts the synthesis procedure. This molecular approach appears to be particularly interesting for solar energy conversion, since the bicon-

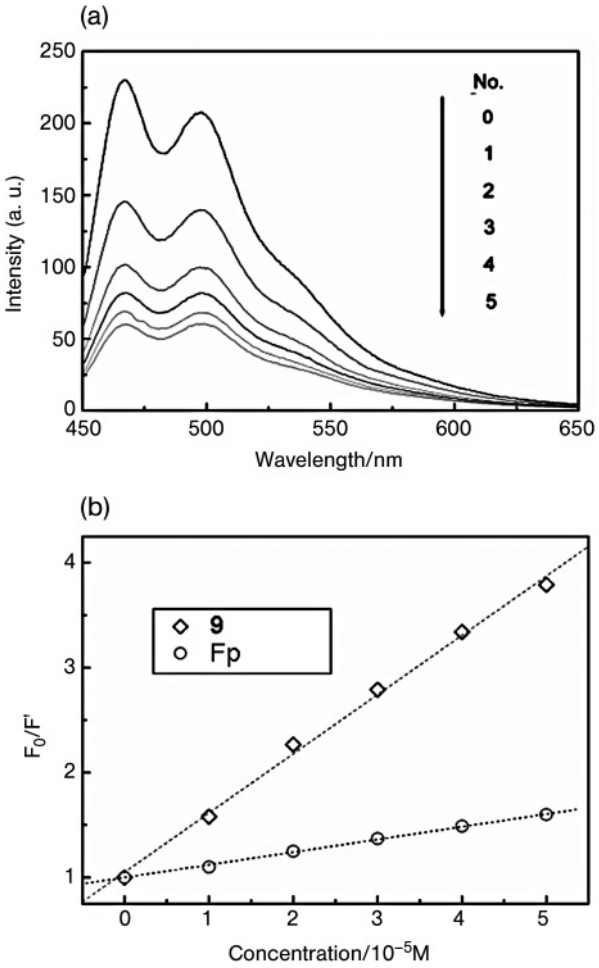

Figure 7.3 (a) Fluorescence of **8** solution (1.0×10^{-5} M) in $CHCl_3$ quenched by **9** solution in $CHCl_3$ ($\lambda_{ex} = 430$ nm) – the concentrations (M) of **9** are (line 0) 0, (1) 1.0×10^{-5}, (2) 2.0×10^{-5}, (3) 3.0×10^{-5}, (4) 4.0×10^{-5} M; (b) dependence of F_0/F' on the concentration of ◇ **9** or ○ *N*-methylfulleropyrrolidine. (Reproduced by permission of the American Chemical Society).

tinuous network obtained by chemically linking the hole-conducting OPE moiety to the electron-conducting fullerene subunit prevents any problems arising from bad contacts at the junction, as observed in polymer/C_{60} blends. Furthermore, this new synthetic approach also offers great versatility for tuning the photovoltaic system. Interestingly, increasing the donor ability of the conjugated oligomer substituents due to the presence of the aniline group increases the efficiency and sensitivity of photovoltaic devices by an order of magnitude.

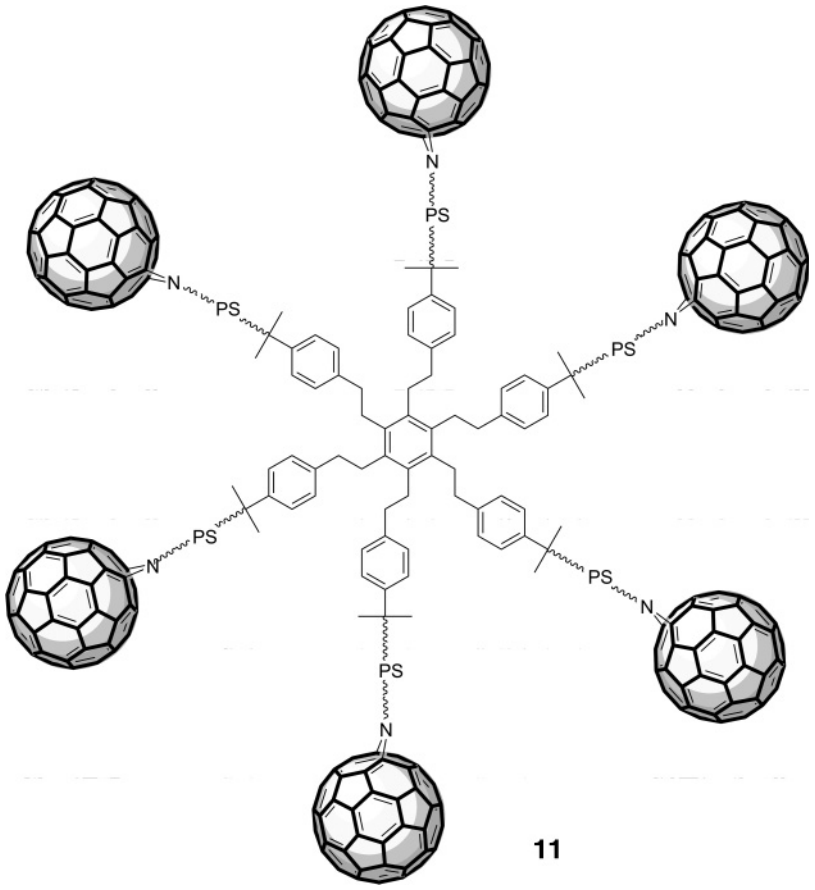

Figure 7.4 A hexafullerene star polymer formed by heating a hexaarm hexaazidopolystyrene star polymer with a twofold excess of C_{60}.

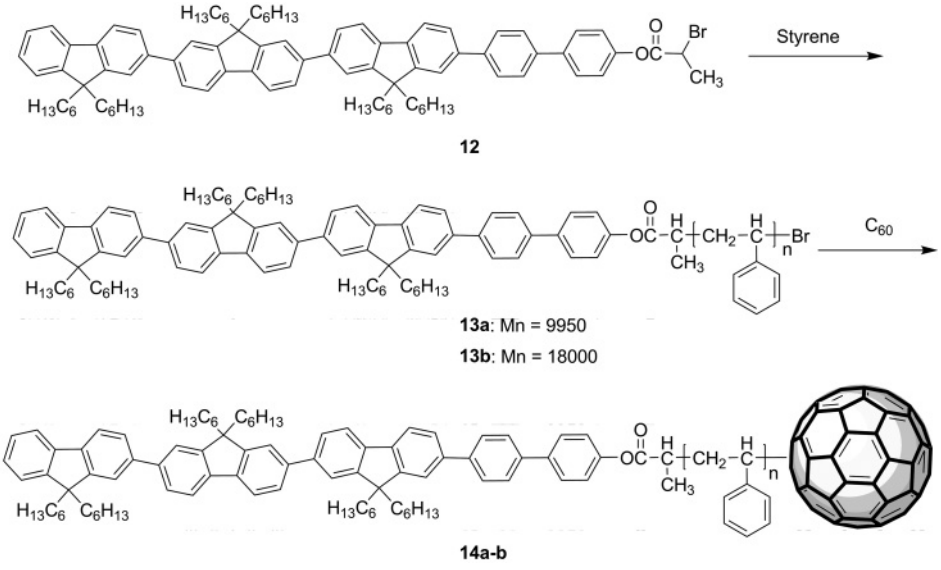

Scheme 7.3

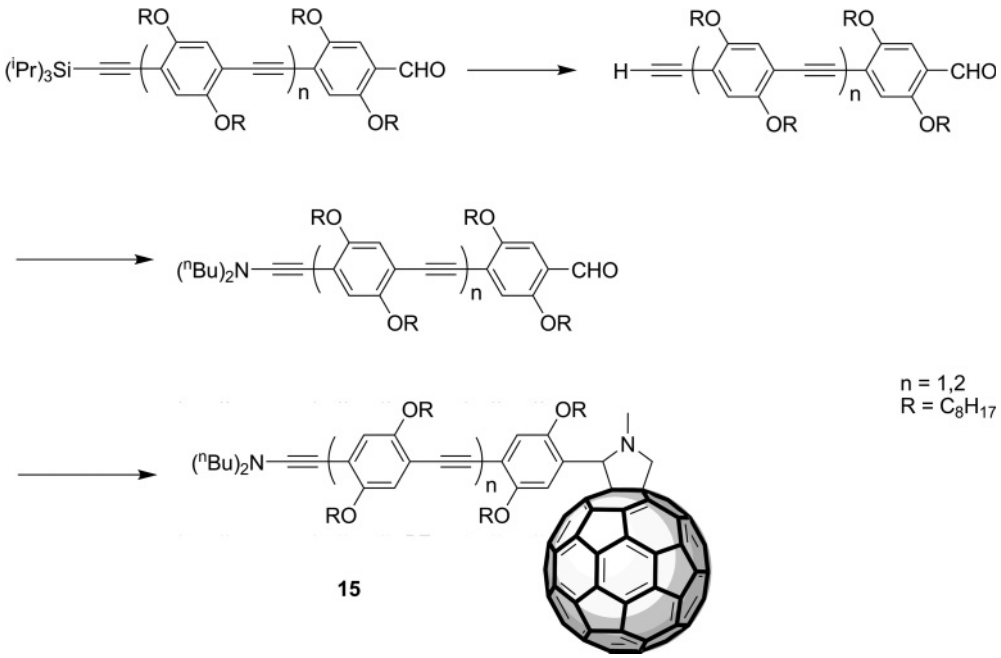

Scheme 7.4

A very interesting strategy has been adopted by Hiorns *et al.* for the synthesis of C_{60} star block copolymers C_{60}(PS-*b*-PPP)$_6$ (**19**) and C_{60}(styrene-PPP-*b*-PS)$_6$ (**23**) [22]. As depicted in Scheme 7.5, they first prepared poly(1,3-cyclohexadiene) (PCHD, **16**) by living anionic polymerization as precursor for the block copolymer PS-PCHD (**17**), which was in turn reacted with C_{60} and oxidized with DDQ to afford C_{60}(PS-*b*-PPP)$_6$ (**19**). An analogous route was followed for C_{60}(styrene-PPP-*b*-PS)$_6$ (**23**). Again, C_{60} was observed to limit the number of linked polymeric chains to six even if a 10 : 1 stoichiometry of arm : C_{60} is used, probably due to the strong steric hindrance around the fullerene core. The use of a PS "shell" around PPP, themselves spaced about an internal C_{60} core, resulted in materials that consisted of highly conjugated PPP segments yet remained soluble in common organic solvents. Furthermore, **23** had an effective quenching of PPP fluorescence that was considered indicative for a charge transfer from the donor fragment PPP to the acceptor C_{60}. The photoconductivity indicated to occur in these systems may provide a starting point in the design of photovoltaic devices. However, a combination of C_{60} and PPP will probably require the use of different molecular structures to provide the necessary capabilities of complete electron and hole separation and transfer.

Chiang and coworkers have described the gradual synthesis of hexaarm oligoaniline and polyaniline-C_{60} star polymer [23]. The polymers were prepared by nucleophilic substitution of the tertiary NO_2 groups (used as good leaving groups)

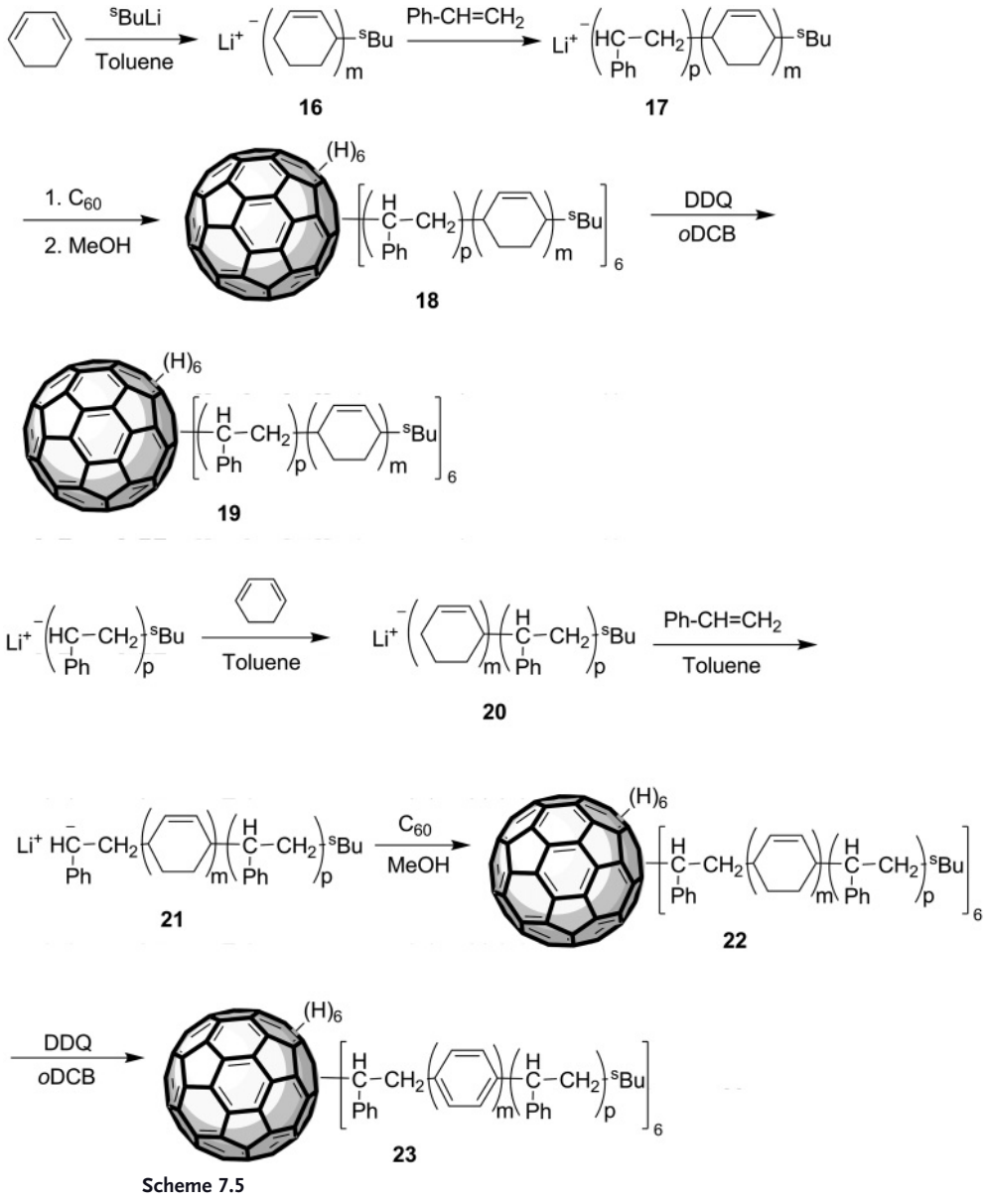
sBuLi
Toluene
Ph-CH=CH2
16
17
1. C60
2. MeOH
(H)6
DDQ
oDCB
18
19
Toluene
20
21
C60
MeOH
22
23

Scheme 7.5

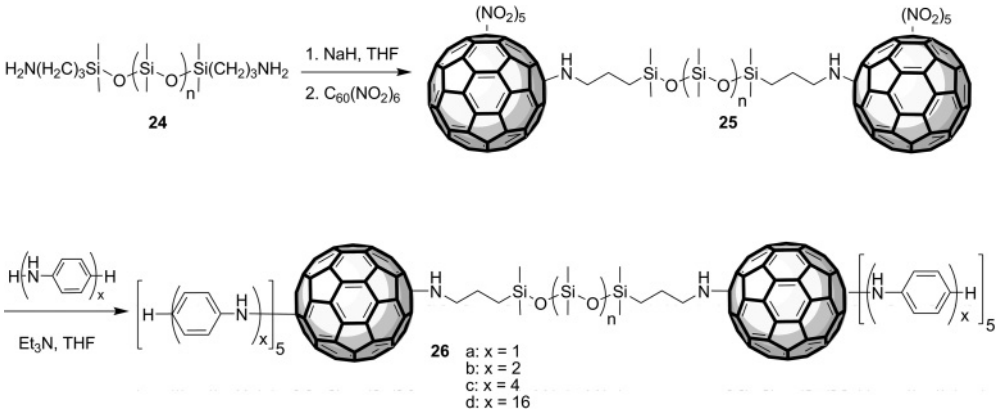

Scheme 7.6

in hexanitrofullerene C_{60}—$(NO_2)_6$ with aniline, oligoaniline and polyaniline. Photoexcitation of such materials produced photoinduced intramolecular electron transfer from benzenoid moieties of oligoaniline arms to the C_{60} sphere [24]. The same authors have synthesized a palm-tree polymer series **26a–d** by capping the poly(dimethylsiloxane) **25** with hexanitro[60]fullerene followed by substitution with oligoaniline (Scheme 7.6) [25]. In polar solvents, these macromolecules aggregated into submicron to nanoparticles consisting of an elastic poly(dimethylsiloxane) core and a conjugate oligoaniline shell, from observation of the SEM images. These aggregation structures may be useful for conducting electrode printing applications on flexible substrates.

Anantharaj *et al.* (Scheme 7.7) [26] have prepared another six-arm star-shaped fullerene polymer from hexanitrofullerene (HNF) as a reactive precursor molecule. A synthetic approach was developed for the production of oligoanilinated fullerenes as intramolecular donor–acceptor A-$(D)_6$ starburst macromolecules with a well-defined arm number and chain length. Only an equal molar quantity of tetraaniline and hexadecaaniline was necessary for a complete reaction with HNF under mild conditions. The NMR data confirmed the structure of tetraanilinated and hexadecaanilinated fullerenes, containing tetraanilino and hexadecaanilino arms per C_{60}, respectively. The optical properties of hexa(hexadecaanilino) [60] fullerenes revealed a close similarity to that of high molecular weight polyanilines.

In 1992, Loy and Assink reported the first example of in-chain C_{60} polymers [27]. The solubility of these polymers is low due to crosslinking through multiple benzylations on the C_{60} sphere. The electrochemical synthesis of a copolymer consisting of phenylene vinylene units and C_{60} has been carried out by Kvarnström *et al.* [28, 29]. In 2006, Saigo *et al.* have prepared a pearl-necklace polyiminofullerene, starting from enantiopure equatorial bis(formylmethano)[60]fullerenes (**31**) and the aromatic diamine 4,4″-diamino-2′,5′-bis(dodecyloxy)-*p*-terphenyl (**32**)

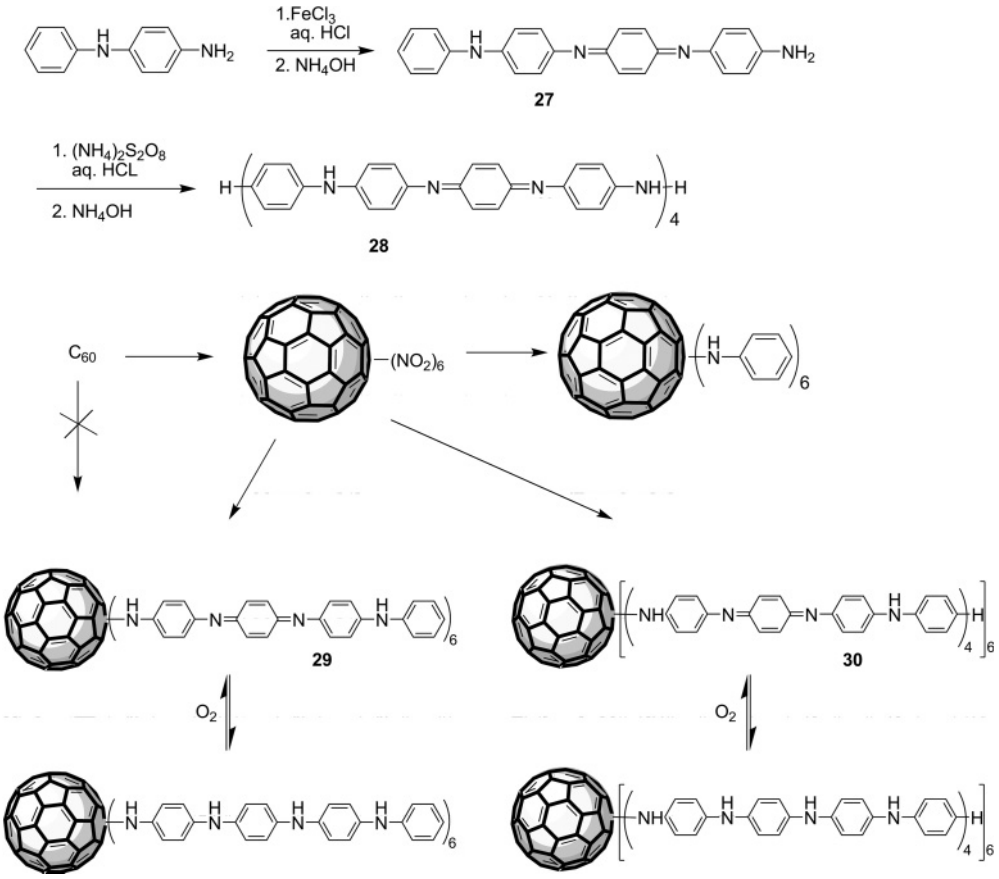

Scheme 7.7

(Scheme 7.8) [30]. This polymer showed excellent processability. On the other hand, a C_{60} derivative, benzylaminofullerene (BZAF) with a stoichiometry of $[C_{60}H_{1.9}(NHC_6H_5)_{1.9}]$, has been synthesized by nucleophilic addition of fullerene with benzylamine in DMSO/*o*-dichlorobenzene. Free radical copolymerization of BZAF with methyl methacrylate or ethyl methacrylate gave high yields of copolymers. The optical limiting threshold of BZAF is comparable to that of C_{60} and stronger than those of the copolymers [31].

7.3 Organic Solar Cells

Fossil fuel alternatives, such as solar energy, are moving to the forefront in various research fields. Polymer-based organic photovoltaic systems hold the promise of a cost-effective, lightweight solar energy conversion platform, which could benefit

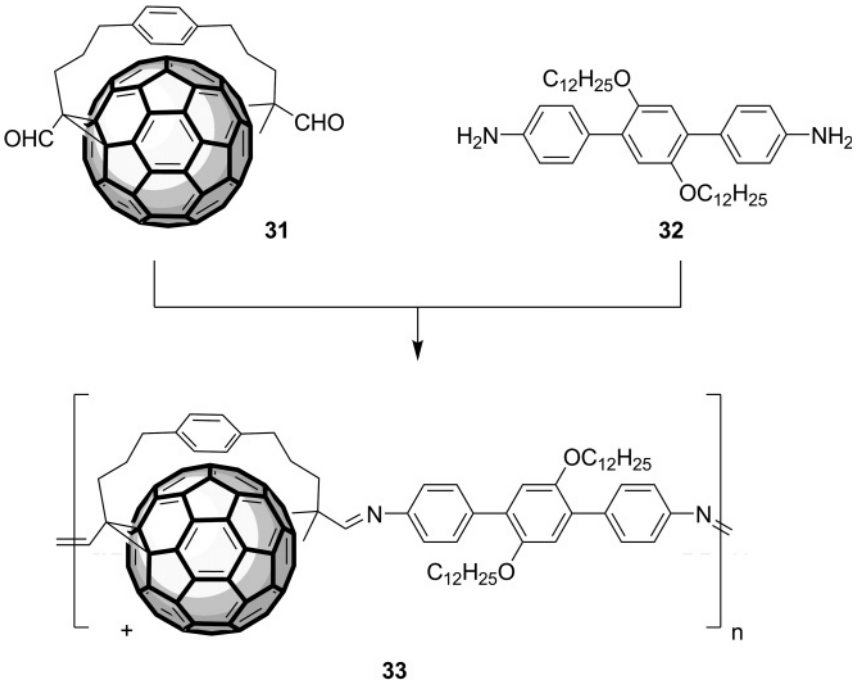

Scheme 7.8

from simple solution processing of the active layer. The function of such excitonic solar cells is based on photoinduced electron transfer from a donor to an acceptor. Materials having a delocalized π electron system can absorb sunlight, create photogenerated charge carriers and transport these charge carriers [32–35]. Research on organic solar cells generally focuses either on solution processable organic semiconducting molecules/polymers or on vacuum-deposited small-molecular materials [36]. Photoinduced electron transfer from donor-type semiconducting polymers onto acceptor-type polymers or molecules, such as fullerenes [37], are utilized in these organic solar cells. Fullerenes have become the ubiquitous acceptors because of their high electron affinity and ability to transport charge effectively. The best solar cells currently achieve an efficiency of about 5% [38–43]; thus, significant advances in the fundamental understanding of the complex interplay between the active layer morphology and electronic properties are required if this technology is to find viable application (Figure 7.5).

Schanze *et al*. have described the layer-by-layer (LBL) fabrication of multilayer films and photovoltaic cells using poly(phenylene ethynylene)-based anionic conjugated polyelectrolytes as electron donors and water-soluble cationic fullerene C_{60} derivatives as acceptors [44]. LBL film deposition was found to be linearly related to the number of bilayers, as monitored by UV/vis absorption. Atomic force microscopy (AFM) and scanning electron microscopy (SEM) of the multilayer

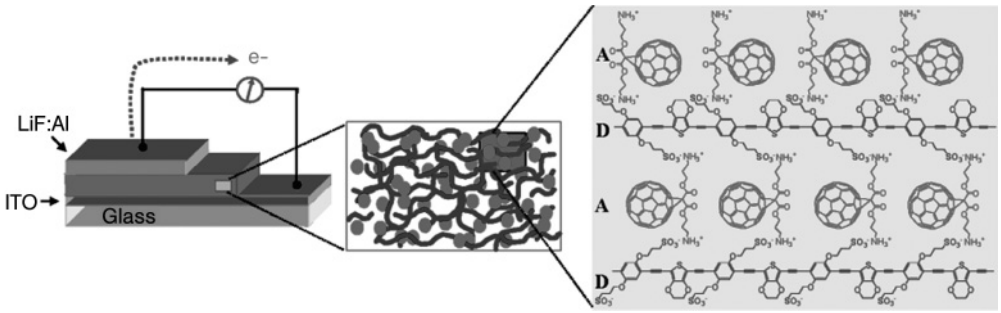

Figure 7.5 Schematic representation of the photovoltaic cell structure, showing the alternating donor and acceptor layers forming the active material (Reproduced by permission of the American Chemical Society).

films revealed an aggregated but relatively uniform morphology devoid of any long-range phase separation. The maximum incident monochromatic photon to current conversion efficiency (IPCE) of the photovoltaic cells was 5.5%, the highest efficiency reported to date for cells fabricated using the LBL fabrication technique; since the thin film cells do not provide complete absorption of the incident light, the current generation per photon absorbed may be as much as 10%. The cells exhibited open circuit voltages of 200–250 mV with the highest measured short circuit currents up to 0.5 mA cm^{-2} and fill factors around 30%. The power conversion efficiencies measured at AM 1.5 solar conditions (100 mW cm^{-2}) varied between 0.01 and 0.04%, and similar to the IPCE results the efficiency is a function of the thickness of the PV active layer.

Donor–acceptor materials based on random polynorbornenes bearing pendant phthalocyanine and fullerene units have been synthesized by Grubbs and his group (Scheme 7.9) [45]. Preliminary solar cells built with copolymer **36** as the active layer have shown only a moderate power-conversion efficiency of about 0.07% under simulated solar illumination (AM 1.5, 100 mW cm^{-2}). The good match between the photocurrent (IPCE) and the absorption spectra of thin films of copolymer **36** confirms the ability of the material to create charge carriers from absorbed photons with a wavelength of up to 800 nm. Their present investigations are directed at the optimization of the devices by improving the film morphology. Furthermore, the influence of the donor/acceptor ratio on the performance will also be studied, as the fullerene content may be too low relative to bulk heterojunction solar cells with conjugated polymers.

Photoexcitation spectroscopic investigations have shown that double-cables in their solid state undergo photoinduced electron transfer, leading to long-lived, mobile charge carriers, as observed earlier in conjugated polymer/fullerene composites [46–51]. Since in double-cable polymers phase separation cannot occur, these materials are indeed appealing as a way to control both electronic and morphological properties within the photoactive layer of plastic solar cells.

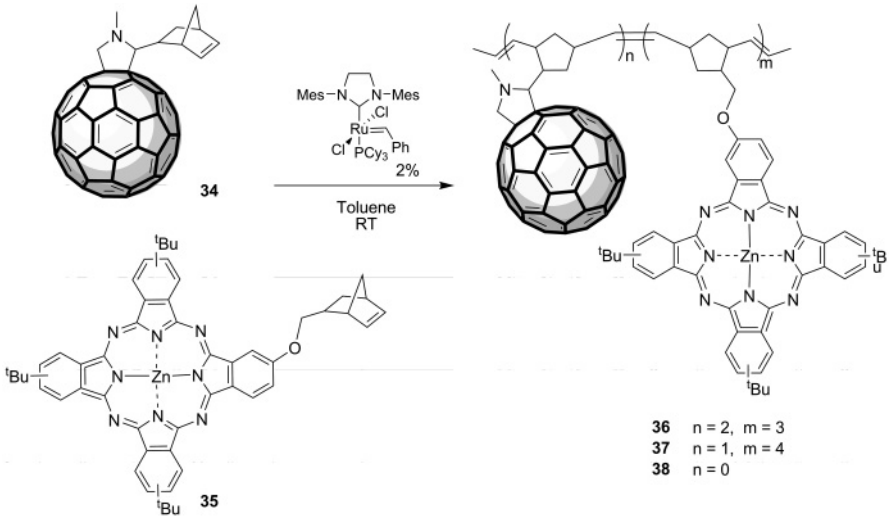

Scheme 7.9

A class of soluble double-cables has been described by Xiao *et al.* [52] and by Wang *et al.* [53, 54]. Based on the well established photoconducting as well as electrochemical properties of carbazole, they synthesized a soluble regular copolymer containing *p*-phenylene vinylene and carbazole units, the latter bearing a pendant azido functionality (Figure 7.6). Reaction with C_{60} in chlorobenzene gave a soluble fraction (CCl_4) with a fullerene percentage estimated spectroscopically as 19.9 wt%. (**39**). Similarly, they synthesized a double-cable containing also triphenylamine moieties (**41**). In this case, the fullerene content was about 21 wt%. The weight-average M_w values were determined by gel permeation chromatography as 3810 for **39** and 5051 for **41**. Based on these values, these double-cables clearly consist of only a few repeating units. A highly fullerene loaded double-cable has been prepared by Wang's group (**40**) [53]. In this latter material, the fullerene percentage has been estimated as high as 68.8 wt%. This value seems to be overestimated, since, based on the repeating unit, the calculated maximum fullerene loading is ca. 57 wt%. Nevertheless, this is a high fullerene loading, approaching that of conjugated polymer/fullerene composites used for the fabrication of "bulk heterojunction" solar cells with improved efficiency. By means of thermal gravimetric analysis, these copolymers have been found to be stable up to about 350 °C, and moderate weight losses occurred only within the range 380–460 °C. Spectroscopic and electrochemical studies allowed the authors to conclude that the electronic properties of the fullerene moieties were substantially preserved in all cases. Photoinduced electron transfer has been claimed to occur due to photoluminescence quenching observed in chloroform solutions. These double cable polymers are presently being tested as material for plastic PV energy conversion.

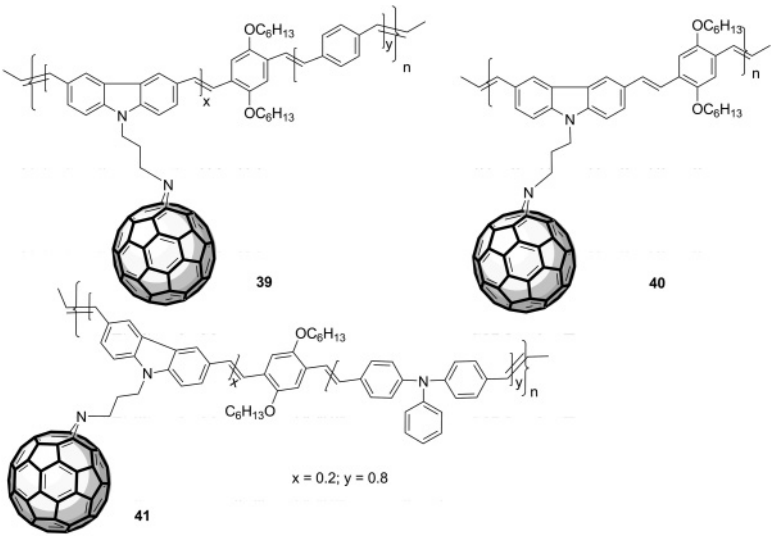

Figure 7.6 Some soluble double-cables compounds.

These three copolymers have an interesting increasing C_{60} content, that is, 19.9 wt% for **41**, 21% for **39**, and a remarkable 57% for **40**. The last molecule had very good properties as a dopant for poly-l,4-[2-(3,7-dimethyloctyloxy)-3,5,6-trimethoxylphenylenevinylene] (POMPV) in polymer OLED [54]. In fact, blending 1 wt% of **40** into conjugated polymer POMPV matrix resulted in an increase of LED luminescence and luminescence effect, making this dopant polymer one of the more promising hole-trapping candidates in polymer LEDs for further optimization.

However, on examining the M_w values of PPV-based polymers **39–41** it seems surprising that they move in the 2307–5838 amu range. Although the authors ascribed this to the partial solubility of such polymers in THF, the more soluble polymer precursors showed exactly the same M_w range.

Li and coworkers have described synthetic methods for fabricating conjugated polymer systems containing porphyrin, PPV and/or pendant fullerene units by means of the Wittig reaction (Scheme 7.10) [55]. Notably, the reduction potentials of fullerene attached to the conjugated backbone are decreased compared to the corresponding reduction process of the monomer, which indicates better electron-accepting ability. The first reduction potential of the polymers decreased when the content of the fullerene unit in the polymers increased. Although the first oxidation potential of the polymers is bigger than the corresponding oxidation peak potential of the fullerene, the potential gaps between the first oxidation peak potential and reduction peak potential of the polymers gradually decrease when the fullerene content in the polymers increases. These results show that the polymer with pendent fullerene, porphyrin and PPV units is a good candidate for a photoinduced electron-transfer system.

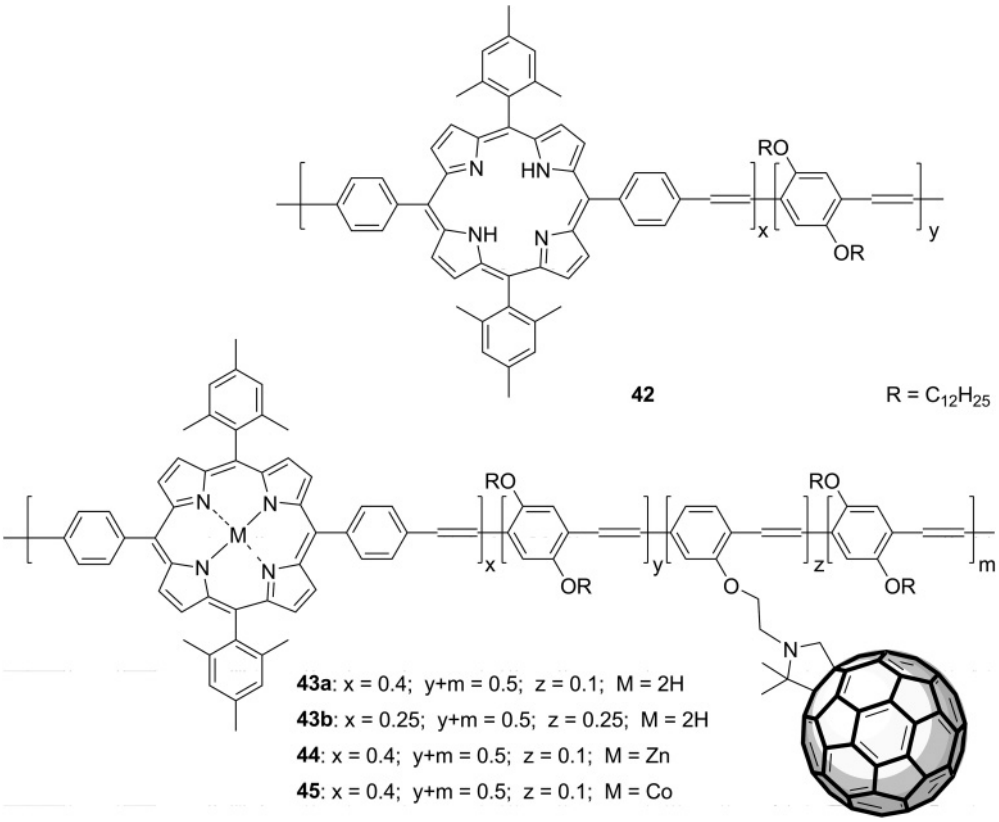

Scheme 7.10

A conventional three-electrode cell has been used to measure the photoelectrochemical properties of the monolayer film deposited on indium-tin oxide (ITO) glass. The photocurrent of the polymer monolayer film deposited on ITO electrode was measured separately at white light irradiation of 20.7 mW cm^{-2}. As shown in Figure 7.7a and b, a steady and rapid photocurrent response was produced when irradiation of the monolayer film was switched on and off. More interestingly, the photocurrent was enhanced when the content of the fullerene unit in the polymers increased. This was due to the increase of the component of fullerene electron acceptor in the polymers.

Figure 7.8 shows the chemical structures of four novel DC polymers in which the C_{60} moiety has been connected via Prato's reaction [56–58].

Photovoltaic cells have been prepared using polymers **46–48** in which the fullerene content varies between ~3% for **46a** and ~28% for **47** [59]. An ITO/PEDOT:PSS/polymer blend/Al architecture was employed in which the polymers were blended 1:1 by weight with MEH-PPV. However, the most efficient device in which the active layer was constituted solely by **46b** showed an overall conversion efficiency of only 0.01%.

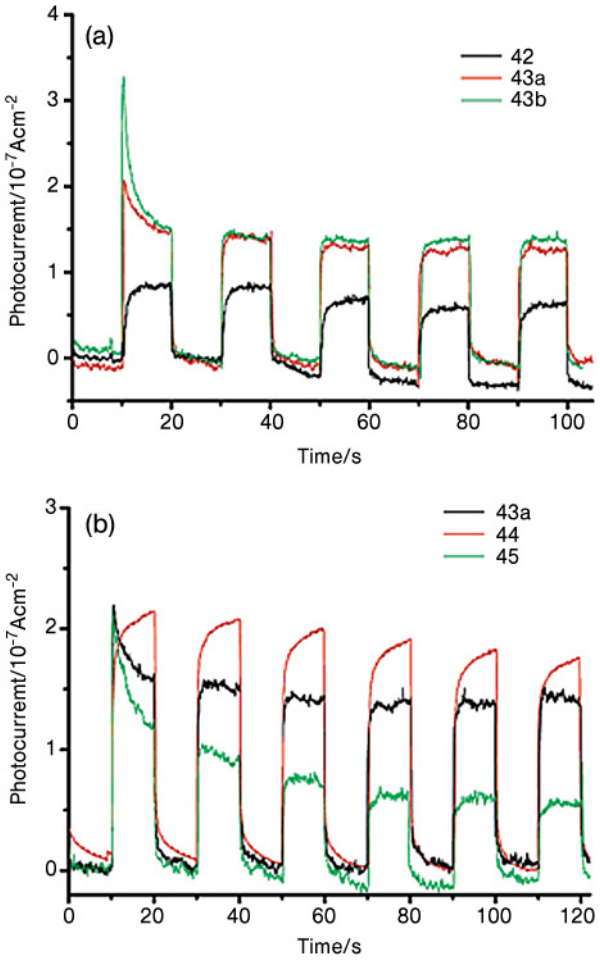

Figure 7.7 (a) PP ((Porphyrin)(phenylenevinylene)), $P_4P_5F_1$ ((Porphyrin)$_4$(phenylenevinylene)$_5$(Fullerene)$_1$), $P_1P_2F_1$ ((Porphyrin)$_1$(phenylenevinylene)$_2$(Fullerene)$_1$) and (b) $P_4P_5F_1$ ((Porphyrin)(phenylenevinylene)), $ZnP_4P_5F_1$ ((Zn-Porphyrin)$_4$(phenylenevinylene)(Fullerene)$_1$), $CoP_4P_5F_1$ ((Co-Porphyrin)$_4$(phenylenevinylene)). Photocurrent generation of monolayer films upon irradiation with 20.7 mW cm^{-2} white light in 0.5 M KCl solution.

Since polyacetylene derivatives exhibit unique properties such as semiconductivity, high gas permeability, helix inversion and nonlinear optical properties [60, 61] they represent an interesting class of macromolecules to be investigated as polymeric backbone in double-cable polymers. In fact, it is expected that attaching side electroactive groups (i.e., fullerenes and porphyrins) to the well-defined π-conjugated system [62–67] will improve the light-harvesting capacity and charge-separation efficiency for potential applications in solar cells (based on synergistic actions of pendant and main-chain conjugation). In this light, Li and

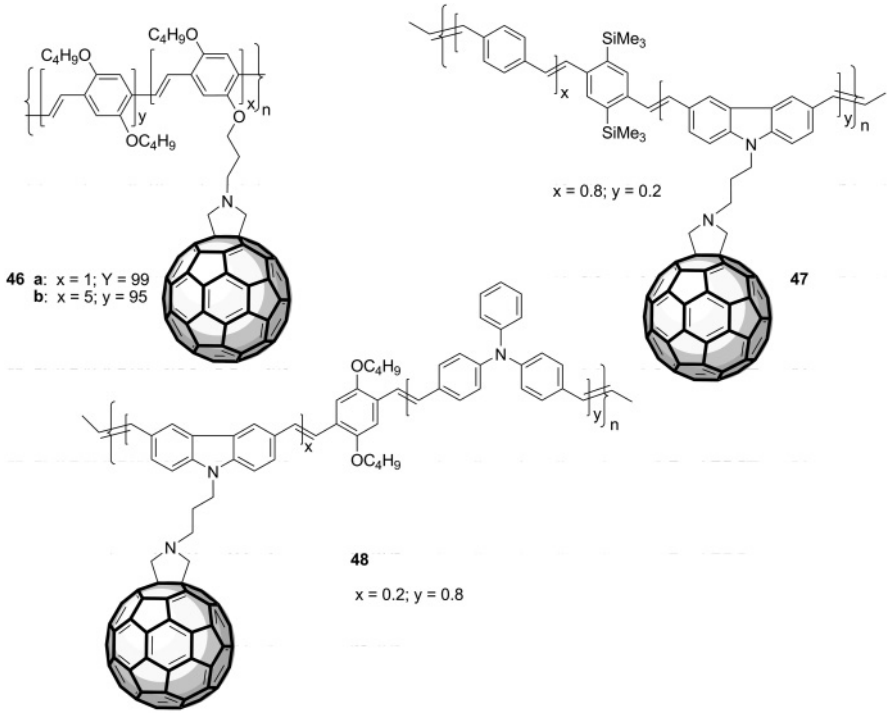

Figure 7.8 Chemical structures of some novel DC polymers.

coworkers have prepared several polyacetylene-based DC bearing fullerene and zinc-porphyrin (ZnP, **53**) [68, 69], fullerene and perylenebisimide (**56**) [70], or only fullerene (**55**) as the pendant groups (Scheme 7.11).

Polymers **51** and **52** are synthesized by reacting monomers **49** and **50** in the presence of norbornandienerhodium(I) chloride dimer ($[Rh(nbd)Cl]_2$) in dry chloroform (Scheme 7.11). The ^1H NMR spectra for all DC polyacetylenes show a signal at 5.3 ppm, which is assignable to the main-chain olefinic protons, indicating a cis-trans structure. However, the broadening of such peaks reveals that the large C_{60}, ZnP and perylene units induce distortion of the stereoregularity of the main chain.

7.4 Other Applications

In 2005, an amphiphilic ABA triblock polymer capped with C_{60} at both ends was prepared by Gan *et al.* via the ATRP strategy (Figure 7.9) [71]. C_{60} was successfully incorporated at both ends of the polymer chain via azido cycloaddition. In aqueous solution, **57** aggregates to form flower micelles that can potentially be used as carriers for drug/gene delivery application.

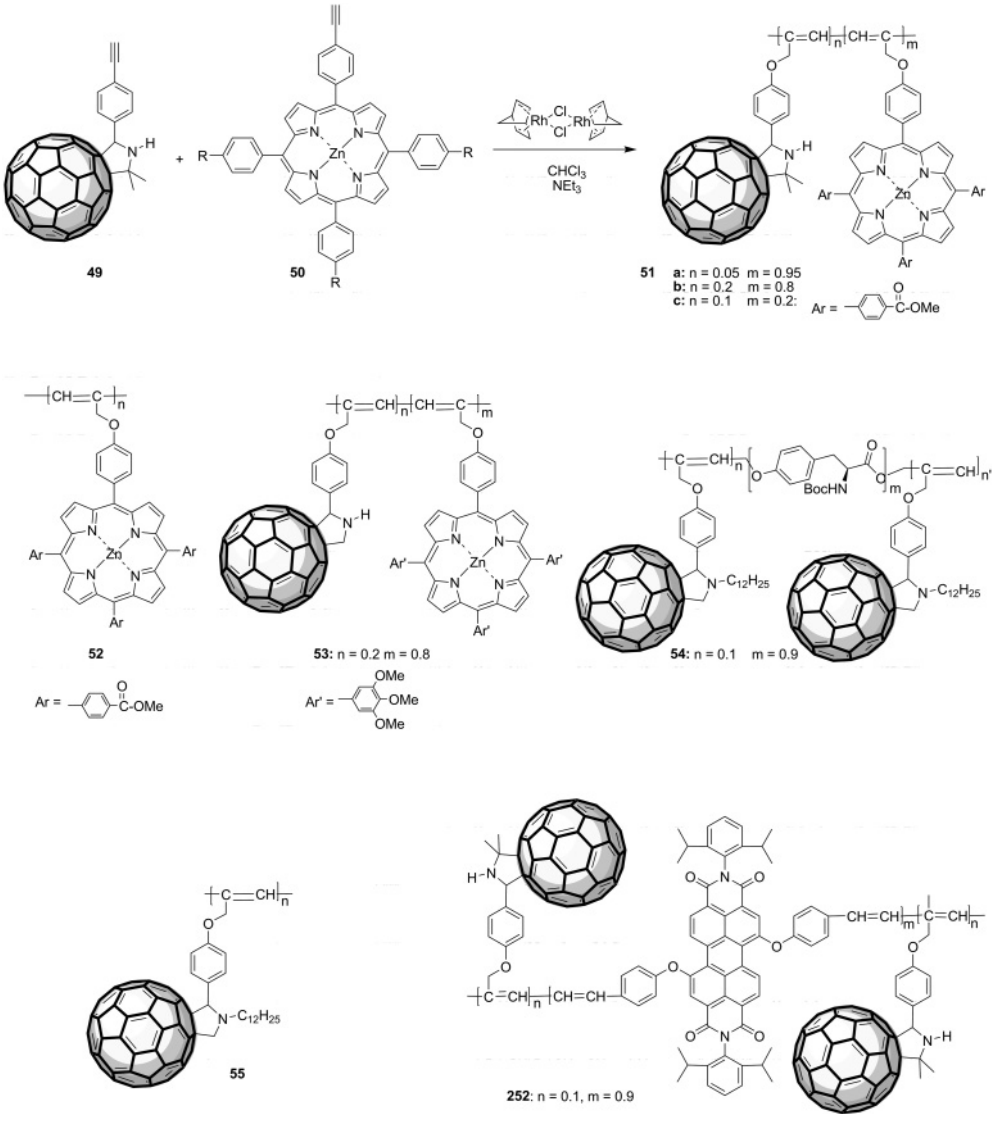

Scheme 7.11

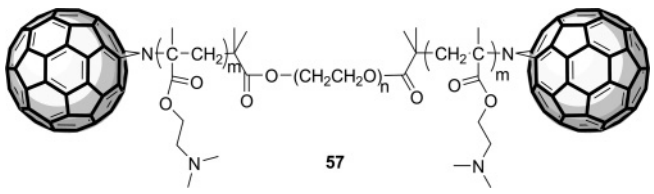

Figure 7.9 An amphiphilic ABA triblock polymer capped with C_{60} at both ends.

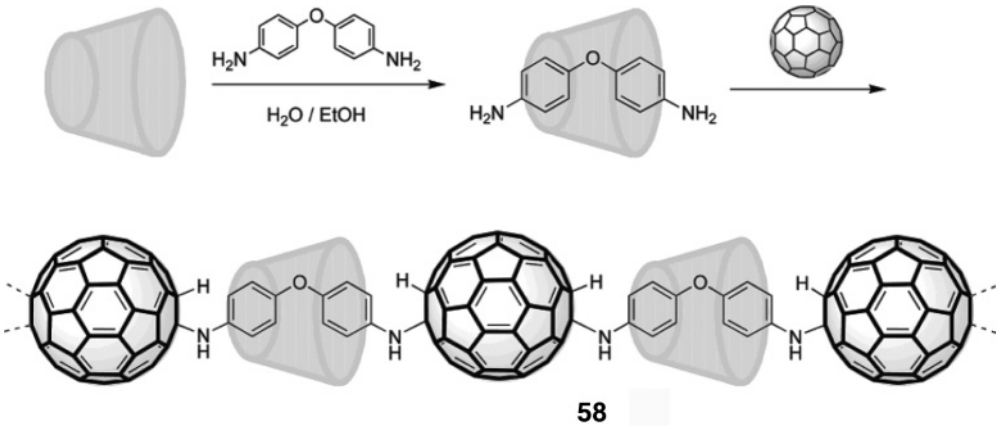

Scheme 7.12 (Reproduced by permission of the Royal Society of Chemistry).

The first water-soluble main-chain C_{60} polymers have been prepared by Geckeler *et al.* (Scheme 7.12) [72]. Polymer **58** was synthesized by nucleophilic reaction of the α-cyclodextrin-bis(*p*-aminophenyl) ether complex (CD-BPE) with C_{60}. The resulting polymer **58** exhibited an extraordinary solubility in water (>10 mg mL^{-1}) as well as a very narrow polydispersity index of 1.06. Meanwhile, the CD moieties play a crucial function since they not only furnished water solubility to the final polymer but also prevented further branching in the C_{60} cage due to their bulkiness. Interestingly, this polymer has been successfully employed as a highly efficient DNA cleaving agent under visible light conditions [73]. The quantitative DNA-cleaving achieved suggests strong application prospects of water-soluble C_{60}-polymers in photodynamic cancer therapy.

In one example, Liu and coworkers have prepared a water-soluble fullerene assembly with a coordinated metal center via end-to-end intermolecular inclusion complexation of fullerene with a cyclodextrin dimer [74].

Figure 7.10 shows the supramolecular polymer **59**, whose TEM micrographs display the presence of linear structures with a length in the range 150–250 nm. Moreover, this complex showed biological activity since it had an effective DNA-cleavage ability under light irradiation, representing a potential application of **59** in medicinal chemistry.

In another investigation, fullerene-containing star-shaped polymers prepared by Sun and coworkers displayed optical magnetic properties. These polymers were synthesized using the diazo salt derived from bithiazole (**60**) and [60]fullerene (Scheme 7.13) [75]. After copolymerization, the same workers also prepared the corresponding ferro complexes by treating polymer **61** with $FeSO_4$ in DMSO solution at 60 °C. Interestingly, the so-obtained derivative **62** exhibited soft magnetic behavior, whereas the precursor polymer **61** behaves as an anti-ferromagnetic material.

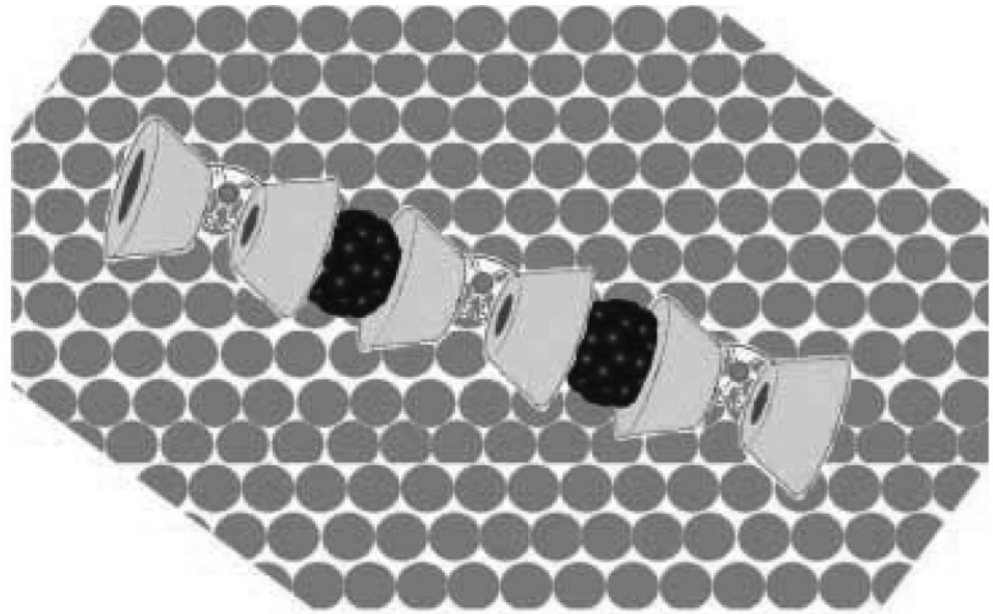

59

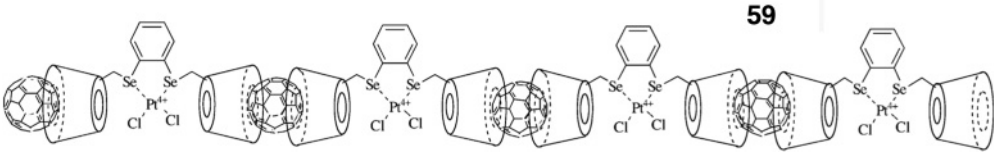

Figure 7.10 Supramolecular polymer **59** (Reproduced by permission of Wiley-VCH).

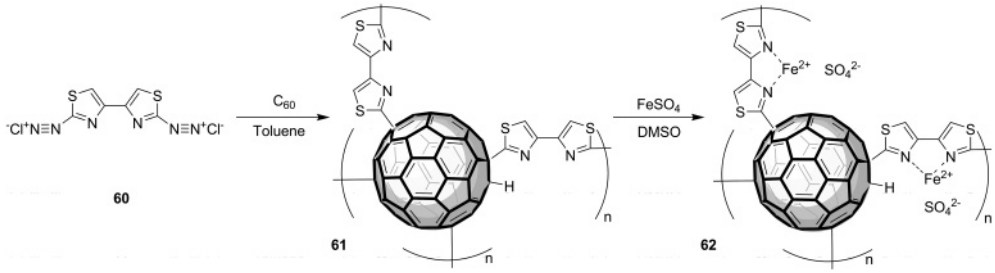

Scheme 7.13

7.5 Summary

C_{60}-based polymers will furnish unprecedented materials in which the integration of fullerenes as a photo- and electroactive building blocks into the polymer structure should result in new properties for development of realistic applications. In this regard, after the discovery of fullerenes, the scientific community is looking for real applications of this new carbon allotrope. Once more, the ease of processability and availability of polymers could be the key for application of fullerenes for practical purposes.

With the development of fullerene organic chemistry, many low-molecular organic reactions can be used in polymeric modification of fullerene. By controlling the functional groups in polymers, and the reaction conditions, many well-defined fullerene polymers can be produced, such as crosslinked fullerene polymers, end-capped fullerene polymers, star-shaped fullerene polymers, main-chain fullerene polymers, side-chain fullerene polymers, double-cable fullerene polymers, supramolecular fullerene polymers. At the same time, many living polymerization methods have been introduced into the preparation of the polymer fullerenes. Thus it is now possible to control the architecture of fullerene polymers precisely by methods that constitute a good platform for the practical applications of fullerene derivatives. Implementing the chemistry of fullerenes into macromolecular chemistry has allowed the preparation of new polymer materials that exhibit outstanding structural, electrochemical and photophysical properties that might find application, and in some cases are currently under intensive and competitive research, in different fields.

References

1 Kroto, H.W., Heath, J.R., O'Brien, S.C., Curl, R.F. and Smalley, R.E. (1985) *Nature*, **318**, 162.

2 Kratschmer, W., Lamb, L.D., Fostiropoulos, K. and Huffman, D.R. (1990) *Nature*, **347**, 354.

3 (a) Hammond, G.S. and Kuck, V.J. (eds) (1992) *Fullerenes: Synthesis, Properties, and Chemistry of Large Carbon Clusters*, ACS Symposium Series 481, American Chemical Society, Washington, DC.
(b) Hebard, A.F. (1993) *Annu. Rev. Mater. Sci.*, **23**, 159.

4 (a) Allemand, P.M., Khemani, K.C., Koch, A., Wudl, F., Holczer, K., Donovan, S., Grüner, G. and Thompson, J.D. (1991) *Science*, **253**, 301.
(b) Lappas, A., Prassides, K., Vavekis, K., Arcon, D., Blinc, R., Cevc, P., Amato, A., Feyerherm, R., Gygax, F.N. and Schenck, A. (1995) *Science*, **267**, 1799.
(c) Narymbetov, B., Omerzu, A., Kabanov, V.V., Tokumoto, M., Kobayashi, H. and Mihailovic, D. (2000) *Nature*, **407**, 883.
(d) Makarova, T.L., Sundqvist, B., Hohne, R., Esquinazi, P., Kopelevich, Y., Scharff, P., Davydov, V.A., Kashevarova, L.S. and Rakhmanina, A.V. (2001) *Nature*, **413**, 716.

5 (a) Hebard, A.F., Rosseinsky, M.J., Haddon, R.C., Murphy, D.W., Glarum, S.H., Palstra, T.T.M., Ramirez, A.P. and Kortan, A.R. (1991) *Nature*, **350**, 600.
(b) Schon, J., Kloc, C. and Batlogg, B. (2001) *Science*, **293**, 2432.
(c) Dagotto, E. (2001) *Science*, **293**, 2410.
(d) Grant, P. (2001) *Nature*, **413**, 264.

6 (a) Xie, Q., Pérez-Cordero, E. and Echegoyen, L.J. (1992) *J. Am. Chem. Soc.*,

114, 3978.(b) Echegoyen, L. and Echegoyen, L.E. (1998) *Acc. Chem. Res.*, **31**, 593.

7 (a) Guldi, D.M. (2000) *Chem. Commun.*, 321.
(b) Guldi, D.M. and Prato, M. (2000) *Acc. Chem. Res.*, **33**, 695.

8 Guldi, D.M. and Martín, N. (eds) (2002) *Fullerenes: From Synthesis to Optoelectronic Properties*, Kluwer Academic Publishers, Dordrecht, The Netherlands.

9 (a) Giacalone, F. and Martín, N. (2006) *Chem. Rev.*, **106**, 5136.
(b) Nakamura, E. and Isobe, H. (2003) *Acc. Chem. Res.*, **36**, 807.
(c) Wang, C., Guo, Z.-X., Fu, S., Wu, W. and Zhu, D. (2004) *Prog. Polym. Sci.*, **29**, 1079.
(d) Dai, L. and Mau, A.W.H. (2001) *Adv. Mater*, **13**, 899.
(e) Thompson, B.C. and Fréchet, J.M.J. (2008) *Angew. Chem. Int. Ed.*, **47**, 58.
(f) Cravino, A. and Sariciftci, N.S. (2002) *J. Mater. Chem.*, **12**, 1931–43.

10 Anderson, H.L., Boudon, C., Diederich, F., Gisselbrecht, J.-P., Gross, M. and Seiler, P. (1994) *Angew. Chem. Int. Ed. Engl.*, **33**, 1628.

11 Ferraris, J.P., Yassar, A., Loveday, D. and Hmyene, M. (1998) *Opt. Mater. (Amsterdam)*, **9**, 34.

12 Cravino, A., Zerza, C., Maggini, M., Bucella, S., Svensson, M., Andersson, M.R., Neugebauer, H. and Sariciftci, N.S. (2000) *Chem. Commun.*, 2487.

13 Cravino, A., Zerza, G., Neugebauer, H., Bucella, S., Maggini, M., Menna, E., Svensson, M., Andersson, M.R. and Sariciftci, N.S. (2001) *Synth. Met.*, **121**, 1555.

14 Cravino, A., Zerza, G., Neugebauer, H., Maggini, M., Bucella, S., Menna, E., Svensson, M., Andersson, M.R., Brabec, C.J. and Sariciftci, N.S. (2002) *J. Phys. Chem. B*, **106**, 70.

15 Sonmez, G., Shen, C.K.F., Rubin, Y. and Wudl, F. (2005) *Adv. Mater.*, **17**, 897.

16 Fang, H., Wang, S., Xiao, S., Yang, J., Li, Y., Shi, Z., Li, H., Liu, H., Xiao, S. and Zhu, D. (2003) *Chem. Mater.*, **15**, 1593.

17 Fang, H., Shi, Z., Li, Y., Xiao, S., Li, H., Liu, H. and Zhu, D. (2003) *Synth. Met.*, **135–136**, 843.

18 (a) Cloutet, E., Fillaut, J.-L., Gnanou, Y. and Astruc, D. (1994) *J. Chem. Soc. Chem. Commun.*, 2433.
(b) Cloutet, E., Fillaut, J.-L., Gnanou, Y. and Astruc, D. (1996) *Chem. Commun.*, 1565.
(c) Cloutet, E., Fillaut, J.-L., Astruc, D. and Gnanou, Y. (1999) *Macromolecules*, **32**, 1043.

19 Arias, F., Echegoyen, L., Wilson, S.R. and Lu, Q. (1995) *J. Am. Chem. Soc.*, **117**, 1422.

20 Chochos, C.L., Kallitsis, J.K. and Gregoriou, V.G. (2005) *J. Phys. Chem. B*, **109**, 8755.

21 Gu, T., Tsamouras, D., Melzer, C., Krasnikov, V., Gisselbrecht, P., Gross, M., Hadziioannou, G. and Nierengarten, J.-F. (2002) *ChemPhysChem*, **3**, 124.

22 Mignard, E., Hiorns, R.C. and François, B. (2002) *Macromolecules*, **35**, 6132.

23 (a) Anantharaj, V., Wang, L.Y., Cateenwala, L. and Chiang, L.Y. (1999) *J. Chem. Soc. Perkin Trans.1*, 3357.
(b) Wang, L.Y., Anantharaj, V., Ashok, K. and Chiang, L.Y. (1999) *Synth. Met.*, **103**, 2350.

24 Canteenwala, L., Anantharaj, V., Patil, S.V., Haldar, M. and Chiang, L.Y. (2002) *J. Macromol. Sci.-Pure Appl. Chem. A*, **39**, 1069.

25 (a) Canteenwala, T., Patil, S.V., Haldar, M., Padmawar, P.A., Verma, S. and Chiang, L.Y. (2003) *J. Macromol. Sci.-Pure Appl. Chem. A*, **40**, 1263.
(b) Canteenwala, T., Padmawar, P.A., Patil, S.V., Haldar, M. and Chiang, L.Y. (2005) *Synth. Met.*, **154**, 5.

26 Anantharaj, V., Wang, L.Y., Canteenwala, T. and Chiang, L.Y. (1999) *J. Chem. Soc., Perkin Trans. 1*, 3357.

27 Loy, D.A. and Assink, R.A. (1992) *J. Am. Chem. Soc.*, **114**, 3977.

28 Kvarnström, C., Kulovaara, H., Damlin, P., Vuorinen, T., Lemmetyinen, H. and Ivaska, A. (2005) *Synth. Met.*, **149**, 39.

29 Kvarnström, C., Hulovaara, H., Damlin, P. and Ivaska, A. (2003) *Synth. Met.*, **135–136**, 783.

30 Ito, H., Ishida, Y. and Saigo, K. (2006) *Tetrahedron Lett.*, **47**, 3095.

31 Lu, Z., Goh, S.H., Lee, S.Y., Sun, X. and Ji, W. (1999) *Polymer*, **40**, 2863.

32 Coenjarts, C., Garcia, O., Llauger, L., Palfreyman, J., Vinette, A.L. and

Scaiano, J.C. (2003) *J. Am. Chem. Soc.*, **125**, 620.
33 Mondal, R., Shah, B.K. and Neckers, D.C. (2006) *J. Am. Chem. Soc.*, **128**, 9612.
34 Saeki, A., Seki, S., Koizumi, Y., Sunagawa, T., Ushida, K. and Tagawa, S. (2005) *J. Phys. Chem. B*, **109**, 10015.
35 Yan, X.Z. and Goodson, T. III (2006) *J. Phys. Chem. B*, **110**, 14667.
36 Hoppe, H. and Sariciftci, N.S. (2004) *J. Mater. Chem.*, **19**, 1924.
37 Nunzi, J.M. (2002) *C. R. Physique*, **3**, 523.
38 Kim, J.Y., Lee, K., Coates, N.E., Moses, D., Nguyen, T.-Q., Dante, M. and Heeger, A.J. (2007) *Science*, **317**, 222.
39 Kim, J.Y., Kim, S.H., Lee, H.-H., Lee, K., Ma, W., Gong, X. and Heeger, A.J. (2006) *Adv. Mater.*, **18**, 572.
40 Kim, K., Liu, J., Namboothiry, M.A.G. and Carroll, D.L. (2007) *Appl. Phys.Lett.*, **90**, 163511.
41 Ma, W., Yang, C., Gong, X., Lee, K. and Heeger, A.J. (2005) *Adv. Funct. Mater.*, **15**, 1617.
42 Li, G., Shrotriya, V., Huang, J., Yao, Y., Moriarty, T., Emery, K. and Yang, Y. (2005) *Nat. Mater.*, **4**, 864.
43 Xue, J., Rand, B.P., Uchida, S. and Forrest, S.R. (2005) *Adv. Mater.*, **17**, 66.
44 Mwaura, J.K., Pinto, M.R., Witker, D., Ananthakrishnan, N., Schanze, K.S. and Reynolds, J.R. (2005) *Langmuir*, **21**, 10119.
45 Neugebauer, C., Winder, M., Drees and Sariciftci, N.S. (2007) *Chem. Asian J.*, **1–2**, 148.
46 Gunes, S., Neugebauer, H. and Sariciftci, N.S. (2007) *Chem. Rev.*, **107**, 1324.
47 Luzzati, S., Scharber, M., Catellani, M., Giacalone, F., Segura, J.L., Martín, N., Neugebauer, H. and Sariciftci, N.S. (2006) *J. Phys. Chem. B*, **110**, 5351.
48 Guldi, D.M., Luo, C., Swartz, A., Gómez, R., Segura, J.L., Martín, N., Brabec, C. and Sariciftci, N.S. (2002) *J. Org. Chem.*, **67**, 1141.
49 Zerza, G., Cravino, A., Neugebauer, H., Sariciftci, N.S., Gómez, R., Segura, J.L., Martín, N., Svensson, M. and Andersson, M.R. (2001) *J. Phys. Chem. A*, **105**, 4172.
50 Cravino, A., Neugebauer, H., Petr, A., Skabara, P.J., Spencer, H.J., McDouall, J.J.W., Dunsch, L. and Sariciftci, N.S. (2006) *J. Phys. Chem. B*, **110**, 2662.
51 Roquet, S., Cravino, A., Leriche, P., Aleveque, O., Frere, P. and Roncali, J. (2006) *J. Am. Chem. Soc.*, **128**, 3459.
52 Xiao, S., Wang, S., Fang, H., Li, Y., Shi, Z., Du, C. and Zhu, D. (2001) *Macromol. Rapid Commun.*, **22**, 1313.
53 Wang, S., Xiao, S., Li, Y., Shi, Z., Du, C., Fang, H. and Zhu, D. (2002) *Polymer*, **43**, 2049.
54 Wang, S., Yang, J., Li, Y., Lin, H., Guo, Z., Xiao, S., Shi, Z., Zhu, D., Woo, H.-S., Carroll, D.L., Kee, L.-S. and Lee, J.-H. (2002) *Appl. Phys. Lett.*, **80**, 3847.
55 Huang, C.S., Wang, N., Li, Y.L., Li, C.H., Li, J.B., Liu, H.B. and Zhu, D.B. (2006) *Macromolecules*, **39**, 5319.
56 Maggini, M., Prato, M. and Scorrano, G. (1993) *J. Am. Chem. Soc.*, **115**, 9798.
57 Prato, M. and Maggini, M. (1998) *Acc. Chem. Res.*, **31**, 519.
58 Tagmatarchis, N. and Prato, M. (2003) *Synlett*, 768.
59 Yang, C., Li, H., Sun, Q., Qiao, J., Li, Y., Li, Y. and Zhu, D. (2005) *Sol. Energy Mater. Sol. Cells*, **85**, 241.
60 Nagai, K., Masuda, T., Nakagawa, T., Freeman, B.D. and Pinnau, I. (2001) *Prog. Polym. Sci.*, **26**, 721.
61 Masuda, T. (1996) Acelylenic polymers, in *Polymeric Material Encyclopedia*, Vol. **1** (ed. J.C. Salamone), CRC, New York, p. 32.
62 Yashima, E., Huang, S.L., Matsushima, T. and Okamoto, Y. (1995) *Macromolecules*, **28**, 4184.
63 Teraguchi, M. and Masuda, T. (2000) *Macromolecules*, **33**, 240.
64 Ikeda, A., Hatano, T., Shinkai, S., Akiyama, T. and Yamada, S. (2001) *J. Am. Chem. Soc.*, **123**, 4855.
65 Nishimura, T., Takatani, K., Sakurai, S.L., Maeda, K. and Yashima, E. (2002) *Angew. Chem. Int. Ed.*, **41**, 3602.
66 Sanda, F., Kawaguchi, T., Masuda, T. and Kobayashi, N. (2003) *Macromolecules*, **36**, 2224.
67 Konishi, T., Ikeda, A., Asai, M., Hatano, T., Shinkai, S., Fujitsuka, M., Ito, O., Tsuchiya, Y. and Kikuchi, J.I. (2003) *J. Phys. Chem. B*, **107**, 11261.
68 Lu, F., Xiao, S., Li, Y., Liu, H., Li, H., Zhuang, J., Liu, Y., Wang, N., He, X., Li, X., Can, L. and Zhu, D. (2004) *Macromolecules*, **37**, 7444.

69 Wang, N., Li, Y., Lu, F., Liu, Y., He, X., Jiang, L., Zhuang, J., Li, X., Li, Y., Wang, S., Liu, H. and Zhu, D. (2005) *J. Polym. Sci, Part A: Polym. Chem.*, **43**, 2851.
70 Liu, Y., Wang, N., Li, Y., Liu, H., Li, Y., Xiao, J., Xu, X., Huang, C., Cui, S. and Zhu, D. (2005) *Macromolecules*, **38**, 4880.
71 Yu, H., Gan, L.H., Hu, X., Venkatraman, S.S., Tam, K.C. and Gan, Y.Y. (2005) *Macromolecules*, **38**, 9889.
72 Samal, S., Choi, B.-J. and Geckeler, K.E. (2000) *Chem. Commun.*, 1373.
73 Samal, S., Choi, B.-J. and Geckeler, K.E. (2001) *Macromol. Biosci.*, **1**, 329.
74 Liu, Y., Yang, Y.-W., Chen, Y. and Zou, H.-X. (2005) *Macromolecules*, **38**, 5838.
75 Jiang, L., Sun, W., Weng, J. and Shen, Z. (2002) *Polymer*, **43**, 1563.

8
Polyfullerenes for Organic Photovoltaics

Antonio Cravino and Niyazi Serdar Sariciftci

8.1
Introduction

Organic semiconductors are emerging materials for innovative and "soft" optoelectronics applications, including photodetection and photovoltaic energy conversion. Using thin films of blended conjugated polymers and fullerene derivatives as electron donor (D) and acceptor (A), respectively, (solar light to electrical) power conversion efficiencies above 5% are currently obtained. This approach, known as D–A bulk-heterojunction (bulk heterojunction), has inspired the design of intrinsically ambipolar polymers to simultaneously control the electronic properties and the degree of D–A phase separation within the photoactive layer. The covalent grafting of acceptor moieties such as fullerenes onto π-conjugated polymeric backbones appeared as the first choice toward the preparation of such ambipolar organic semiconductors (pictorially called double-cable polymers). In this chapter, we review, along with examples, such double cable materials and their electronic and device properties. Furthermore, the concept of double-cable materials is critically revisited on the basis of the present understanding of organic photovoltaics and bulk-heterojunction solar cells.

8.1.1
Background

Converting solar light into electrical power with an efficiency above 5%, organic, plastic, electron donor (D) and acceptor (A) bulk-heterojunction solar cells are promising for a new kind of large area, flexible, light-weight-portable and eventually disposable photovoltaic applications. More importantly, on a longer time-scale, these devices could cost-effectively replace inorganic solar cells (mainly because of the low cost manufacturing processes, such as printing techniques etc.) [1–10] and contribute to ease the increasing energy problem [11].

Usually, the photoactive layer of bulk heterojunction solar cells is a physical blend [1–3] of a π-conjugated polymer [12] and a fullerene derivative [13–17]. This bulk heterojunction structure inspired the design and preparation of donor

Fullerene Polymers. Synthesis, Properties and Applications. Edited by Nazario Martín and Francesco Giacalone

ISBN: 978-3-527-32282-4

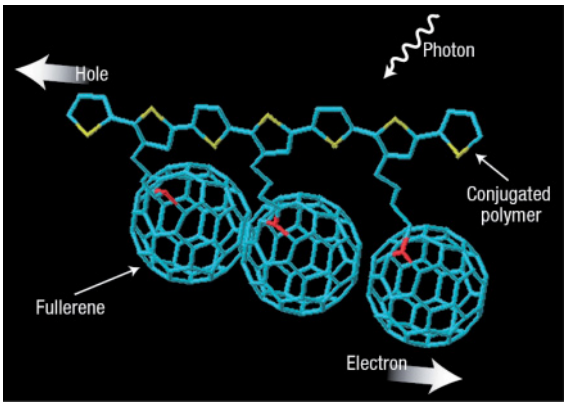

Figure 8.1 A double-cable polyfullerene consisting of fullerene pendants attached to a polythiophene conjugated chain. (Reproduced with permission of Nature Publishing from Reference [18a].)

conjugated polymers with covalently tethered acceptor fullerene moieties (Figure 8.1). Such donor–acceptor blends undergo a photoinduced charge transfer [19–21] leading to metastable positive and negative charged species on the donor and acceptor phases, respectively [18, 22, 23].

In addition, polyfullerenes such as double-cables were expected to lead to an intimate contact between the D and the A by preventing the phase separation often observed in blended layers. Provided that the driving forces are actually established in these devices (as discussed below), in double-cable polymers the holes should drift in-chain [24] then further continue their motion to the collecting positive electrode by inter-chain hopping, while the electrons jump between the pending A units in the opposite direction.

However, a fully homogeneous distribution of D and A "sites" might not represent the optimum topology/morphology for bulk heterojunction solar cells; rather, an optimized nano-scale D–A phase separation might be necessary. Still, double-cable polyfullerenes might lead to the simultaneous control of the electronic properties and nanomorphology within the active layer of photodetectors and bulk heterojunction solar cells, or in ambipolar field-effect transistors [25]. Although the polyfullerene double-cables approach has not, so far, led to spectacular solar power conversion efficiencies it remains a very stimulating concept for chemists and the materials scientists who dedicate their research to novel organic photovoltaic materials. This approach has been also taken into account in theoretical work modeling bulk heterojunction solar cells, and surely serves as a tool for a better comprehension and design of organic solar energy materials and solar cells.

We first, briefly, introduce the concept of bulk heterojunction solar cells, with the aim of pointing out the importance of the nanomorphology and the degree of D–A separation within the photoactive layer. Then, with no claims of completeness, we select examples of polyfullerene double-cables from the recent literature,

discussing their main spectroscopic, photophysical and photovoltaic properties. Finally, we critically review the concept of double-cable polymers on the basis of the present understanding of D–A heterojunctions, taking into account both recent experimental and theoretical results.

8.1.2
Organic D-A Photovoltaics and Bulk-Heterojunction Solar Cells

After the seminal work of Tang [26], great research activity has been devoted to the improvement of heterojunctions consisting of thin films of conjugated D and A molecules sandwiched between metal contacts (usually with different work functions, Figure 8.2a) [27–30].

Under illumination, following a π–π^* transition, neutral excitons are formed either in one or both materials. If the energy off-set between the lowest unoccupied molecular orbital (LUMO) of the donor and LUMO level of the acceptor is large enough, these excitons will dissociate – via an electron transfer – into metastable long-lived charged species, namely the radical-cations (polarons) of the D and the radical-anions of the A [19, 20]. A complete analogous process of photoinduced hole transfer can occur, when the offset between the highest occupied molecular orbital (HOMO) levels of the donor and of the acceptor is large enough. These

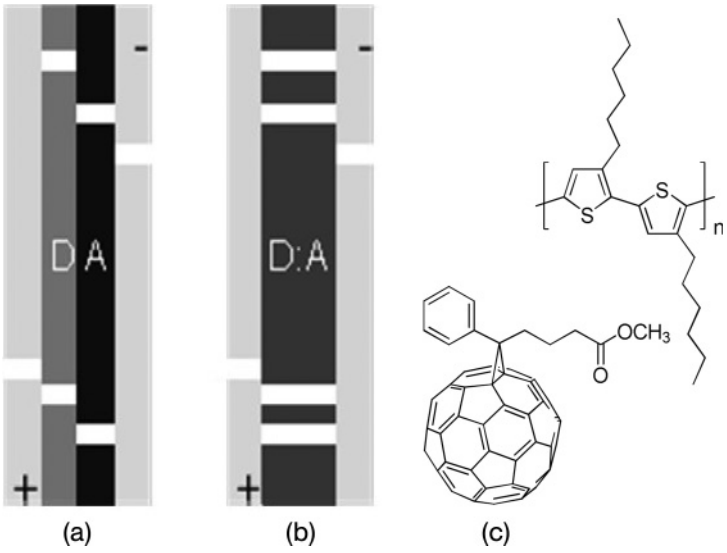

Figure 8.2 (a) Schematic representation of a D/A bilayer heterojunction, consisting of two molecules with HOMO and LUMO energetic offsets sandwiched between electrodes with different work functions; (b) in a bulk heterojunction solar cells, the D and the A are blended, providing a larger interface for photoinduced charge carrier generation; the energetic levels of the systems are shown by the white bars; (c) typical D:A couple, rr-poly(3-hexylthiophene) and the fullerene derivative 1-(3-methoxycarbonyl)propyl-1-phenyl-[6,6]-methanofullerene (PCBM).

photoactive heterojunctions might lead to diode-like rectification in current–voltage characteristics and to photovoltaic effects. Energy conversion efficiencies as high as 5% have been reached by optimizing such architectures [30].

In a bulk heterojunction, the D and A components are physically mixed so that they can interact through the entire device's volume (therefore called "bulk" heterojunction). Indeed, this approach enhances the process of photoinduced charge carrier generation and, thus, short circuit current and power conversion efficiency [1–7, 31, 32]. The driving forces relevant for the operation of both D/A bilayer and D:A bulk-heterojunction devices are discussed in Section 8.3.

8.1.3
D-A Phase Separation–Device Performance Relationship

This subsection points out the relationship between the D–A phase separation and performance in bulk heterojunction cells, providing the "original" motivation for the design of double-cable polyfullerenes. An in-depth coverage of the topic can be found in a recent review [33]. Until 2001, the best performing bulk heterojunction solar cells were devices based on a poly(*para*-phenylenevinylene) (so-called MDMO-PPV) and a soluble fullerene (PCBM) blended in a 1 : 3 wt-ratio [3, 9, 10]. Such an excess of fullerene was thought to be necessary to counterbalance its tendency to phase-segregate, and that only in exceeding amounts could it provide some intercontacts between the formed fullerene A domains. Preparing such devices using different solvents for spin-casting the active layer, Shaheen *et al.* obtained solar cells with remarkably different power conversion efficiencies [32]. As clarified by atomic force microscopy, chlorobenzene induced the formation of more homogenous blends, with finer domain size, and, thus, a larger D–A interfacial area, an effect beneficial for photoinduced charge carrier generation [34]. Such devices from chlorobenzene were indeed far superior to those with large scale nanodomains obtained from, for example, toluene as solvent.

In particular, maximizing the D–A interface was sought intensively, by modulating processing parameters such as the casting solvent, concentration, spinning speed, temperature and so on. It was also exciting to think of the synthesis of D conjugated polymers with covalently tethered A moieties (double cable polymers). The preparation of double-cable polyfullerenes, as well as systems such as D–A diblock copolymers, is a synthetically rather demanding task, as well as was an intellectually stimulating challenge. This class of polymers can have a degree of D–A phase separation ("secondary and tertiary structure") – at least in principle – engineered by their "primary structure" [18, 35, 36].

8.2
Double-Cable Polyfullerenes

Double-cables are members of the charm-bracelet polyfullerene family [15], with the specificity that their bracelet is a π-conjugated chain. Electrochemical polymerization is among the most straightforward methods to synthesize π-conjugated

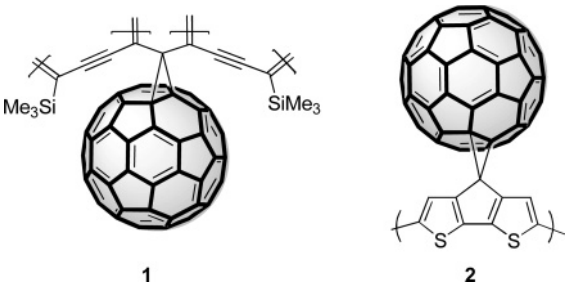

1 2

Figure 8.3 Structures of polymers **1** and **2**.

oligomers and polymers, at least for laboratory studies. Electrochemical synthesis technique were applied to prepare the first polyfullerene double-cables, **1** and **2** (Figure 8.3).

Contrary to what we have stated in a previous publication, the very first example of a double-cable was reported in 1994. Starting from bis(trimethylsilyl)methanofullerene, Anderson *et al*. synthesized the "double-sided" polydiacetylene **1** [37]. Two years later, Benincori *et al*. reported the synthesis of polycyclopentadithiophene **2**, whose electrochemical properties were investigated by cyclic voltammetry [38]. The trace showed one anodic process, ascribed to the reversible oxidation (p-doping) of the conjugated backbone, and three cathodic waves related to the reversible one-electron reduction steps of the fullerene moieties. These results, together with visible electronic absorption spectroscopy data, revealed a rather distorted conjugated chain with an effective conjugation length shorter than the unsubstituted parent polymer, but confirmed that the D and A moieties of the material basically retain their individual electronic and electrochemical properties, that is, no ground-state interaction between them was observed. Analogous results were obtained by Yassar, Ferraris *et al*. [39, 40]. While polybithiophene **3** was also prepared electrochemically, soluble materials **4** and **5** were, for the first time, chemically obtained by reacting head-to-tail copolythiophenes functionalized with azido- or primary amino-groups and fullerene C_{60} (Figure 8.4). In solution, these copolymers showed absorption spectra similar to those of standard polythiophenes, indicating that flexible chains linking the backbone to the pending fullerenes effectively relieved the steric hindrance.

8.2.1
Photoinduced Charge Transfer in Double-Cable Polyfullerenes

Crucial to photovoltaic applications, the first observation of a photoinduced charge transfer in double-cable polyfullerenes was reported in 2000. Polymer **6**, an electrochemically prepared polythiophene carrying fulleropyrrolidine moieties, was studied by means of different techniques, including steady-state photoexcited spectroscopy and light-induced electron spin resonance (Figure 8.5) [22, 23].

The photoinduced absorption spectrum showed two bands at about 1.4 and 0.6 eV, features typical of positive polarons on a thiophene-based backbone. The

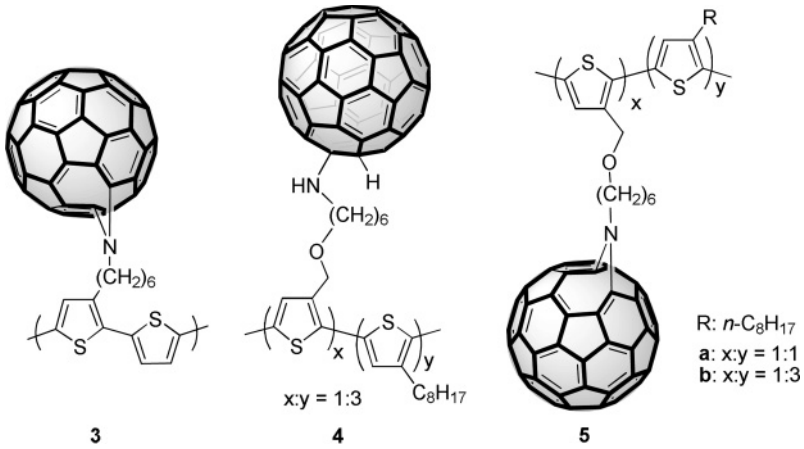

3 4 5

Figure 8.4 Structures of polymers **3–5**.

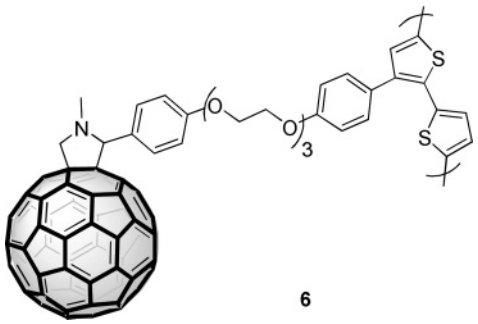

6

Figure 8.5 Structure of polymer **6**.

excitation intensity dependence of both bands showed a square-root relationship [41, 42], indicating a bimolecular recombination and ruling out geminate monomolecular kinetics as the dominant recombination. This suggests that the photoinduced charges move within the samples and, thus, can behave as charge carriers. Definitive proof for a photoinduced charge transfer between the D backbone and the A (pendant fulleropyrrolidines) was obtained by means of light-induced electron spin resonance: photoexciting thin films of **6**, the formation of paramagnetic species such as polythiophene polarons ($g = 2.0022$) and fullerene radical-anions ($g = 2.0004$) was indeed observed (Figure 8.6).

The above results demonstrated that in this class of polyfullerenes (i) the ground-state electronic properties of the D backbone and the tethered fullerene A can retain their individual properties and (ii) a photoinduced electron transfer from the D to the A leads to metastable and mobile charges, that is, the covalent linkage between them does not forcedly enhance geminate monomolecular recombination.

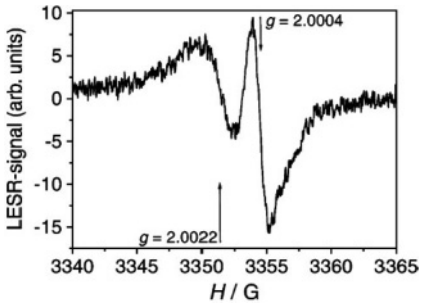

Figure 8.6 LESR (light-on minus light-off) spectrum of **6** on ITO-coated plastic foils. Excitation at 488 nm (20 mW cm^{-2}); $T \sim 77$ K. (Reproduced from Reference [23] with permission of the Royal Society of Chemistry.)

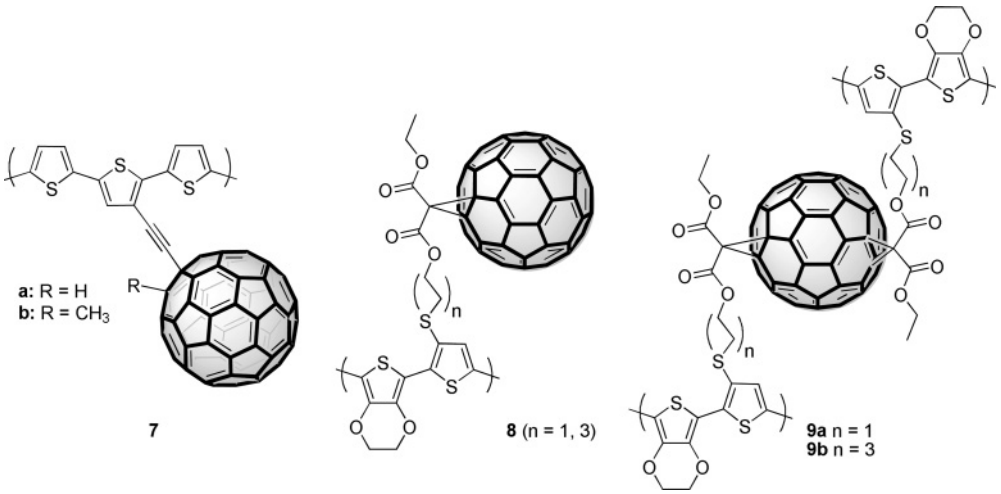

Figure 8.7 Structures of polymers **7–9**.

8.2.2
Electrochemically or Chemically Synthesized Double-Cable Polyfullerenes

In recent years, several examples of electrochemically or chemically synthesized double-cable polyfullerenes have been reported by several groups. For instance, Komatzu *et al.* have electrochemically polymerized two terthiophenes carrying a fullerene cage via an acetylenic bridge, obtaining **7a** and **7b** (Figure 8.7) [43]. While the former was unstable due to the presence of a reactive hydrogen on the fullerene moiety, the latter was electroactive and stable upon both anodic and cathodic cycling processes, and showed an absorption spectrum extending to above 700 nm.

Interesting polyfullerenes such as **8** and **9** have been described by the group of Roncali [44]. These polymers were obtained by electrosynthesis of electron donor 3,4-ethylenedioxythiophene and 3-alkylsulfanylthiophene, carrying fullerene moieties via alkyl spacers of different length. This type of precursor allows for a ready and efficient electropolymerization at low oxidation potentials. Note that **9a, b** are

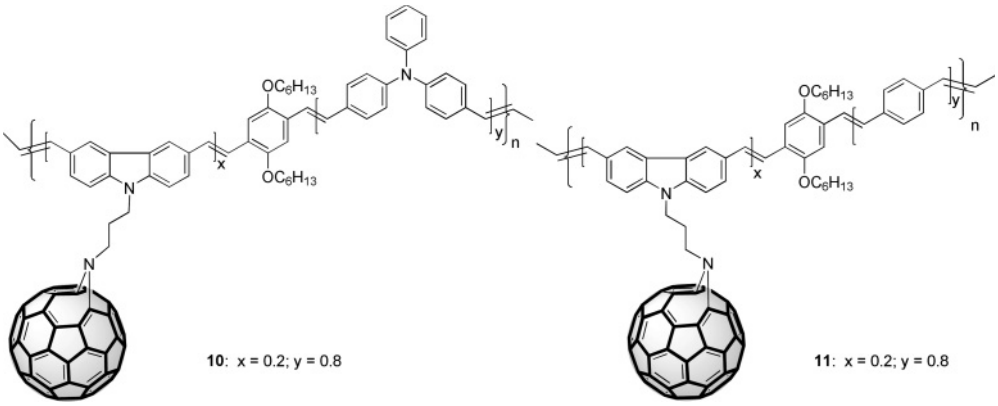

Figure 8.8 Structures of polymers **10** and **11**.

two-site precursors that polymerize in "three-dimensions." Indeed, a comparison of the electrochemical and optical properties of **8** and **9** showed that the latter leads to more robust and porous polymer films. The photoelectrochemical response of films of **9b** deposited on platinum electrodes was three times larger than a control polymer based on the same type of precursor but with no attached fullerene. This indicates a photoinduced charge transfer between the reticulated conjugated chains and the acceptor moieties.

Several chemically prepared and soluble double-cable polymers have been reported by the group of Zhu [45–47]. Among them are polymers with chains other than polythiophenes. As examples, **10** and **11** are copolymers based on alternating poly(*para*-phenylenevinylene) and/or hole transporting carbazole or triphenylamine moieties (Figure 8.8). The materials were found to be rather stable, as demonstrated by thermogravimetric analysis. Moreover, a quenching of the photoluminescence of the unsubstituted backbones by the fullerene tethering indicates a photoinduced charge transfer.

Other examples of interest are the polyfullerenes reported by the group of Yashima. They have synthesized and characterized optically active helical polyphenylacetylenes with tethered achiral fullerene groups (see **12** in Figure 8.9) (see also Chapter 6) [48]. The latter arranges with a dominant screw-sense in a helical array along the conjugated backbone. The copolymer with 10 mol.% fullerene loading exhibited an intense induced circular dichroism. The authors proposed a helical structure with short intercontacts between the fullerene moieties: this is a good example of a double-cable "primary structure" that can dictate a "secondary structure" [49]. Recently, this possible closed and screw-sensed arrangement of fullerenes moieties has been proposed by Ohsawa *et al.* (Figure 8.10, and, as an example, polymer **13**) [50].

For recent and more complete coverage on double-cable polymers, including those containing A moieties other than fullerenes, see Reference [36] and references therein.

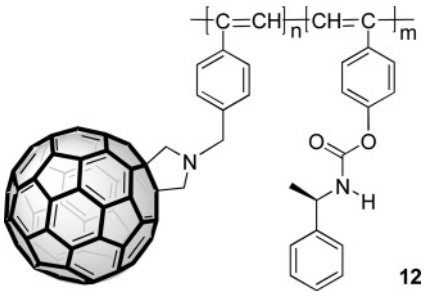

Figure 8.9 Structure of polymer **12**.

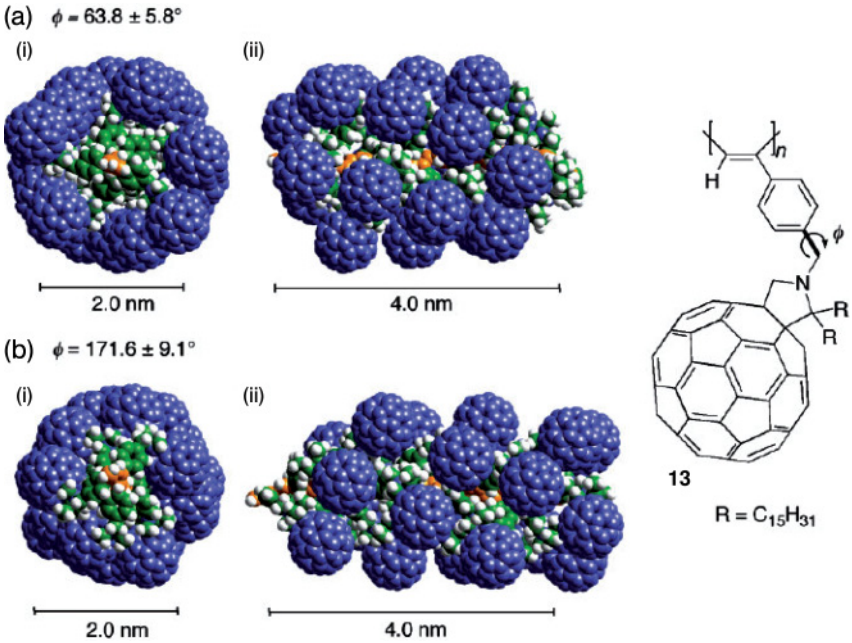

Figure 8.10 Possible helical structures of a copolymer of achiral and chiral bounded phenylacetylenes. Space filling models are shown of the top (i) and side views (ii). The polymer backbones are shown in orange and the pentadecyl groups are omitted for clarity. The main chains have a right-handed helical structure. The fullerene units are arranged in right-handed (a) and left-handed helical arrays (b). The helix-sense of the main-chain is assigned from the Cotton effect sign of the ICD in the main-chain region (ca. 370 nm). The initial dihedral angle between the phenyl group and the fulleropyrrolidine moiety was set to be 60° and 180° in (a) and (b), respectively. The values after optimization are also shown in (a) and (b). (Reproduced from Reference [50] with permission of the American Chemical Society.)

8.2.3
Double-Cables at Work: Photodetectors and Solar Cells

Although several papers report the synthesis of double cables as well as their electrochemical and macromolecular properties, very few have explored the photovoltaic properties in real prototype devices.

Ramos *et al*. [51] have reported a copolymer conjugated backbone, containing *p*-phenylenevinylene and *p*-phenyleneethynylene repeating units, functionalized with pendant methanofullerene moieties (**14**) (Figure 8.11). As observed for polymer **6**, the solid state photoinduced absorption spectrum of **14** exhibited bands typical of methanofullerene radical anions and of positive polarons on a conjugated chain. The photoinduced charge recombination obeyed a non-geminate bimolecular kinetics, and the lifetime of the photogenerated charges extended to the millisecond domain. Using spin-coating, solar cells delivering a short circuit current of 0.4 mA cm^{-2} and an open circuit voltage of 830 mV (under 100 mW cm^{-2} illumination, see Figure 8.12) were prepared.

Soon after this, the synthesis of polymers **15a** and **b** was reported (Figure 8.13) [52]. Random copolymers were obtained by chemical oxidative coupling. Different fullerene loadings were obtained by different fullerene-bearing monomer ratios

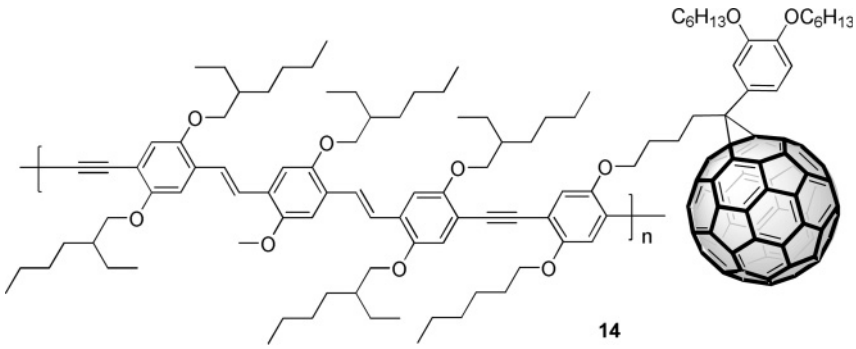

Figure 8.11 Structure of polymer **14**.

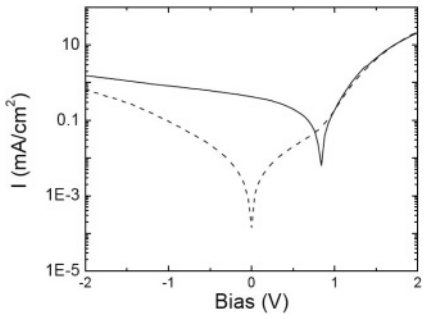

Figure 8.12 Current–voltage characteristics of an ITO/PEDOT:PSS/**14**/Al device in the dark (dashed line) and under white-light illumination (solid line). (Reproduced from Reference [51] with the permission of the American Chemical Society.)

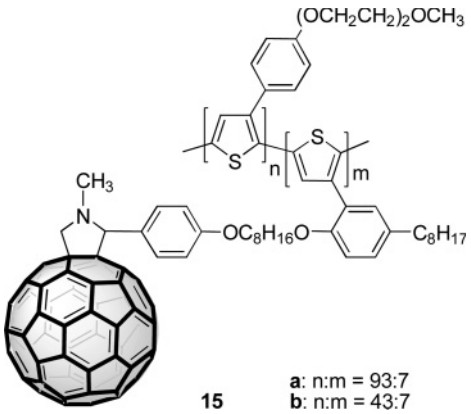

Figure 8.13 Structure of polymer **15**.

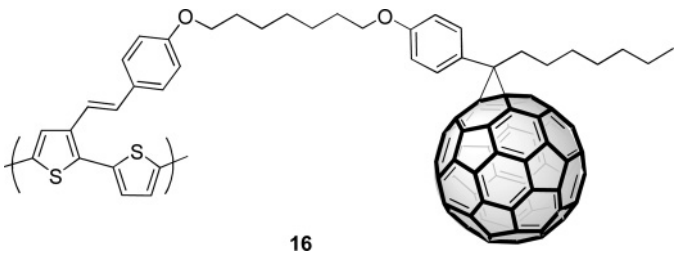

Figure 8.14 Structure of polymer (PT-F) **16**.

in the feed. The copolymers had about 7 and 14 mol.% loading in monomers containing fullerene, respectively. They displayed two phases, blue and orange ones. In the blue phase, the copolymers display a broad electronic absorption band covering a wide range of the solar spectrum. Their solubility allowed for the preparation of photodiodes [52, 53]. Devices based on the double-cable with high fullerene loading (**15b**) showed quantum efficiencies (incident photon to collected electron efficiency, IPCE) more than double that of devices prepared with **15a**. In both cases, the IPCE was improved significantly upon exposure of the photoactive films to chloroform vapor. This effect reflects the change in the absorption spectra while going from the orange- to the blue-phase of the materials. Devices prepared using **15b** were characterized under monochromatic light (λ = 505 nm, 0.1 mW cm^{-2}). Under these conditions, the power conversion efficiency was 0.6%. However, the photodiodes not treated with chloroform delivered a high photovoltage of 750 mV. After treatment with chloroform vapor, the V_{OC} of the device was reduced to 450 mV, behavior that reflects the higher HOMO energy in the blue-phase as compared to that of the orange one, as it will be discussed later.

Recently, the group of Li have described solar cells based on double-cable polyfullerenes [54]. The PT-F (see **16** in Figure 8.14) is based on a polythiophene chain

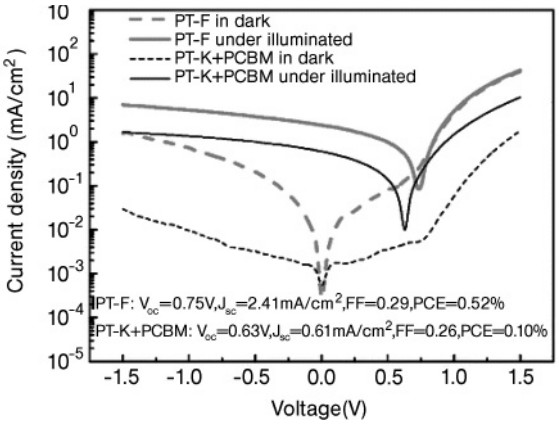

Figure 8.15 *I–V* curves of polymer solar cells based on PT-F (**16**) and reference PT-K blended with PCBM in dark and under the illumination of AM 1.5 (100 mW cm^{-2}). (Reproduced from Reference [54] with the permission of the American Chemical Society.)

substituted with phenylenevinylene pending moieties conceived to increase the overall electron delocalization. Also of interest is the fragment linking the fullerene cage to the rest of the polymer: the authors chose an alkylphenylene motif, as in the case of the PCBM.

As shown in Figure 8.15, under AM1.5 solar simulated illumination (100 mW cm^{-2}), solar cells based on this polyfullerene double-cable provided an open circuit voltage of 750 mV and a short circuit current density of 2.41 mA cm^{-2}, values that together with a filling factor of 0.29 determine a power conversion efficiency of 0.52% [6].

8.3 Revisiting the Double-Cable Approach

The fundamentals and the various factors affecting the physics of bulk heterojunction solar cells have already been studied and modeled in several original research papers [1–3, 28, 30, 57–59]. However, diffusion processes driven by photoinduced chemical potential gradients appear to play a very important role in D–A solar cells, a fact that, at least from a molecular point of view, must be taken into account when designing intrinsic D–A ambipolar materials. As discussed below, this implies that a too intimate, overly homogenous D–A distribution is counterproductive for the operation of bulk heterojunction solar cells.

The open circuit voltage (V_{OC}) of bilayer heterojunction solar cells is governed by the energetics at the D/A interface rather than that involving the electrodes, as pointed out already by Tang in his seminal paper [26]. Conversely, bulk heterojunc-

tion solar cells with interpenetrated D:A structure were originally regarded as classical metal-insulator-metal (MIM) devices. In these devices, the open-circuit voltage is dictated by the difference between the electrode work-functions. However, in 2001, Brabec *et al.* demonstrated that the V_{OC} of bulk heterojunction solar cells can exceed the classical built-in potential (i.e., the difference between electrode work-functions mentioned above) and suggested that it relates to the energetic difference between the D's highest occupied molecular orbital and the A's lowest unoccupied molecular orbital, divided for the elementary charge q (at least in principle, as losses of different nature are observed and are still under investigation by several groups) [57, 58, 60, 61, 71]. This common origin of the open circuit voltage of a D–A bilayer and bulk heterojunction solar cells is also related to the extent of their phase separation. In classical MIM devices, holes and electrons are photogenerated together within the same phase. Thus, an electrical field is necessary to drive them toward the respective opposite electrodes. Conversely, as discussed by Gregg and Hanna, who have proposed the term excitonic solar cells, in all devices in which excitons dissociate across a D–A interface, holes and electrons are formed within their "right" phase; thus, important carrier concentration gradients (photoinduced chemical potential gradients, $\nabla\mu_{h\upsilon}$) that promote the photovoltaic effect are established. Indeed, photovoltaic effects were observed in architecture with no classical built-in potential [55, 56]. This fact is easily visualized in a bilayer heterojunction (Figure 8.16). However, providing a concentration asymmetry is established within the device – (using different electrode work-functions, hole or electron blocking layers at one or both contacts, e.g., Baytron) [62] – $\nabla\mu_{h\upsilon}$ is beneficial for bulk heterojunction solar cells. As a practical example,

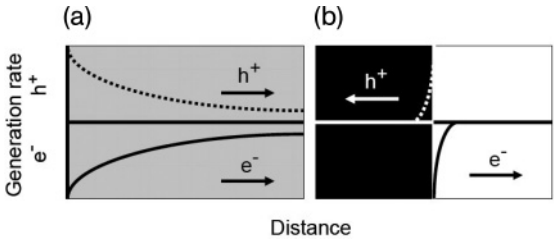

Figure 8.16 Difference in charge-carrier generation in conventional (a) and D–A bilayer (b) solar cells. In conventional solar cells electrons and holes are photogenerated together wherever light is absorbed. Therefore, no photoinduced chemical-potential energy gradient $\nabla\mu h\upsilon$ (represented by arrows) is established. For the cell functioning, an electric field is required. In D–A cells electrons are photogenerated in one phase while holes are generated in the other via interfacial exciton dissociation; $\nabla\mu_{h\upsilon}$ drives electrons and holes in opposite directions, even in absence of a classical built-in electrical potential. See References [55] and [56]. In bulk heterojunction solar cells, and depending on the degree of D–A phase separation, although an electrical field is necessary to "break" the symmetry of the devices, $\nabla\mu_{h\upsilon}$ still provides an additional force beneficial for the photovoltaic effect. Reproduced from Reference [36] with the permission of John Wiley & Sons.

the performance of 1 : 1 rr-poly(3-hexylthiophene):PCBM solar cells after thermal annealing, a process that induces a crystallization of the polymer chains and increases D–A phase separation, is about ten times higher than that of as-cast devices [6, 63, 64]. The thermal treatment results not only in higher short circuit current and filling factor but an increase in open circuit voltage can be observed [31].

Using molecular parameters such as the ionization potential of the D, electron affinity of the A and energy gaps, working models for the bulk heterojunction have been developed. The devices have been represented by D and A nanodomain sites of variable size and distribution, mimicking different situations, such as bilayer cells, bulk heterojunction with considerable phase separation, and very homogenous or even perfectly aligned D–A structures [65, 66]. Structures with the highest D–A interfacial area in 2D simulation were found to perform best in terms of short circuit current. However, the extension of this model in three dimensions revealed that overly homogenous structures are suboptimal [67]. In particular, they suffer from both recombination and reduced open circuit voltage. The authors report that, in accord with the discussion above, for working solar cells and a given D–A pair the maximum open circuit voltage is calculated for simple bilayer heterojunctions.

8.4 Conclusions

Donor, hole conducting, conjugated backbones with tethered fullerene moieties have been reviewed. The experimental results obtained so far evidence that in this class of polyfullerenes a photoinduced electron transfer occurs, resulting in long-lived, mobile holes and electrons. Although the first reports of double-cable polyfullerenes based solar cells and photodetectors were published almost a decade ago, examples of application of these materials in real devices remain scarce. Since in double-cable polyfullerenes the degree of D–A phase separation can be dictated by their primary structure, they could in principle lead to the simultaneous control of the electronic properties and the meso- or nano-structure of the photoactive layer of plastic solar cells.

In D–A solar cells, illumination, combined with donor–acceptor phase separation, establishes a chemical potential gradient that drifts the carriers in addition to the external electrical field of the asymmetrical electrodes. As such, a properly tuned D–A separation is not only topologically required but, also, an optimized phase separation intrinsically maximizes the efficiency of the processes of charge separation and transport of carriers, preserving in addition their electrochemical potential and thus leading to high open circuit potential values. On these bases, a double-cable polyfullerene should guarantee a large surface for D–A contacts, preserving the rest of the device's volume for D-D and A-A contacts. The preparation of double-cable copolymers, so far synthesized to circumvent solubility problems, should indeed now be regarded as a valuable approach. At an extreme of

this strategy, the preparation of D–A diblock copolymers [68–70] should be also pursued.

Although the most appealing feature of ambipolar D–A materials is their potential use as a single component of bulk heterojunction solar cells they could also be proposed as a third ingredient. Within an already rather optimized bulk heterojunction structure, the presence of an ambipolar material might enhance the D–A interfacial area without affecting the morphology too strongly.

Finally, double-cable polymers could be ambipolar materials for photomodulated p-n type organic field effect transistors (OFETs).

References

1 Günes, S., Neugebauer, H. and Sariciftci, N.S. (2007) *Chem. Rev.*, **107**, 1324.

2 Brabec, C.J., Dyakonov, V., Parisi, J. and Sariciftci, N.S. (eds) (2003) *Organic Photovoltaics: Concepts and Realisation*, Springer-Verlag, Berlin.

3 Brabec, C.J., Sariciftci, N.S. and Hummelen, J.C. (2001) *Adv. Funct. Mater.*, **11**, 15.

4 Peet, J., Kim, J.Y., Ma, W.L., Moses, D., Heeger, A.J. and Bazan, G.C. (2007) *Nat. Mater.*, **6**, 497.

5 Kim, Y., Cook, S., Tuladhar, S.M., Choulis, S.A., Nelson, J., Durrant, J.R., Bradley, D.D.C., Giles, M., McCulloch, I., Ha, C.-S. and Ree, M. (2006) *Nat. Mater.*, **5**, 159.

6 Ma, W., Yang, C., Gong, X., Lee, K. and Heeger, A.J. (2005) *Adv. Funct. Mater.*, **15**, 1617.

7 Li, G., Shrotriya, V., Huang, J., Yao, Y., Moriarty, T., Emery, K. and Yang, Y. (2005) *Nat. Mater.*, **4**, 864.

8 Wienk, M.M., Kroon, J.M., Verhees, W.J.H., Knol, J., Hummelen, J.C., van Hal, P.A. and Janssen, R.A.J. (2003) *Angew. Chem. Int. Ed.*, **42**, 3371.

9 Halls, J.J.M., Pickler, K., Friend, R.H., Morati, S.C. and Holmes, A.B. (1995) *Nature*, **376**, 498.

10 Yu, G., Gao, J., Hummelen, J.C., Wudl, F. and Heeger, A.J. (1995) *Science*, **270**, 1789.

11 Armaroli, N. and Balzani, V. (2007) *Angew. Chem. Int. Ed.*, **46**, 52.

12 Nalwa, H.S. (ed.) (1997) *Handbook of Conductive Molecules and Polymers*, Vol. **1–4**, John Wiley & Sons, Ltd, Chichester.

13 Kroto, H.W., Heath, J.R., O'Brien, S.C., Curl, R.F. and Smalley, R.E. (1985) *Nature*, **318**, 162.

14 Dresselhaus, M.S., Dresselhaus, G. and Eklund, P.C. (1996) *Science of Fullerenes and Carbon Nanotubes*, Academic Press, San Diego.

15 (a) Wudl, F. (2002) *J. Mater. Chem.*, **12**, 1959.
(b) Giacalone, F. and Martín, N. (2006) *Chem. Rev.*, **106**, 5136.

16 Hirsch, A. (1999) *Fullerenes and Related Structures, Top. Curr. Chem.*, Vol. **199**, Springer-Verlag, Berlin.

17 Prato, M. (1997) *J. Mater. Chem.*, **7**, 1097 and references therein.

18 (a) Cravino, A. and Sariciftci, N.S. (2003) *Nat. Mater.*, **2**, 360.
(b) Cravino, A. and Sariciftci, N.S. (2002) *J. Mater. Chem.*, **12**, 1931.

19 Sariciftci, N.S., Smilowitz, L., Heeger, A.J. and Wudl, F. (1992) *Science*, **258**, 1474.

20 Morita, S., Zakhidov, A.A. and Yoshino, K. (1992) *Solid State Commun.*, **82**, 249.

21 Brabec, C.J., Zerza, G., Cerullo, G., De Silvestri, S., Luzzati, S., Hummelen, J.C. and Sariciftci, N.S. (2001) *Chem. Phys. Lett.*, **340**, 232.

22 Cravino, A., Zerza, G., Neugebauer, H., Maggini, M., Bucella, S., Menna, E., Svensson, M., Andersson, M.R., Brabec, C.J. and Sariciftci, N.S. (2002) *J. Phys. Chem. B*, **106**, 70.

23 Cravino, A., Zerza, G., Maggini, M., Bucella, S., Svensson, M., Andersson, M.R., Neugebauer, H. and Sariciftci, N.S. (2000) *Chem. Commun.*, 2487.

24 Hoofman, R.J.O.M., De Haas, M.P., Siebbeles, L.D.A. and Warman, J.M. (1998) *Nature*, **392**, 6671.

25 Singh, T.B., Günes, S., Marianović , N., Sariciftci, N.S. and Menon, R. (2005) *J. Appl. Phys.*, **97**, 114508.

26 Tang, C.W. (1986) *Appl. Phys. Lett.*, **48**, 183.

27 Rostalski, J. and Meissner, D. (2000) *Sol. Energy Mater. Sol. Cells*, **87**, 61.

28 Peumans, P., Yakimov, A. and Forrest, S.R. (2003) *J. Appl. Phys.*, **93**, 3693.

29 Drechsel, J., Mannig, B., Kozlowski, F., Pfeiffer, M., Leo, K. and Hoppe, H. (2005) *Appl. Phys. Lett.*, **24**, 86.

30 Xue, J., Uchida, S., Rand, B.P. and Forrest, R.S. (2004) *Appl. Phys. Lett.*, **84**, 3013.

31 Padinger, F., Rittberger, R.S. and Sariciftci, N.S. (2003) *Adv. Funct. Mater.*, **13**, 85.

32 Shaheen, S.E., Brabec, C.J., Padinger, F., Fromherz, T., Hummelen, J.C. and Sariciftci, N.S. (2001) *Appl. Phys. Lett.*, **78**, 841.

33 Hoppe, A. and Sariciftci, N.S. (2006) *J. Mater. Chem.*, **16**, 45 and references therein.

34 Geens, W., Shaheen, S.E., Brabec, C.J., Poortmans, J. and Sariciftci, N.S. (2000) *Electronic Properties of Novel Materials*, Vol. **544** (eds H. Kuzmany, J. Fink, M. Mehring and S. Roth), IOP, Bristol.

35 Roncali, J. (2005) *Chem. Soc. Rev.*, **34**, 483.

36 Cravino, A. (2007) *Polym. Int.*, **56**, 943.

37 Anderson, H.L., Boudon, C., Diederich, F., Gisselbrecht, J.-P., Gross, M. and Seiler, P. (1994) *Angew. Chem. Int. Ed. Engl.*, **33**, 1628.

38 Benincori, T., Brenna, E., Sannicolò, F., Trimarco, L., Zotti, G. and Sozzani, P. (1996) *Angew. Chem. Int. Ed. Engl.*, **35**, 648.

39 Yassar, A., Hmyene, M., Loveday, D.C. and Ferraris, J.P. (1997) *Synth. Met.*, **84**, 231.

40 Ferraris, J.P., Yassar, A., Loveday, D.C. and Hmyene, M. (1998) *Opt. Mater.*, **9**, 34.

41 Dellepiane, G., Cuniberti, C., Comoretto, D., Musso, G.F., Figari, G., Piaggi, A. and Borghesi, A. (1993) *Phys. Rev. B*, **48**, 7850.

42 Botta, C., Luzzati, S., Tubino, R., Bradley, D.D.C. and Friend, R.H. (1993) *Phys. Rev. B*, **48**, 14809.

43 Murata, Y., Mitsuharu, S. and Komatsu, K. (2003) *Org. Biomol. Chem.*, **1**, 2624.

44 Jousselme, B., Blanchard, P., Levillain, E., de Bettignies, R. and Roncali, J. (2003) *Macromolecules*, **36**, 3020.

45 Xiao, S., Wang, S., Fang, H., Li, Y., Shi, Z. Du, C. and Zhu, D. (2001) *Macromol. Rapid. Commun.*, **22**, 1313.

46 Wang, S., Xiao, S., Li, Y., Shi, Z., Du, C., Fang, H. and Zhu, D. (2002) *Polymer*, **43**, 2049.

47 Wang, N., Li, Y., Lu, F., Liu, Y., He, X., Jiang, L., Zhuang, J., Li, X., Li, Y., Wang, S., Liu, H. and Zhu, D. (2005) *J. Polym. Sci. A: Polym. Chem.*, **43**, 2851.

48 Nishimura, T., Takatani, K., Sakurai, S., Maeda, K. and Yashima, E. (2002) *Angew. Chem. Int. Ed.*, **41**, 3602.

49 Nishimura, T., Maeda, K., Ohsawa, S. and Yashima, E. (2005) *Chem. Eur. J.*, **11**, 1181.

50 Ohsawa, S., Maeda, K. and Yashima, E. (2007) *Macromolecules*, **40**, 9244.

51 Marcos Ramos, A., Rispens, M.T., van Duren, J.K.J., Hummelen, J.C. and Janssen, R.A.J. (2001) *J. Am. Chem. Soc.*, **123**, 6714.

52 Cravino, A., Zerza, G., Maggini, M., Bucella, S., Svensson, M., Andersson, M.R., Neugebauer, H., Brabec, C.J. and Sariciftci, N.S. (2003) *Monatsh. Chem., Chem. Mon.*, **134**, 519.

53 Zhang, F., Svensson, M., Andersson, M.R., Maggini, M., Bucella, S., Menna, E. and Inganäs, O. (2001) *Adv. Mater.*, **13**, 171.

54 Tan, Z., Hou, J., He, Y., Zhou, E., Yang, C. and Li, Y. (2007) *Macromolecules*, **40**, 1868.

55 Gregg, B.A. (2003) *J. Phys. Chem. B*, **107**, 4688.

56 Gregg, B.A. and Hanna, M.C. (2003) *J. Appl. Phys.*, **93**, 3605 and references therein.

57 Scharber, M.C., Mühlbacher, D., Koppe, M., Denk, P., Waldauf, C., Heeger, A.J. and Brabec, C.J. (2006) *Adv. Mater.*, **18**, 789.

58 Blom, W.M.P., Mihailetchi, V.D., Koster, L.J.A. and Markov, D.E. (2007) *Adv. Funct. Mater.*, **19**, 1551.

59 (a) Barker, J.A., Ramsdale, C.M. and Greenham, N.C. (2003) *Phys. Rev. B*, **67**, 075205.

(b) McNeill, C.R., Westenhoff, S., Groves, C., Friend, R.H. and Greenham, N.C. (2007) *J. Phys. Chem. C*, **111**, 19153.

60 Cravino, A. (2007) *Appl. Phys. Lett.*, **91**, 243502.

61 Rand, B.P., Burk, D.P. and Forrest, S.R. (2007) *Phys. Rev. B*, **75**, 115327.

62 (a) Gregg, B.A. (2003) *J. Phys. Chem. B*, **107**, 4688.
(b) Kirchmeyer, S. and Reuter, K. (2005) *J. Mater. Chem.*, **15**, 2077.

63 Camaioni, N., Ridolfi, G., Casalbore-Miceli, G., Possamai, G. and Maggini, M. (2002) *Adv. Mater.*, **14**, 1735.

64 Chiu, M.-Y., Jeng, U-S., Su, C.-H., Liang, K.S. and Wei, K.-H. (2008) *Adv. Mater.*, **20**, 2573.

65 Sylvester-Hvid, K.O. and Ratner, M.A. (2004) *J. Phys. Chem. B*, **108**, 4296.

66 Sylvester-Hvid, K.O. and Ratner, M.A. (2005) *J. Phys. Chem. B*, **109**, 200.

67 Koh, S.E., Delley, B., Medvedeva, J.E., Facchetti, A., Freeman, A.J., Marks, T.J. and Ratner, M.A. (2006) *J. Phys. Chem. B*, **110**, 24361.

68 Stalmach, U., de Boer, B., Videlot, C., van Hutten, P.F. and Hadziioannou, G. (2000) *J. Am. Chem. Soc.*, **122**, 5464.

69 Lindner, S.M., Hüttner, S., Chiche, A., Thelakkat, M. and Krausch, G. (2006) *Angew. Chem. Int. Ed.*, **45**, 3364.

70 Richard, F., Brochon, C., Leclerc, N., Eckhardt, D., Heiser, T. and Hadziioannou, G. (2008) *Macromol. Rapid Commun.*, **29**, 885.

71 Brabec, C.J., Cravino, A., Meissner, D., Sariciftci, N.S., Fromherz, T., Rispens, M.T., Sánchez, L. and Hummelen, J.C. (2001) *Adv. Funct. Mater.*, **11**, 374.

9
Fullerene-Containing Supramolecular Polymers

Takeharu Haino

9.1
Introduction

Fullerene is one of the most fascinating classes of carbon clusters [1–3]; it has attracted great interest due to its unique three-dimensional geometry and its outstanding magnetic [4–6], superconducting [7, 8], electrochemical [9–12] and photophysical [13–15] properties. The combination of fullerene chemistry and macromolecular chemistry provides an opportunity to create new fullerene-containing polymers, which show promise for an enormously broad scope of applications [16–18]. Initial attempts to synthesize fullerene-containing polymers have involved polymerizing fullerene molecules directly through [2 + 2] cycloaddition [19–22]. However, the actual products formed – one-, two- and three-dimensional polymeric architectures – are less processable than conventional polymers.

More recently, intense research efforts have been devoted to developing [60]fullerene-polymer hybrids in which [60]fullerene molecules are incorporated onto polymer main chains or side chains [23–25]. These [60]fullerene-polymer hybrids have proven to be innovative materials, functioning as organic solar cells, magnets, photoconductors, optical-limiting devices and semiconductors [26–28]. Synthetically, the 30 highly reactive double bonds of a [60]fullerene molecule limit the possible polymerization reactions [24, 28–31]. However, *supramolecular* methods of incorporating [60]fullerene onto a polymer main chain can overcome this limitation.

A "supramolecular polymer" is any type of self-assembly that creates polymer-like aggregates via reversible interactions of one or more types of components [32–34]. The reversible interactions can allow supramolecular polymers to thermally equilibrate with their monomers, whereas conventional polymers never show such reversibility [35]. For instance, classes of supramolecular polymers include micelles, colloids, liquid crystals, gels, aromatic stacks and hydrogen-bonded polymers. One characteristic they share is the ability to reversibly change their structures at the supramolecular level in response to external stimuli [36, 37], which offers a new way to engineer functional systems at the nano-scale [38]. Thus,

Fullerene Polymers. Synthesis, Properties and Applications. Edited by Nazario Martín and Francesco Giacalone

ISBN: 978-3-527-32282-4

the development of supramolecular [60]fullerene-containing polymers has gained momentum as an effective method for synthesizing functional, carbon-based material.

The control of weak forces to define the size and shape of the resulting supramolecular [60]fullerene ensemble in relation to its function is a major task for various phases: solid state, mesophase, solution and liquid–liquid and liquid–solid interfaces (Figure 9.1). The intermolecular weak forces always compete with solvation in solution. Such competition does not occur, however, in the solid state. For this reason, nanofabrication of [60]fullerene using host–guest chemistry has been studied intensively in the solid state. Another type of approach takes advantage of chemical modification to produce [60]fullerene molecules that are amphiphilic nature, leading to self-organization of the functionalized [60]fullerene molecules in mesophase and in aqueous solution. Microphase separation or amphiphilic interaction can produce liquid crystals, micelles and bilayer structures. These are well-organized supramolecular ensembles of [60]fullerene in which the functionalities attached onto the [60]fullerene surface and the globular [60]fullerene moiety are sufficiently separated to produce segregation at a higher level of organization. In solution, the construction of the [60]fullerene-containing polymers and nano-arrays is the most fascinating topic in the field of supramolecular chemistry. Many noncovalent interactions can be employed; indeed, binding motifs for the construction of [60]fullerene nano-arrays have been carefully optimized to overcome the competing process of solvation. Hydrogen bonding, Coulombic

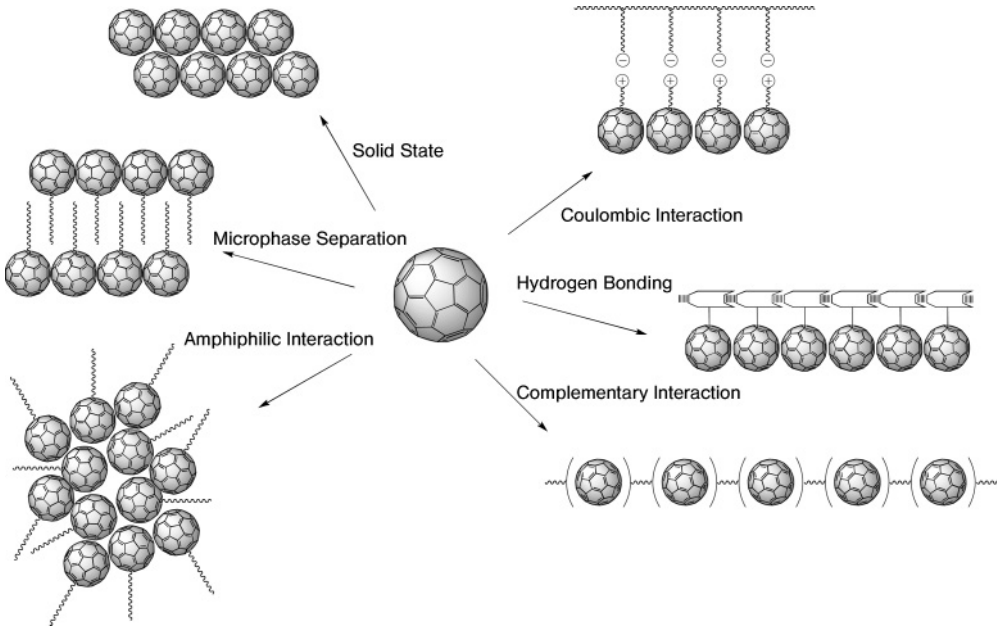

Figure 9.1 Schematic representation of the construction of fullerene-based supramolecular ensembles.

interactions, charge transfer, hydrophobic interactions, aromatic stacking and complementary interactions are choices available to build up well-organized supramolecular ensembles of [60]fullerene.

This chapter focuses on recent developments in the construction of supramolecular polymer-like ensembles incorporating [60]fullerene, including supramolecular polymers, nano-arrays and discrete assemblies of [60]fullerene derivatives. These ensembles have been constructed in various phases: solid state, meso, solution and solid–liquid and liquid–liquid interfaces.

9.2
Nanofabrication of [60]Fullerene in the Solid State

To engineer multimolecular arrays of [60]fullerene on the nanometer scale we can take advantage of noncovalent interactions, including ion–ion, ion–dipole, hydrogen-bond, dipole–dipole, π–π stacking and van der Waals interactions. Typically, these noncovalent interactions have to compete with solvation of the functional group, which is responsible for fullerene association in common organic solvents. In contrast, they appear to be stronger in the solid state because a competitive process of solvation is absent. In this context, the ordering of [60]fullerene molecules into one-, two- and three-dimensional arrays can be controlled in a supramolecular manner. Flat aromatic rings can stack on the smooth and dense surface of the [60]fullerene molecule to create attractive π–π stacking interactions. Thus, aromatic stacking can be utilized effectively to organized [60]fullerene nano-arrays in the solid state. Crystallizing [60]fullerene from a solution of aromatic solvents produces one-dimensional nano-arrays containing [60]fullerene molecules interspersed with solvent molecules [39–42]. The aromatic solvents fill the free spaces formed by the ordering of the [60]fullerene molecules in the crystals. This prevents the [60]fullerene molecules from randomly aggregating in the solid state.

Stacking interactions are effective at assembling fullerene nano-arrays into a supramolecular organization. Co-crystallization of hosts with [60]fullerene has led to an aligned arrangement of [60]fullerene molecules [43, 44]. Balch and coworkers have synthesized [60]fullerene-iridium complex **1**, which has two phenylethylbenzene components and forms a supramolecular polymer in the solid state (Figure 9.2) [45]. The four aromatic rings of **1** create a π-basic cavity in which the smooth,

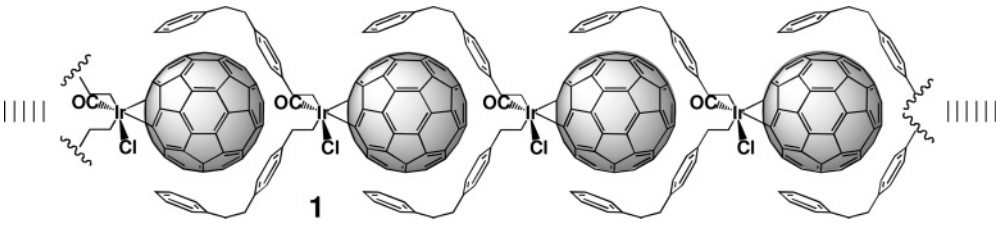

Figure 9.2 Supramolecular polymer of $(\eta^2\text{-}C_{60})Ir(CO)Cl$ (**1**) in solid state.

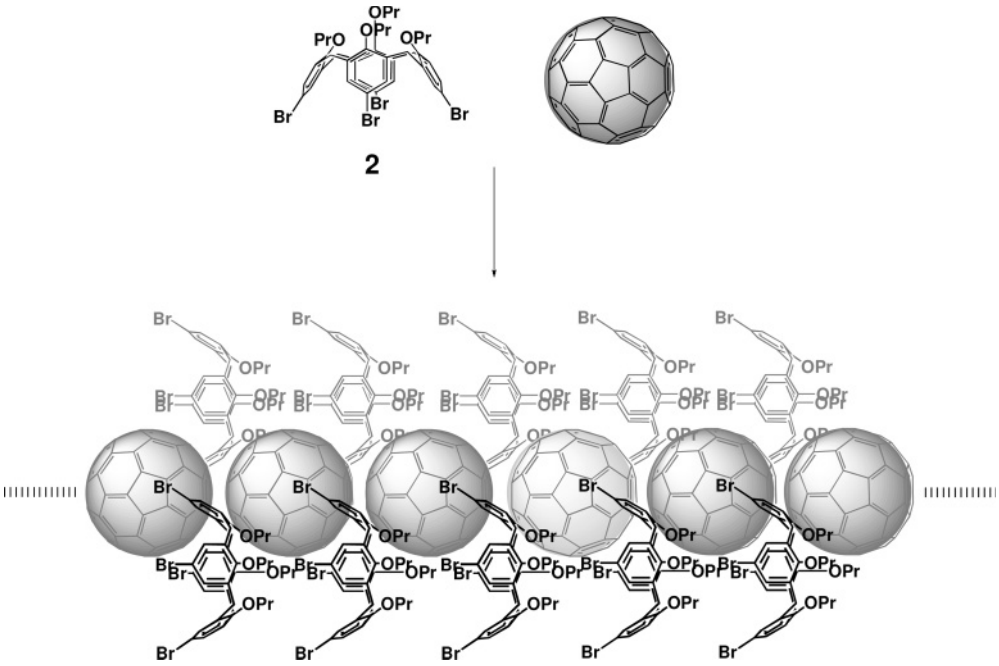

Figure 9.3 Co-crystallization of [60]fullerene with *p*-bromocalix[4]arene propyl ether (**2**).

globular surface of the adjacent [60]fullerene unit is accommodated, giving rise to effective π–π stacking interactions. This complementary interaction is responsible for the formation of the [60]fullerene nano-array.

Co-crystallization of [60]fullerene molecules and calix[4]arene **2** has afforded pre-organized linear columns (Figure 9.3) [46]. Aggregation of the globular [60] fullerene molecules results in residual spaces among them. The calix[4]arene **2** fills this residual space. The bromo, phenyl and propyl groups give rise to effective van der Waals contacts with the smooth surface of the [60]fullerene molecules, which probably drive the formation of the columnar array of [60]fullerene in the solid state. In addition, notably, the well-organized columnar array of [60]fullerene is completely separated by calix[4]arene **2**; intercolumnar communication between [60]fullerene molecules is prevented. This permits the directional polymerization of the [60]fullerene molecules; in fact, the action of heat and pressure on the crystals produced the linear [2 + 2] addition polymer without crosslinking [47].

Calix[5]arenes encapsulate groups of fullerenes into their cone-shaped cavity [48–59]. Atwood, Barbour, Raston and coworkers have reported that calix[5]arene **3**, toluene and the [60]fullerene molecule form co-crystals: one with a 1 : 1 : 1 composition with the [60]fullerene molecules arranged in a supramolecular zigzag and the other with a 4 : 2 : 5 composition, giving rise to a Z-array of the [60]fullerene

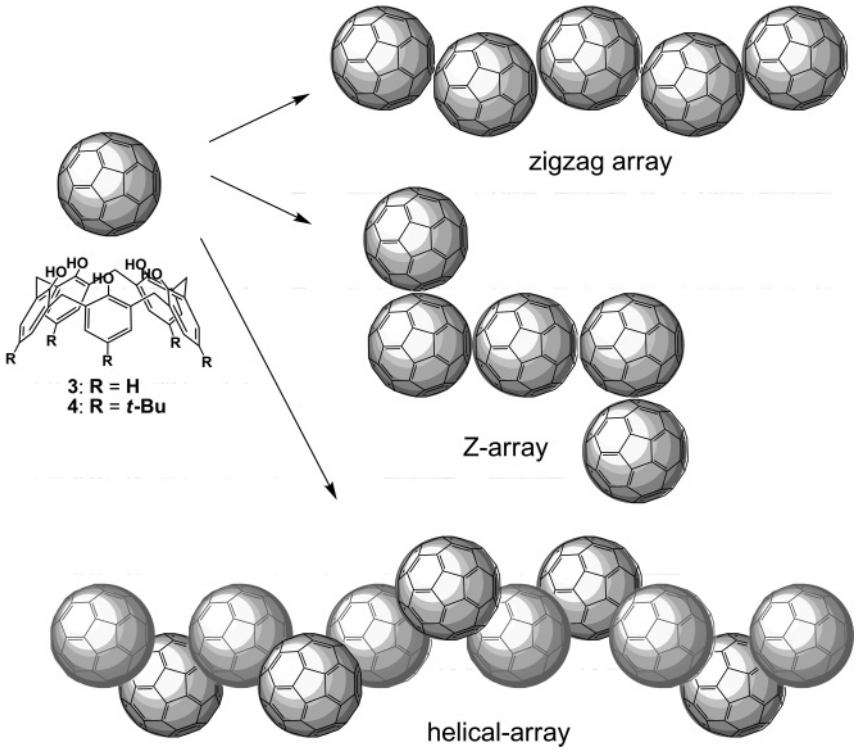

Figure 9.4 Arrangements of the [60]fullerene molecules with calix[5]arene hosts **3** or **4** in the solid state. The calix[5]arene molecules are omitted from the pictures of the assemblies for clarity.

molecules (Figure 9.4) [60, 61]. A helical array of the [60]fullerene molecules has also resulted from using calix[5]arene **4** instead of **3** (Figure 9.4).

In the zigzag array of [60]fullerene molecules in the calix[5]arenes, the exo surfaces of two adjacent calix[5]arenes produce close contacts with each [60]fullerene (Figure 9.5). This can be rationalized by considering the electron-deficient nature of the [60]fullerene and the electron-rich aromatic rings of the calix[5]arenes.

In the Z-array of the [60]fullerene molecules with the calix[5]arenes, the [60]fullerene molecules arrange to form five-fold linear columns along the crystallographic *a* axis. The cross-section of these columns is Z-shaped, and the calix[5]arene and toluene molecules form a boundary between the five-fold fullerene strands (Figure 9.6) [61]. The [60]fullerene-containing channels are not interlinked, meaning that the [60]fullerene molecules in one channel are not in close contact with the [60]fullerenes in an adjacent channel. This fascinating [60]fullerene arrangement in nano-space is driven by shape-complementary molecular recognition. Indeed, the calix[5]arene cavities align to form the highly organized

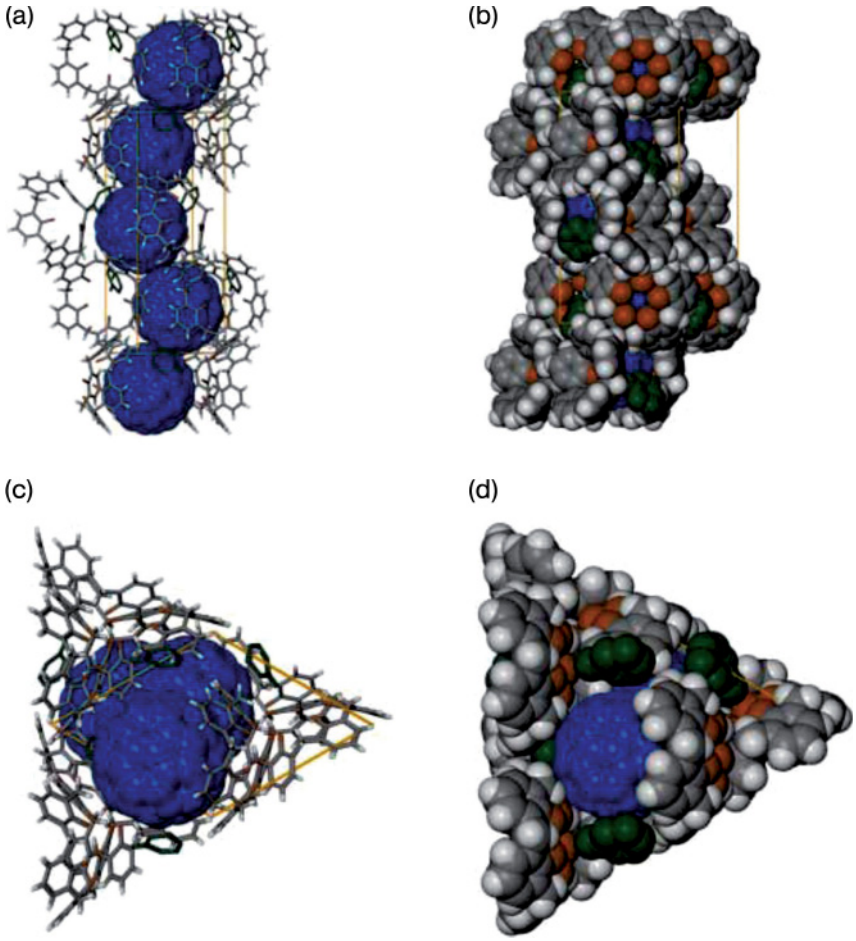

Figure 9.5 X-ray crystal structure of [(C_{60})(calix[5]arene **3**)]·toluene projected at right angles to the zigzag array of fullerenes (a and b), and nearly perpendicular to the array (c and d). Blue = C_{60}; dark and light gray = carbon and hydrogen atoms of the calixarene, respectively; red = oxygen atoms; dark green = toluene. (Reproduced with permission from Reference [60]. Copyright Wiley-VCH Verlag GmbH.)

nano-space in which the [60]fullerene molecules are accommodated by means of van der Waals interactions.

A helical array of the [60]fullerene molecules in the solid state has been obtained with the aid of calix[5]arene complexation [62]. *p-t*-Butyl calix[5]arene **4** was used as a host molecule instead of **3**, giving rise to a 1:1 host–guest complex and linear striations of [60]fullerenes within bundled nanofibers (Figure 9.7). Detailed analysis of the powder X-ray diffraction pattern of the [60]fullerene complex with

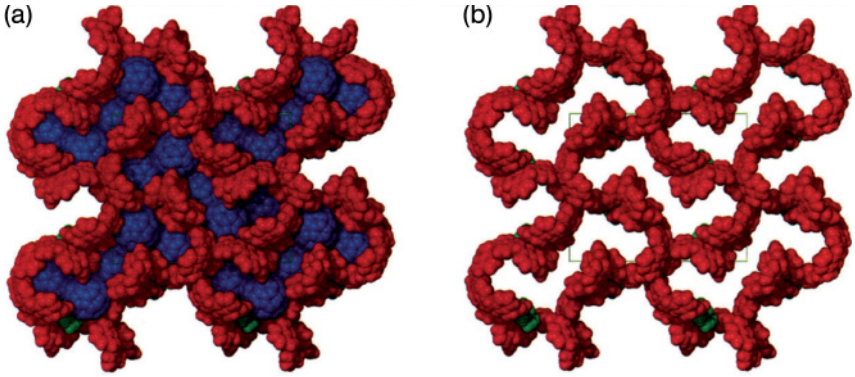

Figure 9.6 Extended structure viewed along [100] (red, calix[5]arene; blue, C_{60}; green, toluene). (a) The direction of the projection is parallel to the five-fold, Z-shaped columns of C_{60}; (b) C_{60} molecules have been removed to show the infinite channels running along [100]. (Reprinted with permission from Reference [61]. Copyright (2002) American Chemical Society.)

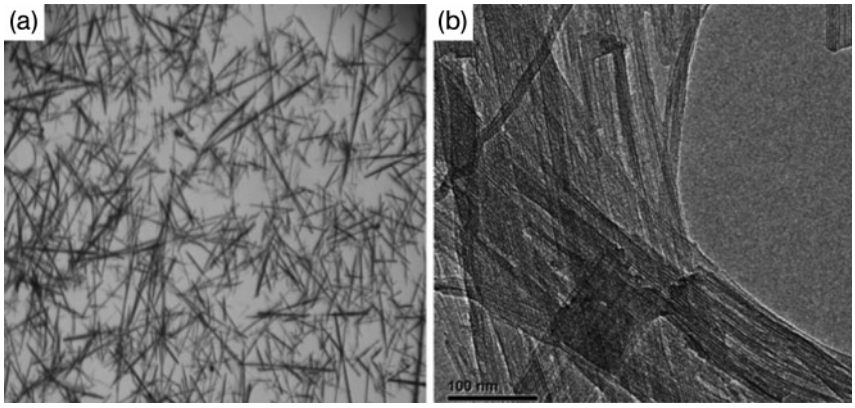

Figure 9.7 Optical micrograph (a) and TEM image (b) of the [60]fullerene@calix[5]arene **4** complex. (Reproduced with permission from Reference [62]. Copyright Wiley-VCH Verlag GmbH.)

calix[5]arene **4** revealed that the [60]fullerene molecules adopt the form of a one-dimensional, helical array in the solid state. Figure 9.8 illustrates the arrangement of the calixarenes in a single helical array. The array grows along its principal axis to form the strands of [60]fullerene fibers seen in Figure 9.7b. *p-t*-Butyl groups fill the residual space produced by the [60]fullerene assemblies, allowing effective van der Waals interactions with the smooth and dense aromatic surface of the [60] fullerene molecules. These interactions probably lead to the dramatic change in the [60]fullerene nano-array.

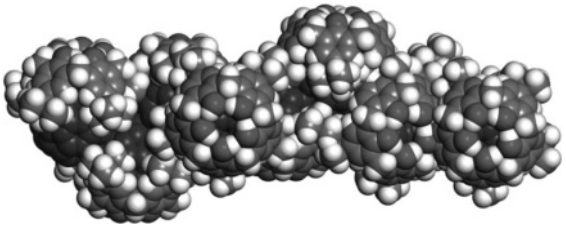

Figure 9.8 Proposed calixarene packing arrangement around a [60]fullerene column. (Reproduced with permission from Reference [62]. Copyright Wiley-VCH Verlag GmbH.)

Double-concave graphene, permethoxylated hexa-peri-hexabenzocoronene (HBC) **5**, co-crystallized with [60]fullerene to form a linear array of [60]fullerene molecules (Figure 9.9) [63]. Permethoxylated HBC **5** is not planar due to steric congestion in the bay region; the outer aromatic rings alternate between "flipped up" and "flipped down" with regard to the inner ring. As a result, HBC **5** has two concave faces and adopts a centrosymmetric conformation. The double-concave structure of **5** has two surfaces complementary to the globular [60]fullerene molecule. The co-crystallization of **5** and [60]fullerene gives rise to a columnar packing arrangement, in which the two [60]fullerene molecules are positioned on each side of HBC **5** through π–π stacking and van der Waals interactions. This is a remarkable example of the construction of a linear nano-array of the [60]fullerene molecule in the solid state.

Template-assisted nano-ordering of [60]fullerene molecules is an intriguing area. The [60]fullerene molecules were encapsulated in a single-wall carbon nanotube (Figure 9.10). Some of them are observed to self-assemble into a supramolecular polymer chain with nearly uniform center-to-center distances, resembling a nano-scale fullerene-peapod [64–66]. The encapsulated fullerene molecules coalesce in the carbon nanotube, probably as a result of strong π–π interactions between the exterior of the [60]fullerene and the interior of the single-wall carbon nanotube.

These above examples are characteristic of the construction of [60]fullerene nano-arrays using weak intermolecular forces in the solid state. Controlling intermolecular weak interactions has proven to be effective for the construction of selectively organized polymeric nano-arrays of [60]fullerene molecules in the solid state.

9.3
Self-Organization of Amphiphilic [60]Fullerenes

The macroscopic morphologies of the self-organized structures derived from the aggregation of [60]fullerene molecules have received considerable attention due to their tunable physical and chemical properties. This section deals with recent approaches seeking to exploit amphiphilic interactions of functionalized [60]fullerene derivatives to build new nano architectures.

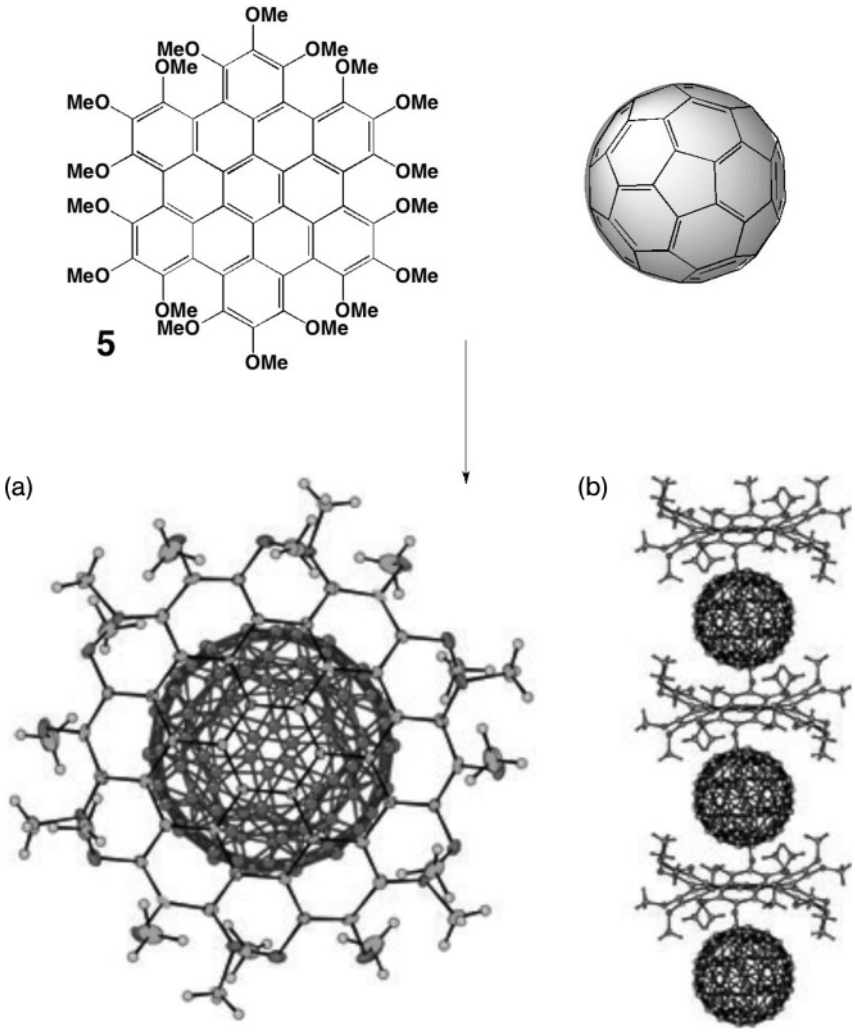

Figure 9.9 Permethoxylated hexa-peri-hexabenzocoronene (**5**) and [60]fullerene, and the crystal structure of the host–guest complex. (Reproduced with permission from Reference [63]. Copyright Wiley-VCH Verlag GmbH.)

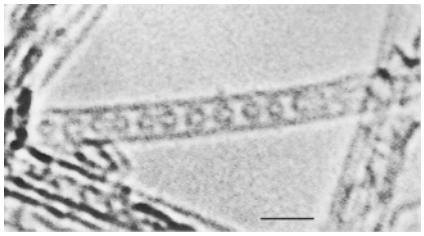

Figure 9.10 A single-walled carbon nanotube containing a row of closed carbon shells concentric with the tubule axis. The diameter and center-to-center spacing of the internal shells are consistent with a chain of C_{60} molecules. The nanotube is surrounded by a vacuum. Scale bar, 2.0 nm. (Reprinted by permission from Macmillan Publishers Ltd: Nature Reference [64], copyright 1998.)

Modification of the [60]fullerene structure is a conventional approach to controlling the morphology of [60]fullerenes. Microphase separation is often observed in liquid crystals. The introduction of long alkyl chains at the [60]fullerene surface creates well-developed fullerene nano-arrays, forming liquid crystalline phases. Deschenaux describes the details of [60]fullerene-based liquid crystals in Chapter 11. Part of this section deals with [60]fullerene-based liquid crystals, with a characteristic example of the supramolecular assemblies resulting from the amphiphilic nature of functionalized [60]fullerenes. Deschenaux and coworkers have intensively studied fullerene-based liquid crystalline materials [67–77]. The introduction of branched long alkyl chains on [60]fullerene molecule (**6**) gives rise to a completely new class of liquid crystalline materials (Figure 9.11). The fullerene moiety is immiscible with the other phase, which is composed of the long alkyl chains; eventually, the immiscibility of the fullerene moiety leads to the formation of a liquid crystalline phase.

Another design for fullerene-based liquid crystalline molecules, shaped like a shuttlecock, has been developed by Nakamura and coworkers (Figure 9.12) [78–80]. The attachment of five aromatic groups to one pentagon of a [60]fullerene molecule gives rise to the deeply conical molecule **7**, which has a cavity complementary to the exterior of the globular surface of a [60]fullerene molecule. The head-to-tail stacking is driven by the attractive noncovalent interactions between the spherical fullerene moiety and the hollow cone formed by the five aromatic side groups of an adjacent molecule in the same column to create an infinite one-dimensional array in a hexagonal columnar liquid crystalline phase.

Amphiphilic [60]fullerenes bearing hydrophilic moieties substituted at the intrinsically hydrophobic [60]fullerene surface are useful components for constructing supramolecular architectures. Chu and coworkers have reported that potassium pentaphenyl fullerene **8** formed spherical bilayer vesicles in water (Figure 9.13) [81]. A laser light scattering study of the aggregate of **8** in water revealed that the hydrocarbon anions **8** form the bilayer structure, forming stable spherical vesicles with an average hydrodynamic radius of about 17 nm, with a very low critical aggregation concentration. The average aggregation number of the associated particles in these large spherical vesicles was approximately 1.2×10^4.

Goh and coworkers have synthesized PEG substituted [60]fullerenes, which formed spherical aggregates in polar solvents [82]. Hydrophilic polymer chains can also be attached to the [60]fullerene surface. Nanometer-sized fullerene particles have been constructed successfully [83, 84]. Certainly, the self-assembly of these nano architectures results from the amphiphilic nature of the [60]fullerene derivatives; thus, the hydrophobic moieties play a key role in their microphase separation during the aggregation process.

Nakanishi and coworkers have reported the first successful control of the hierarchical organization of [60]fullerenes carrying long aliphatic chains [85–88]. Careful adjustment of the solvent polarity successfully induces the self-assembly of a [60]fullerene derivative with long alkyl chains to form hierarchical supramolecular nano objects, such as spherical vesicles, fibers, tapes, discs and conical

Figure 9.11 Schematic representation of the microphase separation of the fullerene-based liquid crystal **6** [76].

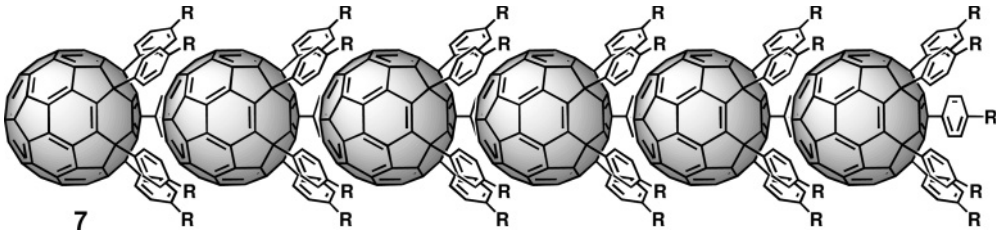

Figure 9.12 Linear array of shuttlecock-like [60]fullerene molecules.

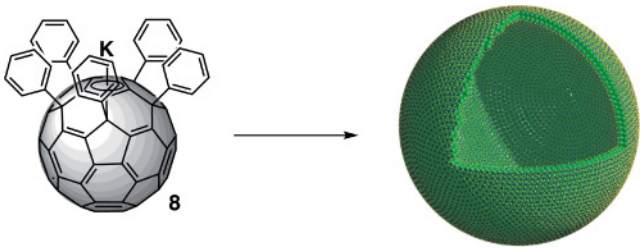

Figure 9.13 A bilayer vesicle model, consisting of N_{outer} = 6693 molecules in an outer shell of radius R_{outer} = 17.6 nm in addition to N_{inner} = 5973 molecules in an inner shell of radius R_{inner} = 16.7 nm. A piece has been cut away for enhanced visibility. The hydrophobic fullerene bodies are shown in green, the hydrophilic-charged cyclopentadienide regions are in blue, and the five substituents are represented as yellow sticks. (Reprinted with permission of the AAAS from Reference [81].)

assemblies. X-ray diffraction measurements, transmission electron microscopy and atomic force microscopy studies have confirmed the formation of a bilayer structure in which the fullerene moiety and alkyl chain are separated to form individual columns due to the microphase separation resulting from the amphiphilic nature of [60]fullerene derivative **9** with long alkyl chains (Figure 9.14). The self-organized bilayer structure of **9** is a fundamental subunit for constructing superstructures in higher dimensions. Two intermolecular forces are present due to the aromatic and aliphatic units of the [60]fullerene derivative: the fullerene moieties interact through strong π–π interactions, while the alkyl chains interact through van der Waals interactions. This amphiphilic interaction should give rise to effective phase separation and thus produce a lamellar bilayer structure.

Modification of the globular aromatic surface of [60]fullerene with various functionalities creates an amphiphilic nature on the [60]fullerene molecule, which allows for the production of liquid crystalline phases, vesicles, colloidal clusters and bilayer structures. The amphiphilic interactions among the [60]fullerene molecules are obviously crucial in determining the supramolecular organization formed.

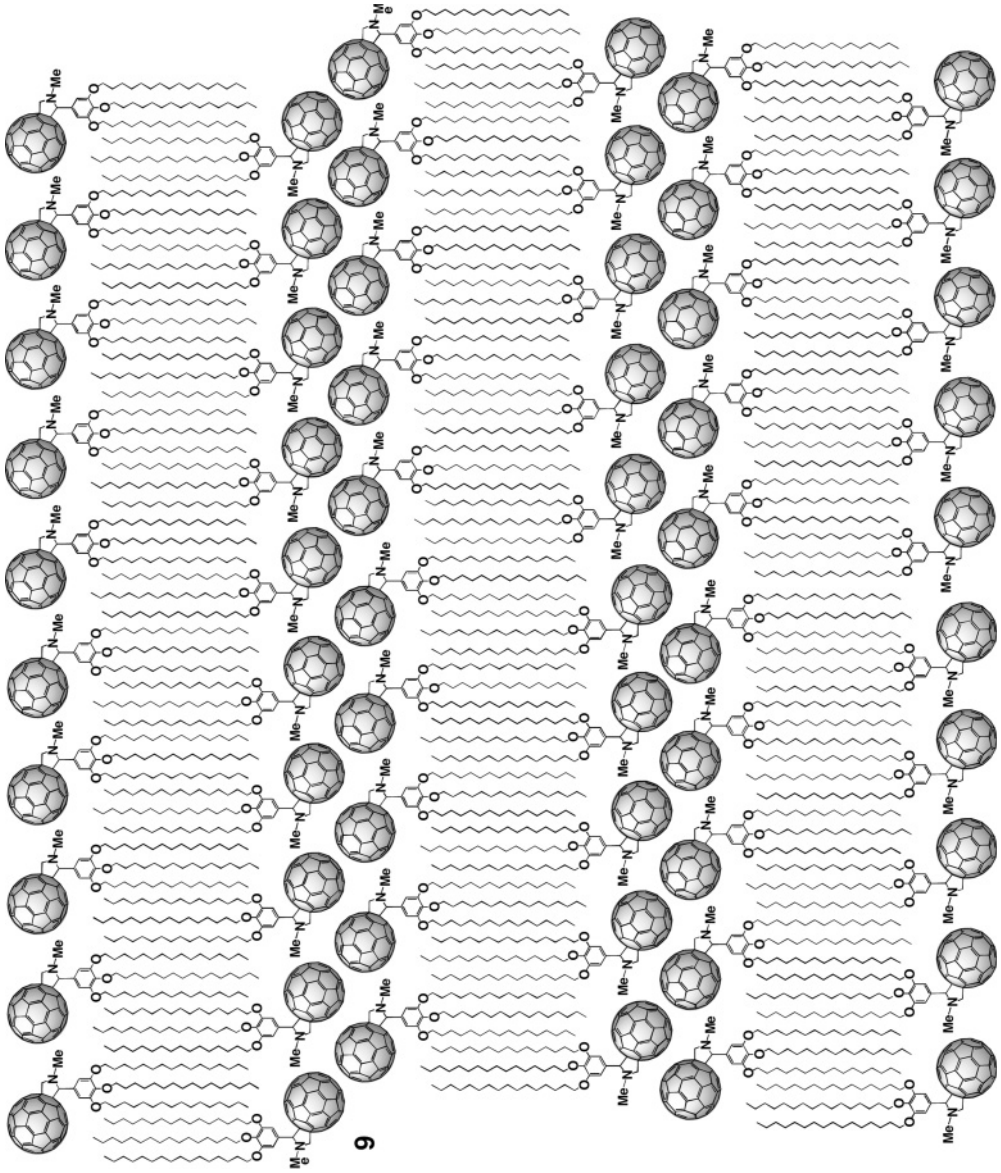

Figure 9.14 Schematic representation of a self-assembled bilayer structure containing [60]fullerene derivatives with long alkyl chains.

9.4
Introduction of [60]Fullerenes onto Polymer Chains via Noncovalent Bonds

This section discusses the scope of [60]fullerene-based polymer chemistry. These approaches may allow for the development, on a supramolecular level, of unprecedented architectures. Previous sections have dealt primarily with the self-assembly of the [60]fullerene and its derivatives as a result of microphase separation and subsequent formation of huge [60]fullerene clusters driven by the weak noncovalent forces in the solid state, mesophase and water. To avoid microphase separation, the introduction of functionalized [60]fullerene derivatives into polymer main chains through noncovalent interactions is a very promising approach. The construction of fullerene-containing supramolecular polymers in organic solution is now presented.

Introduction of [60]fullerene into polymer structures through noncovalent interactions increases the number of strategies that can be used to synthesize them (Figure 9.15) [24]. The synthetic strategies for fullerene-containing supramolecular polymers can be classified into four types (Figure 9.15): (a) functionalized [60]fullerenes attached to conventional polymers through noncovalent interactions, (b) multifunctionalized [60]fullerene-assisted crosslinking of polymer backbones via complementary noncovalent interactions, (c) self-assembly of [60]fullerene-appended nanometer-scale components and (d) molecular recognition driven-polymerization of [60]fullerene and concave hosts.

An initial successful approach to the synthesis of supramolecular fullerene polymers has been reported by Goh and coworkers. Poly(styrene-*co*-4-vinylpyridine) (PSVPy) (**12**) contains proton-accepting units, creating hydrogen bonds to methanofullerene carboxylic acid **10** (Figure 9.16) [89]. A [60]fullerene derivative having a polar functionality is not processable due to poor dispersibility in common organic solvents. However, the materials obtained after mixing **10** and **12** are easily

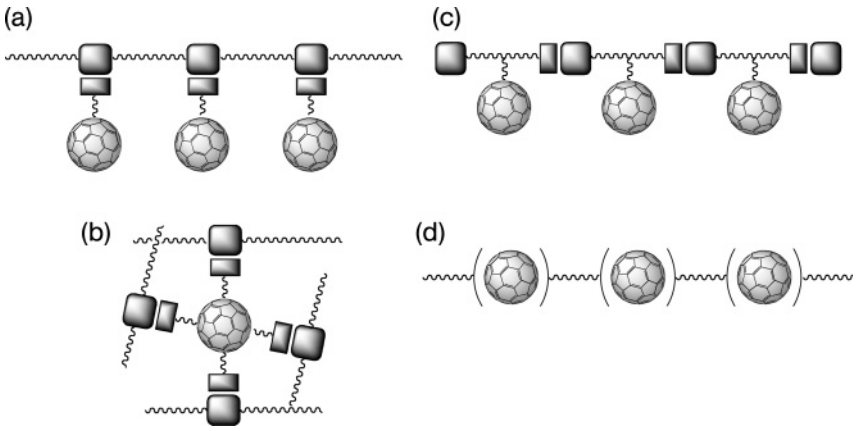

Figure 9.15 Strategies for the synthesis of [60]fullerene-based supramolecular polymers.

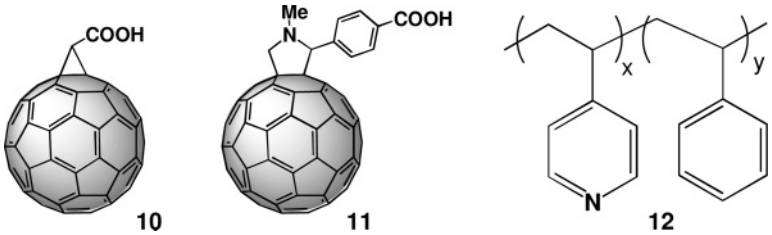

Figure 9.16 [60]fullerene carboxylic acids (**10** and **11**) and PSP4VPy polymer (**12**).

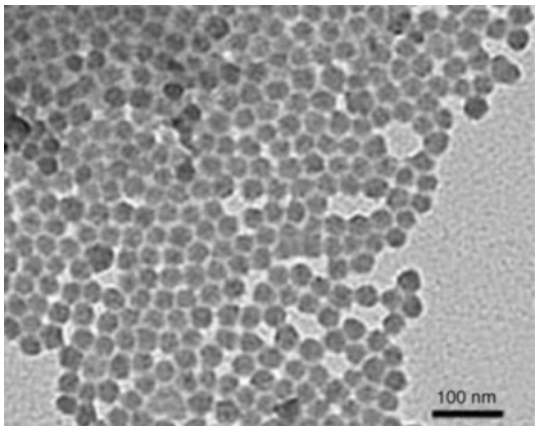

Figure 9.17 TEM image of polymer composite **11·12**. (Reproduced with permission from Reference [90]. Copyright Wiley-VCH Verlag GmbH.)

processed by solution casting, melting and blending. This is probably due to the formation of the hydrogen-bonded supramolecular fullerene polymer. Shinkai and coworkers have taken advantage of diblock copolymer **12** and [60]fullerene carboxylic acid **11** to prepare a fullerene-containing supramolecular polymer, giving rise to micelle-like superstructures (Figure 9.17) [90]. This morphology can be controlled by the reorganization of polymer **12** through the interaction of **11** at supramolecular level. The polymer chain of **12** adopts a random-coil structure in solution in the absence of the fullerene. The hydrogen bonding of **11** to the pyridine moieties forces the polymer to adopt a rigid, rod-like conformation due to the structural bulkiness of the bound fullerene. The poor solubility of the [60]fullerene-complexed polymer and the high solubility of the polystyrene block results in phase separation that causes a large structural transformation in the globular aggregates in which the more soluble polystyrene portion remains outside of the micelle (Figure 9.18). This process affords uniform nanoparticles with a diameter of approximately 20–25 nm.

A molecule of uracil and a 2,6-diacylaminopyridine (DAP) form a heterodimer through complementary three-fold hydrogen bonding, and this has been used to

Figure 9.18 Schematic representation of the formation of supramolecular rod-coil polymer, leading to the generation of micelles. (Reproduced with permission from Reference [90]. Copyright Wiley-VCH Verlag GmbH.)

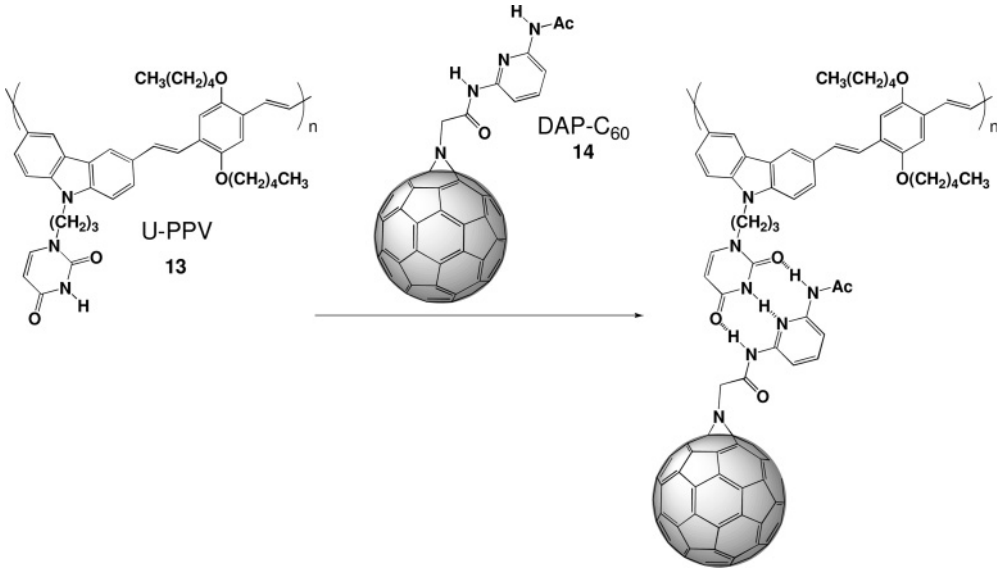

Figure 9.19 Self-complementary hydrogen-bonded supramolecular polymer.

construct a fullerene-containing supramolecular polymer (Figure 9.19) [91, 92]. Introduction of a uracil moiety onto a poly-*p*-phenylenevinylenecarbazole yields U-PPV (**13**). Mixing **13** and DAP-[60]fullerene **14** produces a [60]fullerene-containing supramolecular polymer via selective heterodimerization between the uracil and DAP moieties.

Polymer-templated fullerene nano-arrays can be produced using ionic interactions between charged polymers and fullerene derivatives [93]. Schanze, Reynolds and coworkers have reported that the layer-by-layer self-assembly approach can be used to fabricate an active material layer made up of PPE-SO_3^- **15**, PPE-EDOT-SO_3^- **16** and [60]fullerene **17** for photovoltaic cells (EDOT = 3,4-ethylenedioxythiophene) (Figure 9.20) [94]. Multiple, layer-by-layer deposition of the polymers and com-

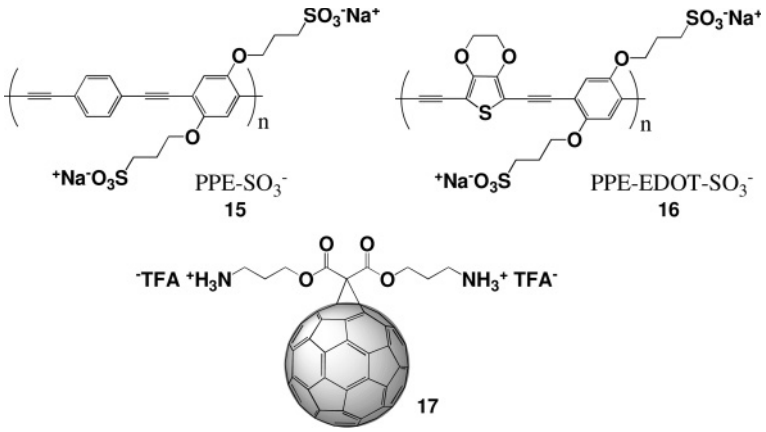

Figure 9.20 Charged polymers and a water-soluble [60]fullerene derivative.

pound **17** produces 50 layers on an ITO electrode, and uniform films are obtained, as confirmed by AFM (atomic force microscopy) studies. This approach yields devices showing a good photovoltaic response. Figure 9.21 shows the ideal layer-by-layer structure. An interpenetration of the polymer chains within the layers leads to a more disordered structure. Disorder within the film leads to intimate mixing of the donor and acceptor components. This creates the possibility of forming a bulk heterojunction, producing effective charge separation and transport through a photovoltaic cell.

Poly(*cis*-phenylacetylene) adopts a helical structure due to steric interaction of the phenyl rings. Chiral [60]fullerene-bisadduct **19** is complexed with anionic polyphenylacetylene **18** to form a fullerene nano-array on the polymer main chain, which induce its macromolecular helicity (Figure 9.22) [95]. Induction of helicity is sensitive to the geometry of the [60]fullerene-bisadducts. The *trans*-3 adduct **19** transfers its chiral information onto the macromolecular helicity, whereas *trans*-2 and *cis*-3 do not (see Chapter 6 for more details of fullerene-containing helical polymers).

Fullerene-containing supramolecular polymers based on DNA templating have been reported by Chu and coworkers [96]. Cationic [60]fullerene derivatives bind onto the DNA main chain through Coulombic interactions, which gives rise to the polymeric nano-array of [60]fullerene. Shinkai and coworkers have reported photocurrent generation in a supramolecular fullerene polymer [97]. A [60]fullerene/porphyrin/DNA ternary complex is deposited on an ITO (indium tin oxide) electrode by oxidative polymerization of EDOT. The effective photocurrent generation is observed by light excitation of the porphyrin.

Multifunctionalized [60]fullerenes can interact with a properly functionalized polymer (Figure 9.15b). Dai and coworkers have utilized Coulombic interactions

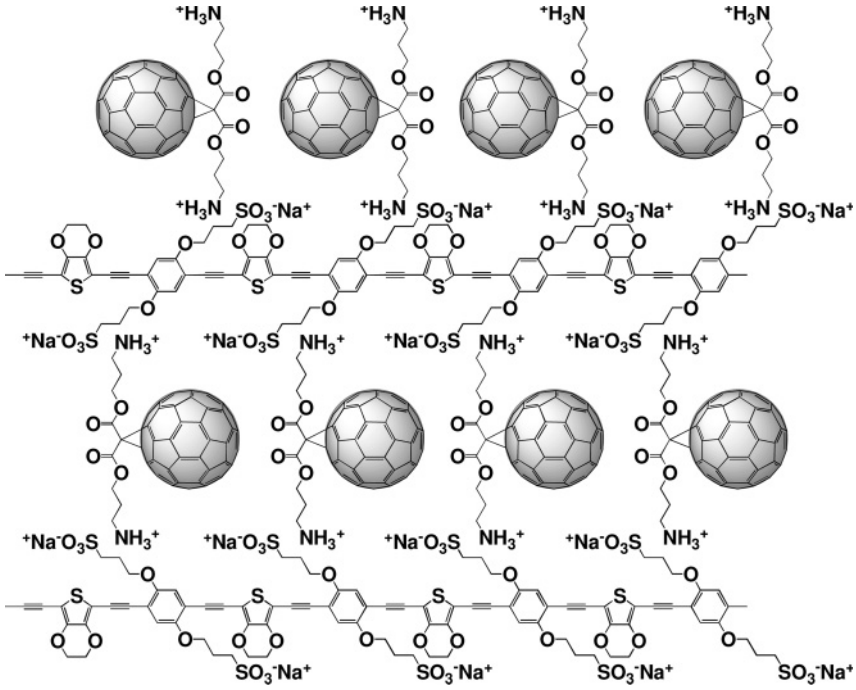

Figure 9.21 Schematic representation of the layer-by-layer structure of the film formed from **16** and **17** (Figure 9.20).

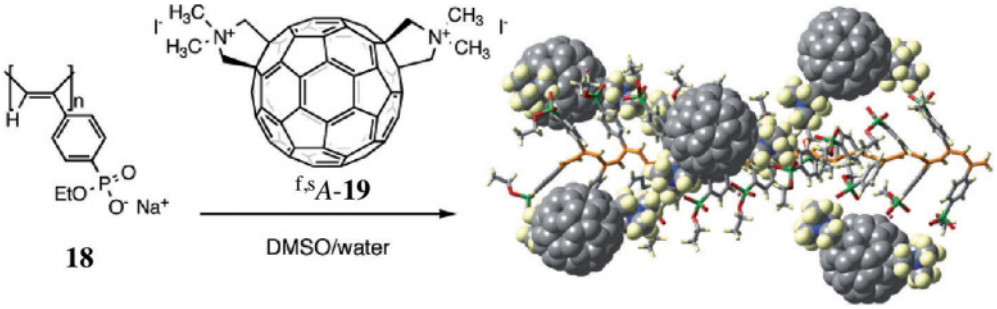

Figure 9.22 Schematic representation of the macromolecular helicity induced in **18** by optically active **19**. (Reprinted with permission from Reference [95]. Copyright (2007) American Chemical Society.)

to introduce hydrogensulfonated fullerenol **21** to PANI-EB polymer **20** (Figure 9.23). The supramolecular polymer shows outstanding electroconductivity, as high as 100 S cm^{-1}, in other words approximately six orders of magnitude higher than the typical value for a fullerene-doped conductive polymer [98, 99].

Multifunctional [60]fullerenes possessing eight pyridyl or morpholine moieties create strong ionic interactions with acidic polymers such as poly(styrenesulfonic

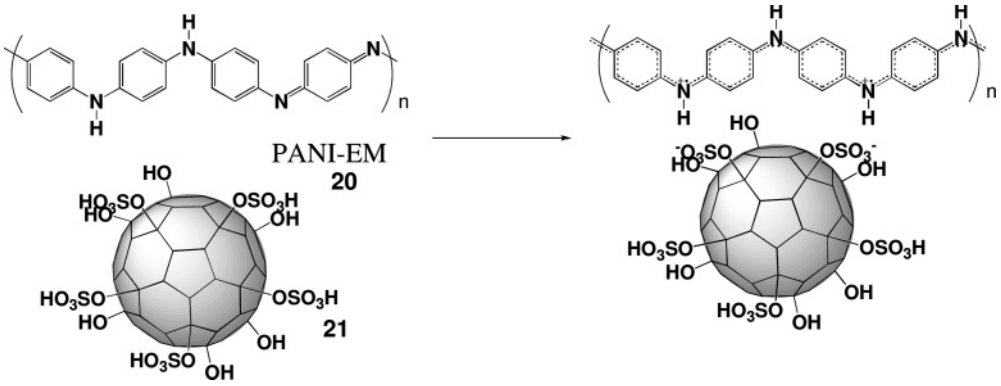

Figure 9.23 Polyaniline emeraldine base (PANI-EB) doped with hydrogensulfonated fullerenol.

acid) (PSSA), poly(vinylphosphonic acid) (PVPA), PAA and PMA [100, 101]. The composites produced give rise to very stable films due to the hydrogen bonding interactions inside each film.

The synthesis of fullerene-containing supramolecular polymers driven by complementary noncovalent interactions has been studied intensively in recent years (Figure 9.15c, d). The degree of polymerization of the supramolecular polymer formed through noncovalent interactions can be controlled by external stimuli; thus, a stimuli-responsive functional polymer can be created. One of the most useful noncovalent interactions is hydrogen bonding.

Bassani's approach utilized [60]fullerene barbituric acid **22** and pentathienylmelamine **23**, which formed hydrogen-bonded supramolecular polymers (Figure 9.24) [102]. The hydrogen-bonded polymer is processed to a thin film for photovoltaic application. The supramolecular polymers are presumably well organized by the complementary hydrogen bonding networks, in which [60]fullerene and the oligothiophene moieties are aligned along different axes. This leads to improvements in both the light harvesting efficiency of the oligothiophene moiety in the visible region and the photovoltaic response.

Hummelen and coworkers have presented a fascinating [60]fullerene-containing polymer built up by hydrogen-bonding interactions (Figure 9.25) [103]. 2-Ureido-4-pyrimidone has a "donor-donor-acceptor-acceptor" (DDAA) hydrogen bonding motif, which gives rise to a very stable hydrogen-bonded dimer. [60] Fullerene derivative **24**, having two 2-ureido-4-pyrimidone components, forms a self-complementary hydrogen-bonded polymer in organic solution.

Bisporphyrin cleft molecule **25**, which has dendritic wedges attached to the [60] fullerene molecules, forms an artificial peapod (Figure 9.26) [104]. [60]Fullerene is encapsulated within the cleft space provided by the two porphyrin components. As a result, the bisporphyrin cleft loses its conformational flexibility, and the two porphyrin units adopt a parallel arrangement, as in encapsulating [60]fullerene. This pre-organized structure assembles to produce a parallel array of the fullerene peapods. A fibrous morphology with a uniform diameter of 15 nm is confirmed by TEM.

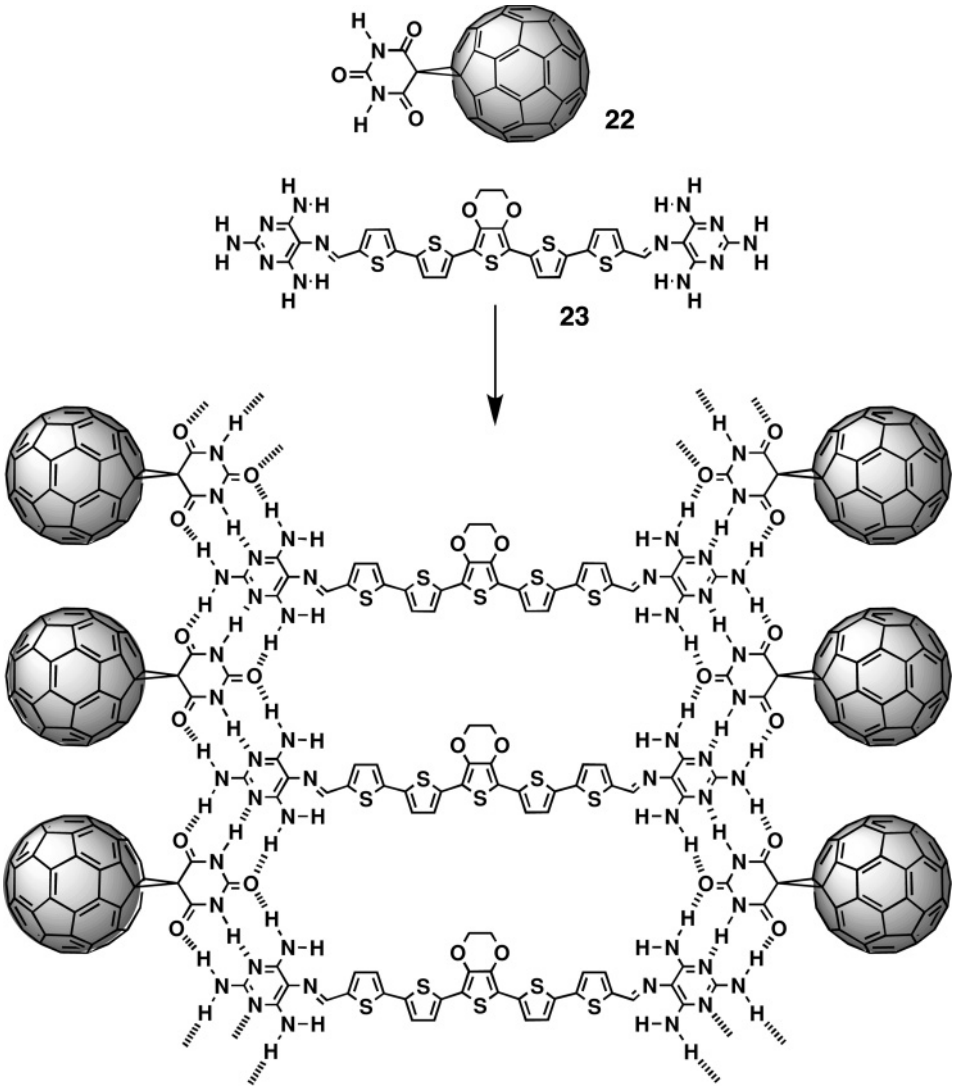

Figure 9.24 Hydrogen-bonded oligothiophene-fullerene polymer.

Another unique approach to create fullerene nano-arrays through hydrogen-bonding-assisted host–guest interaction has been reported by Shinkai and coworkers (Figure 9.27) [105]. Porphyrin **26** has hydrogen-bonding functionalities, which create a sheet-like morphology in the absence of [60]fullerene. In contrast, a 1 : 2 complexation of [60]fullerene and the porphyrin produces nanofibers in which the encapsulated [60]fullerene molecules are arranged in the complementary space formed between the two porphyrin molecules. The supramolecular polymer acts as a gelator for aromatic solvents. SEM observation of the xerogels confirms the

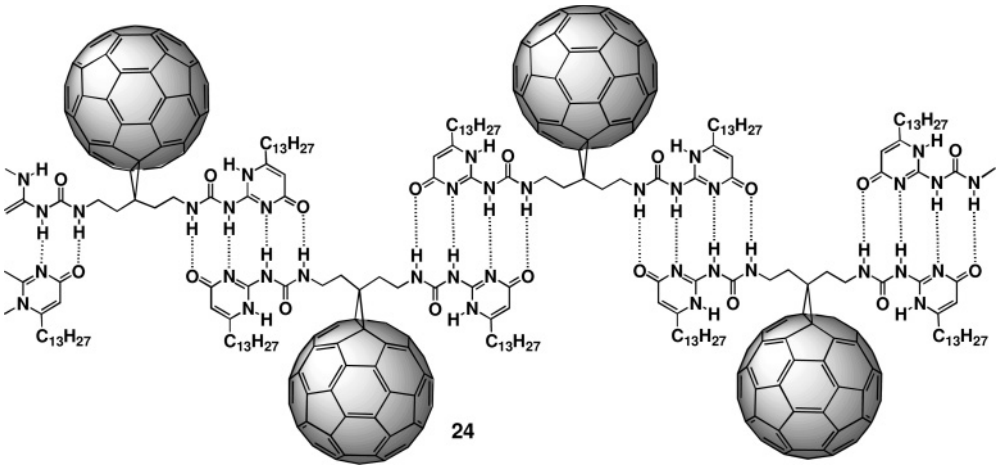

Figure 9.25 Hydrogen-bonded fullerene polymer.

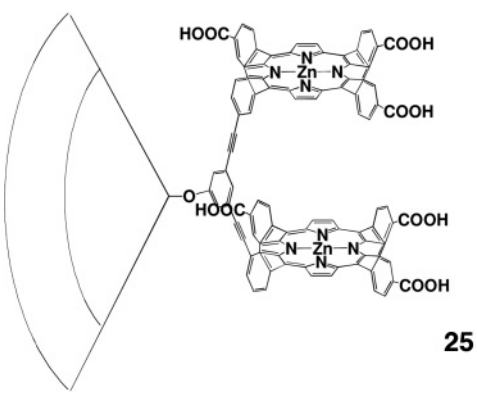

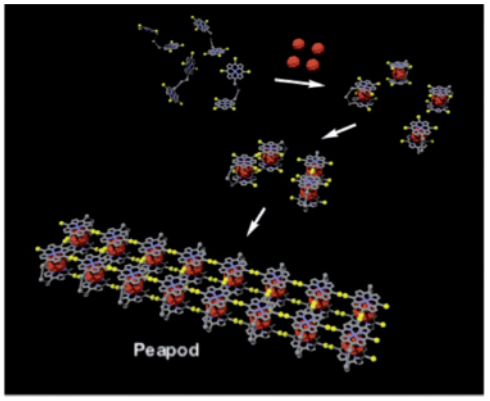

Figure 9.26 Bisporphyrin **25** and fullerene peapod formed by self-assembly of **25** with [60]fullerene. (Reprinted with permission from Reference [104]. Copyright (2003) American Chemical Society.)

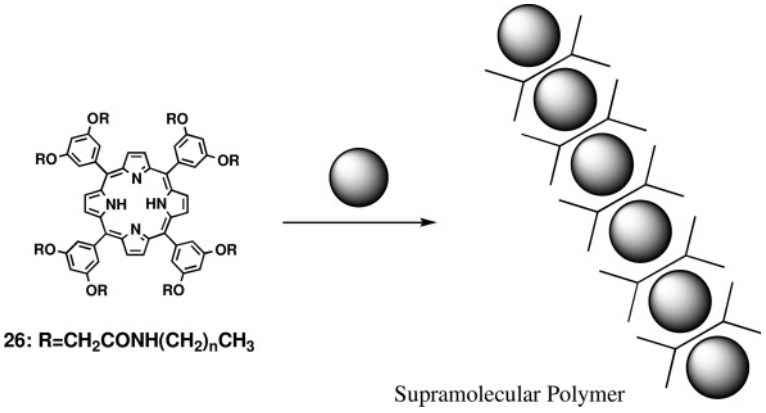

Figure 9.27 Supramolecular polymer formation driven by [60]fullerene complexation.

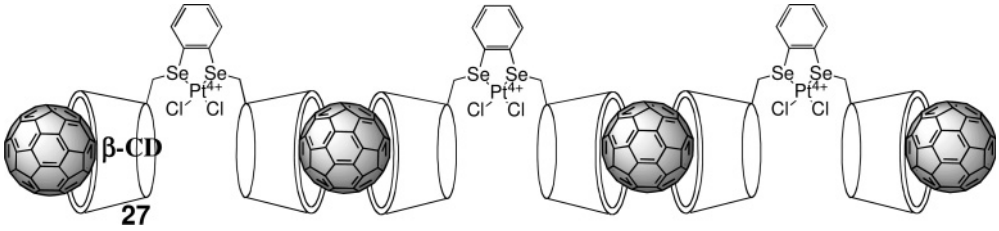

Figure 9.28 A supramolecular polymer whose structure is determined by complementary host–guest interactions.

characteristic morphology in the gel state. This is a very interesting example of fullerene-assisted morphological control of a supramolecular polymer.

Hydrophobic interactions are one of the most reliable forces for producing host–guest complexes. Of course, [60]fullerene is extremely hydrophobic; thus, some of the initial attempts to capture a [60]fullerene molecule were carried out in water. [60]Fullerene is encapsulated within the cavity of cyclodextrin molecules, to form a 2 : 1 complex. Liu and coworkers have synthesized water-soluble double-CD **27**. The end-to-end intermolecular inclusion complexation of [60]fullerene with double-CD **27** forms a supramolecular polymer in water (Figure 9.28) [106]. A STM image of the polymer shows a regular linear arrangement of the [60]fullerene nano-arrays on HOPG (highly ordered pyrolytic graphite) (Figure 9.29). TEM observation of the supramolecular polymer shows the presence of a linear structure with a length in the range 150–250 nm, suggesting that the polymer is composed of 60–80 units of the minimum component.

CD-based polyrotaxane **28** end-capped with β-CD units has been employed to create polymeric aggregates in the presence of [60]fullerene (Figure 9.30) [107]. TEM observation of the [60]fullerene-containing polymer shows the presence of many linear arrays of different lengths, with the longest polymer in the range 600–700 nm (Figure 9.31). The detailed structure of this polymer has been confirmed by STM measurements, which reveal a fine fibrous structure. The estimated length (14.5 nm) of **28** is consistent with the measured length shown in Figure 9.31a, b, and the width and height profiles of the fiber match the outer diameter of β-CD. Based on gel-permeation chromatography analysis, the supramolecular polymer connected by host–guest interactions shows narrow polydispersity and a high M_w (293 000).

Polyrotaxanes **29** associate with [60]fullerene molecules to form interlocked bis(polyrotaxane) with [60]fullerene (Figure 9.32) [108]. Important chiral and electrochemical properties have been demonstrated.

Supramolecular organic/inorganic hybrids have been produced using gold nanoparticles and [60]fullerene [109]. Kaifer and coworkers prepared γ-cyclodextrin-capped gold nanoparticles (3.2 nm diameter), which combined to form water-soluble network aggregates with a diameter of approximately 300 nm in the presence of [60]fullerene. In the particles, complexation of γ-cyclodextrins and [60]

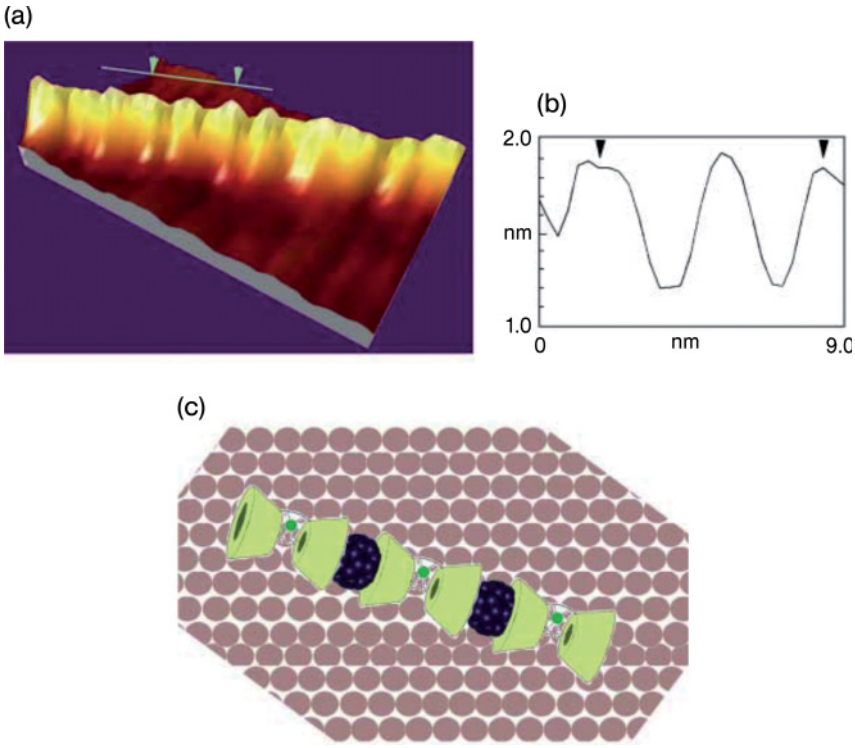

Figure 9.29 (a) STM images of assembly **27** with [60]fullerene on a HOPG surface; (b) line profile of image shown in (a); (c) schematic structure of the assembly. (Reproduced with permission from Reference [106]. Copyright Wiley-VCH Verlag GmbH.)

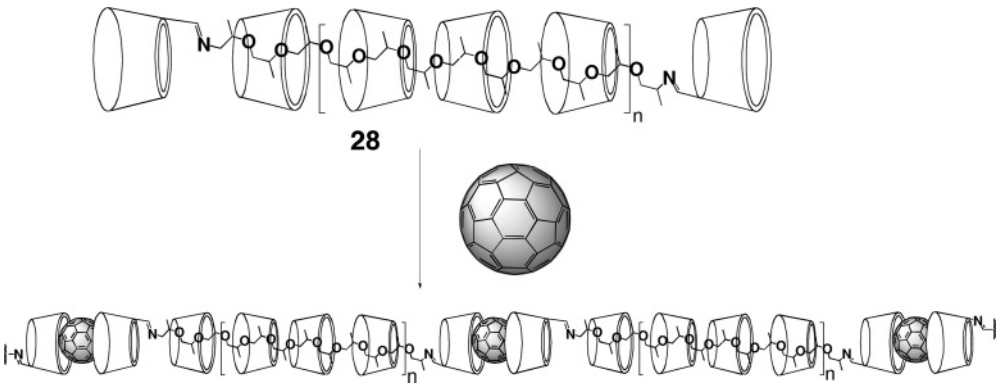

Figure 9.30 Supramolecular polymer formed by assembly of polyrotaxane **28** and [60]fullerene.

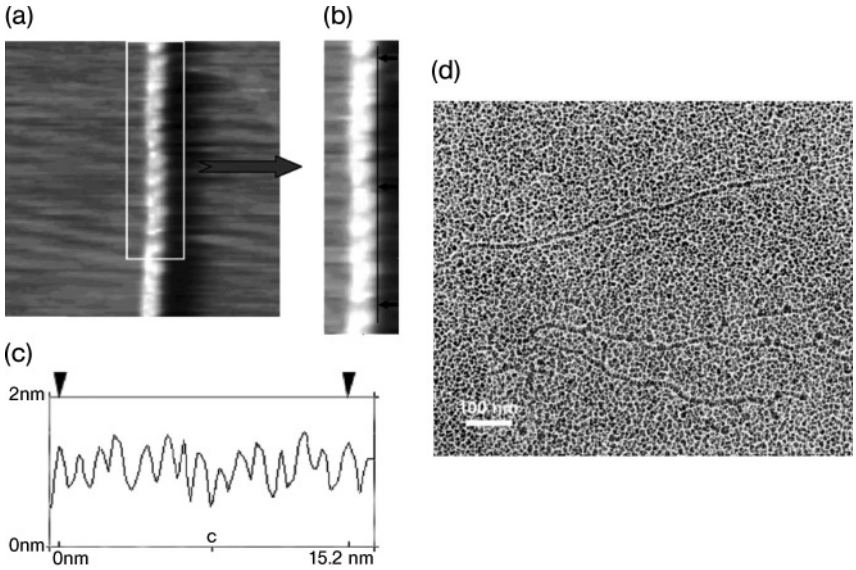

Figure 9.31 STM image of (a) the supramolecular polymer and (b) enlarged image on a HOPG surface; (c) line profile of image (b); (d) TEM image of the polymer. (Reprinted with permission from Reference [107]. Copyright (2005) American Chemical Society.)

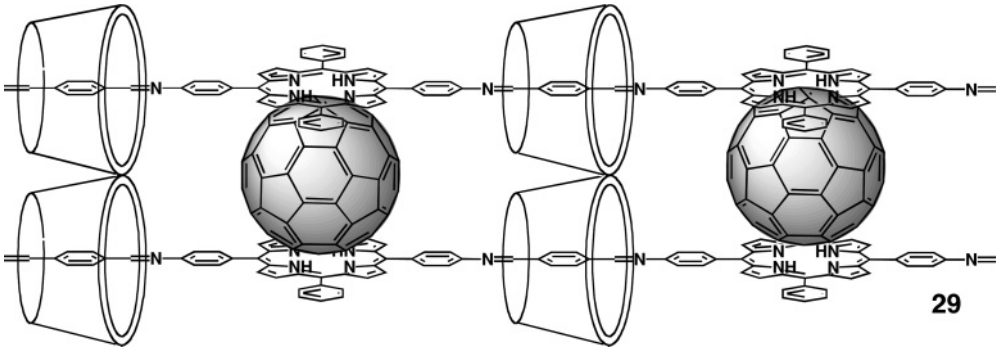

Figure 9.32 Fullerene nano-array formed between polyrotaxanes **29**.

fullerene molecules in a 2:1 molecular ratio via hydrophobic interactions creates supramolecular networks and enhances aggregation of individual particles.

Finally, the complementary molecular affinity between a [60]fullerene component and a complementary host in organic solution has been used to construct supramolecular polymeric nano-arrays of [60]fullerene. Haino and coworkers have developed a supramolecular fullerene polymer through the iterative complexation of ditopic calix[5]arene **30** and dumbbell-shaped [60]fullerene **31** (Figure 9.33) [110]. Although pulsed-field gradient NMR studies indicate that the

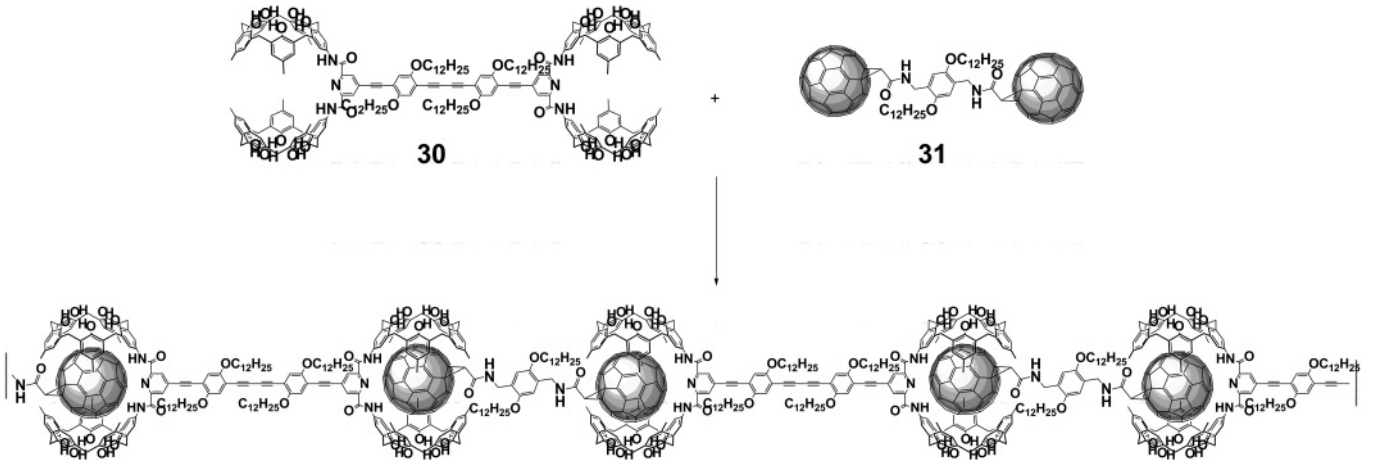

Figure 9.33 Schematic representation of supramolecular polymer formation via the complementary interaction between the double calix[5]arene and [60]fullerene components.

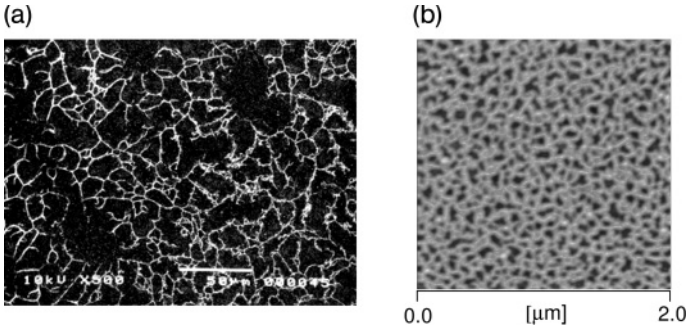

Figure 9.34 SEM (a) and AFM (b) images of the supramolecular polymer produced from the complexation of **30** and **31**. (Reprinted with permission from Reference [110]. Copyright (2005) American Chemical Society.)

trimeric supramolecular copolymer forms in solution, a higher degree of polymerization occurs in the solid state. SEM and AFM observations of the supramolecular polymer networks confirm the formation of entwined fibers 100 nm long and 50–250 nm in diameter (Figure 9.34).

Martín and coworkers have demonstrated that double-armed fullerene hosts possessing the π-extended TTF analogue, 2-[9-(1,3-dithiol-2-ylidene)anthracen-10(9*H*)-ylidene]-1,3-dithiole (exTTF), show good affinity for fullerene [111], and they have recently created a head-to-tail donor–acceptor hybrid that iteratively associates to form a supramolecular fullerene-containing polymer (Figure 9.35) [112]. Self-association studies of **32** using dynamic light scattering and NMR confirm the formation of sizable aggregates containing more than 400 monomers. AFM measurements show the formation of supramolecular polymer networks in the solid state (Figure 9.36). The images show a winding, necklace-like fragment, 15–300 nm long and 1.7–2.5 nm high. These dimensions are consistent with those of assemblies of **32**. A long tubular formation 77 nm long is seen in Figure 9.36b–d.

This section has described precisely designed supramolecular assemblies. Coulombic, hydrogen bonding, π–π stacking, charge transfer and hydrophobic interactions are the main tools for creating these ingenious supramolecular architectures. Some of the examples presented take advantage of unique motifs to generate molecular interactions, and these examples suggest a bright future for nanotechnology and nanoscience based on supramolecular chemistry.

9.5 Outlook

The discovery of fullerenes in 1985 created the new research field of carbon clusters [113]. A major breakthrough in fullerene science came when Krätschmer and

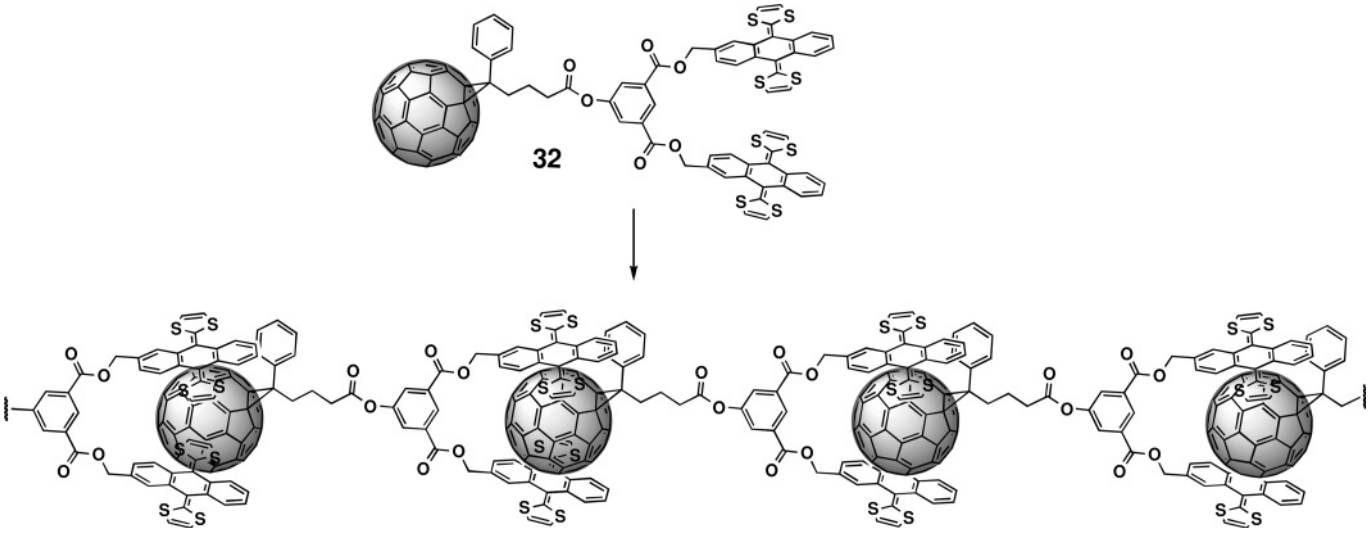

Figure 9.35 Supramolecular polymer driven by head-to-tail donor–acceptor interactions.

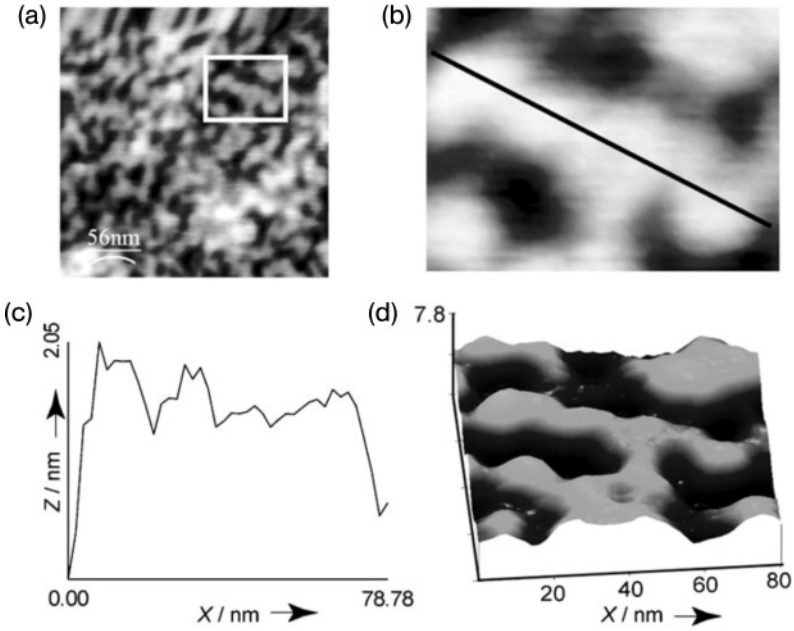

Figure 9.36 AFM images (tapping mode, air, 298 K) of a drop-cast of a dichloromethane solution of **32** on mica: (a) 277 × 277 nm; (b) 80 × 65 nm; (c) profile of the structure shown in (b) (black line); (d) three-dimensional image of (b). (Reproduced with permission from Reference [112]. Copyright Wiley-VCH Verlag GmbH.)

Huffman produced practical amounts of [60]fullerene [114]. This opened up the fullerene world, which chemists expanded by synthesizing new classes of well-organized fullerene architectures. The unique three-dimensional geometry of [60] fullerene, with its 30 highly reactive double bonds, can be chemically modified in various ways. Many unique chemical reactions have been developed to create selectively functionalized [60]fullerenes. The chemistry of [60]fullerene is now considered a well-established field in which most aspects of chemical reactivity are understood. However, more structural variations are required to develop new functional materials, paving the way for new research directions in chemistry as well as creating key materials for the emerging field of nanotechnology.

The impact of [60]fullerene molecules in chemistry, nanotechnology and related fields has been impressive and is expected to grow through the incorporation of concepts and practices from supramolecular chemistry. Chemists have already made significant advances in the supramolecular chemistry of fullerene by generating new, functional "smart" materials. The functionality derives from the supramolecular level, and it is unique to the assembled state. Thus, controlling the supramolecular structures of "smart" materials at the molecular level involves

"bottom-up" approaches that access complex fullerene-based molecular architectures to engineer specific functions. This work will accelerate the progress of fullerene nanoscience.

References

1 Kraetschmer, W. (1995) *Synth. Met.*, **70**, 1309–12.
2 Dresselhaus, M.S., Dresselhaus, G. and Eklund, P.C. (eds) (1996) *Science of Fullerenes and Carbon Nanotubes*, Academic Press Inc., California.
3 Taylor, R. (1999) *Lecture Notes on Fullerene Chemistry: A Handbook for Chemists*, Imperial College Press, London.
4 Coffey, D. and Trugman, S.A. (1992) *Phys. Rev. Lett.*, **69**, 176–9.
5 Politis, C., Buntar, V., Krauss, W. and Gurevich, A. (1992) *Europhys. Lett.*, **17**, 175–9.
6 Lee, G.H., Huh, S.H., Jeong, J.W. and Ri, H.C. (2002) *J. Magn. Magn. Mater.*, **246**, 404–11.
7 Tanigaki, K., Ebbesen, T.W., Saito, S., Mizuki, J., Tsai, J.S., Kubo, Y. and Kuroshima, S. (1991) *Nature*, **352**, 222–3.
8 Wang, H.H., Kini, A.M., Savall, B.M., Carlson, K.D., Williams, J.M., Lathrop, M.W., Lykke, K.R., Parker, D.H., Wurz, P. *et al.* (1991) *Inorg. Chem.*, **30**, 2962–3.
9 Kronholm, D. and Hummelen, J.C. (2007) *Mater. Matters*, **2**, 16–19.
10 Roncali, J. (2005) *Chem. Soc. Rev.*, **34**, 483–95.
11 Shinohara, H. (2000) *Rep. Prog. Phys.*, **63**, 843–92.
12 Garnier, F. (1998) *Chem. Phys.*, **227**, 253–62.
13 Konishi, T., Ikeda, A. and Shinkai, S. (2005) *Tetrahedron*, **61**, 4881–99.
14 Imahori, H. and Fukuzumi, S. (2004) *Adv. Funct. Mater.*, **14**, 525–36.
15 Sariciftci, N.S. (1999) *Curr. Opin. Solid State Mater. Sci.*, **4**, 373–8.
16 Sariciftci, N.S. and Heeger, A.J. (1995) *Synth. Met.*, **70**, 1349–52.
17 Sariciftci, N.S. and Heeger, A.J. (1994) *Mol. Cryst. Liq. Cryst. Sci. Technol. Sect. A*, **256**, 317–26.
18 Wudl, F. (2002) *J. Mater. Chem.*, **12**, 1959–63.
19 Zhou, P., Dong, Z.H., Rao, A.M. and Eklund, P.C. (1993) *Chem. Phys. Lett.*, **211**, 337–40.
20 Wang, Y., Holden, J.M., Dong, Z.H., Bi, X.X. and Eklund, P.C. (1993) *Chem. Phys. Lett.*, **211**, 341–5.
21 Rao, A.M., Zhou, P., Wang, K.A., Hager, G.T., Holden, J.M., Wang, Y., Lee, W.T., Bi, X.X., Eklund, P.C., Cornett, D.S., Duncan, M.A. and Amster, I.J. (1993) *Science*, **259**, 955–7.
22 Iwasa, Y., Arima, T., Fleming, R.M., Siegrist, T., Zhou, O., Haddon, R.C., Rothberg, L.J., Lyons, K.B., Carter, H.L., Hebard, A.F., Tycko, R., Dabbagh, G., Krajewski, J.J., Thomas, G.A. and Yagi, T. (1994) *Science*, **264**, 1570–2.
23 Geckeler, K.E. and Samal, S. (1999) *Polym. Int.*, **48**, 743–57.
24 Giacalone, F. and Martín, N. (2006) *Chem. Rev.*, **106**, 5136–90.
25 Wang, C., Guo, Z.X., Fu, S., Wu, W. and Zhu, D. (2004) *Prog. Polym. Sci.*, **29**, 1079–141.
26 Martin, N. (2006) *Chem. Commun.*, 2093–104.
27 Segura, J.L., Martín, N. and Guldi, D.M. (2005) *Chem. Soc. Rev.*, **34**, 31–47.
28 Dai, L. (1999) *Polym. Adv. Technol.*, **10**, 357–420.
29 Zhou, N., Merschrod, E.F. and Zhao, S.Y. (2005) *J. Am. Chem. Soc.*, **127**, 14154–5.
30 Nishimura, T., Takatani, K., Sakurai, S.I., Maeda, K. and Yashima, E. (2002) *Angew. Chem. Int. Ed.*, **41**, 3602–4.
31 Gutiérrez Nava, M., Setayesh, S., Rameau, A., Masson, P. and Nierengarten, J.F. (2002) *New J. Chem.*, **26**, 1584–9.
32 Brunsveld, L., Folmer, B.J.B., Meijer, E.W. and Sijbesma, R.P. (2001) *Chem. Rev.*, **101**, 4071–97.

33 Sijbesma, R.P. and Meijer, E.W. (2003) *Chem. Commun.*, 5–16.

34 Sijbesma, R.P., Beijer, F.H., Brunsveld, L., Folmer, B.J.B., Lange, J.H.K.K., Hirschberg, R.F.M., Lowe, J.K.L. and Meijer, E.W. (1997) *Science*, **278**, 1601–4.

35 Ciferri, A. (ed.) (2005) *Supramolecular Polymer*, 2nd edn, Taylor & Francis, New York.

36 Castellano, R.K., Clark, R., Craig, S.L., Nuckolls, C. and Rebek, J. (2000) *Proc. Natl. Acad. Sci. U.S.A.*, **97**, 12418–21.

37 Castellano, R.K., Rudkevich, D.M. and Rebek, J. (1997) *Proc. Natl. Acad. Sci. U.S.A.*, **94**, 7132–7.

38 Rudkevich, D.M. (2007) *Eur. J. Org. Chem.*, 3255–70.

39 Ermer, O. (1991) *Helv. Chim. Acta*, **74**, 1339–51.

40 Crane, J.D., Hitchcock, P.B., Kroto, H.W., Taylor, R. and Walton, D.R.M. (1992) *J. Chem. Soc. Chem. Commun.*, 1764–5.

41 Meidine, M.F., Hitchcock, P.B., Kroto, H.W., Taylor, R. and Walton, D.R.M. (1992) *J. Chem. Soc. Chem. Commun.*, 1534–7.

42 Birkett, P.R., Christides, C., Hitchcock, P.B., Kroto, H.W., Prassides, K., Taylor, R. and Walton, D.R.M. (1993) *J. Chem. Soc. Perkin Trans. 2*, 1407–8.

43 Izuoka, A., Tachikawa, T., Sugawara, T., Suzuki, Y., Konno, M., Saito, Y. and Shinohara, H. (1992) *J. Chem. Soc. Chem. Commun.*, 1472–3.

44 Izuoka, A., Tachikawa, T., Sugawara, T., Saito, Y. and Shinohara, H. (1992) *Chem. Lett.*, 1049–52.

45 Balch, A.L., Catalano, V.J., Lee, J.W. and Olmstead, M.M. (1992) *J. Am. Chem. Soc.*, **114**, 5455–7.

46 Barbour, L.J., Orr, G.W. and Atwood, J.L. (1998) *Chem. Commun.*, 1901–2.

47 Sun, D. and Reed, C.A. (2000) *Chem. Commun.*, 2391–2.

48 Haino, T., Fukunaga, C. and Fukazawa, Y. (2007) *J. Nanosci. Nanotechnol.*, **7**, 1386–8.

49 Haino, T., Seyama, J., Fukunaga, C., Murata, Y., Komatsu, K. and Fukazawa, Y. (2005) *Bull. Chem. Soc. Jpn.*, **78**, 768–70.

50 Haino, T., Yanase, M. and Fukazawa, Y. (1997) *Angew. Chem. Int. Ed. Engl.*, **36**, 259–60.

51 Haino, T., Yanase, M. and Fukazawa, Y. (1997) *Tetrahedron Lett.*, **38**, 3739–42.

52 Haino, T., Yanase, M. and Fukazawa, Y. (1998) *Angew. Chem. Int. Ed.*, **37**, 997–8.

53 Haino, T., Araki, H., Fujiwara, Y., Tanimoto, Y. and Fukazawa, Y. (2002) *Chem. Commun.*, 2148–9.

54 Haino, T., Yamanaka, Y., Araki, H. and Fukazawa, Y. (2002) *Chem. Commun.*, 402–3.

55 Haino, T., Yanase, M., Fukunaga, C. and Fukazawa, Y. (2006) *Tetrahedron*, **62**, 2025–35.

56 Haino, T., Fukunaga, C. and Fukazawa, Y. (2006) *Org. Lett.*, **8**, 3545–8.

57 Yanase, M., Haino, T. and Fukazawa, Y. (1999) *Tetrahedron Lett.*, **40**, 2781–4.

58 Haino, T., Mitsuhashi, H., Ishizu, Y. and Fukazawa, Y. (2006) *Tetrahedron Lett.*, **47**, 7915–18.

59 Haino, T., Yanase, M. and Fukazawa, Y. (2005) *Tetrahedron Lett.*, **46**, 1411–14.

60 Atwood, J.L., Barbour, L.J., Heaven, M.W. and Raston, C.L. (2003) *Angew. Chem. Int. Ed.*, **42**, 3254–7.

61 Atwood, J.L., Barbour, L.J. and Raston, C.L. (2002) *Cryst. Grow. Design.*, **2**, 3–6.

62 Hubble, L.J. and Raston, C.L. (2007) *Chem. Eur. J.*, **13**, 6755–60.

63 Wang, Z., Dötz, F., Enkelmann, V. and Müllen, K. (2005) *Angew. Chem. Int. Ed.*, **44**, 1247–50.

64 Smith, B.W., Monthioux, M. and Luzzi, D.E. (1998) *Nature*, **396**, 323–4.

65 Smith, B.W., Monthioux, M. and Luzzi, D.E. (1999) *Chem. Phys. Lett.*, **315**, 31–6.

66 Burteaux, B., Claye, A., Smith, B.W., Monthioux, M., Luzzi, D.E. and Fischer, J.E. (1999) *Chem. Phys. Lett.*, **310**, 21–4.

67 Chuard, T. and Deschenaux, R. (1996) *Helv. Chim. Acta*, **79**, 736–41.

68 Chuard, T., Deschenaux, R., Hirsch, A. and Schonberger, H. (1999) *Chem. Commun.*, 2103–4.

69 Deschenaux, R., Even, M. and Guillon, D. (1998) *Chem. Commun.*, 537–8.

70 Dardel, B., Guillon, D., Heinrich, B. and Deschenaux, R. (2001) *J. Mater. Chem.*, **11**, 2814–31.

71 Chuard, T. and Deschenaux, R. (2002) *J. Mater. Chem.*, **12**, 1944–51.
72 Campidelli, S. and Deschenaux, R. (2001) *Helv. Chim. Acta*, **84**, 589–93.
73 Dardel, B., Deschenaux, R., Even, M. and Serrano, E. (1999) *Macromolecules*, **32**, 5193–8.
74 Chuard, T., Dardel, B., Deschenaux, R. and Even, M. (2000) *Carbon*, **38**, 1573–6.
75 Even, M., Heinrich, B., Guillon, D., Guldi, D.M., Prato, M. and Deschenaux, R. (2001) *Chem. Eur. J.*, **7**, 2595–604.
76 Campidelli, S., Lenoble, J., Barbera, J., Paolucci, F., Marcaccio, M., Paolucci, D. and Deschenaux, R. (2005) *Macromolecules*, **38**, 7915–25.
77 Campidelli, S., Vazquez, E., Milic, D., Lenoble, J., Castellanos, C.A., Sarova, G., Guldi, D.M., Deschenaux, R. and Prato, M. (2006) *J. Org. Chem.*, **71**, 7603–10.
78 Sawamura, M., Kawai, K., Matsuo, Y., Kanie, K., Kato, T. and Nakamura, E. (2002) *Nature*, **419**, 702–5.
79 Matsuo, Y., Muramatsu, A., Hamasaki, R., Mizoshita, N., Kato, T. and Nakamura, E. (2004) *J. Am. Chem. Soc.*, **126**, 432–3.
80 Zhong, Y.W., Matsuo, Y. and Nakamura, E. (2007) *J. Am. Chem. Soc.*, **129**, 3052–3.
81 Zhou, S., Burger, C., Chu, B., Sawamura, M., Nagahama, N., Toganoh, M., Hackler, U.E., Isobe, H. and Nakamura, E. (2001) *Science*, **291**, 1944–7.
82 Song, T., Dai, S., Tam, K.C., Lee, S.Y. and Goh, S.H. (2003) *Polymer*. **44**, 2529–36.
83 Zhou, G., Harruna, I.I., Zhou, W.L., Aicher, W.K. and Geckeler, K.E. (2007) *Chem. Eur. J.*, **13**, 569–73.
84 Wang, C., Ravi, P. and Tam, K.C. (2007) *Langmuir*, **23**, 8798–805.
85 Nakanishi, T., Schmitt, W., Michinobu, T., Kurth, D.G. and Ariga, K. (2005) *Chem. Commun.*, 5982–4.
86 Nakanishi, T., Miyashita, N., Michinobu, T., Wakayama, Y., Tsuruoka, T., Ariga, K. and Kurth, D.G. (2006) *J. Am. Chem. Soc.*, **128**, 6328–9.
87 Nakanishi, T., Ariga, K., Michinobu, T., Yoshida, K., Takahashi, H., Teranishi, T., Möhwald, H. and Kurth, D.G. (2007) *Small*, **3**, 2019–23.
88 Nakanishi, T., Takahashi, H., Michinobu, T., Hill, J.P., Teranishi, T. and Ariga, K. (2008) *Thin Solid Films*, **516**, 2401–6.
89 Ouyang, J., Goh, S.H. and Li, Y. (2001) *Chem. Phys. Lett.*, **347**, 344–8.
90 Fujita, N., Yamashita, T., Asai, M. and Shinkai, S. (2005) *Angew. Chem. Int. Ed.*, **44**, 1257–61.
91 Fang, H., Wang, S., Xiao, S., Yang, J., Li, Y., Shi, Z., Li, H., Liu, H. and Zhu, D. (2003) *Chem. Mater.*, **15**, 1593–7.
92 Fang, H., Shi, Z., Li, Y., Xiao, S., Li, H., Liu, H. and Zhu, D. (2003) *Synth. Met.*, **135–136**, 843–4.
93 Lu, F., Li, Y., Liu, H., Zhuang, J., Gan, L. and Zhu, D. (2005) *Synth. Met.*, **153**, 317–20.
94 Mwaura, J.K., Pinto, M.R., Witker, D., Ananthakrishnan, N., Schanze, K.S. and Reynolds, J.R. (2005) *Langmuir*, **21**, 10119–26.
95 Nishimura, T., Tsuchiya, K., Ohsawa, S., Maeda, K., Yashima, E., Nakamura, Y. and Nishimura, J. (2004) *J. Am. Chem. Soc.*, **126**, 11711–17.
96 Ying, Q., Zhang, J., Liang, D., Nakanishi, W., Isobe, H., Nakamura, E. and Chu, B. (2005) *Langmuir*, **21**, 9824–31.
97 Bae, A.H., Hatano, T., Sugiyasu, K., Kishida, T., Takeuchi, M. and Shinkai, S. (2005) *Tetrahedron Lett.*, **46**, 3169–73.
98 Dai, L., Lu, J., Matthews, B. and Mau, A.W.H. (1998) *J. Phys. Chem. B*, **102**, 4049–53.
99 Lu, J., Dai, L. and Mau, A.W.H. (1998) *Acta Polym.*, **49**, 371–5.
100 Lu, Z., Goh, S.H. and Lee, S.Y. (1999) *Macromol. Chem. Phys.*, **200**, 1515–22.
101 Goh, S.H., Lee, S.Y., Lu, Z.H. and Huan, C.H.A. (2000) *Macromol. Chem. Phys.*, **201**, 1037–47.
102 Huang, C.H., McClenaghan, N.D., Kuhn, A., Hofstraat, J.W. and Bassani, D.M. (2005) *Org. Lett.*, **7**, 3409–12.
103 Sánchez, L., Rispens, M.T. and Hummelen, J.C. (2002) *Angew. Chem. Int. Ed.*, **41**, 838–40.
104 Yamaguchi, T., Ishii, N., Tashiro, K. and Aida, T. (2003) *J. Am. Chem. Soc.*, **125**, 13934–5.
105 Shirakawa, M., Fujita, N. and Shinkai, S. (2003) *J. Am. Chem. Soc.*, **125**, 9902–3.

106 Liu, Y., Wang, H., Liang, P. and Zhang, H.-Y. (2004) *Angew. Chem. Int. Ed.*, **43**, 2690–4.
107 Liu, Y., Yang, Y.W., Chen, Y. and Zou, H.X. (2005) *Macromolecules*, **38**, 5838–40.
108 Liu, Y., Liang, P., Chen, Y., Zhang, Y.M., Zheng, J.Y. and Yue, H. (2005) *Macromolecules*, **38**, 9095–9.
109 Liu, J., Alvarez, J., Ong, W. and Kaifer, A.E. (2001) *Nano Lett.*, **1**, 57–60.
110 Haino, T., Matsumoto, Y. and Fukazawa, Y. (2005) *J. Am. Chem. Soc.*, **127**, 8936–7.
111 Pérez, E.M., Sánchez, L., Fernández, G. and Martín, N. (2006) *J. Am. Chem. Soc.*, **128**, 7172–3.
112 Fernández, G., Pérez, E.M., Sánchez, L. and Martín, N. (2008) *Angew. Chem. Int. Ed.*, **47**, 1094–7.
113 Kroto, H.W., Heath, J.R., O'Brien, S.C., Curl, R.F. and Smalley, R.E. (1985) *Nature*, **318**, 162–3.
114 Krätschmer, W., Lamb, L.D., Fostiropoulos, K. and Huffman, D.R. (1990) *Nature*, **347**, 354–8.

10
Fullerene-Rich Dendrons and Dendrimers

Jean-François Nierengarten

10.1
Introduction

Nanosized molecules are attracting a considerable attention, with particular emphasize on a special class of polymers named dendrimers. Indeed, dendritic macromolecules made of well-defined branching units emanating from a central core constitute a major field of research [1]. In recent years, rapid advances in dendrimer synthetic chemistry have moved toward the creation of functional systems with increased attention on potential applications [1]. Among many molecular subunits used for dendrimer chemistry, C_{60} has proven to be a versatile building block [2]. Actually, fullerene-functionalized dendrimers have generated significant research activities in recent years [3, 4]. In particular, the peculiar physical properties of fullerene derivatives make fullerodendrimers attractive candidates for various interesting features in supramolecular chemistry and materials science [5]. C_{60} itself is a convenient core for dendrimer chemistry [3] and the functionalization of C_{60} with a controlled number of dendrons dramatically improves the solubility of the fullerenes [6]. Furthermore, variable degrees of addition about the fullerene core are possible and its almost spherical shape leads to globular systems even with low-generation dendrons [7]. On the other hand, specific advantages are brought about by the encapsulation of a fullerene moiety in the middle of a dendritic structure [8]. The shielding effect resulting from the presence of the surrounding shell has been found useful to optimize the optical limiting properties of C_{60} derivatives [9], to obtain amphiphilic derivatives with good spreading characteristics [10] or to prepare fullerene-containing liquid crystalline materials [11]. The use of the fullerene sphere as a photoactive core unit has also been reported [12]. In particular, the special photophysical properties of C_{60} have been used to evidence dendritic shielding effects [13] and to prepare dendrimer-based light-harvesting systems [14]. Whereas most fullerene-containing dendrimers reported so far have been prepared with a C_{60} core, dendritic structures with fullerene units at their surface or with C_{60} spheres in the dendritic branches have been essentially ignored. This is mainly associated with the difficulties related to the synthesis of

Fullerene Polymers. Synthesis, Properties and Applications. Edited by Nazario Martín and Francesco Giacalone

ISBN: 978-3-527-32282-4

fullerene-rich molecules [4]. Indeed, the two major problems for the preparation of such dendrimers are the low solubility of C_{60} and its chemical reactivity limiting the range of reactions that can be used for the synthesis of branched structures bearing multiple C_{60} units. This chapter presents the most recent developments on the molecular engineering of fullerene-rich dendrons and dendrimers. The aim is not to give an exhaustive review on such systems but to present significant examples to illustrate the current state-of-the-art of fullerene chemistry for the development of new nanostructures.

10.2
Fullerene-Rich Dendrons

10.2.1
Synthesis of Fullerene-Rich Dendrons and Their Incorporation in Langmuir and Langmuir–Blodgett Films

The first example of convergent preparation of dendritic branches with fullerene subunits at the periphery was reported by Nierengarten and coworkers [15]. Scheme 10.1 depicts the synthesis of these fullerodendrons. The starting fullerene derivative **1** is easily obtained on a multi-gram scale and is highly soluble in common organic solvents owing to the presence of the four long alkyl chains. The iterative reaction sequence used for the preparation of the subsequent dendrimer generations relies upon successive cleavage of a *t*-butyl ester moiety under acidic conditions followed by a *N*,*N*′-dicyclohexylcarbodiimide (DCC)-mediated esterification reaction with the A_2B building block **3** possessing two benzylic alcohol functions and a protected carboxylic acid group [15].

The *t*-butyl ester group in **1** was cleaved selectively by treatment with an excess of CF_3COOH (trifluoroacetic acid, TFA) in CH_2Cl_2 to afford **2** in quantitative yield. Reaction of diol **3** with carboxylic acid **2** under esterification conditions using DCC, 4-dimethylaminopyridine (DMAP) and 1-hydroxybenzotriazole (HOBt) in CH_2Cl_2 gave the protected dendron of second generation (**4**) in 90% yield. Hydrolysis of the *t*-butyl ester moiety under acidic conditions then afforded the corresponding carboxylic acid **5** in quantitative yield. Esterification of **5** with diol **3** (DCC, HOBt, DMAP) afforded the *t*-butyl-protected fullerodendron **6** in 95% yield. Selective hydrolysis of the *t*-butyl ester under acidic conditions afforded acid **7** in 97% yield. Dendrons **2**, **5** and **7** are easily prepared on a multi-gram scale and are highly soluble in common organic solvents.

Following the successful preparation of dendritic branches with peripheral C_{60} subunits, Nierengarten and coworkers also reported several synthesis of fullerodendrons with C_{60} groups at each branching units [16]. Scheme 10.2 shows a typical example. Reaction of acid **9** with **8** under esterification conditions using DCC, DMAP and BtOH afforded **10** in 65% yield. Subsequent cleavage of the *t*-butyl ester moiety with CF_3CO_2H (TFA) in CH_2Cl_2 gave fullerodendron **11** in 96% yield.

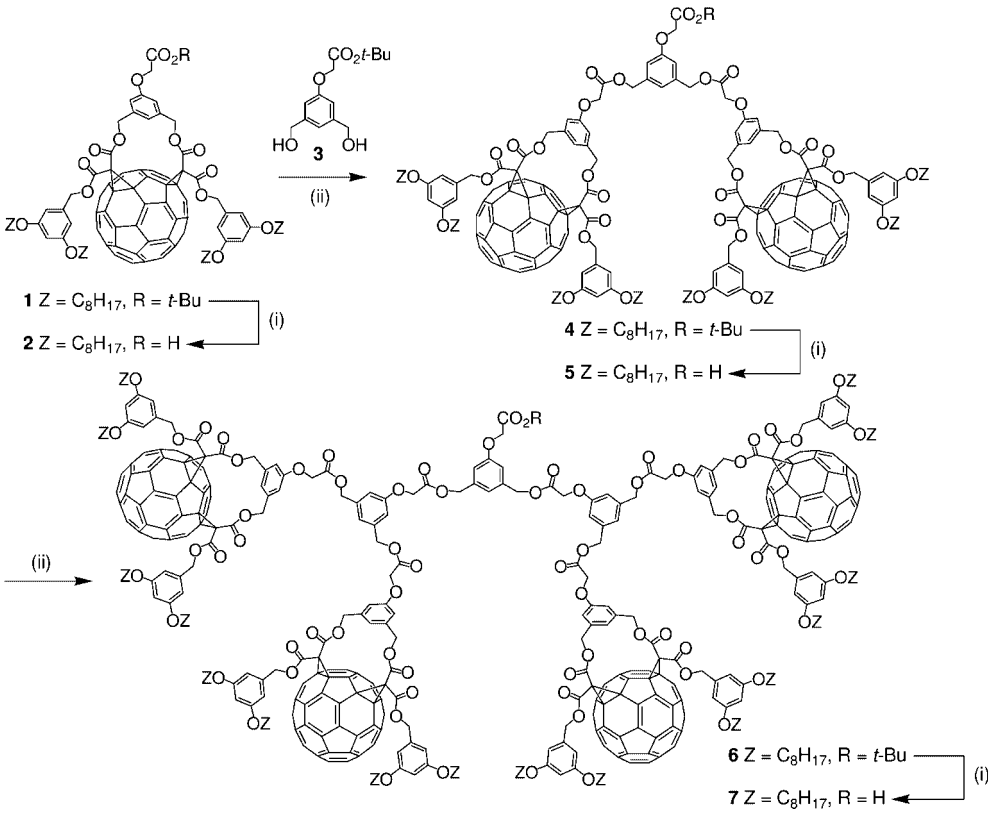

Scheme 10.1 Preparation of fullerodendrons **4**–**7**; reagents and conditions: (i) TFA, CH_2Cl_2, rt, 4 h (**2**: 99%; **5**: 99%; **7**: 97%); (ii) DCC, DMAP, HOBt, CH_2Cl_2, 0 °C to rt, 12 h (**4**: 90%; **6**: 95%).

Fullerodendrons **2, 5, 7** and **11** are amphiphilic compounds and their incorporation in Langmuir films has been investigated [17]. Indeed, the preparation of thin ordered films appears to be an important issue for applications in nanotechnology and materials science. Compounds **2, 5** and **7** form good quality Langmuir films at the air–water interface and the isotherms taken at 20 °C are depicted in Figure 10.1. Dendrons **2** and **7** can withstand pressures up to $\Pi \approx 20\,\mathrm{mN\,m^{-1}}$, the collapse of the films being indicated by the rounding of the curve, while the film prepared with **5** begins to collapse around $30\,\mathrm{mN\,m^{-1}}$. The molecular areas for **2, 5** and **7** extrapolated at zero pressure are 140 ± 7, 310 ± 15 and 560 ± 30 Å^2, respectively. They are in the expected 1 : 2 : 4 proportion given the structure of the dendrimers and are in good agreement with the values estimated by molecular modeling. Compound **11** can also form Langmuir films at the air–water interface and the general shape of the isotherm is similar to that obtained with **7**.

The authors also succeeded in forming Langmuir–Blodgett (LB) films by transferring monolayers of **2, 5, 7** and **11** onto solid substrates. However, due to the difference in size between the hydrophobic and hydrophilic groups, the Langmuir

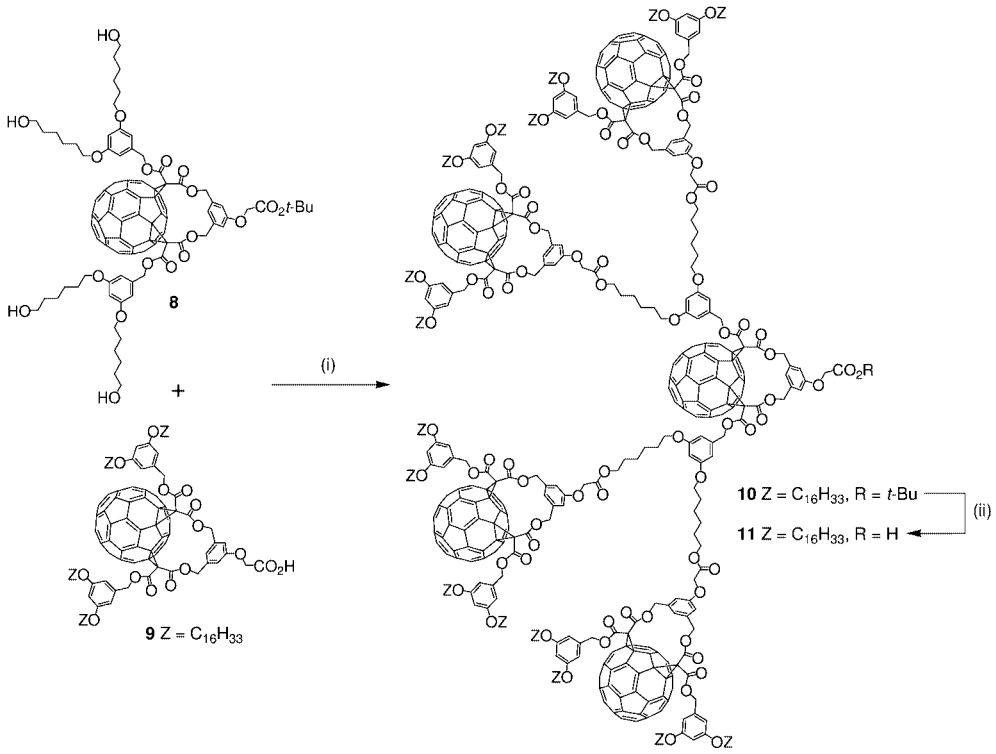

Scheme 10.2 Preparation of fullerodendron **12**; reagents and conditions: (i) DCC, DMAP, HOBt, CH_2Cl_2, 0 °C to rt; 96 h (65%); (ii) TFA, CH_2Cl_2, rt, 2 h (96%).

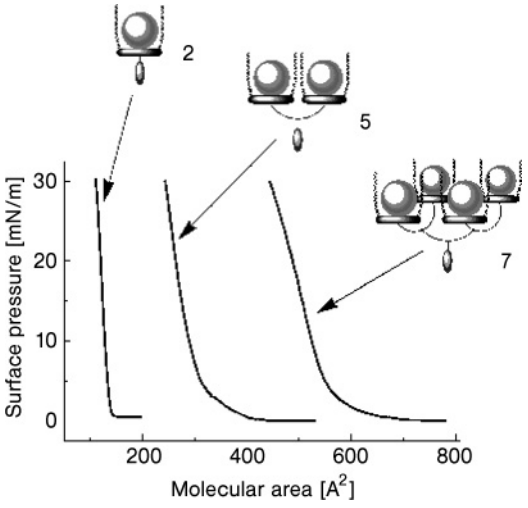

Figure 10.1 Pressure–area isotherms for **2, 5** and **7** at 20 °C.

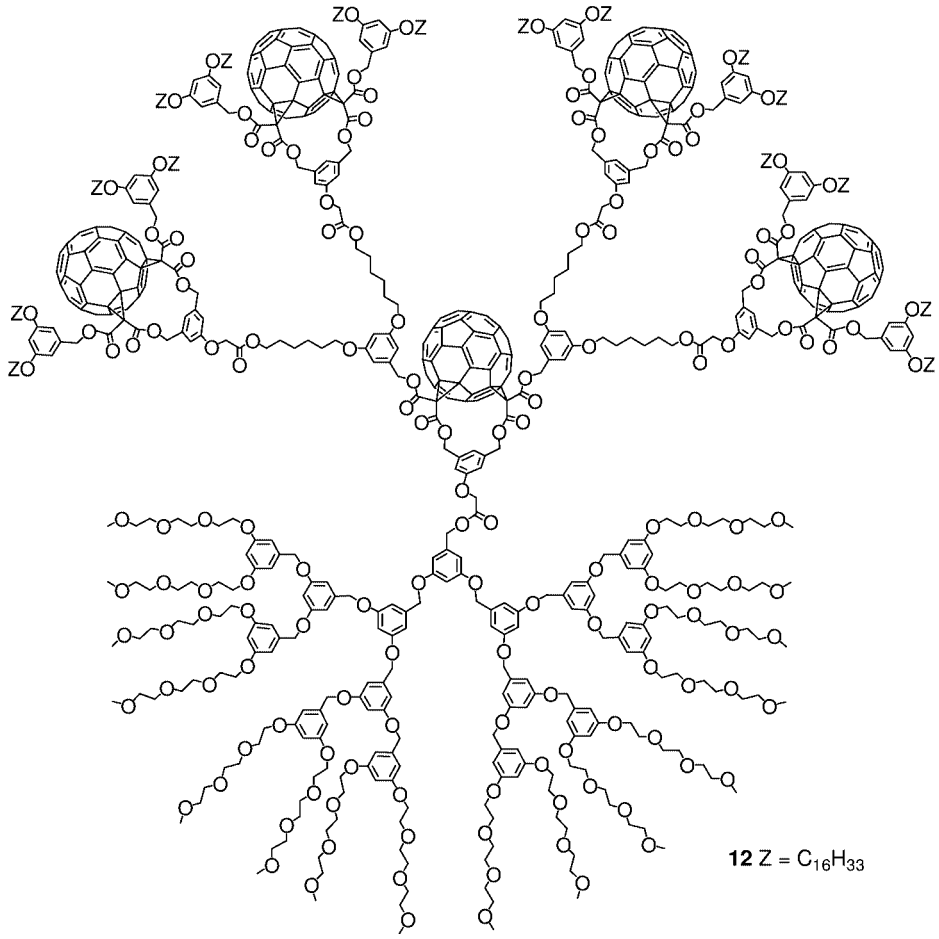

Figure 10.2 Amphiphilic fullerodendrimer **12**.

films of the largest derivatives are not sufficiently stable to stand the pressure over a long period of time. Therefore, the preparation of multilayered films was found to be difficult. To stabilize the films, it was decided to functionalize fullerodendron **11** with a large polar head group. A Fréchet-type dendron functionalized with peripheral ethylene glycol chains was attached to the focal point of compound **11**, leading to the diblock globular dendrimer **12** (Figure 10.2) [18].

Peripheral substitution with hydrophobic chains on one hemisphere and hydrophilic groups on the other provides the perfect hydrophobic/hydrophilic balance, allowing the formation of stable Langmuir films. In addition, a perfect reversibility has been observed in successive compression/decompression cycles (Figure 10.3).

Transfer experiments of the Langmuir films onto solid substrates and the preparation of LB films have been investigated for **12**. The deposition of films of **12**

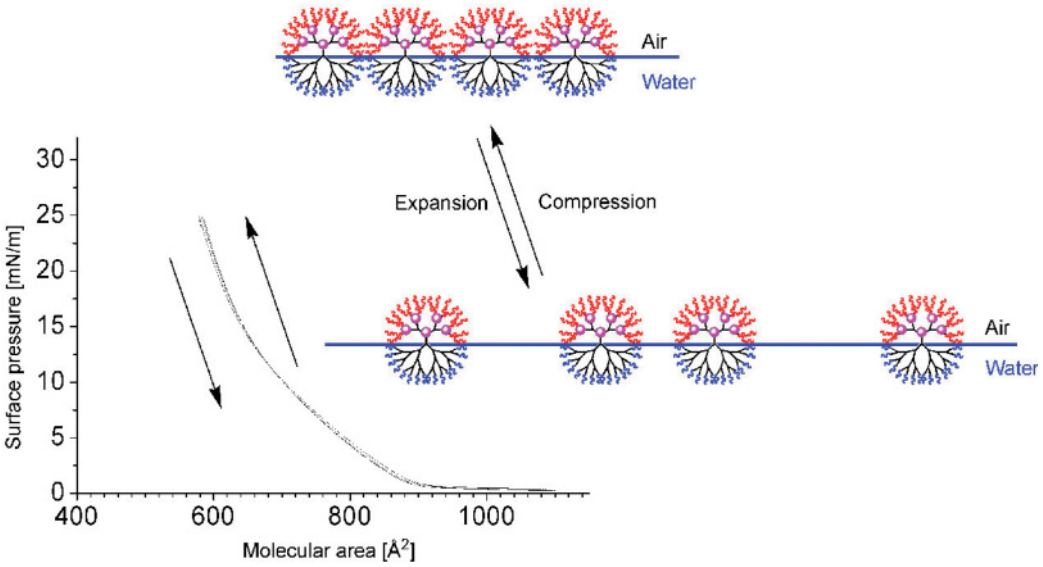

Figure 10.3 Four successive compression/expansion cycles with a monolayer of **12**, showing the perfect reversibility of the process.

occurred regularly on quartz slides or silicon wafers with a transfer ratio of 1 ± 0.05. The diblock structure of dendrimer **12** appeared also crucial for efficient transfers of the Langmuir films in order to obtain well-ordered multilayered LB films. Effectively, the transfer of the Langmuir films of **11** with a small polar head group was difficult, with a transfer ratio of about 0.5–0.7. The structural quality of mono- and multilayer films of **11** and **12** was investigated by grazing incidence X-ray diffraction. The quality of the LB films made with **11** was not very good and only allowed an estimation of their thickness, with the roughness being always in the 3 Å range. For LB films of **12**, the presence of low-angle Kiessig fringes in the grazing X-ray patterns indicates that the overall quality of the films is good. The best fit of the grazing X-ray pattern obtained for a monomolecular film gives a thickness of 36 ± 1 Å and a roughness of about 2 Å. For the multilayer films, the average layer thickness was found to be ca. 36 Å, indicating no or little interpenetration of successive layers. The excellent quality of the LB films prepared with **12** is also deduced from the plot of their UV/Vis absorbance as a function of the layer number: a straight line is obtained, indicating an efficient stacking of the layers. The peripheral substitution of a globular dendrimer with hydrophobic chains on one hemisphere and hydrophilic groups on the other provides the perfect hydrophobic/hydrophilic balance allowing the formation of stable Langmuir films. On the one hand, this approach shows some of the fundamental architectural requirements for obtaining stable films with amphiphilic dendrimers. On the other hand, functional groups not well adapted for the preparation of

Langmuir and LB films such as fullerenes can be attached into the branching shell of the dendritic structure and, thus, efficiently incorporated in thin ordered films.

10.2.2 Synthesis of Fullerene-Rich Dendrons and Photoelectrochemical Properties of Their Nanoclusters

The synthesis of high generation dendritic branches from building blocks **7** and **11** was found to be difficult due to steric hindrance problems. This prompted Nierengarten and coworkers to further explore the development of new fullerodendrons starting from a less hindered fullerene derivative (Schemes 10.3 and 10.4) [19]. The iterative reaction sequence used for the synthesis of the successive dendrimer generations is the same as that described for the preparation of dendrons **4**–**7**.

Cleavage of the *t*-butyl ester group in **13** by treatment with an excess of TFA followed by reaction of the resulting **14** with diol **3** under esterification conditions (DCC, DMAP, HOBt) gave the protected dendron of second generation **15** in 90% yield. Hydrolysis of the *t*-butyl ester moiety under acidic conditions then afforded the corresponding carboxylic acid **16** in quantitative yield. Esterification of **16** with diol **3** (DCC, HOBt, DMAP) gave **17** in 87% yield. Subsequent treatment with TFA afforded acid **18** in 99% yield. Reaction of **18** with diol **3** in the presence of DCC, HOBt and DMAP yielded fullerodendron **19** (95%), which after treatment with TFA gave **20** (97%). By repeating the same reaction sequence from **20**, the fifth generation derivatives **21** and **22** were also prepared (Scheme 10.4). It is important to highlight here that the time needed to consume all the reactants during the esterification step increased as the generation number increased. However, *N*-acyldicyclohexylurea by-products resulting from the rearrangement of the activated acid intermediates [19] were quite limited even for the highest generation compound, thus allowing the preparation of the fifth generation protected dendron **21** under DCC-mediated esterification conditions in a good yield (76%). This synthetic methodology is therefore efficient for the preparation of fullerene-rich derivatives **15**–**22** and does not suffer from the reduced accessibility of the reactive group located at the focal point of the dendritic structure as observed for the first series of dendrimers synthesized under similar esterification conditions.

Absorption spectra of **13**–**22** in toluene/acetonitrile (1/6 = v/v) mixed solvent exhibit structureless broad absorption in the range 300–800 nm. These results suggest that these compounds aggregate and form large clusters in the mixed solvents [20]. The particle size of these clusters in the mixed solvent has been measured by dynamic light scattering (DLS). In a mixture (1/6) of toluene/acetonitrile at an incubation period of 15 min after the injection of the toluene solution into acetonitrile, the size distribution of **13**, **15**, **17**, **19** and **21** was found to be relatively narrow, with different mean diameters of 790 nm for $(\mathbf{13})_m$, 210 nm for $(\mathbf{15})_m$, 170 nm for $(\mathbf{17})_m$, 100 nm for $(\mathbf{19})_m$ and 90 nm for $(\mathbf{21})_m$. The order of the mean diameters is not consistent with that of their molecular sizes. Dendrimers and dendrons are known to become a compact, rigid structure with increasing the

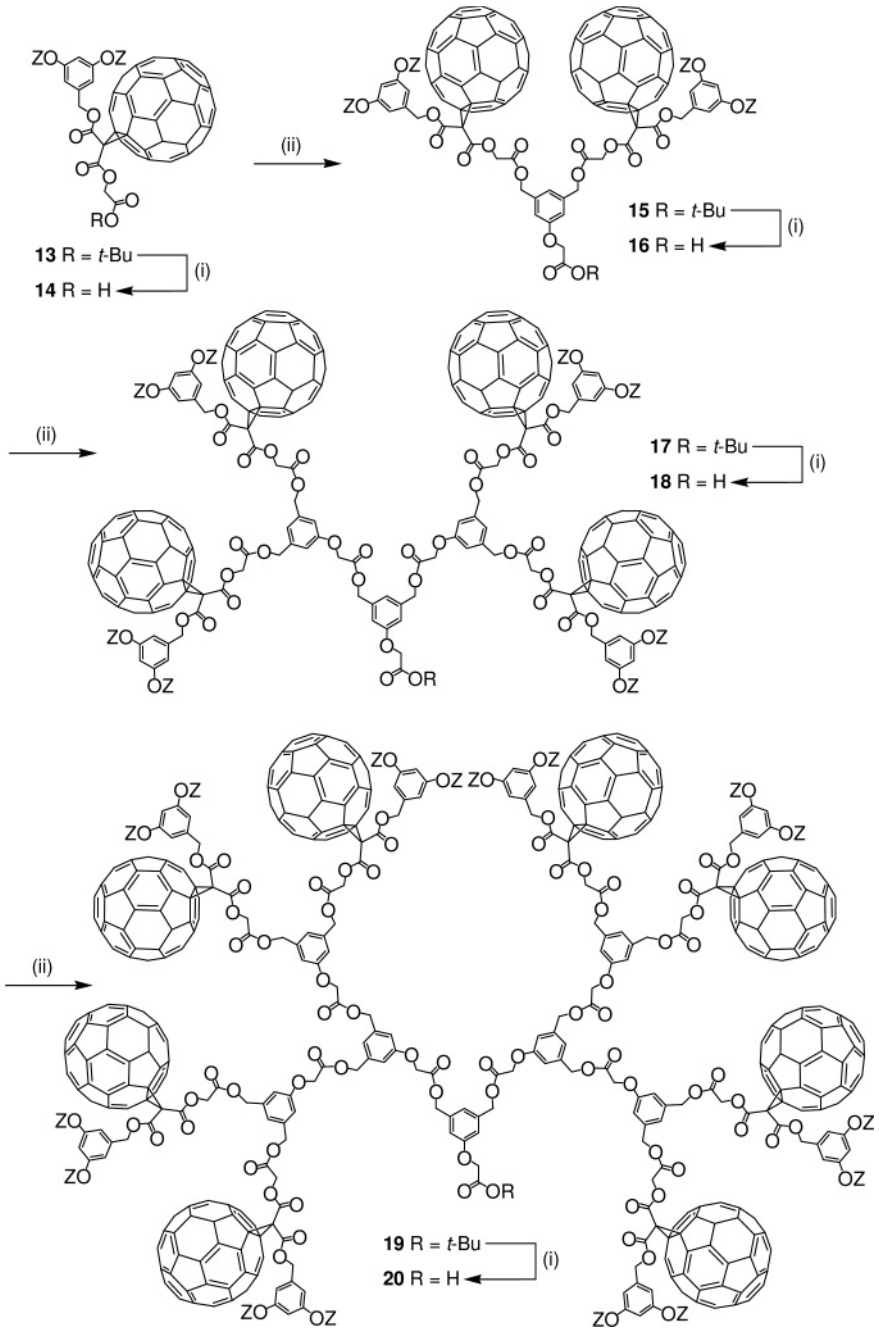

Scheme 10.3 Preparation of fullerodendrons **15**–**20** ($Z = C_8H_{17}$); reagents and conditions: (i) TFA, CH_2Cl_2, rt, 4 h (**14**: 99%; **16**: 99%; **18**: 99%; **20**: 97%); (ii) DCC, DMAP, HOBt, CH_2Cl_2, 0 °C to rt, 24 h (**15**: 90%; **17**: 87%; **19**: 95%).

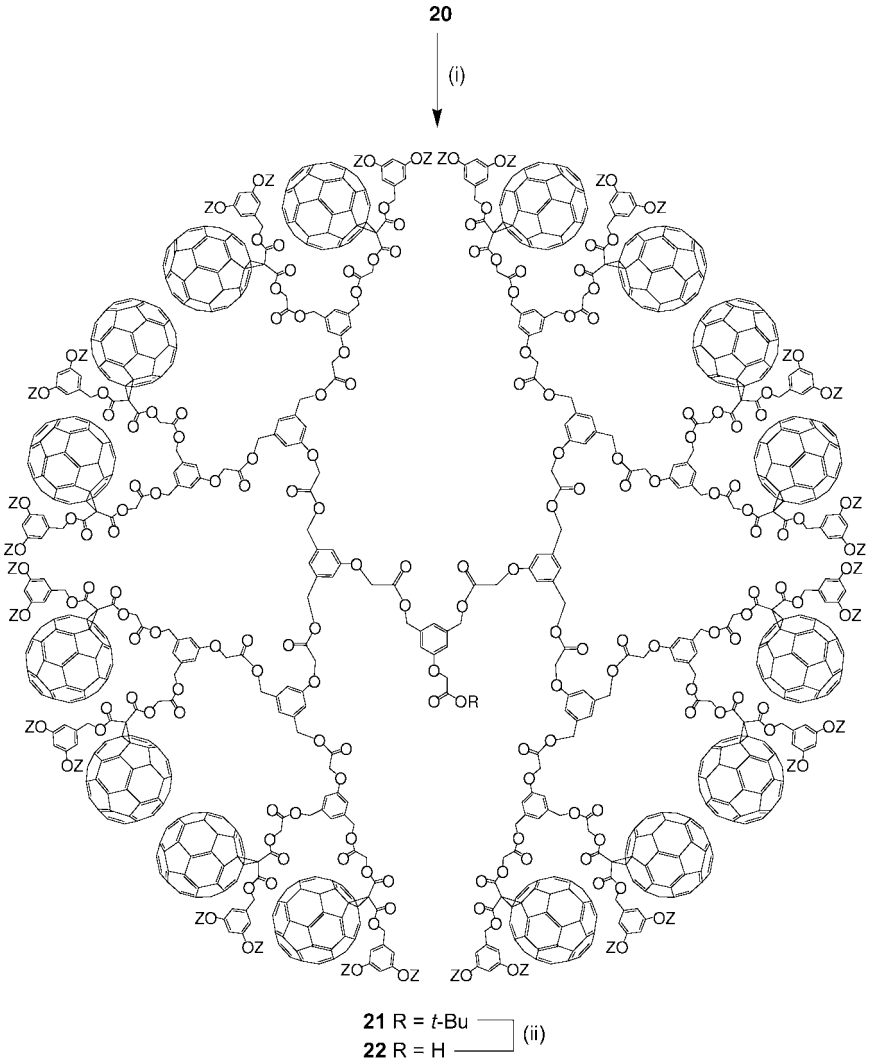

Scheme 10.4 Preparation of fullerodendrons **21** and **22** (Z = C_8H_{17}); reagents and conditions: (i) **3**, DCC, DMAP, HOBt, CH_2Cl_2, 0°C to rt, 96 h (76%); (ii) TFA, CH_2Cl_2, rt, 4 h (88%).

generation number. This suggests that, in the process of cluster formation with the higher dendrimer generation, each dendritic branch is subject to interactions with branches belonging to the same dendrimer molecule (*intramolecular*) rather than to other molecules (*intermolecular*), resulting in the formation of densely packed dendrimer clusters with a small, compact size (i.e., 90–100 nm). In other words, in the lower dendrimer generations *intermolecular* interactions among branches prevail, leading to the formation of poorly packed dendrimer clusters with a large size. To assess the shape and morphology of (**13**, **15**, **17**, **19** and **21**)$_m$

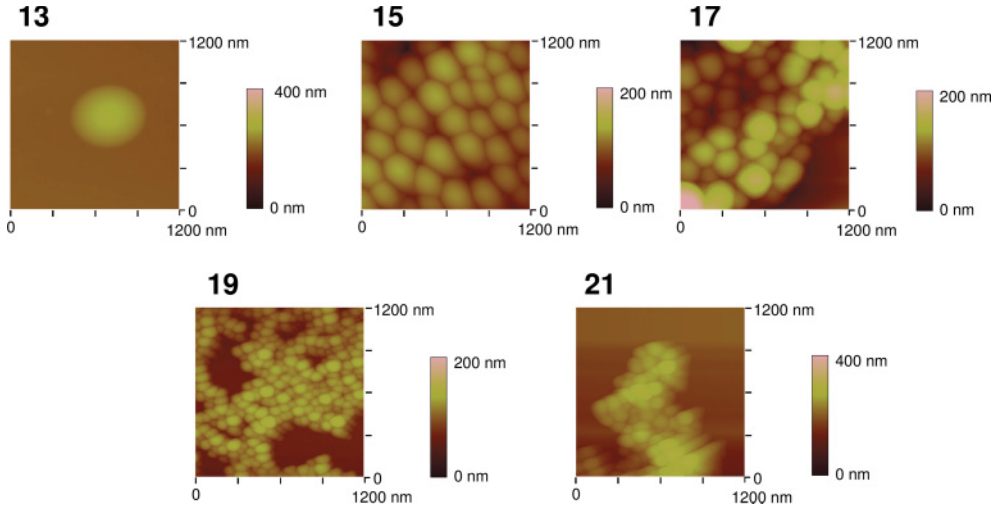

Figure 10.4 AFM images of (**13, 15, 17, 19** and **21**)$_m$ on mica.

clusters, atomic force microscopy (AFM) measurements have been carried out. Figure 10.4 shows the AFM images of clusters prepared by spin-coating of the (**13, 15, 17, 19** and **21**)$_m$ cluster solutions on mica surface. To remove solvent, the resulting substrates were heated under reduced pressure. The (**13, 15, 17, 19** and **21**)$_m$ clusters are spherical with an average horizontal diameter of 900 nm for (**13**)$_m$, 200 nm for (**15**)$_m$, 200 nm for (**17**)$_m$, 100 nm for (**19**)$_m$ and 100 nm for (**21**)$_m$. The size of the clusters agrees well with the values obtained from the DLS measurements. The vertical size of the clusters on mica correlates largely with the horizontal size of the clusters, except the case of (**13**)$_m$. The AFM image of the (**13**)$_m$ cluster reveals a rather disc-like structure with an average diameter of 900 nm and an average maximum thickness of 170 nm. Namely, the vertical size of the (**13**)$_m$ cluster is much smaller than the horizontal size. Although detailed structure at the molecular level is not yet clear, self-organization of **13** in the mixed solvent would lead to the formation of a multilayer vesicle. In such a case solvent evaporation from the inner space of the multilayer vesicle may yield the disk-like structure. Similar proposed structures have been reported for amphiphilic fullerene derivatives in water, mixed organic solvents and cast films [21].

To see if the differences observed in the size of the nanoclusters obtained from **13, 15, 17, 19** and **21** can have an influence on their macroscopic properties, photoelectrochemical cells have been prepared. The clusters have been deposited electrophoretically onto ITO/SnO_2 electrodes (ITO = indium tin oxide) by applying a DC voltage to the electrode [22]. After the electrophoretic deposition, the ITO/SnO_2 electrode turned brown, whereas discoloration of the cluster solution took place. As a result, cluster films 4–5 μm thick could be obtained. AFM was used to evaluate the surface morphology of the films deposited on the electrodes. The ITO/SnO_2/(**13, 15, 17, 19** and **21**)$_m$ films are composed of closely packed clusters with

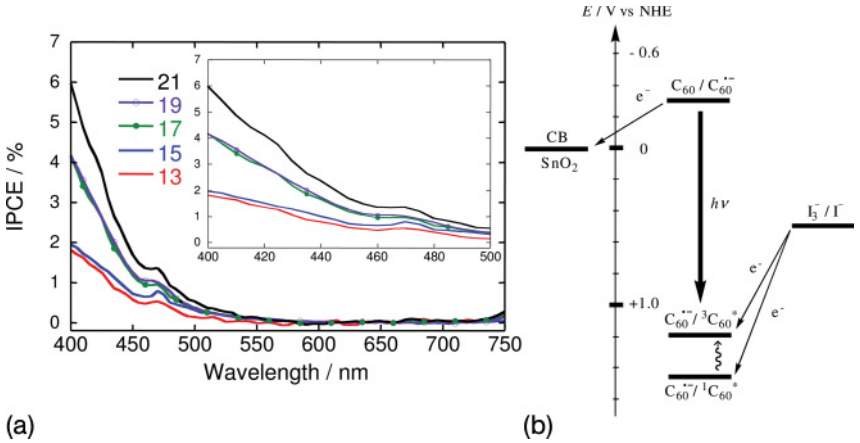

Figure 10.5 (a) Photocurrent action spectra of ITO/SnO_2/(G1-5CO_2*t*Bu)$_m$ (**13, 15, 17, 19** and **21**)$_m$; applied potential: +0.11 V vs SCE; 0.5 M LiI and 0.01 M I_2 in acetonitrile; (b) photocurrent generation diagram.

a size in nm of 800 (**13**), 200 (**15**), 200 (**17**), 100 (**19**) and 100 (**21**). The size of the clusters largely agrees with the diameters of the clusters on the mica obtained from the cluster solutions. These results also confirm that fullerene dendrimer clusters are successfully transferred onto the nanostructured SnO_2 electrodes. Photoelectrochemical measurements were performed in deaerated acetonitrile containing 0.5 M LiI and 0.01 M I_2 with ITO/SnO_2/(**13, 15, 17, 19** and **21**)$_m$ as a working electrode, a platinum wire as a counter electrode and an I^-/I^{3-} reference electrode. The photocurrent responses are prompt, steady and reproducible during repeated on/off cycles of visible light illumination. Blank experiments conducted with a bare ITO/SnO_2 electrode yield no detectable photocurrent under similar experimental conditions. A series of photocurrent action spectra were recorded to evaluate the response of fullerodendron clusters towards photocurrent generation. Figure 10.5 shows the photocurrent action spectra of ITO/SnO_2/(**13, 15, 17, 19** and **21**)$_m$ devices. Incident photon-to-photocurrent efficiency (IPCE) was calculated by normalizing the photocurrent density for incident light energy and intensity using the expression:

$$\mathrm{IPCE}(\%) = 100 \times 1240 \times i/(W_{\mathrm{in}} \times \lambda)$$

where i is the photocurrent density (A cm^{-2}), W_{in} is the incident light intensity (W cm^{-2}) and λ is the excitation wavelength (nm). The action spectra of ITO/SnO_2/(**13, 15, 17, 19** and **21**)$_m$ devices largely agree with the absorption spectra on ITO/SnO_2, supporting the involvement of the C_{60} moieties for photocurrent generation. These results are consistent with the photoelectrochemical properties of the clusters of fullerene derivatives on SnO_2 electrodes [22]. The IPCE values of ITO/SnO_2/

(**13**, **15**, **17**, **19** and **21**)$_m$ devices are compared under the same conditions. The IPCE at an excitation wavelength of 400 nm increases with increasing generation number: 1.7% for ITO/SnO_2/(**13**)$_m$, 1.9% for ITO/SnO_2/(**15**)$_m$, 4.1% for ITO/SnO_2/(**17**)$_m$, 4.1% for ITO/SnO_2/(**19**)$_m$ and 6.0% for ITO/SnO_2/(**21**)$_m$ devices.

Based on previous studies on a similar photoelectrochemical system of C_{60} and C_{60} derivatives [22], a photocurrent generation diagram is illustrated in Figure 10.5b. The primary step in the photocurrent generation is initiated by photoinduced electron transfer from I^- (I^{3-}/I^-, 0.5 V vs NHE) in the electrolyte solution to the excited states of fullerodendrimer clusters ($C_{60}^{\bullet-}/{}^1C_{60}^*$ = 1.45 V vs NHE, $C_{60}^{\bullet-}/{}^3C_{60}^*$ = 1.2 V vs NHE) [22]. The electron transfer rate is controlled by diffusion of I^- (~$109\,s^{-1}$) in the electrolyte solution. The resulting reduced C_{60} ($C_{60}^{\bullet-}/C_{60}$ = −0.3 V vs NHE) injects an electron directly into the SnO_2 nanocrystallites (ECB = 0 V vs NHE) or the electron is injected into the SnO_2 nanocrystallites through electron hopping process between the C_{60} molecules [22]. The electron transferred to the semiconductor is driven to the counter electrode via external circuit to regenerate the redox couple. Notably, the IPCE values depend on the dendritic generation. With increasing dendritic generation the IPCE increases. Structural investigation on the fullerodendrimers revealed that the higher dendrimer generation leads to the formation of densely packed clusters with a smaller, compact size (*vide supra*). Such structures of fullerene dendrimer clusters on ITO/SnO_2 in the higher generation would make it possible to accelerate the electron injection process from the reduced C_{60} to the conduction band of SnO_2 via the more efficient electron hopping through the C_{60} moieties where the average distance between the C_{60} moieties is smaller.

10.3 Fullerene-Rich Dendrimers

10.3.1 Divergent Synthesis

The results described in the previous section are a strong driving force to develop new efficient synthetic strategies for the preparation of large fullerene-rich dendritic molecules. In this respect, the divergent preparation of fullerodendrimers by grafting C_{60} units on the peripheral reactive groups of commercially available dendrimers is the easiest way to produce large dendritic structures. This synthetic approach has been applied to prepare compounds **23–25** (Figure 10.6) from fullerene derivative **1** and polypropyleneimine (PPI) dendrimers [23].

The choice of appropriate activating group for the carboxylic acid function of the C_{60} building block **1** was the key to this synthesis. Effectively, the reaction conditions for the activation step may not be strongly acid or basic, to preserve the ester functions. Furthermore, the grafting onto the dendritic polyamines requires an extremely efficient reaction to obtain the corresponding functionalized derivatives with good yields and to avoid the formation of defective dendrimers. The prepara-

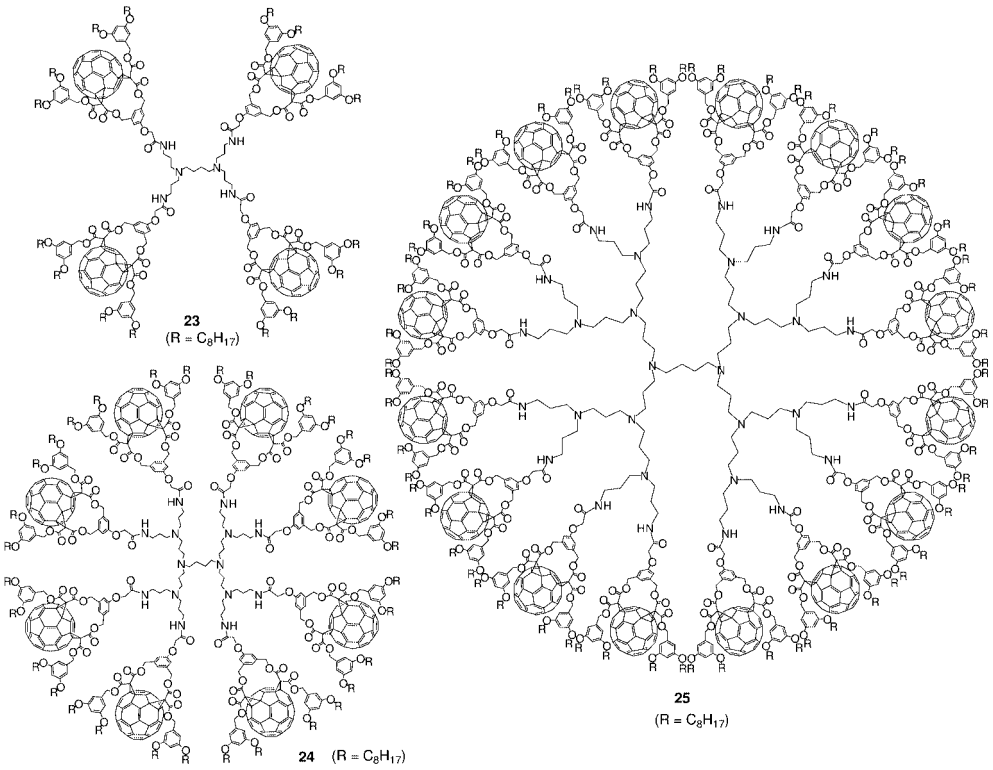

Figure 10.6 Fullerene-rich dendrimers **23**–**25**.

tion of the pentafluorothiophenolester derived from compound **1** and pentafluorothiophenol under DCC-mediated esterification conditions appeared as a good choice. Indeed, the reaction conditions for the preparation of this activated acid are mild and the efficient grafting of pentafluorothiophenolesters onto PPI dendrimers has already been reported [1]. The activated acid was obtained in nearly quantitative yields by reaction of carboxylic acid **1** with pentathiofluorothiophenol in the presence of DCC and a catalytic amount of 4-dimethylaminopyridine (DMAP). Subsequent reaction of the resulting pentafluorothiophenolester with the PPI dendrimers of 1st, 2nd and 3rd generation in the presence of triethylamine provided the corresponding dendritic derivatives **23**–**25** in good yields. Owing to the presence of four pendant alkyl chains per fullerene moiety, **23**–**25** are all well soluble in common organic solvents such as CH_2Cl_2, $CHCl_3$, THF or toluene, and spectroscopic characterization was easily achieved. The ^{1}H NMR spectra of dendrimers **23**–**25** show the typical pattern of the fullerene *cis*-2 bis-adduct with the expected additional signals arising from the PPI skeleton. The integration ratios are also consistent with the proposed molecular structures. The structure of **23** and **24** was further confirmed by MALDI-TOF mass spectrometry. The expected molecular ion peaks were clearly observed for both compounds. Notably, no peaks

corresponding to defective dendrimers were observed in the mass spectra of **23** and **24**, thus providing clear evidence for their monodispersity. For **25**, a high level of fragmentation prevented the observation of the expected molecular ion peak and its monodispersity could not be unambiguously demonstrated.

10.3.2 Convergent Synthesis

In the divergent strategy, dendrimers are constructed from the central core to the periphery [24]. In each repeat cycle, the *n* reactive groups on the dendrimer periphery react with *n* monomer units to add a new generation to the dendrimer. However, owing to the increasing number of reactive terminal units, defects in the structures appear rapidly. In the convergent strategy, which has been introduced by Hawker and Fréchet [25], dendritic branches are first built up, then attached to the central core in the final step. In this case, the number of coupling reactions needed to add each new generation, usually 2 or 3, is the same throughout the synthesis, making defective products easier to separate. Whereas exactly the same number of steps is required by using a divergent or a convergent approach for the preparation of a given dendrimer, the convergent one appears to be more efficient for the construction of monodisperse dendrimers. This approach has been used to produce several fullerene-rich dendrimers from the fullerodendrons described in Section 10.2 [26, 27]. For example, Nierengarten and coworkers have prepared alkyne **27–29** by reaction of diol **26** with fullerodendrons **2, 5** and **7**, respectively, under esterification conditions using DCC, HOBt and DMAP (Scheme 10.5). Cyclotrimerization of the resulting dendronized bis-arylalkynes was a perfect tool for the synthesis of fullerene-rich dendrimers **30** and **31** [27].

The reaction conditions for the cyclotrimerization were first optimized for the first generation compound. The choice of the appropriate catalyst was the key to this synthesis. Indeed, $Co_2(CO)_8$ appeared as a good candidate. It is a known catalyst for the cyclotrimerization of alkynes [28] and Martín and coworkers have shown that C_{60} is only reactive in the presence of $Co_2(CO)_8$ under Pauson–Khand conditions when a very specific stereochemical orientation is possible [29]. It was effectively found that $Co_2(CO)_8$ is an efficient catalyst for the preparation of **30** from alkyne **27**. Under optimized conditions, treatment of **27** with a catalytic amount of $Co_2(CO)_8$ in dioxane at room temperature for 24 h afforded **30** in 93% yield. The same conditions were used for the preparation of the highest generation compounds. The reaction of the second-generation derivative **28** was finished after one day and compound **31** was isolated in 62% yield. In contrast, the reaction of the highest generation precursor was very slow, most probably as a result of steric effects. After 5 days, the starting material was not completely consumed but the reaction was stopped since significant degradation was evidenced. After purification by column chromatography on SiO_2 followed by gel permeation chromatography, compound **32** (Figure 10.7) was isolated in 24% yield.

Having shown that the construction of dendrimers containing multiple C_{60} subunits is successful, the next challenge was to prepare fullerene-rich

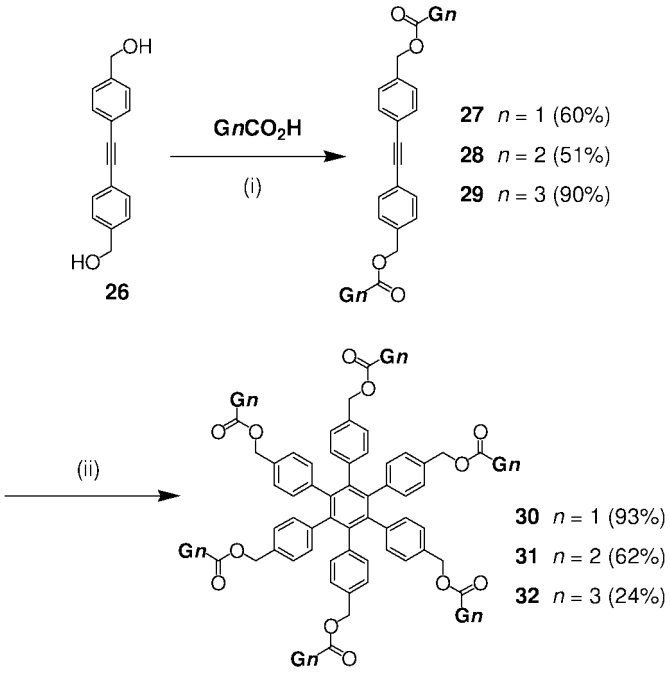

Scheme 10.5 Preparation of fullerene-rich dendrimers **30**–**32**; reagents and conditions: (i) DCC, DMAP, HOBt, CH_2Cl_2, 0 °C to rh, 24 to 120 h; (ii) $Co_2(CO)_8$, dioxane, rt, 24 to 120 h.

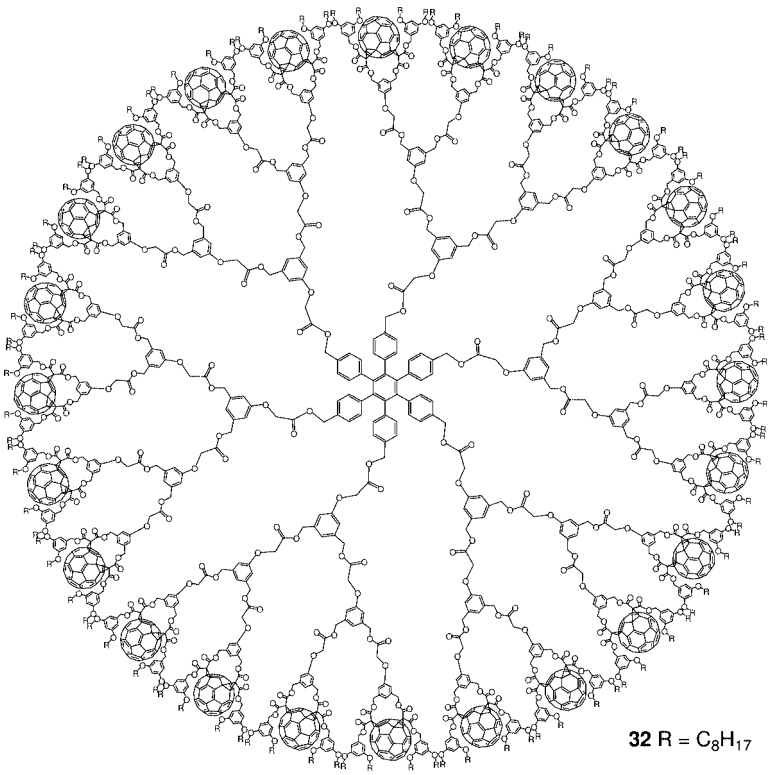

Figure 10.7 Fullerene-rich dendrimer **32**.

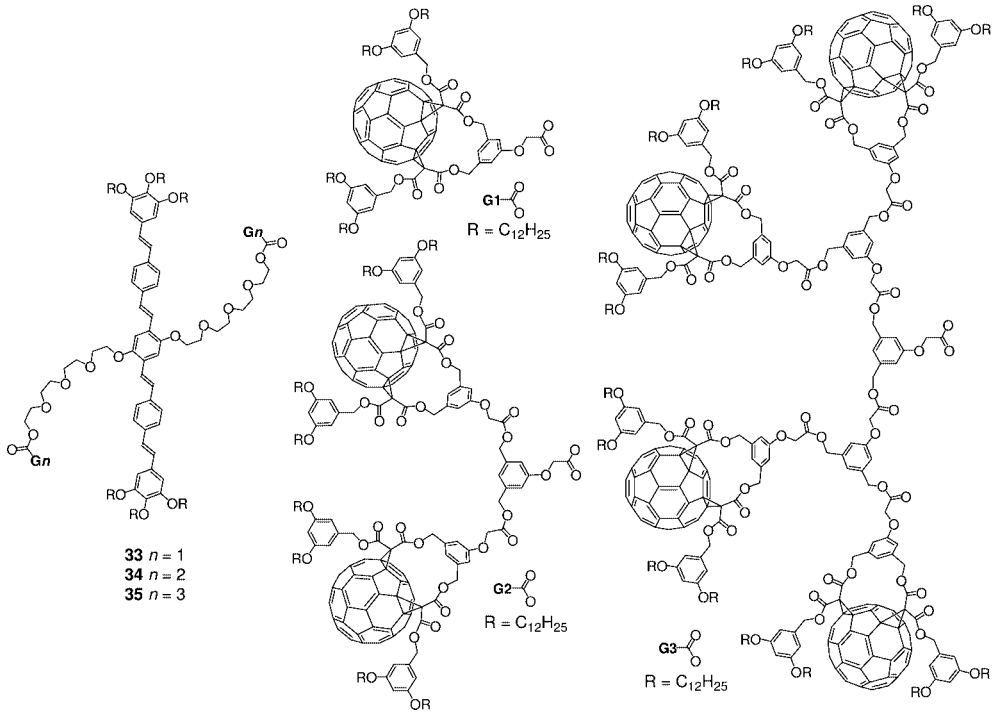

Figure 10.8 Fullerodendrimers **33**–**35**.

nanostructures with new properties. With this idea in mind, the dodecyloxy analogues of dendritic branches **2, 5** and **7** have been attached to an oligophenylenevinylene (OPV) core bearing two alcohol functions to yield dendrimers **33, 34** and **35** with two, four and eight peripheral C_{60} groups, respectively (Figure 10.8) [30].

The photophysical properties of **33**–**35** have been systematically investigated in solvents of increasing polarity, that is, toluene, dichloromethane and benzonitrile. Ultrafast OPV→C_{60} singlet energy transfer takes place upon photoexcitation of the OPV core for the whole series of dendrimers, whatever the solvent is. Electron transfer from the fullerene singlet is thermodynamically allowed in CH_2Cl_2 and benzonitrile, but not in apolar toluene. For a given solvent, the extent of electron transfer, signaled by the quenching of the fullerene fluorescence, is not the same along the series, despite the fact that identical electron transfer partners are present. By increasing the dendrimer size, electron transfer is progressively more difficult. Practically no electron transfer from the fullerene singlet occurs for **35** in CH_2Cl_2, whereas some of it is still detected in the more polar PhCN. These trends can be rationalized by considering increasingly compact dendrimer structures in more polar solvents [31]. This implies that the actual polarity experienced by the involved electron transfer partners, particularly the central OPV, is no longer that of the bulk solvent. This strongly affects electron transfer thermody-

namics which, being reasonably located in the normal region of the Marcus parabola, becomes less exergonic and thus slower and less competitive toward intrinsic deactivation of the fullerene singlet state. This dendritic effect is in line with molecular dynamics studies that suggest that the central OPV unit is more and more protected by the dendritic branches when the generation number is increased. Actually, the calculated structure of **35** shows that the two dendrons of third generation are able to fully cover the central OPV core.

10.4
Self-Assembly of Fullerene-Rich Dendrimers

The self-assembly of dendrons using noncovalent interactions is particularly well-suited for the preparation of fullerene-rich macromolecules [32]. Indeed, the synthesis itself is restricted to the preparation of dendrons and self-aggregation leads to the dendritic superstructure, thus avoiding tedious final synthetic steps with precursors incorporating potentially reactive functional groups such as C_{60}. For example, Nierengarten and coworkers have shown that C_{60} derivatives bearing a carboxylic acid function undergo self-assembly with *n*-butylstannonic acid, *n*BuSn(O)OH, to produce fullerene-rich nanostructures with a stannoxane core [33]. The reaction conditions were first adjusted with compound **14** (Scheme 10.6).

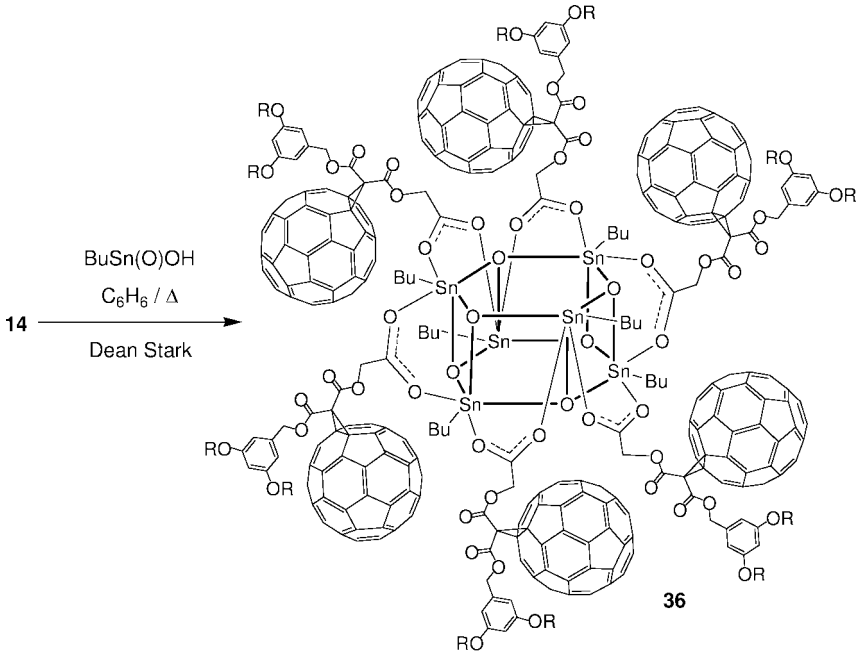

Scheme 10.6 Preparation of compound **36**.

Under optimized conditions, a mixture of **14** (1 equiv.) and *n*BuSn(O)OH (1 equiv.) in benzene was refluxed for 12 h using a Dean-Stark trap. After cooling, the solution was filtered and evaporated to dryness to afford the hexameric organostannoxane derivative **36** in 99% yield.

The reaction conditions used for the preparation of **36** from carboxylic acid **14** were then applied to fullerodendrons **16** and **18**. The corresponding organostannoxane derivatives **37** and **38** were thus obtained in almost quantitative yields (Figure 10.9). Interestingly, the self-assembly process is not affected by the increased size of the starting carboxylic acids when going from the first to the third generation derivative. Whatever the generation number is, the reaction was finished after 12 h and the hexameric assembly was obtained in a very high yield. The latter observations contrast with the previous examples described in Section 10.3 – effectively, the reactions were significantly slower and, in most cases, only moderate yields were obtained for the third generation derivatives when compared to the corresponding first and second generation ones.

These compounds are well soluble in common organic solvents such as CH_2Cl_2, $CHCl_3$, C_6H_6 or toluene and complete spectroscopic characterization was easily achieved. The ^1H and ^{13}C NMR spectra of **36–38** clearly reveal the characteristic signals of the starting carboxylic acid precursors as well as the expected additional resonances arising from the *n*-butyl chains. Importantly, the spectra clearly showed that all the peripheral fullerene subunits are equivalent in **36–38**, as expected for a six-fold symmetric assembly with a drum-shaped organostannoxane core. In addition, a single resonance is observed at approx. –480 ppm in the ^{119}Sn NMR spectra of **36–38** recorded in C_6D_6. This characteristic signature of tin-drum clusters provides definitive evidence for the formation of **36–38**.

C_{60} itself and simple fullerene derivatives have also been assembled on dendritic templates by using purely electrostatic interactions. For example, Astruc and coworkers have taken advantage of the electrochemical properties of C_{60} to assemble a fullerene-rich supramolecular dendritic structure [34]. When a toluene solution of C_{60} (64 equiv.) was added to an acetonitrile solution of the 64-Fe(I) dendrimer **39** (1 equiv.), a black precipitate of **40** was obtained (Scheme 10.7). Tentative extraction of this precipitate with toluene yielded a colorless solution, thus indicating that no C_{60} was present. The Mössbauer spectrum of this black solid (**40**) is a clean quadrupole doublet whose parameters at 77 K are consistent with the presence of an Fe(II) sandwich complex. Its EPR spectrum recorded at 298 K shows the characteristic feature observed for a model compound obtained from the reaction of C_{60} with the 19-electron complex [Fe(I)Cp(η^6-C_6Me_6)] [35]. It can thus be concluded that C_{60} has been reduced to its monoanion, as designed for a process that is exergonic by 0.9 eV. The peripheral cationic Fe(II) units with their C_{60}^- counteranion being very large are, most likely, located at the dendrimer periphery, presumably with rather tight ion pairs although the number of fullerene layers and overall molecular size are unknown.

Another system based on electrostatic interactions has been reported by van Koten and coworkers [36]. A core–shell dendrimer with a cationic tetra[bis(benzylammonium)aryl]silane core has been used as a template for the

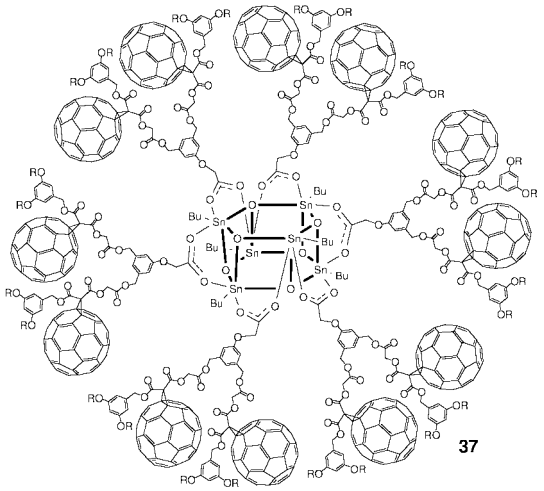

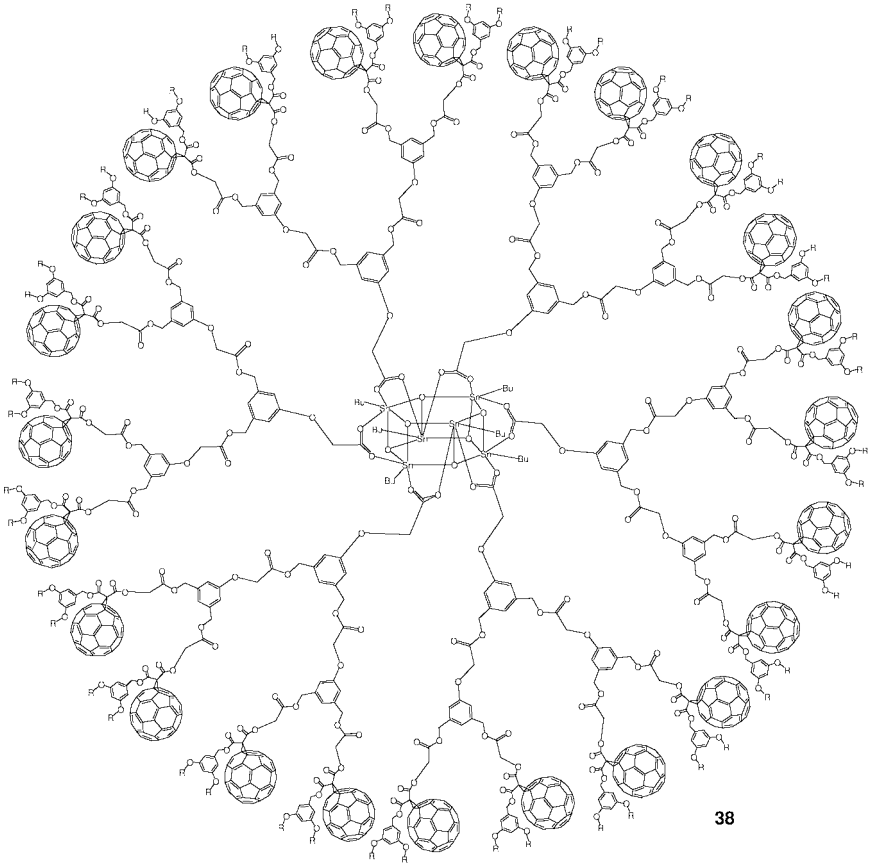

Figure 10.9 Fullerene-rich dendrimers **37** and **38**.

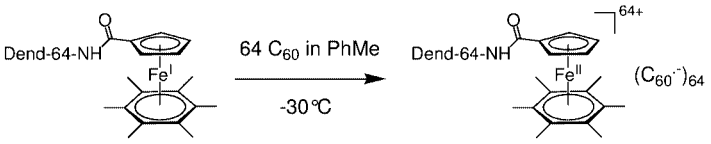

39 in MeCN **40** (black precipitate)

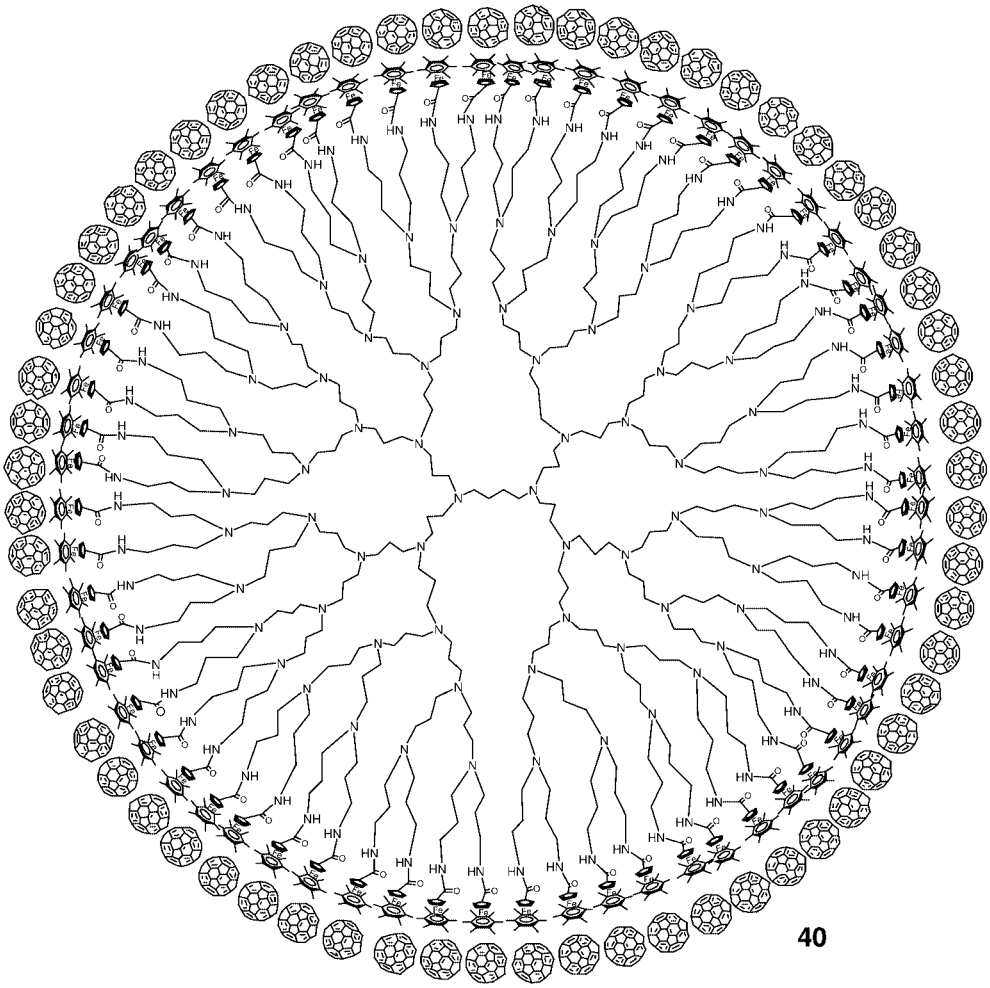

Scheme 10.7 Dendrimer **40** resulting from the reaction of **39** (1 equiv.) with C_{60} (64 equiv.) in MeCN/PhMe at –30 °C.

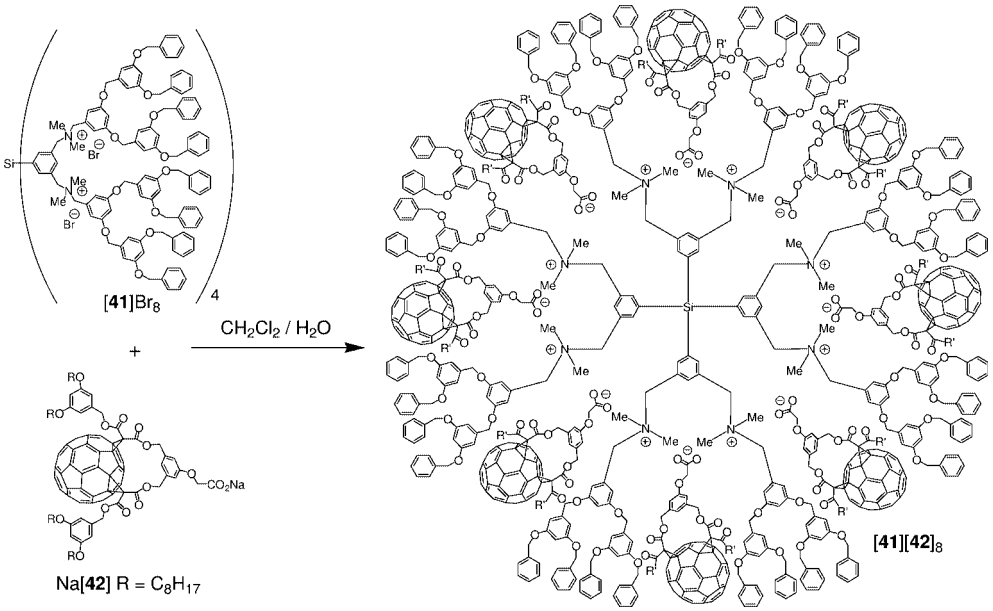

Scheme 10.8 Anion exchange reaction of [**41**]Br_8 with Na[**42**] leading to the fullerene-rich dendrimer [**41**][**42**]$_8$.

assembly of fullerene-carboxylate derivatives via a straightforward anion exchange reaction of [**41**]Br_8 with Na[**42**] (Scheme 10.8). In contrast to dendrimer **40**, the supramolecular fullerene-rich assembly [**41**][**42**]$_8$ thus prepared is soluble in common organic solvents and its spectroscopic characterization could be easily achieved. In the ^{1}H NMR spectrum of a solution of [**41**][**42**]$_8$ in $CDCl_3$, the diagnostic signals of both [**41**]$^{8+}$ and [**42**]$^-$ can clearly be observed. Furthermore, specific peak integrals show that the octa-cationic dendritic moiety [**41**]$^{8+}$ and the anions [**42**]$^-$ are present in a 1 : 8 molar ratio.

The UV-absorption spectrum of a solution of [**41**][**42**]$_8$ in CH_2Cl_2 shows characteristic absorption features that can be ascribed to the fullerene units as well as a band diagnostic for the cationic dendrimer. Actually, the UV-absorption spectrum of [**41**][**42**]$_8$ matches the spectral profile of a 1 : 8 molar mixture of authentic [**41**]Br_8 and the *t*-butyl ester (**1**) of the [**8**]$^-$ anion, which is unable to self-assemble. The similarity of these spectra indicates that there are no significant ground state interactions between the respective chromophores in the supramolecular complex [**41**][**42**]$_8$. The luminescence properties of solutions of [**41**][**42**]$_8$ in CH_2Cl_2 were also investigated and compared to the behavior of an iso-absorbing model mixture of authentic [**41**]Br_8 and **1**. Upon excitation of the latter model mixture, in the UV-region where the main part of the light is absorbed by the dendritic wedges of the octa-cationic moiety [**41**]$^{8+}$, the characteristic emission of the polybenzyl aryl ether dendritic wedges is observed. In contrast, complete quenching of this emission of

$[\mathbf{41}]^{8+}$ is observed in $[\mathbf{41}][\mathbf{42}]_8$, which suggests that upon excitation intramolecular energy transfer occurs from the lowest singlet excited state of the Fréchet-type dendritic branch to the low lying fullerene singlet excited state. The latter observation provides further evidence for the association of $[\mathbf{41}]^{8+}$ and $[\mathbf{42}]^{-}$. To establish the molecular weight of the host–guest assembly, gel-permeation chromatography coupled to a low-angle laser light scattering (GPC/LALLS) instrument was performed using THF as eluent. The chromatogram displayed three peaks. The first corresponds to a mass of 21 780 g mol^{-1} (M_w/M_n = 1.27), which was identified as the 1:8 host–guest octa-fullero-dendrimer assembly $[\mathbf{41}][\mathbf{42}]_8$ (calculated M_w = 20 960.05 g mol^{-1}). The molecular weights associated to the two additional peaks are higher: 38 670 (M_w/M_n = 1.04) and 94 070 g mol^{-1} (M_w/M_n = 1.02), respectively. These fractions are attributed to superstructures consisting of aggregated assemblies derived from $[\mathbf{41}][\mathbf{42}]_8$. Such behavior is commonly observed during the GPC analysis of poly-ionic macromolecules when an organic solvent is used as eluent. Importantly, no peaks corresponding to compounds with a molecular weight lower than $[\mathbf{41}][\mathbf{42}]_8$ were detected, which further substantiates the formation of a stoichiometric assembly between octa-cationic $[\mathbf{41}]^{8+}$ and eight $[\mathbf{42}]^{-}$ anions.

10.5 Conclusions

Efficient methodologies allowing the preparation of dendrons substituted with several fullerene moieties have been developed. These fullerodendrons are interesting building blocks for the preparation of large fullerene-rich dendritic molecules. Substantial research efforts have also been carried out to organize such compounds onto surfaces or to study their electronic properties. For example, it has been shown that dendrimers bearing multiple C_{60} units are good candidates for solar energy conversion. Importantly, significant changes in the photoelectrochemical properties have been evidenced by increasing the generation number. In particular, the incident photon-to-photocurrent efficiency (IPCE) of the devices is significantly increased by increasing the generation number and thus the number of C_{60} subunits of the dendritic molecules used in the photoactive layer. The latter observation is a strong driving force to develop new fullerene-rich dendritic molecules. Recent results on the self-assembly of fullerene-containing components by using supramolecular interactions rather than covalent bonds clearly demonstrate that this strategy is an attractive alternative for their preparation. Indeed, fullerene-rich derivatives are thus easier to produce and the range of systems that can be prepared is not severely limited by the synthetic route. In this way, in-depth investigations of their properties is possible and one can really start to envisage the use of fullerene-rich materials for specific applications. Clearly, despite some remarkable recent achievements, the examples discussed herein represent only the first steps towards the design of fullerene-rich molecular assemblies that can display functionality at the macroscopic level. More research in this

area is clearly needed to fully explore the possibilities offered by these materials, for example, in nanotechnology or in photovoltaics.

Acknowledgments

This research was supported by the CNRS. I warmly thank all my coworkers and collaborators for their outstanding contributions; their names are cited in the references.

References

1 (a) Newkome, G.R., Moorefield, C.N. and Vögtle, F. (2001) *Dendrimers and Dendrons: Concepts, Syntheses, Applications*, VCH, Weinheim.
(b) Fréchet, J.M.J. and Tomalia, D.A. (eds) (2001) *Dendrimers and Other Dendritic Polymers*, John Wiley & Sons, Ltd, Chichester.
2 Nierengarten, J.-F. (2000) *Chem. Eur. J.*, **6**, 3667.
3 Hirsch, A. and Vostrowsky, O. (2001) *Top. Curr. Chem.*, **217**, 51.
4 Nierengarten, J.-F. (2003) *Top. Curr. Chem.*, **228**, 87.
5 (a) Nierengarten, J.-F. (2004) *New J. Chem.*, **28**, 1177.
(b) Imahori, H. and Fukuzumi, S. (2004) *Adv. Funct. Mater.*, **14**, 525.
(c) Martin, N. (2006) *Chem. Commun.*, 2093.
6 (a) Wooley, K.L., Hawker, C.J., Fréchet, J.M.J., Wudl, F., Srdanov, G., Shi, S., Li, C. and Kao, M. (1993) *J. Am. Chem. Soc.*, **115**, 9836.
(b) Hawker, C.J., Wooley, K.L. and Fréchet, J.M.J. (1994) *J. Chem. Soc. Chem. Commun.*, 925.
(c) Nierengarten, J.-F., Habicher, T., Kessinger, R., Cardullo, F., Diederich, F., Gramlich, V., Gisselbrecht, J.-P., Boudon, C. and Gross, M. (1997) *Helv. Chim. Acta*, **80**, 2238.
(d) Brettreich, M. and Hirsch, A. (1998) *Tetrahedron Lett.*, **39**, 2731.
(e) Rio, Y., Nicoud, J.-F., Rehspringer, J.-L. and Nierengarten, J.-F. (2000) *Tetrahedron Lett.*, **41**, 10207.
7 (a) Camps, X. and Hirsch, A. (1997) *J. Chem. Soc. Perkin Trans. 1*, 1595.
(b) Camps, X., Schönberger, H. and Hirsch, A. (1997) *Chem. Eur. J.*, **3**, 561.
(c) Herzog, A., Hirsch, A. and Vostrowsky, O. (2000) *Eur. J. Org. Chem.*, 171.
8 Nierengarten, J.-F. (2003) *Comptes Rendus Chim.*, **6**, 725.
9 Rio, Y., Accorsi, G., Nierengarten, H., Rehspringer, J.-L., Hönerlage, B., Kopitkovas, G., Chugreev, A., Van Dorsselaer, A., Armaroli, N. and Nierengarten, J.-F. (2002) *New J. Chem.*, **26**, 1146.
10 (a) Cardullo, F., Diederich, F., Echegoyen, L., Habicher, T., Jayaraman, N., Leblanc, R.M., Stoddart, J.F. and Wang, S. (1998) *Langmuir*, **14**, 1955.
(b) Zhang, S., Rio, Y., Cardinali, F., Bourgogne, C., Gallani, J.-L. and Nierengarten, J.-F. (2003) *J. Org. Chem.*, **68**, 9787.
11 Chuard, T. and Deschenaux, R. (2002) *J. Mater. Chem.*, **12**, 1944 and references therein.
12 Nierengarten, J.-F., Armaroli, N., Accorsi, G., Rio, Y. and Eckert, J.-F. (2003) *Chem. Eur. J.*, **9**, 36.
13 (a) Kunieda, R., Fujitsuka, M., Ito, O., Ito, M., Murata, Y. and Komatsu, K. (2002) *J. Phys. Chem. B*, **106**, 7193.
(b) Murata, Y., Ito, M. and Komatsu, K. (2002) *J. Mater. Chem.*, **12**, 2009.
(c) Rio, Y., Accorsi, G., Nierengarten, H., Bourgogne, C., Strub, J.-M., Van Dorsselaer, A., Armaroli, N. and Nierengarten, J.-F. (2003) *Tetrahedron*, **59**, 3833.
14 (a) Armaroli, N., Barigelletti, F., Ceroni, P., Eckert, J.-F., Nicoud, J.-F. and

Nierengarten, J.-F. (2000) *Chem. Commun.*, 599.
(b) Segura, J.L., Gomez, R., Martin, N., Luo, C.P., Swartz, A. and Guldi, D.M. (2001) *Chem. Commun.*, 707.
(c) Accorsi, G., Armaroli, N., Eckert, J.-F. and Nierengarten, J.-F. (2002) *Tetrahedron Lett.*, **43**, 65.
(d) Langa, F., Gómez-Escalonilla, M.J., Díez-Barra, E., García-Martínez, J.C., Rodríguez-López, A., de la Hoz, J., González-Cortés, A. and López-Arza, V. (2001) *Tetrahedron Lett.*, **42**, 3435.
(e) Guldi, D.M., Swartz, A., Luo, C., Gomez, R., Segura, J.L. and Martin, N. (2002) *J. Am. Chem. Soc.*, **124**, 10875.
(f) Pérez, L., Garcia-Martinez, J.C., Diez-Barra, E., Atienzar, P., Garcia, H., Rodriguez-Lopez, J. and Langa, F. (2006) *Chem. Eur. J.*, **12**, 5149.
(g) Armaroli, N., Accorsi, G., Clifford, J.N., Eckert, J.-F. and Nierengarten, J.-F. (2006) *Chem. Asian J.*, **1**, 564.

15 Nierengarten, J.-F., Felder, D. and Nicoud, J.-F. (1999) *Tetrahedron Lett.*, **40**, 269.

16 (a) Nierengarten, J.-F., Felder, D. and Nicoud, J.-F. (2000) *Tetrahedron Lett.*, **41**, 41.
(b) Felder, D., Nierengarten, H., Gisselbrecht, J.-P., Boudon, C., Leize, E., Nicoud, J.-F., Gross, M., Van Dorsselaer, A. and Nierengarten, J.-F. (2000) *New J. Chem.*, **24**, 687.

17 Felder, D., Gallani, J.-L., Guillon, D., Heinrich, B., Nicoud, J.-F. and Nierengarten, J.-F. (2000) *Angew. Chem. Int. Ed.*, **39**, 201.

18 Nierengarten, J.-F., Eckert, J.-F., Rio, Y., Carreon, M.P., Gallani, J.-L. and Guillon, D. (2001) *J. Am. Chem. Soc.*, **123**, 9743.

19 (a) Hahn, U., Hosomizu, K., Imahori, H. and Nierengarten, J.-F. (2006) *Eur. J. Org. Chem.*, 85.
(b) Herschbach, H., Hosomizu, K., Hahn, U., Leize, E., Van Dorsselaer, A., Imahori, H. and Nierengarten, J.-F. (2006) *Anal. Bioanal. Chem.*, **386**, 46.

20 Hosomizu, K., Imahori, H., Hahn, U., Nierengarten, J.-F., Listorti, A., Armaroli, N., Nemoto, T. and Isoda, S. (2007) *J. Phys. Chem. C*, **111**, 2777.

21 Zhou, S., Burger, C., Chu, B., Sawamura, M., Nagahama, N., Toganoh, M., Hackler, U.E., Isobe, H. and Nakamura, E. (2001) *Science*, **291**, 1944.

22 (a) Kamat, P.V., Barazzouk, S., Thomas, K.G. and Hötchandani, S. (2000) *J. Phys. Chem. B*, **104**, 4014.
(b) Hotta, H., Kang, S., Umeyama, T., Matano, Y., Yoshida, K., Isoda, S. and Imahori, H. (2005) *J. Phys. Chem. B*, **109**, 5700.

23 Hahn, U., Nierengarten, J.-F., Vögtle, F., Listorti, A., Monti, F. and Armaroli, N. (2009) *New J. Chem.*, **33**, 337.

24 (a) Buhleier, E., Wehner, W. and Vögtle, F. (1978) *Synthesis*, 155.
(b) Newkome, G.R., Yao, Z.-Q., Baker, G.R. and Gupta, V.K. (1985) *J. Org. Chem.*, **50**, 2003.

25 Hawker, C. and Fréchet, J.M.J. (1990) *J. Chem. Soc. Chem. Commun.*, 1010.

26 (a) Nierengarten, J.-F., Felder, D. and Nicoud, J.-F. (1999) *Tetrahedron Lett.*, **40**, 273.
(b) Armaroli, N., Boudon, C., Felder, D., Gisselbrecht, J.-P., Gross, M., Marconi, G., Nicoud, J.-F., Nierengarten, J.-F. and Vicinelli, V. (1999) *Angew. Chem. Int. Ed.*, **38**, 3730.
(c) Hahn, U., González, J.J., Huerta, E., Segura, M., Eckert, J.-F., Cardinali, F., de Mendoza, J. and Nierengarten, J.-F. (2005) *Chem. Eur. J.*, **11**, 6666.
(d) Elhabiri, M., Trabolsi, A., Cardinali, F., Hahn, U., Albrecht-Gary, A.-M. and Nierengarten, J.-F. (2005) *Chem. Eur. J.*, **11**, 4793.
(e) Nierengarten, J.-F., Hahn, U., Trabolsi, A., Herschbach, H., Cardinali, F., Elhabiri, M., Leize, E., Van Dorsselaer, A. and Albrecht-Gary, A.-M. (2006) *Chem. Eur. J.*, **12**, 3365.

27 Hahn, U., Maisonhaute, E., Amatore, C. and Nierengarten, J.-F. (2007) *Angew. Chem. Int. Ed.*, **46**, 951.

28 (a) Schore, N.E. (1988) *Chem. Rev.*, **88**, 1081.
(b) Lautens, M., Klute, W. and Tam, W. (1996) *Chem. Rev.*, **96**, 49.
(c) Kotha, S., Brahmachary, E. and Lahiri, K. (2005) *Eur. J. Org. Chem.*, 4741.

29 Martín, N., Altable, M., Filippone, S., Martín-Domenech, Á., Poater, A. and Solà, M. (2005) *Chem. Eur. J.*, **11**, 2716.

30 Gutiérrez-Nava, M., Accorsi, G., Masson, P., Armaroli, N. and Nierengarten, J.-F. (2004) *Chem. Eur. J.*, **10**, 5076.

31 Figueira-Duarte, T.M., Gégout, A. and Nierengarten, J.-F. (2007) *Chem. Commun.*, 109.
32 Hahn, U., Cardinali, F. and Nierengarten, J.-F. (2007) *New J. Chem.*, **31**, 1128.
33 (a) Hahn, U., Gégout, A., Duhayon, C., Coppel, Y., Saquet, A. and Nierengarten, J.-F. (2007) *Chem. Commun.*, 516.
(b) Delavaux-Nicot, B., Kaeser, A., Hahn, U., Gégout, A., Brandli, P.-E., Duhayon, C., Coppel, Y., Saquet, A. and Nierengarten, J.-F. (2008) *J. Mater. Chem.*, **18**, 1547.
34 Ruiz, J., Pradet, C., Varret, F. and Astruc, D. (2002) *Chem. Commun.*, 1108.
35 Bossard, C., Rigaut, S., Astruc, D., Delville, M.-H., Félix, G., Février-Bouvier, A., Amiell, J., Flandrois, S. and Delhaès, P. (1993) *J. Chem. Soc. Chem. Commun.*, 333.
36 van de Coevering, R., Kreiter, R., Cardinali, F., van Koten, G., Nierengarten, J.-F. and Gebbink Klein, R.J.M. (2005) *Tetrahedron Lett.*, **46**, 3353.

11
Liquid-Crystalline Fullerodendrimers and Fullero(codendrimers)

Daniel Guillon, Bertrand Donnio, and Robert Deschenaux

11.1
Introduction

The expected nanotechnology revolution shall probably not occur without the prior emergence of reliable self-assembling techniques. Clearly, despite their incredible progress, top-down technologies and lithographic techniques are now reaching their limits. With the promise of lower cost and high impact, self-assembling techniques stand unrivaled, the mere existence of self-assembled living creatures being an obvious proof of their ultimate efficiency. Moreover, as space is no longer a problem in nanoscale devices, such systems can be less sensitive to damages or fabrication errors than the present ones. On the other hand, liquid crystals are the typical example of self-organizing nano-objects. The rules governing the formation and stability of the various mesophases are now well understood, and their fluid nature makes these materials intrinsically defect tolerant.

The bottom-up approach is the appropriate one to build up nanostructures from the assembly of individual atoms, molecules or macromolecules [1]. With this in view, dendrimers have been considered, during the last decade, as promising materials for the elaboration and assembly of nanostructures, such as, Langmuir and Langmuir–Blodgett films [2], micelles [3] and membranes [4]. As such, dendrimers represent an interesting alternative towards the development of materials in which information at the molecular level is transferred from an initiator core to the periphery (or vice versa) at the nanometer scale, with the expectation of complementary and synergic phenomena, that is, induction of new properties, and/or cooperative effects, that is, amplification of the existing properties.

It was thus logical and of interest to functionalize dendrimers with mesogenic elements to obtain new classes of liquid-crystalline materials [5, 6]. Among them, liquid-crystalline fullerodendrimers are an interesting family of functional materials. Indeed, the incorporation of [60]fullerene (C_{60}) into liquid-crystalline structures may open the way to novel molecular devices and molecular switches showing outstanding performances by combining the electrochemical and photophysical properties of C_{60} [7] with the self-assembling features of liquid crystals [8]. The use

Fullerene Polymers. Synthesis, Properties and Applications. Edited by Nazario Martín and Francesco Giacalone

ISBN: 978-3-527-32282-4

of liquid-crystalline dendrimers as mesomorphic promoters to functionalize C_{60} has two advantages: firstly, C_{60}–C_{60} interactions, which are responsible for the formation of aggregates, are reduced or even suppressed [9], and, secondly, the supramolecular organization within the liquid crystal state can be controlled owing to the many possibilities that can be used to modify the structure of the dendrimers (generation, polarity and stiffness of the core, number of branching units, nature of the end-groups) [6, 10].

This chapter highlights with *selected* examples some relevant results we have obtained in the field of fullerene-containing thermotropic liquid-crystalline dendrimers. These examples will demonstrate the wide application of dendrimers in designing supramolecular fullerene materials. In the following sections, the structures and properties will be presented according to the nature of the dendrimers and mesogenic units.

11.2
Liquid-Crystalline Fullerodendrimers

11.2.1
Poly(Aryl Ester) Dendrons Carrying Cyanobiphenyl Mesogenic Groups

Induction of liquid-crystalline phase formation into a priori "anti-mesogenic" bulky structures such as octahedral metal complexes [11] or lanthanides [12] often requires the design of strongly mesomorphic ligands. The principle of this strategy consists in counterbalancing the unfavorable molecular shape of such functional cores and associated geometrical constraints by modifying and improving the molecular interface (area compatibilities between both the hard and soft organic moieties), consequently enhancing microsegregation by the embedding of the hard nucleus and possibly yielding liquid-crystalline materials. This strategy has been successfully applied to bulky cores other than C_{60} [13] such as silsesquioxanes [14], polymetallic cages [15], nanoparticles [16] and large supramolecular objects [17].

In the case of C_{60}, the connection of straight mesogens, such as cholesterol [18] or ferrocenomesogens [19] indeed produced mesophases, although in most cases the liquid-crystalline phases were either transient or monotropic [20]. Conversely, the use of mesomorphic dendritic addends led to liquid-crystalline materials with accessible and stable mesomorphic properties.

Addition reaction of various generations of malonate-based dendritic addends, bearing cyanobiphenyl end-groups, onto C_{60} led to methanofullerodendrimers **1**–**4** [21]. All of them, **1** (first generation; Tg 48 SmA 179 I), **2** (second generation; Tg: not detected; SmA 183 N 184 I), **3** (third generation; Tg: not detected; SmA 212 I) and **4** (fourth generation; Tg: not detected; SmA 252 I), exhibit a broad SmA phase, with the mesophase stability increasing with the dendrimer generation. In all cases, periodicities are of the order of 100 Å.

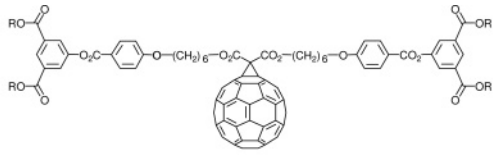

1

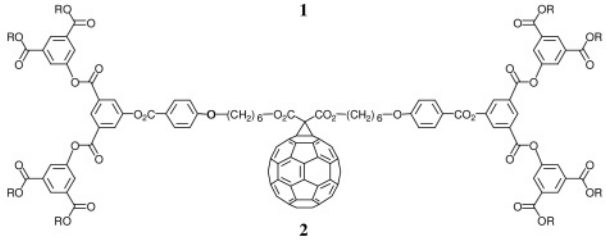

2

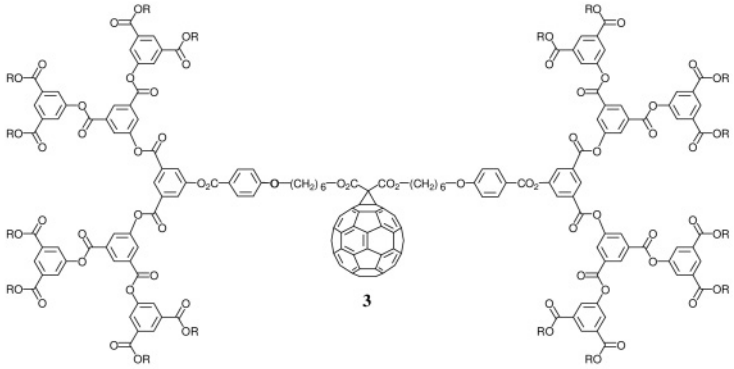

3

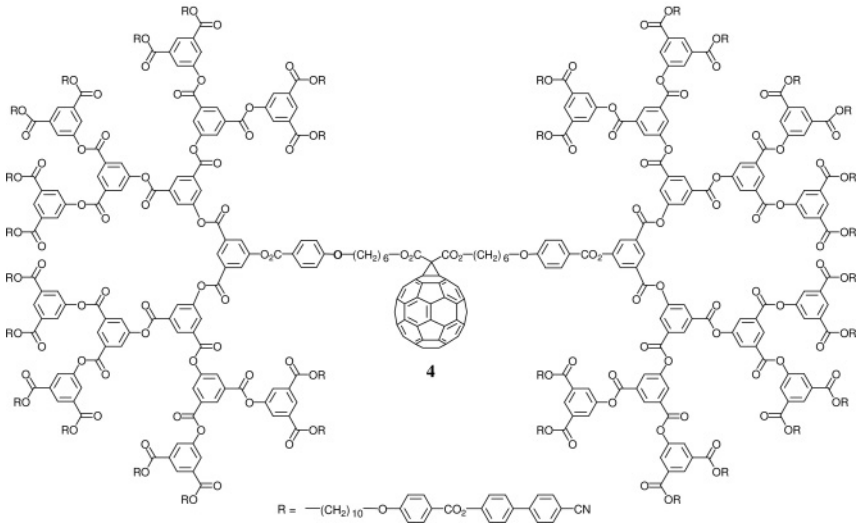

4

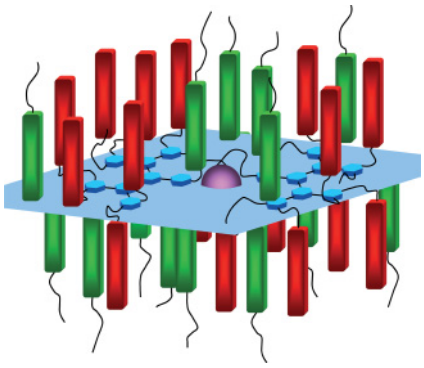

Figure 11.1 Proposed supramolecular organization of **3** within the smectic A phase. The interdigitation is illustrated by the red and green cyanobiphenyl units: the red units belong to the dendrimer that is displayed on the drawing, and the green units belong to dendrimers of adjacent layers. Compounds **2** and **4** show a similar supramolecular organization.

The supramolecular organization of these dendrimers was deduced and understood from X-ray diffraction analysis and molecular simulation. For **1**, the molecules adopt a V-shape (constituted by pairs of mesogenic groups), and arrange in a head-to-tail fashion favored by the antiparallel packing of the polar end-groups. For **2**, the branching part begins to have significant lateral extension with respect to the layer normal, and the two branches extend on both sides of C_{60}. Then, for **3** and **4** (Figure 11.1), the structure is solely governed by the polar cyano groups. The central part of the layer is constituted by the fullerene moiety embedded by the dendritic segments, and the layer interface is formed by partial interdigitation of the mesogenic groups. In all cases, the mesophase is stabilized by dipolar interactions (antiparallel arrangement of the cyanobiphenyl units). Thus, in **1–4**, C_{60} is buried within the dendritic branches, at least above the second generation, and as a consequence the supramolecular organization of these fullerodendrimers is independent of the change of the generation number of the dendrimer and both the thermal behavior and mesophase organization are similar to that of the corresponding mesomorphic malonate precursors (structures not shown).

The corresponding hemi-dendrimers of first and second generations were also prepared for comparison purposes (structures not shown). The same type of supramolecular organization was suggested. Interestingly, the mesomorphic temperature range was strongly reduced in the hemi-dendrimers compared to that of the corresponding dendrimers. It was also shown by electro-optical Kerr effect and hydrodynamics methods that the hemi-dendrimers are more sensitive than dendrimers to the presence of C_{60} in their structure (viscosity, shape changes) [22].

Fulleropyrrolidines are an important family of C_{60} derivatives that have the advantage over methanofullerenes of leading to stable reduced species – an essential feature for integration into electro-active devices. To promote mesomorphism in fulleropyrrolidines, C_{60} was modified with dendritic addends bearing cyanobiphenyl groups, leading to four generations of fulleropyrrolidines (**5–8**) [23]. This appeared to be the right strategy since, with the exception of first generation **5**, which is non-mesomorphic (Cr 178 I), all other fullerene-based dendrimers give rise to a SmA phase (**6**: Tg 44 SmA 168 I; **7**: Tg 51 SmA 196 I; **8**: Tg 36 SmA 231

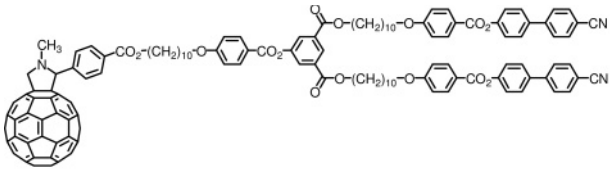

5

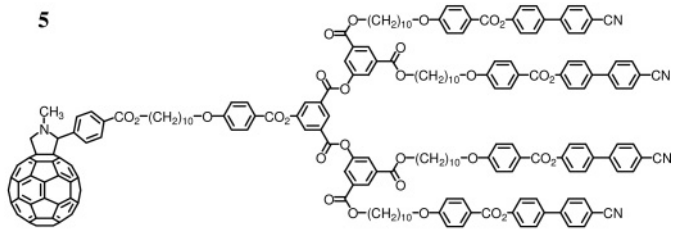

6

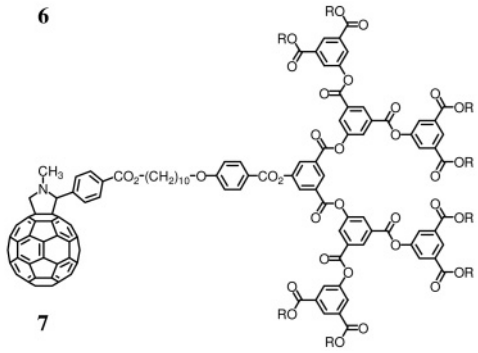

7

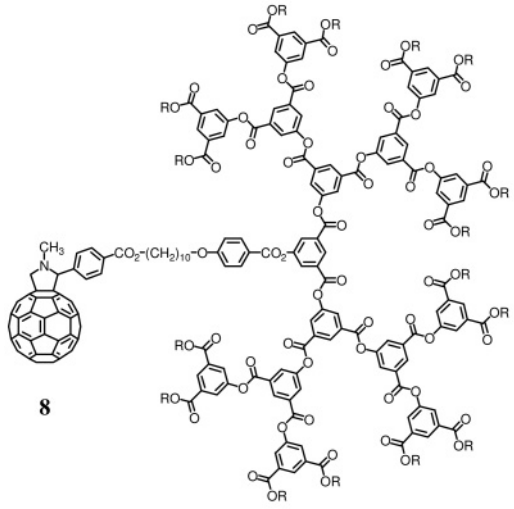

8

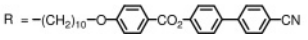

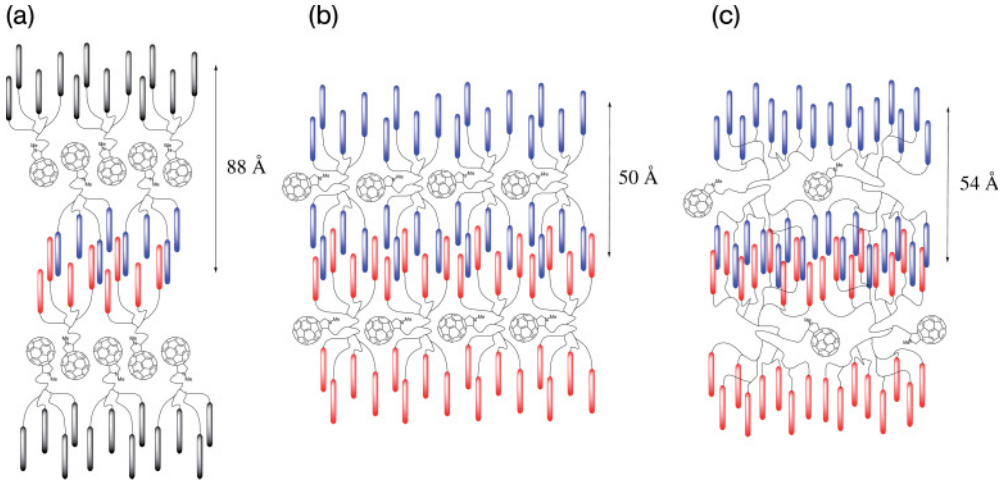

Figure 11.2 Postulated supramolecular organization of fulleropyrrolidines **6** (a), **7** (b) and **8** (c) within the smectic A phase.

I), the stability of which increases with the generation number. The aldehyde precursors show a broad SmA phase, except the one of first generation, which shows a nematic phase. As for the molecular organization within the SmA phase (Figure 11.2), the second generation molecules **6** are oriented in a head-to-tail fashion within the layers, and for each molecule the mesogenic groups point in the same direction, interdigitating with mesogenic groups of adjacent layers. For the higher generations, that is, **7** and **8**, the mesogenic units are positioned above and below the dendritic core, and interdigitation occurs between layers; C_{60} is hidden in the dendritic core and has no influence on the supramolecular organization, as was the case for the methanofullerodendrimers discussed above.

With a view to exploiting C_{60} as a synthetic platform for the design of liquid-crystalline materials with unconventional shapes, the mesomorphic properties of fullerodendrimers based on the bis-addition pattern were also investigated [24]. Indeed, bisadducts of C_{60} retain most of the properties of C_{60}, considering that the major drawback of the poly-addition pattern [25, 26] is that the properties of C_{60} are considerably altered [7]. The bis-addition led to various isomeric structures, including V-shaped structures with different angles. The same second-generation cyanobiphenyl-based dendrimer was used as liquid-crystalline promoter for the synthesis of mesomorphic bisadducts of C_{60}. Liquid-crystalline *trans*-2 (**10**), *trans*-3 (**11**) and equatorial (**12**) bisadducts were obtained by condensation of the liquid-crystalline promoter, which carries a carboxylic acid function, with the corresponding bisaminofullerene derivatives. A monoadduct of fullerene (**9**) was prepared for comparative purposes.

The molecular organization of monoadduct **9** (Cr 44 SmA 153 I) within the smectic layers is mainly governed by steric factors, that is, the required adequacy

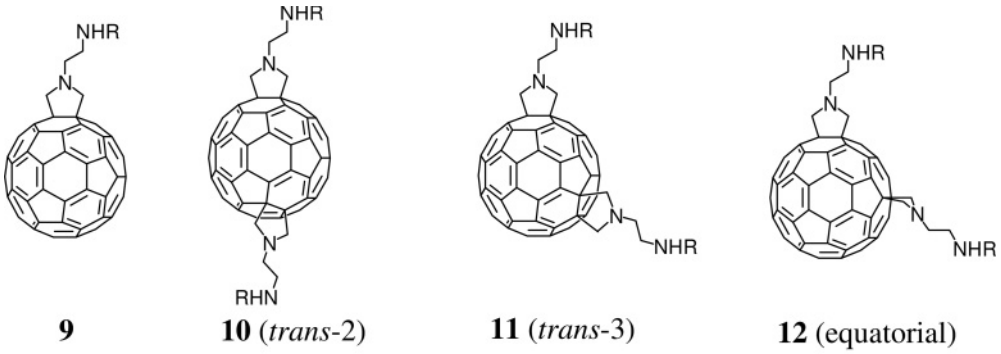

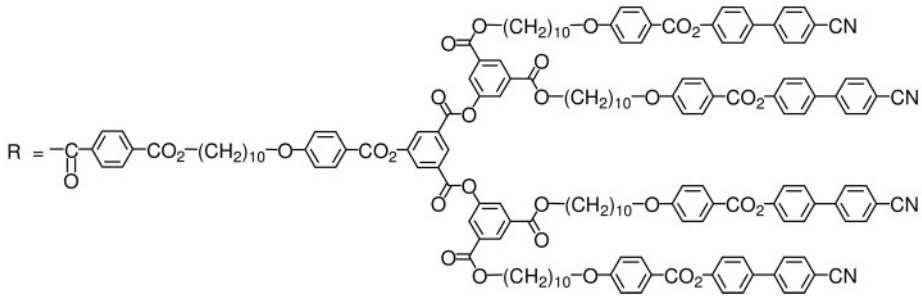

between the cross-sectional areas of C_{60} (90–100 Å^2) and that of the mesogenic units (22–25 Å^2 per mesogenic unit). Thus, the cyanobiphenyl units of one molecule point in the same direction, and the molecules are organized in a head-to-tail fashion, forming a bilayered smectic A phase. As for that of bisadducts **10** (Tg 60 SmA 167 M 170 I, M: unidentified mesophase), **11** (Tg 61 SmA 169 I) and **12** (Cr 42 SmA 166 I), the two dendrons expand laterally with respect to C_{60} so that the latter is embedded within the layers formed by the dendrimers and has no influence on the supramolecular organization. The bisadduct derivatives are organized into a monolayered smectic A phase, similar to that obtained for fulleropyrrolidines and methanofullerenes functionalized by analogous liquid-crystalline dendrimers (Figures 11.1 and 11.2). For bisadducts **10–12**, the supramolecular organization is essentially governed by the nature and the structure of the mesogenic units and of the dendritic core. A comprehensive investigation of the photophysical properties of several of these fulleropyrrolidine dendrimers revealed that the basic fullerene features are largely preserved, and no spectroscopic evidence for strong π–π interactions between individual fullerenes could be detected.

Thus, the smectic mesomorphism obtained for **1–12** is determined by the nature of the terminal groups, as in other classical dendrimers [5, 10].

11.2.2
Poly(Aryl Ester) Dendrons Carrying Optically-Active Mesogenic Groups

Liquid-crystalline chiral systems are generally designed for their ferroelectric and/or pyroelectric properties [14]. Chirality has been introduced into C_{60} systems by addition of dendritic malonates carrying chiral nematic mesogens attached in a side-on fashion onto C_{60} [14, 27]. Fullerodendrimer **13** shows an enantiotropic chiral nematic phase with the following phase sequence: Tg 26 N* 69 I [27]. The value of the pitch of the helix is $5 \pm 0.5\,\mu m$ and does not depend on temperature. This value indicates that C_{60} fits within the helical structure formed by the mesogens themselves without causing any significant perturbation of the pitch itself. Interestingly, the dendritic moiety also exhibits a chiral nematic phase with a helical pitch of $2.5 \pm 0.5\,\mu m$. Thus, C_{60} and the dendritic unit act as diluents to the self-organizing system provided by the unsubstituted mesogenic addends. Although C_{60} may strongly disturb the mesogenic interactions, it can nevertheless be encapsulated within the self-organizing chiral nematic medium. For **14** (g 24.3 N* 80.6 I), where the number of the mesogenic groups is doubled, thereby reducing the weight fraction of C_{60} in the dendritic supermolecule, the chiral nematic phase is more stable, in agreement with the decreasing influence of C_{60}, which is totally buried within the liquid-crystalline matrix [14].

11.2.3
Poly(Benzyl Ether) Dendrons Carrying Flexible Alkyl Chains

For fundamental aspects as well as for potential applications, it is of interest to control the nature and symmetry of the mesophases with, for instance, the induction of mesophases with curved interfaces. Indeed, fullerene-containing liquid crystals displaying columnar phases are candidates of choice for the development of new electronic and optoelectronic devices [28]. This can be achieved by modifying the molecular structures of the dendritic addends; poly(benzyl ether) dendrons were selected since they give rise to either spherical or cylindrical supramolecular dendrimers: due to their inherent fan, conical or even spherical conformation, they subsequently self-organize into cubic or columnar lattices [29]. Functionalization of C_{60} with poly(benzyl ether) dendrons equipped with an aldehyde function, which exhibit columnar mesomorphism, and *N*-methylglycine led to fullerodendrimers **15** (Tg not detected, Col_r 80 I) and **16** (Tg 46 Col_r 74 I) which exhibit a Col_r phase with a *c2mm* symmetry, with rather large lattice parameters ($a = 128.6$ Å, $b = 86.0$ Å for **15**, and $a = 129.6$ Å, $b = 89.4$ Å for **16**) [30].

Considering a hexagonal close compact packing of the C_{60} spheres along the columnar axis, surrounded by the flexible dendritic shell, the number of molecules included in an elementary columnar slice (8.7 Å thick) was calculated. From the values of the lattice parameters and the estimated molecular volumes (4550 and 4700 $Å^3$ for **15** and **16**, respectively), this number turned out to be about ten for each compound. The supramolecular organization thus results in bundles of ten dendrimers superimposed one over the other to form an elliptic columnar core,

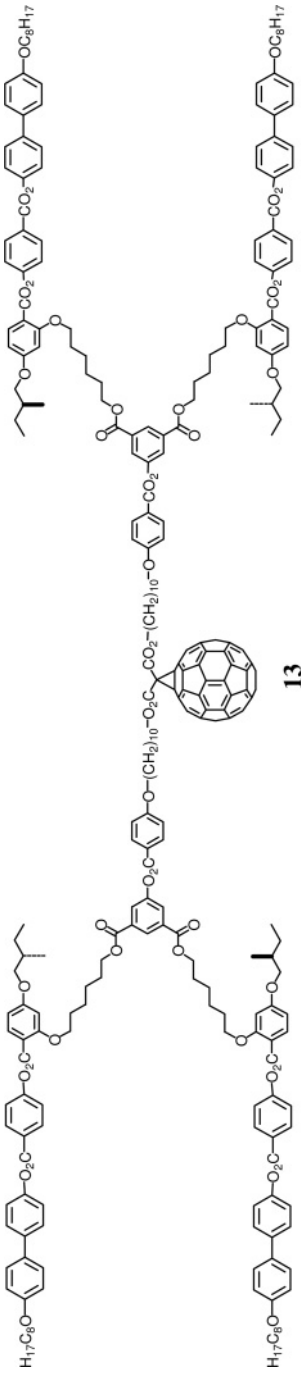

13

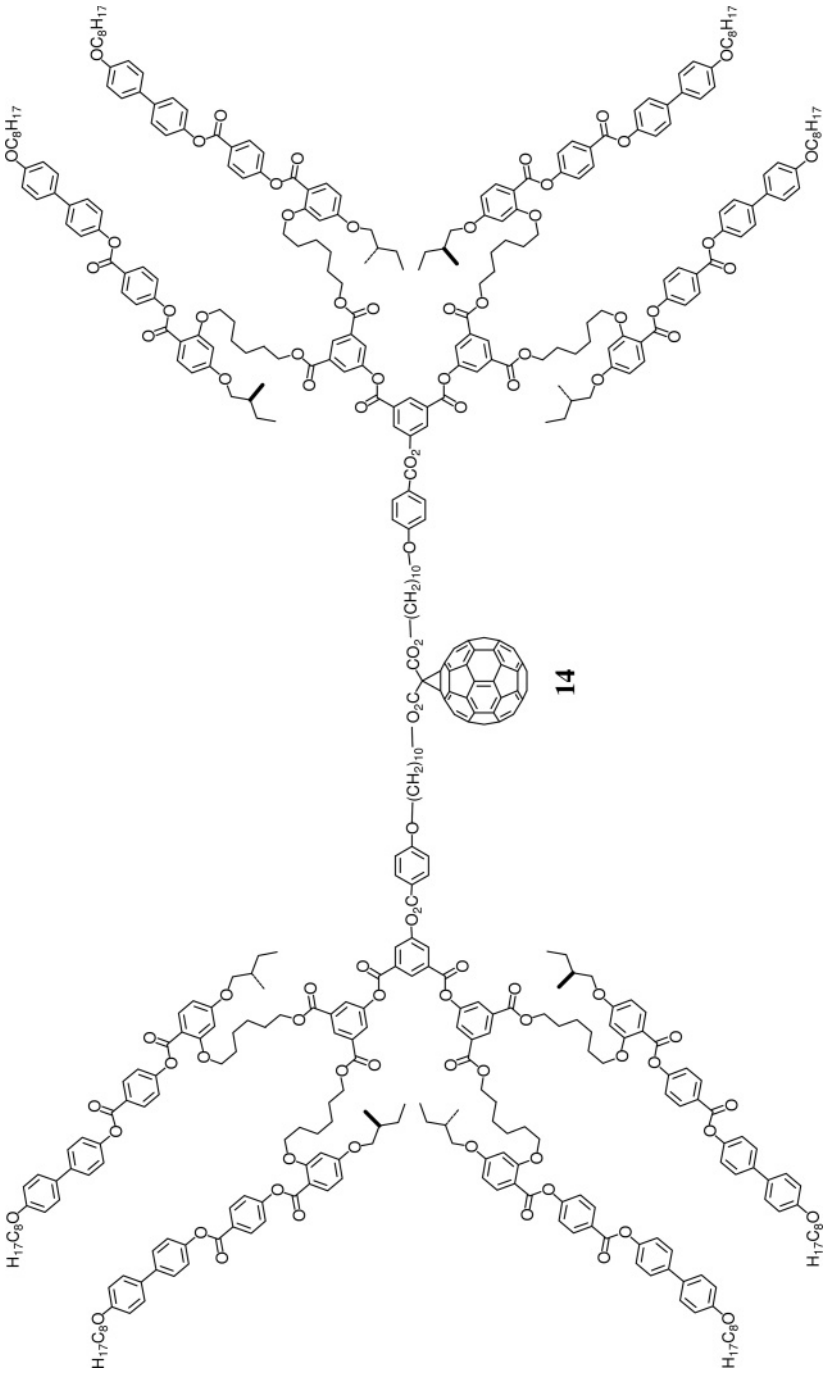
OC8H17
H17C8O
CO2
(CH2)10
O2C
14

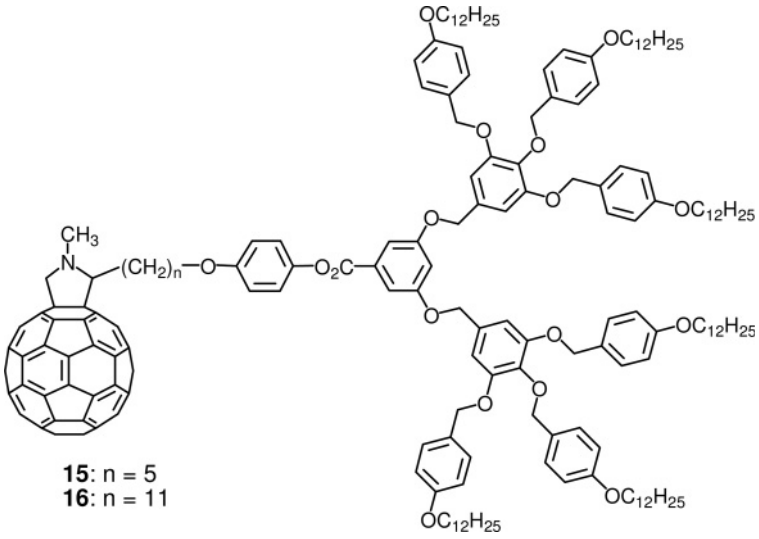

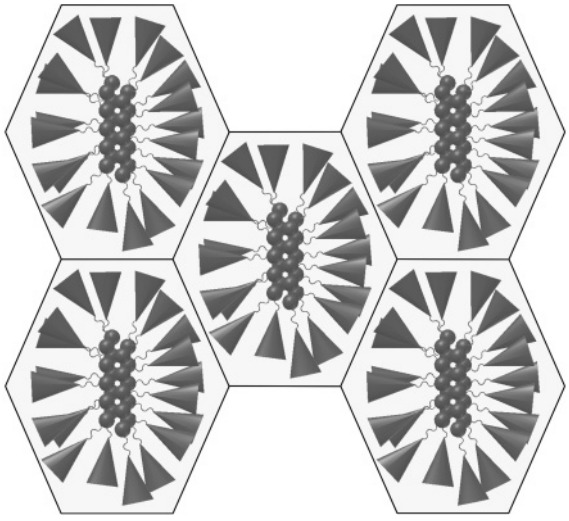

Figure 11.3 Postulated supramolecular organization of **15** and **16** within the rectangular columnar phase.

the shape and orientation of which are in agreement with the *c2mm* symmetry. The dendritic moieties are arranged around this elliptic core to fill the intercolumnar space (Figure 11.3). This result demonstrates that C_{60} can be organized along one single direction (here, the columnar axis) provided a suitable molecular design is achieved.

To further investigate the formation of columnar phases, methanofullerenes carrying simultaneously at both extremities either two identical poly(benzyl ether)

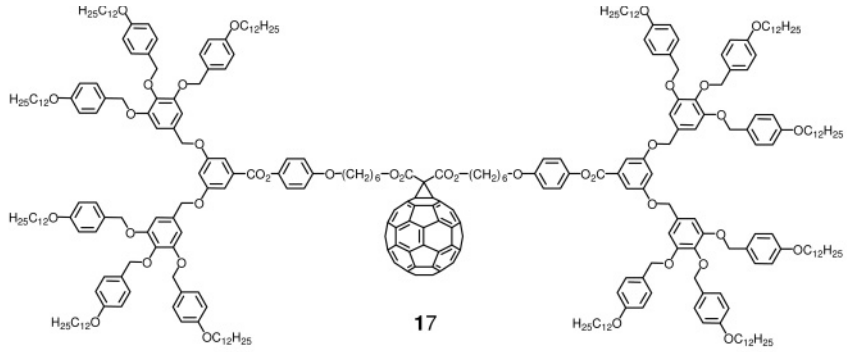

17

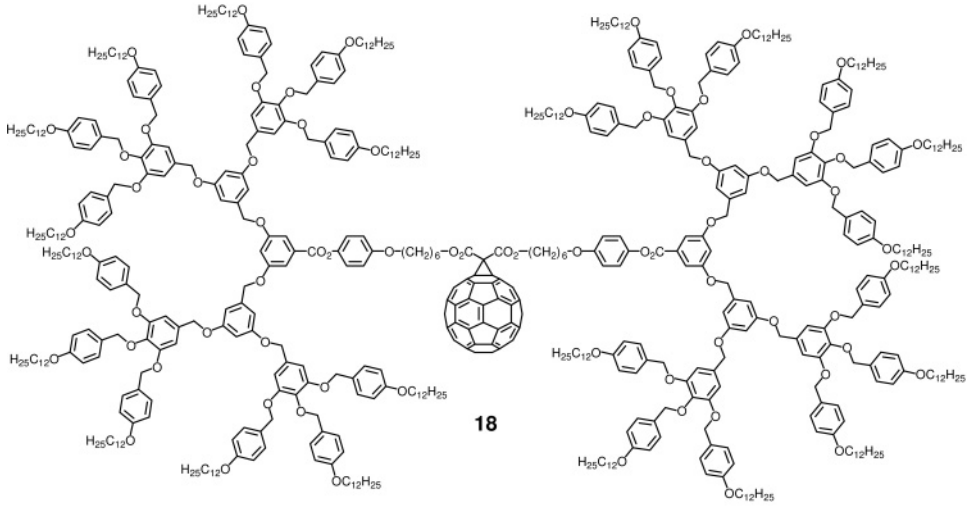

18

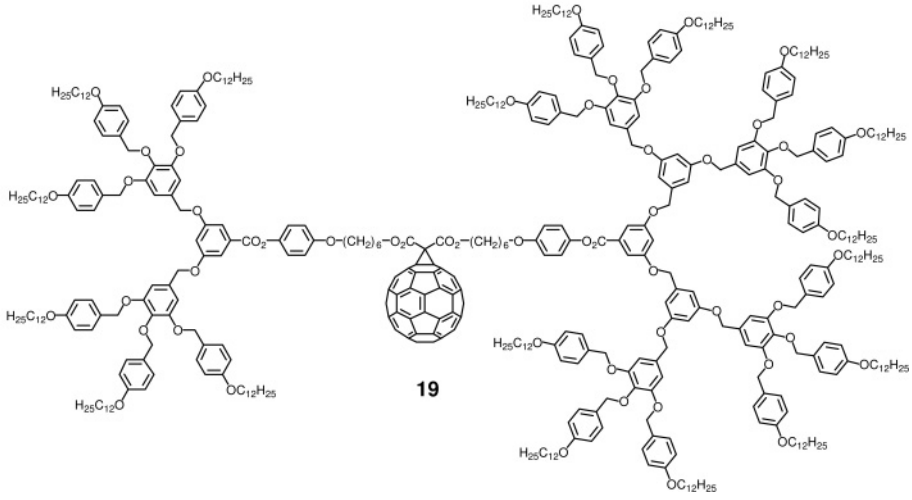

19

dendrons (**17**: two second-generation dendrons; **18**: two third-generation dendrons) or two poly(benzyl ether) dendrons of different generations (**19**: second- and third-generation dendrons) have been synthesized [31]. All the dendritic malonate precursors exhibit a Col_h phase, with a large increase in phase stability as the size of the dendrons increases. However, while compound **17** (Cr 52 I) does not show liquid-crystalline properties, **18** (Tg 44 Col_h 93 I) and **19** (Tg 64 Col_h 74 I) display hexagonal columnar phases, clearly identified by XRD diffraction. Thus, C_{60} has no (or little) influence on the structure of the mesophases, but its impact is detrimental on the mesophase stability. The parameters of the two-dimensional hexagonal lattices (*p6mm* symmetry) are consistent with the dimensions of the basic dendritic branches, a = 47.05 and 46.65 Å for **18** or **19**, respectively, and are similar to that of the malonate precursors, suggesting that a similar supramolecular organization is maintained. The fan-like conformation of the dendrons forces the fullerodendrimers (and the malonates) to arrange in cylindrical columns, with the C_{60} units inside the organic shell. Depending on the combination of dendritic branches and on the geometrical parameters, two molecules of **18** and **19** self-associate into a disc to pave the hexagonal 2D network. In both cases, the C_{60} units are located towards the interior of the column, and loosely stacked along the columnar axis, surrounded by the dendritic part. Molecular dynamic experiments on compound **19** confirmed this supramolecular organization (Figures 11.4 and 11.5) – a lattice parameter comparable to that of the X-ray experiments and a density close to unity were found. The non-mesomorphic character of **17** indicates that mesophase induction in such bulky materials requires the connection of stronger liquid-crystalline promoters. The corresponding hemidendritic homologues, malonates and fullerodendrimers (structures not shown) also exhibit a Col_h phase, except one compound, which shows a Col_r phase.

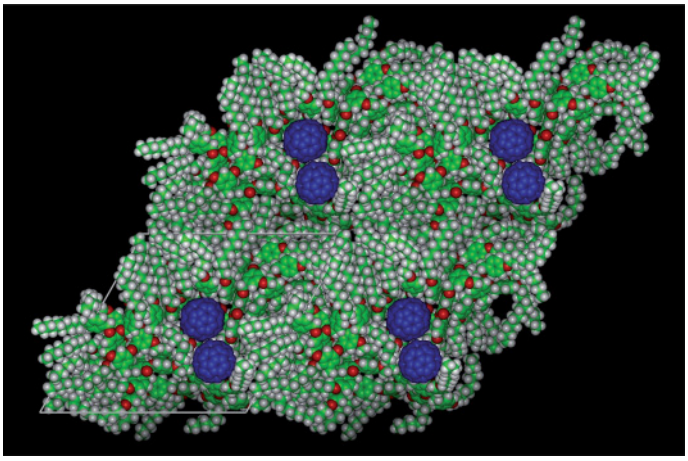

Figure 11.4 Top view of the supramolecular organization of **19** within the hexagonal columnar phase of *p6mm* symmetry.

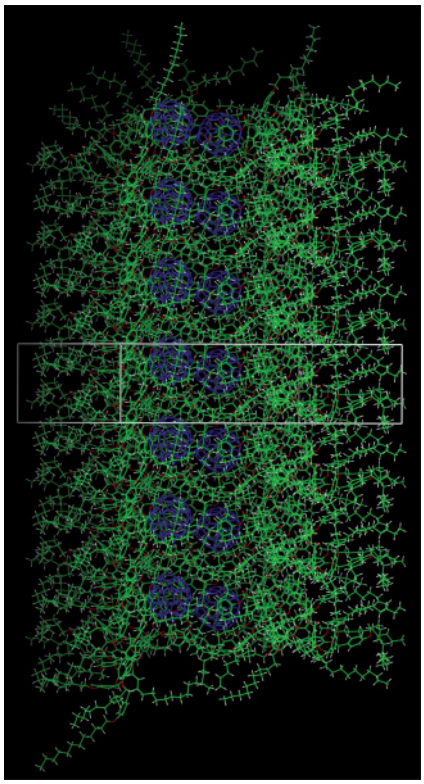

Figure 11.5 Side view of the supramolecular organization of **19** within the hexagonal columnar phase of *p6mm* symmetry.

Thus, essentially all the malonate and fullerene derivatives equipped with such flexible poly(benzyl ether) dendrons give rise to columnar phases, and their supramolecular organization within the columnar phases is governed by the dendrimer, providing that the size of the dendritic addends is large enough to compensate and circumvent the large area of the bulky C_{60}.

11.3
Liquid-Crystalline Fullero(codendrimers)

As reported above, grafting of fan-like shaped poly(benzyl ether) dendrimers onto C_{60} yielded fullerodendrimers exhibiting columnar phases with either hexagonal or rectangular symmetry, while the use of dendrons bearing calamitic end-groups promoted the formation of smectic phases. As this was just evoked, it seems that there are more possibilities to control the liquid-crystalline properties in codendrimers than in homodendrimers, and this approach may represent an attractive way for the design of fullerene-containing liquid crystals with tailor-made mesomorphic properties. For example, when two different dendrons are assembled,

their generation, relative proportion and location within the molecule can be varied independently, and each modification can be used, in principle, to control the nature of the mesophases. By exploiting this modular construction, we envisioned that the liquid-crystalline properties of fullero(codendrimers) could be tuned by changing the generation and the nature of the dendrons located on C_{60}. Therefore, the assembly of poly(aryl ester) dendrons functionalized with cyanobiphenyl groups and poly(benzyl ether) dendrons carrying alkyl chains was attempted. These dendrimers were selected with the expectation that their different structural characteristics and properties would influence the overall liquid-crystalline behavior. In such voluminous structures, C_{60} is hidden in the organic matrix, and the supramolecular organization should only depend on the dendrons and should not be altered by the presence of the isotropic C_{60} hard sphere. Furthermore, owing to the different nature of the dendrons, multilevel microsegregation should be obtained, leading to long-range organization within the liquid crystal state.

Six fullero(codendrimers) (**20–25**) have been prepared [32] and can be classified within two families from the point of view of their liquid-crystalline properties: the compounds that give rise to columnar phases, that is, **20** (Tg 31 $Col_{r\text{-}c2mm}$ 105 I′ 108 I), **21** (Tg: not detected; $Col_{r\text{-}p2gg}$ 109 I) and **22** (Tg: not detected; $Col_{r\text{-}c2mm}$ 152 I), and those showing smectic phases, that is, **23** (Tg: not detected; SmC 116 SmA 155 I), **24** (Tg: not detected; SmA 210 I) and **25** (Tg: not detected; SmA 209 I).

The liquid-crystalline properties of **20–25** clearly depend on the generation of each dendron. When the generation of the poly(benzyl ether) dendron is higher than that of the poly(aryl ester) dendron, columnar mesomorphism is observed (i.e., for **20–22**); conversely, when the generation of the poly(aryl ester) dendron is higher (i.e., for **24**) than or the same as (i.e., for **23** and **25**) that of the poly(benzyl ether) dendron, smectic mesomorphism is observed. The liquid-crystalline properties of **20–25** can thus be tuned by design.

Comparison of the isotropization temperatures emphasizes the influence of the poly(aryl ester) dendrons on the thermal stability of the liquid-crystalline phases. Compounds **24** and **25**, with third generation poly(aryl ester) dendron, show the highest isotropization temperatures (210 °C for **24** and 209 °C for **25**); in contrast, the size of the poly(benzyl ether) dendron (second generation for **24** and third generation for **25**) has no influence on the isotropization temperature. Decreasing the poly(aryl ester) dendron generation results in a decrease in the clearing point [155 °C for **23**, and 152 °C for **22**, both second generation poly(aryl ester) dendron], independent of the observed mesophase. Finally, the clearing point of **20** and **21** confirm that the poly(benzyl ether) dendron has no influence on the isotropization temperature (105 °C for **20** and 109 °C for **21**).

The formation of smectic phases for **23–25** results from the antiparallel arrangement of the fullerodendrimers forming one central sublayer containing the cyanobiphenyl groups, and the poly(benzyl ether) dendrons being ejected to another sublayer. Such an intramolecular segregation occurs above the glass transition, giving enough flexibility to the poly(benzyl ether) dendron and the aliphatic spacers of the poly(aryl ester) dendron to deform in order to favor a parallel arrangement of the mesogenic groups, thus producing well-developed lamellar structures.

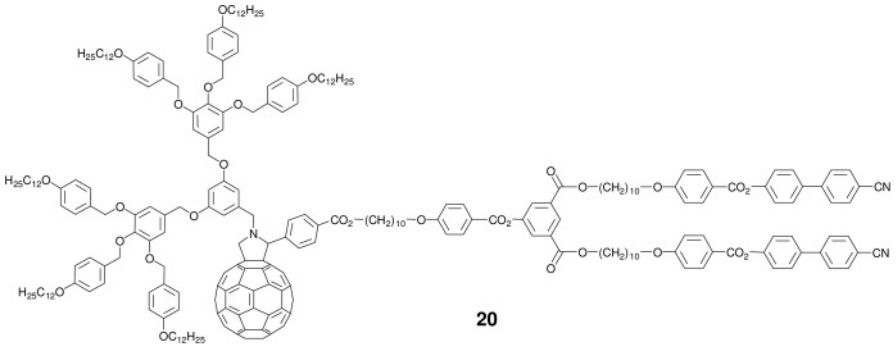

20

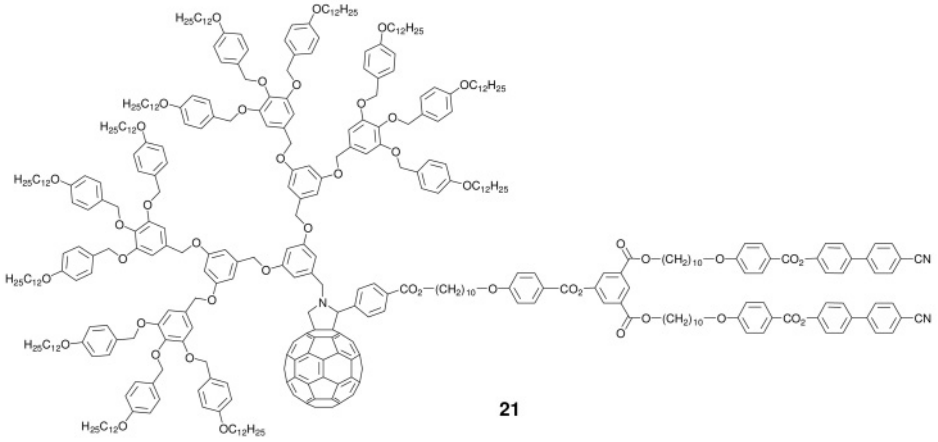

21

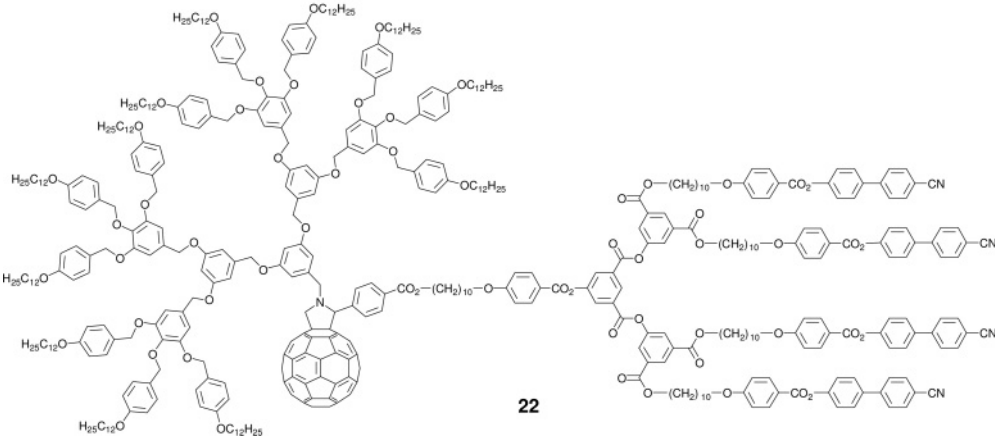

22

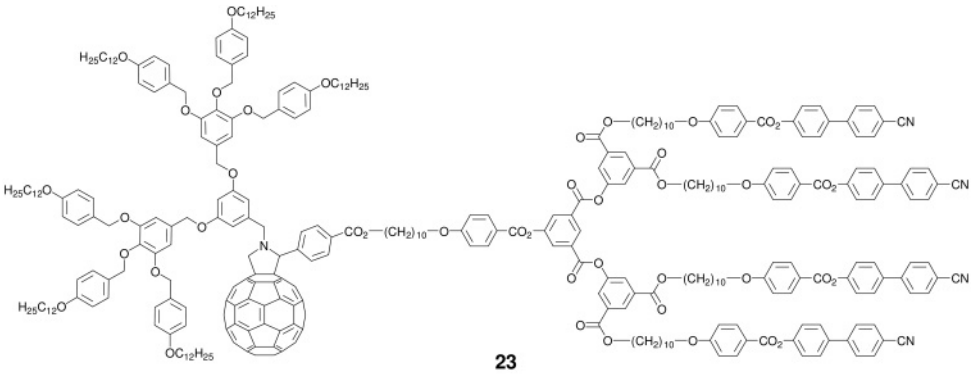

23

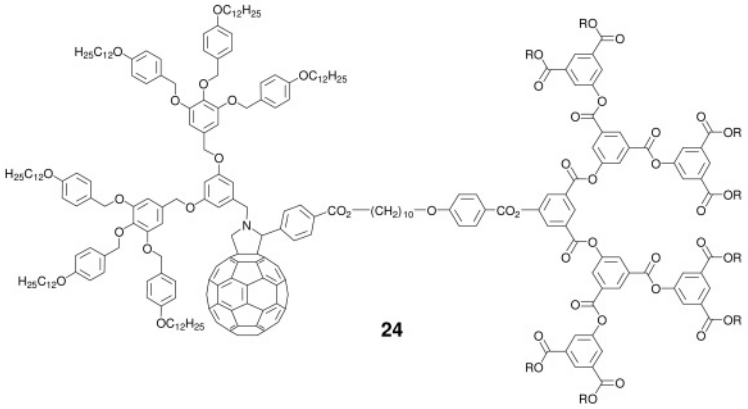

24

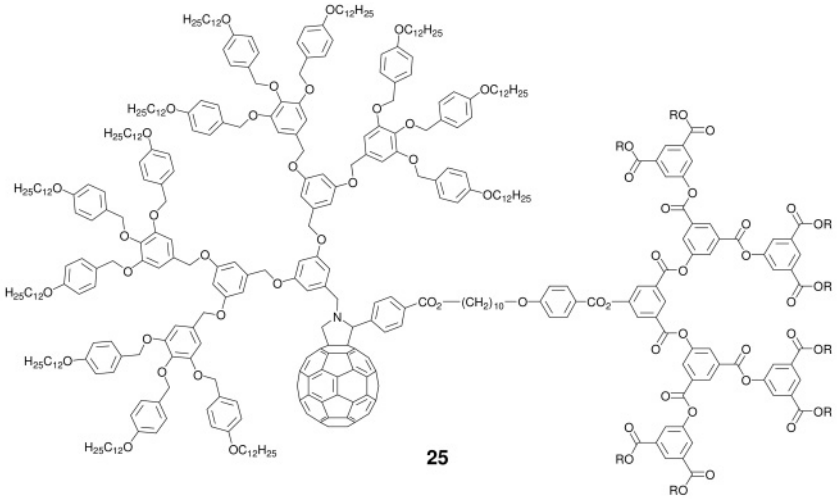

25

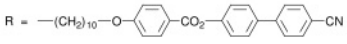

The values of the layer periodicities, which increase only slightly with increasing molecular weight (121.5, 125.9 and 136.0 Å for **23**, **24** and **25**, respectively), and molecular areas permit us to understand the molecular organization within the layers. A bilayered structure (molecules arranged head-to-head) is thus envisaged, where the central slab of the layer is made up of the cyanobiphenyl mesogenic groups arranged in an antiparallel fashion and the aliphatic chains of the poly(benzylether) dendrons point out at both interfaces of the layer (Figure 11.6). In this model, the area available for the aliphatic chains is compensated by that of the cyanobiphenyl mesogenic groups. In the center of the layer, the mesogenic groups are either tilted or normal to the smectic plane, depending on *R*, that is, the "aliphatic terminal chains/mesogenic groups" ratio. In these layers, the C_{60} units are confined within well-defined sublayers, located on both sides of the central layer formed by the cyanobiphenyl groups; the poly(benzyl ether) dendritic portion is confined within external sublayers. The absence of X-ray signals corresponding to the C_{60} units suggests the absence of long-range organization and a random disposition of fullerene within the sublayers.

The supramolecular organization of **20**–**22** extend over long distances despite the high molecular weight of the compounds (4.3–7.7 kDa) and in the absence of any molecular shape specificity. The values of the ratio *R*, which is 3 for **20** and **22**, and 6 for **21**, are consistent with an induced curvature in the structures (the number of aliphatic chains is larger than the number of cyanobiphenyl mesogenic groups, and thus the transverse molecular areas of both molecular moieties are significantly different, and therefore a stable lamellar structure cannot be obtained), leading to columnar phases. In addition, they develop only above

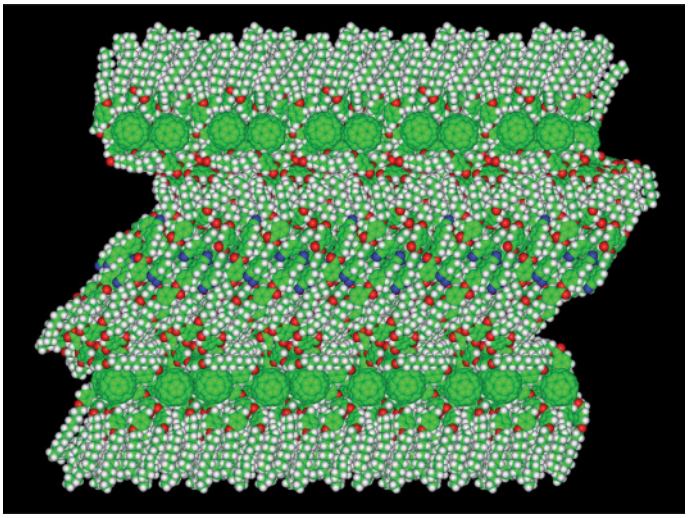

Figure 11.6 Postulated supramolecular organization of **23** obtained by molecular dynamics. Compounds **24** and **25** gave similar results.

certain temperatures in such a way that the conformation of the aliphatic spacers and the dendritic moieties can adapt to the most stable condensed phase.

The number of molecules per unit length along the columnar axis (*ca.* 10 Å thick, corresponding to the diameter of C_{60}) was calculated from the rectangular lattice parameters and the estimated molecular volumes. A columnar slice contains 14 molecules of **20** and ten molecules of the larger dendrimers **21** and **22**. The postulated model of the molecular organization is derived from that of the lamellar organization although the increasing *R* value destabilizes the layering by breaking the layers into ribbons, as previously observed for lamellar-to-columnar phase transitions exhibited by polycatenar liquid crystals [33], fifth-generation carbosilane dendrimers [34] and statistical liquid-crystalline codendrimers [35]. Each columnar core is made up of mesogenic groups interacting through the cyanobiphenyl groups and is surrounded by the poly(benzyl ether) dendrons including the C_{60} units. Competition occurs between the tendency of the cyanobiphenyl subunits to form layers via a head-to-head arrangement and the bulky dendrons forcing a columnar arrangement. This competition is dominated by the bulky dendrons, as evidenced by the presence of strong layer undulations with large amplitudes, which results in the destruction of the layers into ribbons. The symmetry of these 2D arrangements (*c2mm* or *p2gg*) is clearly associated with the ratio *R*. The absence of X-ray signals corresponding to C_{60} suggests a loose disposition of the latter. This arrangement was confirmed by molecular dynamics calculations on **20** (Figure 11.7).

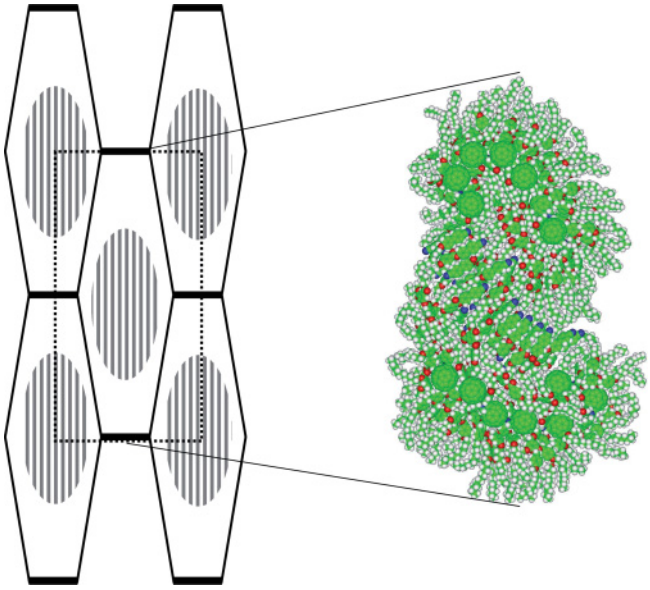

Figure 11.7 Postulated supramolecular organization of **20** within the rectangular columnar phase of *c2mm* symmetry. Compounds **21** ($Col_{r\text{-}p2gg}$) and **22** ($Col_{r\text{-}c2mm}$) gave a similar organization.

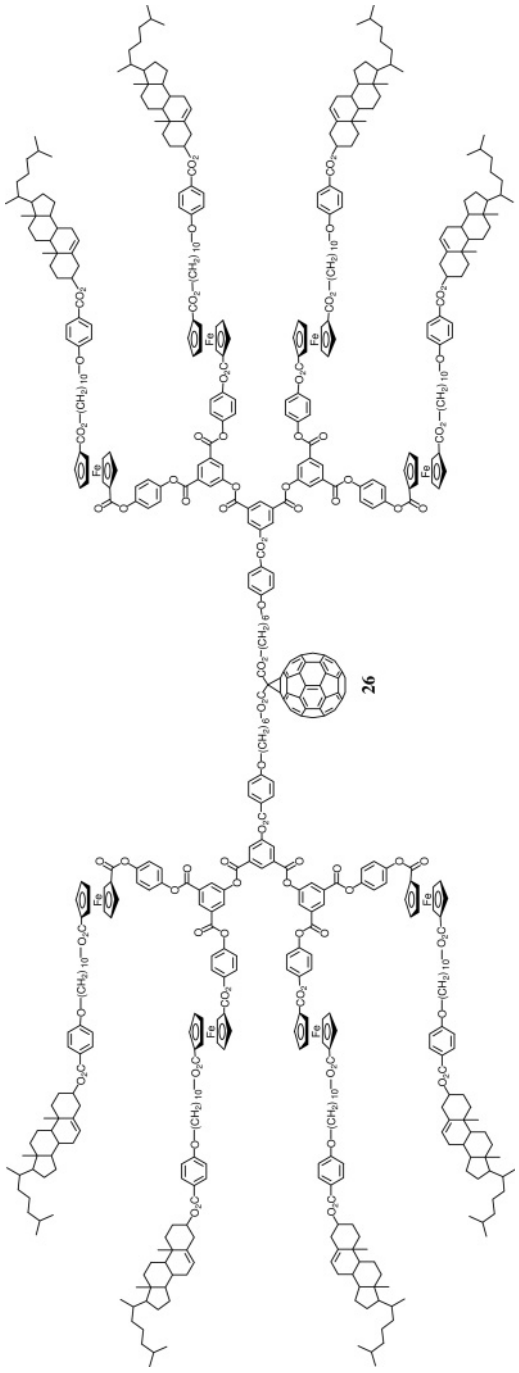

26

The beneficial effect of co-dendritic architectures to generate mesomorphism for fullerodendrimers is therefore clearly demonstrated in these systems. Thus, XRD investigations, molecular modeling and solution studies revealed that the supramolecular organization of compounds **20–25** is governed by (i) the "aliphatic terminal chains/mesogenic groups" ratio, (ii) the effective lateral intra- and intermolecular interactions between the cyanobiphenyl mesogenic groups, (iii) the effective microsegregation of the dendrons and (iv) the deformation of the dendritic core. Notably, the supramolecular organization within the mesophases extends over long distances, as evidenced by the presence of a large number of sharp and intense small-angle XRD peaks.

11.4 Conclusion

The results presented above, and those published by other research groups [36–42] that have described different strategies to obtain liquid-crystalline fullerenes, demonstrate that fullerene-containing liquid crystals have reached a high degree of sophistication both from the point of view of their structure and mesomorphic properties. The association of C_{60} with redox-active units, such as ferrocene (smectic A phase) [43], OPV (smectic A phase) [44] or TTF (smectic A and smectic B phases) [45] and a second-generation liquid-crystalline dendron, has led to polyfunctional liquid-crystalline materials for application as supramolecular switches and in solar cell technology. Indeed, such materials combine the self-organizing characteristics of liquid crystals and the properties of the subunits (e.g., photoinduced electron transfer). Obviously, liquid-crystalline fullerenes are promising compounds for the development of nanotechnology by the bottom-up approach. Future investigations will be devoted to the study of the physicochemical properties within the liquid-crystalline phases for dyads such as compound **26** (Tg not detected; SmA 157 I) [46].

Acknowledgments

R. D. acknowledges the Swiss National Science Foundation for financial support. D. G. and B. D. thank UDS and CNRS for their support.

Abbreviations

Tg	glass transition
Cr	crystalline or semi-crystalline solid
N	nematic phase
N*	chiral nematic phase
SmA	smectic A phase

SmC	smectic C phase
Col_h	hexagonal columnar phases
Col_r	rectangular columnar phase
$Col_{r\text{-}c2mm}$	rectangular columnar phase of *c2mm* symmetry
$Col_{r\text{-}p2gg}$	rectangular columnar phase of *p2gg* symmetry
I	isotropic liquid; temperatures given in °C.

References

1 Yong, P. (2003) *The Chemistry of Nanostructured Materials*, World Scientific, Singapore.

2 (a) Cardullo, F., Diederich, F., Echegoyen, L., Habicher, T., Jayaraman, N., Leblanc, R.M., Stoddart, J.F. and Wang, S. (1998) *Langmuir*, **14**, 1955.
(b) Nierengarten, J.-F., Eckert, J.-F., Rio, Y., del Pilar Carreon, M., Gallani, J.-L. and Guillon, D. (2001) *J. Am. Chem. Soc*, **123**, 9743.

3 Burghardt, S., Hirsch, A., Schade, B., Ludwig, K. and Böttcher, C. (2005) *Angew. Chem. Int. Ed.*, **44**, 2976.

4 Brettreich, M., Burghardt, S., Böttcher, C., Bayerl, T., Bayerl, S. and Hirsch, A. (2000) *Angew. Chem. Int. Ed.*, **39**, 1845.

5 (a) Ponomarenko, S.A., Boiko, N.I. and Shibaev, V.P. (2001) *Polym. Sci. Ser. C*, **43**, 1.
(b) Guillon, D. and Deschenaux, R. (2002) *Curr. Opin. Solid State Mater. Sci.*, **6**, 515.

6 (a) Saez, I.M. and Goodby, J.W. (2005) *J. Mater. Chem.*, **15**, 26.
(b) Saez, I.M. and Goodby, J.W. (2008) *Struct. Bond.*, **128**, 1.

7 Guldi, D.M. (2000) *Chem. Commun.*, 321.

8 Kato, T., Mizoshita, N. and Kishimoto, K. (2006) *Angew. Chem. Int. Ed.*, **45**, 38.

9 Nierengarten, J.-F., Solladié, N. and Deschenaux, R. (2007) *Fullerenes: Principles and Applications* (eds F. Langa and J.-F. Nierengarten), RSC Publishing, Cambridge, pp. 127–51.

10 (a) Donnio, B. and Guillon, D. (2006) *Adv. Polym. Sci.*, **201**, 45.
(b) Donnio, B., Buathong, S., Bury, I. and Guillon, D. (2007) *Chem. Soc. Rev.*, **36**, 1495.

11 (a) Date, R.W., Iglesias, E.F., Rowe, K.E., Elliott, J.M. and Bruce, D.W. (2003) *Dalton Trans.*, 1914.
(b) Donnio, B., Guillon, D., Bruce, D.W. and Deschenaux, R. (2003) Metallomesogens, in *From the Molecular to the Nanoscale: Synthesis, Structure, and Properties* (eds M. Fujita, A. Powell, and C. Creutz), Comprehensive Coordination Chemistry II: From Biology to Nanotechnology (series eds J.A. McCleverty and T.J. Meyer), Elsevier, Oxford, UK, Volume **7**, Chapter 7.9, pp. 357–627.
(c) Deschenaux, R. (2008) *Ferrocenes: Ligands, Materials and Biomolecules* (ed. P. Štěpnička), John Wiley & Sons, Ltd, Chichester, pp. 447–63.

12 (a) Cardinaels, T., Driesen, K., Parac-Vogt, T.N., Heinrich, B., Bourgogne, C., Guillon, D., Donnio, B. and Binnemans, K. (2005) *Chem. Mater.*, **17**, 6589.
(b) Binnemans, K. and Görller-Walrand, C. (2002) *Chem. Rev.*, **102**, 2303.
(c) Piguet, C., Bünzli, J.-C., Donnio, B. and Guillon, D. (2006) *Chem. Commun.*, 3755.
(d) Terazzi, E., Bocquet, B., Campidelli, S., Donnio, B., Guillon, D., Deschenaux, R. and Piguet, C. (2006) *Chem. Commun.*, 2922.
(e) Jensen, T.B., Terazzi, E., Donnio, B., Guillon, D. and Piguet, C. (2008) *Chem. Commun.*, 181.

13 (a) Chuard, T. and Deschenaux, R. (2002) *J. Mater. Chem.*, **12**, 1944.
(b) Deschenaux, R., Donnio, B. and Guillon, D. (2007) *New. J. Chem*, **31**, 1064.

14 Goodby, J.W., Saez, I.M., Cowling, S.J., Görtz, V., Draper, M., Hall, A.W., Sia, S., Cosquer, G., Lee, S.-E. and Raynes, E.P. (2008) *Angew. Chem. Int. Ed.*, **47**, 2754.

15 Terazzi, E., Bourgogne, C., Welter, R., Gallani, J.-L., Guillon, D., Rogez, G. and

Donnio, B. (2008) *Angew. Chem. Int. Ed.*, **47**, 490.

16 (a) Kanayama, N., Tsutsumi, O., Kanazawa, A. and Ikeda, T. (2001) *Chem. Commun.*, 2640.
(b) Kanie, K. and Sugimoto, T. (2003) *J. Am. Chem. Soc.*, **125**, 10518.
(c) Kanie, K. and Muramatsu, A. (2005) *J. Am. Chem. Soc.*, **127**, 11578.
(d) Cseh, L. and Mehl, G.H. (2006) *J. Am. Chem. Soc.*, **128**, 13376.
(e) Donnio, B., García-Vázquez, P., Gallani, J.-L., Guillon, D. and Terazzi, E. (2007) *Adv. Mater.*, **19**, 3534.

17 (a) Aprahamian, I., Yasuda, T., Ikeda, T., Saha, S., Dichtel, W.R., Isoda, K., Kato, T. and Stoddart, J.F. (2007) *Angew. Chem. Int. Ed.*, **46**, 4675.
(b) Baranoff, E.D., Voignier, J., Yasuda, T., Heitz, V., Sauvage, J.-P. and Kato, T. (2007) *Angew. Chem. Int. Ed.*, **46**, 4680.

18 Chuard, T. and Deschenaux, R. (1996) *Helv. Chim. Acta*, **79**, 736.

19 (a) Deschenaux, R., Even, M. and Guillon, D. (1998) *Chem. Commun.*, 537.
(b) Even, M., Heinrich, B., Guillon, D., Guldi, D.M., Prato, M. and Deschenaux, R. (2001) *Chem. Eur. J.*, **7**, 2595.

20 Tirelli, N., Cardullo, F., Habicher, T., Suter, U.W. and Diederich, F. (2000) *J. Chem. Soc. Perkin Trans.*, **2**, 193.

21 Dardel, B., Guillon, D., Heinrich, B. and Deschenaux, R. (2001) *J. Mater. Chem.*, **11**, 2814.

22 (a) Yevlampieva, N.P., Dardel, B., Lavrenko, P. and Deschenaux, R. (2003) *Chem. Phys. Lett.*, **382**, 32.
(b) Lavrenko, P., Yevlampieva, N., Dardel, B. and Deschenaux, R. (2004) *Prog. Colloid Polym. Sci.*, **127**, 61.

23 Campidelli, S., Lenoble, J., Barberá, J., Paolucci, F., Marcaccio, M., Paolucci, D. and Deschenaux, R. (2005) *Macromolecules*, **38**, 7915.

24 Campidelli, S., Vázquez, E., Milic, D., Lenoble, J., Atienza Castellanos, C., Sarova, G., Guldi, D.M., Deschenaux, R. and Prato, M. (2006) *J. Org. Chem.*, **71**, 7603.

25 (a) Chuard, T., Deschenaux, R., Hirsch, A. and Schönberger, H. (1999) *Chem. Commun.*, 2103.
(b) Campidelli, S., Brandmüller, T., Hirsch, A., Saez, I.M., Goodby, J.W. and Deschenaux, R. (2006) *Chem. Commun.*, 4282.
(c) Gottis, S., Kopp, C., Allard, E. and Deschenaux, R. (2007) *Helv. Chim. Acta*, **90**, 957.

26 (a) Felder-Flesch, D., Rupnicki, L., Bourgogne, C., Donnio, B. and Guillon, D. (2006) *J. Mater. Chem.*, **16**, 304.
(b) Mamlouk, H., Heinrich, B., Bourgogne, C., Donnio, B., Guillon, D. and Felder-Flesch, D. (2007) *J. Mater. Chem.*, **17**, 2199.

27 Campidelli, S., Eng, C., Saez, I.M., Goodby, J.W. and Deschenaux, R. (2003) *Chem. Commun.*, 1520.

28 (a) Laschat, S., Baro, A., Steinke, N., Giesselmann, F., Hägele, C., Scalia, G., Judele, R., Kapatsina, E., Sauer, S., Schreivogel, A. and Tosoni, M. (2007) *Angew. Chem. Int. Ed.*, **46**, 4832.
(b) Sergeyev, S., Pisula, W. and Geerts, Y.H. (2007) *Chem. Soc. Rev.*, **36**, 1902.

29 (a) Percec, V., Ahn, C.H., Cho, W.-D., Jamieson, A.M., Kim, J., Leman, T., Schmidt, M., Gerle, M., Möller, M., Prokhorova, S.A., Sheiko, S.S., Cheng, S.Z.D., Zhang, A., Ungar, G. and Yeardley, D.J.P. (1998) *J. Am. Chem. Soc.*, **120**, 8619.
(b) Percec, V., Cho, W.-D., Ungar, G. and Yeardley, D.J.P. (2001) *J. Am. Chem. Soc.*, **123**, 1302.
(c) Percec, V., Glodde, M., Bera, T.K., Miura, Y., Shiyanovskaya, I., Singer, K.D., Balagurusamy, V.S.K., Heiney, P.A., Schnell, I., Rapp, A., Spiess, H.-W., Hudson, S.D. and Duan, H. (2002) *Nature*, **419**, 384.
(d) Ungar, G., Liu, Y., Zeng, X., Percec, V. and Cho, W.-D. (2003) *Science*, **299**, 1208.
(e) Percec, V., Imam, M.R., Bera, T.K., Balagurusamy, V.S.K., Peterca, M. and Heiney, P.A. (2005) *Angew. Chem. Int. Ed.*, **44**, 4739.
(f) Percec, V., Dulcey, A.E., Peterca, M., Ilies, M., Sienkowska, M.J. and Heiney, P.A. (2005) *J. Am. Chem. Soc.*, **127**, 17902.

30 Lenoble, J., Maringa, N., Campidelli, S., Donnio, B., Guillon, D. and Deschenaux, R. (2006) *Org. Lett.*, **8**, 1851.

31 Maringa, N., Lenoble, J., Donnio, B., Guillon, D. and Deschenaux, R. (2008) *J. Mater. Chem.*, **18**, 1524.

32 Lenoble, J., Campidelli, S., Maringa, N., Donnio, B., Guillon, D., Yevlampieva, N. and Deschenaux, R. (2007) *J. Am. Chem. Soc.*, **129**, 9941.

33 Nguyen, H.-T., Destrade, C. and Malthête, J. (1997) *Adv. Mater.*, **9**, 375.

34 Richardson, R.M., Ponomarenko, S.A., Boiko, N.I. and Shibaev, V.P. (1999) *Liq. Cryst.*, **26**, 101.

35 Rueff, J.-M., Barberá, J., Donnio, B., Guillon, D., Marcos, M. and Serrano, J.-L. (2003) *Macromolecules*, **36**, 8368.

36 Felder, D., Heinrich, B., Guillon, D., Nicoud, J.-F. and Nierengarten, J.-F. (2000) *Chem. Eur. J.*, **6**, 3501.

37 (a) Sawamura, M., Kawai, K., Matsuo, Y., Kanie, K., Kato, T. and Nakamura, E. (2002) *Nature*, **419**, 702.
(b) Matsuo, Y., Muramatsu, A., Hamasaki, R., Mizoshita, N., Kato, T. and Nakamura, E. (2004) *J. Am. Chem. Soc.*, **126**, 432.
(c) Matsuo, Y., Muramatsu, A., Kamikawa, Y., Kato, T. and Nakamura, E. (2006) *J. Am. Chem. Soc.*, **128**, 9586.
(d) Zhong, Y.-W., Matsuo, Y. and Nakamura, E. (2007) *J. Am. Chem. Soc*, **129**, 3052.

38 Kimura, M., Saito, Y., Ohta, K., Hanabusa, K., Shirai, H. and Kobayashi, N. (2002) *J. Am. Chem. Soc*, **124**, 5274.

39 Busby, R.J., Hamley, I.W., Liu, Q., Lozman, O.R. and Lydon, J.E. (2005) *J. Mater. Chem.*, **15**, 4429.

40 de la Escosura, A., Martínez-Díaz, M.V., Barberá, J. and Torres, T. (2008) *J. Org. Chem.*, **73**, 1475.

41 Nakanishi, T., Shen, Y., Wang, J., Yagai, S., Funahashi, M., Kato, T., Fernandes, P., Möwald, H. and Kurth, D.G. (2008) *J. Am. Chem. Soc.*, **130**, 9236.

42 Li, W.-S., Yamamoto, Y., Fukushima, T., Saeki, A., Seki, S., Tagawa, S., Masunaga, H., Sasaki, S., Takata, M. and Aida, T. (2008) *J. Am. Chem. Soc.*, **130**, 8886.

43 (a) Campidelli, S., Vázquez, E., Milic, D., Prato, M., Barberá, J., Guldi, D.M., Marcaccio, M., Paolucci, D., Paolucci, F. and Deschenaux, R. (2004) *J. Mater. Chem.*, **14**, 1266.
(b) Campidelli, S., Pérez, L., Rodríguez-López, J., Barberá, J., Langa, F. and Deschenaux, R. (2006) *Tetrahedron*, **62**, 2115.
(c) Campidelli, S., Séverac, M., Scanu, D., Deschenaux, R., Vázquez, E., Milic, D., Prato, M., Carano, M., Marcaccio, M., Paolucci, F., Aminur Rahman, G.M. and Guldi, D.M. (2008) *J. Mater. Chem.*, **18**, 1504.

44 Campidelli, S., Deschenaux, R., Eckert, J.-F., Guillon, D. and Nierengarten, J.-F. (2002) *Chem. Commun.*, 656.

45 Allard, E., Oswald, F., Donnio, B., Guillon, D., Delgado, J.L., Langa, F. and Deschenaux, R. (2005) *Org. Lett.*, **7**, 383.

46 Dardel, B., Deschenaux, R., Even, M. and Serrano, E. (1999) *Macromolecules*, **32**, 5193.

12
Polymers Based on Carbon Nanotubes

Mª Ángeles Herranz and Nazario Martín

12.1
Introduction

Since carbon nanotubes (NTs) were reported by Iijima in 1991 [1] they have generated huge activity in most areas of science and engineering due to their unprecedented mechanical, electrical and thermal properties [2]. In fact, among the different forms of carbon nanostructures [3], NTs show the most potential in terms of applications. The intrinsic features of NTs – which determine their properties – are strongly influenced by the production method, as well as by the experimental conditions in which the preparation has been carried out. Two main types of carbon nanotubes are available today: (i) single-walled carbon nanotubes (SWNTs) [4], which consist of a single sheet of graphene rolled seamlessly to form a cylinder with a diameter of the order of 1 nm and length of up to centimeters, and (ii) multi-walled carbon nanotubes (MWNTs), which consist of an array of such cylinders formed concentrically and separated by 0.35 nm, similar to the basal plane separation in graphite [1]. MWNTs have diameters from 2 to 100 nm and lengths of tens of microns (Figure 12.1).

Presently, MWNTs and SWNTs are mainly produced by three techniques: the arc-discharge (AD) method [5], which implies the arc evaporation of pure or metal-doped carbon electrodes, laser vaporization of metal-doped carbon targets [6] and chemical vapor deposition (CVD) [7], which consists of the decomposition of carbon-containing molecules such as ethane, methane and carbon monoxide on supported nanoparticles of metal that play the role of catalyst for NTs growth. Compared with the other methods, CVD might offer more control over the length and structure of the produced nanotubes, and the process appears scalable to industrial quantities. Among reported CVD methods, the so-called high-pressure carbon oxide (HiPCO) process [8] is particularly successful and produces high-quality SWNTs of small lengths and narrow diameter with rather high yield.

However, the bottleneck that still hampers the real incorporation of SWNTs in different technological applications in that the as-produced SWNTs are held together in bundles of 50 to a few hundred individual SWNTs by very strong van

Fullerene Polymers. Synthesis, Properties and Applications. Edited by Nazario Martín and Francesco Giacalone

ISBN: 978-3-527-32282-4

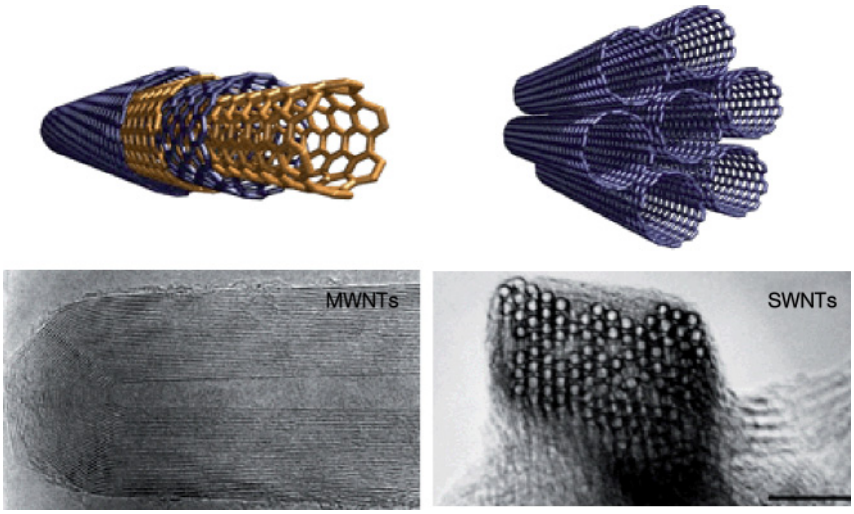

Figure 12.1 Cartoon representing SWNT and MWNT structures and transmission electron microscopy (TEM) images. The SWNT rope consists of about 100 SWNTs (Figure courtesy of Professor Andreas Hirsch.)

der Waals interactions (Figure 12.1). In addition, they are mixtures that exhibit different chiralities, diameters and length, and also non-NT carbon and metal catalysts are present in the final material.

Considerable effort is being directed towards combining polymers and fullerenes [9], as well as carbon nanotubes [10] into composites with exceptional mechanical and electrical properties. While significant insights have been achieved, there are still many unresolved issues that need to be addressed to harness the maximum benefits from NTs in polymer composite systems. In this chapter we discuss the progress, remaining challengers and future directions of nanotube/polymer research. First, we review the properties of NTs and the different approaches followed for their combination with polymers [11]. This leads us to study the many potential applications of NTs able to respond to relevant stimuli [12]. Finally, we discuss the advances made so far in the very promising application of NT/polymer composites for artificial photosynthesis and in the preparation of NT-modified electrodes for solar energy conversion [13, 14].

12.2
Carbon Nanotube Properties

Because of the different ways of rolling a graphene sheet into a cylinder, achiral zigzag and armchair tubes and helical chiral nanotubes are distinguished [2]. Each individual NT is uniquely specified by a chiral vector, defined in terms of graphene

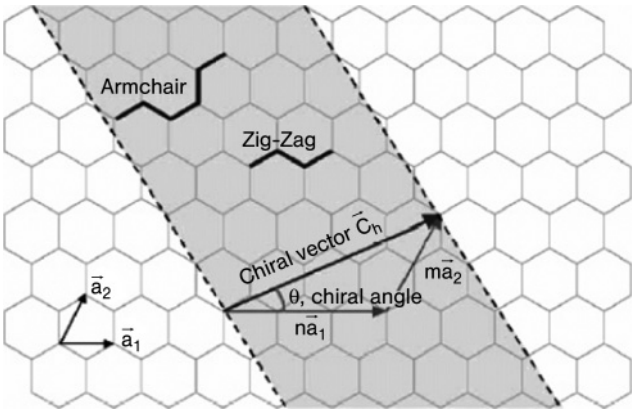

Figure 12.2 Schematic diagram showing how a hexagonal sheet of graphene is "rolled" to form a carbon nanotube. The rolling shown in the diagram will form a (3,2) nanotube. (Reprinted with permission from Reference [15]. Copyright 2001 Elsevier.)

sheet unit vectors $C_h = na_1 + ma_2$, where the integers (n, m) are the number of steps along the unit vectors (a_1 and a_2) of the hexagonal lattice (Figure 12.2) [15]. Using this naming scheme, the three types of orientation of the carbon atoms around the nanotube circumference are specified as armchair ($n = m$), zigzag ($n = 0$ or $m = 0$), or chiral (all others). The chirality of nanotubes has a significant impact on their transport properties, particularly the electronic properties. All armchair SWNTs are metallic with a bandgap of 0 eV. SWNTs with n-$m = 3i$ (i being an integer different from 0) are semi-metallic with a band gap on the order of a few meV, while SWNTs with n-m different from $3i$ are semiconductors with a band gap of approximately 0.5–1.5 eV [16]. Each MWNT contains various tube chiralities, so their physical properties are not easy to predict.

12.2.1 Electrical and Thermal Conductivity

Pristine carbon nanotubes are extremely conductive. Owing to their one-dimensional nature, charge carriers can travel through nanotubes without scattering resulting in ballistic transport. Dai and coworkers [17] obtained $R \approx 32\,k\Omega$ at 290 K for a metallic SWNT ($l = 4\,\mu m$, $d = 1.7$ nm), yielding a conductivity of $0.9 \times 10^6\,S\,cm^{-1}$ (Figure 12.3). This should not be considered a limiting value, as significantly larger conductivities should be achievable for thinner and longer ideal metallic SWNTs [18]. NTs can also carry very large current densities of up to $100\,MA\,cm^{-2}$ [19], with observed carrier mobilities as high as $10^5\,cm^2\,V^{-1}\,s^{-1}$ for semiconducting NTs [20]. Superconductivity has also been observed in SWNTs, albeit with transition temperatures of 5 K [21].

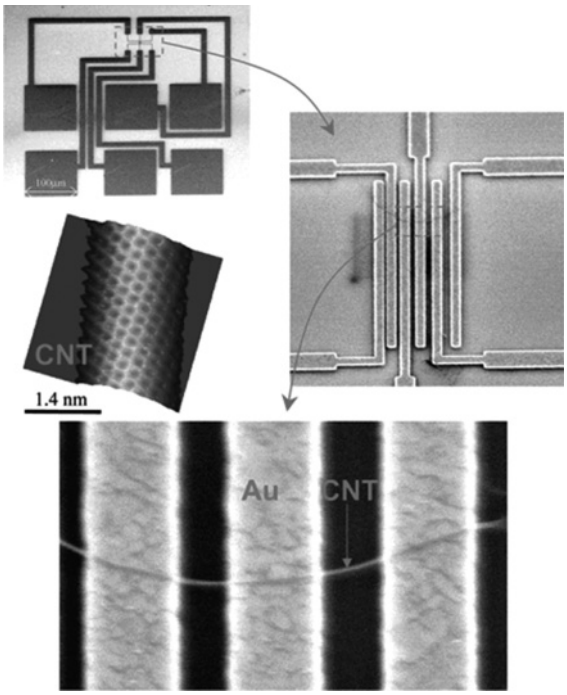

Figure 12.3 Electron microscope image of the metal electrodes used to measure the electrical properties of individual NTs. Inset: atomic resolution scanning tunneling microscope (STM) image of a NT. (Reprinted with permission from Reference [18]. Copyright 2002 American Chemical Society.)

In addition, it has been demonstrated that individual semiconducting SWNTs exhibit excellent transistor characteristics ($I_{ON}/I_{OFF} = 10^6$) [22]. However, these devices can not be prepared through controlled synthesis. Using carbon nanotubes organized into a network is a way around the synthesis problem as the properties then depend on all of the nanotubes (semiconducting and metallic). However, this comes at a cost as the properties are reduced by several orders of magnitude (conductivity = $10^3\,S\,cm^{-1}$; transistor characteristics, $I_{ON}/I_{OFF} = 10^4$) [23]. The conductivity of nanotube fibers is similar to that of the nanotube network, but is still several orders of magnitude below the possible maximum (ballistic transport).

Nanotubes are thermally stable at temperatures exceeding 1000 °C and also very conductive for phonons. Theory predicted a room temperature thermal conductivity of up to $6000\,W\,mK^{-1}$ (twice that of diamond) [24], a value that has recently been measured [25].

12.2.2
Mechanical Properties

Since the discovery of NTs it was expected that they would display superlative mechanical properties by analogy with graphite. In fact, NTs exhibit a unique tensile strength (100 times stronger than steel and ten times stronger than Kevlar) and an outstanding elastic Young's modulus (seven times that of steel).

The first direct mechanical measurements on NTs were made by Wong *et al.* in 1997 [26]. They used an atomic force microscope (AFM) to measure the stiffness constant of arc-MWNTs pinned at one end. This gave an average value for Young's modulus of 1.28 TPa. More importantly, they also managed to make the first strength measurements, obtaining an average bending strength of 14 GPa. Salvetat *et al.* have used an AFM to bend an arc-MWNT pinned at each end over a hole, obtaining an average modulus value of 810 GPa [27]. However, the ultimate measurements were carried out by Yu *et al.* in 2000 when they managed to perform stress–strain measurements on individual arc-MWNTs inside an electron microscope [28]. For a range of tubes they obtained modulus values of 0.27–0.95 TPa. Fracture of MWNTs occurred at strains of up to 12% and with strengths in the range 11–63 GPa. This allows the toughness of nanotube to be estimated as ~1240 J g^{-1}.

Measurements on SWNTs took longer due to difficulties in handling them. The first measurements were carried out by Salvetat *et al.* using their AFM method [29]. They observed a tensile modulus of ~1 TPa for small diameter SWNT bundles by bending methods. However, the properties of larger diameter bundles were dominated by shear slippage of individual nanotubes within the bundle. Yu *et al.* were able to measure the tensile properties of bundles by the same method they used for their MWNTs study. Moduli in the range 0.32–1.47 TPa were observed and strengths between 10 and 52 GPa.

The evaluated electrical, thermal and mechanical properties of NTs clearly surpass those of electroactive polymers. The challenge has been to incorporate NTs into polymer composite materials and achieve enhanced properties.

12.3
Carbon Nanotube-Polymer Composites

Nanotubes, in particular SWNTs, are typically held together as bundles, resulting in poor NT dispersion in polymer matrices. Since, due to the relatively smooth graphene like surface of NTs, there is a lack of interfacial bonding between polymer matrix and carbon nanotubes, surface modification by chemical means of NTs has been envisaged as a very important factor to overcome this problem and to facilitate NTs processing and applications [30].

There are two main approaches for the surface modification of NTs. One is the covalent attachment of functional groups to the walls and/or rims of the NTs, and the other is the noncovalent attachment of molecules [31].

In particular, when considering the covalent modification of NTs with polymers, two main strategies have been reported: "grafting to" and "grafting from." The "grafting to" approach is based on the attachment of already preformed end-functionalized polymer molecules to functional groups on the NT surface via different chemical reactions. The "grafting from" method is based on the initial immobilization of initiators onto the nanotube surface followed by the *in situ* polymerization of appropriate monomers with the formation of polymer molecules bound to the NT. Covalent attachment of functional groups to the surface of NTs can improve the efficiency of load transfer. However, these functional groups might introduce defects on the walls of the NT, modifying its electrical and mechanical properties. In contrast, the noncovalent attachment of polymers has the advantage of preserving the electronic properties of NTs. The main potential disadvantage of this methodology is that the forces between the polymer and the NT might be weak; thus, as a filler in a composite material, the efficiency of the load transfer might be low.

We now assess the progress made, considering both types of chemical approaches for the incorporation of NTs and polymers into composites.

12.3.1 Covalent Attachment

Carbon nanotubes can be separated and dispersed by chemical oxidation in acidic media [30], where the acid, however, not only dissolves any remaining metal catalyst but also removes the NT caps, leaving carboxylic acid (—COOH) residues behind. These groups allow the covalent linkage of oligomers or polymers to the nanotubes.

12.3.1.1 "Grafting to" Method

One of the first examples of the "grafting to" approach was published by Sun *et al.* in 2001 [32]. In this work carboxylic acid groups on the nanotube surface were converted into acyl chlorides by refluxing the samples in thionyl chloride. Then the acid chloride functionalized carbon nanotubes were reacted with hydroxyl groups of dendritic PEG polymers via esterification reactions. Similarly, many polymers terminated with amino or hydroxyl moieties have been used in amidation and esterification reactions with acid chloride modified NTs: poly(propionylethylenimine-*co*-ethylenimine) (PPEI-EI) [33], poly(styrene-*co*-aminomethylstyrene) (PSN) [34], poly-(amic acid) containing bithiazole rings [35], monoamine-terminated poly(ethylene oxide) (PEO) [36], poly(styrene-*co*-hydroxymethylstyrene) (PSA) [37], poly(styrene-*co*-*p*-[4-(4′-vinylphenyl)-3-oxabutanol]) (PSV) [38], poly(vinyl alcohol) (PVA) [39], poly(vinyl acetate-*co*-vinyl alcohol) (PVA-VA) [40] or poly[3-(2-hydroxyethyl)-2,5-thienylene] (PHET) [41].

In a recent example, the interfacial grafting reaction between MWNTs and a newly designed non-fluorinated polyetherimide (BisADA-DCB) (Scheme 12.1) was carried out using simple carboxylic acid-functionalized MWNTs [42]. The tensile strength and modulus of the BisADA-DCB films grafted with carboxylic acid-

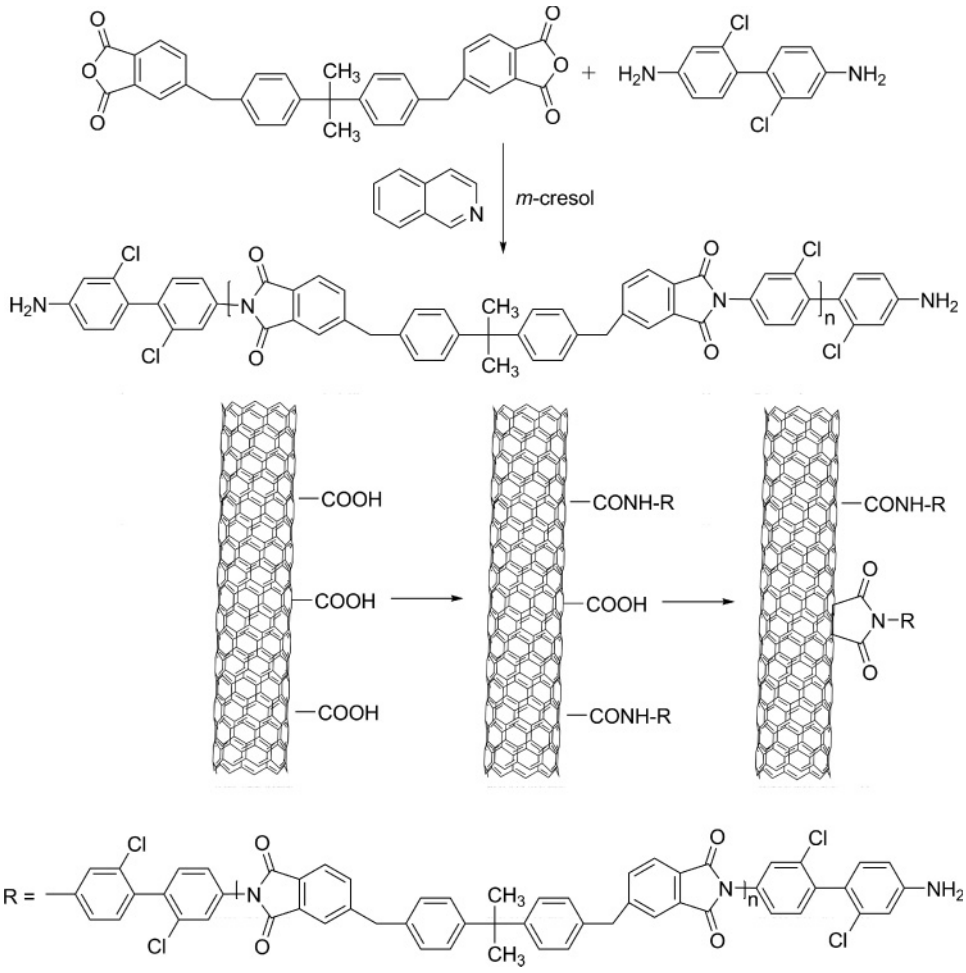

Scheme 12.1 Schematic representation for the chemical grafting of the aromatic polyimide synthesized from BisADA and DCB onto MWNTs.

functionalized MWNTs increase with MWNTs concentration (0.14–0.38 wt%). The tensile strength ranges between 131 and 194 MPa, the modulus between 3.7 and 4.4 GPa and the elongation at break (ϵ_b) between 10% and 7%. These compare with 121 MPa and 2.9 GPa, respectively, with an ϵ_b of 16% without the MWNTs. The improvement in the mechanical properties is therefore significant.

Covalent modification of NTs considering these straightforward reactions has also resulted in composites with potential biomedical applications. In this sense, Dwyer and coworkers have presented the use of amino-terminated DNA stands in functionalizing the open ends and defect sites of oxidatively prepared SWNTs, an

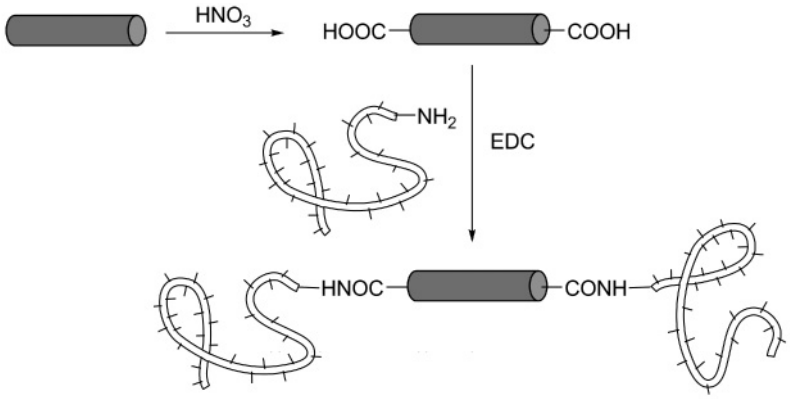

Scheme 12.2 Capped NTs are oxidatively opened and then reacted with amine-terminated single-stranded DNA.

important first step in realizing a DNA-guided self-assembly process for NTs (Scheme 12.2) [43].

Ferritin and bovine serum albumin (BSA) proteins can also chemically bond to nitrogen-doped MWNTs (CNx-MWNTs) through a two-step process of diimide-activated amidation. Firstly, carboxylated CNx-MWNTs were activated by *N*-ethyl-*N*′-(3-dimethylaminopropyl)carbodiimide hydrochloride (EDAC), forming a stable active ester in the presence of *N*-hydroxysuccinimide (NHS). Secondly, the active ester was reacted with the amine groups on the proteins of ferritin or BSA, forming an amide bond between the CNx-MWNTs and proteins. This two-step process avoids the intermolecular conjugation of proteins, and guarantees the uniform attachment of proteins on NTs (Scheme 12.3) [44].

Wong *et al*. have demonstrated that NT tips with the capability of chemical and biological discrimination can be created with acidic functionality and by coupling basic or hydrophobic functionalities or biomolecular probes to the carboxyl groups that are present at the open tip ends. These modified NTs have been used as AFM tips to titrate acid and base groups, to measure the binding force between single protein–ligand pairs and to image patterned samples based on molecular interactions [40].

In addition to acyl chloride functionalized NTs, the covalent "grafting to" of polymers onto NTs has been carried out for other reactions. A polystyrene azide ($PSt\text{-}N_3$) with a designed molecular weight and a narrow molecular weight distribution was synthesized by atom transfer radical polymerization of styrene followed by end group transformation and then added to SWNTs via a cycloaddition reaction (Scheme 12.4) [45].

A radical polymerization has been developed by Liu *et al*. [46] to prepare polymer or copolymer grafted SWNTs. The radical chains of polystyrene and poly(*tert*-butyl acrylate-*b*-styrene) with well-defined molecular weights and polydispersities, prepared by nitroxide-mediated free-radical polymerization, were successfully used to

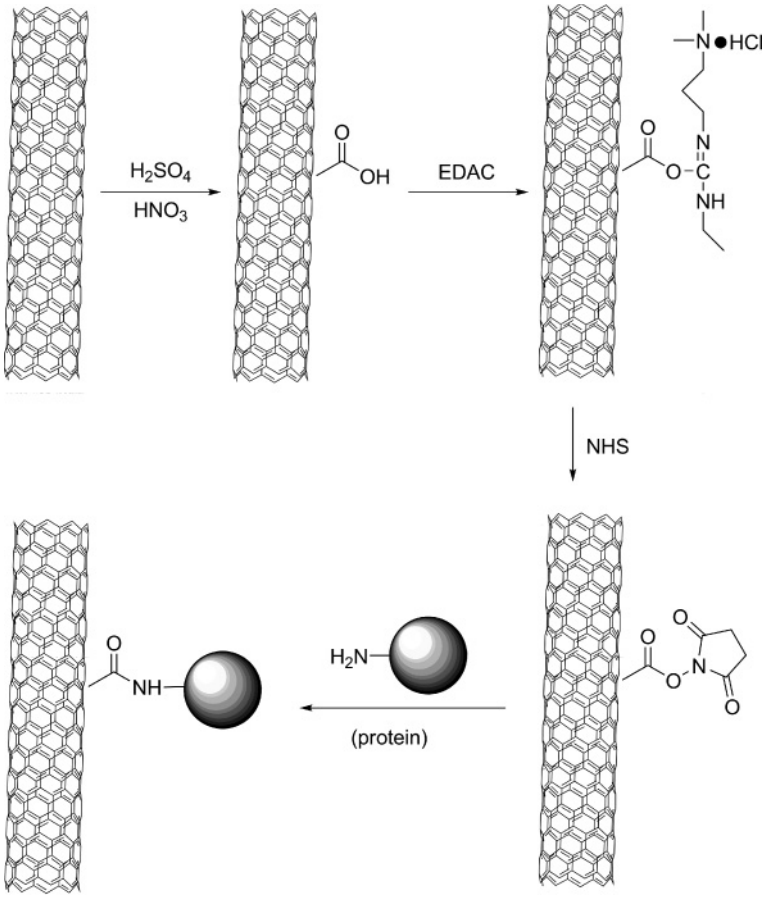

Scheme 12.3 Attachment of proteins to NTs via a two-step process of diimide-activated amidation.

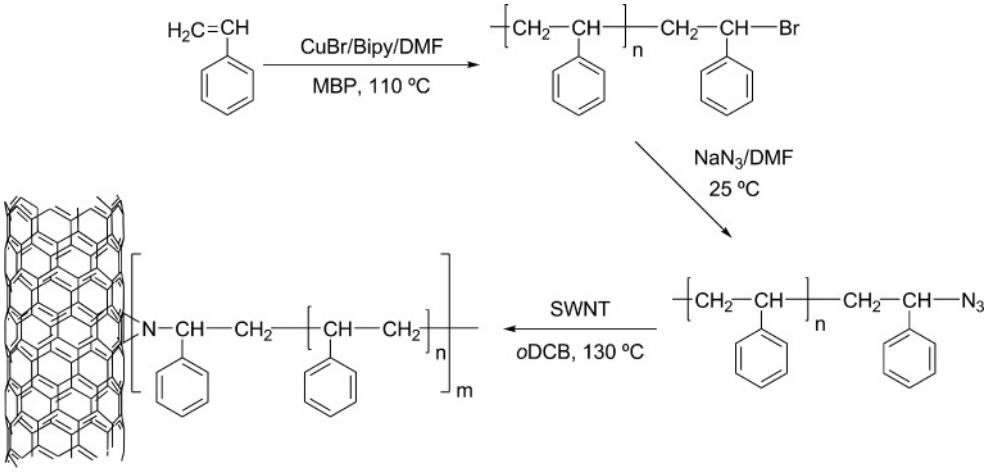

Scheme 12.4 Addition of PSt-N_3 to SWNTs.

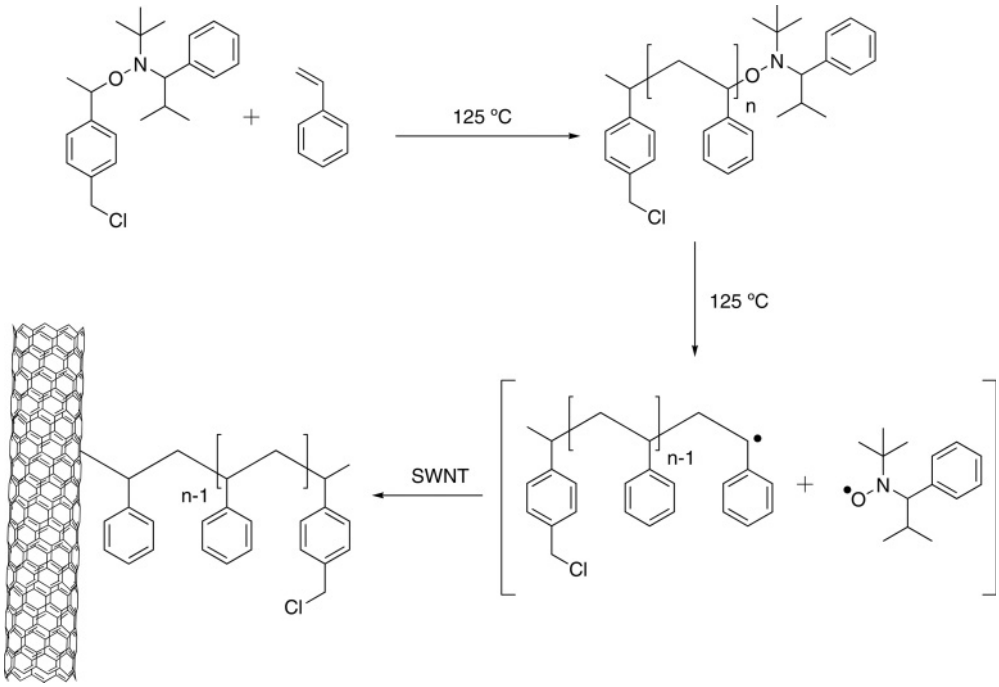

Scheme 12.5 Functionalization of SWNTs with polymers by radical coupling.

functionalize the SWNTs through a radical coupling reaction involving polymer-centered radicals at 125 °C via loss of a stable free-radical nitroxide capping agent (Scheme 12.5).

The covalent functionalization of NTs via 1,3-dipolar cycloadditions [47] is a powerful method for enhancing the ability to process NTs and facilitating the preparation of hybrid composites. Pantarotto *et al.* have used this synthetic approach for the preparation of peptide-NTs **1** and **2** (Figure 12.4). The bound peptide to the foot-and-mount disease virus (FMDV) (**2**) retained the structural integrity of the virus and was recognized by monoclonal and polyclonal antibodies [48]. The peptide-NT conjugate **2** is immunogenic, eliciting antibody responses of the right specificity. Such a system could be greatly advantageous for diagnostic purposes and could find future applications in vaccine delivery.

Concerning 1,3-dipolar cycloadditions, Prato and coworkers have also functionalized MWNTs with phenol groups, providing stable dispersions in a range of polar solvents, including water. An advantage of the phenolic functionalities is that they allow post-functionalization of the MWNTs with other molecules that can be employed in preparing customized products (**3** and **4** in Figure 12.4) or in combination with polymers and layered aluminosilicate clay minerals to give homogeneous, coherent and transparent NT thin films and gels [49].

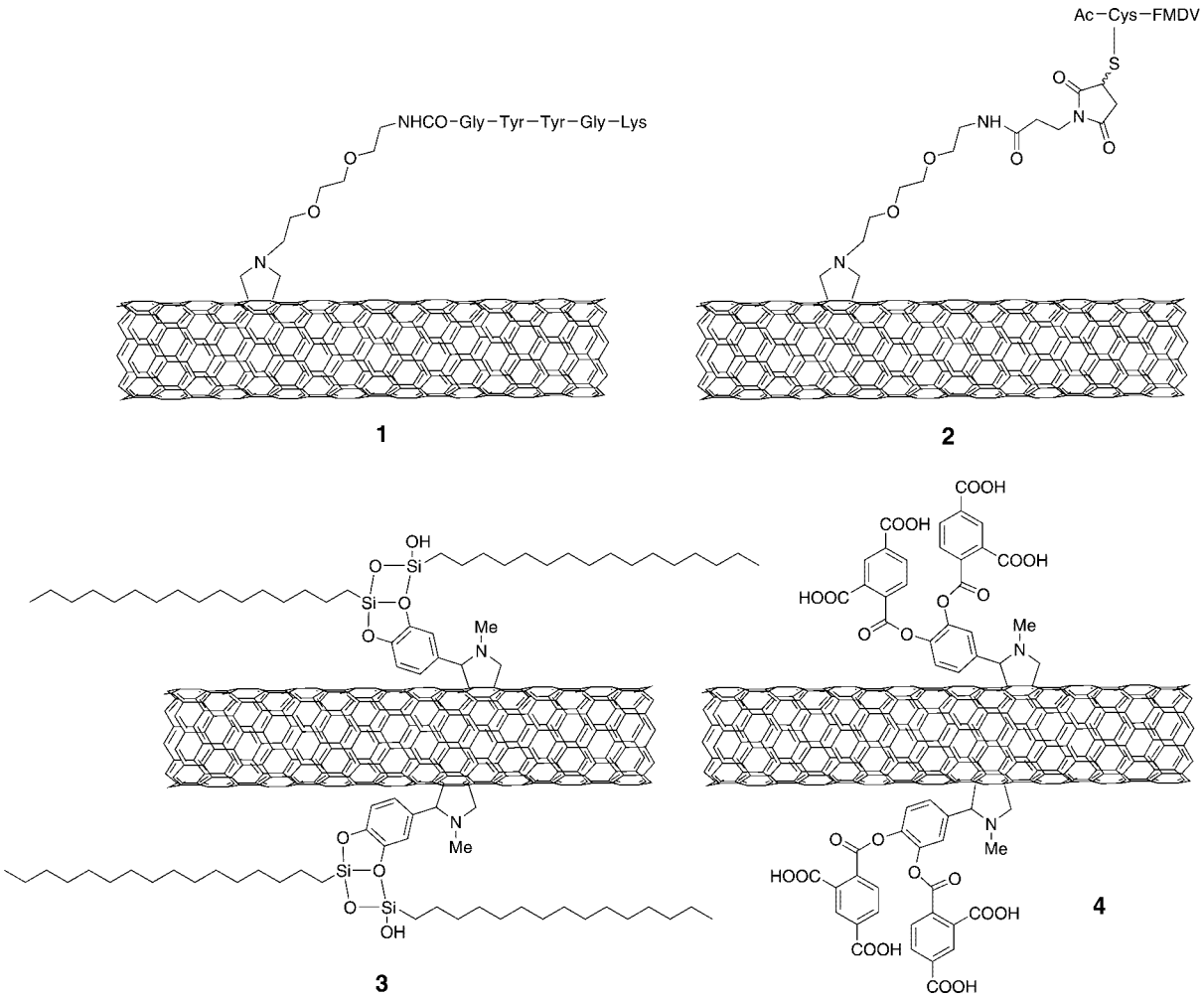

Figure 12.4 NT conjugates obtained by 1,3-dipolar cycloaddition reactions.

12.3.1.2 "Grafting from" Method

An example of the "grafting from" strategy is the treatment of SWNTs with *sec*-butyllithium, which generates carbanions on the nanotube surface. These carbanions serve as initiators of anionic polymerization of styrene for *in situ* preparation of polystyrene-grafted NTs [50]. This procedure allows the debundling of SWNTs and produces homogeneous dispersions of NTs in polystyrene solutions.

Guan *et al.* have reported the synthesis of an individual poly-acrylamide-NTs (PAMNTs) copolymer by an *in situ* UV radiation initiated polymerization of acrylamide in aqueous solution in the presence of MWNTs [51].

Using the "grafting from" approach Tong *et al.* have modified SWNTs with polyethylene (PE) by *in situ* Ziegler–Natta polymerization. In this work the surface of the SWNTs was initially functionalized with the catalyst ($MgCl_2/TiCl_4$), and then the ethylene was polymerized, thereby giving PE-grafted SWNTs, which were mixed with commercial PE by melt blending [52].

The "grafting from" technique is widely used for the preparation of poly(methyl methacrylate) (PMMA) and related polymer grafted NTs. For example, Qin *et al.* have reported the preparation of poly(*n*-butyl methacrylate) grafted SWNTs by attaching *n*-butyl methacrylate (*n*BMA) to the ends and sidewalls of SWNTs via atom transfer radical polymerization (ATRP) using methyl 2-hydroxyethyl 2-bromopropionate as the free radical initiator (Scheme 12.6) [53]. A similar approach has been reported by Hwang *et al.* for the synthesis of PMMA grafted MWNTs by using potassium persulfate as initiator [54] and, by Xia *et al.* for the modification of MWNTs with poly(butyl acrylate) PBA) and PMMA polymers [55]. The PBA and PMMA polymer encapsulated NTs could be used to reinforce Nylon 6 matrices [55].

In another example, Baskaran *et al.* used MWNT-COOH to attach the ATRP initiator, hydroxyethyl 2-bromoisobutyrate; the initiator-modified MWNT was then used for the *in situ* ATRP of PS and PMMA from MWNTs [56].

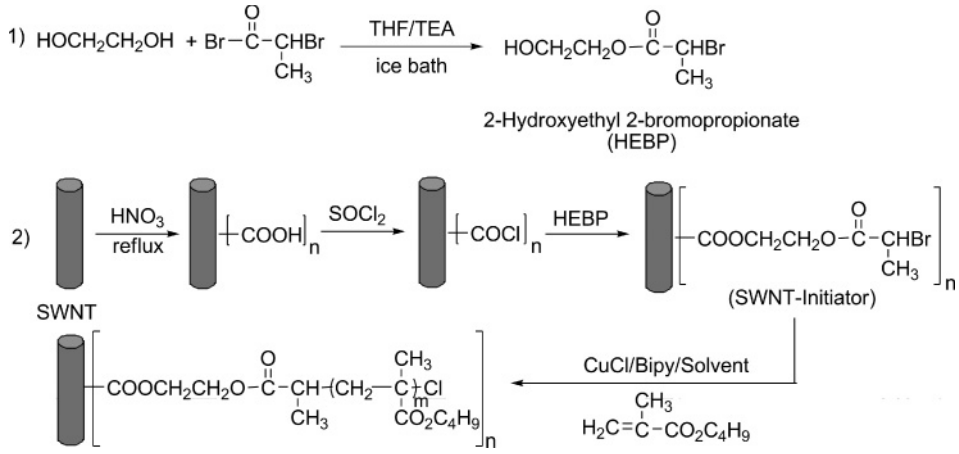

Scheme 12.6 Polymer grafted SWNTs by ATRP of *n*-butyl methacrylate.

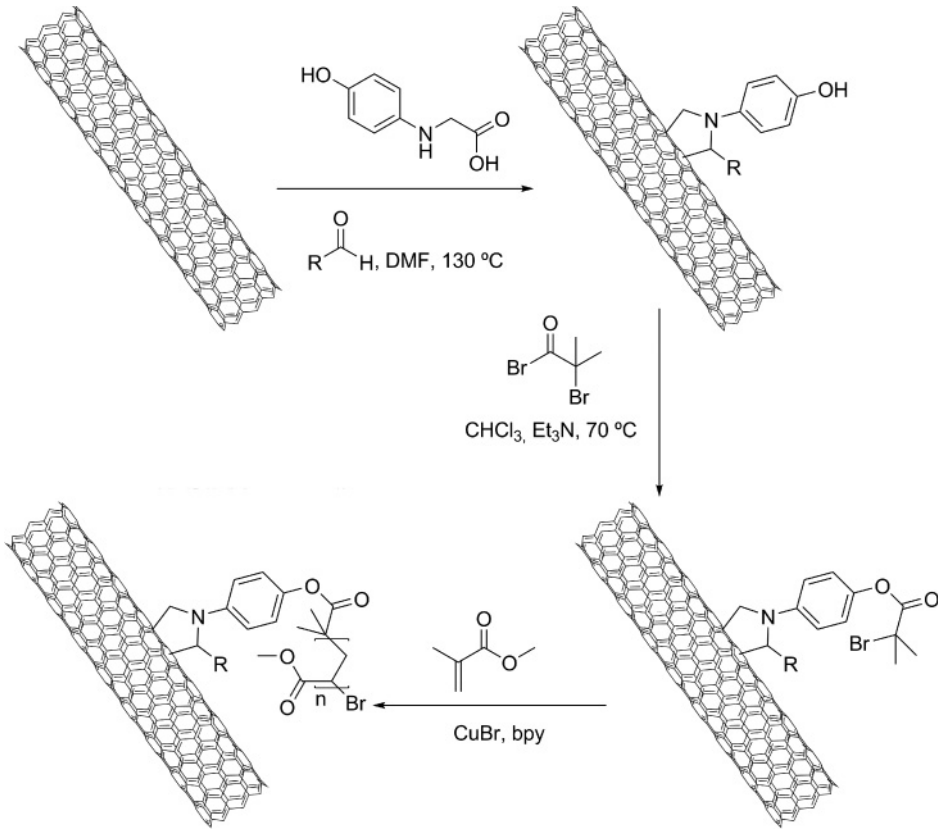

Scheme 12.7 Functionalization of shortened SWNTs with ATRP initiators and the ATRP of MMA.

The 1,3-dipolar cycloaddition reaction has also been used in "grafting from" approaches for the preparation of NT-polymer composites. In this respect, SWNTs were functionalized along their sidewalls with phenol groups, which were further derivatized with 2-bromoisobutyryl bromide, resulting in the attachment of ATRP initiators to the sidewalls of the nanotubes. These initiators were active in the polymerization of methyl methacrylate (MMA) and *tert*-butyl acrylate (*t*-BA) from the surface of the NTs (Scheme 12.7) [57].

12.3.2
Noncovalent Attachment

In a different approach towards the preparation of polymer/NTs composites, polymers have been used in the formation of supramolecular complexes with NTs. Besides possibly improving the mechanical and electrical properties of polymers,

the formation of polymer/NTs composites is considered to be a useful approach for incorporating NTs into polymer based devices [58].

In particular, the rate of scientific publications on conducting polymers and NTs has steadily increased since their discoveries in 1977 [59] and 1991 [1], respectively, to around 120 articles per week, indicating that interest in polymers, NTs and their composites continues to grow. (The number of publications was obtained from the Web of Science database for the term "carbon nanotubes or conducting polymers": www.isiwebofknowledge.com.)

In initial experiments, SWNTs were added to a solution of poly-(*m*-phenylenevinylene) (PmPV) substituted with octyloxy alkyl chains, and a stable suspension of NTs was obtained upon sonication due to the wrapping of the polymer around NTs [58c, 60]. The SWNT/PmPV complex exhibits a conductivity eight-times higher than that of the pure polymer, without any restriction on its luminescence properties. Similar conjugated luminescent polymers, such as poly(*m*-phenylenevinylene-*co*-2,5-dioctyloxy-*p*-phenylene vinylene) (PmPV-*co*-DOctOPV) [61] and its derivatives, such as poly(2,6-pyridinylenevinylene-*co*-2,5-dioctyloxy-*p*-phenylene vinylene) (PPyPV-*co*-DOctOPV) [62] and poly(5-alkoxy-*m*-phenylenevinylene)-*co*-2,5-dioctyloxy-*p*-phenylene vinylene) (PAmPV-*co*-DOctOPV) (Figure 12.5) [63] have formed supramolecular complexes with NTs. Stoddart *et al.* [64] have also synthesized stilbenoid dendrimers, a hyperbranched variant of the PmPV polymer, which exhibits an appropriate degree of branching; they were found to be more efficient at breaking up nanotube bundles, provided they are employed at higher polymer-to-NTs ratios than the parent PmPV polymer.

Homogeneous nanocomposites of poly(phenyleneethynylene) (PEE)-SWNTs/polystyrene (PS) and PPE-SWNTs/polycarbonate were noncovalently functionalized and revealed dramatic improvements in the electric conductivity with very low percolation thresholds (i.e., 0.05–0.1 wt% SWNTs loading) [65].

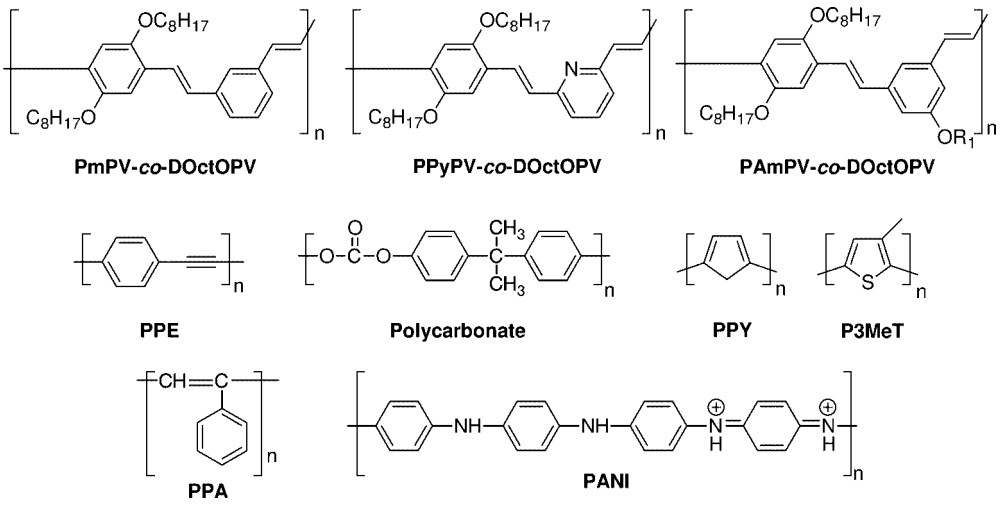

Figure 12.5 Conductive polymers that wrap around NTs.

Among the many conducting polymers, polypyrrole (PPY) stands out as a material of great promise in terms of commercial applications. Notable properties include high conductivity, air stability and ease of preparation. Nanotubular MWNTs/PPY materials have been prepared using *in situ* polymerization [66]. While no meaningful chemical interactions were observed to arise between MWNTs and PPY, the conducting PPY modified the physical properties of NTs. When applying electrochemical polymerization conditions, MWNTs were simultaneously co-deposited with PPY and poly(3-methylthiophene) (P3MeT) to yield nanoporous composite films [67].

Tang and Xu [68] have prepared soluble MWNT-containing photoconductive poly(phenylacetylenes) (NTs/PPAs) by *in situ* polymerizations of phenylacetylene catalyzed by WCl_6-Ph_4Sn and $[Rh(nbd)Cl]_2$ (nbd = 2,5-norbornardiene) in the presence of the NTs. They demonstrated that the NTs in the composite solutions can be easily aligned by mechanical shear, and an efficient optical limiting property was observed in these nanocomposite materials.

Molecular dynamics studies carried out on the interactions of PS, PPA, PmPV (Figure 12.5) and *p*-phenylene vinylene (PPV) with SWNTs in vacuum indicate that the interaction between the NTs and the polymer is strongly influenced by the specific monomer structure [69]. NT–polymer interactions are strongest for conjugated polymers with aromatic rings on the polymer backbone, as these rings can align parallel to the NT surface and thereby provide strong interfacial adhesion. In the presence of well-separated NTs, different polymer chains become disentangled and align the NTs to cover their surface. This is a general observation for all investigated polymers, although the effect is most pronounced for PmPV, which combines a certain flexibility in the backbone structure, flexible side chains and strong interaction with the NTs surface.

Another fascinating class of composites arises from the combination of NTs and aniline. Polyaniline (PANI) has particularly great possibilities in synthesizing polymer/CNT composites due to its environmental stability, good processability and reversible control of conductivity both by protonation and charge-transfer doping. Several recent reports have focused on the design and fabrication of PANI/NTs composites [10b, 70]. For example, Wu *et al.* [71] have described the synthesis of doped polyaniline in its emeraldine salt form (polyaniline emeraldine salt, PANI-ES) with MWNTs fabricated by *in situ* polymerization. The as-prepared MWNTs were treated using a 3 : 1 mixture of concentrated H_2SO_4 : HNO_3, which produced carboxylic acid groups at the defect sites. Based on the π–π electron interaction between aniline monomers and MWNTs and hydrogen bonding interactions between the amino group of aniline monomers and the carboxylic acid groups of the modified MWNTs, aniline molecules were adsorbed and polymerized on the surface of MWNTs. Structural analysis of the composites formed by spectroscopic techniques showed the formation of tubular structures with diameters of several tens to hundreds of nanometers, depending on the PANI content. The electric conductivities at room temperature of PANI-ES/MWNTs composites are 50–70% higher than those of PANI without MWNTs [71].

Although poly(9,9-dialkylfluorenes) exhibit the extended conjugation required for π-stacking to the NTs surface, they have thus far attracted limited attention as

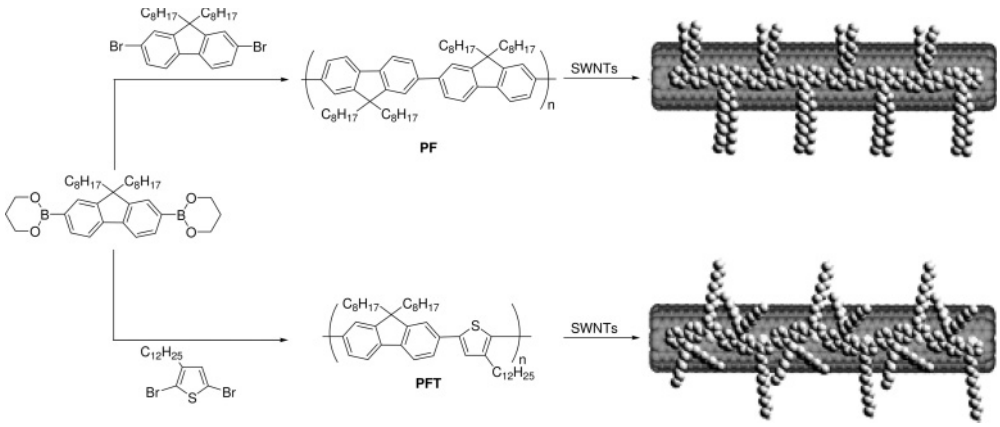

Scheme 12.8 Preparation of conjugated PF and PFT polymers and a cartoon representation of their interaction with SWNTs. (Reprinted with permission from Reference [73]. Copyright 2008 American Chemical Society.)

supramolecular attends for SWNTs [72]. Only recently, have poly(9,9-dialkylfluorene) (PF) and poly(9,9-dialkylfluorene-*co*-3-alkylthiophene) (PFT) been used to prepare discrete polymer-SWNTs complexes which showed excellent solubilities in organic solvents in the absence of excess free polymer (Scheme 12.8) [73]. Both the polymer structure and the solvent used strongly influence the dispersion of the NTs; it is not only possible to prepare SWNT solutions with different solubilities but also to perform selective solubilization of SWNTs with the ability to selectively tune the distribution of NT species that are solubilized [74].

In addition, much research has been carried out with non-conducting polymers. Linear polymers that bear polar octyloxy alkyl side-chains, such as poly(vinyl pyrrolidine) (PVP) and polystyrene sulfonate (PSS) (Figure 12.6), also form stable composite materials with NTs [75].

Various approaches have been developed to improve the solubility of NTs in different polymer matrices. The addition of 1 wt% non-ionic surfactants improves, for instance, the glass transition temperature. Moreover, the elastic modulus increased by more than 30% relative to the absence of a surfactant [76]. In the presence of 0.5 wt% poly(vinylene fluoride) (PVDF) the storage modulus of MWNTs/PMMA composites was significantly improved at low temperatures [77].

Water-soluble poly(diallyl-dimethylammonium chloride) (PDDA)/MWNTs aggregates have been also obtained by mild sonication [78]. In these composites, it has been suggested that the interaction between PDDA and MWNTs is not electrostatic in nature but, instead, the presence of unsaturated impurities in the PDDA chain drives π–π interactions. Thus, NTs coated with PDDA function as positively charged polyelectrolytes that exhibit electrostatic repulsion between NTs/PDDA, thereby guaranteeing the NTs hydrophilicity.

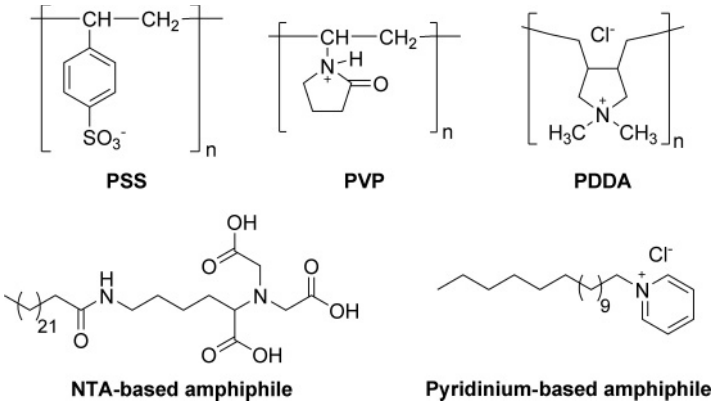

Figure 12.6 Polyelectrolytes and amphiphiles that noncovalently functionalize NTs.

Surfactants and analogous systems also self-assemble on the surface of NTs [79]. When amphiphilic surfactants are mixed with NTs at a concentration greater than the critical micellar concentration (CMC) they self-organize as hemimicelles on the NT surface. While the hydrophobic portion of the amphiphile is adsorbed on NTs walls by van der Waals interactions, its hydrophilic headgroup is oriented towards the aqueous phase, producing half-cylinders that prevent aggregation and induce stable nanotube suspensions in water. Amphiphiles containing a long alkyl chains and polar heads made of either nitrolotriacetic acid (NTA) or pyridinium (Figure 12.6) efficiently solubilized NTs and provided an effective template for the homogeneous and dense deposition of noble metal nanoparticles (NPs) on the NTs surface [80]. Electrocatalytic applications of the resulting nanohybrids were evaluated, and superior activity in certain oxidation reactions, compared to similar systems, was observed.

It is essential to solubilize NTs in aqueous media to improve their biocompatibility and enable their environmentally friendly characterization, separation and self-assembly. To exploit the unique properties of NTs in biologically relevant systems, SWNTs have been suspended in water-soluble amylose in the presence of iodine [81]. Very likely, iodine plays a key role in the initial preorganization of amylose in support of a helical conformation. Since this process is reversible at high temperatures, it opens up the exciting opportunity of employing the strategy to separate SWNTs from amorphous carbon.

DNA molecules may be also encapsulated inside, or wrap around, NTs owing to van der Waals attraction between DNA and NTs. Advances in this field have been reviewed by Gao and Kong [82].

Considering other important biological molecules, an amphiphilic α-helical peptide has been coated successfully to NTs by folding. The peptide can disperse the NTs in aqueous solutions by noncovalent interactions with their surface [83]. Analysis of the aggregates formed showed the presence of individual peptide wrapped SWNTs, possibly connected end-to-end, into long fibrillar structures [84].

12.4
Applications of NT-Polymer Composites

The functionalization of NTs with polymers via covalent or supramolecular methods has played a vital role in tailoring the engineering of NT-based nanodevices and nanosensors [12]. Several research groups have reported the functionalization of NTs with different polymers, which not only increased the solubility and processability of NTs but also endowed them with new properties [85]. In this section we present some representative examples of modified NTs responsive to stimuli, which have interest in different areas, such as materials science and biological applications.

12.4.1
Thermo- and pH-Responsive NT-Polymer Composites

Poly(*N*-isopropylacrylamide) (PNIPAM) has been widely investigated for biomedical applications owing to the entropy change of the polymer from a water-soluble coil to a hydrophobic globule at ~32 °C. For this reason, modification of NTs with PNIPAM chains can make NTs responsive to temperature (Scheme 12.9a). NTs have been functionalized with PNIPAM by considering different approaches: (i) a reversible addition–fragmentation chain transfer (RAFT) agent was immobilized onto the surface of MWNTs, and subsequently PNIPAM chains were grafted onto

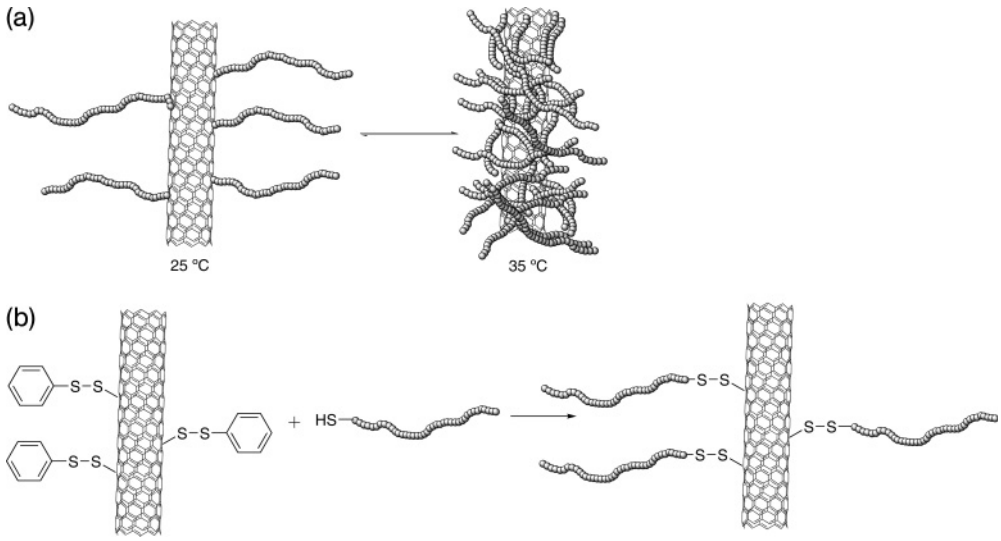

Scheme 12.9 Schematic representations of:
(a) conformational changes of PNIPAM chains on NTs;
(b) the modification of NTs with a temperature-responsive polymer via glutathione-sensitive linkages.

the NTs via surface RAFT polymerization of NIPAM [86], (ii) via ATRP of NIPAM using NT-supported ATRP initiators [87] and (iii) the noncovalent modification of NTs with PNIPAM [88].

The NT-PNIPAM dispersion/aggregation states controlled by temperature were completely reversible, and have potential application in smart sensors and probes, reusable catalysts, delivery of drugs and proteins, smart separators and scaffolds to target different tissues. In a recent example, PNIPAM-S-S-NTs conjugates (Scheme 12.9b) were obtained via a thiol coupling reaction of the thiol ends of PNIPAM and the pyridyldithio functionalities previously introduced on the surface of the NTs [89]. The PNIPAM-S-S-NTs conjugates have temperature-responsive PNIPAM chains, and the disulfide linkages between PNIPAM and the NTs are sensitive to bio-stimuli such as glutathione; therefore, dually-responsive PNIPAM-NT conjugates have been obtained.

Polymers with pyrene-terminal functionalities and containing poly(ethylene glycol) methacrylate (PEGMA) and 2-(2-methoxyethoxy)ethyl methacrylate (DEGMA) (Scheme 12.10) have also demonstrated a thermo-responsive water-dispersant ability of NTs, with a tunable capability between 29 and 91 °C by modification of the copolymer composition [90].

Zhao *et al*. were one of the first to observe that the optical absorption of semiconducting NTs reversibly responded to pH changes after surface modification with carboxylate groups [91]. PSS-functionalized NTs can also be transformed into water-soluble structures through sulfonation of the grafted PSS chains using acetyl sulfate; the resulting sulfonated composites are pH responsive. They are soluble in water between pH 3 and 13, and insoluble outside of this range, precipitating from the solution [92].

Another example is the composites formed by poly(acrylic acid) (PAA)-modified SWNTs [93]; the viscosity of these aggregate suspensions is responsive to pH. At low shear rates ($<100\,s^{-1}$) the viscosity increased as the pH rose from 2.9 to 9.2. The reversibility of these changes was observed when the pH of the suspension was reduced progressively from 9.2 to 2.9; this effect arises from the chemical and conformational changes in PAA that take place with changes in pH.

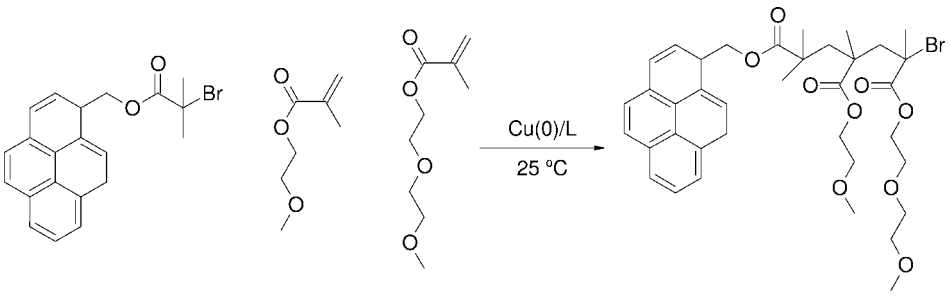

Scheme 12.10 Synthesis of pyrene-terminal polymers for the thermo-responsive functionalization of NTs.

Stable NT-lysozyme (LSZ) complexes can be obtained by dispersing NTs in an aqueous solution of LSZ (isoelectric point at pH 10.02); they exhibit pH-responsive properties [94]. The NT-LSZ remains in a highly dispersed state at pH < 8 and at pH > 11 (lysozyme highly charged), whereas in the pH range 8–11 (lysozyme not charged) the NT-LSZ aggregates become insoluble. The secondary and tertiary structures of most of the lysozyme are well preserved – a feature that holds promise for the development of NT-based biomedical devices.

12.4.2 Molecular Sensors

The conductivity and fluorescent properties of NTs have been well developed to detect trace molecules in solution [95]. For example, NT-DNA aggregates can be used to detect trace amounts of metal ions in whole blood, opaque solutions and living mammalian cells owing to the change in shape that occurs on the DNA structure after the recognition event. The NT surface covered by the DNA is thus modified, and the electronic structure of the NT is perturbed, shifting the natural near-infrared fluorescence to a lower energy [96]. The process is reversible and reusable and has also been used for the recognition of biological molecules [97].

The chiral properties of NTs have, however, not been particularly well studied and applied. Only recently has a new type of sensor been designed to detect trace Hg(II) ions at the nM level by monitoring the induced circular dichroism (ICD) of SWNT-DNA aggregates [98]. In this sensor, the Hg ions coordinate to the bases of single-stand DNA, causing the interaction between the DNA and SWNTs to weaken, and the ICD signal to greatly decrease (Figure 12.7).

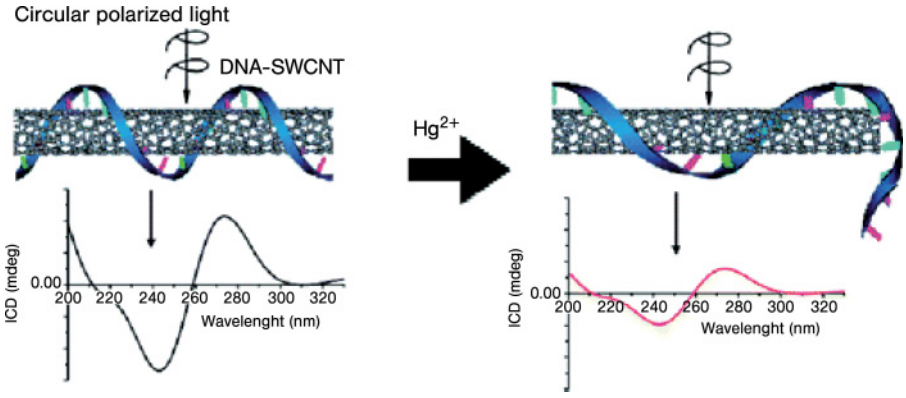

Figure 12.7 Illustration of Hg-induced ICD signal intensity change of SWNT-DNA aggregates. (Reproduced with permission from Reference [98]. Copyright 2008 American Chemical Society.)

Another kind of sensor has been developed by Strano and Barone for glucose [99]. SWNTs were first decorated with phenoxy-derivatized dextran via a noncovalent method, forming dextran-NT complexes, which can be well suspended in aqueous solution, and are responsive to concanavalin A (conA). The dextran-NTs assemble, due to the formation of ConA-dextran-NT complexes, and undergo a concomitant decrease in NT photoluminescence. Moreover, the ConA-dextran-NT complexes are responsive to glucose – they decomplexed after adding mM amounts of glucose owing to competitive binding between the glucose and dextran for ConA binding sites. At the same time, the photoluminescence of the NTs was recovered and the aggregates reformed after glucose was removed through dialysis.

12.4.3
Hybrid Gels

Recently, reports have appeared on the interaction of NTs with ionic liquids, organic molecules or OPVs to form composite gels [100]. In particular, the self-assembly of OPV molecules is accelerated through physical interaction with NTs in hydrocarbon solvents. As a result, the NTs are dispersed in the solvent, which facilitates the self-assembly processes and leads to the formation of hybrid π-conjugated gels. The individually dispersed NTs are significantly aligned within the OPV gel, thereby reinforcing the OPV supramolecular tapes and enhancing the gel stability.

Harada *et al*. have prepared supramolecular NT hydrogels via host–guest interactions between β-cyclodextrins (CDs) and guest dodecyl groups in PAA [101]. Pyrene-modified β-CDs were initially immobilized onto SWNTs surfaces via π–π stacking interactions, and the vacant CD cavities of the supramolecular aggregates formed were able to capture polymer-carrying guest moieties, such as PAA. The supramolecular hydrogel is chemically responsive and undergoes gel-to-sol transitions on adding competitive guest or hosts as shown in Figure 12.8. A gel-to-sol transition was observed after addition of sodium adamantane carboxylate (AdCNa), since this guest strongly interacts with β-CDs and the dodecyl groups are displaced. A gel-to-sol transition was also observed after the addition of α-CDs, a competitive host that complexes dodecyl moieties more favorably than β-CDs.

12.5
NT-Polymer Composites for Solar Energy Conversion

Here we focus on probably one of the most promising applications of NTs: their ability to transport electrons or holes efficiently when modified by photoactive molecules, forming donor–acceptor nanohybrid models as a building block in optoelectronic devices [14, 30].

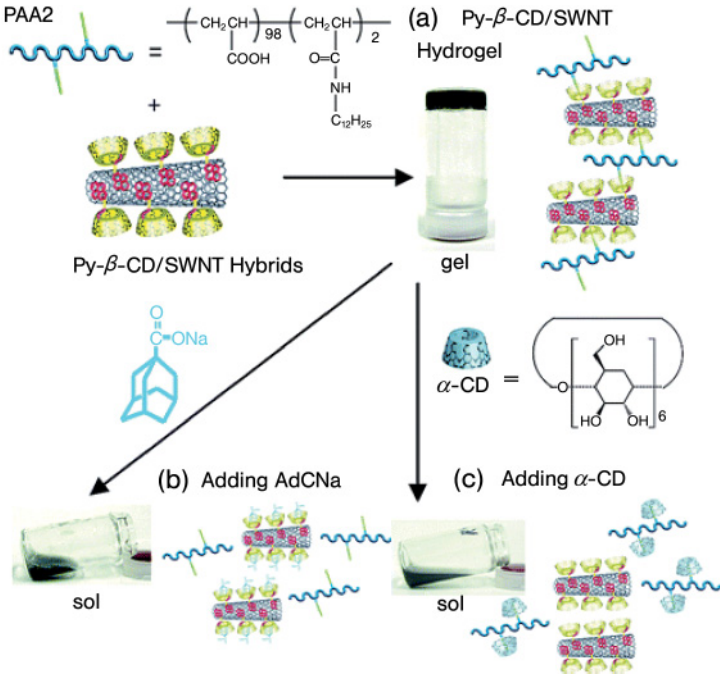

Figure 12.8 (a) Pyrene-β-CD-NT hydrogel with PAA. Gel-to-sol transitions upon addition of (b) competitive guest AdCNa and (c) competitive host α-CD. (Reproduced with permission from Reference [101]. Copyright 2007 American Chemical Society.)

12.5.1
NTs as Electron Acceptors in Donor–Acceptor Systems

The combination of NTs with oligomers or polymers bearing porphyrins that serve as visible light harvesting chromophores has been particularly beneficial. SWNTs were found to strongly interact with Zn-porphyrins (ZnPs) in ZnP conjugated polymers [102], triply fused ZnP-trimers [103] and just ZnP (Figure 12.9) [104]. Successful complexation with, for example, the ZnP-polymer was manifested in a 127 nm bathochromic shift of the Q-band absorption. Additional evidence for interactions of ZnP-polymer, ZnP-trimer and ZnP with SWNTs was obtained from fluorescence spectra, where the ZnP fluorescence was significantly quenched. The fluorescence quenching has been ascribed to energy transfer between the photo-excited porphyrin and SWNTs.

The formation of large scale donor–acceptor ensembles is also possible by π–π interactions between a porphyrin-peptide hexadecamer [$P(H_2P)_{16}$] (Figure 12.10) and SWNTs [105]. In this case, supramolecular formation occurs through π–π interaction between porphyrins and NTs together with wrapping of the peptidic backbone in $P(H_2P)_{16}$; this makes it possible to extract the large-diameter NTs (*ca.*

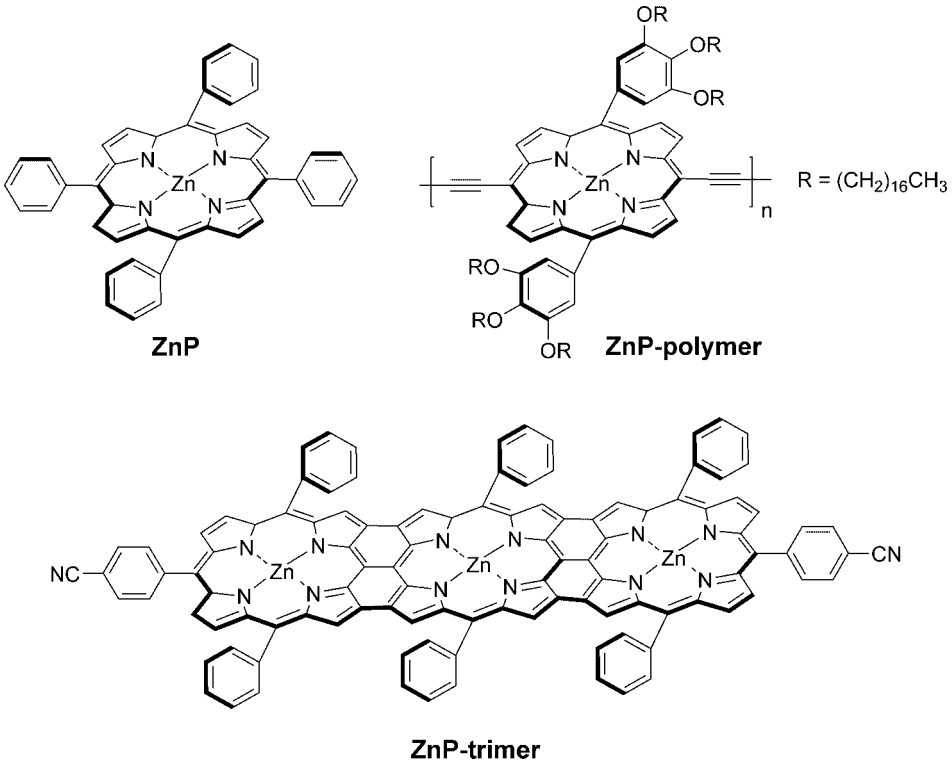

Figure 12.9 Leading examples of ZnP for the preparation of SWNT charge transfer nanohybrids.

1.3 nm), as revealed by ultraviolet/visible/near infrared and Raman spectroscopy as well as high-resolution transmission electron microscopy. This supramolecular approach enables not only the achievement of non-destructive and diameter-selective SWNT extraction methods but also the development of an efficient light energy conversion system. Laser photoexcitation of the $P(H_2P)_{16}$/SWNTs nanohybrids in DMF affords a long-lived charge-separated (CS) state (370 μs) that opens up a new strategy towards efficient light energy conversion [105].

A versatile approach to form donor–acceptor aggregates between NTs and porphyrins, preserving the unique electronic structure of the NTs, involves grafting SWNTs with polymers such as PSS (Figure 12.11a) [106]. The attached PSS^{n-} functionalities also assist in exfoliating individual SWNT-PSS^{n-} from the larger bundles. AFM and TEM analysis corroborated the presence of SWNTs with lengths reaching several micrometers and diameters around 1.2 nm. Coulomb complex formation with porphyrins was achieved between SWNT-$PSS^{n-}$and an octapyridinium H_2P salt (H_2P^{8+}) (Figure 12.11a). Several spectroscopic techniques were used to monitor the complex formation between SWNT-PSS^{n-} and H_2P^{8+} yielding nanohybrids that, after photoexcitation, generated an efficient CS state (14 μs) [106].

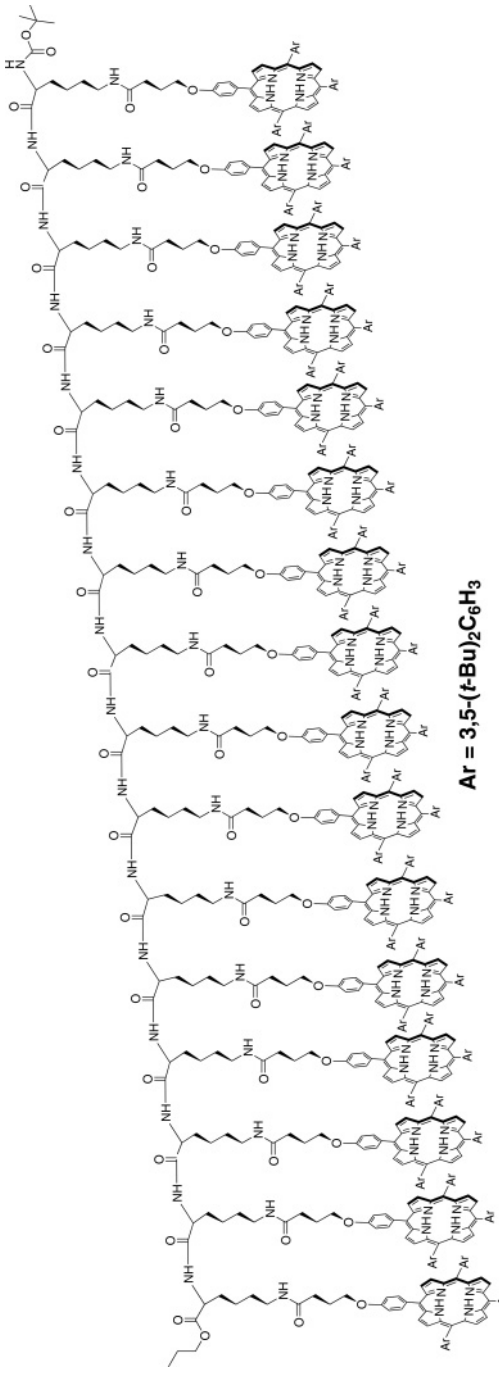

Figure 12.10 Structure of porphyrin-peptide hexadecamer [$P(H_2P)_{16}$].

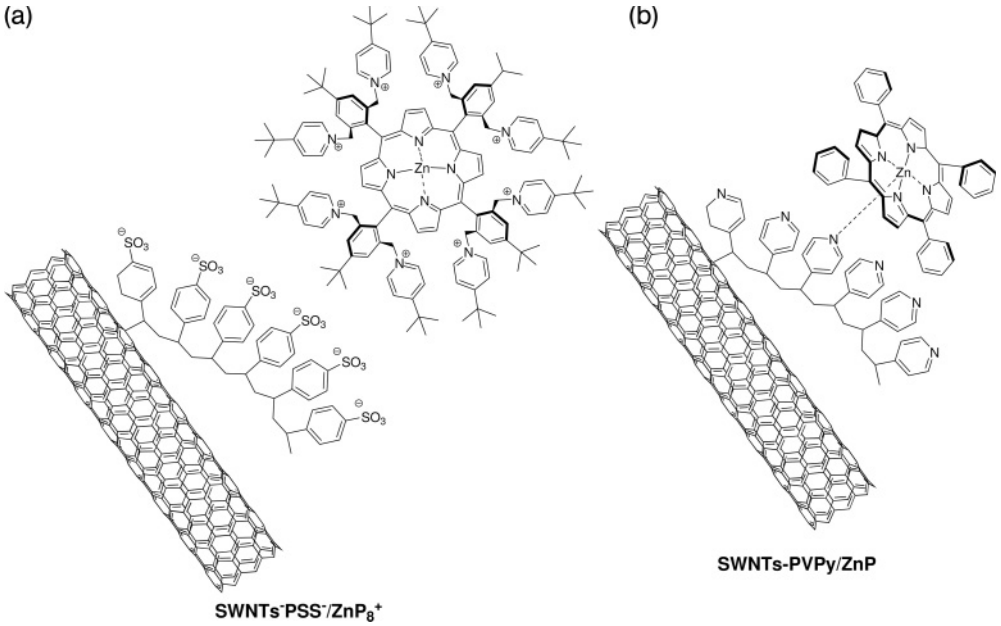

Figure 12.11 SWNT-based nanohybrids: (a) SWNT-PSS^{-}/ZnP^{8+}; (b) SWNT-PVPy/ZnP.

Similarly, dispersible SWNTs grafted with poly(4-vinylpyridine) (PVPy) have been coordinated with ZnP (Figure 12.11b). Support for the grafting of the polymers to the sidewalls of SWNTs came from Raman and near-infrared spectra, and the composition of the resulting SWNT-PVPy was estimated as 61/39. Kinetic and spectroscopic evidence corroborates the successful formation of SWNT-PVPy/ZnP nanohybrids in solution, which upon photoexcitation generate a μs-lived radical ion pair state [107].

12.5.2
NT-Polymer Composites in Photoelectrochemical Devices

For the systematic and molecularly controlled organization of SWNTs and electron donor molecules onto electrodes, Guldi *et al.* have used van der Waals and electrostatic interaction to prepare photoelectrochemical devices (Figure 12.12) [108]. First, PDDA^{n+} and PSS^{n-} were adsorbed sequentially onto indium tin oxide (ITO) substrates as base layers and then the substrate was immersed in the solution of SWNTs dispersed by pyrene derivatives bearing an ammonium group (pyrene^{+}) to deposit the composite SWNT-pyrene^{+} onto the base layer. Next, the negatively charged zinc porphyrin (ZnP^{8-}) was deposited to yield a layer-by-layer assembled film of ITO/PDDA^{n+}/PSS^{n-}/SWNT-pyrene^{+}/ZnP^{8-}. Photoelectrochemical measurements with a standard three-electrode system revealed an action spectrum with a shape similar to that of the absorption spectrum of ZnP^{8-}. The maximum

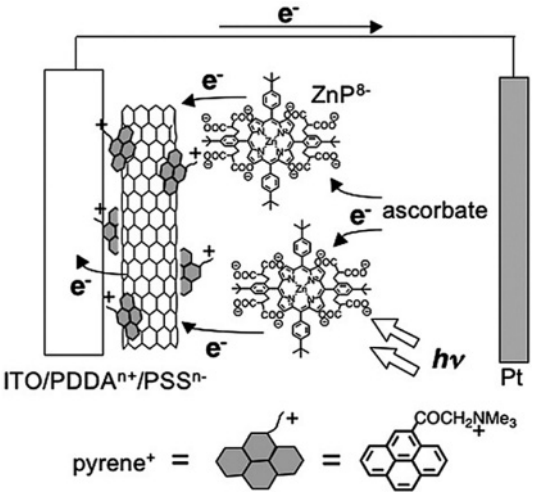

Figure 12.12 Schematic illustration for photocurrent generation in a photoelectrochemical cell using a ITO/PDDA^{n+}/PSS^{n-}/SWNT-pyrene^{+}/ZnP^{8-} electrode. (Reproduced with permission from Reference [14b]. Copyright 2008 Royal Society of Chemistry.)

incident photon-to-photocurrent efficiency (IPCE) was 4.2%, which is much higher than the 0.08% of the ITO/PDDA^{n+}/PSS^{n-}/ZnP^{8-} device without SWNTs. Furthermore, repetitive deposition steps allows modification of the base layer with multiply stacked SWNT-pyrene^{+}/ZnP^{8-}. The absorption property was enhanced linearly up to ten stacks and the maximum IPCE reached approx. 8.5% at an applied potential of 0.2 V vs. SCE, which is twice that of the device with a single layer of SWNT-pyrene^{+}/ZnP^{8-} [108].

Considering this approach, a polythiophene derivative (PSCOOH) and SWNT-pyrene^{+} were also integrated into photoactive ITO electrodes [109]. In the device, polythiophene can function as the light-harvesting chromophore that donates an electron to the electron-accepting SWNTs by photoinduced electron transfer. A higher maximum IPCE (9.3%) was obtained with eight layers of SWNT-pyrene^{+}/PSCOOH than that of the ITO/PDDA^{n+}/PSS^{n-}/SWNT-pyrene^{+}/ZnP^{8-} device [109].

Kamat *et al.* have shown that the composite of protonated porphyrin (H_4P^{2+}) and SWNTs form rod structures by sonication that disperses well in acidified THF [110]. In addition, when photocurrent measurements were performed using the ITO/SnO_2/SWNT-H_4P^{2+} as a photoanode, under the standard three-electrode conditions, a maximum IPCE of 13% was obtained at a bias potential of 0.2 V vs. SCE.

In this manner, layer-by-layer approaches using van der Waals and electrostatic interactions are universal and can be extended to the combination of SWNTs with various photoactive molecules. Hopefully, optimization of the molecular structure would achieve a further improvement in the photocurrent generation efficiency.

12.5.3
NT-Polymer Composites in Photovoltaic Cells

Polymeric solar cells have attracted great interest over the past 20 years [111]. This technology offers various advantages, including the absence of liquid electrolyte, mechanical flexibility and ease of large-area processing. NTs have been typically incorporated into active layers of polymer solar cells by the dispersion of NTs in a solution of an electron-donating conjugated polymer, such as PT or PPV derivatives, and spin-coating the composites onto a transparent conductive electrode, typically ITO, covered with a hole-blocking layer [112].

Friend *et al*. described the first investigation on the electronic properties of the composite formed by MWNTs and PPV derivatives [112a]. On the other hand, Kymakis *et al*. demonstrated an increase in cell performance by blending poly(3-octylthiophene) (P3OT) with only 1 wt% of SWNTs [112b]. Since their pioneering work, many groups have exploited NTs in bulk heterojunction solar cells [112c, 14]. However, the power conversion efficiencies of polymer–NT solar cells are only as high as approx. 0.2%, which is much lower than typical values of high-performance bulk heterojunction solar cells (3–6%) with a combination of π-conjugated polymers and fullerene derivatives, including PCBM ([6,6]-phenyl-C_{61}-butyric acid methyl ester) [113] and diphenylmethanofullerenes (DPMs) [114].

Recently, several groups have come up with an idea of employing SWNTs and MWNTs as the transparent conductive electrode [115], since high quality ITO is expensive due to the resource constraint of indium. In addition, ITO is not compatible with the roll-to-roll fabrication processing of today's market requirements for a full printable solar cell. For example, Rowell *et al*. have fabricated flexible transparent conducting electrodes by printing films of SWNT networks on a flexible poly(ethylene terephthalate) (PET) substrate and used them as transparent electrodes for poly(3-hexylthiophene) (P3HT)-PCBM bulk heterojunction solar cells [115a]. The power conversion efficiency was 2.5% under AM1.5 conditions, which is close to that of the ITO/glass system under their optimized conditions (3%). Further improvement of the performance may be possible through optimization of the SWNT network structure considering the high mobility of individual SWNTs.

12.6
Summary and Conclusions

In this chapter we have provided a general picture of the research carried out into carbon nanotubes polymer composites, from their chemical construction – considering both covalent and noncovalent approaches – to revision of the factors that ultimately control their properties, with particular emphasis on the promising properties of NTs in the cell performance of photoelectrochemical and NT-based solar cells.

For the successful future development of new polymer/NT composites, however, it is important to improve the quality of the NT raw material, with particular emphasis on the uniformity of the samples in terms of geometrical and electronic features. In this regard, a major challenge in the preparation of SWNTs is the production of NTs according to their metallic or semiconducting electrical properties. Furthermore, comparative studies on individual NTs before and after functionalization are necessary, so that both the dependence of reactivity on electronic structure and the effect of chemical modification on the electronic and mechanical properties can be determined. The ultimate challenge is to produce composites that allow access to the properties of individual NTs.

Acknowledgment

The authors wish to express their gratitude to the MEC of Spain (projects CTQ2005-02609/BQU and Consolider-Ingenio 2010 CSD2007-0010 Nanociencia Molecular), the CAM (project P-PPQ-000225-0505) and the ESF (project 05-SONS-FP-021) for generous financial support.

References

1 Iijima, S. (1991) *Nature*, **354**, 56–8.

2 (a) Popov, V.N. and Lambin, P. (2006) *Carbon Nanotubes*, Springer, Dordrecht.
(b) Reich, S., Thomsen, C. and Maultzsch, J. (2004) *Carbon Nanotubes: Basic Concepts and Physical Properties*, Wiley-VCH Verlag GmbH, Weinheim, Germany.
(c) Special issue on carbon nanotubes (2002) *Acc. Chem. Res.*, **35**, 997–1113.
(d) Harris, P.J.F. (2001) *Carbon Nanotubes and Related Structures: New Materials for the Twenty-First Century*, Cambridge University Press, Cambridge.

3 For a recent review on the nanoforms of carbon, see: Delgado, J.L., Herranz, M.A. and Martín, N. (2008) *J. Mater. Chem.*, **18**, 1417–26.

4 (a) Bethune, D.S., Kiang, C.H., Devries, M.S., Gorman, G., Savoy, R., Vazquez, J. and Beyers, R. (1993) *Nature*, **363**, 605–7.
(b) Iijima, S. and Ichihashi, T. (1993) *Nature*, **363**, 603–5.

5 (a) Journet, C., Maser, W.K., Bernier, P., Loiseau, A., Delachapelle, M.L., Lefrant, S., Deniard, P., Lee, R. and Fischer, J.E. (1997) *Nature*, **388**, 756–8.
(b) Jung, S.H., Kim, M.R., Jeong, S.H., Kim, S.U., Lee, O.J., Lee, K.H., Suh, J.H. and Park, C.K. (2003) *Appl. Phys. Lett.*, **76**, 285–6.

6 (a) Guo, T., Nikolaev, P., Thess, A., Colbert, D.T. and Smalley, R.E. (1995) *Chem. Phys. Lett.*, **243**, 49–54.
(b) Thess, A., Lee, R., Nikolaev, P., Dai, H., Petit, P., Xu, C., Robert, J., Lee, Y.H., Kim, S.G., Rinzler, A.G., Colbert, D.T., Scuseria, G.E., Tomanek, D., Fischer, J.E. and Smalley, R.E. (1996) *Science*, **273**, 483–8.

7 Hafner, J.H., Bronikowski, M.J., Azamian, B.R., Nikolaev, P., Rinzler, A.G., Colbert, D.T., Smith, K.A. and Smalley, R.E. (1998) *Chem. Phys. Lett.*, **296**, 195–202.

8 Nikolaev, P., Bronikowski, M.J., Bradley, R.K., Rohmund, F., Colbert, D.T., Smith, K.A. and Smalley, R.E. (1999) *Chem. Phys. Lett.*, **313**, 91–7.

9 Giacalone, F. and Martín, N. (2006) *Chem. Rev.*, **106**, 5136–90.

10 (a) Moniruzzaman, M. and Winey, K.I. (2006) *Macromolecules*, **39**, 5194–205.
(b) in het Panhuis, M. (2006) *J. Mater. Chem.*, **16**, 3598–605.

(c) For reviews on mechanical reinforcement, see: Coleman, J.N., Khan, U. and Gun'ko, Y.K. (2006) *Adv. Mater.*, **18**, 689–706.
(d) Coleman, J.N., Khan, U., Blau, W.J. and Gun'ko, Y.K. (2006) *Carbon*, **44**, 1624–52.
(e) For reviews on conductive composites, see: Grossiord, N., Loos, J., Regev, O. and Koning, C.E. (2006) *Chem. Mater.*, **18**, 1089–99.
11 Liu, P. (2005) *Eur. Polym. J.*, **41**, 2693–703.
12 Hong, C.-Y. and Pan, C.-Y. (2008) *J. Mater. Chem.*, **18**, 1831–6.
13 Kamat, P.V. (2007) *J. Phys. Chem. C*, **111**, 2834–60.
14 (a) Sgobba, V. and Guldi, D.M. (2008) *J. Mater. Chem.*, **18**, 153–7.
(b) Umeyama, T. and Imahori, H. (2008) *Energy Environ. Sci.*, **1**, 120–33.
15 Thostenson, E.T., Zhifeng, R. and Chou, T.-W. (2001) *Compos. Sci. Technol.*, **61**, 1899–912.
16 Dyke, C.A. and Tour, J.M. (2004) *J. Phys. Chem. A*, **108**, 11151–9.
17 Mann, D., Javey, A., Kong, J., Wang, Q. and Dai, H. (2003) *Nano Lett.*, **3**, 1541.
18 Avouris, P. (2002) *Acc. Chem. Res.*, **35**, 1026–34.
19 Wei, B.Q., Vajtai, R. and Ajayan, P.M. (2001) *Appl. Phys. Lett.*, **79**, 1172–4.
20 Kim, B.M. and Fuhrer, A.M.S. (2004) *J. Phys.: Condens. Matter*, **16**, R553–80.
21 Tang, Z.K., Zhang, L.Y., Wang, N., Zhang, X.X., Wen, G.H., Li, G.D., Wang, J.N., Chan, C.T. and Sheng, P. (2001) *Science*, **292**, 2462–5.
22 Javey, A., Guo, J., Wang, Q., Lundstrom, M. and Dai, H. (2003) *Nature*, **424**, 654–7.
23 (a) Dettlaff-Weglikowska, U., Skakalov, V., Graupner, R., Jhang, S.H., Kim, B.H., Lee, H.J., Ley, L., Park, Y.W., Berber, S., Tomanek, D. and Roth, S. (2005) *J. Am. Chem. Soc.*, **127**, 5125–31.
(b) in het Panhuis, M., Gowrisanker, S., Vanesko, D.J., Mire, C.A., Jia, H., Xie, H., Baughman, R.H., Musselman, I.H., Gnade, B.E., Dieckmann, G.R. and Draper, R.K. (2005) *Small*, **1**, 820–3.
(c) Bradley, K., Gabriel, J.-P.C. and Grüner, G. (2003) *Nano Lett.*, **3**, 1353–5.
24 (a) Che, J.W., Cagin, T. and Goddard, W.A. (2000) *Nanotechnology*, **11**, 65–9.
(b) Osman, M.A. and Srivastava, D. (2001) *Nanotechnology*, **12**, 21–4.
(c) Berber, S., Kwon, Y. and Tománek, D. (2000) *Phys. Rev. Lett.*, **84**, 4613–16.
25 Pop, E., Mann, D., Wang, Q., Goodson, K. and Dai, H. (2006) *Nano Lett.*, **6**, 96–100.
26 Wong, E.W., Sheehan, P.E. and Lieber, C.M. (1997) *Science*, **277**, 1971–5.
27 Salvetat, J.P., Kulik, A.J., Bonard, J.M., Briggs, G.A.D., Stckli, T., Metenier, K., Bonnamy, S., Béguin, F., Burnham, N.A. and Forró, L. (1999) *Adv. Mater.*, **11**, 161–5.
28 Yu, M., Lourie, O., Dyer, M.J., Kelly, T.F. and Ruoff, R.S. (2000) *Science*, **287**, 637–40.
29 Salvetat, J.P., Briggs, G.A.D., Bonard, J.M., Bacsa, R.R., Kulik, A.J., Stockli, T., Burhman, N.A. and Forró, L. (1999) *Phys. Rev. Lett.*, **82**, 944–7.
30 For reviews on the functionalization of NTs, see: (a) Hirsch, A. (2002) *Angew. Chem. Int. Ed.*, **41**, 1853–9.
(b) Barh, J.L. and Tour, J.M. (2002) *J. Mater. Chem.*, **12**, 1952–8.
(c) Nigoyi, S., Hamon, M.A., Hu, H., Zhao, B., Bhomwik, P., Sen, R., Itkis, M.E. and Haddon, R.C. (2002) *Acc. Chem. Res.*, **35**, 1105–13.
(d) Sun, Y.-P., Fu, K., Lin, Y. and Huang, W. (2002) *Acc. Chem. Res.*, **35**, 1096–104.
(e) Banerjee, S., Kahn, M.G.C. and Wong, S.S. (2003) *Chem. Eur. J.*, **9**, 1898–908.
(f) Tasis, D., Tagmatarchis, N., Georgakilas, V. and Prato, M. (2003) *Chem. Eur. J.*, **9**, 4001–8.
(g) Dyke, C.A. and Tour, J.M. (2004) *Chem. Eur. J.*, **10**, 812–17.
(h) Banerjee, S., Hemraj-Benny, T. and Wong, S.S. (2005) *Adv. Mater.*, **17**, 17–29.
(i) Guldi, D.M., Rahman, G.M.A., Zerbetto, F. and Prato, M. (2005) *Acc. Chem. Res.*, **38**, 871–8.
(j) Hirsch, A. and Vostrowsky, O. (2005) *Top. Curr. Chem.*, **245**, 193–237.
(k) Tasis, D., Tagmatarchis, N., Bianco, A. and Prato, M. (2006) *Chem. Rev.*, **106**, 1105–36.

(l) Guldi, D.M., Rahman, G.M.A., Sgobba, V. and Ehli, C. (2006) *Chem. Soc. Rev.*, **35**, 471–87.
(m) Guldi, D.M. (2007) *Phys. Chem. Chem. Phys*, 1400–20.

31 (a) For recent examples of covalent and supramolecular connectivity of an electron donor (π-extended tetrathiafulvalene) to SWNTs, see: Herranz, M.A., Martín, N., Campidelli, S., Prato, M. and Brehm, G. (2006) *Angew. Chem. Int. Ed.*, **45**, 4478–82.
(b) Herranz, M.A., Ehli, C., Campidelli, S., Gutiérrez, M., Hug, G.L., Ohkubo, K., Fukuzumi, S. and Prato, M. (2008) *J. Am. Chem. Soc.*, **130**, 66–73.
(c) Ehli, C., Guldi, D.M., Herranz, M.A., Martín, N., Campidelli, S. and Prato, M. (2008) *J. Mater. Chem.*, **18**, 1498–503.

32 Fu, K., Huang, W., Lin, Y., Riddle, L.A., Carroll, D.L. and Sun, Y.P. (2001) *Nano Lett.*, **1**, 438–41.

33 (a) Riggs, J.E., Guo, Z.X., Carroll, D.L. and Sun, Y.P. (2000) *J. Am. Chem. Soc.*, **122**, 5879–80.
(b) Huang, W.J., Lin, Y., Taylor, S., Gaillard, J., Rao, A.M. and Sun, Y.P. (2002) *Nano Lett.*, **2**, 231–4.

34 Hill, D.E., Lin, Y., Allard, L.F. and Sun, Y.P. (2002) *Int. J. Nanosci.*, **1**, 213–21.

35 He, B.J., Sun, W.L., Wang, M., Liu, S. and Shen, Z.Q. (2004) *Mater. Chem. Phys.*, **84**, 140–5.

36 Sano, M., Kamino, A., Okamura, J. and Shinkai, S. (2001) *Langmuir*, **17**, 5125–8.

37 Chen, J., Hamon, M.A., Hu, H., Chen, Y., Rao, A.M., Eklund, P.C. and Haddon, R.C. (1998) *Science*, **282**, 95–8.

38 Hill, D.E., Lin, Y., Rao, A.M., Allard, L.F. and Sun, Y.P. (2002) *Macromolecules*, **35**, 9466–71.

39 Lin, Y., Zhou, B., Fernando, K.A.S., Liu, P., Allard, L.F. and Sun, Y.P. (2003) *Macromolecules*, **36**, 7199–204.

40 Wong, S.S., Joselevich, E., Woolley, A.T., Cheung, C.L. and Lieber, C.M. (1998) *Nature*, **394**, 52–5.

41 Philip, B., Xie, J.N., Chandrasekhar, A., Abraham, J. and Varadan, V.K. (2004) *Smart Mater. Struct.*, **13**, 295–8.

42 Ge, J.J., Zhang, D., Li, Q., Hou, H., Graham, M.J., Dai, L., Harris, F.W. and Cheng, S.Z.D. (2008) *J. Am. Chem. Soc.*, **127**, 9984–5.

43 Dwyer, C., Guthold, M., Falvo, M., Washburn, S., Superfine, R. and Erie, D. (2002) *Nanotechnology*, **13**, 601–4.

44 Jiang, K.Y., Schadler, L.S., Siegel, R.W., Zhang, X.J., Zhang, H.F. and Terrones, M. (2004) *J. Mater. Chem.*, **14**, 37–9.

45 Qin, S.H., Qin, D.Q., Ford, W.T., Resaco, D.E. and Herrera, J.E. (2004) *Macromolecules*, **37**, 752–7.

46 Liu, Y.Q., Yao, Z.L. and Adronov, A. (2005) *Macromolecules*, **38**, 1172–9.

47 (a) Georgakilas, V., Kordatos, K., Prato, M., Guldi, D.M., Holzinger, M. and Hirsch, A. (2002) *J. Am. Chem. Soc.*, **124**, 760–1.
(b) Georgakilas, V., Tagmatarchis, N., Pantarotto, D., Bianco, A., Briand, J.-P. and Prato, M. (2002) *Chem. Commun.*, 3050–1.

48 Pantarotto, D., Partidos, C.D., Graff, R., Hoebeke, J., Briand, J.P. and Prato, M. (2003) *J. Am. Chem. Soc.*, **125**, 6160–4.

49 Georgakilas, V., Bourlinos, A., Gournis, D., Tsoufis, T., Trapalis, C., Mateo-Alonso, A. and Prato, M. (2008) *J. Am. Chem. Soc.*, **130**, 8733–40.

50 Viswanathan, G., Chakrapani, N., Yang, H., Wei, B., Chung, H., Cho, K., Ryu, C. and Ajayan, P.M. (2003) *J. Am. Chem. Soc.*, **125**, 9258–9.

51 Li, X.F., Guan, W.C., Yan, H.B. and Huang, L. (2004) *Mater. Chem. Phys.*, **88**, 53–8.

52 Tong, X., Liu, C., Cheng, H.-M., Zhao, H., Yang, F. and Zhang, X. (2004) *J. Appl. Polym. Sci.*, **92**, 3697–700.

53 Qin, S.H., Qin, D.Q., Ford, W.T., Resasco, D.E. and Herrera, J.E. (2004) *J. Am. Chem. Soc.*, **126**, 170–6.

54 Hwang, G.L., Shieh, Y.-T. and Hwang, K.C. (2004) *Adv. Funct. Mater.*, **14**, 487–91.

55 Xia, H., Wang, Q. and Qiu, G. (2003) *Chem. Mater.*, **15**, 3879–86.

56 Baskaran, D., Mays, J.W. and Bratcher, M.S. (2004) *Angew. Chem. Int. Ed.*, **43**, 2138–42.

57 Yao, Z.L., Braidy, N., Botton, G.A. and Adronov, A. (2003) *J. Am. Chem. Soc.*, **125**, 16015–24.

58 (a) Curran, S.A., Ajayan, P.M., Blau, W.J., Carroll, D.L., Coleman, J.N.,

Dalton, A.B., Davey, A.P., Drury, A., McCarthy, B., Maier, S. and Stevens, A. (1998) *Adv. Mater.*, **10**, 1091–3.
(b) Ago, H., Petritsch, K., Shaffer, M.S.P., Windle, A.H. and Friend, R.H. (1999) *Adv. Mater.*, **11**, 1281–5.
(c) Kymakis, E. and Amaratunga, G.A. (2002) *J. Appl. Phys. Lett.*, **80**, 112–14.

59 Shirakawa, H., Louis, E.J., MacDiarmid, A.G., Chiang, C.K. and Heeger, A.J. (1977) *J. Chem. Soc. Chem. Commun.*, 578–9.

60 Coleman, J.M., Dalton, A.B., Curran, S., Rubio, A., Davey, A.P., Drury, A., MacCarthy, B., Lahr, B., Ajayan, P.M., Roth, S., Barklie, R.C. and Blau, W.J. (2000) *Adv. Mater.*, **12**, 213–16.

61 Star, A., Stoddart, J.F., Steuerman, D., Diehl, M., Boukai, A., Wong, E.W., Yang, X., Chung, S.-W., Choi, H. and Heath, J.R. (2001) *Angew. Chem. Int. Ed.*, **40**, 1721–5.

62 Steuerman, D.W., Star, A., Narizzano, R., Choi, H., Ries, R.S., Nicolini, C., Stoddart, J.F. and Heath, J.R. (2002) *J. Phys. Chem. B*, **106**, 3124–30.

63 Star, A., Liu, Y., Grant, K., Ridvan, L., Stoddart, J.F., Steuerman, D.W., Diehl, M.R., Boukai, A. and Heath, J.R. (2003) *Macromolecules*, **36**, 553–60.

64 Star, A. and Stoddart, J.F. (2002) *Macromolecules*, **35**, 7516–20.

65 (a) Ramasubramanian, R., Chen, J. and Liu, J. (2003) *Appl. Phys. Lett.*, **83**, 2928–30.
(b) Curran, S., Davey, A.P., Coleman, J.N., Czerw, R., Dalton, A.B., McCarthy, B., Maier, S., Drury, A., Gray, D., Brennan, M., Ryder, K., Lamy de la Chapelle, M., Journet, C., Bernier, P., Byrne, H.J. Carroll, D., Ajayan, P.M., Lefrant, S. and Blau, W.J. (1999) *Synth. Met.*, **103**, 2559–62.

66 Fan, J., Wan, M., Zhu, D., Chang, B., Pan, Z. and Xie, S. (1999) *J. Appl. Polym. Sci.*, **74**, 2605–10.

67 Hughes, M., Chen, G.Z., Shaffer, M.S.P., Fray, D.J. and Windle, A.H. (2004) *Comp. Sci. Technol.*, **64**, 2325–31.

68 Tang, B.Z. and Xu, H.Y. (1999) *Macromolecules*, **32**, 2569–76.

69 Yang, M., Koutsos, V. and Zaiser, M. (2005) *J. Phys. Chem. B*, **109**, 10009–14.

70 Wei, Z.X., Wan, M.X., Lin, T. and Dai, L.M. (2003) *Adv. Mater.*, **15**, 136–9.

71 Wu, T.-M., Lin, Y.-W. and Liao, C.-S. (2005) *Carbon*, **43**, 734–40.

72 Chen, F.M., Wang, B., Chen, Y. and Li, L.J. (2007) *Nano Lett.*, **7**, 3013–17.

73 Cheng, F., Imin, P., Maunders, C., Botton, G. and Adronov, A. (2008) *Macromolecules*, **41**, 2304–8.

74 Hwang, J.-Y., Nish, A., Doig, J., Douven, S., Chen, C.-W., Chen, L.-C. and Nicholas, R.J. (2008) *J. Am. Chem. Soc.*, **130**, 3543–53.

75 O'Connel, R.J., Boul, P.J., Ericson, L.M., Huffman, C., Wang, Y., Haroz, E., Kuper, C., Tour, J., Ausman, K.D. and Smalley, R.E. (2001) *Chem. Phys. Lett.*, **342**, 265–71.

76 Gong, X., Liu, J., Baskaran, S., Voise, R.D. and Young, J.S. (2000) *Chem. Mater.*, **12**, 1049–52.

77 Jin, Z., Pramoda, K.P., Goh, S.H. and Xu, G. (2002) *Mater. Res. Bull.*, **37**, 271–8.

78 Yang, D.-Q., Rochette, J.-F. and Sacher, E. (2005) *J. Phys. Chem. B*, **109**, 4481–4.

79 Richard, C., Balavoine, F., Schultz, P., Ebbesen, T.W. and Mioskowski, C. (2003) *Science*, **300**, 775–8.

80 Mackiewicz, N., Surendran, G., Remita, H., Keita, B., Zhang, G., Nadjo, L., Hagège, A., Doris, E. and Mioskowski, C. (2008) *J. Am. Chem. Soc.*, **130**, 8110–11.

81 Star, A., Steuerman, D.W., Heath, J.R. and Stoddart, J.F. (2002) *Angew. Chem. Int. Ed.*, **41**, 2508–12.

82 Gao, H.J. and Kong, Y. (2004) *Ann. Rev. Mater. Res.*, **34**, 123–50.

83 Dieckmann, G.R., Dalton, A.B., Johnson, P.A., Razal, J., Chen, J., Giordano, G.M., Munoz, E., Musselman, I.H., Baughman, R.H. and Draper, R.K. (2003) *J. Am. Chem. Soc.*, **125**, 1770–7.

84 Zorbas, V., Ortiz-Acevedo, A., Dalton, A.B., Yoshida, M.M., Dieckmann, G.R., Draper, R.K., Baughman, K.R.H., Jose-Yacaman, M. and Musselman, I.H. (2004) *J. Am. Chem. Soc.*, **126**, 7222–7.

85 (a) Park, S., Yang, H.-S., Kim, D., Jo, K. and Jon, S. (2008) *Chem. Commun.*, 2876–8.
(b) Srinivasan, S., Praveen, V.K., Philip, R. and Ajayaghosh, A. (2008) *Angew. Chem. Int. Ed.*, **47**, 5750–4.

86 (a) Hong, C.Y., You, Y.Z. and Pan, C.Y. (2005) *Chem. Mater.*, **17**, 2247–54.
(b) Xu, G.Y., Wu, W.T., Wang, Y.S., Pang, W.M., Wang, P.H., Zhu, Q.R. and Lu, F. (2006) *Nanotechnology*, **17**, 2458–65.

87 Kong, H., Li, W.W., Yan, D.Y., Jin, Y.Z., Walton, D.R.M. and Kroto, H.W. (2004) *Macromolecules*, **37**, 6683–6.

88 Wang, D. and Chen, L.W. (2007) *Nano. Lett.*, **7**, 1480–4.

89 You, Y.Z., Hong, C.Y. and Pan, C.Y. (2007) *Adv. Funct. Mater.*, **17**, 2470–7.

90 Chen, G., Wright, P.M., Geng, J., Mantovani, G. and Haddleton, D.M. (2008) *Chem. Commun.*, 1097–9.

91 Zhao, W., Song, C. and Pehrsson, P.E. (2002) *J. Am. Chem. Soc.*, **124**, 12418–19.

92 Li, H. and Adronov, A. (2007) *Carbon*, **45**, 984–90.

93 Grunlan, J.C., Liu, L. and Kim, Y.S. (2006) *Nano Lett.*, **6**, 911–15.

94 Nepal, D. and Geckeler, K.E. (2006) *Small*, **2**, 406–12.

95 (a) Kim, S.N., Rusling, J.F. and Papadimitrakopoulos, F. (2007) *Adv. Mater.*, **19**, 3214–28.
(b) Star, A., Tu, E., Niemann, J., Gabriel, J.P., Joiner, C.S. and Valcke, C. (2006) *Proc. Natl. Acad. Sci. U.S.A.*, **103**, 921–6.
(c) Satishkumar, B.C., Brown, L.O., Gao, Y., Wang, C.C., Wang, H.L. and Doorn, S.K. (2007) *Nat. Nanotechnol.*, **2**, 560–4.

96 Heller, D.A., Jeng, E.S., Yeung, T.K., Martinez, B.M., Moll, A.E., Gastala, J.B. and Strano. M.S. (2006) *Science*, **311**, 508–11.

97 Jeng, E.S., Moll, A.E., Roy, A.C., Gastala, J.B. and Strano, M.S. (2006) *Nano Lett.*, **6**, 371–5.

98 Gao, X., Xing, G., Yang, Y., Shi, X., Liu, R., Chu, W., Jing, L., Zhao, F., Ye, C., Yuan, H., Fang, X., Wang, C. and Zhao, Y. (2008) *J. Am. Chem. Soc.*, **130**, 9190–1.

99 Barone, P.W. and Strano, M.S. (2006) *Angew. Chem. Int. Ed.*, **45**, 8138–41.

100 Srinivasan, S., Babu, S.S., Praveen, V.K. and Ajayaghosh, A. (2008) *Angew. Chem. Int. Ed.*, **47**, 5746–9.

101 Ogoshi, T., Takashima, Y., Yamaguchi, H. and Harada, A. (2007) *J. Am. Chem. Soc.*, **129**, 4878–9.

102 (a) Cheng, F. and Adronov, A. (2006) *Chem. Eur. J.*, **12**, 5053–9.
(b) Satake, A., Miyajima, Y. and Kobuke, Y. (2005) *Chem. Mater.*, **17**, 716–24.
(c) Li, H., Zhou, B., Lin, Y., Gu, L., Wang, W., Fernando, K.A.S., Kumar, S., Allard, L.F. and Sun, Y.-P. (2004) *J. Am. Chem. Soc.*, **126**, 1014–15.
(d) Chen, J. and Collier, C.P. (2005) *J. Phys. Chem. B*, **109**, 7605–9.

103 Cheng, F., Zhang, S., Adronov, A., Echegoyen, L. and Diederich, F. (2006) *Chem. Eur. J.*, **12**, 6062–70.

104 (a) Murakami, H., Nomura, T. and Nakashima, N. (2003) *Chem. Phys. Lett.*, **378**, 481–5.
(b) Rahman, G.M.A., Guldi, D.M., Campidelli, S. and Prato, M. (2006) *J. Mater. Chem.*, **16**, 62–5.

105 (a) Saito, K., Troiani, V., Qiu, H., Solladié, N., Sakata, T., Mori, H., Ohama, M. and Fukuzumi, S. (2007) *J. Phys. Chem. C*, **111**, 1194–9.
(b) Fukuzumi, S. and Kojima, T. (2008) *J. Mater. Chem.*, **18**, 1427–39.

106 (a) Qin, S., Qin, D., Ford, W.T., Herrera, J.E., Resasco, D.E., Bachilo, S.M. and Weisman, R.B. (2004) *Macromolecules*, **35**, 3965–70.
(b) Guldi, D.M., Rahman, G.M.A., Ramey, J., Marcaccio, M., Paolucci, D., Paolucci, F., Qin, S., Ford, W.T., Balbinot, D., Jux, N., Tagmatarchis, N. and Prato, M. (2004) *Chem. Commun.*, 2034–5.

107 Guldi, D.M., Rahman, G.M.A., Qin, S., Tchoul, M., Ford, W.T., Marcaccio, M., Paolucci, D., Paolucci, F., Campidelli, S. and Prato, M. (2006) *Chem. Eur. J.*, **12**, 2152–61.

108 (a) Guldi, D.M., Rahman, G.M.A., Prato, M., Jux, N., Qin, S. and Ford, W. (2005) *Angew. Chem. Int. Ed.*, **44**, 2015–18.
(b) Sgobba, V., Rahman, G.M.A., Guldi, D.M., Jux, N., Campidelli, S. and Prato, M. (2006) *Adv. Mater.*, **18**, 2264–9.

109 Rahman, G.M.A., Guldi, D.M., Cagnoli, R., Mucci, A., Schenetti, L., Vaccari, L. and Prato, M. (2005) *J. Am. Chem. Soc.*, **127**, 10051–7.

110 (a) Hasobe, T., Fukuzumi, S. and Kamat, P.V. (2005) *J. Am. Chem. Soc.*, **127**, 11884–5.

(b) Hasobe, T., Fukuzumi, S. and Kamat, P.V. (2006) *J. Phys. Chem. B*, **110**, 25477–84.

111 (a) Brabec, C.J., Sariciftci, N.S. and Hummelen, J.C. (2001) *Adv. Funct. Mater.*, **11**, 15–26.
(b) Coakley, K.M. and McGehee, M.D. (2004) *Chem. Mater.*, **16**, 4533–42.
(c) Günes, S. and Neugebauer, H. (2007) *Chem. Rev.*, **107**, 1324–38.
(d) Armaroli, N. and Balzani, V. (2007) *Angew. Chem. Int. Ed.*, **46**, 52–66.
(e) Cravino, A. (2007) *Polym. Int.*, **56**, 943–56.
(f) Thompson, B.C. and Fréchet, J.M.J. (2008) *Angew. Chem. Int. Ed.*, **47**, 58–77.
(g) Balzani, V., Credi, A. and Venturi, M. (2008) *ChemSusChem*, **1**, 26–58.

112 (a) Ago, H., Petritsch, K., Shaffer, M.S.P., Windle, A.H. and Friend, R.H. (1999) *Adv. Mater.*, **11**, 1281–5.
(b) Kymakis, E., Stratakis, E. and Koudoumas, E. (2007) *Thin Solid Films*, **515**, 8589–600.
(c) Berson, S., Bettingbies, R., Bailly, S., Guillerez, S. and Jousselme, B. (2007) *Adv. Funct. Mater.*, **17**, 3363–70.

113 (a) For recent examples of high efficiency PV devices, see: Ma, W., Yang, C., Gong, X., Lee, K. and Heeger, A.J. (2005) *Adv. Funct. Mater.*, **15**, 1617–22.
(b) Kim, Y., Cook, S., Tuladhar, S.M., Choulis, S.A., Nelson, J., Durrant, J.R., Bradley, D.D.C., Giles, M., McCulloch, I., Ha, C.-S. and Ree, M. (2006) *Nat. Mater.*, **5**, 197–203.
(c) Hoppe, H. and Sariciftci, N.S. (2006) *J. Mater. Chem.*, **16**, 45–61.
(d) Kim, J.Y., Lee, K., Coates, N.E., Moses, D., Nguyen, T.-Q., Dante, M. and Heeger, A.J. (2007) *Science*, **317**, 222–5.

114 (a) Riedel, I., von Hauff, E., Parisi, J., Martín, N., Giacalone, F. and Dyakonov, V. (2005) *Adv. Funct. Mater.*, **15**, 1979–87.
(b) Catellani, M., Luzzati, S., Lupsac, N.O., Mendichi, R., Consonni, R., Giacalone, F., Segura, J.L. and Martín, N. (2004) *Thin Solid Films*, **452**, 43–7.

115 (a) Rowell, M.W., Topinka, M.A., McGehee, M.D., Prall, H.J., Dennler, G., Sariciftci, N.S., Hu, L.B. and Gruner, G. (2006) *Appl. Phys. Lett.*, **88**, 233506-233506-3.
(b) Pasquier, A.D., Unalan, H.E., Kanwal, A., Miller, S. and Chhowalla, M. (2006) *Appl. Phys. Lett.*, **87**, 203511-203511-3.

Index

Fullerene Polymers. Synthesis, Properties and Applications. Edited by Nazario Martín and Francesco Giacalone

ISBN: 978-3-527-32282-4

d